DATE LABEL

145

Acc. No.

Class No.

Book No.

Author

Title

Borrower's No.	Issue Date	Borrower's No.	Issue Date

Acc. No. _____

Class No. _____ Book No. _____

Author _____

Title _____

Borrower's No.	Issue Date	Borrower's No.	Issue Date

DIFFUSION IN AND THROUGH SOLIDS

DIFFUSION
IN AND THROUGH
SOLIDS

BY

RICHARD M. BARRER
D.Sc. (N.Z.), Ph.D. (Cantab.), F.I.C.

*Head of the Chemistry Department, The Technical
College, Bradford; formerly Research
Fellow, Clare College, Cambridge*

PRINTED IN GREAT BRITAIN

CONTENTS

PAGE

FOREWORD

The general theory of diffusion is based upon analogy to the flow of heat through solid media, as is exemplified in the classical treatments of Fourier and also of Lord Kelvin in the *Encyclopedia*. In the actual process of diffusion of molecules and ions through and in solids a whole set of new phenomena is observed. For example, limitations on the magnitude of the diffusion potential are much more frequently imposed on these material systems by such factors as solubility or compound formation than are observed in systems in which the flow of heat alone is concerned. Again the flow of matter through solids is frequently composite in character, the various modes of transport being dependent on microheterogeneity, as is exemplified by lattice diffusion and movement along crystal boundaries, canals and capillaries, or even on molecular discontinuity as is the case when migration depends on the existence of molecular or ionic "holes" or vacant lattice points in a crystal. In studying the movement of material particles through a solid, we must consider the nature of the interaction between diffusing material and diffusion medium. We may in a somewhat general manner note that either only dispersive or Van der Waals interactions are involved, or that electronic switches have taken place leading to chemi-sorption or chemical combination. Migration across a surface or through a solid medium may thus involve movement across an energy barrier from one position of minimum potential energy to another. At sufficiently high temperatures in the higher energy levels activated surface migration naturally merges into free migration, with a consequent change in the temperature dependence of the diffusion.

The mechanism of the transfer of material across phase boundaries likewise presents a number of novel and interesting problems. Here we have to consider firstly the abnormal

distribution of diffusing material at the phase boundary. We note that the Donnan membrane equilibrium may apply to electrolytic systems diffusing through a solid membrane, the Gibbs relation for a non-electrolyte or· the adsorption isotherm for a gas permeating a solid. Diffusion must then take place into and out of the boundary layer from the homogeneous phases on both sides. Energies of activation are involved which may differ considerably from those required for the diffusion process in the homogeneous phases. Dr Barrer has been interested in these problems for a number of years, from the theoretical as well as from the experimental point of view. I pointed out to him that they were the concern of many who would find a monograph on the subject invaluable in their work, and I experienced a deep sense of satisfaction when my colleague assented to the suggestion of writing a book.

E. K. RIDEAL

LABORATORY OF COLLOID SCIENCE
THE UNIVERSITY
CAMBRIDGE

12 *February* 1941

AUTHOR'S PREFACE

Diffusion processes are related to chemical kinetics on the one hand, and to sorption and solution equilibria on the other. There are available excellent surveys dealing with chemical kinetics and also with sorption equilibria. No previous text has attempted to correlate and summarise diffusion data in condensed phases, save briefly and in relation to one or other of these fields. It is apparent that the study of diffusion touches upon numerous aspects of physico-chemical research. There are in general two states of flow by diffusion—the so-called stationary and non-stationary states. From the former one derives the *permeability constant* (quantity transferred/unit time/unit area of unit thickness under a standard concentration or pressure difference) and from the latter the *diffusion constant*. The permeability constant, P, and the diffusion constant, D, are related by

$$P = -D \frac{\partial C}{\partial x},$$

when $\partial C / \partial x$ is a standard concentration gradient. One therefore has to do also with the solubility of the diffusing substance in the solvent. The aim of this book has been to study the permeability of materials to solutes, and the diffusion constants of solutes within them, and not specifically the sorption equilibria partly controlling the permeability. However, wherever the permeability and diffusion constants are discussed it becomes essential to outline also the data on solubility, and this has been done throughout the book.

In treating the data, the author has tried to keep a balance between experimental methods and their mathematical and physical interpretation; the listing of adequate numerical values of permeability and diffusion constants which may serve as reference material, and as starting points for further investigations; and outlines of current theories of processes of

permeation, solution and diffusion in solids. Many problems remain partially or completely unsolved, but if this book directs attention to them, and produces further work in a very fruitful field of research, it will adequately repay the time and trouble involved in its preparation.

In Chapter I is given a number of solutions of the diffusion equation suitable for treating the various diffusion problems that may arise. The solutions are as explicit as possible, so that they may be employed at once, or with the aid of tables of Gauss or Bessel functions. The purpose of this chapter is to provide ready-made integrals of the diffusion equation, thus avoiding too long a search through a scattered literature for suitable solutions. Not all experimentalists have the mathematical training to derive at will solutions to suit the boundary conditions of their particular problem. Chapter II is devoted to a survey of the different types of gas flow in capillary systems, from the study of which interesting methods of fractionating gas mixtures have been evolved. The peculiar permeability of some glasses to certain gases has been known for a considerable time, and Chapter III considers gas flow through glasses, and in crystals. These diffusions are much more selective than those considered in capillary systems, but they are not specific as are the processes of diffusion of gases through and in metals, discussed in Chapters IV and V. The uptake and evolution of gases by metals is a subject of technical importance concerning which a great body of experimental evidence has been amassed. These chapters, however, show that many problems remain unsolved.

Chapters VI and VII describe the phenomena of conductivity and diffusion of ions and atoms in ionic lattices and metals. The first of these chapters has to do with reversible diffusion phenomena, and the second with irreversible diffusion processes depending upon the past history of the system concerned. Many of the problems discussed in Chapter VII have to do with diffusion processes down grain boundaries or internal surfaces, so that it is but a step to the treatment of numerous and interesting surface diffusions, described in

Chapter VIII. Finally, in Chapters IX and X the problems of gas and vapour flow through and diffusion in organic polymers are considered. In these chapters a large number of permeability and diffusion constants are collected for systems of technical importance. As examples one may cite the passage of gases and vapours through rubbers, proteins and celluloses, and of water through leather, or insulating substances such as vulcanite, ebonite, rubber, or guttapercha.

B D

CHAPTER I

SOLUTIONS OF THE DIFFUSION EQUATION

DIFFERENTIAL FORMS OF FICK'S LAWS

No adequate compilation of those solutions of the diffusion equation applicable to the diffusion of matter has as yet been made. The author has become aware of the difficulty of obtaining suitable solutions in a number of studies of diffusion, and it is hoped that this chapter will provide a source of reference for such solutions. Equations of chemical kinetics can be used readily in differential or integral form, but the equations of diffusion kinetics require for their treatment a special and often laborious technique. Many of the cases which can arise have not yet been solved rigorously, though the field is a rich one both from the mathematical and the experimental viewpoints. The present chapter aims at giving some solutions of the diffusion equation in a form in which they may be applied, together with cases of diffusion systems in which the boundary conditions are those of the diffusion equation solved.

Two familiar differential forms of Fick's laws of diffusion are:

$$P = -D \frac{\partial C}{\partial x} \tag{1}$$

and

$$\frac{\partial C}{\partial t} = D \frac{\partial^2 C}{\partial x^2}. \tag{2}$$

Equation (1) gives the rate of permeation, in the steady state of flow, through unit area of any medium, in terms of the concentration gradient across the medium, and a constant called the diffusion constant D. The second equation refers to the accumulation of matter at a given point in a medium as a function of time. That is, it refers to a non-stationary state of flow. This second equation may be derived from the first, by considering diffusion in the $+x$ direction of a cylinder of unit cross-section. The accumulation of matter within an element of volume dx bounded by two planes, 1 and 2, normal

to the axis of the cylinder, dx apart, may be estimated as follows:

The rate of accumulation is

$$(P_1 - P_2) = -D\frac{\partial(C)}{\partial x} + D\frac{\partial}{\partial x}\left(C + \frac{\partial C}{\partial x}dx\right) = \frac{\partial C}{\partial t}dx,$$

which gives

$$\frac{\partial C}{\partial t} = D\frac{\partial^2 C}{\partial x^2}.$$

In two dimensions the above equation becomes

$$\frac{\partial C}{\partial t} = D\frac{\partial^2 C}{\partial x^2} + D\frac{\partial^2 C}{\partial y^2}, \tag{3}$$

and in three dimensions

$$\frac{\partial C}{\partial t} = D\frac{\partial^2 C}{\partial x^2} + D\frac{\partial^2 C}{\partial y^2} + D\frac{\partial^2 C}{\partial z^2} \tag{4}$$

or

$$\frac{\partial C}{\partial t} = D\nabla^2 C \tag{5}$$

or

$$\frac{\partial C}{\partial t} = D\,(\text{div grad})\,C, \tag{6}$$

as it may alternatively be written. All the equations (3)–(6) assume an isotropic medium, but if the medium is not isotropic one may simply write

$$\frac{\partial C}{\partial t} = D_x\frac{\partial^2 C}{\partial x^2} + D_y\frac{\partial^2 C}{\partial y^2} + D_z\frac{\partial^2 C}{\partial z^2}, \tag{7}$$

and then make the substitution

$$\xi = \frac{x\sqrt{D}}{\sqrt{D_x}}; \quad \eta = \frac{y\sqrt{D}}{\sqrt{D_y}}; \quad \zeta = \frac{z\sqrt{D}}{\sqrt{D_z}}$$

to bring the equation to the form of (4):

$$\frac{\partial C}{\partial t} = D\left\{\frac{\partial^2 C}{\partial \xi^2} + \frac{\partial^2 C}{\partial \eta^2} + \frac{\partial^2 C}{\partial \zeta^2}\right\}. \tag{8}$$

This transformation involves then a change of co-ordinates, after which methods suitable for the solution of (4) apply also to (8).

In many cases the diffusion constant, D, depends itself upon the concentration in the medium, e.g. the interdiffusion of

metals (Chap. VI), the diffusion of water in certain zeolites (Chap. III), the surface diffusion of caesium, sodium, potassium, or thorium on tungsten (Chap. VIII), or the diffusion of organic vapours in media such as rubber which swell during the permeation process (Chap. X). It is now necessary to solve an equation of the form

$$\frac{\partial C}{\partial t} = \frac{\partial}{\partial x}\left[D\frac{\partial C}{\partial x}\right] + \frac{\partial}{\partial y}\left[D\frac{\partial C}{\partial y}\right] + \frac{\partial}{\partial z}\left[D\frac{\partial C}{\partial z}\right]. \tag{9}$$

Equation (4) may be expressed in spherical polar co-ordinates r, θ, and ϕ, by means of the transformation equations

$$\left.\begin{aligned} x &= r\sin\theta\cos\phi, \\ y &= r\sin\theta\sin\phi, \\ z &= r\cos\theta. \end{aligned}\right\} \tag{10}$$

Equation (4) then becomes

$$\frac{\partial C}{\partial t} = \frac{D}{r^2}\left[\frac{\partial}{\partial r}\left(r^2\frac{\partial C}{\partial r}\right) + \frac{1}{\sin\theta}\frac{\partial}{\partial\theta}\left(\sin\theta\frac{\partial C}{\partial\theta}\right) + \frac{1}{\sin^2\theta}\frac{\partial^2 C}{\partial\phi^2}\right]. \tag{11}$$

Equation (11), for a spherically symmetrical diffusion, reduces to

$$\frac{\partial C}{\partial t} = D\left[\frac{\partial^2 C}{\partial r^2} + \frac{2}{r}\frac{\partial C}{\partial r}\right], \tag{12}$$

for then $\partial C/\partial\theta = 0$ and $\partial^2 C/\partial\phi^2 = 0$.

If one desires to express equation (4) in cylindrical co-ordinates r, θ and z, the transformation equations are

$$\left.\begin{aligned} x &= r\cos\theta, \\ y &= r\sin\theta, \end{aligned}\right\} \tag{13}$$

so that the equation becomes

$$\frac{\partial C}{\partial t} = \frac{D}{r}\left[\frac{\partial}{\partial r}\left(r\frac{\partial C}{\partial r}\right) + \frac{\partial}{\partial\theta}\left(\frac{1}{r}\frac{\partial C}{\partial\theta}\right) + \frac{\partial}{\partial z}\left(r\frac{\partial C}{\partial z}\right)\right]. \tag{14}$$

Equation (14) again takes simpler forms in certain cases. In problems concerning the sorption and desorption of gases in

and from long metal wires, for example, where end-effects are small, the equation reduces to

$$\frac{\partial C}{\partial t} = D\left[\frac{1}{r}\frac{\partial}{\partial r}\left(r\frac{\partial C}{\partial r}\right)\right], \tag{15}$$

because $\partial C/\partial \theta = 0$, and $\partial^2 C/\partial z^2 = 0$. For examples of the use of the full equations (11) and (14) text-books on the conduction of heat may be consulted (e.g. Carslaw, *Mathematical Theory of the Conduction of Heat*, Macmillan, 1921; Ingersoll and Zobell, *Mathematical Theory of Heat Conduction*, Boston, 1913). The equations (1)–(15) serve to show most of the differential forms of the diffusion equation which may be encountered in studies of diffusion kinetics.

Various solutions taken from different fields of diffusion kinetics may now be given. In order, the solutions given will be for

A. The steady state of flow.

B. The non-stationary state of flow:

    (1) Diffusion in one dimension—the infinite, semi-infinite, and finite solid.

    (2) Radial diffusion.

    (3) Diffusion in cylinders.

    (4) Surface reaction and diffusion simultaneously.

    (5) Instantaneous point, surface, and volume sources.

    (6) Diffusion when D depends on the concentration.

The solutions given cover a great variety of diffusion systems, and with the aid of appropriate tables for error and Bessel functions may be readily applied to practical problems.

A. The steady state of flow

The diffusion equation takes particularly simple forms when the term $\partial C/\partial t = 0$, i.e. as much solute leaves a given volume element as enters it per unit of time. The equations of flow then become:

Through a plate: $$D\frac{\partial^2 C}{\partial x^2} = 0. \tag{16}$$

Through a hollow spherical shell:

$$\frac{1}{r}\frac{\partial^2(rC)}{\partial r^2} = 0. \tag{17}$$

Through a cylindrical tube:

$$\frac{1}{r}\frac{\partial(r\,\partial C/\partial r)}{\partial r} = 0. \tag{18}$$

The plate. Consider the diffusion of a gas through a plate of thickness l. If the boundary conditions are

$$C = C_1 \text{ at } x = 0 \text{ for all } t,$$

$$C = C_2 \text{ at } x = l \text{ for all } t,$$

the solution $\qquad C = Ax + B \qquad$ (19)

of equation (16) may be further elucidated by putting $x = 0$, and $x = l$, and eliminating A and B. This procedure leads to the expression

$$\frac{C - C_1}{C_2 - C_1} = \frac{x}{l}, \tag{20}$$

where C denotes the steady state concentration at any value of x. The flow through unit area of the plate is

$$V\frac{\partial C_g}{\partial t} = -D\left(\frac{\partial C}{\partial x}\right)_{x=l} = D\frac{C_1 - C_2}{l}, \tag{21}$$

where C_g denotes the concentration of the gas which has diffused through the plate into a volume V at a time t (the condition $C = C_2$ at $x = l$ for all t naturally makes it necessary that $C_g \ll C_2$). Then the amount of gas which has diffused in time t is

$$VC_g = D\frac{C_1 - C_2}{l}t. \tag{22}$$

The hollow sphere. For the diffusion of a gas through a hollow spherical shell of internal and external radii b and a respectively, with boundary conditions

$$C = C_1 \text{ at } r = b \text{ for all } t,$$

$$C = C_2 \text{ at } r = a \text{ for all } t,$$

the solution of (17) is

$$\frac{C_1 - C}{C_1 - C_2} = \frac{a\,(r - b)}{r\,(a - b)}, \tag{23}$$

where C is the steady state concentration at any value of r. The outward flow of gas per unit time and per unit area of the shell is then

$$-D\left(\frac{\partial C}{\partial r}\right)_{r=a} = D(C_1 - C_2)\frac{b}{a}\frac{1}{(a - b)}. \tag{24}$$

Over the whole area of the shell the expression is

$$q = -4\pi a^2 D\left(\frac{\partial C}{\partial r}\right)_{r=a} = 4\pi D(C_1 - C_2)\frac{ab}{(a - b)}, \tag{25}$$

and the quantity diffused in time t, $Q = \int_0^t q\,dt$, is

$$Q = 4\pi D(C_1 - C_2)\frac{ab}{(a - b)}t. \tag{26}$$

The cylindrical tube. The solution of equation (18) is

$$C = A \ln r + B,$$

and if the boundary conditions are

$$C = C_1 \text{ at } r = b \text{ for all } t,$$

$$C = C_2 \text{ at } r = a \text{ for all } t,$$

where b and a are respectively the internal and external radii of the tube, one may as for (20) and (23) eliminate A and B and obtain

$$C = \frac{C_1 - C_2}{\ln b - \ln a}\ln r + \frac{C_2 \ln b - C_1 \ln a}{\ln b - \ln a}. \tag{27}$$

This leads to an expression for Q, the quantity which diffuses through unit length of the wall of the cylinder in time t:

$$Q = \frac{2\pi D(C_2 - C_1)\,t}{\ln a - \ln b}. \tag{28}$$

The equations given will be found useful in evaluating the permeability constants of various types of membrane. The diffusion constants may also be evaluated when the absolute values of C_1 and C_2 are known. The permeability constant

may conveniently be defined as the quantity of gas diffusing per unit of time through unit area of the outgoing surface of a plate, cylinder, or hollow sphere when unit concentration gradient exists at that surface. Other equivalent definitions may be found more practical, and will be used in later chapters (e.g. Chap. II). The permeability constant as defined above is *numerically* equal to the diffusion constant. The dimensions are, however, different.

B. THE NON-STATIONARY STATE OF FLOW

(1) *Solutions of the linear diffusion law*

Solutions of the Fick law for diffusion in the x-direction may be divided into those for infinite, semi-infinite, and finite solids. The infinite solid extends to infinity in $+$ and $-x$ directions, the semi-infinite solid extends from a bounding plane at $x = 0$ to $x = +\infty$, and the finite solid is bounded by planes at $x = 0$, $x = l$ and sometimes $x = (l+h)$. All these solutions are exemplified by physical systems, which will be illustrated in the text.

(a) *The infinite solid.*

We have to solve the equation

$$\frac{\partial C}{\partial t} = D\frac{\partial^2 C}{\partial x^2},$$

given that $\quad C = C(x,t), \quad$ when $t > 0$,

$\quad C = f(x), \quad$ when $t = 0$,

$f(x)$ can be differentiated when $t > 0$.

The solution may be written as

$$C = \phi(x)\,F(t), \tag{29}$$

which allows one to separate the variables in Fick's law. $\phi(x)$ and $F(t)$ take the forms

$$\left.\begin{aligned}\phi(x) &= A\cos kx + B\sin kx,\\ F(t) &= \alpha e^{-k^2 Dt},\end{aligned}\right\} \tag{30}$$

where A, B, α and k are real constants. Any sum of solutions is also a solution, and a new solution is therefore obtained when the equations (30) are integrated over all values of k:

$$C = \int_0^\infty [g(k) \cos kx + h(k) \sin kx]\, e^{-k^2 Dt}\, dk. \qquad (31)$$

In (31) $g(k)$, $h(k)$ are functions chosen to fulfil the condition $C = f(x)$ where $t = 0$, and Fourier showed that these functions took the forms

$$\left. \begin{aligned} g(k) &= \frac{1}{\pi} \int_{-\infty}^{+\infty} f(x') \cos(x'k)\, dx', \\ h(k) &= \frac{1}{\pi} \int_{-\infty}^{+\infty} f(x') \sin(x'k)\, dx'. \end{aligned} \right\} \qquad (32)$$

Thus when the equations (32) are substituted in (31) one has as a general solution

$$C = \frac{1}{\pi} \int_0^\infty e^{-k^2 Dt}\, dk \int_{-\infty}^{+\infty} f(x') \cos k(x' - x)\, dx'. \qquad (33)$$

This equation, by an integration process, can be brought to the form

$$C = \frac{1}{2\sqrt{(\pi Dt)}} \int_{-\infty}^{+\infty} f(x') \exp\left[-\frac{(x - x')^2}{4Dt} \right] dx'. \qquad (34)$$

Case 1. Suppose we have diffusion of a solute across a sharp boundary at $x = 0$ from a solution into a solvent. The solute may be a salt dissolved in water; it may be radioactive lead dissolved in lead diffusing into pure lead; or it may be an ion in an ionic lattice diffusing into another lattice, e.g. silver diffusing from silver sulphide into copper sulphide, while copper passes in the opposite direction. For the equation (34) to hold we know that D must not be a function of C; and that the amounts of solution and solvent must be great enough, the diffusion slow enough, or the time short enough, so that no appreciable amount of solute diffuses from the far extremity of the solution, or reaches the far extremity of the solvent (Fig. 1). In these systems, at $t = 0$, $C = C_0$ for $x < 0$, $C = 0$

for $x > 0$. For all positive values of x, the concentration at time t and at a point x becomes

$$C = \frac{C_0}{2\sqrt{(\pi Dt)}} \int_0^\infty \exp\left[-\frac{(x-x')^2}{4Dt}\right] dx' \qquad (35)$$

$$= \frac{C_0}{\sqrt{\pi}} \int_{x/2\sqrt{(Dt)}}^\infty e^{-y^2} dy, \text{ if } y^2 = \frac{(x-x')^2}{4Dt}, \qquad (36)$$

$$= \frac{C_0}{2}\left[1 - \frac{2}{\sqrt{\pi}} \int_0^{x/2\sqrt{(Dt)}} e^{-y^2} dy\right]. \qquad (37)$$
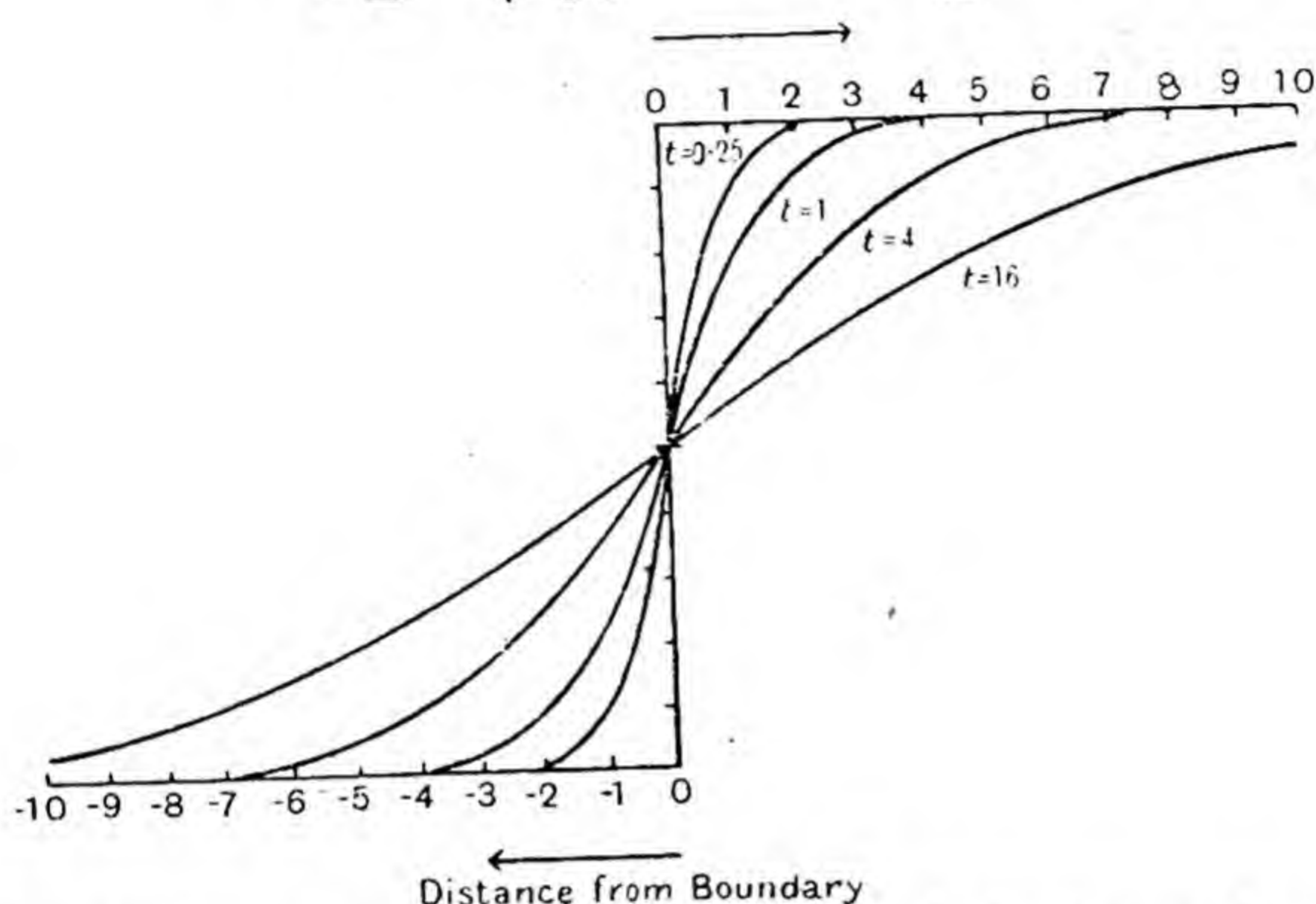
Fig. 1. Diffusion across a boundary from a solution into a solvent.

The second term is the Gaussian error function, erf (y), and may be evaluated from mathematical tables. Equation (37) may be expanded as a series:

$$C = \frac{C_0}{2}\left[1 - \frac{2}{\sqrt{\pi}}\left\{\frac{x}{2\sqrt{(Dt)}} - \frac{x^3}{3.1!\{2\sqrt{(Dt)}\}^3} + \frac{x^5}{5.2!\{2\sqrt{(Dt)}\}^5} - \frac{x^7}{7.3!\{2\sqrt{(Dt)}\}^7} + \ldots\right\}\right]. \qquad (38)$$

The solution for $x < 0$ is correspondingly

$$C = \frac{C_0}{2}[1 + \text{erf}(y)]$$

$$= \frac{C_0}{2}\left[1 + \frac{2}{\sqrt{\pi}}\left\{\frac{x}{2\sqrt{(Dt)}} - \frac{x^3}{3.1!\{2\sqrt{(Dt)}\}^3} + \frac{x^5}{5.2!\{2\sqrt{(Dt)}\}^5} - \frac{x^7}{7.3!\{2\sqrt{(Dt)}\}^7} + \ldots\right\}\right]. \qquad (39)$$

Case 2. It is necessary to have a readily applicable solution of Fick's law for systems in which two diffusion media are present. In many instances, when metals interdiffuse for example, a number of solid phases occur, as alloys, with sharp phase boundaries. This is true when molybdenum diffuses into iron[1] at a temperature of 1300° C., for there is a diffusion of molybdenum dissolved in a molybdenum-iron alloy formed in the outer layer of the iron, and a diffusion of molybdenum also in the purer iron at the core of the rod. This diffusion system is complicated further by a movement inwards of the alloy-iron phase boundary. The simpler case of a stationary phase boundary can be easily treated by the methods already outlined[2].

The boundary conditions are

(i) $\dfrac{\partial C_1}{\partial t} = D_1 \dfrac{\partial^2 C_1}{\partial x^2}$ for the first solvent; $\dfrac{\partial C_2}{\partial t} = D_2 \dfrac{\partial^2 C_2}{\partial x^2}$ for the second solvent.

Fig. 2. Diffusion in two phases I and II where $k = 3$ and $D_1 = D_2$.
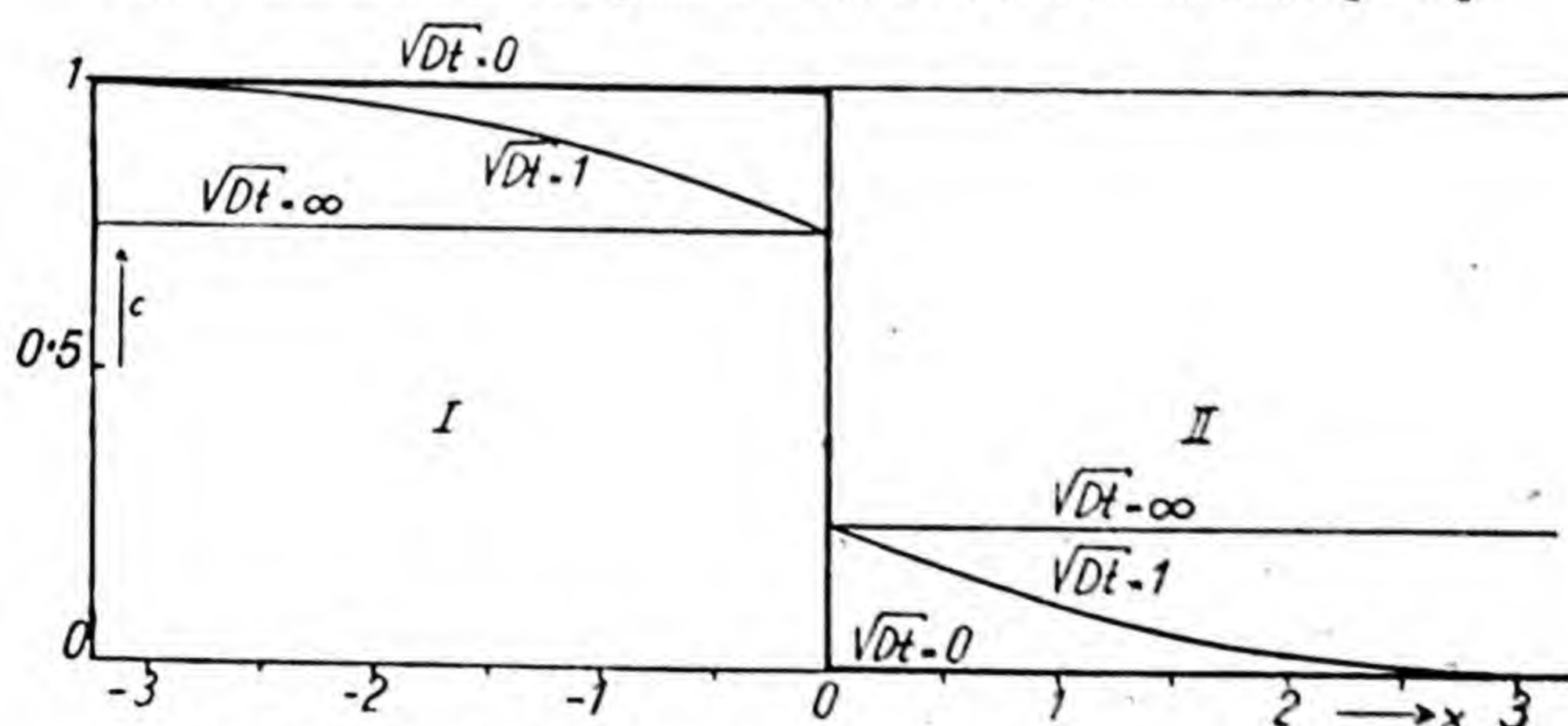
Fig. 3. Diffusion in two phases I and II where $k = \frac{1}{3}$ and $D_1 = D_2$.

(ii) $C_1 = C_0$ for $t = 0$ and $x < 0$; $C_2 = 0$ for $t = 0$ and $x > 0$.

(iii) $D_1\left(\dfrac{\partial x_1}{\partial x}\right)_{x=0} = D_2\left(\dfrac{\partial x_2}{\partial x}\right)_{x=0}$ at the interface between the solvents for all t.

(iv) $\displaystyle\int_{-\infty}^{0}(C_0 - C_1)\,dx = \int_{0}^{\infty} C_2\,dt$ = the total amount diffused.

(v) $C_2/C_1 = k$, the partition coefficient, in the equilibrium state.

The solutions of the problem for $x > 0$ and $x < 0$ are

$$C_1 = C_0\left[1 - \frac{k\sqrt{D_2}}{k\sqrt{D_2}+\sqrt{D_1}}\left\{1 + \frac{2}{\sqrt{\pi}}\int_{0}^{x/2\sqrt{(Dt)}} e^{-y^2}\,dy\right\}\right], \quad (40)$$
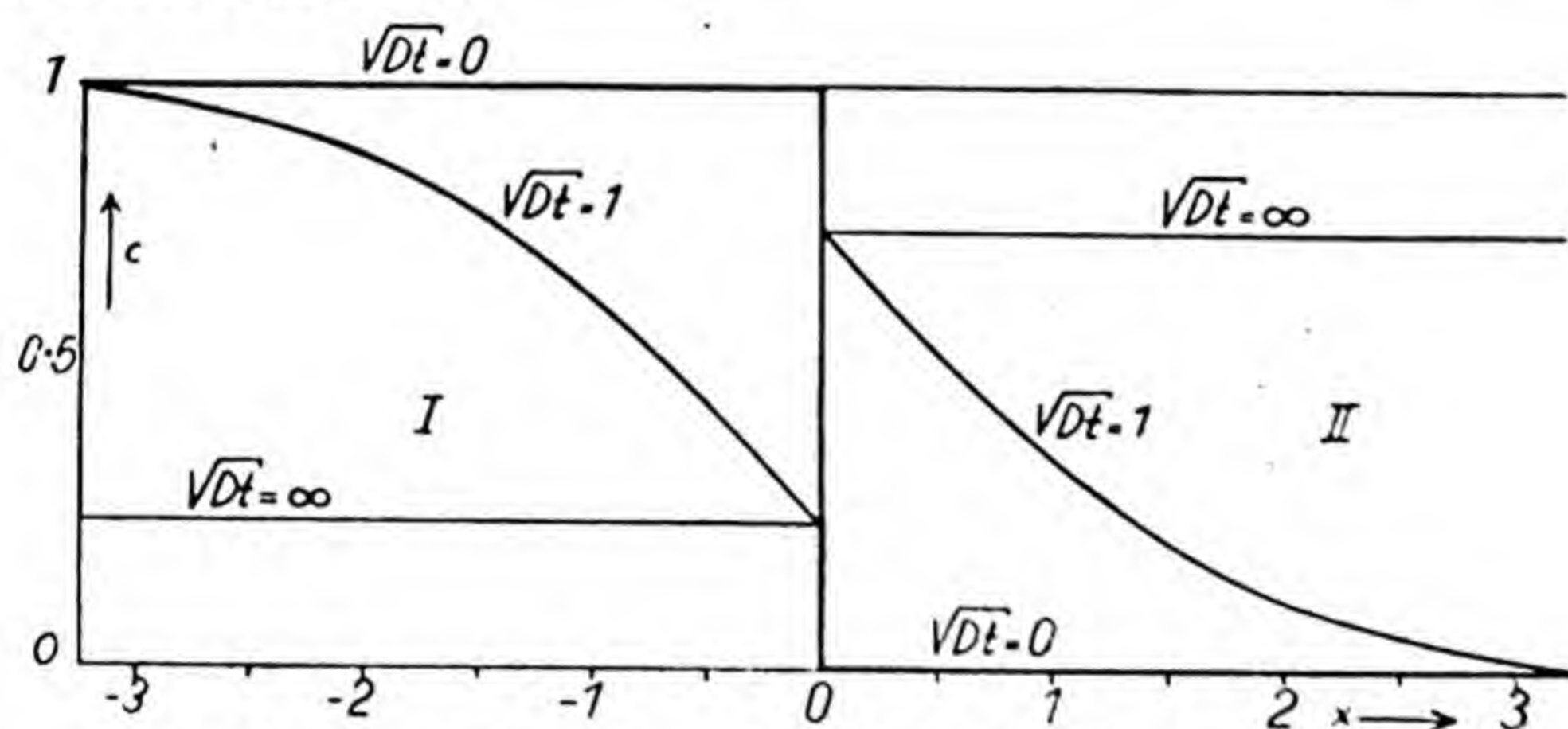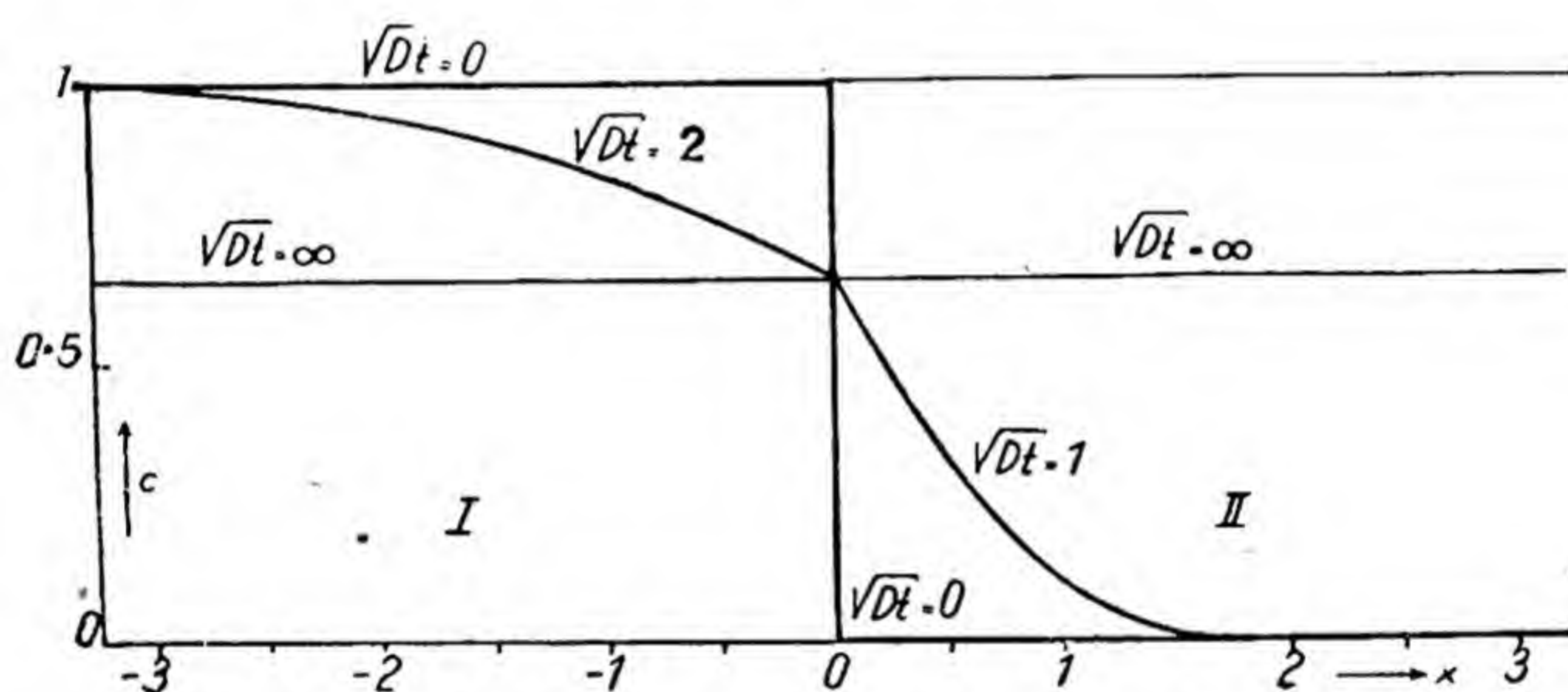

Fig. 4. Diffusion in two phases I and II where $k = 1$ and $D_1 = 4D_2$.
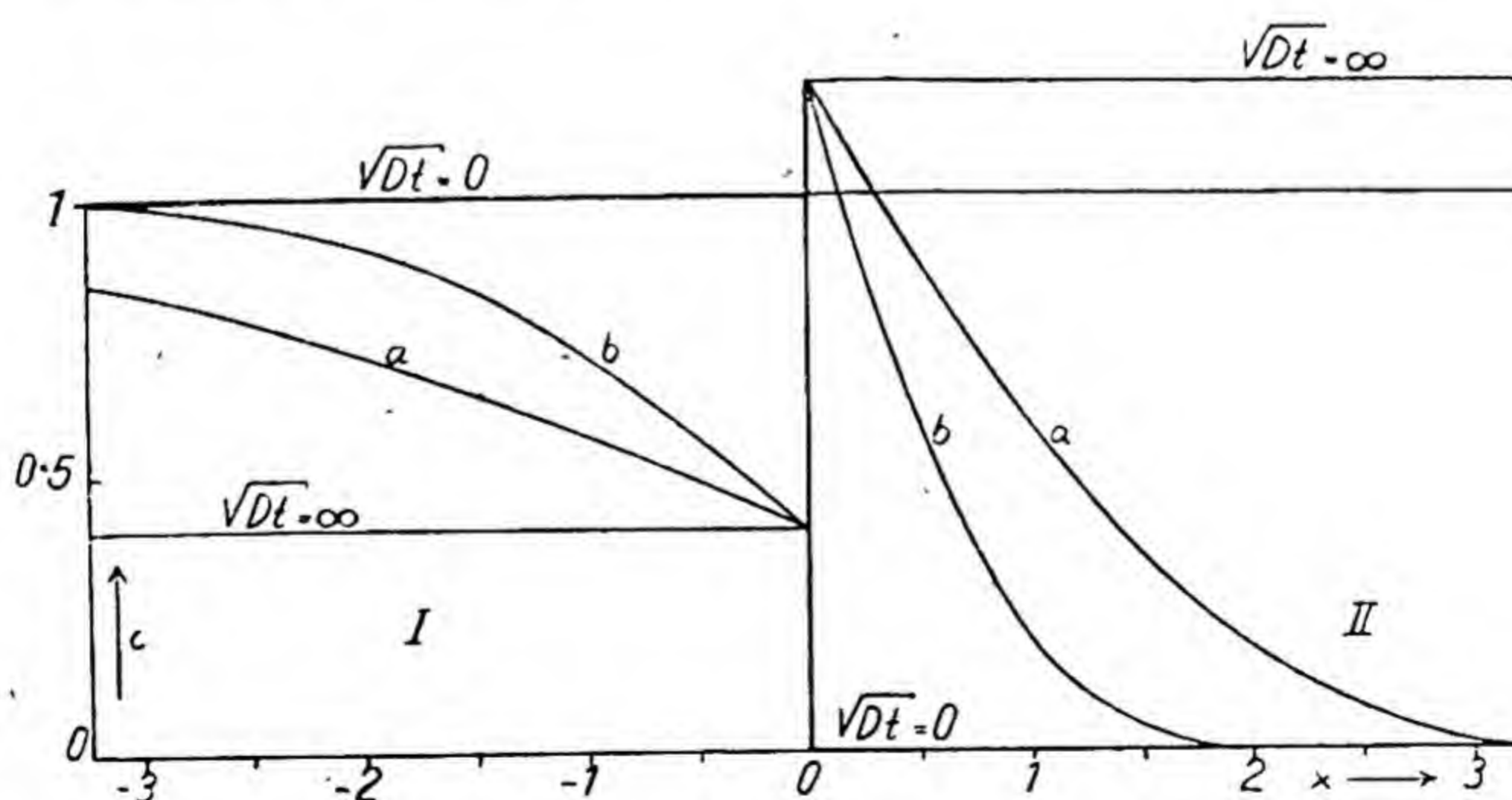
Fig. 5. Diffusion in two phases I and II where $k = 3$, $D_1 = 4D_2$, and for the curves (a) $\sqrt{(D_2 t)} = 1$, $\sqrt{(D_1 t)} = 2$, while for the curves (b) $\sqrt{(D_2 t)} = 0.5$, $\sqrt{(D_1 t)} = 1$.

$$C_2 = C_0\left[\frac{k\sqrt{D_1}}{k\sqrt{D_2}+\sqrt{D_1}}\left\{1 - \frac{2}{\sqrt{\pi}}\int_0^{x/2\sqrt{(Dt)}} e^{-v^2}\,dy\right\}\right]. \tag{41}$$

Some solutions of the equations (40) and (41) are illustrated graphically [3] in Figs. 2–5.

(b) The semi-infinite solid.

The medium now extends from $x = 0$ to $x = +\infty$, and the general equation takes the form

$$C = \frac{1}{\sqrt{(\pi Dt)}}\int_0^{+\infty} f(x')\exp\left[-\frac{(x-x')^2}{4Dt}\right]dx'. \tag{42}$$

Case 1. At the plane $x = 0$ one may generate a supply of solute, in which the rate of supply is any function of time. Instances where the supply is constant will be of the greatest practical significance. Examples would be the sorption of gas at constant pressure in a *large* amount of a solid* (oxygen in silver, hydrogen in palladium, nitrogen in iron, ammonia in analcite) or a crystal in contact with a quiescent solvent liquid.

When the supply at the plane $x = 0$ is constant the boundary conditions are

$$C = C_0 \text{ at } x = 0 \text{ for all } t,$$

$$C = 0 \text{ at } x > 0 \text{ and } t = 0,$$

$$C = C(x, t) \text{ at } x > 0 \text{ and } t > 0,$$

and the solution giving the concentration C at a point x and a time t is

$$C(x, t) = \frac{C_0}{\sqrt{(\pi Dt)}}\int_0^{\infty} \exp\left[-\frac{(x-x')^2}{4Dt}\right]dx' \tag{43}$$

$$= C_0\left[1 - \frac{2}{\sqrt{\pi}}\int_0^{x/2\sqrt{(Dt)}} e^{-v^2}\,dy\right], \tag{44}$$

where $\qquad y = \dfrac{x'-x}{2\sqrt{(Dt)}}.$

* Neglecting for the moment the possibility of a rate controlling process at the interface gas-solid.

(c) *Finite solid.*

We have been concerned hitherto with so much solvent that its amount for practical computations of D can be reckoned as infinite. Such a supposition limits the applicability of the equations given, for it will be much more usual to work with small amounts of diffusion media. The solutions now to be given will concern themselves with problems such as the following. A solute diffuses from a solution bounded between the planes $x = 0$, $x = h$ into a solvent bounded between the planes $x = h$ and $x = l$. The concentration-distance-time curves may be measured readily enough and have now to be interpreted so that the diffusion constants, D, may be evaluated. The new solutions of Fick's law will apply to numerous cases of the interdiffusion of metals, and salts, so long as D does not depend on the concentration, and whenever the amount of metal or salt is limited.

Another group of solutions will be given for the problems involving diffusion into, through, and out of a slab bounded by the planes $x = 0$ and $x = l$. This group has to do with the diffusion of gases or liquids through membranes, organic (rubber, cellulose, gelatin, plastics) or inorganic (metals, crystals, and glasses). It is necessary in applying the solutions that the surface processes should be sufficiently rapid not to interfere with the internal diffusion process. This is true when gases diffuse through organic membranes, or inorganic glasses and crystals, but it is not true of gas-metal systems such as H_2-palladium, to which solutions of the diffusion equation must be applied with caution.

The general solution for diffusion within parallel boundaries which obeys the conditions

(i) $\dfrac{\partial C}{\partial t} = D \dfrac{\partial^2 C}{\partial x^2}$, (ii) at $t = 0$, $C = f(x)$ for $0 \leqslant x \leqslant l$,

(iii) $C = 0$ at $x = 0$ and $x = l$ for all t,

may be written as follows:

$$C = \frac{2}{l} \sum_{n=1}^{n=\infty} e^{-(n\pi/l)^2 Dt} \sin \frac{n\pi x}{l} \int_0^l f(x') \sin \frac{n\pi x'}{l} \, dx'. \qquad (45)$$

Case 1. Diffusion from one layer to another may be treated by regarding the system as being a single layer with impermeable boundaries in which the distribution at time $t = 0$ is as follows:

$$f(x) = C_0 \text{ for } 0 < x < h,$$

$$f(x) = 0 \text{ for } h < x < l, \quad (l > h).$$

The solution for this particular case is

$$C = C_0\left(\frac{h}{l} + \frac{2}{\pi}\sum_1^\infty \frac{1}{n} e^{-(n\pi/l)^2 Dt}\cos\frac{n\pi x}{l}\sin\frac{n\pi h}{l}\right). \qquad (46)$$

For any numerical ratio of h/l, equation (46) may now readily be expanded as a series, each term of which may be given a numerical value. These numerical values have been worked out when $\frac{1}{4}l = h$ by Stefan[4] and Kawalki[5] whose tables may be consulted.

Case 2. For some purposes it may be necessary to evaluate D from measurements as a function of time of the total solute which has diffused across the boundary. This quantity, Q, is given by the equation

$$Q = -\int_0^t D\left(\frac{\partial C}{\partial x}\right)_{x=h} dt. \qquad (47)$$

From equation (46) one has, at $x = h$,

$$\frac{\partial C}{\partial x} = -C_0\frac{2}{l}\sum_1^\infty e^{-(n\pi/l)^2 Dt}\sin^2\frac{n\pi h}{l}. \qquad (48)$$

Thence, substituting (48) in (47) and integrating,

$$Q = C_0\frac{l}{2\pi^2}\sum_1^\infty \frac{1}{n^2}\sin^2\frac{n\pi h}{l}\left[1 - \exp\left\{-\frac{Dn^2\pi^2 t}{l^2}\right\}\right]. \qquad (49)$$

Equation (49) may be evaluated for various ratios of h/l. For instance, when $h/l = \frac{1}{2}$, equation (49) reduces to

$$Q = \frac{C_0 l}{4}\left[1 - \frac{8}{\pi^2}\sum_{m=0}^\infty \frac{1}{(2m+1)^2}\exp\left\{-\frac{D(2m+1)^2\pi^2 t}{l^2}\right\}\right], \qquad (50)$$

which may again be expanded as a series and readily employed.

The various possibilities which arise when a solute at a constant concentration diffuses into a slab may now be con-

sidered. The slab, as before, is bounded by the planes $x = 0$ and $x = l$, and the boundary conditions are

$$C = C_1 \text{ at } x = 0 \text{ for all } t,$$
$$C = C_2 \text{ at } x = l \text{ for all } t,$$
$$C = f(x) \text{ at } t = 0 \text{ for } 0 < x < l.$$

The general solution of this problem is(6)

$$C = C_1 + (C_2 - C_1)\frac{x}{l} + \frac{2}{\pi}\sum_1^\infty \frac{C_2\cos n\pi - C_1}{n}\sin\frac{n\pi x}{l}\exp\left[-\frac{Dn^2\pi^2 t}{l^2}\right]$$
$$+ \frac{2}{l}\sum_1^\infty \sin\frac{n\pi x}{l}\exp\left[-\frac{Dn^2\pi^2 t}{l^2}\right]\int_0^l f(x')\sin\frac{n\pi x'}{l}\,dx'. \quad (51)$$

Case 3. When the slab is initially free of solute, and the concentrations of solute at the faces are C_1 (at $x = 0$) and C_2 (at $x = l$), one has the example of diffusion of gas at constant pressure into a membrane of solid free of gas. Here $f(x') = 0$ and the solution is

$$C = C_1 + (C_2 - C_1)\frac{x}{l} + \frac{2}{\pi}\sum_1^\infty \frac{C_2\cos n\pi - C_1}{n}\sin\frac{n\pi x}{l}\exp\left[-\frac{Dn^2\pi^2 t}{l^2}\right]. \quad (52)$$

If instead of the membrane being initially free of gas there is an initial uniform concentration, C_0, of gas in the membrane, the solution is

$$C = C_1 + (C_2 - C_1)\frac{x}{l} + \frac{2}{\pi}\sum_1^\infty \frac{C_2\cos n\pi - C_1}{n}\sin\frac{n\pi x}{l}\exp\left[-\frac{Dn^2\pi^2 t}{l^2}\right]$$
$$+ \frac{4C_0}{\pi}\sum_{m=0}^\infty \frac{1}{(2m+1)}\sin\frac{(2m+1)\pi x}{l}\exp\left[-\frac{D(2m+1)^2\pi^2 t}{l^2}\right]. \quad (53)$$

Again, if $C_1 = 0$ for all t, and $C_0 = 0$ at $t = 0$, the solution is

$$C = C_2\left[\frac{x}{l} + \frac{2}{\pi}\sum_1^\infty \frac{(-1)^n}{n}\sin\frac{n\pi x}{l}\exp\left\{-\frac{Dn^2\pi^2 t}{l^2}\right\}\right]. \quad (54)$$

Also, when $C_1 = C_2$ for all t, and $C_0 = 0$ at $t = 0$, the solution becomes

$$C = C_1\left[1 - \frac{4}{\pi}\sum_{m=0}^\infty \frac{1}{2m+1}\sin\frac{(2m+1)\pi x}{l}\exp\left\{-\frac{D(2m+1)^2\pi^2 t}{l^2}\right\}\right]. \quad (55)$$

The reader may work out other examples from the general equation (51), simply by giving C_1, C_2 and $f(x')$ their appropriate initial values. Special cases of equations (52)–(55) follow with equal ease. For instance, in equation (55) the concentration at the mid-plane of the slab $(x = \frac{1}{2}l)$ is given by putting $x = \frac{1}{2}l$ and so getting

$$(C)_{x=\frac{1}{2}l} = C_1\left[1 - \frac{4}{\pi}\sum_{m=0}^{\infty}\frac{1}{(2m+1)}\exp\left\{-\frac{D(2m+1)^2\pi^2 t}{l^2}\right\}\right]. \quad (56)$$

All the equations (52)–(56) have to do with the flow of gas or other solute into a membrane. The use of these equations presents no difficulty. They may be expanded term by term, and all terms save the first two or three can be neglected, because the series converges rapidly. In this form the equations become of special interest in the field of sorption kinetics.

Case 4. The desorption of gas from a membrane is an equally important example of the application of equation (51). Suppose at the time $t = 0$ the membrane contains a uniform concentration C_0 of solute throughout, from $x = 0$ to $x = l$ and $C_1 = C_2 = 0$. The solution in this case by substitution in (51) becomes

$$C = \frac{2C_0}{l}\sum_{1}^{\infty}\sin\frac{n\pi x}{l}\exp\left[-\frac{Dn^2\pi^2 t}{l^2}\right]\int_0^l\sin\frac{n\pi x'}{l}dx'$$

$$= \frac{4C_0}{\pi}\sum_{m=0}^{\infty}\frac{1}{(2m+1)}\sin\frac{(2m+1)\pi x}{l}\exp\left[-\frac{D(2m+1)^2\pi^2 t}{l^2}\right]. \quad (57)$$

At the midpoint of the membrane $(x = \frac{1}{2}l)$ equation (57) reduces to

$$C = \frac{4}{\pi}C_0\sum_{m=0}^{\infty}\frac{-(-1)^{m+1}}{(2m+1)}\exp\left[-\frac{D(2m+1)^2\pi^2 t}{l^2}\right]. \quad (58)$$

Should the gas desorb from the slab not into a vacuum, as in (58), but into a gas atmosphere where at $x = 0$ and $x = l$ the concentration is C_1, the solution of (58) becomes

$$C = C_1 + (C_0 - C_1)\frac{4}{\pi}\sum_{m=0}^{\infty}\frac{-(-1)^{m+1}}{(2m+1)}\exp\left[-\frac{D(2m+1)^2\pi^2 t}{l^2}\right]. \quad (59)$$

Case 5. In the study of sorption kinetics one frequently requires an expression for the amount of gas (or other solute) left in a membrane at any time t, or alternatively, for the quantity which has diffused out of the membrane. The total amount of sorbed gas at the time t is given by the expression

$$Q_1 = \int_0^l C(x, t)\, dx$$

$$= \frac{4C_0}{\pi} \int_0^l \sum_{m=0}^{\infty} \frac{1}{(2m+1)} \sin \frac{(2m+1)\pi x}{l} \exp\left[-\frac{D(2m+1)^2\pi^2 t}{l^2}\right].$$

(60)

When the integration is carried out one gets

$$Q_1 = \frac{8lC_0}{\pi^2} \sum_0^{\infty} \frac{1}{(2m+1)^2} \exp\left[-\frac{D(2m+1)^2\pi^2 t}{l^2}\right]. \tag{61}$$

Corresponding to equation (61), the amount of gas which has been desorbed is

$$Q_2 = Q_0 - \int_0^l C(x, t)\, dx$$

$$= lC_0\left[1 - \frac{8}{\pi^2} \sum_{m=0}^{\infty} \frac{1}{(2m+1)^2} \exp\left\{-\frac{D(2m+1)^2\pi^2 t}{l^2}\right\}\right]. \tag{62}$$

The corresponding problem of the quantity of gas which has been sorbed in the membrane after a given time t appears from either of the two relationships

$$Q_2 = \int_0^l C(x, t)\, dx - Q_0 = -\int_0^t D\left[\left(\frac{\partial C}{\partial x}\right)_{x=0} - \left(\frac{\partial C}{\partial x}\right)_{x=l}\right] dt,$$

when the boundary conditions in the most general practical case are those which led to equation (53). The solution when $C_0 = 0$ is simply equation (98), if u_1 and u_2 are the constant concentrations at $x = 0$ and $x = l$ respectively. The solution for the general case (concentrations C_1 at $x = 0$, C_2 at $x = l$, and $C = C_0$ at $t = 0$) is

$$Q = l\left[\frac{C_1 + C_2}{2} + C_0\right]$$

$$\times \left[1 - \frac{8}{\pi^2} \sum_{m=0}^{\infty} \frac{1}{(2m+1)^2} \exp\left\{-\frac{D(2m+1)^2\pi^2 t}{l^2}\right\}\right]. \tag{63}$$

Case 6.   If one is measuring the rate of flow of a gas (or any other solute) through a membrane in which the gas dissolves, there will be an interval from the moment the gas comes into contact with the membrane until it emerges at a constant rate on the other side. By analysing stationary and non-stationary states of flow it is possible to measure the diffusion constant, the permeability constant, and the solubility of the gas in the membrane. Once more one may employ equation (53) to determine the intercept (L), in terms of D, l, and C, which the pressure-time curve makes on the axis of time.

The boundary conditions are

$$C = C_1 \text{ at } x = 0 \text{ for all } t,$$
$$C = C_2 \text{ at } x = l \text{ for all } t,$$
$$C = C_0 \text{ for } 0 < x < l \text{ and at } t = 0,$$

giving as solution

$$C = C_1 + (C_2 - C_1)\frac{x}{l} + \frac{2}{\pi}\sum_1^\infty \frac{C_2 \cos n\pi - C_1}{n}\sin\frac{n\pi x}{l}\exp\left[-\frac{Dn^2\pi^2 t}{l^2}\right]$$
$$+ \frac{4C_0}{\pi}\sum_{m=0}^\infty \frac{1}{(2m+1)}\sin\frac{(2m+1)\pi x}{l}\exp\left[-\frac{D(2m+1)^2\pi^2 t}{l^2}\right].$$

$$(53)$$

Equation (53) may be differentiated, and one obtains at $x = 0$

$$\left(\frac{\partial C}{\partial x}\right)_{x=0} = \frac{C_2 - C_1}{l} + \frac{2}{l}\sum_1^\infty (C_2 \cos n\pi - C_1)\exp\left[-\frac{Dn^2\pi^2 t}{l^2}\right]$$
$$+ \frac{4C_0}{l}\sum_{m=0}^\infty \exp\left[-\frac{D(2m+1)^2\pi^2 t}{l^2}\right]. \quad (64)$$

But if the gas flows through a membrane into a volume V, the flow of gas is given by

$$V\frac{\partial C_0}{\partial t} = D\left(\frac{\partial C}{\partial x}\right)_{x=0}. \quad (65)$$

Substitute (64) in (65) and integrate between the limits 0 and t, and so obtain

$$C_0 = D\frac{C_2 - C_1}{l}\frac{t}{V} + \frac{2l}{\pi^2 V}\sum_1^\infty \frac{C_2 \cos n\pi - C_1}{n^2}\left(1 - \exp\left[-\frac{Dn^2\pi^2 t}{l^2}\right]\right)$$
$$+ \frac{4C_0 l}{\pi^2 V}\sum_{m=0}^\infty \frac{1}{(2m+1)^2}\left(1 - \exp\left[-\frac{D(2m+1)^2\pi^2 t}{l^2}\right]\right). \quad (66)$$

Equation (53) as $t \to \infty$ approaches the line

$$C_g = \frac{D}{lV}\left[(C_2 - C_1)t + \frac{2l^2}{D\pi^2}\sum_1^\infty \left(\frac{C_2 \cos n\pi}{n^2} - \frac{C_1}{n^2}\right) \right.$$

$$\left. + \frac{4C_0 l}{\pi^2 D}\sum_{m=0}^\infty \frac{1}{(2m+1)^2}\right] \qquad (67)$$

$$= \frac{D}{lV}\left[(C_2 - C_1)t - \frac{C_2 l^2}{6D} - \frac{C_1 l^2}{3D} + \frac{C_0 l^2}{2D}\right]. \qquad (67a)$$

Had there been no time lag, C_g would be expressed by

$$C_g = \frac{D}{lV}(C_2 - C_1)t, \qquad (68)$$

so that the intercept, L, on the time axis is given by

$$L = \frac{1}{(C_2 - C_1)}\left[\frac{C_2 l^2}{6D} + \frac{C_1 l^2}{3D} - \frac{C_0 l^2}{2D}\right]. \qquad (69)$$

In the case where $C_0 = 0$ at $t = 0$

$$L = \frac{1}{(C_2 - C_1)}\left[\frac{C_2 l^2}{6D} + \frac{C_1 l^2}{3D}\right], \qquad (69a)$$

and where $C_0 = 0$ and C_1 is very small ($\simeq 0$)

$$L = \frac{l^2}{6D}. \qquad (69b)$$

In equations (69), (69a) and (69b), one is provided with an easy means of measuring D.

(d) *Finite solids with surface concentration a function of time.*

Case 1. In many experiments, e.g. the uptake of gases by solids, the surface concentration is a function of time if sorption occurs at constant volume or variable pressure. The following considerations will apply to systems such as O_2-Ag, H_2-Cu, N_2-Mo, NH_3-, H_2O-zeolite, where sorption occurs in a sheet of metal or crystal, provided there is no rate controlling interface reaction. Then the boundary conditions are for the most general case:

$$C = \phi_1(t) \text{ at } x = 0,$$
$$C = \phi_2(t) \text{ at } x = l,$$
$$C = f(x) \text{ when } t = 0,$$

and the solution becomes [7]

$$C = \frac{2}{l} \sum_1^\infty \exp\left[-\frac{Dn^2\pi^2 t}{l^2}\right] \sin\frac{n\pi x}{l} \left\{ \int_0^l f(x') \sin\frac{n\pi x'}{l} dx' \right.$$

$$\left. + \frac{nD\pi}{l} \int_0^t \exp\left[\frac{Dn^2\pi^2 t'}{l^2}\right] \{\phi_1(t') - (-1)^n \phi_2(t')\} dt' \right\}. \quad (70)$$

When the slab is initially gas free and $\phi_1(t') = \phi_2(t')$ the concentration becomes

$$C = \frac{2}{l} \sum_{m=0}^\infty \sin\frac{(2m+1)\pi x}{l} \frac{(2m+1)D\pi}{l}$$

$$\times \int_0^t \exp\left[-\frac{D(2m+1)^2\pi^2(t-t')}{l^2}\right] \phi(t') dt', \quad (71)$$

and Q, the amount sorbed in unit area at time t, is

$$Q = \int_0^l C(x, t)$$

$$= \frac{4D}{l} \sum_{m=0}^\infty \int_0^t \exp\left[-\frac{D(2m+1)^2\pi^2(t-t')}{l^2}\right] \phi(t') dt'. \quad (72)$$

If in the interval $t' = 0$ to t it is possible to represent $\phi(t')$ by

$$\phi(t') = C_0\{1 + At' + B(t')^2\},$$

where C_0 is the initial surface concentration and A and B are constants, one obtains

$$Q = \frac{lC_0}{2}(1 + At + Bt^2) - \frac{4lC_0}{\pi^2} \sum_{m=0}^\infty \frac{1}{(2m+1)^2}$$

$$\times \left[\frac{A}{\alpha} + \frac{2Bt}{\alpha} + \frac{2B}{\alpha^2} - \left(1 - \frac{A}{\alpha} + \frac{2B}{\alpha^2}\right)e^{-\alpha t}\right], \quad (72a)$$

where

$$\alpha = \frac{D(2m+1)^2\pi^2}{l^2}.$$

It is possible, however, to solve the diffusion equation completely for this type of sorption problem, without recourse to empirical expressions for $\phi(t')$, as the method of case (2) will show.

Case 2. If one has a plate enclosed between the planes $x = 0$ and $x = l$ with the face $x = 0$ impermeable, and an initial

concentration C_0 of solute in it; and if another plate enclosed between the planes $x = l$ and $x = h + l$ is made of the same material with an initial concentration zero, then the solution of the problem of flow from one plate into the other is given by equation (46).

Suppose, however, that the solute in the plate between $x = l$ and $x = h + l$ could be kept at the same concentration throughout by some process of stirring. The concentration in this plate would then be a function of time only. The diffusion equation in this instance is to be solved for the important case of desorption from a slab into a constant gaseous volume. Thus the desorption of water, ammonia, or another gas from a plate of a zeolitic crystal would be examples of diffusion systems of the kind postulated, save that the distribution coefficient $k = \dfrac{C \text{ (in the solid)}}{C \text{ (in the gas)}}$ is not unity. Another example where $k = 1$ is the diffusion of urea from a layer of aqueous gel into a stirred aqueous layer.

The adaptation of the solution which will be obtained for the case where $k \neq 1$ is very simply made, by supposing the actual plate between $x = l$ and $x = (l + h)$ replaced by a plate between $x = l$ and $x = (l + h/k)$ in which the partition coefficient is now unity.

The outline of the solution for this interesting system may now be given. The equation $\dfrac{\partial C}{\partial t} = D \dfrac{\partial^2 C}{\partial x^2}$ has to be solved for the boundary conditions

(i) $\partial C/\partial t = 0$ at $x = 0$, $t > 0$,

(ii) $C = f(x)$ for $0 < x < l$ and $t = 0$,

(iii) contact between solid and gas gives at $x = l$

$$C(l, t) = kC_g(t),$$

where k is the distribution coefficient and $C_g(t)$ denotes the concentration at time t in the space between $x = l$ and $x = l + h$.

First take $k = 1$ and write the solution as the sum of two terms
$$C = C_1 + C_2,$$

where

(iv) $\partial C_1/\partial x = 0$ at $x = 0$; $C_1(l, t) = 0$; $C_1(x, t) = C_0(x)$ at $t = 0$,

(v) $\partial C_2/\partial x = 0$ at $x = 0$; $C_2(l, t) = C_g(t)$, $t > 0$; $C_2(x, t) = 0$ at $t = 0$.

The solutions obtained by March and Weaver[8] then were

$$C(x, t) = C_g - \frac{4}{\pi} \sum_{n=0}^{\infty} \frac{(-1)^n}{2n+1} \cos\left(\frac{2n+1}{2} \frac{\pi x}{l}\right)$$

$$\times \sum_{i=0}^{\infty} \frac{B_i e^{-\beta_i t}}{\left(\frac{D(2n+1)^2 \pi^2}{4 \quad l^2} - \beta_i\right)}, \quad (73)$$

$$C_g(t) = C_g(\infty) - \Sigma \frac{B_i}{\beta_i} e^{-\beta_i t}, \quad (74)$$

where B_i and β_i are constants which can be evaluated for the various ratios λ, defined by

$$\lambda = \frac{h}{l} = \frac{\text{Volume from } x = l \text{ to } x = h}{\text{Volume from } x = 0 \text{ to } x = l} = \frac{V_g}{V_s}.$$

The quantities B_i, β_i contain the constant λ (see below).

In the case of urea diffusing from gel (volume V_s) into an aqueous layer (volume V_g), where $\lambda = V_g/V_s$, equation (74) reduces to

$$C_g(t) = \frac{C_g(0) + C_0(x)\,(V_s/V_g)}{1 + V_s/V_g} - \sum_1^{\infty} \frac{B_i}{\beta_i} e^{-\beta_i t}. \quad (75)$$

Equation (75) becomes

$$C_g(t) = \frac{C_g(0) + C_0(x)}{2} - [0 \cdot 327 e^{-4 \cdot 117 Dt/l^2} + 0 \cdot 0766 e^{-24 \cdot 14 Dt/l^2}$$

$$+ 0 \cdot 0306 e^{-63 \cdot 68 Dt/l^2} + 0 \cdot 0160 e^{-123 Dt/l^2} + \ldots], \quad (75a)$$

if $V_s/V_g = 1$.

Should, however, the distribution coefficient k not be unity

$$\lambda = \frac{\text{Volume from } x = l \text{ to } x = h/k}{\text{Volume from } x = 0 \text{ to } x = l} = \frac{h}{lk},$$

and this value of λ must be used in evaluating B_i and β_i; and also $C_g(\infty)$ in equation (74) becomes

$$C_g(\infty) = \frac{C_g(0) + C_0(x)\,V_s/V_g}{1 + (V_s/V_g)\,k}. \tag{76}$$

The constants β_i and B_i are obtained in terms of D by means of the equations (77)–(81). The β_i's are found from the positive roots of the transcendental equation

$$\tan z + \lambda z = 0, \tag{77}$$

which are easily obtained graphically by plotting the curves $y = -\lambda z$ and $y = \tan z$. The solutions are the points of intersection of the curves.

One may now evaluate the constants $B_i,\, \beta_i$. In equation (74)

$$\beta_i = D\frac{z}{l^2}, \tag{78}$$

when

$$\lambda = \frac{h}{lk}. \tag{79}$$

The constants B_i may be evaluated from the relationships

$$B_i\!\left(\frac{4l^2}{\pi^2 D}\right) = B_i', \tag{80}$$

and the equations

$$\left.\begin{array}{l}
B_0' = -0{\cdot}099\lambda + 0{\cdot}644 - \epsilon_0, \\[4pt]
B_1' = -0{\cdot}146\lambda + 0{\cdot}894 - \epsilon_1, \\[4pt]
B_2' = -0{\cdot}157\lambda + 0{\cdot}946 - \epsilon_2, \\[4pt]
B_3' = -0{\cdot}159\lambda + 0{\cdot}958 - \epsilon_3,
\end{array}\right\} \tag{81}$$

and for all B_i' where $i > 3$

$$B_i' = -0{\cdot}162\lambda + 0{\cdot}972 - \epsilon_3.$$

The quantities ϵ_i are then read from Fig. 6 for all values of λ between 0 and 5. Then in the final expression D disappears from the ratio $\Sigma B_i/\beta_i$.

One now sees that it is easily possible to evaluate D, the diffusion constant, from desorption experiments at constant volume, provided $1 < \lambda < 5$, and that no rate controlling interface reaction intervenes. The advantage of this method over the method outlined in equations (72)–(72a) is that one does

not need to represent a $\phi(t) - t$ curve by means of an empirical equation, in order to obtain an expression for Q, the amount sorbed by the plate. Accordingly, the method of March and Weaver[8] has been treated fully as far as practical details for determining the constants in the solution of the diffusion equation are concerned. This method, however, applies only to systems where the diffusing molecule exists in the same molecular state in both phases. For instance, it cannot be applied to systems such as H_2-Pd, where in the gas phase one has molecules, and in the solid phase, atoms. The earlier method of equations (72)–(72a) is, however, still available.
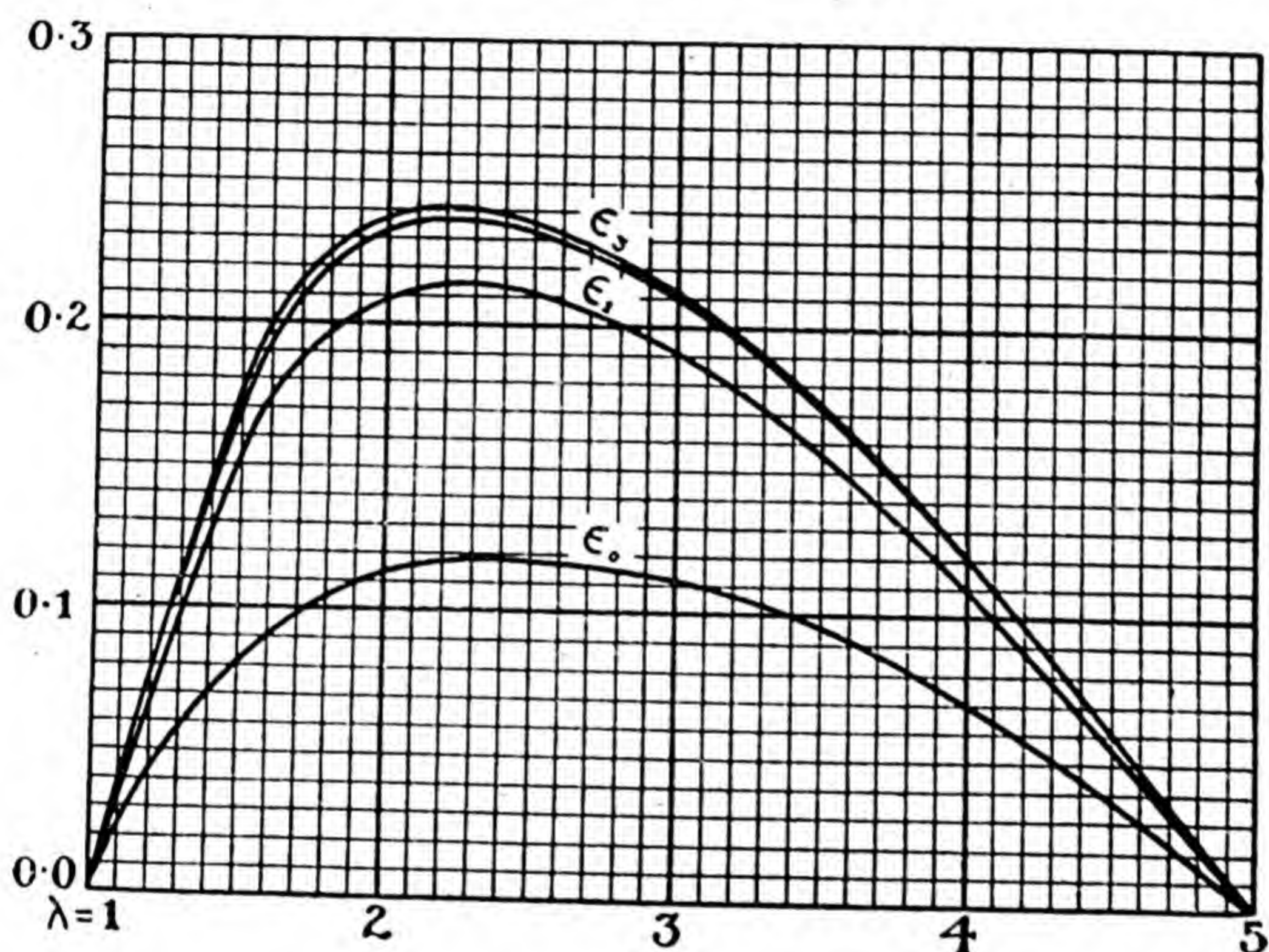
Fig. 6.

Case 3. It is easy to set up a diffusion cell so that one has a porous membrane separating two well-stirred solutions, or two gas volumes. The gas or solution on either side of the membrane contains the same constituents. This system is an important one biologically, as well as chemically. The membrane may be organic or inorganic if it separates two stirred solutions or two gas phases; or it may also be a crystal if it separates two gas phases only.

The exact interpretation of the data to give diffusion constants may now be given (9). The general method of solution is similar to that of March and Weaver given in the previous section. One has a membrane between the planes $x = 0$ and $x = l$; and well-stirred solutions of concentrations $_gC_0$, $_hC_0$ are in contact with the planes $x = 0$ and $x = l$ respectively. The solution in contact with the plane $x = 0$ extends from $x = 0$ to $x = -g$; the solution in contact with $x = l$ extends from $x = l$ to $x = l+h$. Then the boundary conditions for which the equation

$$\frac{\partial C}{\partial t} = D\frac{\partial^2 C}{\partial x^2}$$

is to be solved are

(i) $C = C_0(x)$ at $t = 0$ for $0 < x < l$.

(ii) $C(0, t) = {}_gC(t)$; $C(l, t) = {}_hC(t)$ for $t > 0$.

(iii) $C = {}_gC_0$ at $t = 0$ for $0 < x < -g$, and $C = {}_hC_0$ at $t = 0$ for $l < x < l+h$.

(iv) $\dfrac{\partial({}_gC)}{\partial t} = \dfrac{D}{g}\left(\dfrac{\partial C}{\partial x}\right)_{x=0}$; $\dfrac{\partial({}_hC)}{\partial t} = -\dfrac{D}{h}\left(\dfrac{\partial C}{\partial x}\right)_{x=0}$.

For this system Barnes (9) found solutions in the form

$$_gC = C_\infty - \Sigma\frac{A_i}{\xi_i}e^{-\xi_i t}, \tag{82}$$

$$_hC = C_\infty - \Sigma\frac{B_i}{\xi_i}e^{-\xi_i t}, \tag{83}$$

where C_∞ denotes the uniform final concentration in the solution or gas phases. When the distribution coefficient between membrane and solution is unity,

$$C_\infty(g+l+h) = ({}_gC_0)g + \int_0^l C_0(x)\,dx + ({}_hC_0)h. \tag{84}$$

Also, where $t = 0$,

$$C_\infty - {}_gC_0 = \Sigma\frac{A_i}{\xi_i};   C_\infty - {}_hC_0 = \Sigma\frac{B_i}{\xi_i}. \tag{85}$$

There are three more relationships available for determining the A's, B's and ξ's which are

$$\left.\begin{aligned} A_i\left(\frac{1}{\lambda_1} - \frac{\cot z_i}{z_i}\right) &= - B_i \frac{1}{z_i \sin z_i}, \\ B_i\left(\frac{1}{\lambda_2} - \frac{\cot z_i}{z_i}\right) &= - A_i \frac{1}{z_i \sin z_i}, \end{aligned}\right\} \quad (86)$$

and

$$\frac{D}{l^2}\left[{}_0C_0 - (-1)^n \, {}_hC_0 - \frac{n\pi}{l}\int_0^l C_0(x)\sin\frac{n\pi x}{l}\,dx\right]$$

$$= \sum_i\left(\frac{A_i - (-1)^n B_i}{n^2\pi^2 - z_i^2}\right), \quad (87)$$

where $z_i = \frac{\xi_i l^2}{D}$. From equations (86) one may form the equations

$$\frac{A_i}{B_i} = \sqrt{\frac{1/\lambda_2 - \cot z_i/z_i}{1/\lambda_1 - \cot z_i/z_i}}, \quad (88)$$

and

$$z^2 - (\lambda_1 + \lambda_2) z \cot z - \lambda_1 \lambda_2 = 0. \quad (89)$$

By finding the points of intersection of the graphs $y = z^2 - \lambda_1\lambda_2$ and $y = (\lambda_1 + \lambda_2)z\cot z$, one can readily determine the z's, for which real positive values only are taken. From the infinite set of linear equations (87), whose form is greatly simplified when $C_0(x) = C_0$ (i.e. when there is a uniform concentration within the membrane at $t = 0$), and (88) and (85), one may determine B_i and A_i in terms of z_i and D. In the ratios $\Sigma A_i/\xi_i$, $\Sigma B_i/\xi_i$ which appear before the exponential terms of (82) and (83), the D cancels, since it is a simple multiplier in A_i, B_i and ξ_i. As with all diffusion problems, at large values of t, all the exponential terms save the first become small, so that if one plots $\log\left({}_0C - C_\infty\right)$ against t one obtains a curve such as that in Fig. 7, in which the curve approaches asymptotically a straight line of slope $-\xi_1$. In any case even at small values of t it will not be necessary to take many terms of the exponential series, in solving for A_i and B_i.

The complete solutions of (82) and (83) for the case when $g = h$ (i.e. $\lambda_1 = \lambda_2 = \lambda$, $k = 1$, $C_0(x) = 0 = {}_gC_0$) are

$$
{}_gC = \frac{{}_gC_0}{2}\left[1 - \frac{\lambda}{2} + \frac{\lambda^2}{4} + \left(1 - \frac{\lambda}{6} + \frac{\lambda^2}{60}\right)\exp\left\{-\frac{2\lambda Dt}{l^2}\left(1 - \frac{\lambda}{6} + \frac{\lambda^2}{45}\right)\right\}\right.
$$

$$
\left. + \sum_{i=1}^{\infty}\frac{4\lambda}{i^2\pi^2}\left(1 - \frac{6\lambda}{i^2\pi^2}\right)\exp\left\{-\frac{Dt}{l^2}(i^2\pi^2 + 4\lambda)\right\}\right], \quad (90)
$$

$$
{}_hC = \frac{{}_hC_0}{2}\left[1 - \frac{\lambda}{2} + \frac{\lambda^2}{4} - \left(1 - \frac{\lambda}{6} + \frac{\lambda^2}{60}\right)\exp\left\{-\frac{2\lambda Dt}{l^2}\left(1 - \frac{\lambda}{6} + \frac{\lambda^2}{45}\right)\right\}\right.
$$

$$
\left. - \sum_{i=1}^{\infty}(-1)^i\frac{4\lambda}{i^2\pi^2}\left(1 - \frac{6\lambda}{i^2\pi}\right)\exp\left\{-\frac{Dt}{l^2}(i^2\pi^2 + 4\lambda)\right\}\right], \quad (91)
$$
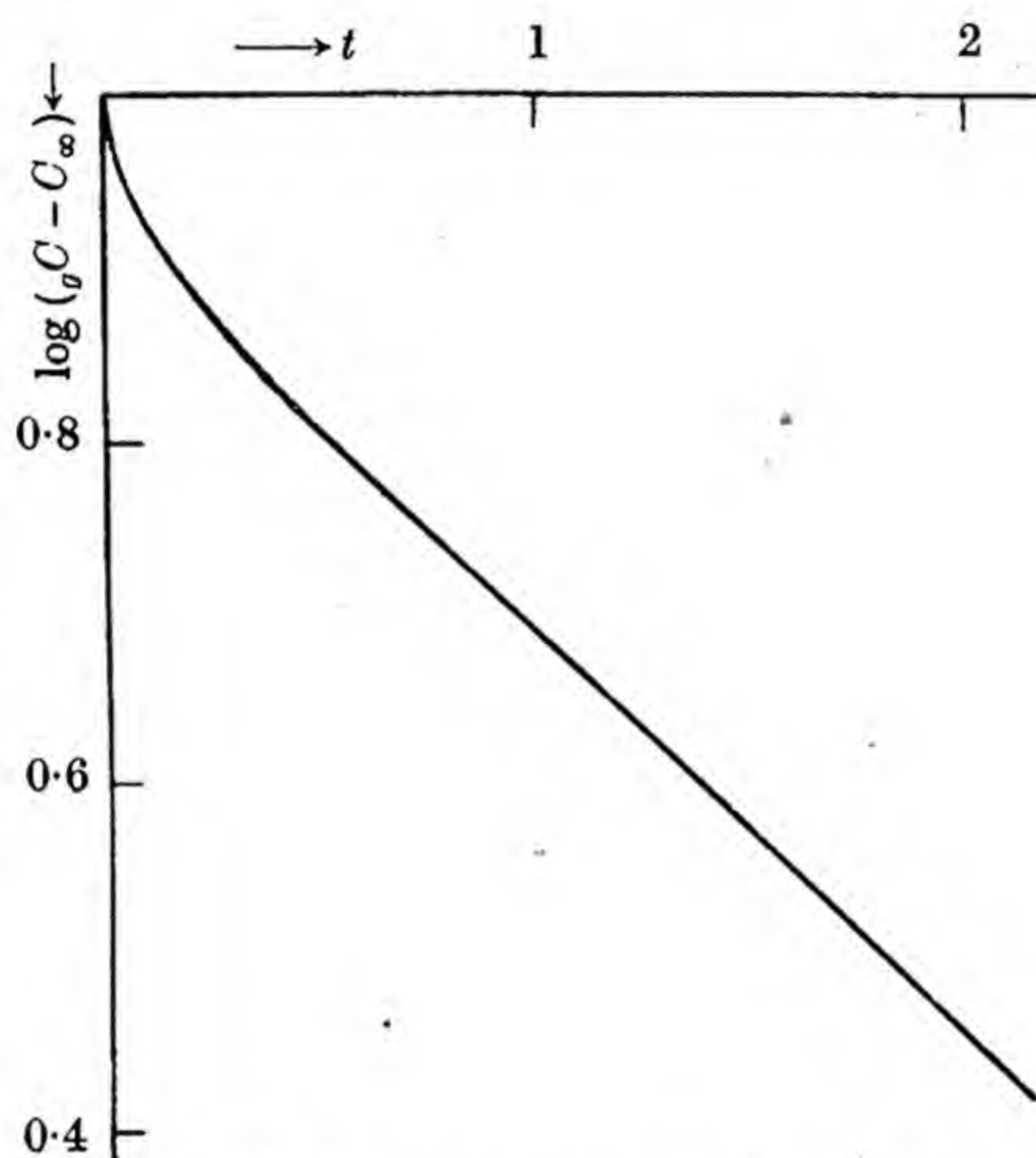
Fig. 7. A typical diffusion rate curve of log $({}_gC - C_\infty)$ against time. The units of ordinates and abcissae are arbitrary.

which reduce as illustrated in Fig. 7 for small values of λ and large t to

$$
{}_gC = \frac{{}_gC_0}{2}[1 + e^{-2\lambda Dt/l^2}], \quad (90a)
$$

$$
{}_hC = \frac{{}_hC_0}{2}[1 - e^{-2\lambda Dt/l^2}]. \quad (91a)
$$

When the distribution coefficient of solute between the membrane and the solvent is not unity, but $k = \dfrac{C \text{ in solid}}{C \text{ in gas}}$, the problem can be treated identically by writing

$$\left.\begin{aligned} \lambda_1 &= \frac{y}{lk}, \\[2mm] \lambda_2 &= \frac{h}{lk}, \end{aligned}\right\} \tag{92}$$

and using for C_∞ the equation (93) instead of (84),

$$C_\infty(g + kl + h) = (_yC_0)\,g + \int_0^l C_0(x)\,dx + (_hC_0)\,h. \tag{93}$$

If the diffusing solute exists in the membrane in atomic form, and in the gas phase (or in solution) in molecular form (e.g. H_2-Pd), then the treatment of Barnes must be further modified.

(2) Solutions of the radial diffusion equation

We may restrict ourselves to considerations of diffusions such that the spherical surfaces of constant concentration are concentric; in this case the equation of diffusion is (12):

$$\frac{\partial C}{\partial t} = D\left(\frac{\partial^2 C}{\partial r^2} + \frac{2}{r}\frac{\partial C}{\partial r}\right). \tag{12}$$

Examples of diffusion in spheres may then be treated in a very simple manner by making the substitution

$$u = Cr,$$

which gives

$$\frac{\partial u}{\partial t} = D\frac{\partial^2 u}{\partial r^2}. \tag{94}$$

The methods used in the previous pages for all the linear cases may then be employed, and analogous solutions obtained. Some examples of these solutions of the diffusion equation will now be given.

Suppose one has a sphere of radius a, and containing solute at an initial concentration $C = f(r)$. The surface of the sphere is kept at a constant concentration C_2. The substitution

$u = Cr$ in equation (12) leads to equation (94) which must be solved for the boundary conditions:

$$u_1 = 0 \text{ at } r = 0 \text{ for all } t,$$

$$u_2 = aC_2 \text{ at } r = a \text{ for all } t,$$

$$u = rf(r) \text{ at } t = 0 \text{ and for } 0 < r < a.$$

These are the conditions for diffusion in a plate of thickness l and with surface concentrations at $x = 0$ and $x = l$ of 0 and aC_0. The solution is therefore (51) in the form (51 a)

$$u = \frac{u_2 r}{a} + \frac{2}{\pi} \sum_1^\infty \frac{u_2 \cos n\pi}{n} \sin \frac{n\pi r}{a} \exp\left[-\frac{Dn^2\pi^2 t}{a^2}\right]$$

$$+ \frac{2}{a} \sum_1^\infty \sin \frac{n\pi r}{a} \exp\left[-\frac{Dn^2\pi^2 t}{a^2}\right] \int_0^a r'f(r') \sin \frac{n\pi r'}{a} dr'. \quad (51\,a)$$

Case 1. The amount of absorption or desorption in spheres can easily be derived from (51 a) for some important examples. For instance, when $f(r) = C_0$ throughout the sphere at $t = 0$, equation (51 a) becomes

$$C = C_2 + \frac{2a}{\pi} \sum_1^\infty \frac{(-1)^n}{n} \sin \frac{n\pi r}{a} \exp\left[-\frac{Dn^2\pi^2 t}{a^2}\right](C_2 - C_0). \quad (95)$$

Equation (95) corresponds to absorption with $C_2 > C_0$, and desorption with $C_0 > C_2$, and from it by means of the equation

$$Q = -\int_0^t D\left(\frac{\partial C}{\partial r}\right)_{r=a} dt,$$

the quantity Q which has been absorbed or desorbed may be found. The necessary differentiation and integration leads to (96):

$$Q = \frac{(C_2 - C_0)a^2}{4}\left(1 - \frac{8}{\pi^2}\sum_1^\infty \frac{1}{n^2}\exp\left[-\frac{Dn^2\pi^2 t}{a^2}\right]\right). \quad (96)$$

Case 2. In the problem of diffusion into or out of the wall of a hollow spherical shell of inside radius b and outside radius a, one may proceed analogously. The solution of $\partial u/\partial t = D\partial^2 u/\partial r^2$ is to be found for the boundary conditions:

$$u = u_1 = bC_1 \text{ at } r = b \text{ for all } t,$$

$$u = u_2 = aC_2 \text{ at } r = a \text{ for all } t,$$

and $\qquad C_0 = 0$ for $b < r < a$ and at $t = 0$.

When one also makes the substitution $r = b + x$, the problem reduces to the case of flow into a plate of thickness $l = (a - b)$, and with constant concentrations u_1 and u_2 at the faces $x = 0$ and $x = l$. Thus the solution is that given by equation (51), with appropriate substitutions:

$$u = u_1 + (u_2 - u_1)\frac{x}{l} + \frac{2}{\pi}\sum_1^\infty \frac{u_2 \cos n\pi - u_1}{n} \sin \frac{n\pi x}{l} \exp\left[-\frac{Dn^2\pi^2 t}{l^2}\right],$$

(52 b)

where $u_1 = bC_1$ at $x = 0$, $u_2 = aC_2$ at $x = (a - b) = l$, $x = r - b$, $u = rf(r) = 0$ at $t = 0$ $(b < r < a)$.

The quantity Q which has flowed into the slab at any time t is given by

$$Q = -D\int_0^t\left[\left(\frac{\partial u}{\partial x}\right)_{x=0} - \left(\frac{\partial u}{\partial x}\right)_{x=l}\right]dt$$

$$= -\frac{2l}{\pi^2}\sum_1^\infty\left(\frac{1-(-1)^n}{n^2}\right)\{u_2(-1)^n - u_1\}\left(1-\exp\left\{-\frac{Dn^2\pi^2 t}{l^2}\right\}\right)\quad (97)$$

$$= (u_2 + u_1)\frac{4l}{\pi^2}\sum_{m=0}^\infty \frac{1}{(2m+1)^2}\left(1-\exp\left\{-\frac{D(2m+1)^2\pi^2 t}{l^2}\right\}\right).\quad (98)$$

Also, $\sum_{m=0}^\infty \dfrac{1}{(2m+1)^2} = \dfrac{\pi^2}{8}$, and so

$$Q = (aC_2 + bC_1)\left(\frac{a-b}{2}\right)$$

$$\left[1 - \frac{8}{\pi^2}\sum_{m=0}^\infty \frac{1}{(2m+1)^2}\exp\left\{-\frac{D(2m+1)^2\pi^2 t}{(a-b)^2}\right\}\right],\quad (99)$$

for sorption in the spherical shell, on resubstituting aC_2 for u_2, bC_1 for u_1 and $(a - b)$ for l. Equation (99) for the case when $C_2 = C_1$ reduces to

$$Q = C_2\frac{(a^2 - b^2)}{2}\left[1 - \frac{8}{\pi^2}\sum_{m=0}^\infty \frac{1}{(2m+1)^2}\exp\left\{-\frac{D(2m+1)^2\pi^2 t}{(a-b)^2}\right\}\right].$$

(99 a)

It is to be noted that the equations (97)–(99a) refer to the quantity Q which has diffused into unit area of thickness l of the slab, i.e. into a volume l of the spherical shell, and that the total quantity $Q_{\text{total}} = Q[\frac{4}{3}\pi(a^3 - b^3)]$.

Case 3. The intercept L upon the t-axis of the curve, where C_g (the concentration built up in the gas phase by permeation of gas through the hollow spherical shell of Case 2) is plotted against t, is given by the theory of equations (63)–(69 b). One has only to make the substitutions of Case 2 (equations (69 a) and (97)–(99 a)) to obtain for the boundary conditions of these equations:

$$L = \frac{1}{u_2 - u_1} \left[\frac{u_2(a-b)^2}{6D} + \frac{u_1(a-b)^2}{3D} \right] \qquad (100)$$

$$= \frac{1}{aC_2 - bC_1} \left[\frac{aC_2(a-b)^2}{6D} + \frac{bC_1(a-b)^2}{3D} \right]. \qquad (101)$$

If $C_1 \simeq 0$, which will be the case when diffusion occurs into a vacuum or near vacuum from the exterior of the shell to the interior, the lag L reduces to

$$L = \frac{(a-b)^2}{6D}, \qquad (102)$$

which is just the same as for a plate. It must be remembered that in the equations (100)–(102) it is supposed that the initial concentration, C_0, of gas in the shell is zero. The equations (101) and (102) provide a very easy method of evaluating D, the diffusion constant.

(3) *Diffusion in cylindrical media*

Examples of diffusion problems in wires are fairly common. Of practical importance is the outgassing of metal filaments, and the converse process of sorption in wires. It is necessary to know how much gas remains in the filaments, or how much has diffused away under vacuum conditions. The diffusion of metals such as thorium into or out of tungsten filaments has a profound effect upon the thermionic and photoelectric emission of the filament, and this in its turn is of importance in various types of valve. The quantitative expression for the flow of thorium can be obtained by integration of the differential equation for flow in a cylinder, using appropriate boundary conditions. Sometimes a supply of a solute may be

generated chemically or physically at the surface of a wire at a concentration which is a function of time. This provides a more complex example of diffusion into a cylinder. For example, a supply of carbon may be generated by the decomposition of hydrocarbons at the surface of an iron wire and the carbon may then diffuse into the wire. Often analogous problems will arise in which gases are sorbed in, desorbed from, or diffuse through the walls of cylindrical tubes.

The equation for radial flow in a cylinder is

$$\frac{\partial C}{\partial t} = D\left[\frac{1}{r}\frac{\partial}{\partial r}\left(r\frac{\partial C}{\partial r}\right)\right], \tag{15}$$

and by making the substitution $C = ue^{-D\alpha^2 t}$, the equation (15) is transformed to

$$\frac{\partial^2 u}{\partial r^2} + \frac{1}{r}\frac{\partial u}{\partial r} + \alpha^2 u = 0, \tag{103}$$

which is Bessel's equation of zero order. Solutions of Bessel's equation may be obtained in terms of the appropriate Bessel functions whose choice is governed by the boundary conditions.

Case 1. A circular cylinder of radius $r = a$ is the diffusion medium, at its surface a constant concentration C_1 is maintained, and the medium is initially free of solute. In this example the solution may be given in terms of Bessel's function of the first kind and of zero order $J_0(x)$ and its differential $J_0'(x)$. The solution is

$$C = C_1\left(1 + \frac{2}{a}\sum_1^\infty \frac{1}{\alpha_n}\frac{J_0(\alpha_n r)}{J_0'(\alpha_n a)} e^{-D\alpha_n^2 t}\right), \tag{104}$$

where α_n is the nth root of the equation $J_0(\alpha_n a) = 0$. The first four roots of $J_0(\alpha_n a) = 0$ are

$$\alpha_1 = \frac{2\cdot405}{a}, \quad \alpha_2 = \frac{5\cdot520}{a}, \quad \alpha_3 = \frac{8\cdot654}{a}, \quad \alpha_4 = \frac{11\cdot7915}{a}. \tag{105}$$

These roots give four exponential terms in an infinite series, and it will be found as a rule that these terms are adequate to express the diffusion process. Indeed, for larger values of the

time, t, a single term will be sufficient. The functions $J_0(x)$
and $J_0'(x)$ are given by the series

$$\left.\begin{aligned}J_0(x) &= 1 - (\tfrac{1}{2}x)^2 + \frac{(\tfrac{1}{2}x)^4}{1^2 2^2} - \frac{(\tfrac{1}{2}x)^6}{1^2 2^2 3^2} + \cdots, \\ J_0'(x) &= -(\tfrac{1}{2}x) + \frac{(\tfrac{1}{2}x)^3}{1^2 2} - \frac{(\tfrac{1}{2}x)^5}{1^2 2^2 3} + \cdots,\end{aligned}\right\} \quad (106)$$

and their values for any values of x are given in tables.*

For most purposes it will be more important to know the
mean concentration in the cylinder, or alternatively the
quantity Q which has diffused into the cylinder, per unit
length. $\bar{C}$, the mean concentration in the cylinder, is given by

$$\left.\begin{aligned}\bar{C} &= \frac{1}{\pi a^2}\int_0^a 2\pi r C\, dr = \frac{2}{a^2}\int_0^a Cr\, dr \\ Q &= 2\pi\int_0^a Cr\, dr, \text{ per unit length.}\end{aligned}\right\} \quad (107)$$

and

The integration of (107) in which (104) has been substituted
leads to the equations

$$\left.\begin{aligned}\bar{C} &= C_1\left(1 - \frac{4}{a^2}\sum_1^\infty \frac{1}{\alpha_n^2}e^{-D\alpha_n^2 t}\right), \\ Q &= \pi a^2 C_1\left(1 - \frac{4}{a^2}\sum_1^\infty \frac{1}{\alpha_n^2}e^{-D\alpha_n^2 t}\right),\end{aligned}\right\} \quad (108)$$

where the first four values of α_n are given by equation (105).
Equations (108) follow easily from the relation

$$-\int_0^a r J_0(\alpha_n r) = \frac{a}{\alpha_n}J_0'(\alpha_n a),$$

and by substitution of (105) lead to a value for the mean
concentration $\bar{C}$ in the filament:

$$\frac{Q}{\pi a^2} = \bar{C} = C_1\left(1 - \frac{4}{(2\cdot405)^2}\exp\left\{-\frac{D(2\cdot405)^2 t}{a^2}\right\} - \frac{4}{(5\cdot520)^2}\right.$$
$$\left.\times\exp\left\{-\frac{D(5\cdot520)^2 t}{a^2}\right\} - \frac{4}{(8\cdot654)^2}\exp\left\{-\frac{D(8\cdot654)^2 t}{a^2}\right\} - \cdots\right).$$
$$(108a)$$

* References to suitable tables are given at the end of this Chapter.

Case 2. If the cylindrical diffusion medium is of radius a and the boundary conditions are

$$C_1 = 0 \text{ at } r = a \text{ for all } t,$$
$$C = f(r) \text{ for } a < r < 0 \text{ at } t = 0,$$

the general solution is

$$C = \frac{2}{a^2} \sum_1^\infty e^{-D\alpha_n^2 t} \frac{\int_0^a rf(r) J_0(\alpha_n r)\, dr}{[J_0'(\alpha_n a)]^2} J_0(\alpha_n r). \qquad (109)$$

When $f(r) = C_0$, the solution is

$$C = -\frac{2C_0}{a} \sum_1^\infty \frac{1}{\alpha_n} e^{-D\alpha_n^2 t} \frac{J_0(\alpha_n r)}{J_0'(\alpha_n a)}. \qquad (109a)$$

By using the relations

$$\bar{C} = \frac{2}{a^2} \int_0^a Cr\, dr \quad \text{and} \quad Q = \pi a^2 C_0 - 2\pi \int_0^a Cr\, dr, \qquad (107a)$$

where Q is now the quantity of solute which has diffused out of the cylindrical medium per unit length, one obtains the solutions for $\bar{C}$ and Q just as for Case 1, equations (108):

$$\left. \begin{array}{l} \bar{C} = \dfrac{4C_0}{a^2} \sum \dfrac{1}{\alpha_n^2} e^{-D\alpha_n^2 t}, \\[3mm] Q = \pi a^2 C_0 \left(1 - \dfrac{4}{a^2} \sum \dfrac{1}{\alpha_n^2} e^{-D\alpha_n^2 t} \right). \end{array} \right\} \qquad (110)$$

Since the α's are given by (105) it is an easy matter to write the first four terms of equations (110), and so to employ them in practice.

Case 3. If in the cylindrical medium of radius a the boundary conditions are

$$C = C_1 \text{ at } r = a \text{ for all } t,$$
$$C = f(r) \text{ for } a < r < 0 \text{ and } t = 0,$$

the general solution is

$$C = C_1 \left(1 + \frac{2}{a} \sum_1^\infty \frac{1}{\alpha_n} \frac{J_0(\alpha_n r)}{J_0'(\alpha_n a)} e^{-D\alpha_n^2 t} \right)$$

$$+ \frac{2}{a^2} \sum_1^\infty e^{-D\alpha_n^2 t} \frac{\int_0^a rf(r) J_0(\alpha_n r)\, dr}{[J_0'(\alpha_n a)]^2} J_0(\alpha_n r). \qquad (111)$$

If $f(r) = C_0$ for $a < r < 0$ and at $t = 0$ (which would correspond to the sorption equilibrium of a gas in a wire before admitting another dose of gas at constant concentration C_1), equation (111) reduces to

$$C = C_1 + \frac{2}{a} \sum_1^\infty \frac{1}{\alpha_n} e^{-D\alpha_n^2 t} \frac{J_0(\alpha_n r)}{J_0'(\alpha_n a)} (C_1 - C_0). \qquad (112)$$

In turn, equation (112) gives for the mean concentration $\bar{C}$ in the cylinder, or the quantity Q of gas which has diffused into or out of the cylinder per unit length,

$$\frac{Q}{\pi a^2} = \bar{C} = C_1 - \frac{2(C_1 - C_0)}{a^2} \sum \frac{1}{\alpha_n^2} e^{-D\alpha_n^2 t}, \qquad (113)$$

where the values of α_1, α_2, α_3 and α_4 are given by (105), and permit four exponential terms of the series to be used.

Case 4. If the surface concentration of solute is $C = At$, where A is a constant, and there is an initial solute concentration C_0 in the cylinder of radius a at $t = 0$, the general solution is (9a)

$$C = -\frac{A}{D} \left[\tfrac{1}{4}(a^2 - r^2 - Dt) + \frac{2}{a} \sum_1^\infty \frac{1}{\alpha_n^3} \frac{J_0(\alpha_n r)}{J_0'(\alpha_n a)} e^{-D\alpha_n^2 t} \right]$$
$$+ \frac{2C_0}{a} \sum_1^\infty \frac{1}{\alpha_n} \frac{J_0(\alpha_n r)}{J_0'(\alpha_n a)} e^{-D\alpha_n^2 t}, \qquad (114)$$

and so one finds for Q and $\bar{C}$ the expression

$$\frac{Q}{\pi a^2} = \bar{C} = A \left[t - \frac{a^2}{8D} + \frac{4}{a^2 D} \sum_1^\infty \frac{1}{\alpha_n^4} e^{-D\alpha_n^2 t} \right] + \frac{2C_0}{a^2} \sum \frac{1}{\alpha_n^2} e^{-D\alpha_n^2 t}. \qquad (115)$$

Case 5. If one has a hollow cylinder of external and internal radii b and a respectively, the initial concentration in the cylinder is $f(r)$ for $a < r < b$, and the concentrations at the surfaces at $r = b$ and $r = a$ are zero for all time t, the general solution for the concentration as a function of time (10) is

$$C = \frac{\pi^2}{2} \sum_1^\infty \alpha_n^2 \frac{J_0^2(\alpha_n a)}{J_0^2(\alpha_n b) - J_0^2(\alpha_n a)} e^{-D\alpha_n^2 t} U_0(\alpha_n r) \int_a^b r f(r) U_0(\alpha_n r) \, dr. \qquad (116)$$

In this equation the α_n's are the roots of the equation

$$J_0(\alpha a) H_0^{(\prime)}(\alpha b) - J_0(\alpha b) H_0^{(\prime)}(\alpha a) = 0,$$

in which $H_0^{(\prime)}(\alpha r)$ denotes a Bessel function of the third kind, for $U_0(\alpha r) = J_0(\alpha r) H_0^{(\prime)}(\alpha b) - J_0(\alpha b) H_0^{(\prime)}(\alpha r)$, and with the above meaning of α_n, $U_0(\alpha_n a) = U_0(\alpha_n b) = 0$, satisfying the boundary condition that at $r = a$ and $r = b$ the concentration is zero.

When $f(r) = C_0$, equation (116) reduces* to

$$C = \frac{\pi^2}{2} C_0 \sum_{a=1}^{\infty} \alpha_n^2 \frac{J_0^2(\alpha_n a)}{J_0^2(\alpha_n b) - J_0^2(\alpha_n a)} e^{-D\alpha_n^2 l} U_0(\alpha_n r)$$
$$\times \left[-\frac{2i}{\pi \alpha_n^2} \left(1 - \frac{J_0(\alpha_n b)}{J_0(\alpha_n a)} \right) \right]. \quad (117)$$

From this equation by means of the relation

$$Q = \pi(b^2 - a^2) C_0 - 2\pi \int_a^b Cr\, dr$$

one may find Q, the amount of material which has diffused out of unit length of the walls of the cylindrical tube, as a function of time,

$$Q = \pi(b^2 - a^2) C_0 \left[1 - \frac{4}{(b^2 - a^2)} \sum_{n=1}^{\infty} \frac{1}{\alpha_n^2} \frac{J_0(\alpha_n b) - J_0(\alpha_n a)}{J_0(\alpha_n b) + J_0(\alpha_n a)} e^{-D\alpha_n^2 l} \right]. \quad (118)$$

The roots of the equation $U_0(\alpha_n b) = 0 = U_0(\alpha_n a)$ are computed from the expression[11]

$$\alpha_n = \frac{n\pi}{(\rho - 1)} - \frac{(\rho - 1)}{8\rho(n\pi)} + \left[\frac{100(\rho^3 - 1)}{3(8\rho)^3 (\rho - 1)} + \frac{1}{(8\rho)^2} \right] \frac{(\rho - 1)^3}{(n\pi)^3}$$
$$+ \left[-\frac{32(1073)(\rho^5 - 1)}{5(8\rho)^5 (\rho - 1)} + \frac{50(\rho^3 - 1)}{3\rho(8\rho)^3 (\rho - 1)} - \frac{2}{(8\rho)^3} \right] \frac{(\rho - 1)^5}{(n\pi)^5} + \dots,$$

---

* This integration makes use of the relationships

$$\int_a^b r\, U_0(\alpha_n r) = \left[\frac{r}{\alpha_n} U_1(\alpha_n r) \right]_a^b,$$

$$U_1(\alpha_n r) = -\frac{\partial U_0(\alpha_n r)}{\partial(\alpha_n r)},$$

$$\left[r \frac{\partial U_0(\alpha_n r)}{\partial r} \right]_{r=b} = -\frac{2i}{\pi},$$

$$\left[r \frac{\partial U_0(\alpha_n r)}{\partial r} \right]_{r=a} = -\frac{2i}{\pi} \frac{J_0(\alpha_n b)}{J_0(\alpha_n a)},$$

the first of which will be found in Watson[10a] and the others in Carslaw[10].

where $\rho = b/a$. The values of $J_0(\alpha_n b)$ and $J_0(\alpha_n a)$ may then be found from tables of Bessel functions.

Case 6. If one has a hollow cylinder of internal and external radii a and b respectively, and there is a concentration C_1 at $r = a$ and C_2 at $r = b$, and a concentration C_0 in the wall of the cylinder, one may treat equation (116) in the same way as was done in equations (63)–(69b) to find the rate of approach to the steady state of flow through the wall of the cylinder. The intercept L made on the time axis by the asymptote to the curve of the quantity diffused plotted against the time is now given by

$$L = -\frac{\pi^2 a}{2D}\frac{\log a/b}{(C_1 - C_2)}\sum_1^\infty \frac{J_0^2(\alpha_n a)}{J_0^2(\alpha_n b) - J_0^2(\alpha_n a)} I[U_0'\alpha_n r]_{r=a}, \quad (119)$$

if

$$I = \int_a^b r U_0(\alpha_n r)\left[C_0 - \left\{\frac{(C_1 - C_2)\log r + C_2 \log a - C_1 \log b}{\log a - \log b}\right\}\right] dr,$$

when $C_0 = 0$, $C_1 = 0$ the most important experimental case arises, and the equation above reduces to

$$L = \frac{2}{D}\sum_1^\infty \frac{1}{\alpha_n^2}\frac{J_0(\alpha_n a) J_0(\alpha_n b)}{J_0^2(\alpha_n b) - J_0^2(\alpha_n a)}\ln\frac{b}{a}, \quad (120)$$

where α_n is as before the nth positive root of

$$U_0(\alpha_n b) = 0 = U_0(\alpha_n a),$$

and one has once more a useful method of measuring the diffusion constant (cf. equations (69), (69a), (69b) for plates, and equation (101) for a hollow spherical shell).

(4) *Diffusion processes coupled with interface reactions*

Sometimes there are slow processes at the surface of the diffusion medium which may sensibly alter the rate at which the diffusing substance leaves or enters the medium. For instance, under certain conditions the diffusion of hydrogen in palladium is fast compared with its rate of entry into the solid from the sorption layer. In this case it will be necessary to include a term to allow for the leaving or entering of hydrogen at the surface. In general two cases will have to be considered:

(a) the solute is dissociated on entering the diffusion medium, and (b) the molecular condition is the same inside as outside the diffusion medium. The first condition will be encountered in systems such as O_2-silver, H_2-palladium, N_2-iron or molybdenum; and the second when ammonia, water or gases diffuse into an alkali halide lattice, or a zeolite lattice. It will be possible to attempt a solution for the conditions of (b).

Case 1. The diffusion of ammonia gas occurs from a sphere of a zeolite (analcite). The initial ammonia concentration in the sphere is $f(r)$; the radius of the sphere is a, and the concentration at $r = a$ is maintained very low (by condensing evolved ammonia in liquid air). One has thus to solve the equation

$$\frac{\partial C}{\partial t} = D\left(\frac{\partial^2 C}{\partial r^2} + \frac{2}{r}\frac{\partial C}{\partial r}\right) \quad \text{for } 0 < r < a, \qquad (a)$$

when

$$C = f(r) \text{ at } t = 0, \qquad (b)$$

and

$$D\frac{\partial C}{\partial r} + kC = 0 \text{ at } r = a. \qquad (c)$$

The substitution $u = Cr$ gives

$$\frac{\partial u}{\partial t} = D\frac{\partial^2 u}{\partial r^2} \quad (0 < r < a), \qquad (d)$$

$$\frac{\partial u}{\partial r} + (h - 1/a)\,u = 0 \text{ at } r = a \text{ when } h = k/D, \qquad (e)$$

$$u = rf(r) \text{ at } t = 0. \qquad (f)$$

The problem is analogous to the process of cooling of a sphere with radiation at its surface(12), the radiation corresponding to the surface desorption. Proceeding therefore along analogous lines to those adopted in the problem of the cooling of the earth(13), one obtains

$$C = \frac{2}{ar}\sum_{n=1}^{\infty}\frac{\alpha_n^2 a^2 + (ah-1)^2}{\alpha_n^2 a^2 + ah(ah-1)}\left(\int_0^a r'f(r')\sin\alpha_n r'\,dr'\right)\sin\alpha_n r\, e^{-D\alpha_n^2 t},$$

$$(121)$$

where α_n is the nth root of

$$\tan\alpha a = \frac{\alpha a}{1 - ah}.$$

When $f(r) = C_0$ the equation reduces to

$$C = \frac{2C_0 h}{1} \sum_1^\infty \frac{1}{\alpha_n^2} \frac{\alpha_n^2 a^2 + (ah-1)^2}{\alpha_n^2 a^2 + ah(ah-1)} \sin \alpha a \frac{\sin \alpha r}{r} e^{-D\alpha_n^2 t}. \quad (122)$$

The quantity Q which has been desorbed from the sphere is then

$$Q = \tfrac{4}{3}\pi a^3 C_0 - 4\pi \int_0^a Cr^2\, dr = Q_0 - 4\pi \int_0^a Cr^2\, dr$$

$$= Q_0\left(1 - \frac{6h^2}{a^2}\right) \sum_{n=1}^\infty \frac{1}{\alpha_n^4} \frac{\alpha_n^2 a^2 + (ah-1)^2}{\alpha_n^2 a^2 + ah(ah-1)} (\sin^2 \alpha a)\, e^{-D\alpha_n^2 t}. \quad (123)$$

When one plots $\ln \dfrac{(Q_0 - Q)}{Q_0}$ against t, the curve for large values

of t approaches a line of slope $-D\alpha_1^2$, for which the intercept on the axis of t is

$$\ln\left[\frac{6h^2}{a^2} \frac{1}{\alpha_1^4} \frac{\alpha_1^2 a^2 + (ah-1)^2}{\alpha_1^2 a^2 + ah(ah-1)} \sin^2 \alpha_1 a\right].$$

These two equations can be solved for D and k with the aid of the equation

$$\tan(\alpha a) = \frac{\alpha a}{1 - ah},$$

i.e. $\tan z + \lambda z = 0$, where $\lambda = \dfrac{1}{a(h-1)}$ and $\overline{\alpha a} = z$. The roots

of this equation [8] are given by

$$z_n = (n + \tfrac{1}{2})\pi + \frac{1}{\lambda(n + \tfrac{1}{2})\pi} - \frac{3\lambda - 1}{3\lambda^3[(n + \tfrac{1}{2})\pi]^3}$$

$$- \frac{1575\lambda^3 + 1575\lambda^2 + 483\lambda + 45}{315\lambda^7[(n + \tfrac{1}{2})\pi]^7}$$

$$+ \frac{39690\lambda^4 + 52920\lambda^3 + 24696\lambda^2 + 3834\lambda + 9}{2835\lambda^9[(n + \tfrac{1}{2})\pi]^9} - \ldots \quad (124)$$

In Fig. 8 are shown the first four roots of the equation $\tan z + \lambda z = 0$ for λ between 1 and 5 [8], i.e. when ak/D lies between 2 and 1·2. The radius a may of course be varied.

When the desorption process at the surface depends on the square of the concentration, the problem cannot be solved along analogous lines.

Case 2. If desorption into a vacuum occurs at the surfaces $x = 0$ and $x = l$ of a slab, the conditions of Case 1 become(14)

(i)
$$\frac{\partial C}{\partial t} = D \frac{\partial^2 C}{\partial x^2},$$

(ii)
$$-\frac{\partial C}{\partial x} + hc = 0 \text{ at } x = 0,$$

(iii)
$$+\frac{\partial C}{\partial x} + hc = 0 \text{ at } x = l, \text{ where } h = k/D,$$

(iv)
$$C = f(x) \text{ at } t = 0.$$
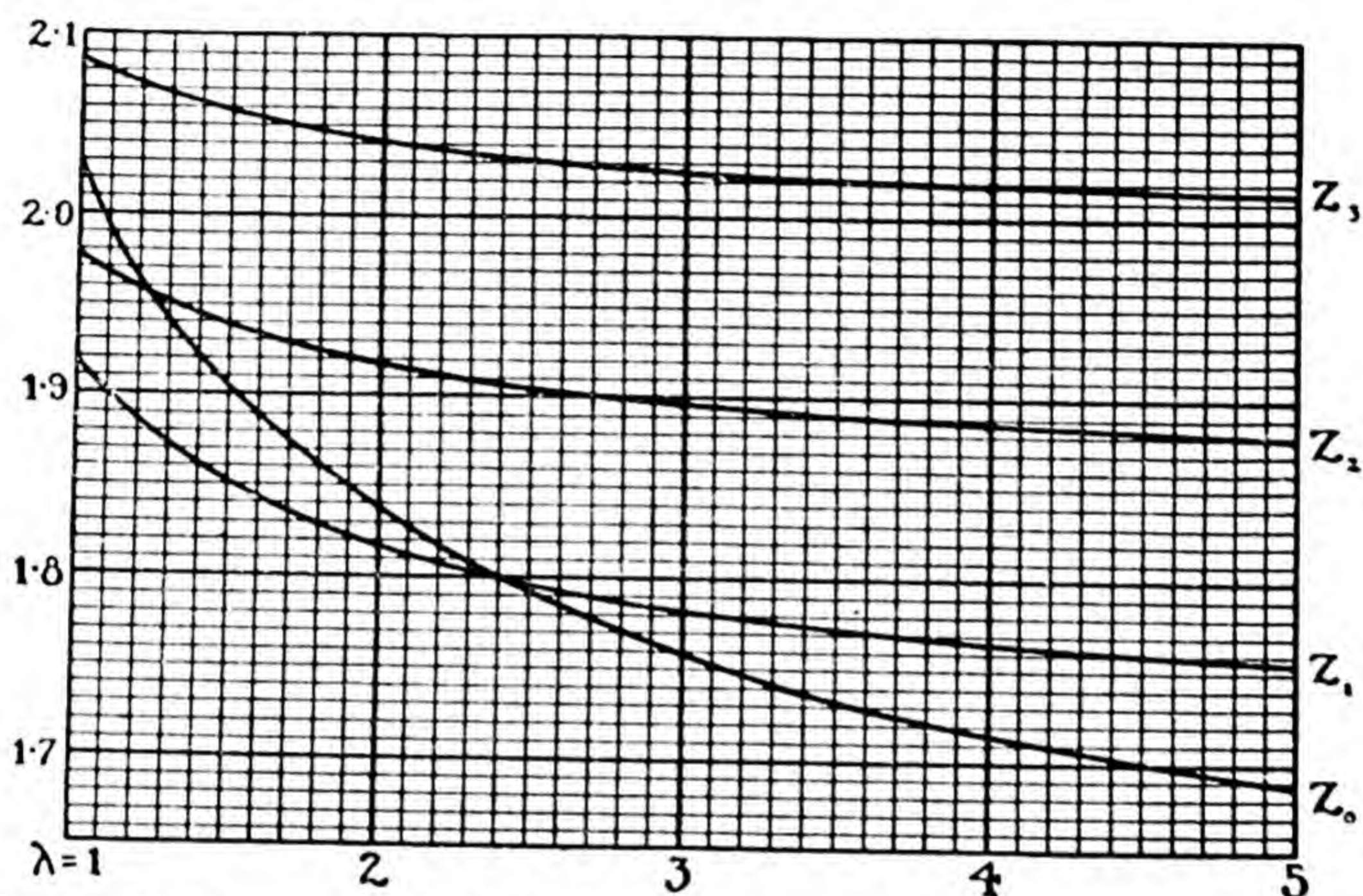
Fig. 8. This figure gives the first four roots, z_0, z_1, z_2, z_3, of the equation $\tan z + \lambda z = 0$, for values of λ ranging from 1 to 5. For the curve z_0 the vertical scale reads as shown. For z_1, the values read from the curve should be increased by 3: for z_2, add 6: for z_3, add 9.

The expression $e^{-D\alpha^2 t}(A \cos \alpha x + B \sin \alpha x)$

may be used to develop the solution, for it satisfies (i), and also (ii) and (iii), when

$$-\alpha B + hA = 0$$

and $\alpha(B \cos \alpha l - A \sin \alpha l) + h(B \sin \alpha l + A \cos \alpha l) = 0,$

which in turn give $\tan \alpha l = \dfrac{2\alpha h}{\alpha^2 - h^2},$ (124a)

$$\frac{A}{\alpha} = \frac{B}{h}.$$ (124b)

The roots of the first expression are the points of intersection of the curves $y = \dfrac{2}{\tan \alpha l}$ and $y = \dfrac{\alpha}{h} - \dfrac{h}{\alpha}$.

The second curve is a hyperbola; the roots of the equation (124a) are all real, not repeated, and only positive values are to be taken.

The solution of the problem is

$$C = 2 \sum_{n=1}^{\infty} e^{-D\alpha_n^2 t} \frac{\alpha_n \cos \alpha_n x + h \sin \alpha_n x}{(\alpha_n^2 + h^2) l + 2h}$$

$$\times \int_0^l f(x')(\alpha_n \cos \alpha_n x' + h \sin \alpha_n x') \, dx, \quad (125)$$

which, if $f(x') = C_0$, reads

$$C = 2C_0 \sum_1^{\infty} e^{-D\alpha_n^2 t} \frac{\alpha_n \cos \alpha_n x + h \sin \alpha_n x}{(\alpha_n^2 + h^2) l + 2h}$$

$$\times \left[\frac{\alpha_n \sin \alpha_n l - h \cos \alpha_n l}{\alpha_n} + \frac{h}{\alpha_n} \right], \quad (126)$$

and gives for Q, the quantity desorbed per unit area,

$$Q = Q_0 - \int C \, dx$$

$$= l C_0 - 2 C_0 \sum_1^{\infty} \frac{1}{\alpha_n^2} \frac{[\alpha_n \sin \alpha_n l - h \cos \alpha_n l + h]^2}{(\alpha_n^2 + h^2) l + 2h} e^{-D\alpha_n^2 t}. \quad (127)$$

Thus, at large values of t one finds in plotting $\ln \dfrac{Q_0 - Q}{Q_0}$ against t that the curve approaches the line of slope $-D\alpha_1^2$, and the intercept upon the t-axis is

$$\ln \left[\frac{2}{l} \frac{1}{\alpha_1^2} \frac{[\alpha_1 \sin \alpha_1 l - h \cos \alpha_1 l + h]^2}{(\alpha_1^2 + h^2) l + 2h} \right].$$

The method outlined is inapplicable when the desorption velocity depends on the square of the concentration at the surface.

Case 3. Barrer[14a] treated the problem of diffusion through a slab of thickness l, when in addition to pure diffusion two other rate-controlling surface processes are important:

(i) The passage of the sorbed atom from the surface to the interior of the plate. Velocity constant k_1.

(ii) The passage of a dissolved atom from the plate to the surface. Velocity constant k_2.

It was assumed in order to treat the problem that the sorption and desorption, with velocity constants k_3 and k_4 respectively, in the gas and the surface layer occurred so rapidly that the surface concentrations were defined by the adsorption isotherm. The distribution of Fig. 9a was subdivided into the two distributions of Figs. 9b and c. In Fig. 9b the gas desorbs into a vacuum; in Fig. 9c one has the steady state of flow through the plate. The complete solution for Fig. 9a was then (employing the notation of Fig. 9)

$$v = u + w.$$

The solution $$u = (Ax + B) \tag{128}$$

for the stationary state of Fig. 9c between $x = 0$ and $x = l$ was given when the constants A and B took the values

$$A = \frac{k_1 k_2 v_2\left(1 - \dfrac{v_1}{v_s}\right) - k_1 k_2 v_1\left(1 - \dfrac{v_2}{v_s}\right)}{\left[k_2\left(1 - \dfrac{v_1}{v_s}\right) + \dfrac{k_1 v_1}{u_s}\right]\left[D + k_2 l\left(1 - \dfrac{v_2}{v_s}\right) + \dfrac{k_1 v_2 l}{u_s}\right]} \\ + D\left[k_2\left(1 - \dfrac{v_2}{v_s}\right) + \dfrac{k_1 v_2}{u_s}\right], \tag{129}$$

$$B = \frac{Dk_1 v_2 + k_1 v_1\left[D + k_2 l\left(1 - \dfrac{v_2}{v_s}\right) + \dfrac{k_1 v_2 l}{u_s}\right]}{\left[k_2\left(1 - \dfrac{v_1}{v_s}\right) + \dfrac{k_1 v_1}{u_s}\right]\left[D + k_2 l\left(1 - \dfrac{v_2}{v_s}\right) + \dfrac{k_1 v_2 l}{u_s}\right]} \\ + D\left[k_2\left(1 - \dfrac{v_2}{v_s}\right) + \dfrac{k_1 v_2}{u_s}\right]. \tag{130}$$

One may work out the different simple types of behaviour that may be encountered. In the equations (129) and (130) v_s denotes the saturation concentration at the surface, and u_s the saturation concentration in the metal. It was observed that very great concentration discontinuities may occur at

the interfaces when diffusion is rapid compared with rates of transport from the surface to the interior of the plate and vice versa.
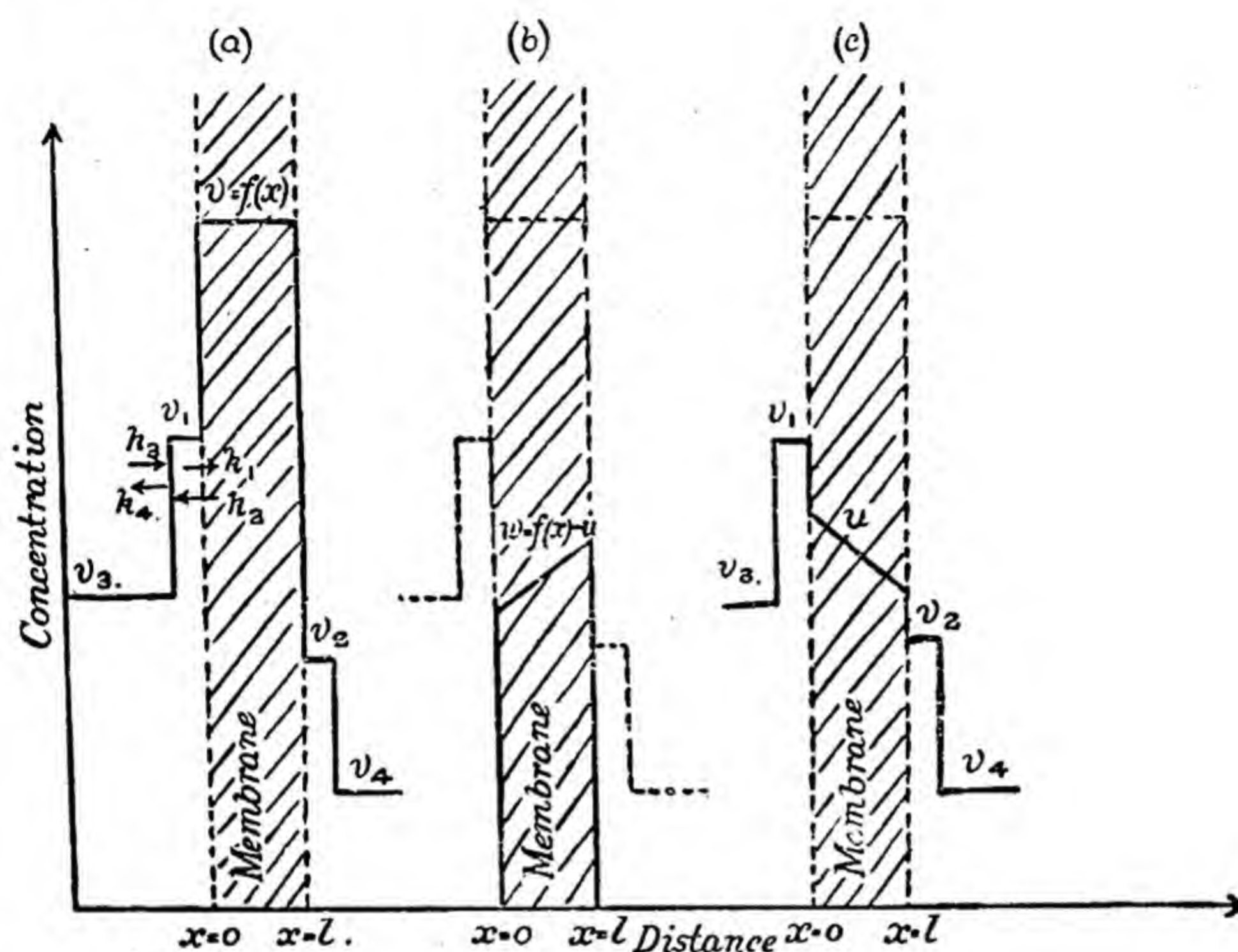
Fig. 9.

The complete solution for the non-stationary state of flow of Fig. 9a is given by

$$v = u + w,$$

where u is defined by equations (128)–(130), and w is given by

$$w = 2 \sum_1^\infty e^{-D\alpha_n^2 t} \frac{\alpha_n \cos \alpha_n x + h \sin \alpha_n x}{(\alpha_n^2 + h^2) l + 2h}$$

$$\times \int_0^x (v_0 - u)(\alpha_n \cos \alpha_n x + h \sin \alpha_n x)\, dx, \quad (131)$$

where α_n is the nth positive root of $\tan \alpha l = \dfrac{2\alpha h}{\alpha^2 - h^2}$, and $h = \dfrac{k_2}{D}$.

(5) *Instantaneous sources*

A number of problems on diffusion into solids require solutions of the diffusion equation for conditions described below. A definite quantity Q of matter is deposited at a point on the

surface of a solid, and left to diffuse into it, or over its surface. Important examples of these diffusion systems are:

(i) Diffusion of caesium along tungsten filaments[15].

(ii) Diffusion of thorium around a tungsten strip[16].

(iii) Diffusions of sodium and potassium into, and over, tungsten strip[17, 18].

It will be seen from the above examples, and in Chap. VIII, that most of our quantitative data on surface diffusions are based on treatments of Fick's law for instantaneous sources.

The solution for an instantaneous plane source in an infinite solid may be derived from equation (34), in which is given the general solution

$$C = \frac{1}{2\sqrt{(\pi D t)}} \int_{-\infty}^{+\infty} f(x') \exp\left[-\frac{(x-x')^2}{4Dt}\right] dx' \qquad (34)$$

to the equation $\dfrac{\partial C}{\partial t} = D\dfrac{\partial^2 C}{\partial x^2}$,

for the boundary conditions

$$C = f(x) \text{ when } t = 0,$$
$$C = f(x, t) \text{ when } t > 0.$$

Suppose in the infinite solid of equation (34) there exists initially a concentration $C = C_0$ between the planes $x = -\frac{1}{2}h$ and $x = +\frac{1}{2}h$. Equation (34) becomes for the new conditions

$$C = \frac{1}{2\sqrt{(\pi D t)}} \int_{-\frac{1}{2}h}^{+\frac{1}{2}h} C_0 \exp\left[-\frac{(x-x')^2}{4Dt}\right] dx', \qquad (132)$$

and if h tends to zero while $C_0 h$ remains constant and equal to Q, one finds

$$C = \frac{Q}{2\sqrt{(\pi D t)}} e^{-x^2/4Dt}. \qquad (133)$$

In Fig. 10 are given[19] a set of curves showing the progress of diffusion according to (133) from a thin layer into a solvent. The curves of Fig. 10 may be compared with those of Fig. 128, Chap. VIII, for sodium diffusing into tungsten.

When the instantaneous source, quantity Q, is deposited at the plane $x = 0$ of a semi-infinite solid, the solution corresponding to (133) is

$$C = \frac{Q}{\sqrt{(\pi Dt)}} e^{-x^2/4Dt}. \tag{134}$$

The variation of C with time at $x = 0$ is given by the equation

$$C = \frac{Q}{\sqrt{(\pi Dt)}} \tag{135}$$

obtained by putting $x = 0$ in (134). Equation (135) gives a very simple method of obtaining D.
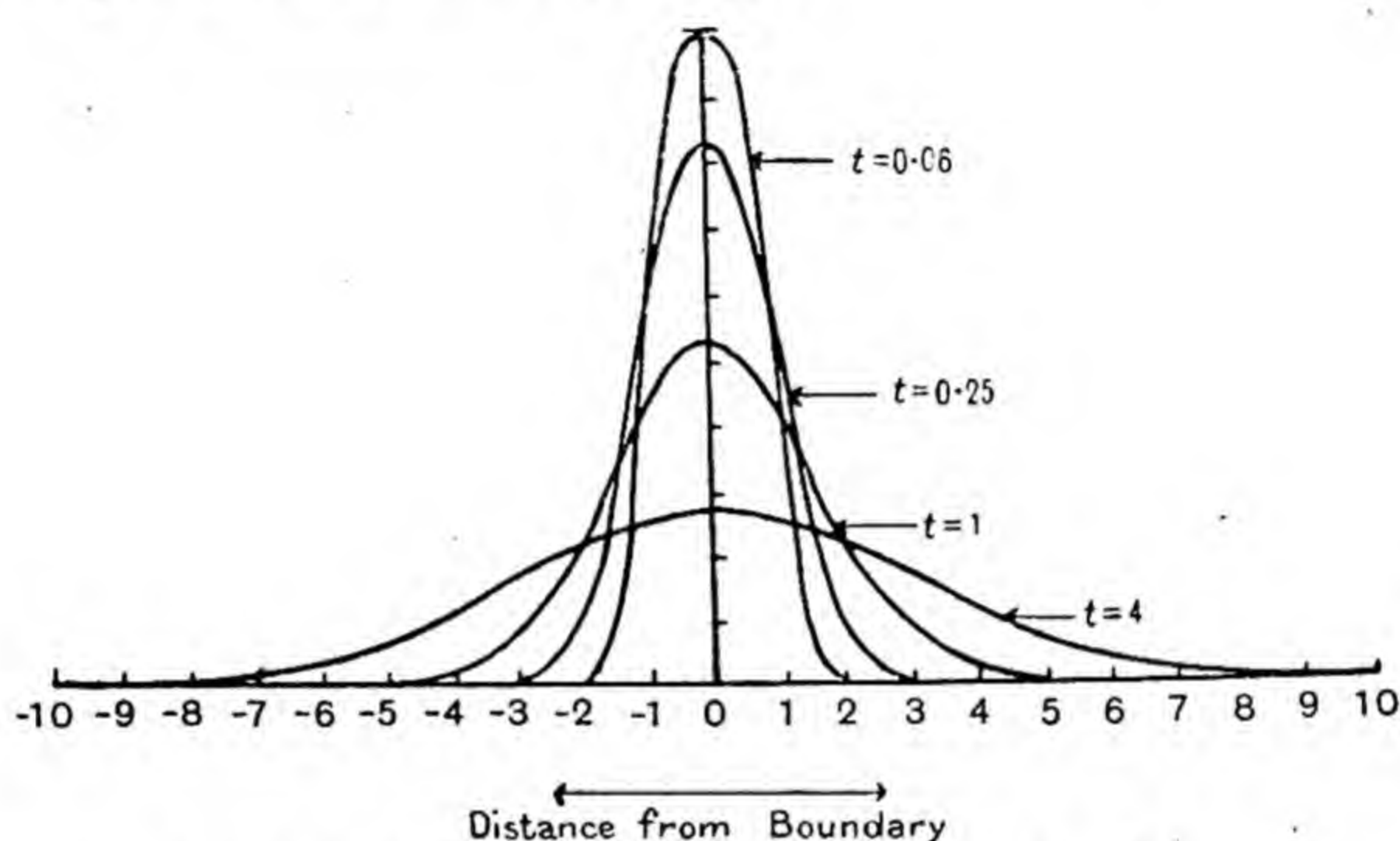
Fig. 10. Diffusion from a thin layer into a solvent.

The solution in two dimensions of the problem treated in the equations (132)–(135) may be deduced in an exactly analogous manner. The equation corresponding to (132) becomes

$$C = \frac{C_0}{4\pi Dt} \int_{-\frac{1}{2}h}^{+\frac{1}{2}h} \int_{-\frac{1}{2}h}^{+\frac{1}{2}h} \exp\left[-\frac{(x-x')^2 + (y-y')^2}{4Dt} \right] dx' dy', \tag{136}$$

and leads to equation (137) for a point source, diffusing over an infinite plane surface:

$$C = \frac{Q}{4\pi Dt} \exp\left[-\frac{(x^2+y^2)}{4Dt} \right] = \frac{Q}{4\pi Dt} \exp\left[-\frac{r^2}{4Dt} \right], \tag{137}$$

if r denotes the radial distance in the plane from the point source.

Similarly, for the point source diffusing in an infinite solid the solution for C in three dimensions is

$$C = \frac{Q}{8(\pi Dt)^{\frac{3}{2}}} e^{-R^2/4Dt}. \tag{138}$$

It will be noted that in the 2- and 3-dimensional cases the value of C at r or $R = 0$ is

$$C = \frac{Q}{4\pi Dt} \tag{139}$$

and

$$C = \frac{Q}{8(\pi Dt)^{\frac{3}{2}}}, \tag{140}$$

respectively. Equation (139) should have ready application in evaluating D in the case of surface diffusion. For instance, one might by a molecular ray method deposit a metal film on a crystal at a point, and heat the crystal. The spreading of the metal could be followed photoelectrically (Chap. VIII).

Equations (138) and (140) are not yet of particular interest in the case of the diffusion of matter, because the conditions of the solution are not capable of easy experimental realisation. One might also have an instantaneous spherical surface source, for which the boundary conditions are that a thin layer of matter exists in the shell

$$a < r < a + h$$

at a concentration C. Then

$$Q = [\tfrac{4}{3}\pi\{(a+h)^3 - a^3\}] C_0,$$

and when, as in (132), we let h tend to zero while Q remains constant, the solution of the general equation

$$C = \frac{C_0}{2r(\pi Dt)^{\frac{1}{2}}} \int_a^{a+h} r' \left[\exp\left\{ -\frac{(r-r')^2}{4Dt} \right\} - \exp\left\{ -\frac{(r+r')^2}{4Dt} \right\} \right] dr' \tag{141}$$

becomes

$$C = \frac{Q}{8\pi ar(\pi Dt)^{\frac{1}{2}}} \left[\exp\left\{ -\frac{(r-a)^2}{4Dt} \right\} - \exp\left\{ -\frac{(r+a)^2}{4Dt} \right\} \right]. \tag{142}$$

Should one have a spherical volume source of radius a, where $\frac{4}{3}\pi a^3 C_0 = Q$, one can obtain the solution by integrating equation (141) between the limits 0 and a, so obtaining (143):

$$C = \frac{3Q}{4a^3\pi^{\frac{3}{2}}} \left[\int_0^{(r+a)/2\sqrt{(Dt)}} e^{-y^2} dy - \int_0^{(r-a)/2\sqrt{(Dt)}} e^{-y^2} dy \right]$$

$$- \frac{3Q}{4a^3\pi^{\frac{3}{2}}} \left(\frac{\sqrt{(Dt)}}{r} \right) \left[\exp\left\{ -\frac{(r-a)^2}{4Dt} \right\} - \exp\left\{ -\frac{(r+a)^2}{4Dt} \right\} \right]. \quad (143)$$

The equations (141)–(143) are more significant in considering flow of heat than of matter, and give the form of temperature waves spreading from areas or volumes through an infinite surrounding medium. Equation (142) would apply to the diffusion of solute from a sphere of aqueous gel into a surrounding medium of solute-free gel. It might also apply to the diffusion of a metal solute from a sphere of a solvent metal embedded in a mass of the solute metal.

(6) Treatment of the equation $\frac{\partial C}{\partial t} = \frac{\partial}{\partial x}\left(D\frac{\partial C}{\partial x} \right)$

Very frequently the diffusion coefficient depends upon the concentration, and it is therefore necessary to solve the equation $\frac{\partial C}{\partial t} = \frac{\partial}{\partial x}\left(D\frac{\partial C}{\partial x} \right)$. The interdiffusion of metal-metal pairs, the diffusion of ammonia or water in certain zeolites, and the diffusion of vapours in media which swell during sorption are typical examples where one must use the above equation. The variation in D with concentration can be very great indeed—a thousandfold or more in some metal-metal systems[20].

The most favoured experimental procedure in following the interdiffusion of metal pairs is to place a slab of each metal in contact, and heat them. The diffusion can be followed by X-ray or chemical analysis of thin layers near the origin, and the slabs may be regarded as of infinite thickness if the diffusion

is slow. The conditions for which a solution is sought are now [21,22]

(i) $$\frac{\partial C}{\partial t} = \frac{\partial}{\partial x}\left(D\frac{\partial C}{\partial x}\right),$$

(ii) $C = C_0$ for $x = 0$ to $x = -\infty$ at $t = 0$,

(iii) $C = 0$ for $x = 0$ to $x = +\infty$ at $t = 0$.

Boltzmann [21] showed that the solution would contain C as a function of a single variable $\lambda = x/\sqrt{t}$. If this variable is substituted in the diffusion equation it becomes

$$-\frac{\lambda}{2}\frac{\partial C}{\partial \lambda} = \frac{\partial}{\partial \lambda}\left(D\frac{\partial C}{\partial \lambda}\right). \tag{144}$$

When some of the diffusing material has passed across the plane $x = 0$, conservation of mass requires that

$$\int_{C_{(x=0)}}^{C_0} x\,dC = \int_0^{C_{(x=0)}} (-x)\,dC; \quad \text{or} \quad \int_0^{C_0} x\,dC = 0. \tag{145}$$

The interdiffusion of two metals in contact is more complicated because each metal acts as both solute and solvent, and after a time the original plane $x = 0$ will no longer satisfy the condition above. It is necessary to choose a new plane at $x' = 0$ so that

$$\int_{C_{(x'=0)}}^{C_0} x'\,dC = \int_0^{C_{(x'=0)}} (-x')\,dC. \tag{146}$$

The zero plane may be chosen when the concentration-distance curve is plotted at a given time. Integration with respect to λ then gives

$$D_{(C=C_1)} = -\frac{1}{2}\frac{d\lambda}{dC}\int_{C=0}^{C=C_1} \lambda\,dC, \quad \text{where} \quad \int_{C=0}^{C=C_0} \lambda\,dC = 0. \tag{147}$$

At any time $t = $ a constant, the equation is

$$D_{(C=C_1)} = \frac{1}{2t}\frac{dx}{dC}\int_{C=C_1}^{C=C_0} x\,dC, \quad \text{where} \quad \int_{C=0}^{C=C_0} x\,dC = 0 \tag{148}$$

and D is easily evaluated, as a function of the concentration, by graphical integration. Boltzmann's original assumption used in treating this problem, that C is a function of $\lambda = x/\sqrt{t}$

only, can be tested by plotting x against $\sqrt{t}$ for a constant value of C. If for each value of C the origin is chosen so that $\int_{C=0}^{C=C_0} \lambda \, dC = 0$, a series of straight lines must be found all of which pass through the origin. Matano [20] showed that this was true of data obtained on the metal pair Ni-Cu.

One can also obtain a solution of the problem with the following boundary conditions:

   (i) $C = 0$ at $x = 0$ for all t,

   (ii) $C = C_0$ at $0 < x < \infty$ and at $t = 0$.

If one writes $C' = \partial C/\partial \lambda$ in equation (144), it may be rewritten in the form

$$-\frac{\lambda}{2D} d\lambda = \frac{d(DC')}{DC'}, \qquad (149)$$

so that

$$\ln(DC') = -\int_0^\lambda \frac{\lambda \, d\lambda}{2D} + \ln a \left. \right\} \qquad (150)$$

or

$$DC' = a \exp\left[-\int_0^\lambda \frac{\lambda \, d\lambda}{2D} \right].$$

Further integration gives

$$C = a \int_0^\lambda \frac{d\lambda}{D} \exp\left[-\int_0^\lambda \frac{\lambda \, d\lambda}{2D} \right] + b, \qquad (151)$$

for which the boundary conditions (i) and (ii) above give $b = 0$ (from (i)) and

$$a = \frac{C_0}{\displaystyle\int_0^\infty \frac{d\lambda}{D} \exp\left[-\int_0^\lambda \frac{\lambda \, d\lambda}{2D} \right]}. \qquad (152)$$

If there is an initial concentration at $x = 0$ of C_1, the integrated equation gives

$$\frac{C_0 - C}{C_0 - C_1} = \frac{\displaystyle\int_0^\lambda \frac{d\lambda}{D} \exp\left[-\int_0^\lambda \frac{\lambda \, d\lambda}{2D} \right]}{\displaystyle\int_0^\infty \frac{d\lambda}{D} \exp\left[-\int_0^\lambda \frac{\lambda \, d\lambda}{2D} \right]}. \qquad (153)$$

Equations such as (151) and (153) are not of the same practical importance as are (147) or (148).

BD

4

(7) *A note on the derivation of diffusion constants from solutions of the diffusion equation*

The solutions which we have given can be expressed, as preceding examples indicate, as a converging series of exponentials:

$$\frac{C - C_0}{C_\infty - C_0} = f_1(A)\, e^{-F_1(b)t} + f_2(A)\, e^{-F_2(b)t} + f_3(A)\, e^{-F_3(b)t} + \ldots.$$

If therefore $\log (C - C_0)/(C_\infty - C_0)$ is plotted against t a curve of the type illustrated in Fig. 7 is obtained. This curve approaches asymptotically to the line

$$\log \frac{C - C_0}{C_\infty - C_0} = \log f_1(A) - \frac{F_1(b)\, t}{2\cdot303},$$

and so the slope, and the intercept on the axis of $\log C$, gives $f_1(A)$ and $\dot{F}_1(b)$. The theory then gives D, and all the other terms. This procedure is available for all converging series of exponentials.

Special methods are available in other instances such as the graphical integration method applied to equation (148). Solutions involving semi-infinite or infinite solids all give

$$C = f\!\left(\frac{x}{\sqrt{(Dt)}}\right),$$

and so one can use the relationship between x and t for a fixed value of C, to measure D. Other methods, or examples of the application of these methods, will be indicated at various points throughout the text (e.g. pp. 97 and 352 *et seq*).

(8) *Some cases for which there is no solution of the diffusion equation*

Nearly all types of system in which the law $\dfrac{\partial C}{\partial t} = D \dfrac{\partial^2 C}{\partial x^2}$ applies have now given an appropriate solution of the diffusion equation. There are one or two outstanding and experimentally important cases:

(i) Sorption or desorption occurs from a diffusion medium into a gas phase where the gas exists as molecules, whilst it exists in the medium as atoms (e.g. H_2-Pd). The desorption-

sorption processes occur into a constant volume system, so that the surface concentration is a function of time. This problem has been solved for the case when the molecular state is the same in gas and diffusion medium (p. 21); but it would now be necessary to have a gas phase volume altering with time also, owing to the existence of an equilibrium

in the gas phase. $H_2 \rightleftharpoons 2H$

(ii) There is the analogous problem of flow through a membrane from one constant volume system into another which has been solved for the case when the molecular state is the same in both gas phases and in the medium. When, however, the gas exists in the medium in the atomic state, consideration of an equilibrium such as ·

$$H_2 \rightleftharpoons 2H$$
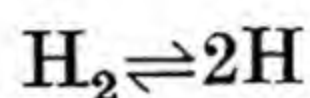
would require, if the same solution were to hold, that the volume of the two gas phases should become functions of time.

(iii) There exist also more complex instances of (i) and (ii) above, when surface reactions occur simultaneously with diffusion. These problems may be solved by the methods outlined on pp. 37 to 43 as soon as the problems (i) and (ii) can be solved.

REFERENCES

For tables of Bessel functions the following may be used:

Watson, G. *Theory of Bessel Functions*, Cambridge Univ. Press (1932).
Gray, A., Mathews, G. and MacRobert, T. *Treatise on Bessel Functions*, Macmillan and Co. (1922).

Values of error functions may be obtained in:

Janke, E. and Emde, F. *Funktionentafeln mit Formeln und Kurven*, Teubner, Berlin (1938).
Pierce, B. *A Short Table of Integrals*, Ginn and Co., Boston (1929).

Further examples of diffusion problems on solids may be worked out by considering analogous problems in heat flow, as given in standard texts on the theory of heat conductivity. Suitable texts are:

Carslaw, H. *Conduction of Heat in Solids*, Macmillan and Co. (1921).
Ingersoll, L. and Zobel, O. *Mathematical Theory of Heat Conduction*, Ginn and Co. (1913).

(1) Jost, W. *Die Chem. Reakt. in Festen Stoffen*, p. 203, Steinkopf (1937).

(2) The method for problems of this type involving spheres and rods is outlined in Carslaw, H., *Theory of Heat Conduction*, pp. 206 *et seq.*, Macmillan and Co. (1921).

(3) Jost, W. *Diffusion ü. Chem. Reakt. in Festen Stoffen*, p. 17 (1937).

(4) Stefan, J. *S.B. Akad. Wiss. Wien*, ii. **79**, 161 (1879).

(5) Kawalki, W. *Ann. Phys., Lpz.*, **52**, 166 (1894).

(6) Carslaw, H. *Theory of Heat Conduction*, p. 67 (1921).

(7) —— *Theory of Heat Conduction*, p. 68 (1921).

(8) March, H. and Weaver, W. *Phys. Rev.* **31**, 1081 (1928).

(9) Barnes, C. *Physics*, **5**, 4 (1934).

(9a) Carslaw, H. *Theory of Heat Conduction*, p. 211 (1921).

(10) —— *Theory of Heat Conduction*, p. 127 (1921).

(10a) Watson, G. *Theory of Bessel Functions*, Cambridge (1932).

(11) Gray, A., Mathews, G. and MacRobert, T. *Treatise on Bessel Functions*, Macmillan and Co. (1922).

(12) Ingersoll, L. and Zobel, O. *Mathematical Theory of Heat Conduction*, p. 136, Ginn and Co. (1913).

(13) Carslaw, H. *Theory of Heat Conduction*, p. 136 (1921).

(14) —— *Theory of Heat Conduction*, p. 74 (1921).

(14a) Barrer, R. *Phil. Mag.* **28**, 148 (1939).

(15) Langmuir, I. and Taylor, J. B. *Phys. Rev.* **40**, 463 (1932).

(16) Becker, J. A. *Trans. Faraday Soc.* **28**, 148 (1932).

(17) Bosworth, R. C. *Proc. Roy. Soc.* **150**A, 58 (1935).

(18) —— *Proc. Roy. Soc.* **154**A, 112 (1936).

(19) Williams, J. and Cady, L. *Chem. Rev.* **14**, 177 (1934).

(20) Matano, C. *Jap. J. Phys.* **8**, 109 (1930–3).

(21) Boltzmann, L. *Ann. Phys., Lpz.*, **53**, 959 (1894).

(22) Wiener, O. *Ann. Phys., Lpz.*, **49**, 105 (1893).

STATIONARY AND NON-STATIONARY STATES OF MOLECULAR FLOW IN CAPILLARY SYSTEMS

TYPES OF FLOW

A number of types of flow have been found to occur in capillary systems, each of which is observed in the appropriate region of pressure difference, absolute pressure, and pore size. Each kind of flow may be characterised by different permeability constants, a fact which has often led to confusion in expressing the data. The nature of gas flow in single capillaries teaches a great deal concerning the more complex permeation processes through porous plates, refractories, and consolidated and unconsolidated sands, so that before discussing flow in these systems the different types of capillary flow will be discussed.

The researches of Warburg[1], Knudsen[2], Gaede[3], Smoluchowski[4], Buckingham[5], and others[6,7] have demonstrated the properties of the following types of flow: (1) Molecular effusion; (2) Molecular streaming, or Knudsen flow; (3) Poiseuille or stream-line flow; (4) Turbulent flow; (5) Orifice flow. These may now be considered in turn.

(1) *Molecular effusion*

If one has an orifice of area A in a thin plane wall such that its diameter is small compared with the mean free path of the gas the number of molecules N effusing up to it in unit time is given by the well-known kinetic theory equations.

$$\left. \begin{aligned} N &= \tfrac{1}{4}AN_0C\overline{w} \\ &= \tfrac{1}{4}AN_0C\left(2\sqrt{\frac{2kT}{\pi m}}\right) \\ &= \frac{AN_0p}{\sqrt{(2\pi MRT)}}. \end{aligned} \right\} \tag{1}$$

In these expressions, N_0 is the Avogadro number, C the concentration, $\overline{w}$ the mean square velocity, k the Boltzmann

constant, m and M the mass of a molecule and of a gram-molecule respectively. This equation may also be written

$$p_1 v_1 = A p_1 \sqrt{\frac{RT}{2\pi M}}, \qquad (1a)$$

since $p_1 v_1 = (N/N_0) RT$, where v_1 is the volume of gas in gram-molecular volumes effusing per second at a pressure p_1.

One sees that the equations for molecular effusion may be used to measure molecular weights, temperatures, or vapour pressures. The emission through such an orifice obeys the cosine law, so that by using two orifices in series, a molecular beam may be defined, whose intensity is given by the effusion equation coupled with Lambert's cosine law.

(2) Molecular streaming, or Knudsen flow

When the orifice is of considerable length molecules will collide with its walls on their way through. If the collisions are elastic the flow through a smooth tube will be identical with the effusion velocity through the hole in the thin plane wall, since no molecules will be turned back in the original direction by collision with the wall. For such a tube therefore the equations of flow are, as before,

$$N = \tfrac{1}{4} A N_0 C \overline{w}$$

$$= \tfrac{1}{4} A N_0 C \left(2 \sqrt{\frac{2kT}{\pi m}} \right) = \frac{A N_0 p}{\sqrt{(2\pi M R T)}}. \qquad (1)$$

Such a flow is independent of the length of the tube, which Knudsen[2] showed was contrary to experiment. Knudsen therefore supposed that of each N molecules striking the wall a fraction f was emitted with random velocity distribution, and a fraction $(1-f)$ was specularly reflected. Some molecules are then returned in the direction from which they came, and more return the greater the length of the tube. The number of molecules striking unit area in unit time at the inlet and outlet sides of the tube are respectively $\tfrac{1}{4} N_0 C_1 \overline{w}$ and $\tfrac{1}{4} N_0 C_2 \overline{w}$. The excess flow of molecules from the inlet to the outlet along the axis x can be shown to be $\tfrac{1}{2} B(dN/dx)$[8], in the stationary state of flow, when B is a constant depending upon the shape

of the tube. N is a linear function of x, in the stationary state, and the nett rate of flow in mol./sec. is given by

$$\frac{dn}{dt} = \tfrac{1}{2}B\frac{1}{\sqrt{(2\pi MR)}}\left(\frac{p_1}{\sqrt{T_1}} - \frac{p_2}{\sqrt{T_2}}\right)\frac{1}{L}\left(\frac{2-f}{f}\right), \qquad (2)$$

where L is the length of the tube. The derivation of the factor $(2-f)/f$ will be found in numerous places [6, 2, 3, 4], and will not be considered here. For tubes of circular cross-section the constant B takes the value $\frac{16}{3}r^3\pi$, where r denotes the radius of the capillary.

(3) Poiseuille or stream-line flow

When an incompressible fluid flows down a tube without turbulence, the volume of fluid passing through a cylindrical tube in unit time [10] is

$$\frac{d^4\pi(p_1-p_2)}{128\eta L} \quad \text{(Poiseuille's law)} \qquad (3)$$

(where $d =$ the pore diameter,

$\eta =$ the viscosity of the fluid,

and $L =$ the tube length).

On the basis of the kinetic theory [10] the flow in mol./sec. is

$$\frac{dn}{dt} = \frac{d^2\pi}{12}\frac{3d^2}{32\varLambda}\bar{w}\frac{\partial C}{\partial x}, \qquad (4)$$

where $\partial C/\partial x$ denotes the concentration gradient in the direction of flow x, and the other terms have already been defined (except $\varLambda$, the mean free path). These equations are valid for an incompressible fluid throughout the pore length; but for a compressible fluid obeying the gas law the equation must be written

$$\frac{dn}{dt} = \frac{d^4\pi}{128L}\int\frac{1}{\eta RT}p\,dp, \qquad (5)$$

which for an isothermal process, with $\eta =$ a constant, becomes

$$\frac{dn}{dt} = \frac{d^4\pi}{128L\eta}\frac{1}{RT}\frac{p_1^2-p_2^2}{2}. \qquad (6)$$

Equation (6) may take the form

$$\frac{dn}{dt} = \frac{d^4\pi}{128L\eta}\frac{1}{RT}\bar{p}(p_1 - p_2), \tag{7}$$

where $\bar{p} = \frac{1}{2}(p_1 + p_2)$ is the mean pressure in the tube. Also

$$\frac{dn}{dt} = \frac{d^4\pi}{128L\eta}\frac{\bar{\rho}}{M}(p_1 - p_2), \tag{8}$$

since $\dfrac{p_1 + p_2}{2}\dfrac{M}{RT} = \bar{\rho}$, the mean density of the gas.

A complete equation of flow.

Two corrections may be applied to Poiseuille's formula:

(i) Only part of the pressure difference is used in over- coming friction; a fraction which must be subtracted from the original pressure difference produces kinetic energy of motion (10, 11, 12).

(ii) In the boundary layer of gas, of thickness Λ, equal to the mean free path, there may be specular reflection at the surface, those molecules specularly reflected having the streaming velocity component of the flowing gas. A fraction f only is emitted in random directions. The coefficient of slippage is then $\dfrac{2-f}{f}\Lambda$ (l.c.).

The equation of flow then becomes

$$\frac{dn}{dt} = \frac{1}{8\eta L}\left(1 + \frac{8(2-f)}{f}\frac{\Lambda}{d}\right)\left[\frac{\pi d^4}{16RT}\frac{p_1^2 - p_2^2}{2} - \frac{M}{\pi}\left(\frac{dn}{dt}\right)^2\right], \tag{9}$$

in which expression the last term gives the correction due to (i). It transpires, however, that this is only a small term; and also when the pores are small, or the pressures are low, that $\dfrac{2-f}{f}\dfrac{\Lambda}{d} \gg 1$. Thus the equation becomes

$$\frac{dn}{dt} = \frac{1}{L}\frac{3\pi^2 d^3}{32}\frac{1}{\sqrt{(2\pi MRT)}}(p_1 - p_2)\left(\frac{2-f}{f}\right), \tag{10}$$

which is the equation given for Knudsen's molecular streaming save that the numerical constants are somewhat different.

(4) *Turbulent flow*

The type of flow known as viscous, stream-line or Poiseuille flow changes when a certain limiting mass velocity W is reached. We will define a quantity $[R]$ (13), called the "Reynold's number", by

$$[R] = \frac{r_h W \rho}{\eta}, \tag{11}$$

where r_h denotes the ratio $\dfrac{\text{cross-section}}{\text{periphery}}$ and is the so-called hydraulic radius, which for circular tubes is one-quarter of the diameter d. ρ and η have their usual significance as fluid density and viscosity respectively. Then for such circular tubes it is found that Poiseuille's equation no longer applies when $[R]$ is greater than 580. In tubes of such a length that any nozzle effect may be neglected, the differential equation of flow is (14, 15, 16)

$$-\frac{d\rho}{dx} = \frac{\beta \rho W^2}{2r_h}, \tag{12}$$

wherein β is a constant. For smooth tubes of glass or steel (17)

$$\beta = 0.056 \frac{1}{\sqrt[4]{[R]}}, \tag{13}$$

but is higher, and follows a different law for rough tubes. For some tubes β may be taken as independent of $[R]$.

There is a formal connection between stream-line and viscous-flow formulae which may be brought out as follows. An alternative form of the above equation of flow is

$$(v\rho)^2 = -\frac{\pi^2(2r_h)\,d^4}{16\beta} \rho \frac{d\rho}{dx} \tag{14}$$

$$= -\left[\frac{\pi^2 r_h d^4}{16\beta} \frac{1}{RT}\right] \frac{d(p^2)}{dx}, \tag{15}$$

since the mass velocity W and the volume v of gas transfusing in unit time are related by the expression $v = (\frac{1}{4}\pi d^2)\,W$. When $d(p^2)/dx$ is constant down the length L of the tube, and since

for a gas at constant temperature pv or ρv is also constant, one may write

$$(v\rho)^2 = \left[\frac{\pi^2 r_h d^4}{16\beta L}\frac{1}{RT}\right](p_1^2 - p_2^2) \tag{16}$$

or

$$(vp)^2 = \left[\frac{\pi^2 r_h d^4}{16\beta L}RT\right](p_1^2 - p_2^2), \tag{16a}$$

whilst the equation for Poiseuille flow gives

$$(vp) = \left[\frac{\pi d^4}{128\eta L}\right](p_1^2 - p_2^2). \tag{17}$$

In the general case of isothermal high-pressure flow, whatever the Reynold's number, we may thus say

$$(vp)^n \propto (p_1^2 - p_2^2), \tag{18}$$

and the value of n then determines whether stream-line or turbulent flow is occurring. Never under any conditions have values of n been found such that $2 < n < 1$. Later in this chapter will be given examples of gas flow in porous solids which are partially turbulent (p. 73). The great importance of gas flow or vapour flow in turbine design or in aeronautics can easily be understood, and further information on turbulent flow will be found in references given earlier[14, 15, 16, 17]. Equations for an adiabatic turbulent flow have been given by Stodola[15].

(5) Orifice flow

In designing permeameters for studying gas flow through textiles, Buckingham[5] discussed another type of flow of a fluid through frictionless jets, the flow being supposed to occur adiabatically.

Let v, K, E denote the volume, kinetic energy and internal energy of unit mass of fluid. For adiabatic flow

$$K_1 - K = E - E_1 + pv - p_1 v_1. \tag{19}$$

Let A_1 be a cross-section of the jet at its nozzle, and A be a cross-section farther upstream where the velocity is negligible. Then K at A is negligible and

$$K_1 = E - E_1 + pv - p_1 v_1. \tag{20}$$

If the gas is ideal,

$$\left.\begin{array}{l} pv = RT, \\ C_v = \text{constant}, \\ E = TC_v + \text{constant}, \\ C_p = C_v + R \end{array}\right\} \qquad (21)$$

(C_p and C_v are, respectively, the specific heats at constant pressure and volume), which combined with the original equation give
$$K_1 = C_p(T - T_1).$$

If S denotes the mean speed of unit mass over the cross-section A_1,
$$K_1 = \tfrac{1}{2}S_1^2,$$

i.e.
$$S_1 = \sqrt{\{2C_p(T - T_1)\}}. \qquad (22)$$

As we have assumed the flow to be frictionless, these considerations are limited to short well-formed nozzles. Then one may apply the adiabatic gas laws

$$\left.\begin{array}{l} pv^\gamma = \text{constant}, \\ T = p^{(\gamma-1)/\gamma} \times \text{constant}, \end{array}\right\} \qquad (23)$$

whence
$$\frac{T_1}{T} = \left(\frac{p_1}{p}\right)^{(\gamma-1)/\gamma} = r^{(\gamma-1)/\gamma}$$

or
$$S_1 = \sqrt{\{2TC_p(1 - r^{(\gamma-1)/\gamma})\}}. \qquad (24)$$

The volume passing the cross-section A_1 in unit time is $V_1 = A_1 S_1$, which under the initial conditions of pressure is $V = V_1(v/v_1)$, and thus

$$V = A_1 \frac{v}{v_1}\sqrt{\{2TC_p(1 - r^{(\gamma-1)/\gamma})\}}. \qquad (25)$$

When A_1 is a circular cross-section of diameter d, and since $v/v_1 = r^{1/\gamma}$, one gets

$$V = \frac{\pi}{2\sqrt{2}}d^2\sqrt{\{TC_p r^{2/\gamma}(1 - r^{(\gamma-1)/\gamma})\}}. \qquad (26)$$

The conditions under which this type of flow is most accurately obeyed are known to require short smooth nozzles, or sharp perforations in a plate. The extent to which the law breaks down as the nozzles increase in length has not been studied

experimentally, nor have its possible uses in determining γ, the ratio of specific heats, or C_p, the specific heat at constant pressure. Reference to orifice flow will be made again in considering the permeability of various paper and fibre-board membranes, when it will be seen that it does not in general occur with such membranes (Chap. IX).

PERMEABILITY CONSTANTS, UNITS, AND DIMENSIONS

By considering the flux of gas through porous membranes, as the volume V measured at a pressure p, passing through the membrane in time t, in relation to the equation governing the flow [19, 20], one can define permeability constants of various types, and having various dimensions. The equation of flow for an incompressible fluid in a pore system may be written:

$$\frac{V}{t} = AP_L(p_1 - p_2), \tag{27}$$

where A is the cross-section of a pore. For a compressible fluid it is

$$\frac{Vp}{t} = AP_G \frac{p_1 + p_2}{2}(p_1 - p_2). \tag{28}$$

In these expressions we can call P_L and P_G "permeabilities". As such they will be functions of the membrane thickness, pore type and size, and of the nature of the gas. By multiplying each of these permeabilities by l, the membrane thickness, one gets "permeability coefficients" $P_L l$ and $P_G l$ which are dependent only upon pore type and size, and the nature of the gas. Finally, multiplying each permeability coefficient by the viscosity η, one obtains the "specific permeability" $P_L l \eta$ or $P_G l \eta$, which should depend only on the pore type and size.

In considering the equation of flow of rarefied gases another set of permeability constants is obtained. The Knudsen equation, for a capillary system, may be written

$$\frac{Vp}{t} = AP_M(p_1 - p_2), \tag{29}$$

so that $P_M = P_G \frac{1}{2}(p_1 + p_2)$, and has been called by Manegold [18, 19] the "molecular permeability". By analogy with the previous cases $(P_G l, P_L l)$, one has also a "molecular permeability coefficient" $P_M l$; and finally a "specific molecular permeability" $P_M l \sqrt{(M/RT)}$, which is dependent only upon pore size and type. The equation of molecular effusion through an orifice gives a "molecular effusion coefficient" P_M, and the equation of orifice flow an "adiabatic effusion coefficient" P_A. These relationships may be summarised as in Table 1.

The various constants defined above have, it will be seen, different dimensions. It is important therefore to specify accurately what constants are being employed. When, as is usually done, the permeability constant is formally defined as the number of unit volumes passing in unit time through unit cube having unit pressure difference between its faces, its dimensions are cm.^{3} sec.^{1} g.$^{-1}$, which are those of the "permeability coefficient" of Table 1, for Poiseuille flow. The dimensions of the diffusion constant D defined by Fick's law $\frac{\partial C}{\partial t} = D \frac{\partial^2 C}{\partial x^2}$ are cm.^{2} sec.$^{-1}$, which are those of the molecular permeability coefficient of Table 1.

The numerical measure of the permeability constant is dependent upon the units in which it is expressed. The literature shows a lack of uniformity with respect to units. It is specially important to state the thickness of the membrane used. In some systems it may also be an advantage to give other membrane properties such as porosity, defined by the ratio

$$\frac{\text{Pore volume}}{\text{Total volume}}.$$

SOME EXPERIMENTAL INVESTIGATIONS OF GAS FLOW IN CAPILLARIES

Warburg [1] first established the validity of Poiseuille's law in the region of high pressures. These measurements were made before the development of high vacuum technique, but at the lower pressures it was even then necessary to assume

TABLE 1

Equation of flow	Permeability constants	Properties	Dimensions in C.G.S. units
Poiseuille equation for (i) Liquid $V/t = AP_L(p_1 - p_2)$ (ii) Gas $Vp/t = AP_G(p_1 - p_2)\frac{1}{2}(p_1 + p_2)$	P_L (permeability) P_G (permeability) $P_L l$ (permeability coefficient) $P_G l$ (permeability coefficient) $P_L l\eta$ (specific permeability) $P_G l\eta$ (specific permeability)	Dependent upon type of pore system, on thickness, and on nature of gas Dependent upon pore system, and on nature of gas Dependent upon pore size and type only	cm.² sec.¹ g.⁻¹ cm.³ sec.¹ g.⁻¹ cm.²
Knudsen equation $Vp/t = AP_M(p_1 - p_2)$	P_M (molecular permeability) $P_M l$ (molecular permeability coefficient) $P_M l\sqrt{(M/RT)}$ (specific molecular permeability)	Dependent upon pore type and size, on thickness of membrane and on nature of gas Dependent upon pore size and type, and on nature of gas Dependent upon pore size and type	cm.¹ sec.⁻¹ cm.² sec.⁻¹ cm.¹
Effusion through an orifice (low pressure) $Vp/t = AP_M(p_1 - p_2)$	P_M (molecular effusion coefficient)	Independent of orifice dimensions and shape. Dependent upon the mol. wt. of the gas and T	cm.¹ sec.⁻¹
Orifice flow, adiabatic, high pressure $V^*/t = AP_A \sqrt{\{(p_1/p_2)^{1.0} - (p_1/p_2)^{1.7}\}}$ for air, oxygen, nitrogen, or hydrogen	P_A (adiabatic effusion coefficient)	Independent of orifice dimensions. Dependent upon T and Cp	cm.¹ sec.⁻¹

* V is measured at the pressure on the high pressure side of the orifice.

a slip between the wall of the capillary and the adjacent gas layer due to specular reflection (compare with equation (9)). Warburg expressed his results by the formula

$$G = \left[ap + ap \frac{4\zeta}{r} \right] [p_1 - p_2], \qquad (30)$$

where his G expressed the quantity of gas flowing per unit of time (measured as the product of pressure in bars and volume), a is a constant $= \dfrac{\pi}{8} \dfrac{1}{\eta} \dfrac{r^4}{L}$ (r being the capillary radius), p is the mean pressure $= \frac{1}{2}(p_1 + p_2)$, and ζ is the "coefficient of slip".*
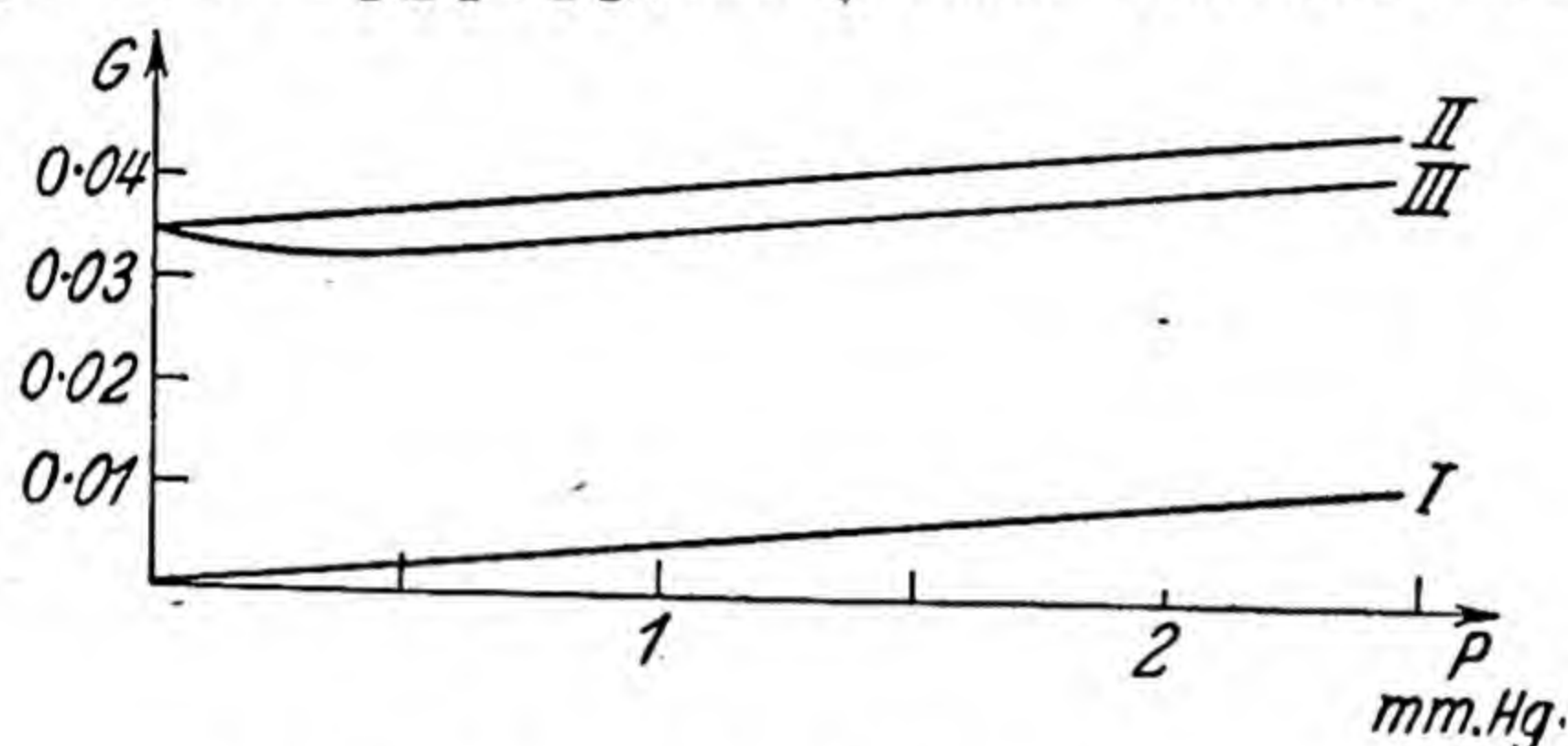

Fig. 11. The gas flow as a function of pressure.

Knudsen (2) expressed his results by the empirical formula

$$G = \left[ap + b\frac{1 + C_1 p}{1 + C_2 p} \right] (p_1 - p_2), \qquad (31)$$

where b was called the "coefficient of molecular streaming" and C_1 and C_2 were two quantities depending upon slip. At high pressure the first term in the square bracket alone is significant, but at the lowest pressure the second term in the bracket was predominant, and so reduced to b. On the basis of the kinetic theory, values may be assigned to b, C_1 and C_2, and to ζ. Fig. 11 (6) gives the quantity of gas flowing as a function of pressure, curve I referring to the simple Poiseuille law $G = ap(p_1 - p_2)$, curve II to the calculated rate of flow according to equation (31), and curve III a typical run by Knudsen. The experimental curve shows a minimum

* $\zeta = \dfrac{2 - f}{f} \Lambda$, as defined on p. 55.

when G is some 5 % less than G at $p = 0$. This minimum, which is characteristic of most of the results obtained(2, 6, 20), being true even for mixtures(21) of gases, does not appear to have been explained. The minimum occurred in this case(6) when the mean free path was about five times as large as the capillary radius. Similarly, Fig. 12(6) gives another series of curves, calculated and experimental, by several authors. Curve I is for simple Poiseuille flow for hydrogen, curve II for Poiseuille flow with slip, curve III for hydrogen employing
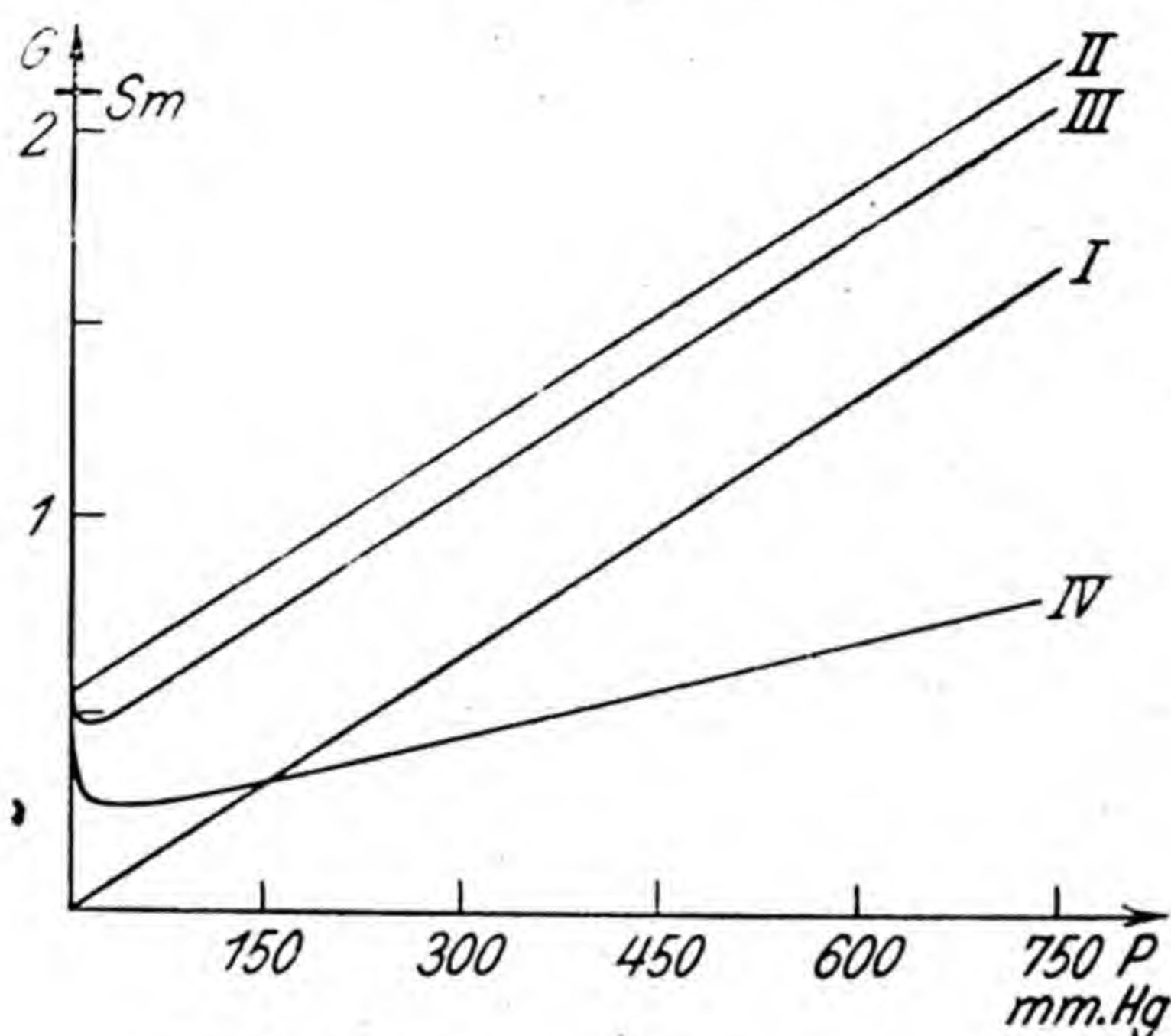
Fig. 12. Gas flow as a function of pressure.

Knudsen's empirical equation for Gaede's(3) apparatus and results (the calculations being made by Klose(6)), while curve IV gives the experimental measurements of Gaede. The point marked "Sm" on the axis of G was calculated by Klose from Smoluchowski's formula for a tube of rectangular cross-section. Fig. 12 shows the degree of divergence in theory and experiment of the various authorities. Clausing's(7) experiments, which are not cited in Figs. 11 or 12, are probably more accurate than any series. In the region of molecular streaming or Knudsen flow he found Knudsen's formula satisfactory, as did Klose, who, however, still noted small deviations which he ascribed to an experimental error.

One may summarise the situation as follows:

(i) For high pressures theory and experiment both lead to the Poiseuille law wherein slip may be neglected.

(ii) For the lowest pressures theory and experiment are agreed on the type of molecular streaming proposed by Knudsen.

(iii) In the region of intermediate pressures theory and experiment do not yet satisfactorily agree, nor is it certain to what extent the deviations are due to experimental errors and to what extent to inadequacies in the theory.

Adzumi[20] has recently tested the Knudsen equation for the mixtures H_2-C_2H_2, H_2-C_3H_6, finding a flow $G = b(p_1 - p_2)$ which was that given by the ideal mixture law $b = n_1 b_1 + n_2 b_2$, the n's being mol. fractions. In the mixtures at the lowest pressures the constituents diffused by molecular streaming independently, but when Poiseuille flow became predominant at high pressure the separation of constituents by flow became negligible.

FLOW OF GASES THROUGH POROUS PLATES

Since a porous plate consists of a medley of pores of different sizes, flow through such a plate need not be of one type. Instead, one would anticipate that flow would be a mixture of the various kinds, reducing to Knudsen flow at the lowest pressures. Effusion through an orifice or molecular streaming down capillaries should occur for all gases at rates inversely proportional to the square root of the molecular weight, the condition for effusion or molecular streaming being a suitably low pressure. It is interesting to see under what conditions the law is fulfilled. Ramsay and Collie[22], by diffusing helium through unglazed clay and comparing the data with the corresponding diffusion of hydrogen, found the atomic weight of helium to be rather low (3·74 compared with 4·00); oxygen, argon and acetylene however obeyed the Knudsen flow formula. Donnan[23] measured the effusion of argon, carbon dioxide, carbon monoxide and oxygen through an orifice, finding small

deviations from the $1/\sqrt{M}$ law, which they attributed in part to orifice flow as described by Buckingham[5] and others. These measurements were made however at pressures approximating to atmospheric.

Recently, Sameshima[24] has measured the rates of flow of various simple gases through a compact unglazed earthenware plate. The rates of flow definitely did not obey the Knudsen formula $t = k\sqrt{M}$, where t denotes the time required for the effusion at constant pressure of a volume V of a gas of molecular weight M, and where k is a constant. On the other hand, the law $t = k\sqrt{M}$ was accurately obeyed when the gases effused through a platinum plate with a single orifice. For the earthenware plate Sameshima found a formula $t = k\eta^n M^{\frac{1}{2}(1-n)}$ to apply. If the wall was very thin n approached zero, and the simple behaviour of the perforated platinum plate was found. If the wall was thick n approached unity and the equation became $t = k\eta$ (η denotes viscosity).

Adzumi[25] has elaborated a semi-empirical theory for flow processes through porous plates, based on the assumption that the plate is perforated by numerous fine holes, the diameters of which can vary down their lengths, so that effectively each capillary is a number of capillaries of very numerous diameters arranged in series; and each such composite capillary is in parallel with all the other capillaries. At high pressures the Poiseuille law $G_v = ap(p_1 - p_2)$ applies (p. 55), and at low pressures the law $G_m = b(p_1 - p_2)$ (p. 54). For medium pressures, or for a porous plate, the two laws may be considered to overlap:

$$G = G_v + \gamma G_m = K(p_1 - p_2), \qquad (32)$$

where γ is a term due to the coefficient of slip, and where $K = A\dfrac{r^4}{l}p + \gamma B\dfrac{r^3}{l}$. If one has n capillaries in parallel,

$$G = K'(p_1 - p_2),$$

$$K' = K_1 + K_2 + \ldots$$

$$= Ap\sum^n \frac{r^4}{l} + \gamma B \sum^n \frac{r^3}{l}. \qquad (33)$$

When one has two capillaries of radii r_1 and r_2 in series,.

$$G_1 = G_{1v} + \gamma G_{1m},$$
$$G_2 = G_{2v} + \gamma G_{2m},$$
$$G = K''(p_1 - p_2) = G_1 = G_2,$$

i.e.
$$\frac{1}{K''} = \frac{1}{K_1 + \dfrac{Ar_1^4}{l_1}\dfrac{p_0 - p_2}{2}} + \frac{1}{K_2 - \dfrac{Ar_2^4}{l_2}\dfrac{p_1 - p_0}{2}}, \tag{34}$$

where p_1 and p_2 are the pressures at the inlet and outlet sides of the capillary, and p_0 the pressure at the junction of its two halves of radii r_1 and r_2.

The last equation takes the form

$$\frac{1}{K''} = \frac{1}{K_1} + \frac{1}{K_2} + \Delta_1, \tag{35}$$

where Δ_1 proves on inserting numerical values for a typical plate to be less than 1 % of $\dfrac{1}{K''}$. This gives

$$K'' \sim \frac{1}{1/K_1 + 1/K_2}, \tag{36}$$

which may in turn be written as

$$K'' \sim Ap\frac{1}{l_1/r_1^4 + l_2/r_2^4} + \gamma B\frac{1}{l_1/r_1^2 + l_2/r_2^3} + \Delta_2, \tag{37}$$

where Δ_2 again proves to be less than 1 % of K''. One obtains therefore as the final constant K'' for m capillaries in series

$$K'' \sim Ap\frac{1}{\overset{m}{\underset{}{\Sigma}}\dfrac{l}{r^4}} + \gamma B\frac{1}{\overset{m}{\underset{}{\Sigma}}\dfrac{l}{r^3}}, \tag{38}$$

while for the series-parallel arrangement of capillaries, presumed to comprise the whole pore system of the plate,

$$K = Ap\overset{n}{\Sigma}\left(\frac{1}{\overset{m}{\underset{}{\Sigma}}\dfrac{l}{r^4}}\right) + \gamma B\overset{n}{\Sigma}\left(\frac{1}{\overset{m}{\underset{}{\Sigma}}\dfrac{l}{r^3}}\right)$$

$$= ApE + \gamma BF. \tag{39}$$

Fig. 13 gives the quantities of gas flowing through a porous plate (expressed as c.c. × atm.) as a function of pressure for

a number of gases. It will be seen that, as the theory requires, the rate of flow is proportional to the pressure, for a constant pressure difference, but with an intercept ($= \gamma BF$) on the K-axis.
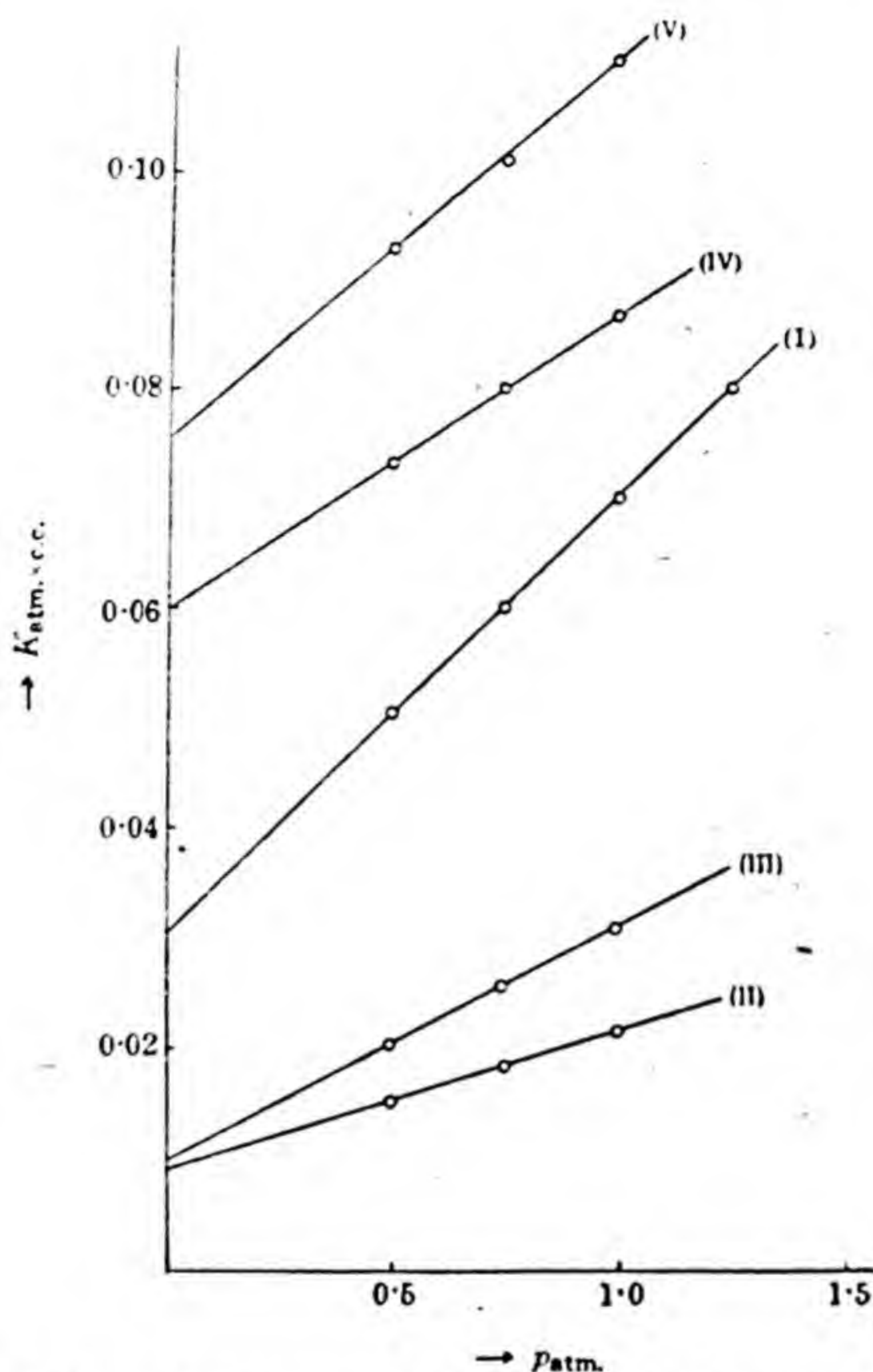

Fig. 13. Gas flow through a porous plate, where K is defined by equation (39).

The treatment of Adzumi allows one to estimate a mean pore size, and the number of pores per unit volume. Should all the n pores be of radius $\bar{r}$,

$$E = n\frac{\bar{r}^4}{l}; \quad F = n\frac{\bar{r}^3}{l} \quad (l = \text{thickness}).$$

If $N =$ the number of pores/unit volume,

$$E_0 = N\bar{r}^4; \quad F_0 = N\bar{r}^3,$$

and one may readily compute E_0 and F_0 from E and F and so find N and $\bar{r}$. This is done for a few permeable plates in Table 2.

For further examples of flow through porous plates one may study the permeability of various refractories, the properties of which, in relation to the diffusion problem, are given in the next section.

TABLE 2. *The mean radii of pores, and the number of pores per unit volume*

Porous plate	Thick-ness cm.	Area cm.^{2}	$E_0 \times 10^{11}$	$F_0 \times 10^7$	$r \times 10^5$ cm.	N
Unglazed earthen-ware	0·15	0·28	0·97	1·83	5·3	$1·2 \times 10^6$
Compact porous pot	0·27	2·22	0·054	0·195	2·77	$2·4 \times 10^5$
Rough porous pot	0·41	2·22	0·154	0·318	4·84	$2·8 \times 10^5$
Mantle of Daniell cell, I	0·2	0·27	0·80	4·98	1·61	$9·6 \times 10^7$
Mantle of Daniell cell, II	0·2	0·27	1·09	6·26	1·74	$1·19 \times 10^8$

PERMEABILITY OF REFRACTORIES

Diffusion through refractories is of technical importance. According to the fineness of the pore structure and the pressure the flow should conform predominantly to the equations for Poiseuille flow or Knudsen flow. In general the numerical value of the permeability depends on a variety of factors[26] which include:

(1) The material of which the refractory is made (silica, fireclay, alumina, chrome, or magnesite).

(2) The physical constitution of the refractory, the grain size of the grog, the percentage of grog to bond, and the method of manufacture.

(3) The nature of the diffusing gas.

(4) The testing temperature, and the thermal expansibility of the solid.

(5) The pressure difference maintained between the ingoing and outgoing surfaces.

(6) The thickness of the specimen being tested.

As a rule the physical constitution produces greater changes in the permeability than the chemical nature of the refractory. Thus one finds a very great range in permeability in different samples of the same chemical nature, as is illustrated in the following data (Table 3) due to Kanz(27). In agreement with

TABLE 3. *The range of permeability in some refractories*

Type of substance	Permeability range (c.c./sec./cm.²/cm./sec./cm. of water difference in pressure)
Fireclay product	0·00278–0·476
Silica product	0·0158 –0·132
Magnesite product	0·0275 –0·265
Chromite product	0·147 –1·42
Insulating product	0·00597–0·539
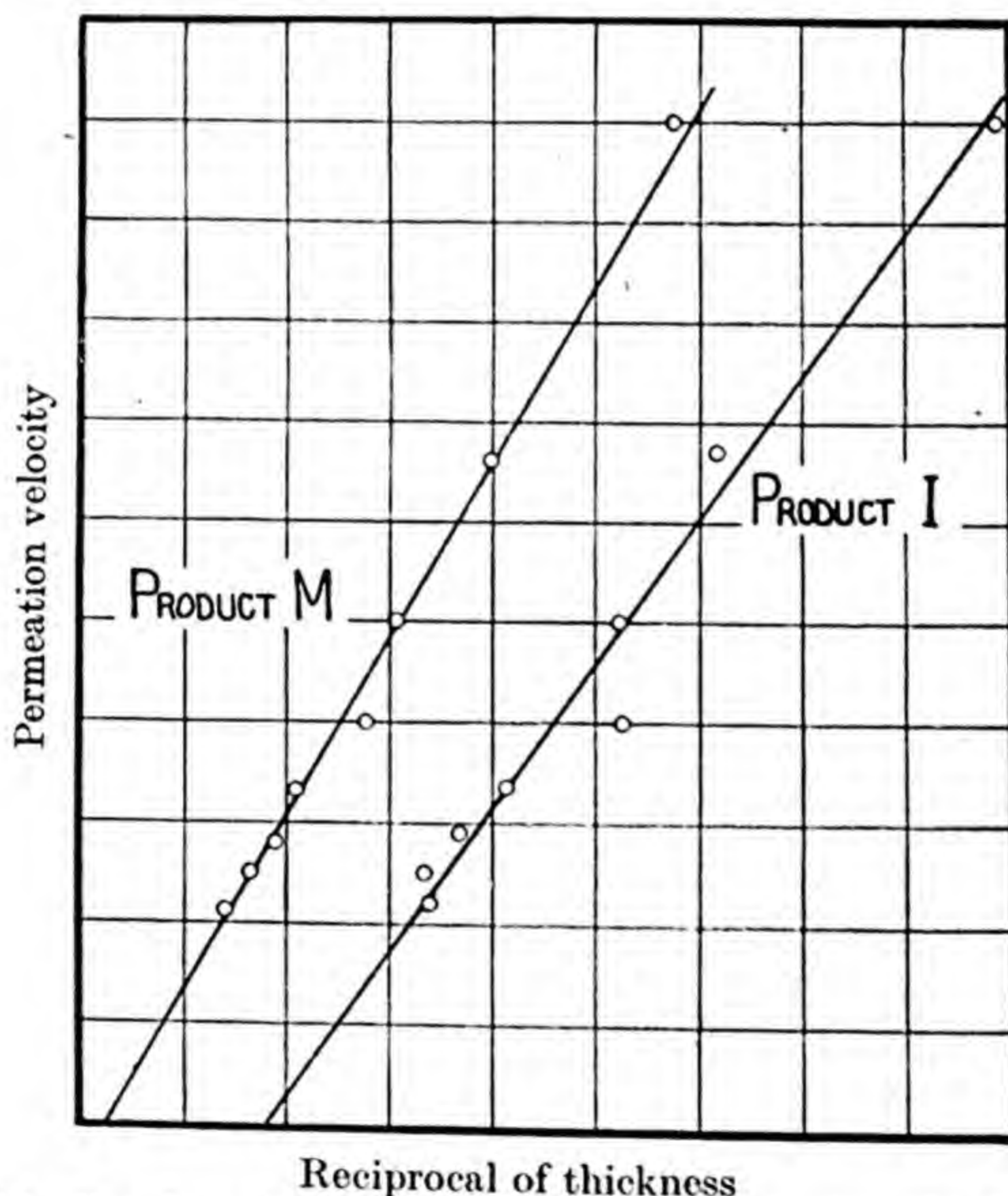
Fig. 14. Gas flow through refractories as a function of thickness.

both Poiseuille's and Knudsen's equations the velocity of transfusion is inversely proportional to L, the thickness of the specimen. Fig. 14, originally due to Clews and Green(28), shows

this relationship for two refractories. The product I shows a gradual change in texture with thickness, so that the curve does not pass through the origin. Usually it appears that the velocity of flow is proportional to the pressure difference causing it, provided in the case of Poiseuille flow one measures the permeation velocity in c.c./unit time at the mean pressure $\frac{1}{2}(p_2 + p_1)$ obtaining inside the material. This proportionality, required by the equation already obtained,

$$\frac{dn}{dt} = \frac{d^4 \pi}{128 L} \frac{1}{\eta} \frac{\bar{\rho}}{M} (p_1 - p_2), \tag{8}$$

was observed by Bansen[29] for a mortar joint, by Kanz [27] for a specimen refractory, and by Clews and Green[28].

Temperature and permeability in refractories

One may look for interesting results by considering the influence of temperature upon the rate of permeation of refractories. The effects of temperature help to sort out the different types of flow, Poiseuille, Knudsen, and activated diffusion. In a refractory should occur large pores and tubes, small pores, and pores of molecular or sub-molecular dimensions. In the large pores one would anticipate Poiseuille flow; the permeability P_G is proportional to $1/\eta$ ($\eta = $ viscosity); and the viscosity increases as temperature increases. Thus Poiseuille flow in capillary systems is marked by a diminution in flow rate with rising temperature. When Knudsen flow is occurring the permeability P_M increases according to a $\sqrt{T}$ relationship. Finally, in a very compact solid where activated diffusion predominates the permeability constant P contains a term $e^{-E/RT}$.

For systems in which Poiseuille flow is important Preston [26] has pointed out that for a given refractory, at all temperatures, the quantity $P_G l \eta$ is constant. Then if $P_G l \eta$ be the specific permeability (p. 62) at a temperature T° C., and $P_G^\circ l$ be the permeability coefficient at a standard temperature, the ratio $P_G \eta / P_G^\circ$ should also be a constant. The data of Clews and Green[28] are summarised by Preston[26] in Table 4, where it

is seen that the product $\eta(P_G/P_G^\circ)$ shows small trends with temperature, but tends to be constant.

The role played by alternative processes of Poiseuille, Knudsen, or activated flow is perhaps to be seen in the data

TABLE 4. *The influence of temperature upon permeability constants*

Temp. °C.	Viscosity of N_2 (poises × 10⁴)	Fireclay product		Silica product	
		P_G/P_G°	$\eta(P_G/P_G^\circ)$	P_G/P_G°	$\eta(P_G/P_G^\circ)$
10	1·71	0·997	1·71	0·992	1·70
100	2·13	0·841	1·79	0·860	1·81
150	2·33	0·785	1·83	0·828	1·93
200	2·52	0·740	1·86	0·759	1·91
250	2·70	0·710	1·92	0·670	1·81
300	2·87	0·687	1·97	0·599	1·72
350	3·03	0·662	2·01	0·546	1·65
400	3·19	0·639	2·04	0·517	1·65
450	3·34	0·613	2·05	0·493	1·65
500	3·48	0·592	2·06	0·473	1·65

TABLE 5. *A comparison of theoretical and experimental permeation rate ratios*

Temp. °C.	$\dfrac{\text{Permeability } CO_2}{\text{Permeability air}}$	$\dfrac{\text{Permeability } H_2}{\text{Permeability air}}$	$\dfrac{\text{Permeability } SO_2}{\text{Permeability air}}$
		Theoretical ratio	
	0·81	3·79	0·67
17	0·80	3·79	0·65
100	0·80	3·82	0·98
145	—	—	1·10
190	—	—	0·95
200	0·79	3·55	0·96
300	0·79	3·07	1·11
400	0·80	2·92	1·13
500	0·83	2·98	—
600	0·84	—	—
700	0·84	—	—

collected by Bremond(30) on the diffusion of gases through unglazed porcelains between 17 and 700° C. This author discovered that for air, carbon dioxide, hydrogen, and sulphur dioxide the permeabilities at first decreased and then increased

with temperature. The temperatures of minimum permeation velocity were:

Gas	Air	CO_2	H_2	SO_2
Temp. °C.	250	240	340	250

The theory of Knudsen flow requires that the ratios of the rates of flow should be in the inverse ratios of the square roots of the molecular weights. Here again the ratios diverge from the requirements of the theory at high temperatures (Table 5). These ratios, as well as the increase in diffusion velocity, may imply a certain amount of activated diffusion at the highest temperatures.

FLOW IN CONSOLIDATED AND UNCONSOLIDATED SANDS

A number of experiments have been carried out upon fluid flow through sands, sandstones, or columns of beads. The experimenters[31] have sought to correlate the phenomena of gas or liquid flow with permeation rates of petroleum and its vapours through oil-bearing sands, and with the possibility of displacing oils from these sands by another fluid. Thus their measurements, whose technical application may become considerable, were carried out at high pressures, and as one would expect cover the regions of Poiseuille flow and of turbulent flow. The quantitative application of Poiseuille's law to each of the pores in sand or a sandstone must have corrections for features such as the following[32,33,34]:

(1) Deviations of the cross-section of an average pore from circular shape.

(2) The increased length of a sinuous path through the medium, as compared with its apparent length, and so the greater pressure gradient across the specimen needed to maintain a flow rate equal to that for a straight path.

(3) The energy consumption due to alternate expansions and contractions of cross-section.

There is little that can be done to allow for (1). Schlichter[35] calculated that in an assembly of spheres the actual path was

1·2–1·5 times the apparent path; while Chilton and Colbourn (36) claimed that 80% of resistance to flow should be due to alternate contractions and expansions of the cross-section, and only 20 % due to the viscosity. However, equations having the form of Poiseuille's law must and do apply, and one has as examples Adzumi's data for flow at moderately small pressures through porous plates (p. 66), and the data cited in the previous pages (69–73) for the permeability of refractories. In papers dealing with the permeabilities of unconsolidated and consolidated sands it has become customary to plot the logarithm of the so-called "friction factor", f, against the logarithm of Reynold's number $[R] = dW\rho/4\eta$(l.c.). The curve is rectilinear at low pressures, but undergoes a smooth continuous transition to another rectilinear portion of smaller slope at the onset of turbulent flow (37, 38) (Fig. 15, p. 75). The friction factor is usually defined by Fanning's (39) equation for a capillary

$$f = \frac{gd}{2\rho}\frac{p_1-p_2}{L}\left(\frac{1}{W^2}\right), \tag{40}$$

where g = the acceleration due to gravity, d = the diameter of a capillary, ρ = the density of the gas at the temperature of the experiment, and the mean pressure $\frac{1}{2}(p_1+p_2)$ of flow, W = the velocity of flow in c.c./sec. Fanning's equation is derivable from an equation of turbulent flow

$$(pv)^2 = \frac{A^2gd}{fRT}(p_1^2-p_2^2), \tag{41}$$

similar to that described on p. 57. A denotes the area of cross-section of the capillary; and v the volume passing through per second measured at pressure p. Stream-line flow obeys a law wherein (ρv) appears only to the power unity (p. 58), and so one sees how the curve $\log(f)$ versus $\log[R]$ is a straight line of slope -1 while stream-line, viscous or Poiseuille flow is occurring; and $-0·5$ when turbulent flow has set in. In Fig. 15, taken from the work of Fancher and Lewis (31), $\log(f)$ versus $\log[R]$ plots have been given for a great variety of porous solids. The pressure at which the experiments were carried out varied from 10 atm. per square
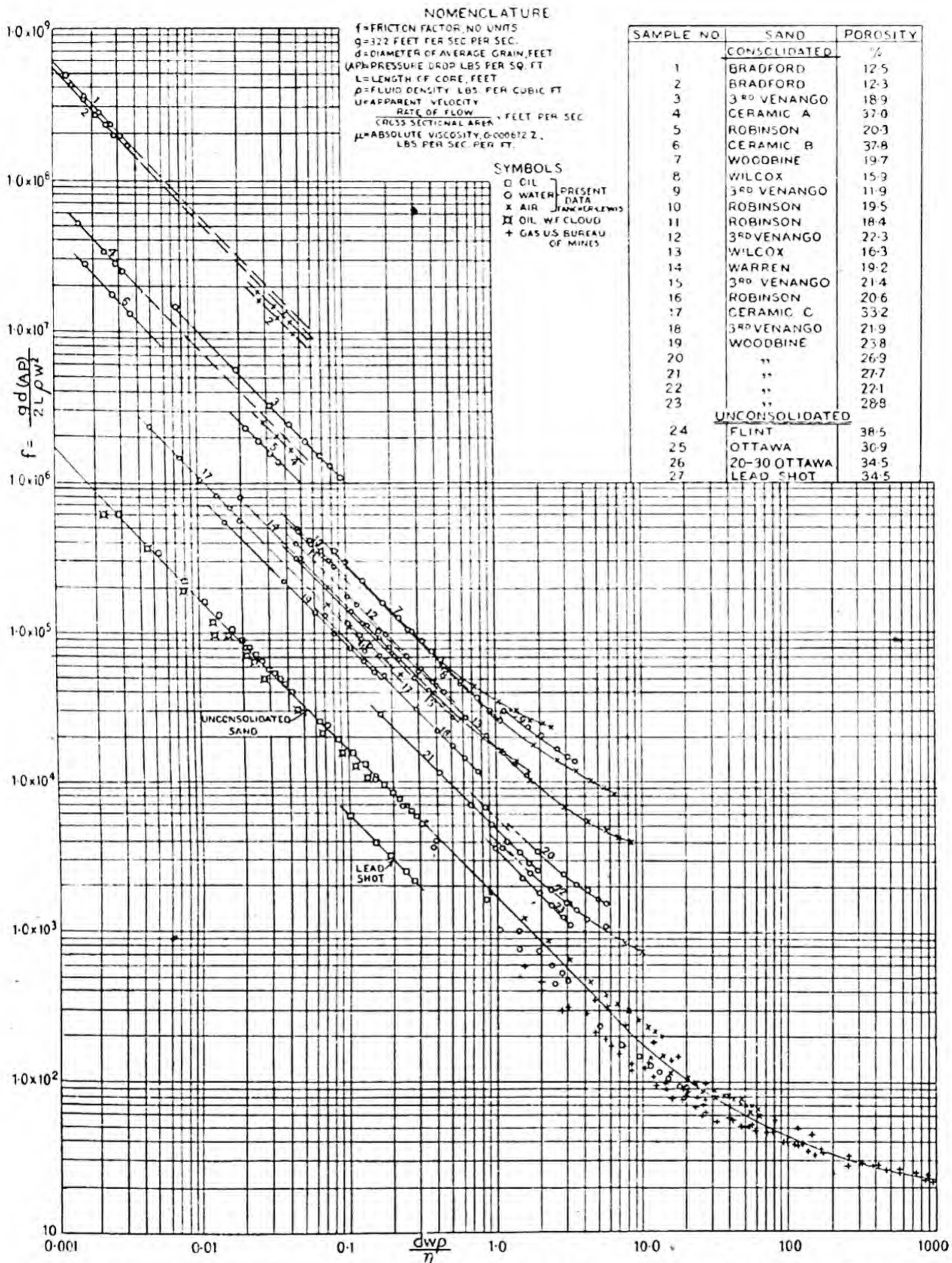
SAMPLE NO.	SAND	POROSITY
	CONSOLIDATED	%
1	BRADFORD	12.5
2	BRADFORD	12.3
3	3RD VENANGO	18.9
4	CERAMIC A	37.0
5	ROBINSON	20.3
6	CERAMIC B	37.8
7	WOODBINE	19.7
8	WILCOX	15.9
9	3RD VENANGO	11.9
10	ROBINSON	19.5
11	ROBINSON	18.4
12	3RD VENANGO	22.3
13	WILCOX	16.3
14	WARREN	19.2
15	3RD VENANGO	21.4
16	ROBINSON	20.6
17	CERAMIC C	33.2
18	3RD VENANGO	21.9
19	WOODBINE	23.8
20	,,	26.9
21	,,	27.7
22	,,	22.1
23	,,	28.9
	UNCONSOLIDATED	
24	FLINT	38.5
25	OTTAWA	30.9
26	20-30 OTTAWA	34.5
27	LEAD SHOT	34.5

$$f = \frac{g d (\Delta P)}{2 L \rho w^2}$$

UNCONSOLIDATED SAND

LEAD SHOT

$$\frac{dw\rho}{\eta}$$

Fig. 15. The curves log (friction factor) versus log (Reynold's number) in the flow of various simple fluids through porous materials.

inch downwards. Fancher and Lewis's notation and the substances used are explained in the figure. It is interesting that, the unconsolidated sands all give curves which fall near a single mean curve, so that they may be said to exhibit a typical behaviour.

Several types of the apparatus[40, 41] devised had arrangements of pressure gauges at intervals down the length of the column of sand through which permeation was occurring. These workers then were able to measure the pressure gradient along the length of the column. It was found that dp^2/dx was constant, and thus equal to $(p_1^2 - p_2^2)/L$. The curves ρv (or pv), against $(p_1^2 - p_2^2)$, obtained by Muskat and Botset[40] for unconsolidated and consolidated sands, emphasise still further that the law of flow is of the form

$$(p_1^2 - p_2^2) = k(\rho v)^n, \qquad (42)$$

where $1 < n < 2$ (see pp. 57 and 58) according to the amount of turbulent or stream-line flow occurring. The chance of turbulent flow occurring decreased with decrease in grain size, whilst of course the permeability decreased as turbulent flow set in, i.e. as n increased from 1 towards 2.

Some typical permeability constants for the stream-line flow of gases and liquids through media such as have just been considered are presented in Tables 6-8. The data recorded in

TABLE 6. *Data of Green and Ampt[42] for flow through unconsolidated media*

Substance	Mean radius cm. $\times 10^{-2}$	Porosity %	Specific permeability c.c./sec./cm.^{2}/mm. thick/cm. Hg/unit viscosity, when, in eq. (28), $2p/(p_1 + p_2) = 1$	
			Specific permeability by gas flow $\times 10^{-6}$	Specific permeability by liquid flow $\times 10^{-6}$
Glass spheres	4·69	36·4	372	357
	3·55	37·3	250	252
	2·49	36·1	113	115
	1·59	36·3	47·6	46·5
	1·25	36·6	28·6	28·3
Quartz sand	4·13	34·7	157·5	154
	1·45	34·7	22·3	22·3
	0·93	37·7	10·1	9·75

TABLE 7. *Data of Muskat, Botset and co-workers* (41); *and Fancher and Lewis* (31). *Stream-line flow through unconsolidated media*

$$2p/(p_1 + p_2) \simeq 1$$

Substance	Mean radius of particles cm. $\times 10^{-2}$	Porosity %	Permeability co-efficient $P_G l$	Specific permeability $P_G l\eta \times 10^{-6}$	$P_L l\eta \times 10^{-6}$
Glass beads	—	33·8	1350	248	—
40–45 mesh sand	—	—	1025	188	188
60–65 mesh sand	—	44·0	233	42·6	—
80–100 mesh sand	—	—	183	33·5	29·6
Heterogeneous sand	—	42·0	271	49·6	—
Lead shot	5	34·5	3190	584	—
Ottawa sand, unsieved	36·7	30·9	1175	215	—
Ottawa sand, sieved	35·7	34·5	1117	204	—
Flint sand, Pennsylvania	18·75	38·5	308	56·3	—

TABLE 8. *Data of Fancher and Lewis* (31). *Stream-line flow through consolidated media. The specific permeabilities are measured with air, water, and crude petroleum;* $2p/(p_1 + p_2) \simeq 1$. *The permeability coefficients are those calculated from* $P_G l\eta$ *for air*

Sandstone	Mean particle radius cm. $\times 10^{-3}$	Porosity %	Permeability coefficient $P_G l$ for air	Specific permeability $P_G l\eta \times 10^{-6}$
Woodbine, Texas	8·11	22·1	24·2	4·62
„ „	8·35	26·9	18·2	3·33
„ „	6·39	28·8	17·3	3·16
Venango, Pennsylvania	12·53	11·9	8·79	1·61
Woodbine, Texas	4·51	22·7	6·35	1·16
Wilcox, Oklahoma	6·99	16·3	4·08	0·75
Venango, Pennsylvania	4·54	21·9	3·32	0·607
Wilcox, Oklahoma	6·97	15·9	2·57	0·47
Venango, Pennsylvania	4·19	21·4	1·78	0·326
Woodbine, Texas	3·13	23·8	1·73	0·317
Warren, Pennsylvania	3·26	19·2	1·03	0·189
Robinson, Illinois	2·74	20·6	0·925	0·170
„ „	2·74	18·4	0·498	0·091
„ „	2·71	19·5	0·466	0·0855
Venango, Pennsylvania	4·90	16·9	0·347	0·0636
Ceramic C (5 % binding agent)	1·43	33·2	0·273	0·0502
Ceramic B (10 % binding agent)	1·43	37·8	0·065	0·0119
Ceramic A (20 % binding agent)	1·43	37·0	0·0380	0·0070
Bradford, Pennsylvania	2·79	12·3	0·0209	0·00384
„ „	2·82	12·5	0·0194	0·00356

these tables show how particle size modifies permeability, at nearly constant porosity (Table 6) and how the nature of the particle (e.g. its smoothness) also controls the gas flow. In general, particle size controls the flow rate more than porosity; and the rate of flow is less through consolidated than through unconsolidated media. The tables also show a good agreement between specific permeabilities determined with liquids and with gases (Tables 7 and 6).

FLOW THROUGH MISCELLANEOUS POROUS SYSTEMS

In the literature will be found measurements on liquid or gas flow through a great variety of substances. The permeability of papers, leathers, textiles, and fibreboards is treated elsewhere (Chap. IX). The permeability of various kinds of wood[43], of a silicic acid gel[44], of building and heat-insulating substances[45, 46], and of various soils[42] illustrate the systems studied. Manegold[19] summarised a number of measurements on these systems, employing the permeabilities or specific permeabilities of Table 1.

SEPARATION OF GAS MIXTURES AND ISOTOPES

Phenomena connected with effusion and molecular streaming through porous plates, and in tubes, have had some interesting applications in separating the components of gas mixtures and, in particular, isotopes. The original method for the separation of isotopes developed by Hertz[47] required a battery of mercury-in-glass diffusion pumps connected in series. Each pump circulates the gas mixture through a clay tube; a greater part of the lighter than of the heavier gas diffuses through the wall in transit down the tube, and enters a counter-current rich in the light fraction on the other side. These lighter fractions tend to enter another higher separating unit, and the heavier fraction a lower unit. The method has served to effect a complete separation of the isotopes of hydrogen (H_2 and D_2)[48], and a partial separation of the isotopes of neon, carbon and nitrogen[49, 50]. A schematic

representation of a Hertz porous wall separation unit is shown in Fig. 16(49).

Recently, however, the type of diffusion unit with a porous wall has been abandoned by Hertz and his collaborators(51), and instead batteries of diffusion pumps are joined together directly, separation occurring by effusion together with mercury vapour through jets. The theory of the separation of
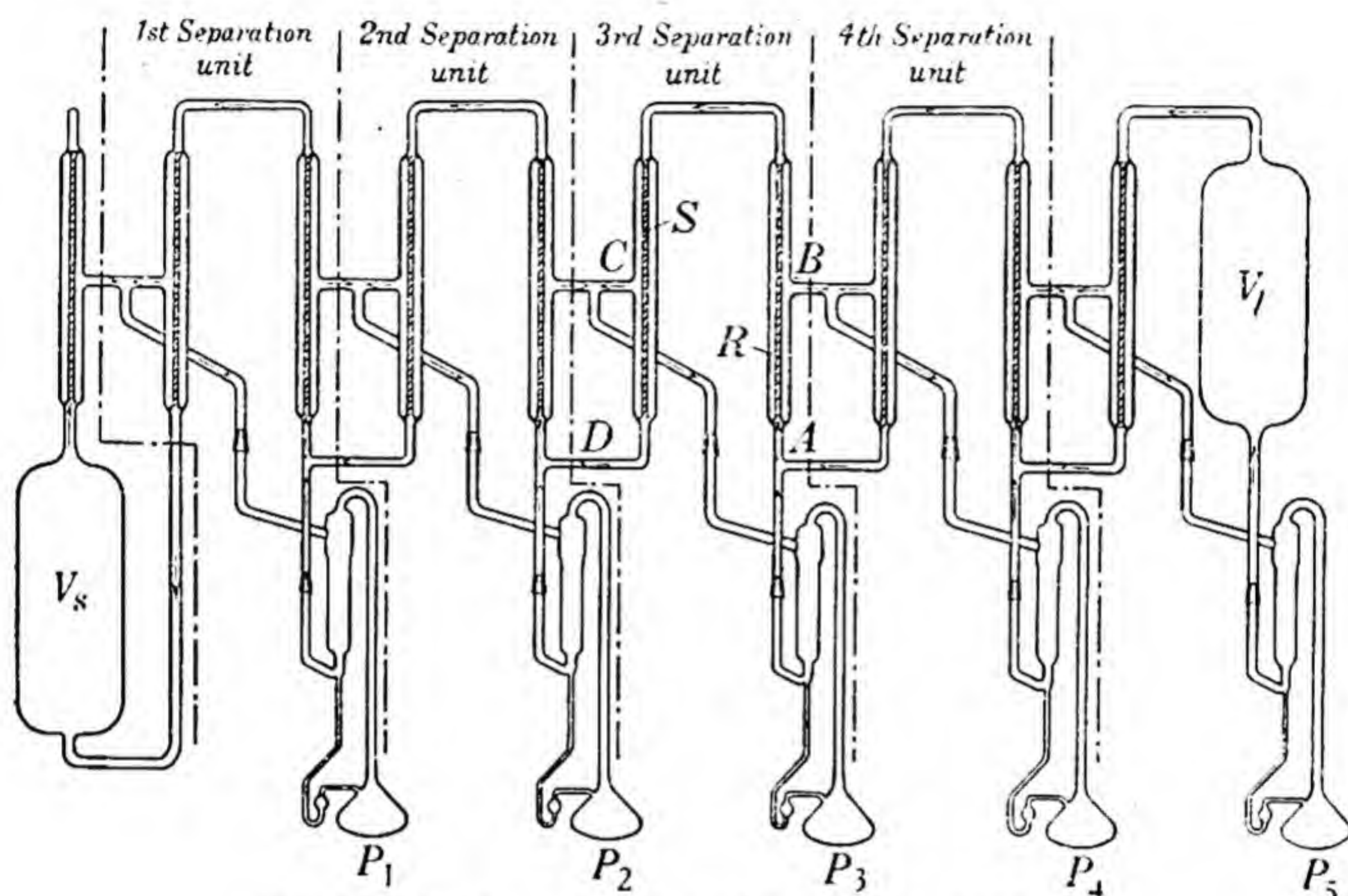
Fig. 16. A Hertz porous wall diffusion apparatus.

isotopes by this method has been given by Barwich(52). For example, one might be employing a battery of pumps to separate the isotopes of carbon, C_{12} and C_{13}, in gaseous form as methane(53). Then according to Barwich one set of conditions gives

$$\ln q = \frac{V}{2}(R - s - x_0)\left[\left(\frac{1}{D_2} - \frac{1}{D_1}\right) + \ln \frac{D_1}{D_2}\right], \qquad (43)$$

where D_1, D_2 denote the diffusion constants of the isotopes, V is the speed of the mercury vapour jet, R, s, and x_0 are geometrical factors of the apparatus, and q is the separation coefficient defined by

$$q = \frac{C_{13}\,(\text{exit})}{C_{12}\,(\text{exit})} \times \frac{C_{12}\,(\text{entrance})}{C_{13}\,(\text{entrance})}. \qquad (44)$$

This equation holds only when the pressure of diffusing gas is high. When the pressure and temperature are such that the densities of the diffusing gases are small compared with the density of the mercury vapour, one has $D = \frac{1}{3}\overline{w}\Lambda$ ($\overline{w}$ = the molecular velocity; Λ = the mean free path), and the expression for the separation of the isotopes becomes

$$\ln q = \text{const.}\,\rho_{Hg}V[(r_2 + r_{Hg})^2 \sqrt{m_2} - (r_1 + r_{Hg})^2 \sqrt{m_1}], \quad (45)$$

where r_1, r_2, r_{Hg} are the molecular radii of the two isotopes and of mercury atoms respectively ($r_1 \simeq r_2$), and ρ_{Hg} is the density of the mercury vapour.

A diagram of the diffusion unit[54] used to separate isotopes by this method is given in Fig. 17. It is not necessary, according to a recent communication[53], to connect the pumps by a capillary tube. With a battery of fifty-one pumps it was found that a 32 % separation of C_{12} and C_{13} could be effected from 300 c.c. of methane at 1·8 mm. pressure. The advantage of this newer arrangement of Hertz's original method is that there is no accumulation of impurities within a porous wall, and that higher separation factors are possible.

Another method of separating liquid and gaseous mixtures, which was first developed by Clusius and Dickel[55], is based upon Chapman's early study of thermo-diffusion in gases[56]. This method promises to be very efficient in separating isotopic mixtures, and is simple to operate. If a hot wire passes axially down a tube containing a mixture of gases, the gases under the combined influence of radial and axial diffusion and of convection undergo a partial separation into the two components[57,58]. Let the separation unit consist of a hot and a cold surface, plane and parallel, between which is confined the solution being disproportionated. The temperature gradient exists across this solution, in the x-direction, and convection occurs in the z-direction. Then the separation velocity is governed by the differential equation[57]

$$D\left(\frac{\partial^2 C}{\partial x^2} + \frac{\partial^2 C}{\partial z^2}\right) + \frac{\partial D}{\partial T}\frac{\partial}{\partial x}\left(C\frac{\partial T}{\partial x}\right) - \frac{\partial}{\partial z}\{Cv(x)\} = \frac{\partial C}{\partial t}, \quad (46)$$

where $v(x)$ denotes the convection velocity as a function of x,

and T the temperature. For a separating unit of length l there is a characteristic time

$$\theta = \frac{l^2}{\pi^2 D},$$

which gives the order of magnitude of the time required for the separation equilibrium to be approached. In a normal
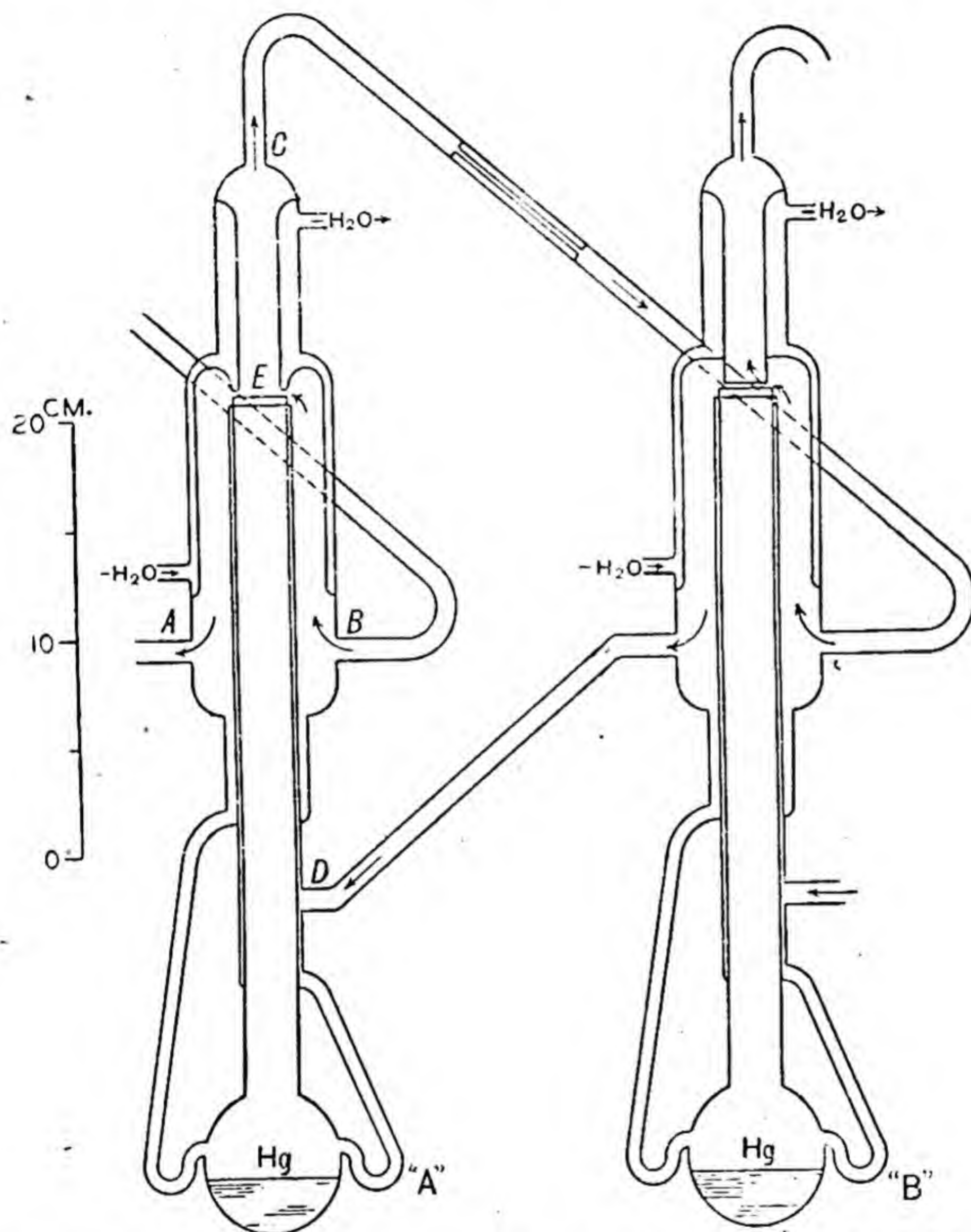
Fig. 17. Mercury diffusion pumps. "A" is the Hertz pump and "B" is a unit with a modified mercury jet. The pumps are connected in series as shown. (Scherr (54).)

apparatus this would be 1000 days for liquids, and < 1 day for gases. The equilibrium state is defined by the equation

$$D\left(\frac{\partial^2 C}{\partial x^2} + \frac{\partial^2 C}{\partial z^2}\right) + \frac{\partial D}{\partial T}\frac{\partial}{\partial x}\left(C\frac{\partial T}{\partial x}\right) - \frac{\partial}{\partial z}\{Cv(x)\} = 0. \quad (47)$$

BD   6

It was found in a liquid mixture $D_2O_{(32°/_o)} + H_2O_{(68°/_o)}$ that a separation of up to 4·8 % was established in two days—about $\frac{1}{10}$ of the equilibrium separation in the stationary state. The method was employed successfully to disproportionate the isotopes Zn_{64}, Zn_{66}, Zn_{68}, as aqueous solutions of zinc sulphate[57]. The isotopes were estimated spectroscopically. The method has also been used[59] in the separation of isotopes of Cl and of Hg. The method is of quite general applicability in disproportionating or sedimenting such mixtures as

$ZnCl_2$, $ZnSO_4$ in H_2O[57], n-Hexane in CCl_4[57],

NaCl, Na_2SO_4 in H_2O[57], C_6H_6 in C_6H_5Cl[57],

Chlorophyll in CCl_4[57].

Table 9 illustrates its efficiency in separating gas mixtures[55].

TABLE 9. *The Clusius-Dickel method of separating gas mixtures*

Total pressure approximately 1 atm.				
Original gas mixture %	Length of separating column cm.	Temp. diff. ° C.	Composition at	
			"Heavy" end	"Light" end
25 Br_2 75 He	65	~ 300	100 % Br_2 (liq.)	100 % He
40 CO_2 60 H_2	100	~ 600	100 % CO_2	—
20 O_2 80 N_2 (air)	(a) 100	~ 600	42 % O_2	—
	(b) 290	~ 600	85 % O_2	—
Normal Ne (at. wt. = 20·18)	260	~ 600	At. wt. 20·68	—
23 $H^{37}Cl$ 77 $H^{35}Cl$	290	~ 600	40 % $H^{37}Cl$ 60 % $H^{35}Cl$	—

NON-STATIONARY STATES OF CAPILLARY GAS FLOW

Stationary streaming proceeds at the same rate whether the molecules have a long life in the adsorbed phase or not, according at any instant to the equation

$$\frac{dn}{dt} = \frac{1}{2}\frac{B}{L}\frac{1}{\sqrt{(2\pi MR)}}\left(\frac{p_1}{\sqrt{T_1}} - \frac{p_2}{\sqrt{T_2}}\right)\frac{(2-f)}{f} \qquad (2)$$

already discussed. In the stationary state every molecule leaving the wall is replaced by one striking the wall. Clausing[7],

however, has shown how non-stationary streaming may be used to determine the lifetime of molecules in the adsorbed phase, and heats of adsorption. His experiments and theoretical treatment are of interest because they obviate any necessity for direct measurement of the very minute quantities adsorbed on certain surfaces such as glass and crystals. The essential apparatus consists of two large flasks connected by a fine capillary. In one flask, for all times $t > 0$ the pressure is p_1; while in the capillary and in the second flask the pressure $p_2 \simeq 0$. At time $t = 0$ the gas enters the capillary. A certain time must elapse before the first molecule enters the second flask, and this time is a function of the lifetime of the molecules in the adsorbed state, being greater the greater this lifetime.

In obtaining a solution for the diffusion into the capillary, Clausing assumed that surface diffusion need not be considered in comparison with bulk diffusion. The diffusion equation is then once more*

$$D \frac{\partial^2 C}{\partial x^2} = \frac{\partial C}{\partial t}. \tag{48}$$

The initial condition is, inside the capillary,

for $t = 0$, $C = 0$.

The boundary conditions are

for $x = 0$, $C = C_1$ for all t,

for $x = L$, $C \simeq 0$ for all t.

The solution of the problem then is

$$C = C_1 \left[\frac{L-x}{L} - \frac{2}{\pi} \left\{ e^{-t/\alpha} \sin \pi \left(\frac{L-x}{L} \right) - \tfrac{1}{2} e^{-4t/\alpha} \sin 2\pi \left(\frac{L-x}{L} \right) \right. \right.$$
$$\left. \left. + \tfrac{1}{3} e^{-9t/\alpha} \sin 3\pi \left(\frac{L-x}{L} \right) - \ldots \right\} \right], \tag{49}$$

if $\alpha = L^2/\pi^2 D$.

When $x = L$

$$\left(\frac{\partial C}{\partial x} \right)_{x=L} = -\frac{C_1}{L} \{ 1 - 2(e^{-t/\alpha} - e^{-4t/\alpha} + e^{-9t/\alpha}) \}. \tag{50}$$

* In equations (48) to (58) C denotes the number of molecules per unit length of the capillary, including those adsorbed on the wall. It is given by equation (55).

Thus in time t there flows into the second vessel a number of molecules N_t given by

$$N_t = \int_0^t D\left(-\frac{\partial C}{\partial x}\right)_{x=L} dt,$$

so that

$$N_t = \frac{DC_1}{L}\left[t - 2\alpha\{(1 - e^{-t/\alpha}) - \tfrac{1}{4}(1 - e^{-4t/\alpha}) + \tfrac{1}{9}(1 - e^{-9t/\alpha}) - \ldots\}\right]. \tag{51}$$

The value of D, Clausing was able to deduce from kinetic theory and from his own consideration of the mean life, τ_e, of an adsorbed molecule. This value of D is

$$D = \frac{4}{3}\frac{r^2}{2r/\overline{w} + \tau_e}, \tag{52}$$

so that

$$\alpha = \frac{3}{\pi^2}\left(\frac{L}{2r}\right)^2\left(\frac{2r}{\overline{w}} + \tau_e\right), \tag{53}$$

and

$$\tau_e = \frac{\pi^2}{3}\left(\frac{2r}{L}\right)^2 \alpha - \frac{2r}{\overline{w}}. \tag{54}$$

It was also shown from simple considerations that

$$C_1 = \frac{\pi}{2}rN_1\overline{w}\left(\frac{2r}{\overline{w}} + \tau_e\right). \tag{55}$$

In equations (52)–(55) r denotes the pore radius, $\overline{w}$ the root mean square velocity of a molecule, and N_1 the number of molecules in the first vessel per c.c.; C_1 is of course the same for stationary as for non-stationary flow. By treating stationary flow as a diffusion, one obtains

$$\frac{dn}{dt} = \frac{8\pi r^3}{3L}\tfrac{1}{4}N_1\overline{w} = -D\frac{\partial C}{\partial x} = P. \tag{56}$$

Thence, by combining (51), (52), (55) and (56), one obtains

$$N_t = Pt\psi\left(\frac{t}{\alpha}\right) = P\alpha\chi\left(\frac{t}{\alpha}\right), \tag{57}$$

in which

$$\psi\left(\frac{t}{\alpha}\right) = 1 - \frac{2\alpha}{t}\{(1 - e^{-t/\alpha}) - \tfrac{1}{4}(1 - e^{-4t/\alpha}) + \tfrac{1}{9}(1 - e^{-9t/\alpha}) - \dots\}$$

and
$$\chi\left(\frac{t}{\alpha}\right) = \frac{t}{\alpha}\,\psi\left(\frac{t}{\alpha}\right).$$

For large values of t

$$N_t = P_t\left(1 - \frac{2\alpha}{t}\{1 - \tfrac{1}{4} + \tfrac{1}{9} - \dots\}\right) = P_t\left(1 - \frac{\pi^2}{6}\frac{\alpha}{t}\right) \simeq P_t. \quad (58)$$

That is, the diffusion rate tends for longer times to become that for stationary streaming, as would be anticipated. The function $\psi(t/\alpha)$ then approaches the asymptote $\psi(t/\alpha) = 1$, corresponding to stationary flow.

In Clausing's apparatus the flow through two capillaries with diameters in the ratio $1:10$ was measured. The pressure on the ingoing side was virtually constant, and on the outgoing side was measured by two ionisation gauges. The current, which was then amplified, was proportional to the pressure, and was registered by a linear galvanometer with a vibration period of $\frac{1}{50}$ sec. Thus the deflection was found as a function of time, and so, from the calibration curve for the instruments, the value of p and therefore of $N_t = P\alpha\psi(t/\alpha)$ was deduced. The record of the diffusion process was obtained photographically on a moving photographic plate. Employing the foregoing theory to interpret his photographs, Clausing obtained the lifetimes of molecules of argon, nitrogen, and neon on glass. He also obtained the lifetime of argon, τ_e, as a function of temperature, his results being expressible as linear $\log\tau_e$ versus $1/T$ curves (T in $^\circ$K.) (Fig. 18). According to the theory of Frenkel[60],

$$\tau_e \simeq \tau_0 e^{\Delta H/RT}, \quad (59)$$

where τ_0 denotes the vibration period of the adsorbed molecule on the solid, and ΔH is the heat of adsorption. Thus the slope of the curve $\log\tau_e$ versus $1/T$ gives the heats of sorption, which are collected for argon on glass in Table 10. The heats of sorption obtained by Kalberer and Mark[61]

for argon on dehydrated silica gel are fairly constant at 2500 cal./atom, a figure somewhat lower than the above value for glass. Clausing remarks that the results are not always easy to reproduce. For argon on glass between 78° and 90° K., the approximate value for τ_e is

$$\tau_e \approx 1 \cdot 7 \times 10^{-14} e^{3800/RT} \text{ sec.} \tag{59a}$$
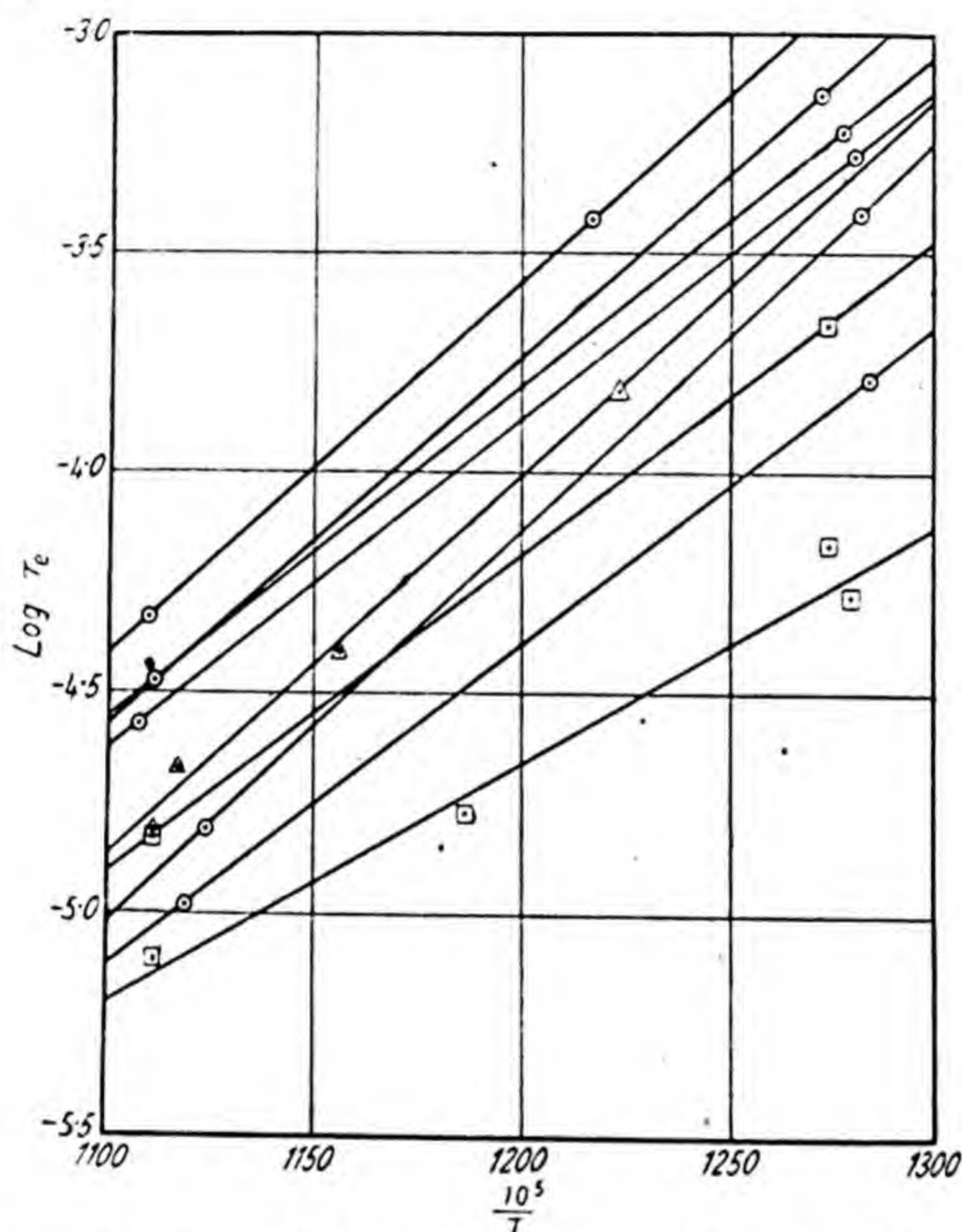
Fig. 18. The linear relationship between $\log \tau_e$ and $1/T$ (T in ° K.). $\odot$, cleaned with chromic acid; $\boxdot$, $\triangle$, cleaned with hydrofluoric acid.

At 78° K., $\tau_e \approx 75 \times 10^{-5}$ sec.; at 90° K. $\tau_e \approx 3 \cdot 1 \times 10^{-5}$ sec. For nitrogen τ_e was of the same order of magnitude, whilst for neon τ_e is less than 2×10^{-7} sec. These lifetimes accord well with our knowledge of the relative adsorbability of these gases.

The establishment of sorption equilibria in porous solids is another very important case of non-stationary flow into capillaries. These capillaries may range in size from molecular dimensions, when activated diffusion occurs, to capillaries

of macroscopic dimensions. Any theoretical treatment is rendered more difficult by the occurrence of an unknown distribution of pore sizes and channel sizes. It is true of a limited number of adsorbents, however, that the pores are nearly all of one size, for example in dehydrated chabasite or analcite crystals(62), from which heat and evacuation removes water without destroying or fundamentally changing the crystal skeleton. A formal treatment based on Fick's law without a kinetic picture of what is happening has been applied

TABLE 10. *The adsorption heat for argon on glass*

Cleaned with hydrofluoric acid		Cleaned with chromic acid	
ΔH (cal./atom)	Remarks	ΔH (cal./atom)	Remarks
2450 2430 3300 3930	The first three results not quite trustworthy, the last result free from objection	3320 3430 4050 3440 3810 3880	The first two results are not so trustworthy, but the last four are free from objection
		Mean of last four results: 3800	

to heulandite and analcite systems by Tiselius(63); and a kinetic theory interpretation of the diffusion has been outlined by Hey (64) (Chap. III). Other attempts have been made, based upon the kinetic theory of gases, to derive formulae for the rate of flow of gases into capillary solids(65, 66). Owing to the complexity of the problem such attempts are not very successful. Often sorption kinetics, after some time has elapsed, tend towards a pseudo-unimolecular law. When oxygen, nitrogen, and hydrogen were sorbed by charcoal(67) at low temperatures, the "unimolecular" velocity constants then stood in the ratio $O_2 : N_2 : H_2 = 1 : 1 \cdot 1 : 3 \cdot 2$. Molecular flow would require $O_2 : N_2 : H_2 = 1 : 1 \cdot 07 : 4 \cdot 0$. Finite sorption velocities may in some cases have their origin in slow dissipation of the heat of sorption, or in the slow displacement of surface

impurity. In the experiments described, however, the first possibility was avoided by using minimal amounts of gas, and the second by the most thorough heat-evacuation treatment. Other authors[68,69,70] have observed finite sorption rates in charcoals, and a number of the equations used to express the velocity of sorption in various adsorbents have been summarised by Swan and Urquhart[71].

REFERENCES

(1) Warburg, E. *Ann. Phys., Lpz.,* **159**, 399 (1876).
(2) Knudsen, M. *Ann. Phys., Lpz.,* **28**, 75 (1909); **35**, 389 (1911).
(3) Gaede, W. *Ann. Phys., Lpz.,* **41**, 289 (1913).
(4) v. Smoluchowski, M. *Ann. Phys., Lpz.,* **33**, 1559 (1910).
(5) Buckingham, E. *Technol. Pap. U.S. Bur. Stand.* No. 183 (1921).
(6) Klose, W. *Phys. Z.* **31**, 503 (1930); *Ann. Phys., Lpz.,* **11**, 73 (1931).
(7) Clausing, P. *Ann. Phys., Lpz.,* **7**, 489, 569 (1930).
(8) Herzfeld, K. and Smallwood, M. In Taylor's *Treatise on Physical Chemistry*, **1**, 169 (1931).
(9) —— —— *Treatise on Physical Chemistry*, **1**, 171 (1931).
(10) Brillouin, M. *Leçons sur la Viscosité*, Paris (1907).
(11) Hagenbach, E. *Ann. Phys., Lpz.,* **109**, 835 (1860).
(12) v. Smoluchowski, M. *Bull. Acad. Krakau*, **143** (1903).
(13) Reynolds, O. *Philos. Trans.* **174**, 935 (1883).
(14) Ackerel, T. *Handb. Phys.* **7**, 304, Berlin (1927).
(15) Stodola, A. and Lowenstein, L. *Steam and Gas Turbines*, **1**, 55–67, New York (1927).
(16) Eason, A. B. *Flow and Measurement of Air and Gases*, London (1919).
(17) Blasins, H. *ForschArb. dtsch. Ing.* **131** (1913).
(18) Manegold, E. *Kolloidzschr.* **81**, 164 (1937).
(19) —— *Kolloidzschr.* **81**, 269 (1937).
(20) Adzumi, H. *Bull. chem. Soc. Japan*, **12**, 285 (1937).
(21) —— *Bull. chem. Soc. Japan*, **12**, 292 (1937).
(22) Ramsay, W. and Collie, N. *Proc. Roy. Soc.* **60**A, 106 (1897).
(23) Donnan, F. *Phil. Mag.* **49**, 423 (1900).
(24) Sameshima, J. *Bull. chem. Soc. Japan*, **1**, 5 (1926).
(25) Adzumi, H. *Bull. chem. Soc. Japan*, **12**, 304 (1937).
(26) Preston, E. *J. Soc. Glass. Tech.* **18**, 336 (1934).
(27) Kanz, A. *Arch. Eisenhüttenw.* **2**, 843 (1929).
(28) Clews, F. and Green, A. *Trans. ceram. Soc.* **32**, 295, 472 (1933).
(29) Bansen, H. *Arch. Eisenhüttenw.* **1**, 687 (1927–8); *Stahl u. Eisen*, **48**, 973 (1928).
(30) Bremond, P. *C.R. Acad. Sci., Paris*, **196**, 1651 (1933).

(31) Fancher, G. and Lewis, J. *Industr. Engng. Chem.* **25**, 1139 (1933).

(32) Bartell, F. *J. phys. Chem.* **15**, 659 (1911); **16**, 318 (1912).
Bartell, F. and Carpenter, D. C. *J. phys. Chem.* **27**, 252 (1923).

(33) Bartell, F. and Miller, F. *Industr. Engng Chem.* **20**, 738 (1928).

(34) Bartell, F. and Osterhof, H. *J. phys. Chem.* **32**, 1553 (1928).

(35) Schlichter, C. *Rep. U.S. geol. Surv.* **2**, 305 (1897–8).

(36) Chilton, J. and Colbourn, A. *Industr. Engng Chem.* **23**, 913 (1931).

(37) Chalmers, J., Taliaferro, D. and Rawlins, E. *Trans. Amer. Inst. min. (metall.) Engrs*, **98**, 375 (1932).

(38) Wilde, H. and Moore, T. *Oil Weekly*, **67**, 34 (1932).

(39) Cf. Fancher, G. and Lewis, J. *Industr. Engng Chem.* **25**, 1139, 1143 (1933).

(40) Muskat, M. and Botset, H. *Physics*, **1**, 27 (1931).

(41) Wyckoff, R., Botset, H., Muskat, M. and Reed, D. *Bull. Amer. Ass. Petrol. Geol.* **18**, 161 (1934).

(42) Green, H. and Ampt, G. *J. Agric. Sci.* **4**, 1 (1911–12); **5**, 1 (1912–13).

(43) Narayanamurti, O. *Z. Ver. dtsch. Ing. Bleiheft*, Nr. **2**, 13 (1936).

(44) Manegold, E. (with Hennenhofer). *Kolloidzschr.* **81**, 278 (1937).

(45) Raisch, E. and Steger, H. *Gesundheitsing*, **57**, 553 (1934).

(46) Raisch, E. *Z. Ver. dtsch. Ing.* **80**, 1257 (1936).

(47) Hertz, G. *Z. Phys.* **79**, 108 (1932).

(48) Farkas, A. *Light and Heavy Hydrogen*, p. 120, Cambridge (1935).

(49) Harmsen, H. *Z. Phys.* **82**, 589 (1933).
Harmsen, H., Hertz, G. and Schutze, W. *Z. Phys.* **90**, 703 (1934).

(50) Wooldridge, D. and Smythe, W. *Phys. Rev.* **50**, 233 (1936).

(51) Hertz, G. *Z. Phys.* **91**, 810 (1934).

(52) Barwich, H. *Z. Phys.* **100**, 166 (1936).

(53) Capron, P., Delfosse, J., Hemptinne, M. de and Taylor, H. S. *J. chem. Phys.* **6**, 656 (1938).
Hemptinne, M. de and Capron, P. *J. Phys. Radium*, **10**, 171 (1939).

(54) Scherr, R. *J. chem. Phys.* **6**, 252 (1938).

(55) Clusius, K. and Dickel, G. *Naturwissenschaften*, **33**, 546 (1938).

(56) Chapman, S. *Phil. Mag.* **7**, 1 (1929).

(57) Korsching, H. and Wirtz, G. *Naturwissenschaften*, **20/21**, 367 (1939).

(58) Waldmann, L. *Naturwissenschaften*, **14**, 230 (1939).
Grinten, W. *Naturwissenschaften*, **19**, 317 (1939).
Wirtz, K. *Naturwissenschaften*, **20/21**, 369 (1939).

(59) Clusius, K. and Dickel, G. *Naturwissenschaften*, **28**, 487, 148 (1939).
Groth, W. and Harteck, P. *Naturwissenschaften*, **34**, 584 (1939).

(60) Frenkel, J. *Z. Phys.* **26**, 117 (1924).

(61) Kalberer, W. and Mark, H. *Z. phys. Chem.* **139** A, 151 (1929).

(62) Barrer, R. *Proc. Roy. Soc.* **167**A, 392 (1938).
(63) Tiselius, A. *Z. phys. Chem.* **169**A, 425 (1934); **174**A, 401 (1935);
    Nature, Lond., **133**, 212 (1934).
(64) Hey, M. *Miner. Mag.* **24**, 99 (1935).
(65) Damköhler, G. *Z. phys. Chem.* **174**A, 222 (1935).
(66) Wicke, E. *Z. Elektrochem.* **44**, 587 (1938).
(67) Barrer, R. and Rideal, E. K. *Proc. Roy. Soc.* **149**A, 231 (1935).
(68) Blythswood, Lord and Allen, H. S. *Phil. Mag.* **10**, 497 (1905).
(69) Herbst, H. *Kolloidchem. Beih.* **21**, 1 (1925).
(70) Dietl, A. *Kolloidchem. Beih.* **6**, 127 (1914).
(71) Swan, E. and Urquhart, A. *J. phys. Chem.* **31**, 251 (1927).

CHAPTER III

GAS FLOW IN AND THROUGH CRYSTALS AND GLASSES

STRUCTURES OF SOME SILICATES AND GLASSES

In this chapter are described the phenomena of gas flow in glasses and in crystals. While the structure of alkali halides and similar more simple crystals is well known, it is not so with the large families of derivatives of silica. Nevertheless, considerable advance has been made towards an understanding of structural relationships in some at least of these families of compounds. Since many silicates are of importance to the present chapter, a few of the known structural relationships will be given for substances such as silica, silicate glasses, zeolites, mica, clays, feldspars and ultramarines, the first four of which are of great importance in discussing the permeability data.

Certain units occur throughout all these substances, for instance, a silicon atom (or Si^{++++} ion) surrounded by four oxygen atoms (or O^{--} ions). Sometimes one finds an analogous aluminium tetrahedron, whose resultant negative charge is balanced by cations, and which, as in the aluminosilicates, may replace the silicon tetrahedron. These tetrahedra are then linked together to form chains and closed rings. Four tetrahedra can form a 4-ring; one can also find analogous 6-rings, and in certain irregular or acrystalline silicates (such as glass) also 5- and 7-rings.

If the structure is composed entirely, or nearly entirely, of linked silicon-oxygen tetrahedra, one can obtain the three crystalline silica structures, showing α- and β-modifications. These are quartz, cristobalite and tridymite. Also the irregular netting of the tetrahedra leads to fused silica glass. Of the crystalline forms, quartz is the most dense; and β-cristobalite, next to fused silica, is the most open. In β-cristobalite, zigzag

chains are cross-linked forming wide 6-rings, about 6 A. across, but in quartz one has spiral chains also cross-linked to give a ring structure, the widest aperture in the lattice being about 4 A. (from ion centre to ion centre).

As already observed, aluminium tetrahedra may replace a part of the silica tetrahedra in the three-dimensional network, which becomes anionic, since Si^{++++} is replaced by Al^{+++}. Cations now enter the lattice to restore electrostatic balance, with a corresponding distortion of the parent structure. In this way nepheline is built up from tridymite. Sometimes more cations are incorporated than are needed for electrostatic balance, and the nett positive charge is then in its turn balanced by the incorporation of anions SO_4'', Cl', S''. This type of structure is typical of the ultramarines, of which lazurite, whose simplest empirical formula is $Na_8Al_6Si_6O_{24}$ (S'', SO_4''), is an example.

These substances in which extra cations or anions are incorporated in the network are called interstitial compounds. Another group of interstitial compounds, of the greatest interest from the viewpoint of gas flow, is the zeolites, in which the very open anionic frameworks, electrostatically balanced by cations, contain also the neutral molecule water. The water may sometimes be replaced with varying lattice changes by the substances NH_3, H_2S, N_2O, H_2, N_2, Ar, He, I_2, Hg, or CH_3OH, so giving rise to very diverse types of diffusion system, and heterogeneous equilibrium. In the zeolites, the ultramarines and the clays, interstitial cations may undergo replacement and diffusion, although these properties are most readily observed in zeolites.

W. H. Taylor[1] has classified the zeolites, according to their structural properties, into

(1) rigid frameworks,

(2) semi-rigid frameworks,

(3) platy frameworks.

In the first class are chabasite and analcite, in which the water-containing interstices do not collapse markedly upon

dehydration at moderate temperatures [1,2]. In these structures the frameworks are thus to a large extent independent of the neutral molecules occupying interstices inside the framework. In the second class are the fibrous zeolites natrolite, scolecite, mesolite and edingtonite, all of which are formed by cross-linking chains of (Si-Al)-O tetrahedra in different ways (Fig. 19). The fibrous zeolites undergo reorganisation around the water-bearing interstices on dehydration, without any appreciable shrinkage of the chain length. The third class of zeolites is exemplified by heulandite, of which the great shrinkage in one dimension on dehydration and the X-ray diffraction patterns are compatible with a platy structure of two-dimensional lattice layers, separated by water molecules and cations. These cations serve to bind the anionic laminae together. In Fig. 20 a possible laminated lattice is shown [1]. Mica is another case of a laminated silicate crystal, while laminar crystals of silica itself have recently been reported [3].

Clays are aluminosilicate structures often having close similarities to the zeolites. Montmorillonite, for example, may be regarded as the counterpart of the zeolites heulandite and stilbite. Like heulandite it swells greatly upon hydration [4], as is indicated by Fig. 21. The clays also show base-exchange properties like the zeolites. In general they contain larger and less definite channels.

Glasses are anhydrous silicates,* in which Al^{+++} or B^{+++} may replace some Si^{++++}, and are based upon the irregular network of silica-glass. Electrostatic balance is restored by the various basic oxides of types M_2O, MO, M_2O_3 which they contain. By varying the proportions of constituents the most diverse properties may be conferred.

Thus one finds in silicate chemistry many examples of complex structures resolved by the classical chemical and X-ray methods. While diffusion phenomena have been little studied in many of the structures (feldspars, ultramarines, and

---

* Experiments upon the diffusion of deuterium through silica glass showed, however, that some hydrogen, probably as hydroxyl groups, still remained in the silica, since the deuterium content of the diffusing gas decreased [4a].
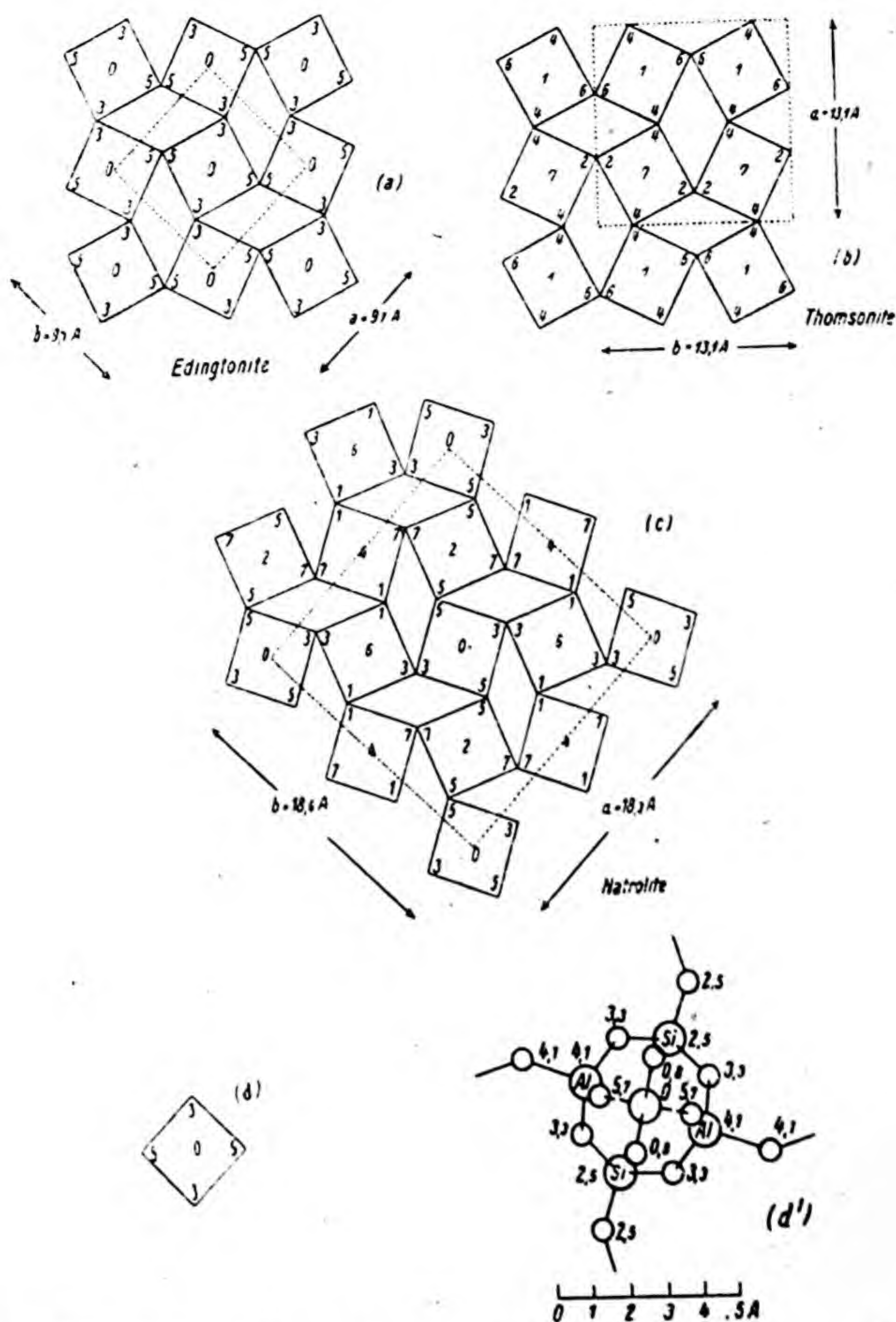
Fig. 19. The structures of some fibrous zeolites. The structure of one tetrahedron chain is shown in (d'), in which the large circles represent silicon or aluminium atoms, the small circles oxygen atoms, and the heights of the atoms are given in A. The same chain is represented diagrammatically in (d), where the numbers show the heights of silicon and aluminium atoms as multiples of $c/8$ (the c-axis is 6·6 A., so that $3c/8 = 2·5$ A., $5c/8 = 4·1$ A.). The linked chains are shown in (a), (b), (c) as arranged in edingtonite, thomsonite and the natrolite group, respectively, and in each the unit cell is indicated by dotted lines.
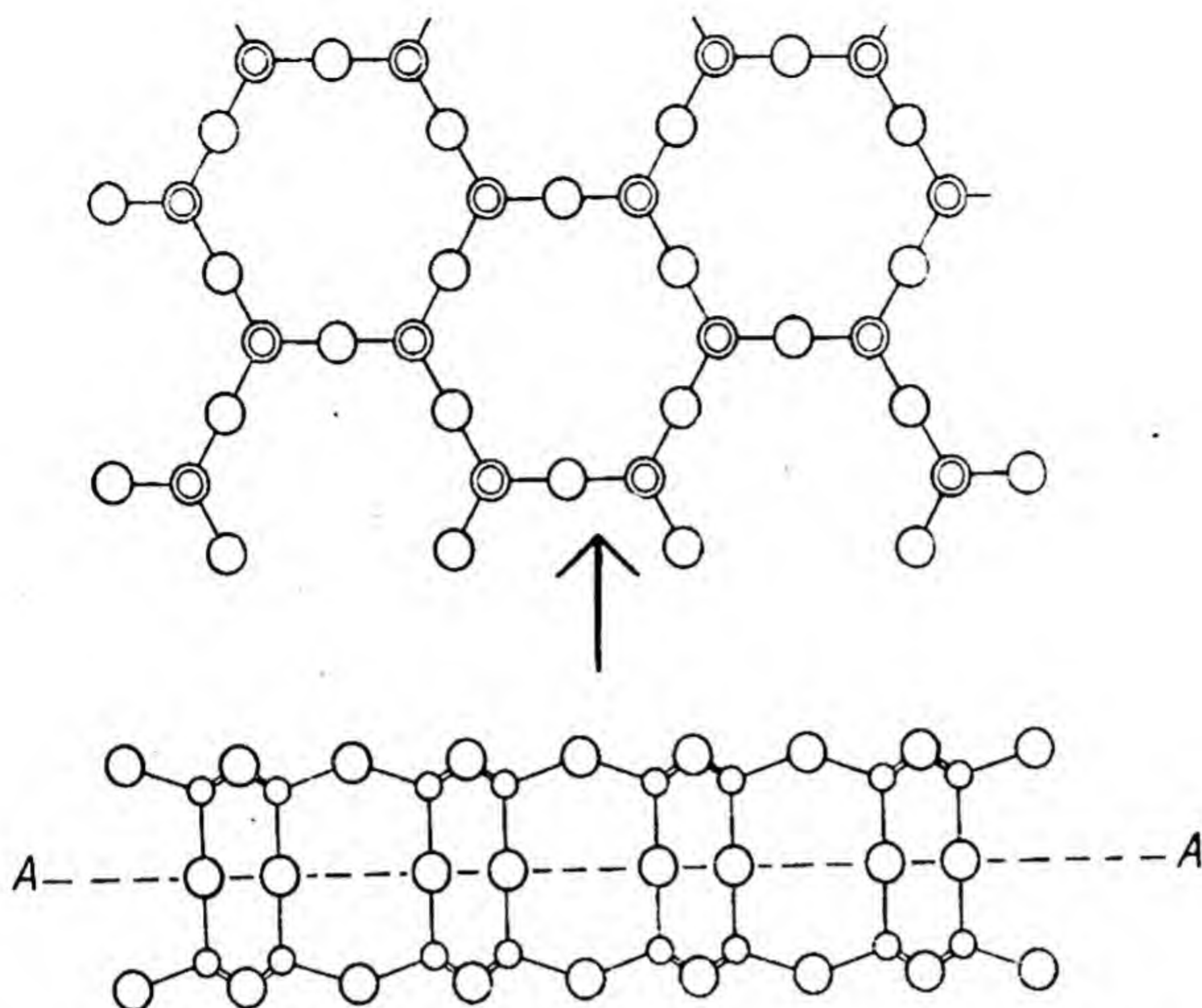
Fig. 20. A lattice of two-dimensional laminae. Large circles represent oxygen atoms, small circles silicon or aluminium atoms. The upper diagram represents a portion of an infinite sheet of tetrahedra in which all vertices are supposed to point upward. If these vertices lie on a reflection plane, a second similar tetrahedron sheet, in which all vertices point down, is linked to the first. The lower diagram represents the appearance of the linked sheets, which form a tetrahedron framework of finite thickness, when viewed in the direction indicated by the arrow in the upper diagram.
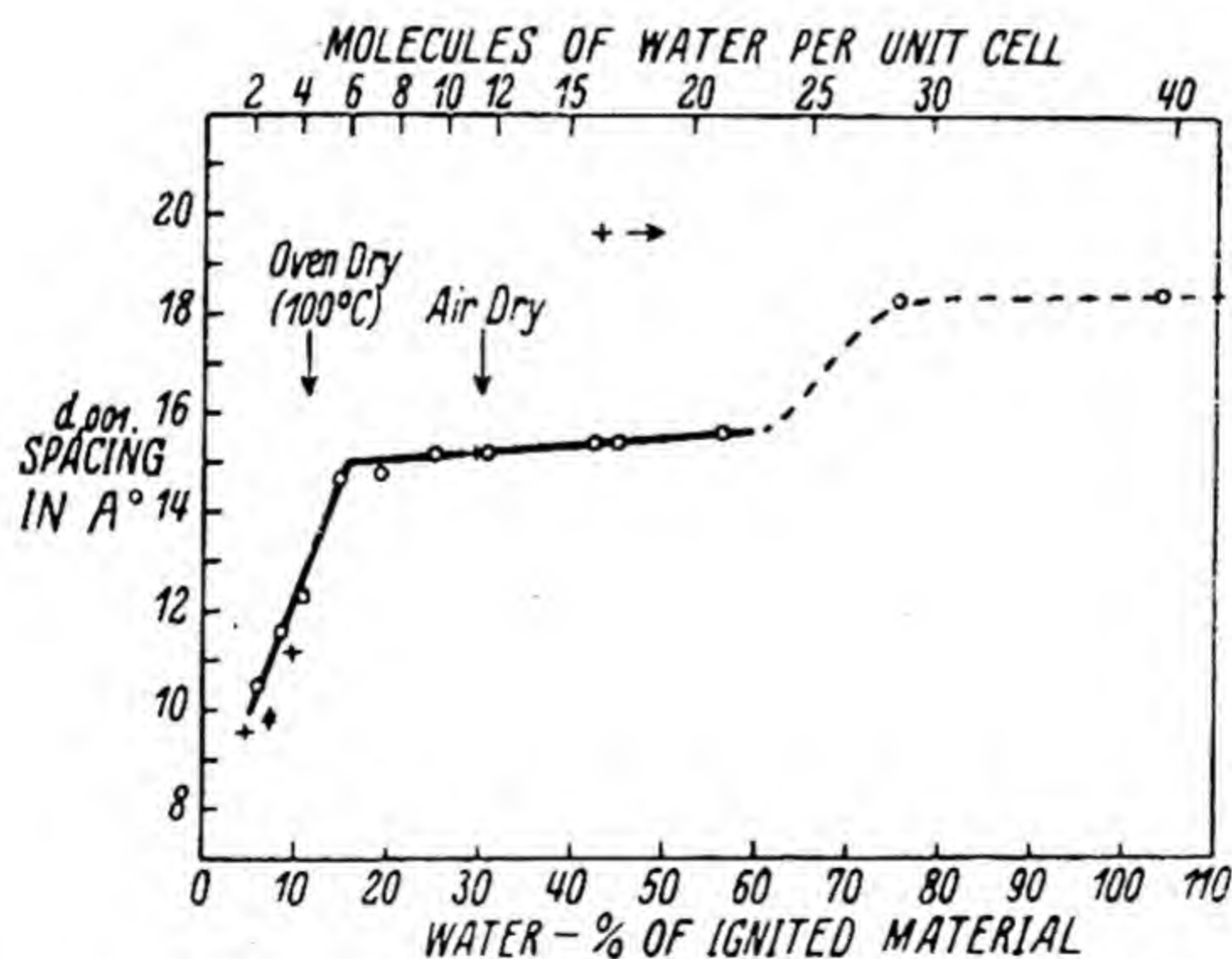
Fig. 21. The one-dimensional swelling of montmorillonite on hydration.

clays), in others (glasses and zeolites) considerable data have been collected. It must be in the light of the main structural features outlined that these data are examined. The mobility of ions has been observed in ultramarines, clays, zeolites and glasses—in the three former groups by base exchange experiments, and in the latter because of its function as a hydrogen electrode, or even as a sodium electrode. The mobility of sodium (and potassium) ions in glass may be demonstrated in an experiment used to prepare pure sodium *in vacuo*. The cell

Cu	NaNO$_3$ (molten)	Na glass	Conducting evacuated space	Glowing tungsten filament
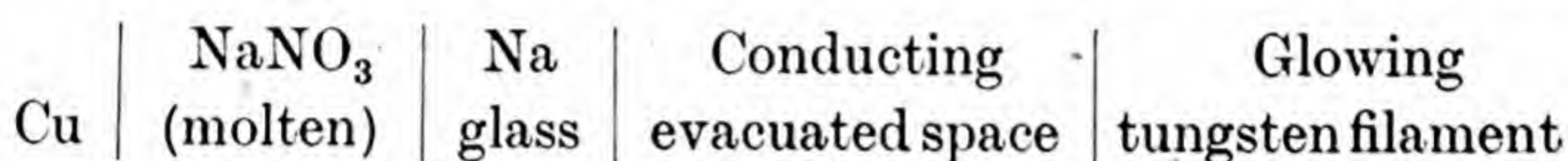
is constructed by dipping an evacuated soda glass bulb into molten sodium nitrate, into which dips a copper electrode. Inside the evacuated bulb is a hot tungsten filament, which, by thermionic emission, renders the evacuated space conducting. On making the tungsten negative with respect to the copper, metallic sodium appears inside the glass bulb.

The diffusion of water and ammonia in zeolites

Introductory

Having briefly reviewed zeolitic structure and properties, one is in a position to consider diffusion within these crystals. The most complete and satisfactory studies are those of A. Tiselius (5, 6), whose methods and data will now be considered. In crystals such as NaCl, lattice diffusion is possible only at elevated temperatures because no channels are available for the diffusion. Very often, as when thorium diffuses in tungsten, diffusion occurs down the only available channels, the grain boundaries and faults in the tungsten crystal. In interstitial compounds such as zeolites there are, when the crystal is dehydrated, numerous channels through the lattice left by the evacuated water, and so diffusion by *spreading* through interstices, as opposed to high temperature processes of diffusion by *place exchange*, may occur.

The experimental and theoretical interpretation of diffusion data

Tiselius[5,6] found that the double refraction of light by these crystals was dependent upon the extent of hydration of the lattice. The crystals were cut for this purpose in the form of thin plates, and the rays were examined in a polarisation microscope. As a first approximation, Tiselius then considered Fick's law to hold. To interpret his data he used the solution of the diffusion equation $\dfrac{\partial C}{\partial t} = D\dfrac{\partial^2 C}{\partial x^2}$ for the diffusion of a substance along the co-ordinate x into a medium of infinite length through a surface normal to its length. The solution is (Chap. I):

$$\frac{C_p - C_x}{C_p - C_0} = \frac{2}{\sqrt{\pi}} \int_0^{\beta} e^{-y^2} dy,$$

where $\beta = x/2\sqrt{(Dt)}$; $C_p =$ the concentration at plane $x = 0$, assumed constant; $C_x =$ the concentration at plane $x = x$ at time t; $C_0 =$ the concentration, constant for all x, at the beginning of diffusion.

For this solution of Fick's equation the boundary conditions are:

$C = C_p$ for $x = 0$ and all times t,

$C = C_0$ for $x > 0$ and $t = 0$,

$C = C_0$ for $x = \infty$ and all t.

The equation provides three methods of obtaining D, the diffusion constant, which are:

(i) Measure x as a function of t for a constant known C;

(ii) Measure C as a function of t for a given x;

(iii) Measure C as a function of x for a given t.

All three methods were employed successfully in Tiselius's experiments.

The laminated lattice of heulandite has the laminae parallel to the 010 plane. The diffusion of water normal to this plane was found to be $D_{010} < 7 \times 10^{-12}$ cm.^{2} sec.$^{-1}$ at 20° C.; but diffusion of water parallel to the 010 plane was rapid, though

proceeding at different rates across 201 planes and 001 planes. Thus one is introduced to the phenomenon of diffusion anisotropy, exhibited also in "platz-wechsel", or place-change, diffusion of ions in salts (4).

The diffusion of water in the 010 plane, normal to the 201 plane

The first of the three methods of determining the diffusion constant, based on Fick's law, depends upon the linear relation between x^2 and t, at constant C. Fig. 22 gives the $x^2 - t$ curve at a constant C_x value of 13·87 % of water in the
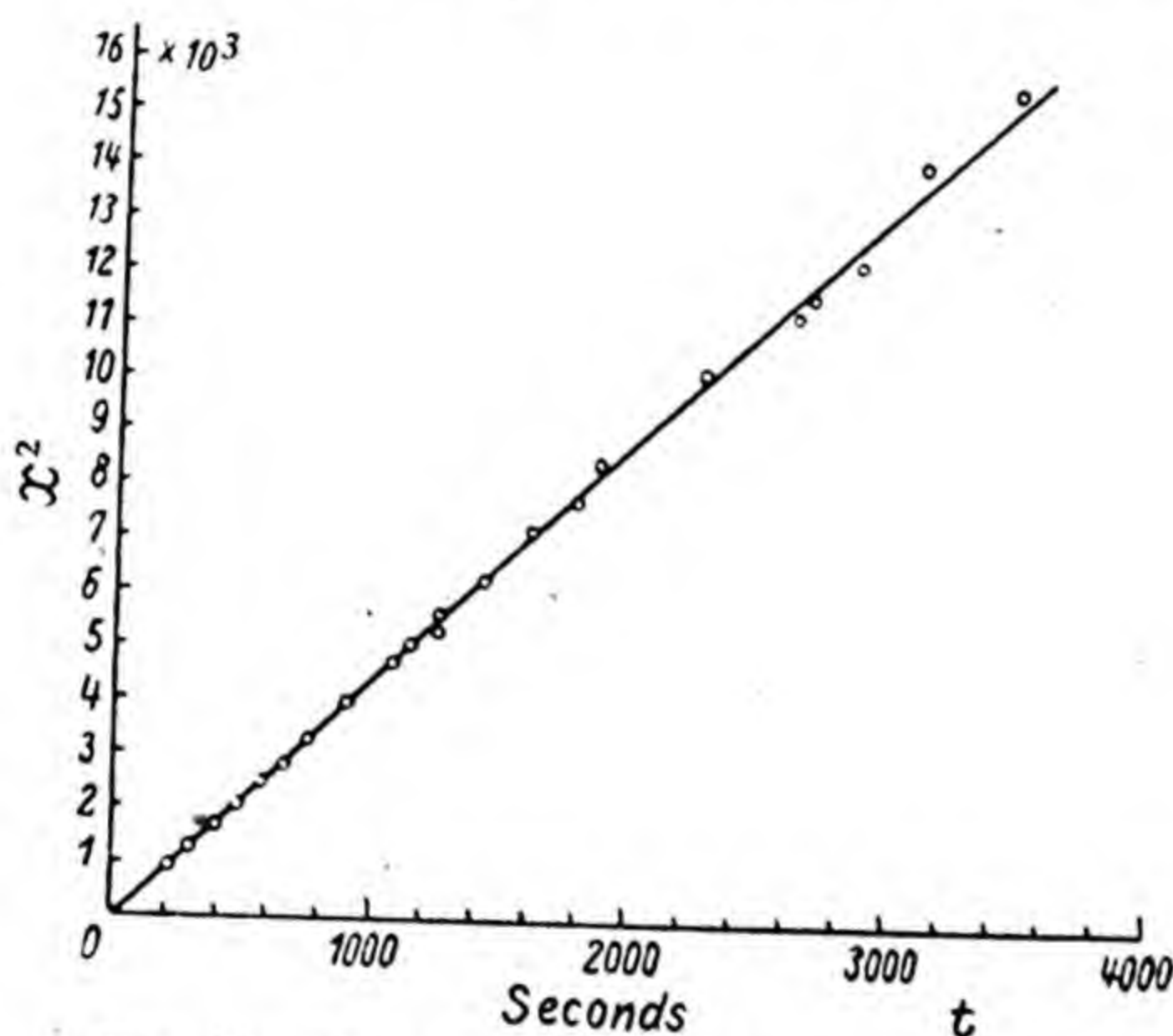
Fig. 22. x^2 as a function of t at constant C.

lattice. Here C_0 was 13·45 % and C_p was 19·67 %, the experiment being performed at 20° C. Thus

$$D_{201} = 3\cdot4 \times 10^{-7} \, cm.^2 \, sec.^{-1}$$

When repeated at different values of C_x, there was evidence that D varied according to the water content of the lattice.

When C was plotted as a function of t at a constant x, the curve of Fig. 23 was found; and when C was plotted as a function of x at constant t, the curve of Fig. 24 was obtained.

In this latter figure the dotted curve gives the value of a $C - x$ curve computed using $D = 3\cdot9 \times 10^{-7} \, cm.^2 \, sec.^{-1}$, and

assuming D to be independent of C. In Tables 11 and 12 are collected the values of D according to these last two methods, as functions of C, using the simple Fick law $\dfrac{\partial C}{\partial x} = D\dfrac{\partial^2 C}{\partial x^2}$ in their evaluation.
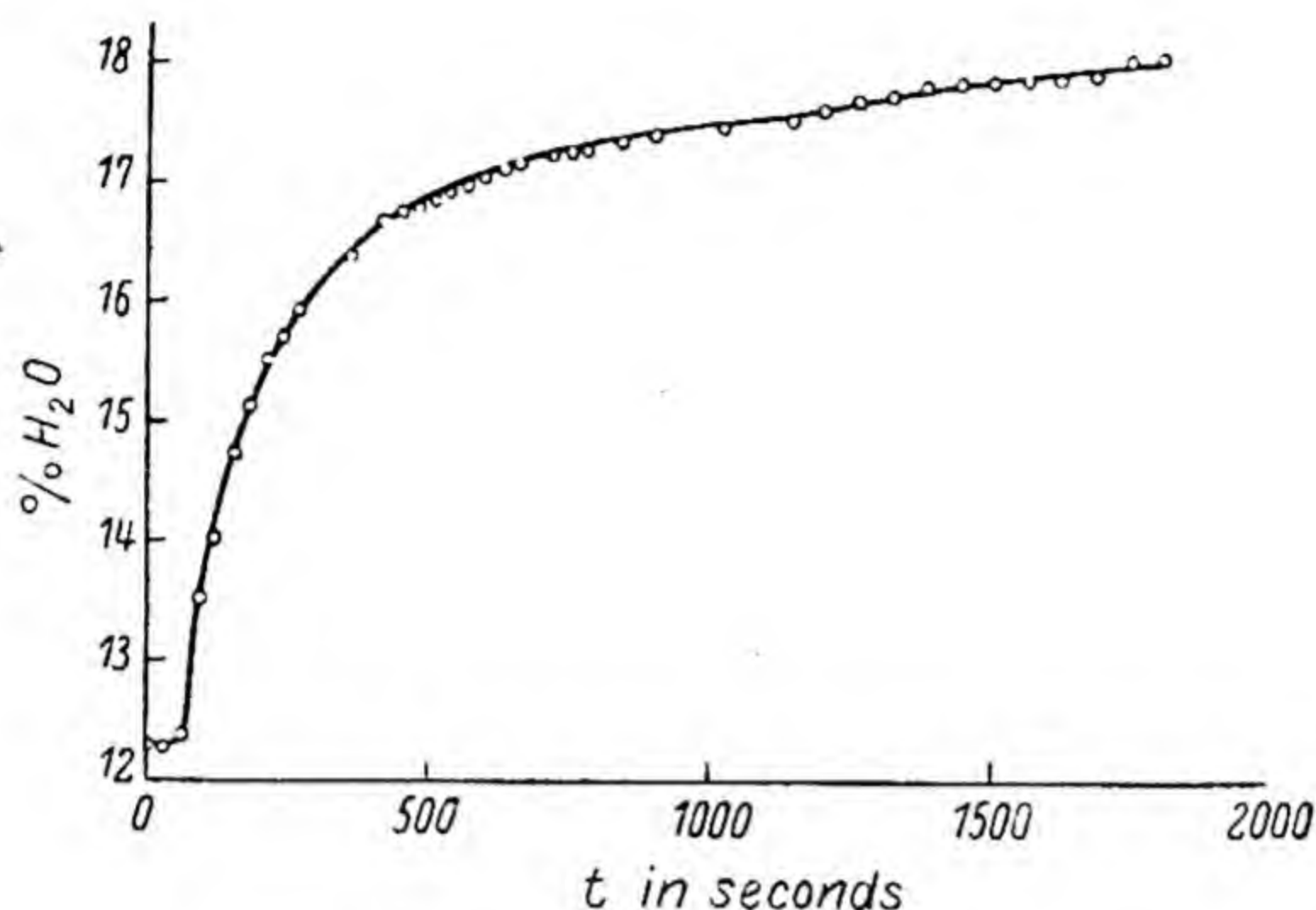
Fig. 23. C as a function of t at constant x.
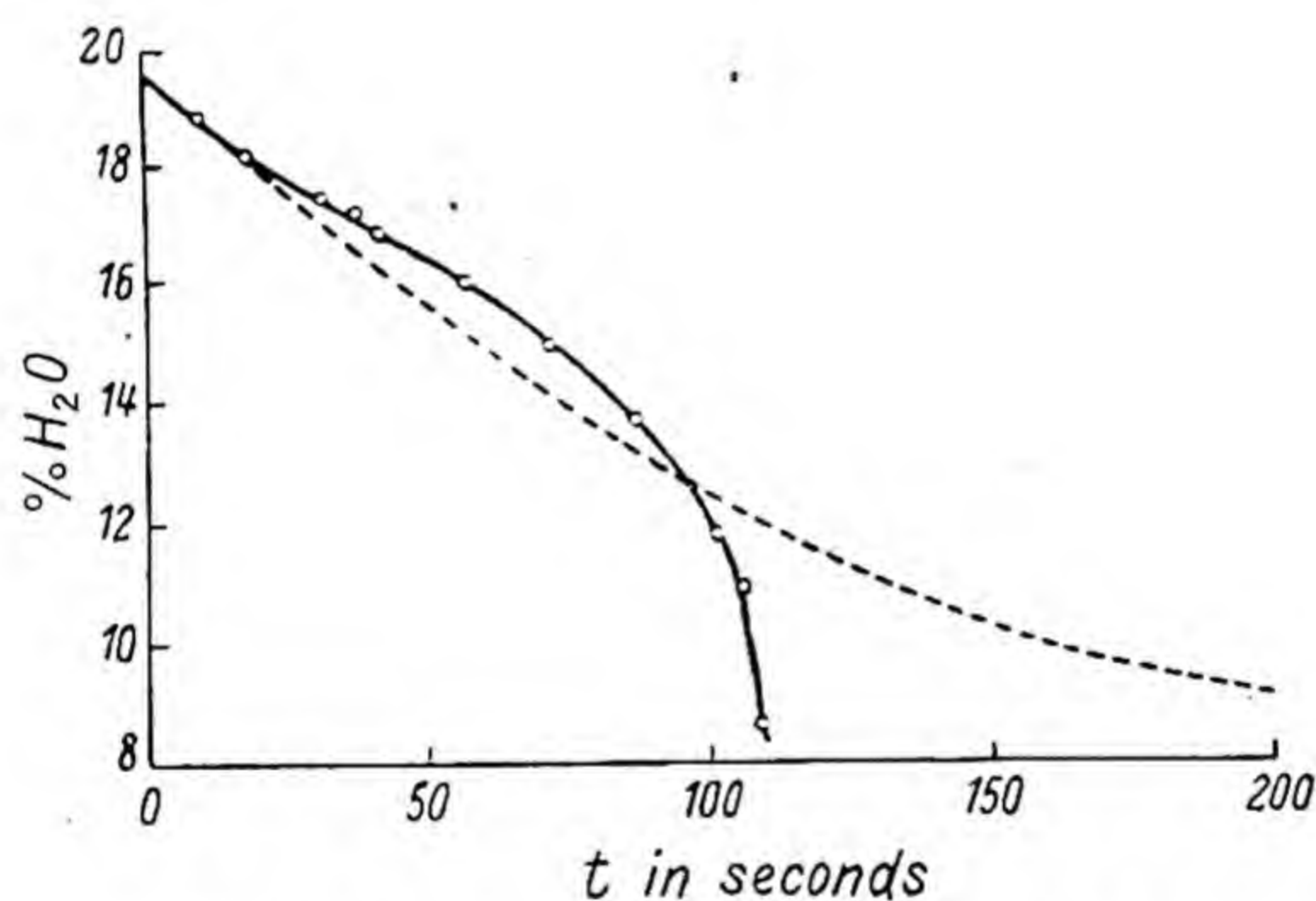
Fig. 24. C as a function of x at constant t.

When the difference between C_p and C_0 was small the values of D were nearly constant, and the simple equation $\dfrac{\partial C}{\partial t} = D\dfrac{\partial^2 C}{\partial x^2}$ more closely obeyed, as is indicated by Table 13.

Hitherto the simplest equation $\dfrac{\partial C}{\partial t} = D\dfrac{\partial^2 C}{\partial x^2}$ has been used.

7-2

TABLE 11. *Diffusion constants from the relation between C as a function of t at constant x*

$C_p = 19 \cdot 67\%$, $C_0 = 12 \cdot 30\%$, $x = 9 \cdot 832 \times 10^{-3}$ cm., $T = 20°$ C.

C_x %	t sec.	$\dfrac{C_p - C_x}{C_p - C_0}$	β	$D \times 10^7$ cm.^{2} sec.$^{-1}$
13·0	81	0·905	1·181	2·4
13·5	93	0·837	0·986	3·0
14·0	112	0·770	0·849	3·4
14·5	140	0·701	0·734	3·6
15·0	169	0·634	0·639	3·9
15·5	212	0·566	0·553	4·2
16·0	283	0·498	0·475	4·2
16·5	377	0·430	0·402	4·4
17·0	577	0·363	0·334	4·4
17·5	1060	0·294	0·267	3·6
18·0	1755	0·227	0·204	3·7

TABLE 12. *Diffusion constants from C as a function of x at constant t*

$C_p = 19 \cdot 67\%$, $C_0 = 8 \cdot 3\%$, $t = 1200$ sec., $T = 20°$ C.

C_x %	x in units $2 \cdot 809 \times 10^{-3}$ cm.	$\dfrac{C_p - C_x}{C_p - C_0}$	$D \times 10^7$ cm.^{2} sec.$^{-1}$
9	108	0·938	1·1
10	107	0·850	1·8
11	105	0·762	2·6
12	99·7	0·675	3·4
13	93·0	0·587	4·2
14	83·0	0·499	5·0
15	70·8	0·411	5·6
16	56·5	0·323	6·0
17	38·0	0·235	5·3
18	21·0	0·147	4·2
19	7·2	0·058	3·3

TABLE 13. *Diffusion constants when the crystal was nearly saturated with water*

$C_p = 19 \cdot 67\%$, $C_0 = 16 \cdot 20\%$, $T = 20°$ C., $x = 11 \cdot 353 \times 10^{-3}$ cm.

C_x %	t sec.	$\dfrac{C_p - C_x}{C_p - C_0}$	β	$D \times 10^7$ cm.^{2} sec.$^{-1}$
16·5	60	0·915	1·218	4·0
17·0	119	0·770	0·894	4·0
17·5	218	0·625	0·627	4·1
18·0	398	0·482	0·457	4·2
18·5	984	0·342	0·313	3·8
19·0	1520	0·266	0·240	4·1

However, there is considerable evidence that D may vary with C (7), in which case the equation to be solved is

$$\frac{\partial C}{\partial t} = \frac{\partial}{\partial x}\left(D\frac{\partial C}{\partial x}\right),$$

for which solutions (5, 6) have been given (Chap. I). Of use in evaluating D is the expression

$$D_{C=C_x} = \frac{1}{2t}\frac{dx}{dC}\int_{C=C_x}^{C=C_0} x\,dC,$$

when C is measured as a function of x for a given time interval. The integral can be evaluated graphically, and the derived value of D refers to that value of C at $x = x_1$. Employing this method, Tiselius succeeded in obtaining a number of diffusion constants for various values of C, which, as Table 14 shows, do indeed depend noticeably on C.

TABLE 14. *Diffusion constants evaluated from* $\dfrac{\partial C}{\partial t} = \dfrac{\partial}{\partial x}\left(D\,\dfrac{\partial C}{\partial x}\right)$

Temp. 20° C., $C_p = 19.67\%$.

C %	$D \times 10^7$ (cm.^{2} sec.$^{-1}$) (exp. with $C_0 = 8.3\%$)	$D \times 10^7$ (cm.^{2} sec.$^{-1}$) (exp. with $C_0 = 13.20\%$)	$D \times 10^7$ (cm.^{2} sec.$^{-1}$) (exp. with $C_0 = 16.20\%$)
10	0.04*	—	—
11	0.2†	—	—
12	0.7	—	—
13	1.3	—	—
14	2.0	2.1	—
15	2.7	2.6	—
16	3.0	3.5	—
17	4.0	4.2	4.0
18	4.0	4.1	4.2
19	3.3	3.5	4.1

* Very uncertain.   † Uncertain.

These results are numerically somewhat different from those obtained earlier with the simple Fick treatment. They show in each case a maximum which might be explained as follows. The heat of sorption is greatest at small C_0; therefore the water molecule is most strongly anchored and is not very mobile. When the lattice has its full complement of water, mobility must also be slight, since few water molecules will

have vacant lattice cells to migrate into, and therefore for intermediate values of C_0 the greatest mobility is possible.

Diffusion anisotropy in heulandite

The permeability perpendicular to the plane of laminae in heulandite is negligible; parallel to this plane it is $> 10^5$ times as rapid, at room temperature. But different directions in the 010 plane have different diffusion constants. This is shown by the photomicrographs in Fig. 25 in which the dark band gives
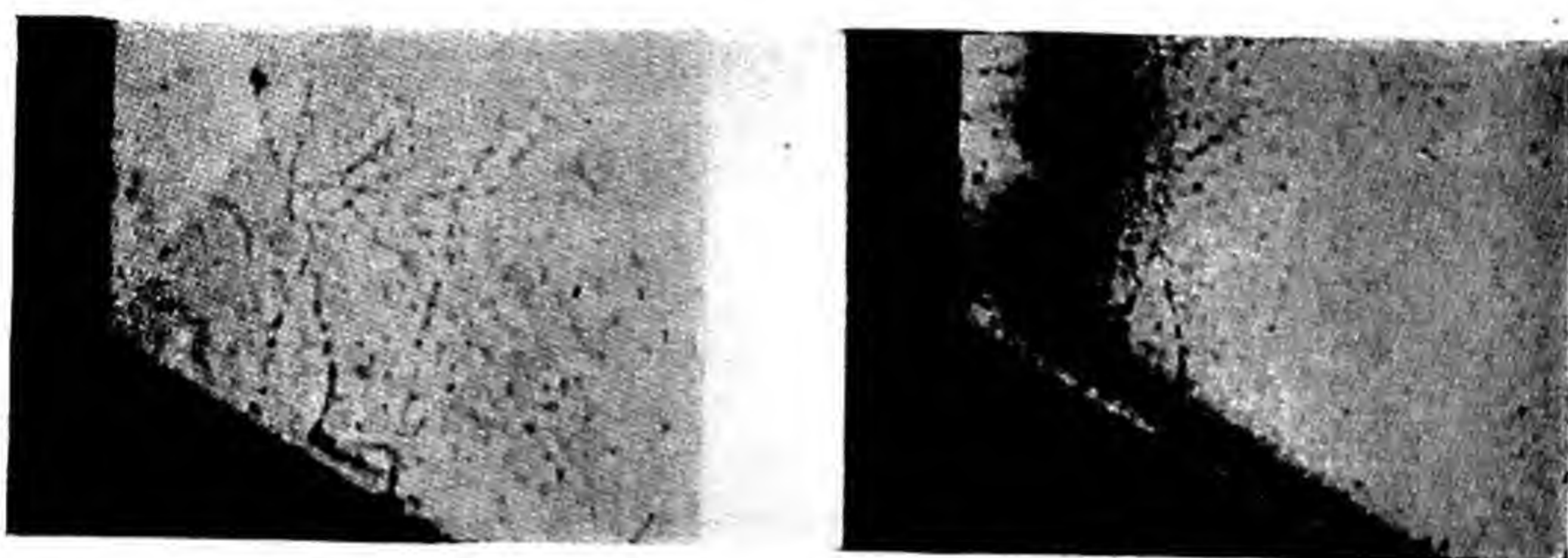
Fig. 25. Progress of diffusion in heulandite, showing diffusion anisotropy.

a measure of the rates of advance of diffusion normal to the 201 and 001 faces, the most rapid advance being found normal to the 201 face. The relative rates of advance of the dark bands are given in Table 5.

TABLE 15. *Diffusion anisotropy*

$C \%$	$x_{201} : x_{001}$
13·21	3·6
14·43	3·4
15·50	3·5
16·25	3·2
17·36	3·4

The ratio $\dfrac{x_{201}^2}{x_{001}^2} = \dfrac{D_{201}}{D_{001}} = 11\cdot 6$, and is constant at a series of values of C_0. When the diffusion velocities normal to the faces 201 and $20\bar{1}$ were measured, it was found that they were equal. Thus for the particular sample of heulandite studied

$$D_{001} : D_{201} : D_{20\bar{1}} = 1 : 11\cdot 6 : 11\cdot 6.$$

The diffusion anisotropy phenomenon was studied in a number of other heulandites, and proved substantially the same in all of them. Always the minimum diffusion rate parallel to the 010 plane was normal to the 001 plane, and the following anisotropy ratios were found:

Heulandite from	D_{201} at 20° C. and $C = 15 \cdot 0\%$	$\dfrac{D_{201}}{D_{001}}$
Dalur, Färoerne	$2 \cdot 7 \times 10^{-7}$	$13 \cdot 6$
Teigarhorn, Iceland	$3 \cdot 7$	15 to 20
Rodefiord, Iceland	$3 \cdot 5$	15 to 20
Sulitelma, Norway	$2 \cdot 3$	15

The energy of activation for the diffusion of water in heulandite

Tiselius measured the diffusion constants at a number of temperatures, finding the values given below:

Temp. ° C.	$D_{201} \times 10^7$ cm.^{2} sec.$^{-1}$	$D_{001} \times 10^7$ cm.^{2} sec.$^{-1}$
$20 \cdot 0$	$2 \cdot 7$	$0 \cdot 23$
$33 \cdot 8$	$4 \cdot 1$	$0 \cdot 45$
$46 \cdot 1$	$4 \cdot 8$	$0 \cdot 66$
$60 \cdot 0$	$7 \cdot 6$	$1 \cdot 45$
$75 \cdot 0$	$11 \cdot 1$	$2 \cdot 8$

From these figures he computed the energy of activation for diffusion normal to the 201 and 001 faces respectively to be 5400 and 9140 cal./mol. The temperature dependence of the diffusion constants he found did not depend appreciably upon the amount of water in the lattice, although we have seen that their absolute magnitudes do.

Diffusion processes in analcite-ammonia

These experiments were made upon a most complex zeolite, heulandite, and were later extended to analcite, which has only one type of lattice hole and a cubic or pseudo-cubic symmetry (7). Once more the optical experiments were performed upon narrow plates cut parallel to cube or diagonal faces. The material was thoroughly outgassed and the sorption processes with ammonia were observed. In Table 16, which

gives the absolute diffusion constants, $\Delta\Gamma$ denotes the difference of the refractive indices of the ordinary and extraordinary rays, which was used as a measure of the amount sorbed.

TABLE 16. *Diffusion of* NH_3 *through* 0·92 *mm. plate cut parallel to cubic surface*

Temp. $= 302°$ C., pressure $= 761·2$ mm., volume of NH_3 sorbed $= 27·5$ c.c./g.

t sec.	$\sqrt{t}$	$\Delta\Gamma \times 10^7$	$D \times 10^8$ cm.² sec.⁻¹
0	0	0	1·4
900	30	40	1·0
3,600	60	66	1·4
8,100	90	119	1·2
14,400	120	151	1·2
22,500	150	183	—

The diffusion rate was the same for a plate cut parallel to the diagonal surface, so that no anisotropy occurs. The temperature dependence of the diffusion velocity was found using powdered analcite, and the equation

$$\Delta Q \propto (C_p - C_0)\sqrt{\frac{Dt}{\pi}},$$

where ΔQ denotes the amount sorbed. This equation supposes that D does not depend upon ΔQ. If one writes

$$\frac{\Delta Q}{C_p - C_0} = \theta = f(D, t)$$

only, the curve θ versus the time, t, or $\sqrt{t}$, should be the same at all pressures. It was shown that this was so for two rate curves at $302°$ C., one with analcite outgassed and $p = 758·6$ mm., the other with the analcite saturated at $p_0 = 578·6$, a further dose of ammonia being admitted at $1385·4$ mm. Then since $\theta = f(D, t)$ only,

$$\frac{D_{T_1}}{D_{T_2}} = \frac{t_{T_1}}{t_{T_2}},$$

and a simple method is available to determine the temperature coefficients and activation energies. The temperature dependence of the diffusion coefficient gave the activation energy for diffusion as 11,480 cal./mol. It was also noted that the

ratio of the diffusion constants at two different temperatures was not dependent upon the amounts of ammonia sorbed.

Other observations on zeolite systems

In a study[2] of sorption by various zeolites, platy, fibrous, and rigid three-dimensional networks, several points of interest were established. Ammonia sorption was most rapid in the lattices of the three dimensional networks (chabasite, analcite). It was least rapid in suitably outgassed fibrous and platy zeolites (natrolite, scolecite, and heulandite). Heulandite, a
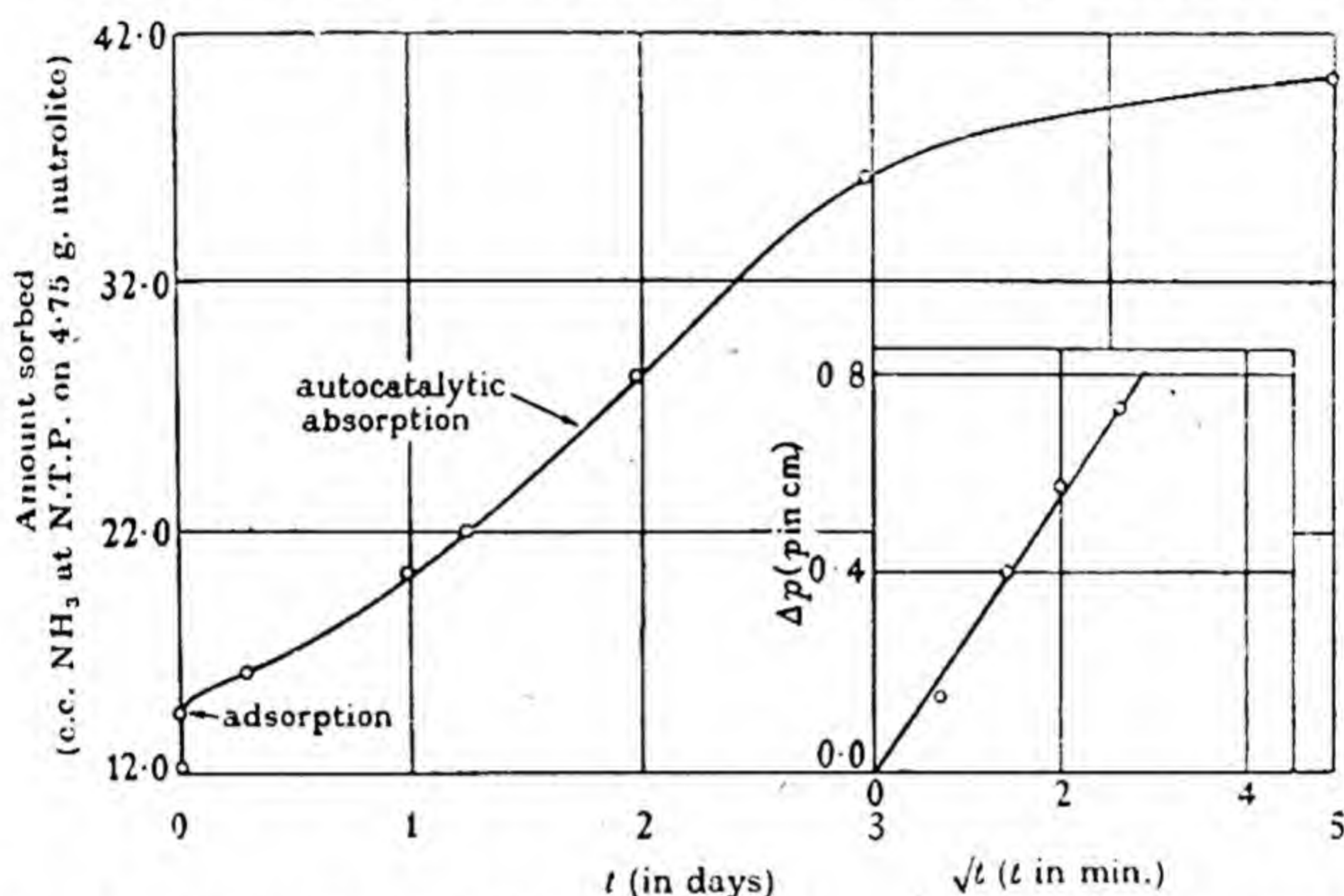
Fig. 26. Sorption velocities. NH_3 on natrolite, showing tendency to autocatalytic sorption rate curves. (NH_3 sorbed before commencing expt. $= 12.11$ c.c. at N.T.P. Inset shows NH_3 on heulandite, sorption rate following the parabolic diffusion law.)

laminated crystal like mica, outgassed at low temperatures (130° C.) to prevent lattice collapse, sorbed ammonia at first rapidly and then more and more slowly, suggesting a rising activation energy with charge. When heated to 330° C., however, heulandite sorbed ammonia much more slowly. Some profound change in the bonding between laminae must have been effected by the high temperatures, associated with the more complete removal of water. For heulandite crystals it will also be seen (Fig. 26) that the sorption rate obeyed the parabolic diffusion law initially, although this law quickly broke down. In natrolite, a fibrous zeolite, sorption in its early

stages was autocatalytic (Fig. 26) and a more or less well-defined ammoniate resulted. The experiments bring out an important point: activated diffusion in zeolites may be a diffusion of interfaces in certain cases (natrolite) and not a diffusion of molecules down a concentration gradient (chabasite, analcite, heulandite).

Another point of interest was the difference in the velocity of ammonia sorption by analcite observed by Barrer[2] and Tiselius[6]. The former found sorption rapid at temperatures as low as 200° C.; the latter found that sorption equilibrium could not be established at 270° C., so slow was the ammonia uptake. These experiments all serve to show the complexity of behaviour of this very interesting series of diffusion systems.

A kinetic theory of diffusion in zeolites

These systems provide a very complete investigation of the diffusion of vapours in zeolites, and the types of phenomena likely to be encountered. They also provide an interesting application of the methods outlined in Chap. I. Kinetic theory may also yield equations of acceptable form for velocities of sorption and for equilibrium data. Such equations were derived by M. Hey[7,8], who expressed Tiselius's data in terms of them and concluded that they were satisfactorily able to represent Tiselius's experiments. Hey derived his equations on the assumptions that water or other vapours may occupy all or part of definite lattice positions, and that the water if given an energy of activation E may become mobile. A plate of zeolite is mounted with a free surface of unit area exposed to the vapour, which diffuses normal to this surface. Water molecules impinging on the surface with an energy E_1 normal to the surface may, if they strike within certain areas, enter that lattice hole nearest the surface. Conversely, molecules in the first lattice hole by acquiring an energy E_2 may re-evaporate, or by acquiring an energy E may diffuse into the lattice. E_2 is usually regarded as being greater than E. In the diffusion problem two extreme cases arise:

(1) Hydration of the zeolite is governed by the sorption and desorption rates at the surface.

(2) Hydration is governed by the diffusion rate into the crystal.

In the latter case
$$D = \frac{d\sqrt{(2E)}}{\pi\chi\sqrt{M}} e^{-E/RT},$$

where d denotes the distance between two successive points of equilibrium of a water molecule in the lattice, χ is a correction term for anharmonicity of vibration of water in the crystal, and the other symbols have their usual significance. When E is a function of x, the vacant fraction of water positions, one may write $E = E_0\{1 + f(x)\}$. The equations involve simplifying assumptions, but were applied to Tiselius's data for water-heulandite diffusion systems. Hey found for this system that for diffusion across the 201 face, from Tiselius's data, $E_{201} = 4{\cdot}79(1 + 0{\cdot}13x) \times 10^3$ cal./mol. from which $d/\chi = 3{\cdot}66$ A., a reasonable value since χ is approximately unity. The diffusion data across the 001 face gave a value of
$$E_{001} = 7{\cdot}3(1 + 0{\cdot}08x) \times 10^3 \text{ cal./mol.} \quad \text{and} \quad d/\chi = 19 \text{ A.},$$
by no means so likely a value. One difficulty is that all the water in heulandite is not held with the same energy; Hey considered three groups of water lattice positions to occur. The data above apply only to the most volatile group ($13{\cdot}11\%$ hydration). Table 17 gives the calculated and observed diffusion constants computed using the data given above.

Similar agreement was found for diffusion across the 001 plane. It may be concluded that an equation of the type deduced by Hey can represent the experimental results when the constants are suitably chosen.

Tiselius's data for ammonia-analcite systems however allow the simplified form
$$D = \frac{d\sqrt{(2E_0)}}{\pi\chi\sqrt{M}} e^{-E_0/RT}$$
to be applied, since E does not appear to vary with x. Hey calculated $E_0 = (1{\cdot}35 \pm 0{\cdot}05) \times 10^4$ cal./mol. of ammonia from Tiselius's data, while from X-ray examination $d = 5{\cdot}93$ A.

Thus $D^{302°C} = (3.5 \pm 2) \times 10^{-8}$ cm.^{2} sec.$^{-1}$, which constant Hey[8] showed for various simple cases was one-third the diffusion constant along a particular set of channels, as measured by Tiselius. Thus from X-ray data and the calculated value of E_0 the diffusion constant was $(1.2 \pm 0.7) \times 10^{-8}$ cm.^{2} sec.$^{-1}$ compared with the directly measured value 1.2×10^{-8} cm.^{2} sec.$^{-1}$, both at 302° C.

TABLE 17. *Diffusion data for heulandite, calculated and observed*

% H_2O ... x ...	19 0.10	18 0.255	17 0.41	16 0.56	15 0.71	14 0.865
$10^7 \times D_{201}^{20°C.}$ cm.^{2} sec.$^{-1}$ (obs.)	3.3, 3.5, 4.1	4.0, 4.1, 4.2	4.0, 4.0, 4.2	3.5, 3.6	2.6, 2.7	2.1, 2.0
$10^7 \times D_{201}^{20°C.}$ cm.^{2} sec.$^{-1}$ (calc.)	4.47	4.27	3.80	3.32	2.70	2.14
Temp. °C. ...	20.0	33.8	46.1	60	75	—
$10^7 \times D_{201}$, for $x = 0.71$, in cm.^{2} sec.$^{-1}$ (obs.)	2.7	4.1	4.8	7.6	11.1	—
$10^7 \times D_{201}$, for $x = 0.71$, in cm.^{2} sec.$^{-1}$ (calc.)	2.70	4.10	5.60	7.90	11.0	—
% H_2O ... x ...	18.5 0.18	17.5 0.33	16.5 0.48	15.5 0.64	14.5 0.79	13.5 0.94
$\dfrac{D_{201}^{16°C.}}{D_{201}^{20°C.}}$ {obs. {calc.	1.7 1.93	2.0 1.93	1.8 1.94	1.8 1.98	1.8 2.03	1.7 2.09

DIFFUSION IN ALKALI HALIDE CRYSTALS

Introductory

Experiments designed to clarify photochemical processes in alkali metal and silver halides have led to some interesting studies on the diffusion of metal vapours[9,10], halogen vapours[11] and hydrogen[12] in alkali halides. It is possible to prepare transparent single crystals of the halides of the greatest chemical purity. It was found that the halides can act as solid solvents for a number of substances, and that the properties of these mixtures or solutions permit one to study photochemical processes and diffusion. Thus, potassium

vapour dissolves in potassium halides giving a number of "colour centres" or "Farbzentren" which give rise to a definite absorption band in the crystal (Fig. 27) [13]. In a similar way, a solution of potassium hydride in potassium bromide gives rise to another typical absorption band (Fig. 27). Exposing a crystal containing colour centres to hydrogen produced a solid solution of potassium hydride in potassium bromide, whereas exposing the hydride-bromide solution to light re-formed the potassium colour centres. What is true for one
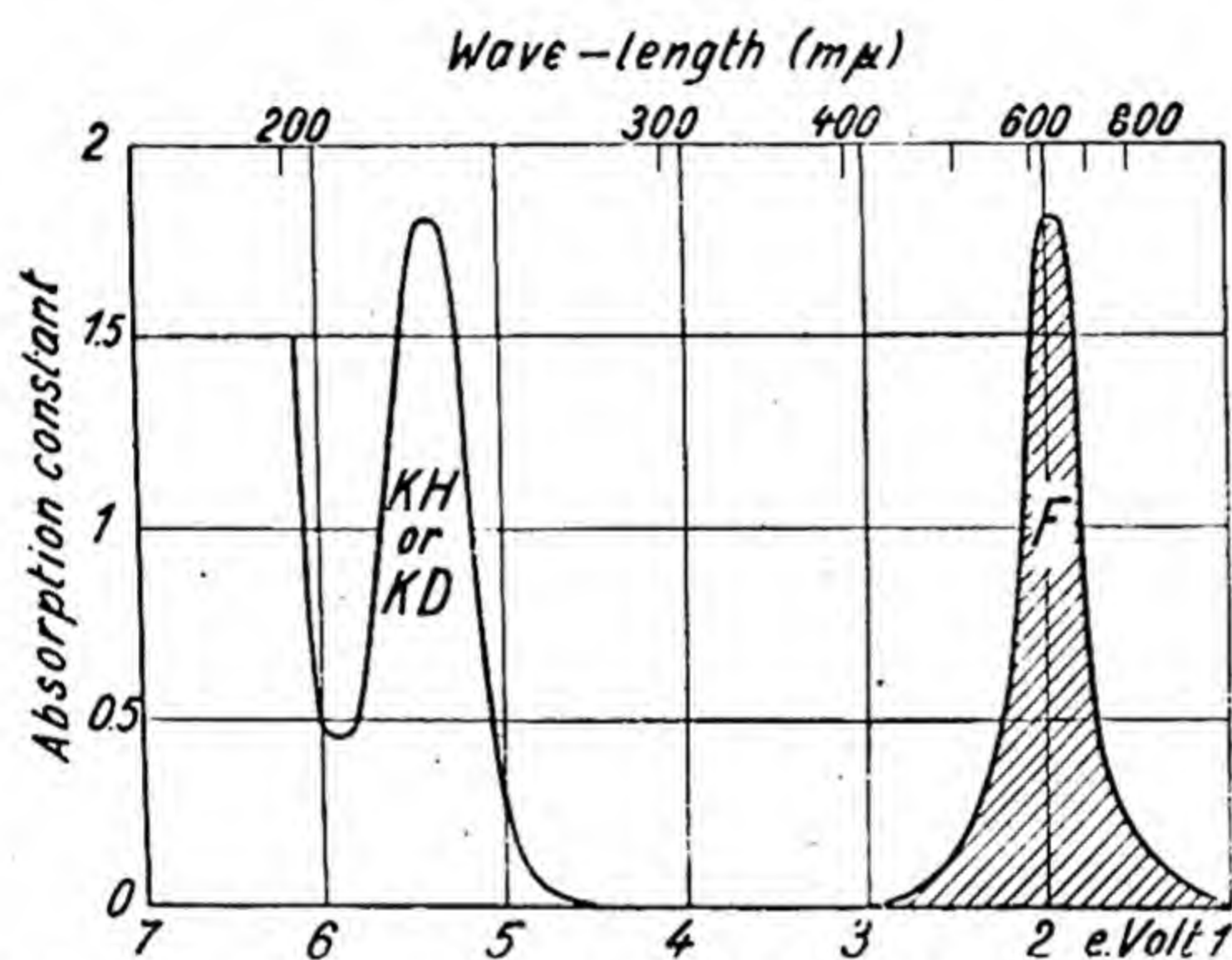
Fig. 27. Optical absorption bands of KH-KBr solid in which about half the KH has been decomposed photochemically giving "Farbzentren".

halide may in general be taken as true for others (RbBr [13], KI [13], KCl [13]). The studies on halides containing potassium and potassium hydride were extended to cover solubility and diffusion of halogens and hydrogen, and it is with these systems as with the mobility of Farbzentren that the data now to be given are concerned.

The number of colour centres per unit volume of halide may be measured optically, after impregnating the crystal with alkali vapour. It can be shown that

$$N = \text{constant} \times K_m \times H$$

$$= \text{constant} \times \text{area of the band "} F \text{" of Fig. 27,}$$

where K_m is the absorption constant at the maximum in the band, and H is the breadth of the band at $K = \frac{1}{2} K_m$.

The concentration of colour centres may also be determined from the conductivity, since each potassium atom can give rise to an electron (e.g. K in KI).

The corresponding investigations upon solutions of the halogens in halide crystals were also attempted using the conductivity of the crystal as a means of estimating the halogen excess (11). For potassium bromide and iodide a rise in conductivity followed their exposure to Br_2 and I_2 vapour respectively, but in Cl_2-KCl systems no rise in conductivity was observed. The diffusion of halogens in halide crystals was also followed by saturating the crystal with thallium vapour, which imparted to it a brown tint. Then, as the halogen subsequently diffused inwards, the brown tint disappeared as the boundary advanced, due to the formation of colourless or white thallium halide. The progress of the colour boundary served to measure the diffusion rate.

In H_2-KBr systems the concentration of hydrogen was very slight, and was best determined by subsequent heating of the crystal containing hydrogen in potassium vapour. In this way potassium hydride was formed, the concentration of which in the mixed crystal KBr + KH can be determined optically, the concentration in atoms per c.c. being

$$(KH) = 5 \cdot 1 \times 10^{16} K_m$$

(K_m = absorption constant of optical absorption maximum). The diffusion of hydrogen was followed by the same method as was employed for the halogens, using as indicator metal potassium and following the movement of the boundary K-KH (blue to colourless) through the crystal.

The experimental results on solubility and diffusion

Potassium dissolved in both potassium bromide and potassium chloride exothermally, the heats of the processes being given by

$$\Delta H_{(K \text{ vap.} \to K \text{ in } KBr)} = -5 \cdot 8 \text{ k.cal./atom of K,}$$

$$\Delta H_{(K \text{ vap.} \to K \text{ in } KCl)} = -2 \cdot 3 \text{ k.cal./atom of K.}$$

At high temperatures the potassium was dispersed in atomic form, but on slow cooling to lower temperatures it could be condensed into colloidal aggregates. The halogens and hydrogen dissolved endothermically in halide lattices, the heats of solution being

$$\Delta H_{(I_2 \text{ vap.} \to I_2 \text{ in } KI)} = 18 \cdot 5 \text{ k.cal./g.mol. } I_2,$$

$$\Delta H_{(Br_2 \text{ vap.} \to Br_2 \text{ in } KBr)} = 27 \cdot 6 \text{ k.cal./g.mol. } Br_2,$$

$$\Delta H_{(H_2 \text{ gas} \to H_2 \text{ in } KBr)} = 16 \text{ k.cal./g.mol. } H_2.$$

The main feature of interest in the results is that the solubility in each case is proportional to the external gas pressure, so that the halogens and hydrogen dissolve in molecular form. The results on diffusion show too that thermal diffusion occurs mainly in molecular form, there being little dissociation, save perhaps for the halogens at the lowest pressures when simultaneous atomic and molecular diffusion takes place (11).

.It is doubtful, when solution occurs as molecules (e.g. H_2, Br_2, Cl_2, in KBr, KCl), whether the molecules are homogeneously dispersed. The "solute" is most likely to be dispersed along faults and glide planes in the crystal. The mere introduction of large foreign molecules into a perfect lattice would distort the lattice locally, and create a fault. Hilsch and Pohl(13), however, pointed out that when KH is formed in KBr the system KH-KBr is a true solution, since the lattice constant of potassium bromide is a linear function of the potassium hydride content.

When both hydrogen and alkali metal vapour were in contact simultaneously with the crystal, which contained a constant amount of potassium, the amount of potassium hydride at the surface was fixed by the equations

$$KH \rightleftharpoons K + \tfrac{1}{2}H_2,$$

$$\kappa = \frac{(K)\sqrt{p_0}}{(KH)} \qquad \text{(Mass Action).}$$

It was established through the optical absorption of successive thin layers of the crystal that the potassium hydride gradient decreased inwards nearly linearly with distance, and it was

then found that two equations for the depth of penetration, x, of hydride could be derived [12] according as the hydrogen diffused as molecules (1) or as atoms (2):

$$\frac{x^2}{t} \simeq 16D\frac{\kappa k}{(K)}\sqrt{p_0}, \qquad (1)$$

$$\frac{x^2}{t} \infty \frac{1}{(K)}. \qquad (2)$$

In the relation (1), k is the Henry's law solubility coefficient for molecular hydrogen in the crystal. Experiment showed [12] that equation (1) was correct, so that hydrogen is both dissolved as molecules and diffuses as molecules. The derived value for D was $2\cdot3 \times 10^{-4}$ cm.^{2} sec.$^{-1}$ at 680° C.
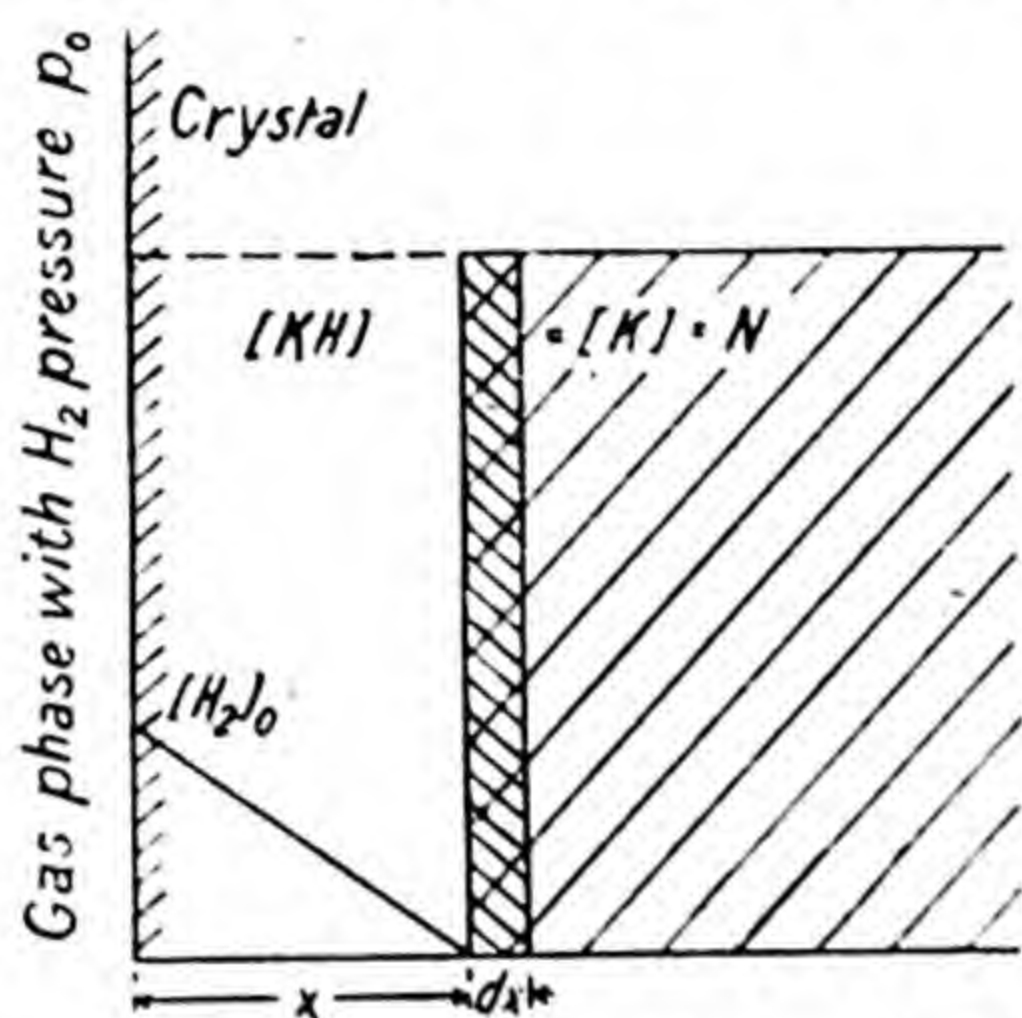
Fig. 28. Diagrammatic representation of penetration by hydrogen of KBr containing an initial uniform excess of K.

If a crystal containing a given uniform concentration, N, of alkali metal is exposed to hydrogen, after the lapse of time t, an approximately linear hydrogen concentration gradient may be assumed to extend into the crystal (Fig. 28) a distance x. During the time interval dt the gradient will extend a further distance dx. If dn/dt denote the hydrogen stream (as molecules),

$$\frac{dn}{dt} = \frac{N}{2}\frac{dx}{dt} = D\frac{(H_2)_{x=0}}{x},$$

whence $D = \dfrac{Nx^2}{p_0 t}\dfrac{1}{4k}$, if k is defined by $(H_2)_{x=0} = kp_0$. Thus Nx^2/t should be a linear function of p_0, a prediction which the

diagrams of Fig. 29 show is substantially correct. The diffusion constants computed from this relationship were

$$D_{600°C.} = 5\cdot5 \times 10^{-4} \text{ cm.}^2 \text{ sec.}^{-1},$$

$$D_{520°C.} = 3\cdot5 \times 10^{-4} \text{ cm.}^2 \text{ sec.}^{-1}$$

The measurements on the movement of bromine and iodine were made along similar lines, the halogen diffusing into the salt containing thallium as indicator. The concentration of
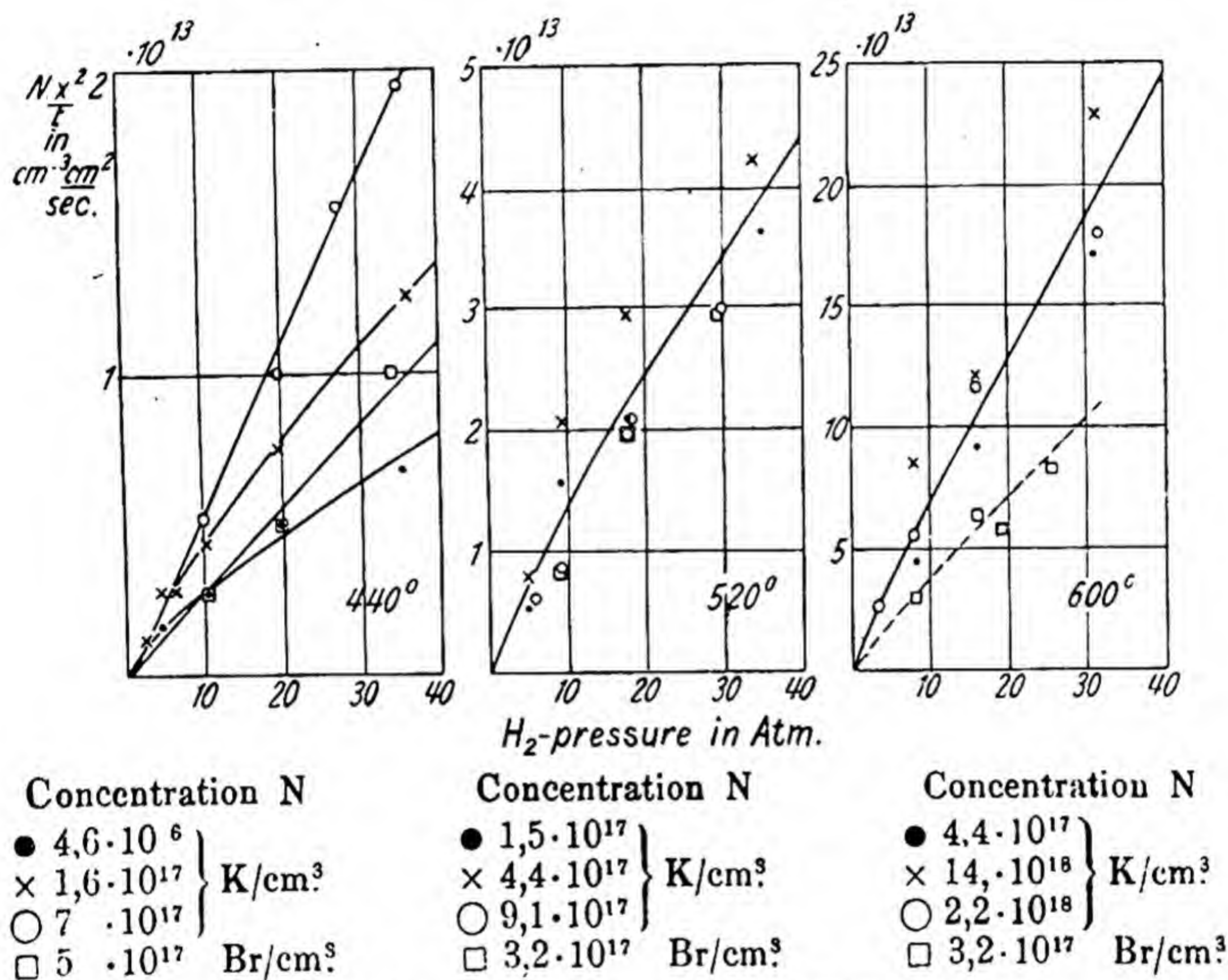
Fig. 29. The linear relation between Nx^2/t and p_0.

Concentration N	Concentration N	Concentration N
● $4,6\cdot10^6$ ⎫	● $1,5\cdot10^{17}$ ⎫	● $4,4\cdot10^{17}$ ⎫
× $1,6\cdot10^{17}$ ⎬ K/cm³	× $4,4\cdot10^{17}$ ⎬ K/cm³	× $14,\cdot10^{18}$ ⎬ K/cm³
○ $7\cdot10^{17}$ ⎭	○ $9,1\cdot10^{17}$ ⎭	○ $2,2\cdot10^{18}$ ⎭
□ $5\cdot10^{17}$ Br/cm³	□ $3,2\cdot10^{17}$ Br/cm³	□ $3,2\cdot10^{17}$ Br/cm³

the thallium within the crystal was large compared with the concentration of absorbed halogen (Fig. 30). If n is the quantity of halogen (expressed in atoms) diffusing through unit cross-section in time t, one may write

$$\frac{dn}{dt} = \frac{dx}{dt} \times N = D\frac{dC}{dx} = D\frac{(C)_{x=0}}{x},$$

since an approximately linear halogen gradient was established. Thus

$$\frac{x^2}{2t}N = D(C)_{x=0},$$

and so according as diffusion occurs as atoms (or ions), or as molecules, one would have $\dfrac{x^2}{2t} N$ a linear function of $\sqrt{p}$ or p respectively. When the experiments were made it was shown that the diffusion occurred mainly as molecules[11]. Table 18 then gives the results for D for several temperatures and at several halogen pressures. In Table 18 are included some diffusion constants for potassium vapour, determined by an electrical method[11]. It is possible that some diffusion of bromine occurs as a diffusion of ions or atoms, but parallel measurements of D_{Br^-} by the electrical conductivity method showed that at high pressures (above 1 atm.) transport of bromine as Br^- was much less important than its transport as Br_2. Below 1 atm. a greater percentage of dissociation occurred, with consequent enhancement of the percentage of transfer as ions.

Fig. 30. Schematic representation of the permeation of thallium-containing halide by halogen.

Since the diffusion of hydrogen and of halogen is mainly as molecules, and since they are dissolved within the halide in the molecular state, one may include them in the same family of diffusion systems as gas-silica (p. 117) and gas-rubber systems, i.e. non-specific activated diffusions. They differ from the latter systems in one respect—the solution processes in the halides are highly endothermic (p. 111) compared with the very slight endothermicity of hydrogen solubility in silica (p. 140) and the slight exothermicity of hydrogen solubility in rubbers (p. 418, Chap. IX). The temperature coefficients of bromine diffusion in potassium bromide are small (Table 18), and correspond to energies from 3 k.cal./g.mol. at 1 atm. pressure to 8 k.cal./g.mol. at 16 atm. pressure. For hydrogen the energy is about 8 k.cal./g.mol. in potassium bromide, while for potassium it is about 16 k.cal./g. atom in the same crystal.

In addition to these studies of solution and diffusion in halide crystals, so important when one considers photochemical and conductivity phenomena in crystals, there has been a number of investigations upon the sorption of dipole gases by alkali halide crystals. That water may penetrate a rock salt crystal has been shown from the infra-red absorption spectrum of the crystal after dipping it in water. In the interior of the

TABLE 18. *Diffusion constants of* Br_2 *and of* K *in* KBr

Temp. ° C.	500			600			700		
Br_2 pressure (atm.)	1	4	16	1	4	16	1	4	16
$D_{Br_2} = N/(C)_{x=0}\, x^2/2t$ in cm.^{2} sec.$^{-1}$ ($\times 10^{-4}$)	2·33	1·33	0·9	2·64	2·28	1·65	3·33	3·0	2·7
D_K from an electrical conductivity method ($\times 10^{-4}$)	0·8			3·0			8·0		

crystal the infra-red spectrum of water may be observed. No study has been made of the velocity of sorption of water by alkali halide crystals, but a number of workers have observed and measured slow sorption processes for the following systems:

$$SO_2 \text{ in } NaCl\,(13a),$$

$$HCl \text{ in } KCl\,(14),$$

$$NH_3 \text{ in } NaCl\,(13b, 13c).$$

In the case of the two latter systems the data obtained showed that a slow activated diffusion occurred into the crystal substance, which followed the Fick diffusion law $\dfrac{\partial C}{\partial t} = D\dfrac{\partial^2 C}{\partial x^2}$, and gave as the temperature coefficient of D

$$E_{HCl-KCl} \sim 7000 \text{ cal./mol.}$$

$$E_{NH_3-NaCl} \sim 6300 \text{ cal./mol.}$$

These experiments were performed upon polycrystalline masses, and it is probable that diffusion occurred down grain boundaries. No experiments upon single crystals designed to

test this point are, however, available. Little experimental work has as yet been carried out upon the diffusion of water in hydrated crystals. The progress of such a diffusion may be followed by using heavy water as diffusing liquid in a crystal with light water of crystallisation. Preliminary measurements of this kind have been made by Kraft (13d) upon the diffusion of D_2O into alum. Kraft obtained data at 75, 65 and 55° C. which conform to the expression

$$D = 0.56 \times 10^{-7} e^{-6000/RT}.$$

DIFFUSION OF HELIUM THROUGH SINGLE CRYSTALS OF IONIC TYPE

The passage of helium gas through a perfect ionic crystal has not so far been detected with any degree of certainty. On account of the laminar structure of mica, and the crystallographic perfection of the laminae, it would be of great interest to establish helium diffusion across the laminae. Rayleigh attempted to measure the helium permeability both at

TABLE 19. *The helium permeabilities of ionic crystals*

Substance	Permeability at ° C. in c.c./hr./cm.²/mm./ thickness/atm. pressure
Quartz (cut ⊥ to optic axis)	$<0.05 \times 10^{-8}$
Mica (cleavage plate)	$<0.06 \times 10^{-9}$
Calcite (cleavage plate)	$<0.05 \times 10^{-8}$
Fluorite	$<0.2 \times 10^{-8}$
Rocksalt	$<0.2 \times 10^{-6}$
Selenite (cleavage plate)	$<0.7 \times 10^{-9}$
Beryl (cut ⊥ to optic axis)	$<0.1 \times 10^{-8}$
Beryl (cut ‖ to optic axis)	$<0.15 \times 10^{-7}$

20° C. (15) and at 415° C. (16). At the latter temperature the permeability was still below 7×10^{-8} c.c./day/cm.²/mm. thickness/atm. pressure, more than 10^{-4} times as small as the helium permeability of silica glass at 20° C. The figure given was about the limit of sensitivity of the apparatus.

No better success has attended the efforts of Urry (17), or of Rayleigh (15) to measure the helium permeability of quartz, the densest of the crystalline forms of silica, and of beryl. The

latter substance is of special interest since channels run parallel to the optic axis, of a diameter slightly greater than that of a helium atom. Table 19 gives the results of Rayleigh's attempts to measure helium permeabilities of a number of crystals. The permeabilities are less than the sensitivity limits of the apparatus.

THE PERMEABILITY OF GLASSES TO GASES

That silica glass is permeable at high temperatures has been known for a considerable time. Reference to this property was made by Watson [18], who used it for the interesting object of purifying helium for an atomic weight determination by means of its selective diffusion through silica glass. Some earlier and some later references have been made by Villard [19], Berthelot [20] and others [21, 22, 23]. Among the earliest quantitative measurements were those of Wüstner [24], who studied both permeation rates and absorption coefficients up to 800 atm. Alty [25] recognised the phenomena as examples of activated diffusion and applied to them a treatment akin to that evolved by Ward [26] and Lennard-Jones [27] for the activated sorption of hydrogen by copper. The experimental and theoretical aspects were extended by Barrer [28] who succeeded in identifying the type of interaction involved in the migration process.

Methods of measurement of gas flow through glasses and crystals

It is usual in the study of gas flow through glasses to use an apparatus which is in essence a chamber containing the gas separated from an evacuated chamber by the membrane whose permeability is being studied. The pressure in the gas-filled chamber is sensibly constant, since the rate of passage of gases through a glass is small, and under ordinary conditions will be varied from one experiment to another from a few centimetres to an atmosphere. The rate of growth of pressure on the high vacuum side is followed by pressure-measuring devices such as the McLeod gauge, Pirani gauge or ionisation

gauge. The problem of mounting the membrane offers little difficulty where soda glass, pyrex, borosilicate glass, silica glass and other glasses are concerned, for these glasses may be blown into double-walled vessels of the types illustrated in Fig. 31. When the glass is available in the form of plates, the latter may be mounted only with difficulty (cf. Fig. 32). Urry (33) mounted flat disks of quartz, basalt, and other rocks upon the ground-glass flanges of a glass tube which led to a gas-analysis apparatus. The specimen was made to adhere to the
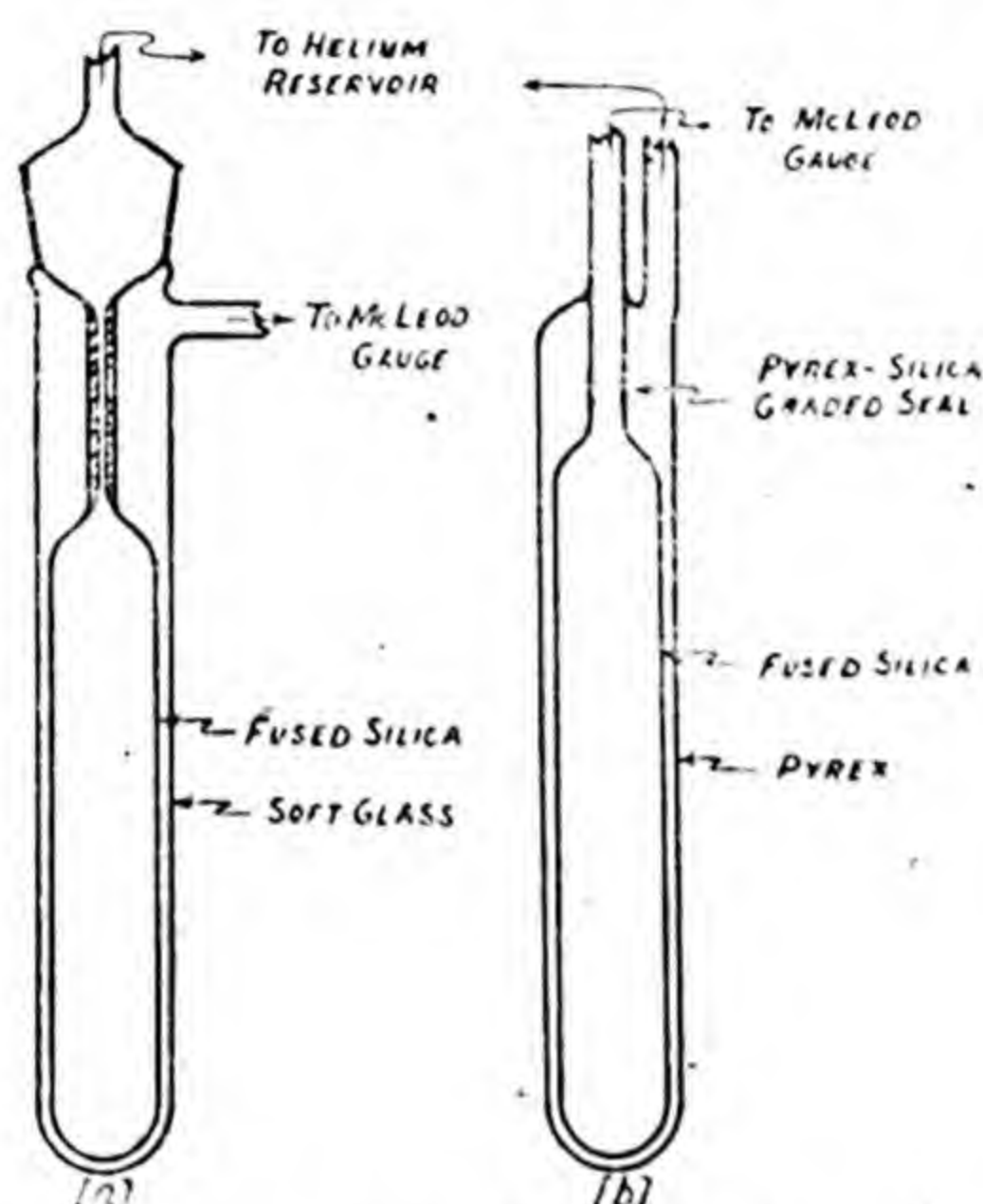
Fig. 31. Types of double-walled diffusion cell.

ground-glass plate by means of a little tap grease, and was sealed off from leakage between it and the ground-glass flanges by filling the apparatus with mercury up to the top edge of the specimen.

The experiments of Wüstner (24) were made at very high pressures and temperatures, so that special requirements had to be met. The diffusion cells were contained in a platinum oven which in turn was in the interior of a steel bomb. The pressure was transmitted to the bomb from the pump (with oil as transmitting fluid), through the separator which was a U-tube containing mercury, to water, which filled the bomb. The requisite temperature within the bomb was reached by the use of the platinum oven. The silica diffusion cells inside

the oven contained the hydrogen imprisoned by mercury seals. This hydrogen was compressed when the pressure was raised, its pressure being given by the gauge, and its temperature by thermo elements leading from the oven. The pressure of hydrogen on one side of the silica was thus high (700–1000 atm.); on the other side it was negligible, and diffusion consequently occurred through the small thin-walled silica bulb into which the hydrogen was compressed. The ingoing and outgoing sides of the silica wall were both open to the pressure-transmitting liquid, so that there was no nett pressure gradient across the wall, and so no danger of mechanical rupture. The volume of hydrogen which diffused through the silica was estimated from the movement of the mercury seal in the silica diffusion cell.

Rayleigh (16) succeeded in the technically difficult task of mounting a mica plate for diffusion experiments at temperatures up to 415° C. The principle of his method was to keep an outer annulus of the plate cold and thermally insulated as far as possible from the inner part of the plate which was kept hot (Fig. 32). The mica plate was held between steel disks, which had a hot inner section and an outside ring water-cooled. The outside ring was separated from the inner disk by narrow
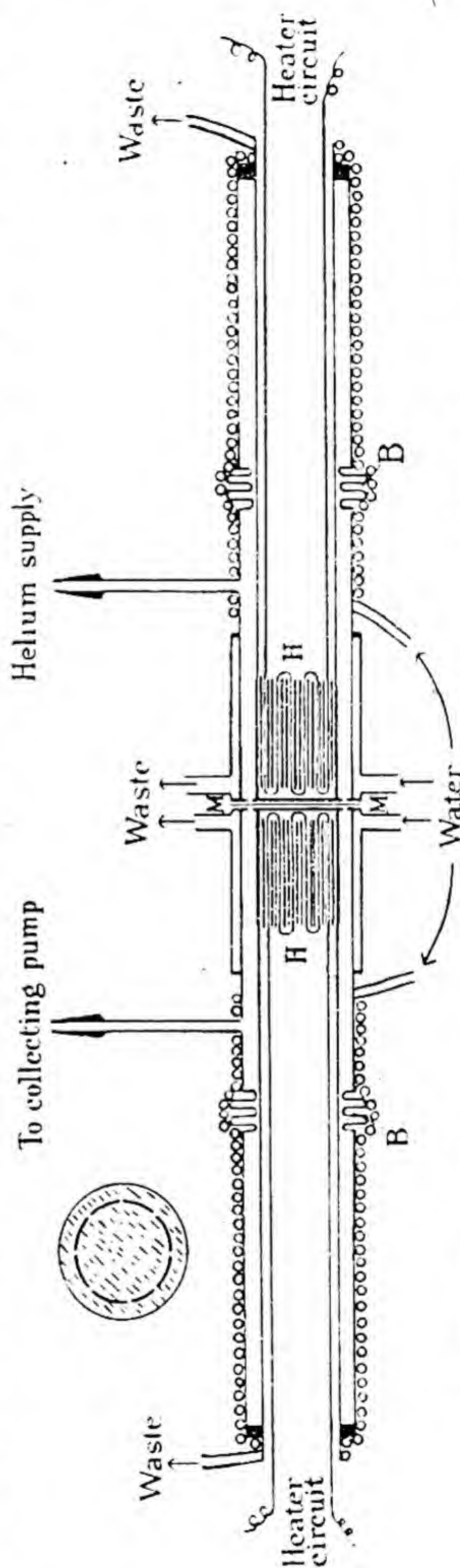
Fig. 32. Rayleigh's apparatus for studying the helium permeability of mica at 415° C.

steel ribs which gave rigidity to the whole, and reduced heat conduction from the hot central disk to the outer annulus. The mica disk was sealed with red wax to the steel annuli on either side of it. In its central part, through which diffusion was to occur, the mica bore sufficiently lightly upon the central steel disks for the helium to pass easily between mica and steel and so to collect in the low-pressure chamber. The mounted membrane was fixed across a steel tube, the two halves so formed serving as chambers to supply the helium at constant pressure, and to collect it. Not only the annuli but also the steel tube was water-cooled. The heating was carried out by means of nichrome wire bent back and forth and passing through silica tubing, there being one heating coil on each side of the mica disk. The diffused gas was removed for analysis by a Toepler pump.

The principal characteristics of the permeation process

The main features observed when one studies the passage of gases through membranes are:

(1) The Fick diffusion law $P = D\dfrac{\partial C}{\partial x}$ (P denotes the permeability and D the diffusion constant) is true in the stationary state (33, 24, 32).

(2) Stationary flow is established in a period of minutes, the actual time depending on the temperatures.

(3) The permeation rates are usually proportional to the pressure and inversely proportional to the thickness of the membrane (29).

(4) The velocity of diffusion is only slightly altered by roughening the outgoing surface (29).

(5) The passage of an electric discharge through either the glass wall or through the gas (hydrogen or helium) has no effect upon the diffusion rate (17).

(6) The process of permeation through these glass membranes is highly selective, and markedly temperature de-

pendent, so that by proper choice of temperature zones one could in theory very effectively separate certain gases (O_2 and He; air and He; argon and He; H_2 and argon, etc.).

Dependence upon pressure of the rate of permeation

A linear pressure dependence of the permeation rate is indicated by the results of various observers [24, 30, 28, 31, 32]. It was immaterial whether the gas was monatomic (He) or diatomic (H_2, O_2, N_2), the same linear relation was obtained. There is one contrary result [33], data on the velocity of permeation of helium through pyrex, soda, lead, and Jena 16[III] glasses being reported as conforming to an equation $dp/dt = \alpha p^n$. The values of n were given as follows:

Pyrex glass $n = 0 \cdot 88$,

Lead glass $n = 0 \cdot 56$,

Soda glass $n = 0 \cdot 64$,

Jena 16[III] glass $n = 0 \cdot 66$.

It was also stated that the value of n was nearly proportional to the amount of $SiO_2 + B_2O_3$. These results need further testing, since helium cannot be dissociated in diffusing (which would give a law $dp/dt = \alpha p^{\frac{1}{2}}$), so that the only possibilities remaining are that helium entered the glass from an adsorbed phase which does not obey a distribution law $x = kp$ (where x denotes the amount adsorbed), or that irreversible changes were occurring in the structure of the glass. At room temperature on glass helium more than all gases should be adsorbed according to Henry's law ($x = kp$).

The nature of the permeation process through silica glass

The observation that the diffusion rate (save for the exceptional data of Urry) is proportional to the pressure is typical of a very wide class of diffusion membranes of silica, glass, basalt, rubber, porcelain, cellulose, collodion, and various polymeric products from styrene, vinyl acetate and similar substances. It may be characteristic of activated diffusion (p. 125) or of various types of flow down tubes (Chap. II). On the other hand, there are

systems where permeation velocities are proportional to $\sqrt{p}$ (p denoting pressure), exemplified by the diffusion of hydrogen through nickel, iron, copper, palladium, platinum and other metals. In this type of system diffusion appears to be a *specific* property of the system considered. No trace of helium will diffuse through palladium [34] or copper [35], though the helium atom is much smaller than the hydrogen molecule. In explanation of all the facts, one may regard specific activated diffusions as occurring when the membrane can dissociate the diffusing molecule into atoms or ions. An insight into the nature of the gas-solid interaction in the case of the non-specific type of activated diffusion is provided by the experiments of Barrer [28] on gas-silica glass systems. It was observed that the temperature dependence of the permeation rate in calories per mole, though much greater than the sublimation energies, follow in the same order (Table 20).

TABLE 20. *Heats of sublimation of gases, and the temperature dependence (in cal./mol.) for flow through silica glass*

Gas	Sublimation heat	Temperature coefficient from $P = P_0 e^{-E/RT}$ for flow
He	126*	5,600
Ne	590	9,500
H_2	529*	10,300
O_2	2150	31,200
N_2	1860	26,000
A	2030	32,100

* Calculated[19] from the force law $E = -\alpha/R^6 + \beta/R^{12}$, when the constants α and β are derived from the virial coefficients of the equation of state of the gas.

Table 20 suggests that van der Waals and repulsive forces contribute to the temperature coefficient of flow (in cal./mol.) just as they do to the latent heat of sublimation; in the latter instance the attractive forces, which are small, are predominant, but in the former the much larger repulsive forces are predominant. This provides a basis for the classification of activated diffusion processes into specific types (H_2-Pd) and non-specific types (He-SiO_2), the basis being the nature of the

interaction between solid and gas. Table 21 attempts a classification of some diffusions having exponential temperature coefficients into specific and non-specific activated diffusions. In addition to these "natural" diffusions there are numerous "forced" diffusions wherein ions may move under an impressed potential. These will be considered separately (Chap. VI).

TABLE 21. *Diffusion processes*

Nature of system	Nature of interaction	
	Specific	Non-specific

Gas-solid	H_2-Pd, Ni, Pt, Cu
	O_2-Ag, Cu_2O, FeO
	N_2-W, Mo, Fe
		H_2-KBr
		H_2-SiO_2, pyrex, rubber,
		    cellulose
		O_2-SiO_2
		N_2-SiO_2
		Ar, Ne, He-SiO_2, B_2O_3,
		    borates, silicates, rubber,
		    cellulose

Vapour-solid	H_2O-zeolites? NH_3-zeolites? HCl, NH_3-NaCl?	NH_3-pure rubber H_2O-pure rubber, cellulose? CO_2-pure rubber

Solid-solid	S-FeS
	Ca^{++}, K^+, Na^+-glass,
	    zeolites, ultramarines,
	    clays
	Metal-metal systems?	

Liquid-liquid	NH_3-H_2O? D_2O-H_2O?	C_6H_5OH-CH_3OH C_6H_5OH-C_6H_6 s-$C_2H_2Br_4$-s-$C_2H_2Cl_4$ D_2O-H_2O?
Gas-liquid	CO_2-NaOH aq.	H_2-H_2O O_2-H_2O, NaOH aq.

The influence of temperature on the permeation rate

Three formulae have been employed to express the permeation rate as a function of temperature. The formulae are

$$-\frac{dn}{dt} = At^m, \tag{1}$$

$$-\frac{dn}{dt} = Be^{aT}, \tag{2}$$

$$-\frac{dn}{dt} = Ce^{-E/RT}, \tag{3}$$

in which A, m; B, a; and C and E/R, are characteristic constants. The most satisfactory agreement over the high
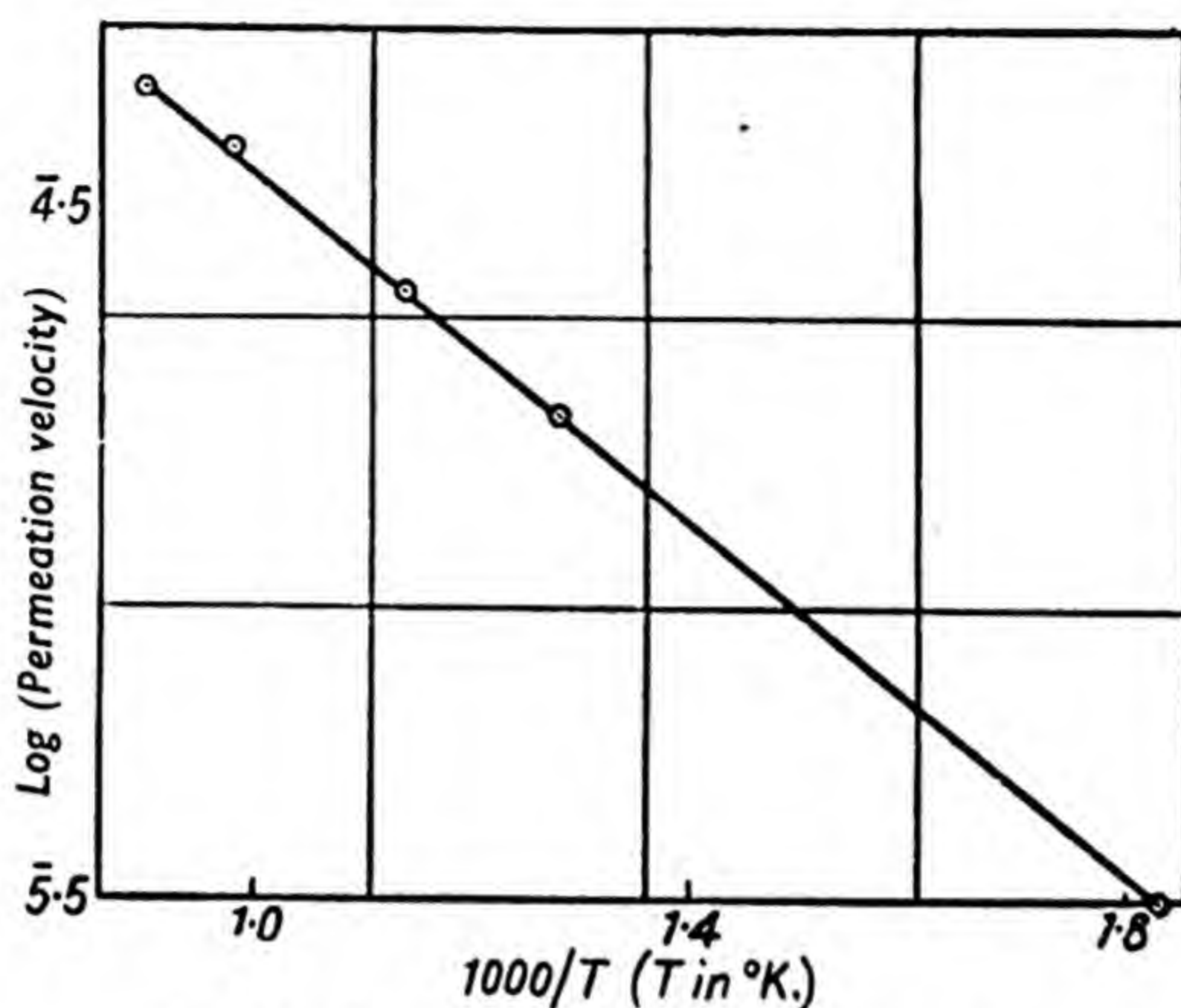
Fig. 33. Passage of helium through silica.
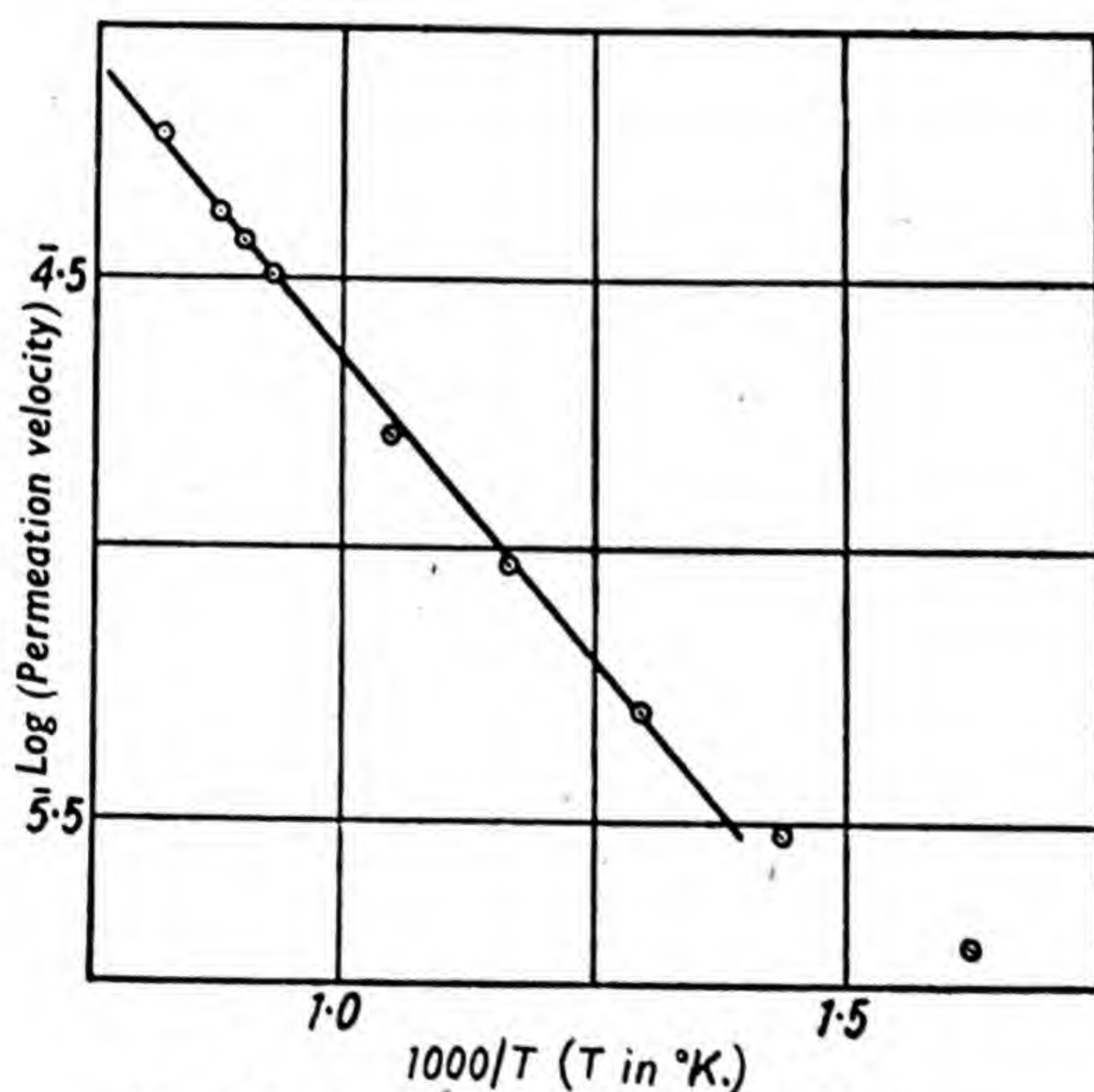
Fig. 34. Passage of hydrogen through silica.

temperature range is undoubtedly given by equation (3) (Figs. 33, 34), which has also the advantage of having a theoretical basis. Thus when an energy of activation is required

to make the molecule enter the pore and to move it along the energetically periodic pore length, one would by analogy with the Arrhenius theory of chemical reactions expect the number entering the pore to be given by

$$N = AN_1 e^{-E/RT},$$

where N_1 denotes the number of molecules available to enter the pore and A denotes the chance that a molecule having a sufficient energy will actually enter the pore. While a kinetic theory of permeation of a more elaborate nature can be derived, the applicability and significance of equation (3) will now be assumed, and from the experimental data the temperature coefficients in cal./mol. for the permeation process are collected in Table 22. These coefficients include the temperature variation of N_1. (which may refer to adsorbed molecules, or even dissolved molecules). Since the heat either of sorption or of solution (p. 140) is small, these temperature coefficients may be approximately identified with activation energies for diffusion within the solid.

Irreversible effects

Several interesting points arose from Barrer's [28] study of the influence of temperature upon the permeation rate. First, the permeability towards the heavier gases is affected by prolonged heating to high temperatures. This is shown by the permeation rates of air through a silica tube, given as a function of temperature for various periods of heat treatment of the silica (Fig. 35). The flowing curves are drawn through points determined in sequence, and the permeability decreases as the heating is prolonged. That the effect was solely a surface one was shown by treatment with hydrofluoric acid, which restored the permeation rate to its original value. This superficial change was probably connected with a visible clouding of the surface, and it was thought that it might be due to the formation of tiny crystals, possibly platy [3] or else of β-cristobalite type. With an ensuing decrease in permeability there was an increase in the activation energy which is clearly indicated

TABLE 22. *The temperature coefficients of permeability constants in glasses in cal./mol.*

Gas	Glass	Energy	Author	Remarks
He	Fused silica	5,600	T'sai and Hogness(30)	The energy of activation increases as the percentage of SiO_2 decreases
	Fused silica	5,700	Barrer(28)	
	Fused silica	5,390	Braaten and Clark(29)	
	Pyrex	8,700	van Voorhis(36)	
	Thuringian	11,300	Piutti and Boggiolera(37)	
	Lead	—	Urry(17)	Permeation observed but influence of temperature not studied
	Soda	—	Urry(17)	
	Jena 16III	8,720	Urry(17)	
Ne	Fused silica	9,500	T'sai and Hogness(30)	
H_2	Fused silica I	9,300	Williams and Ferguson(32)	
	Fused silica II	10,000	Williams and Ferguson(32)	
	Fused silica III	10,000	Williams and Ferguson(32)	
	Fused silica IV	10,800	Williams and Ferguson(32)	
	Fused silica I	10,900	Barrer(28)	
	Fused silica II	10,800	Barrer(28)	After prolonged heating, causing superficial crystallisation
	Fused silica	8,500	Mayer(38)	
	Fused silica	9,200	Johnson and Burt(39)	
	Fused silica	12,000	Wüstner(24)	At up to 800 atm.
	Pyrex	—	Urry(17)	Permeation observable
	Pyrex	—	Williams and Ferguson(32)	Permeation not observed
	Jena	—	Williams and Ferguson(32)	Permeation not observed
N_2	Fused silica	26,000	Johnson and Burt(39)	
	Fused silica	22,000	Barrer(28)	
	Fused silica	29,900	Barrer(28)	After prolonged heating with surface change
O_2	Fused silica	31,200	Barrer(28)	After prolonged heating and cleaning with hydrofluoric acid
Air	Fused silica	[18,500]	Barrer(28)	Apparent energy only
	Fused silica, after prolonged heating	[22,000]	Barrer(28)	A different sample of silica from that used for author's other data
Argon	Fused silica, after prolonged heating	[48,000]	Barrer(28)	A very slow rate of permeation indeed
	Fused silica	32,100	Barrer(28)	A fresh surface obtained by treatment with HF, and much greater permeability

in Table 22. These effects were most marked for the heavy gases (N_2, Ar, and air), whereas for hydrogen and helium the influence of heating upon the permeability was slight. This fact, and the close agreement of the temperature coefficients of the permeability when expressed in cal./mol.,* determined by various
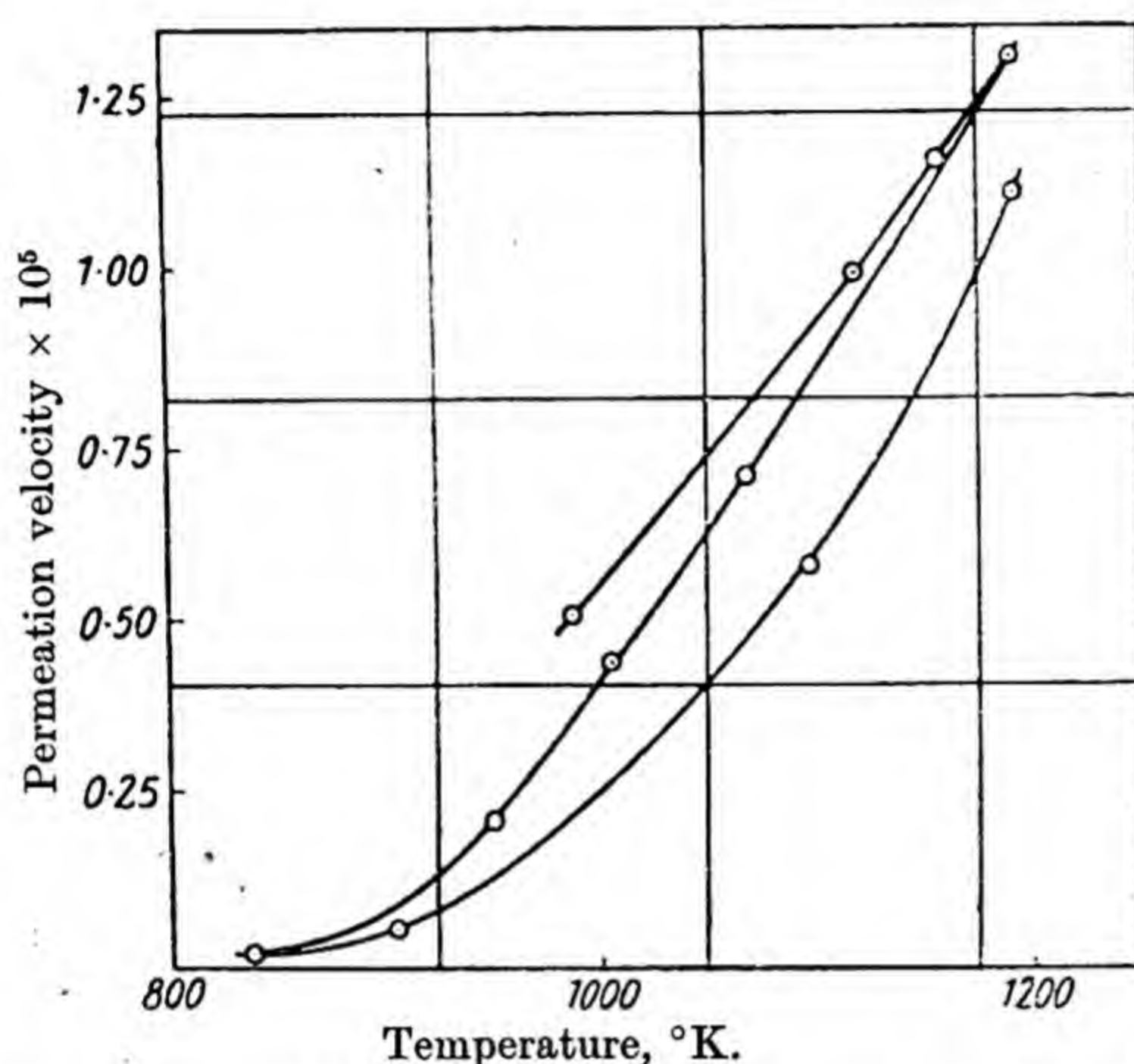
Fig. 35. The rate of flow of air through silica, as affected by temperature and time of heating of the silica.

workers on different samples of silica led to the postulate (28) that there are two types of activated diffusion in silica glass:

(1) A structure sensitive diffusion down faults, and cracks of molecular dimensions, predominant when argon, nitrogen and air diffuse.

(2) A structure insensitive diffusion through the anionic network of the glass itself, and corresponding to a solution process. This diffusion is predominant when helium, neon and hydrogen pass through silica glass.

* The permeability constant P, diffusion constant D and solubility k are related by $P = Dk \, \Delta p / l$, where Δp denotes the pressure difference across, and l the thickness of the specimen. When as for H_2 and He (p. 140) the temperature coefficient of k is small, the temperature coefficient of P in cal./mol. is that for D, i.e. the activation energy for diffusion.

Even for helium, neon and hydrogen, grain boundary diffusion must occur simultaneously with "lattice" diffusion, and the predominance of one or the other is conditioned by the temperature. As the temperature is lowered, the more
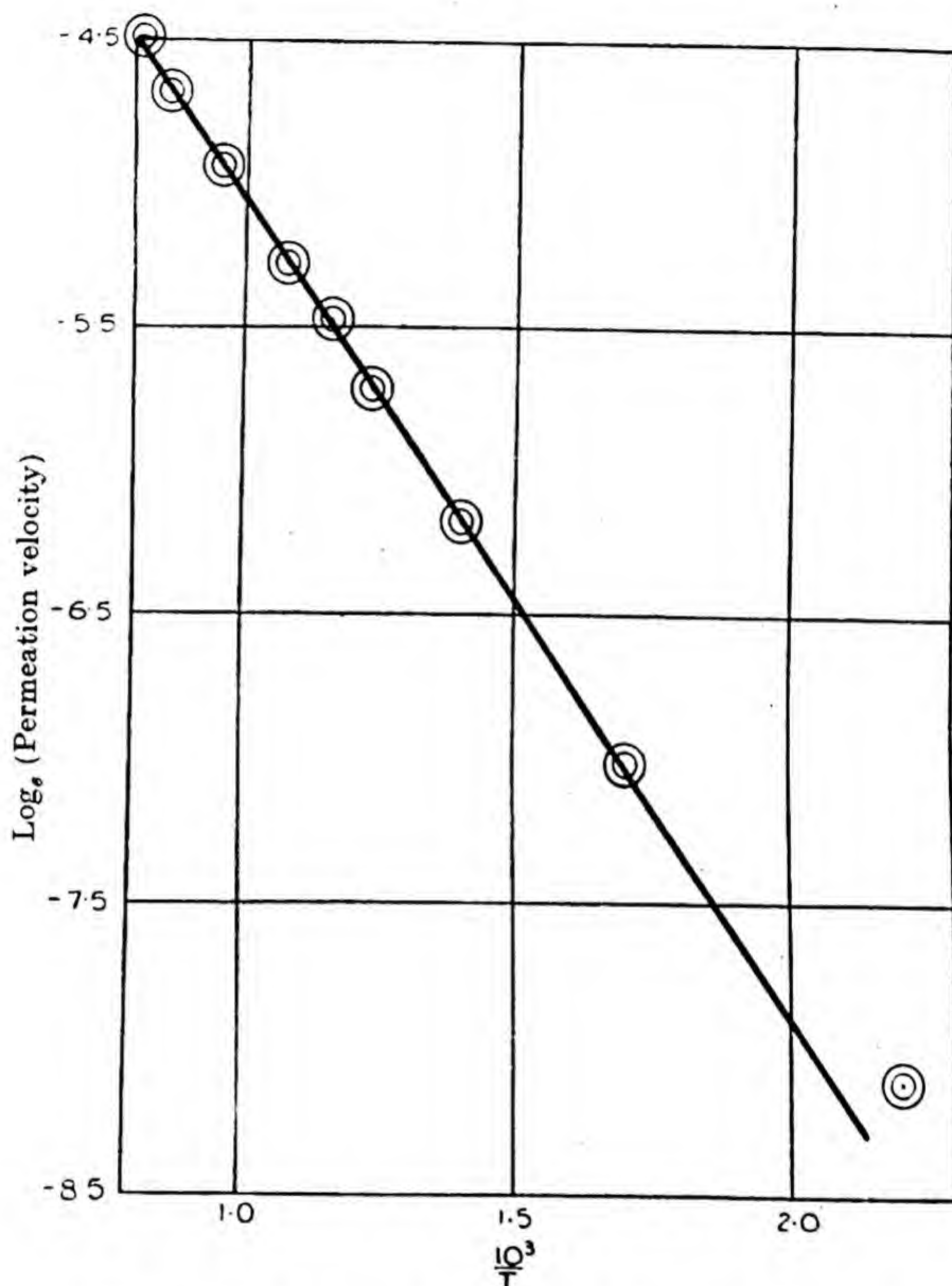
Fig. 36. The structure sensitive and structure insensitive regions in the diffusion of helium in silica glass.

temperature sensitive "lattice" diffusion is increasingly submerged in the grain boundary diffusion. So one should find a flattening of the curve log (permeation rate) against $1/T$ (T in $°$K.) for small values of T. Figs. 34 and 36 show this effect for hydrogen and helium.

On the other hand, a specimen of silica glass which had undergone prolonged heating gave a log (permeation rate) against $1/T$ curve linear even at room temperature, suggesting that the heating had diminished (by the surface change noted (p. 125)) the structure sensitive part of the diffusion.

Table 23 gives mean values of the temperature coefficient of the permeation rate for diffusion processes occurring in various zones of temperature. Table 23 also illustrates in what

TABLE 23. *Temperature coefficients of permeability in cal./mol. at low temperatures**

Gas	Glass	Worker	Nature of predominating diffusion	Energy cal./ mol.	Temp. ° C.
H$_2$	Fused silica	Barrer[28]	Lattice	10,800	>400
	Fused silica	Barrer[28]	Grain boundary	4,300	193
He	Fused silica	T'sai and Hogness[30]	Lattice	5,700	>300
		Burton, Braaten and Wilhelm[31]*	Grain boundary	4,190	110 to 0
				3,040	0 to − 41
				2,310	− 41 to − 78
	Pyrex	van Voorhis[36]	Lattice	8,700	>300
		Urry[17]	Grain boundary	5,840	283 to 172
			Grain boundary	4,540	172 to 81
	Jena 16^{III}	Urry[17]	Uncertain	8,720	283 to 134
			Grain boundary	6,900	134 to 22

* In a later communication[29] two of the authors state that no further diminution in E could be found below − 20° C. Their new values of E were: from 180 to 562° C., 5390 cal.; from 180 to − 78° C., 4800 cal.

way the silica content affects the activation energy for the process. The smaller the silica content, the larger is the activation energy and the smaller the permeation rate (cf. p. 137). The passage of helium through a number of glasses of known composition[36] also revealed that acidic oxides such as B_2O_3 or SiO_2 increased the permeability, while basic oxides such as K_2O, Na_2O, or BaO decreased it approximately in proportion to their amount. Feebly basic or amphoteric oxides such as PbO or Al_2O_3[36] were stated to have little effect upon the permeability. It is to be noted that Al_2O_3 may replace SiO_2 in the anionic network of the silica membrane.

* See footnote, p. 127.

Roeser[40] studied the permeability of various samples of unglazed and glazed porcelain in air. He found many samples with channels so large that stream-line or Knüdsen flow occurred in them; but in other more perfect specimens only a strongly temperature sensitive diffusion was observed. The experiments, which were made up to 1300° C., gave varied agreement with the law

$$\text{Permeability constant*} = P_0 e^{-E/RT},$$

the products of some manufacturers giving linear curves of $\log(P)$ versus $1/T$, while other manufacturers' products behaved more or less capriciously. The slope of the curve $\log(P)$ versus $1/T$ even at the highest temperatures varied from specimen to specimen. The slopes observed at high temperatures for one set of porcelain tubes varied from 29,000 to 63,000 cal. All these results suggest that grain-boundary diffusion is a more usual process than lattice diffusion, in conformity with Barrer's [28] findings for the migration of the heavier gases through silica glass. In this connection it may be mentioned that Roeser's results on silica glass and on glazed and unglazed porcelain give permeability constants of similar magnitude. Porcelain may be considered to consist of crystals of mullite ($3Al_2O_3 . 2SiO_2$) embedded in a glass magna, and often with undissolved quartz or clay in the structure. It is clear that such a chemical will be far from homogeneous, and to this chemical inhomogeneity as well as to its physical inhomogeneity may be ascribed its capricious behaviour.

Further studies on irreversible phenomena associated with helium diffusion through pyrex glass were made by Taylor and Rast [41]. The effects noted by them were not confined to the surface of the glass, as were those observed by Barrer [28]. They found that the permeability constant rose by 10 % at about 550° C., after annealing at that temperature, and that thereafter the new permeability-temperature curve lay above the

---

* Even with a single energy of activation for each gas, this law could not be rigidly obeyed when air diffuses, since air is a mixture of N_2 and O_2 and the law should be $P = P_1 e^{-E_{O_2}/RT} + P_2 e^{-E_{N_2}/RT}$.

old one. The effect was considered to be the result of strain removal in the original glass, the curve log (permeability) against $1/T$ being now continuous into the region where the glass could be regarded as a viscous liquid. The diminution in slope at lower temperatures which have been interpreted [28] as increasingly important contributions of grain-boundary diffusion were also noted, the slopes giving values of

$$E_{440-600°C.} = 7150 \text{ cal./atom},$$

$$E_{350-440°C.} = 6480 \text{ cal./atom},$$

which may be compared with the values of E in Table 23. However, the authors regarded this diminution as due to a loss of rotational or vibrational freedom in the silicate complex, occurring at a critical temperature. As a further change in the slope of the $\log (P)$ versus $1/T$ curve had occurred at $225°$ C., one must on this theory suppose a second loss of rotational or vibrational freedom.

On the relationships between some types of molecular flow

It will be interesting to point out at this stage how several important types of mechanism for gas transference through solids are related. In the normal stream-line flow of fluids the diameter of the pore and the pressure are such that the number of collisions on the pore wall in unit time per unit area is completely outweighed by the number of collisions in unit time and in unit volume of the gas phase. When the pressure and pore diameter are such that collisions with the wall completely outweigh collisions in the gas phase, one finds not stream-line flow but molecular streaming. Also as one continually restricts the pore diameter, the gas molecules must spend a greater and greater fraction of time in the surface field of the solid, that is adsorbed on the solid. Ultimately, as a logical conclusion to this process of restricting the pore diameter, the diffusing molecules are always within the surface fields of the solid. Owing to the periodic or crystalline nature

of the solid, the energy distribution along the surface is also periodic, and a molecule diffusing along the surface finds itself moving to successive energy hollows, separated by energy barriers.

When the periodic fields of the opposite sides of the pore overlap, energy will be needed to make the molecule enter the pore. In illustration of this, Fig. 37 shows the energy needed to
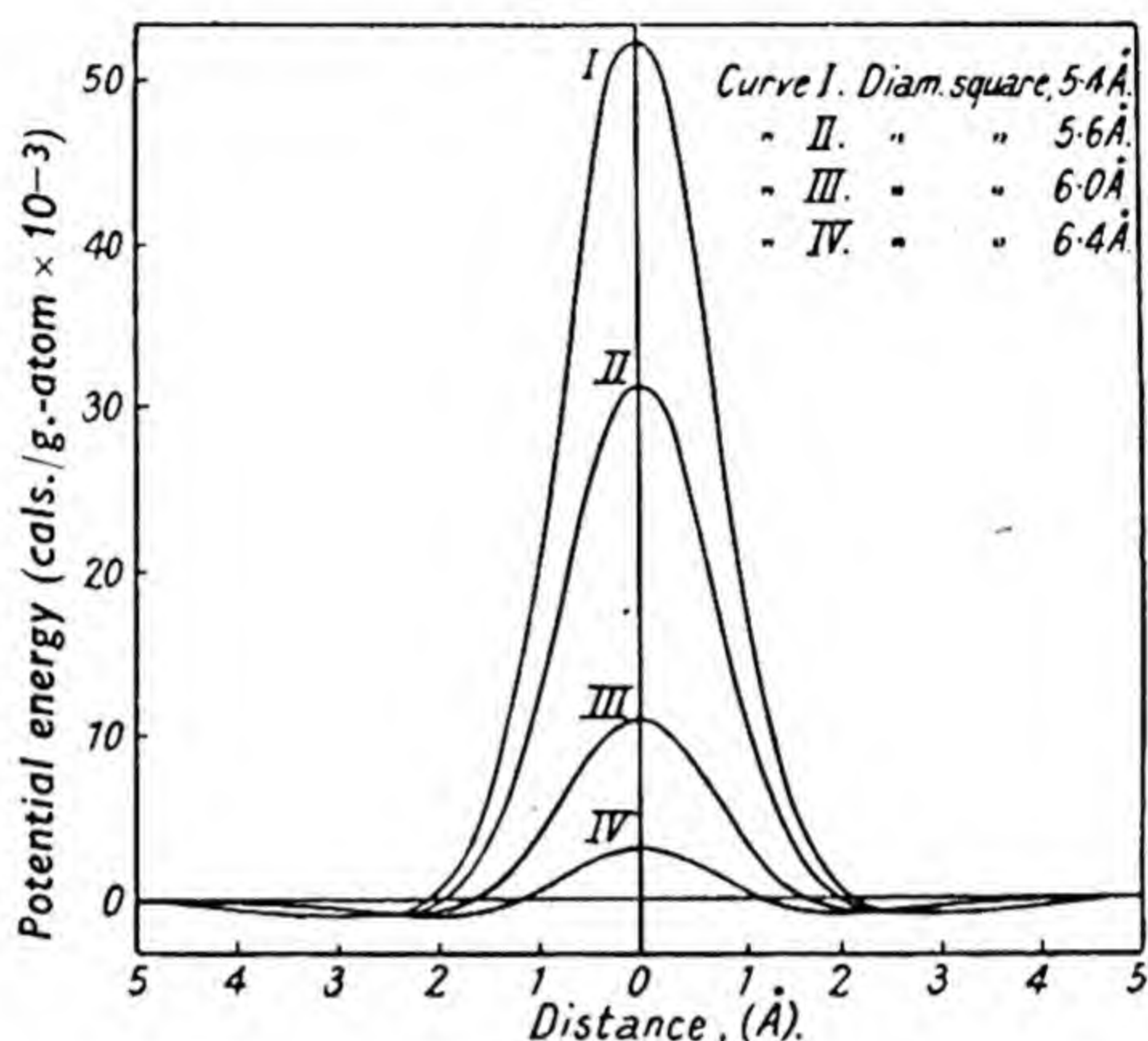
Fig. 37. Energy needed to make an argon atom pass through a square of argon atoms.

make an argon atom pass through a square of argon atoms, when the diameter of the square is varied to make the atomic force fields overlap to varying extents.

Experiments upon the transition region from molecular streaming to activated diffusion are few. Rayleigh[15] has recently made interesting experiments upon the passage of air and helium through very narrow artificial channels. When optically plane glass plates were placed in contact and heated to remove adsorbed gases, but not heated sufficiently to destroy the planeness of the glass, it was found that contact was so intimate that no flow of helium between the two plates could be measured, although the rate of flow of helium through silica glass can be measured at room temperature. In another experiment the plane glass plates were placed in contact,

but not heated. Their distance apart was of the order of 10 A., and the permeation rates for helium and for air were 9.5×10^{-2} cu.mm./day and 1.4×10^{-2} cu.mm./day respectively. The ratio of these velocities is

$$\frac{\text{He}}{\text{Air}} = \frac{6.8}{1}$$

instead of the ratio

$$\frac{\text{He}}{\text{Air}} = \frac{2.7}{1} = \sqrt{\frac{28.8}{4}},$$

which Knudsen's law of molecular streaming would require. That is, Rayleigh succeeded in passing beyond the limits of Knudsen flow into what must be at least a transition region to activated diffusion. In this region the ratio of the permeation rates would be governed principally by a ratio of exponentials:

$$\frac{\text{He}}{\text{Air}} \simeq \frac{e^{-E_{\text{He}}/RT}}{e^{-E_{\text{Air}}/RT}}.$$

Numerical values of the permeabilities

The volumes in c.c. at N.T.P. of gas diffusing per sec./cm.^{2} through a glass wall 1 mm. thick, when a pressure difference of 1 cm. is maintained across the wall, is given in Tables 24–34.

TABLE 24. He-SiO$_2$

Temp. °C.	Permeability constant × 10^9 (c.c. at N.T.P./sec./cm.^{2}/mm./cm. Hg)			
	A	B	C	D
150	0·73	0·78	—	—
200	1·39	1·52	—	0·19
300	3·15	4·13	0·48	0·46
400	6·15	8·25	0·99	0·92
500	10·4	13·8	1·72	2·06
600	16·4	19·3	3·00	4·62
700	21·9	—	4·25	—
800	28·5	—	5·50	—
900	36·2	—	6·72	—
1000	45·4	—	8·42	—

Authors: A = T'sai and Hogness; B = Braaten and Clark; C = Barrer; D = Williams and Ferguson.

TABLE 25. He-SiO$_2$ *from* − 200 *to* 150° C.

Temp. ° C.	Permeability constant × 10⁹ (c.c. at N.T.P./sec./cm.²/mm./cm. Hg)			
	A	A	A	B
− 200	—	—	—	0·0028
− 180	—	—	—	0·0035
− 160	—	—	—	0·0038
− 140	—	—	—	0·0044
− 120	—	—	—	0·0053
− 100	—	—	—	0·0066
− 80	0·00070	—	—	0·0084
− 70	0·00176	—	—	0·0101
− 60	0·00315	—	—	0·0121
− 50	0·0052	—	—	0·0145
− 40	0·0077	—	—	0·0179
− 30	0·0109	—	—	0·0224
− 20	0·0174	—	—	0·028
− 10	0·022	—	—	0·037
0	0·035	0·029	0·028	0·050
10	0·051	0·046	0·040	0·073
20	0·070	0·062	0·055	0·104
30	0·090	0·080	0·073	—
40	0·114	0·106	0·095	—
50	0·135	0·132	0·119	—
70	0·205	0·198	0·176	—
90	0·304	0·29	0·264	0·274
110	0·44	0·42	0·39	0·45
130	0·62	0·59	0·52	0·55
150	0·79	—	—	—

Authors: A = Braaten and Clark; B = Burton, Braaten and Wilhelm.

TABLE 26. Ne-SiO$_2$

Temp. ° C.	Permeability constant × 10⁹ (c.c./sec./cm.²/mm./cm. Hg)
500	0·139
600	0·282
700	0·50
800	0·81
900	1·18
1000	1·63

Authors: T'sai and Hogness.

TABLE 27. *Argon*-SiO_2

Temp. °C.	Permeability constant $\times 10^9$ (c.c./sec./cm.²/mm./cm. Hg)		
	A	A*	B
850	0·0161	—	—
900	—	—	0·58
950	0·062, 0·031	0·00022	—
1000	—	0·00050	—

Authors: A = Barrer; B = Johnson and Burt.

* Decreased permeability due to long heating of silica glass specimen.

TABLE 28. H_2-SiO_2

Temp. °C.	Permeability constant $\times 10^9$ (c.c./sec./cm.²/mm./cm. Hg)						
	A	B	B	B	B	C	D
200	0·022	—	—	—	—	—	—
300	0·099	—	—	—	—	—	0·051
400	0·366	0·48	0·44	—	0·50	—	0·275
500	0·70	0·92	0·84	—	1·06	—	0·58
600	1·43	1·75	1·54	—	2·16	2·00	0·81
700	2·52	3·1	2·70	2·45	3·9	2·76	1·70
800	4·25	4·8	4·4	4·0	6·0	4·5	2·53
900	6·4	—	7·0	5·9	—	—	3·6
1000	10·0	—	—	—	—	—	5·1

Authors: A = Barrer; B = Williams and Ferguson; C = Wüstner; D = Johnson and Burt (mean of three samples).

TABLE 29. N_2-SiO_2

Temp. °C.	Permeability constant $\times 10^9$ (c.c./sec./cm.²/mm./cm. Hg)		
	A	B	B*
650	0·065	0·066	—
700	0·132	0·146	—
750	0·268	0·271	0·161
800	0·43	0·39	—
850	0·80	0·64	—
900	1·19	0·95	—
950	—	1·44	0·65

Authors: A = Johnson and Burt; B = Barrer.

* Decreased permeability due to long heating of silica glass specimen.

TABLE 30. He-*pyrex glass*

Temp. °C.	Permeability constant × 10⁹ (c.c./sec./cm.²/mm./cm. Hg)	
	A	B
0	0·0037	—
20	0·0064	—
50	0·0128	—
100	0·0264	—
150	0·058	—
200	0·124	0·069
250	0·229	—
300	0·38	0·243
400	—	0·70
500	—	1·57

Authors: A = Urry; B = van Voorhis.

TABLE 31. He-*Jena* 16III

Temp. °C.	Permeability constant × 10⁹ (c.c./sec./cm.²/mm./cm. Hg)
20	0·0000095
50	0·0000471
100	0·000071
150	0·000183
200	0·00077
250	0·00176
300	0·00362

Author: Urry.

TABLE 32. He-*miscellaneous glasses*

Temp. °C.	Glass	Permeability constant × 10⁹ (c.c./sec./cm.²/mm./cm. Hg)
283	Lead	0·0037*
283	Soda	0·0098*
610	Pyrex	1·9†

Authors: * = Urry; † = Williams and Ferguson.

TABLE 33. He-*Thuringian glass*

Temp. °C.	Permeability constant × 10⁹ (c.c./sec./cm.²/mm./cm. Hg)
100	0·00000106
200	0·000117
300	0·00084
400	0·0045
500	0·0132

Authors: Piutti and Boggiolera.

TABLE 34. *Air-porcelain*

Temp. °C.	Permeability constant × 10⁹ (c.c./sec./cm.²/mm./cm. Hg)	
	Sample I	Sample II
25	0·00106	—
400	0·00106	—
600	0·00212	—
800	0·0032	—
1000	0·0161	0·0012
1200	0·077	0·022
1300	0·32	0·117

Author: Roeser.

In deriving these permeability data graphs of the experimental measurements were used to obtain figures at comparable temperatures. Several features of this group of tables are interesting. First one may consider the selectivity of the permeability of silica glass towards a number of gases, illustrated by the following series:

For He-SiO$_2$ (30) at 900° C., $\quad P = 36 \cdot 2 \times 10^{-9}$,

$\quad$ H$_2$-SiO$_2$ (28) at 900° C., $\quad P = 6 \cdot 4 \times 10^{-9}$,

$\quad$ Ne-SiO$_2$ (30) at 900° C., $\quad P = 1 \cdot 18 \times 10^{-9}$,

$\quad$ N$_2$-SiO$_2$ (28) at 900° C., $\quad P = 0 \cdot 95 \times 10^{-9}$,

$\quad$ Ar-SiO$_2$ (39) at 900° C., $\quad P = 0 \cdot 58 \times 10^{-9}$.

It must, however, be remembered that permeabilities towards certain of the gases vary from specimen to specimen of glass; thus much smaller permeabilities both to argon and to helium have been reported (28). In yet another series may be given the permeability of a number of glasses to helium:

For He-SiO$_2$ (30) at 300° C., $\quad\quad P = 3 \cdot 15 \times 10^{-9}$,

$\quad$ He-pyrex (17) at 300° C., $\quad\quad P = 0 \cdot 38 \times 10^{-9}$,

$\quad$ He-soda glass (17) at 283° C., $\quad\quad P = 0 \cdot 0098 \times 10^{-9}$,

$\quad$ He-lead glass (17) at 283° C., $\quad\quad P = 0 \cdot 0037 \times 10^{-9}$,

$\quad$ He-Jena 16^{III} (17) at 300° C., $\quad\quad P = 0 \cdot 0036 \times 10^{-9}$,

$\quad$ He-Thuringian glass at 300° C., $\quad P = 0 \cdot 00084 \times 10^{-9}$,

and from the series one observes the high sensitivity of permeability to chemical composition (cf. p. 129). Further data along these lines are provided by Rayleigh's studies on the helium permeability of membranes, including silicate glasses, silica glass, and boron trioxide melts, as well as a number of metallic and organic membranes. The following Tables (35 and 36) give the helium permeabilities of a number of glasses; and also allow a comparison of the permeabilities

TABLE 35. *The helium permeability of glasses at room temperature in c.c./sec./cm.²/mm. thick/cm. Hg pressure difference*

Substance	Permeability	Substance	Permeability
Silica	0.058×10^{-9}	Fused B_2O_3	0.055×10^{-9}
Optical silica	0.043×10^{-9}	Fused B_2O_3	0.056×10^{-9}
Silica sheet	0.025×10^{-9}	Fused borax	$<0.000103 \times 10^{-11}$
Thin silica tube	0.053×10^{-9}	glass	
Pyrex	0.0040×10^{-9}		
Corex glass (mainly $Ca_3(PO_4)_2$)	$<0.000040 \times 10^{-9}$		
Extra white sheet glass	$<0.000025 \times 10^{-10}$		
Micro cover glass	$<0.000020 \times 10^{-10}$		
Flint glass	$<0.000030 \times 10^{-11}$		
Soda glass	$<0.000043 \times 10^{-13}$		

TABLE 36. *The helium and air permeabilities of various kinds of membrane at room temperature in c.c./sec./cm.²/mm. thick/cm. Hg pressure difference*

Substance	Helium permeability	Air permeability	Ratio of permeabilities
Cellophane	0.023×10^{-9}	0.049×10^{-11}	48
Silica	0.052×10^{-9}	$<0.052 \times 10^{-13}$	$>10,000$
Gelatin	0.14×10^{-9}	0.077×10^{-11}	184
Celluloid	6.1×10^{-9}	0.305×10^{-9}	20
Rubber	12×10^{-9}	4.16×10^{-9}	2.9

of certain organic membranes with the inorganic glasses. All the measurements reported were at room temperature,

and the constants have been converted to c.c./sec./cm.^{2}/mm. thickness/cm. of mercury.

Examination of Table 35 shows an extreme variation in the helium permeability of the silica membranes of only 2·3-fold at room temperature, while Table 24 indicates an extreme variation of 6·4-fold at 500° C. The sensitivity of the permeability to the composition of the glass is again apparent, and it may be that the variations in Table 24 are due to small amounts of the alkali metal oxides in the less permeable of the silica glasses as well as to a greater amount of grain-boundary diffusion in the more permeable glasses. It is interesting that fused B_2O_3 compares with fused SiO_2 in permeability, and also that the organic membranes cellophane and gelatin have permeabilities of the same order as the inorganic oxides. The ratio of helium to air permeability clearly bears no relationship to molecular masses, being mainly governed by the ratio of exponential terms of the type $e^{-E/RT}$.

THE SOLUBILITY OF GASES IN SILICA AND DIFFUSION CONSTANTS WITHIN IT

When discussing the temperature coefficients of the permeabilities, we considered these temperature coefficients to be approximately those for the activated diffusion process within the silica. This viewpoint was justified because, as the data now to be given show, the solubility of hydrogen and helium in silica varies only to a very minor extent with temperature, and the permeability constant (P), diffusion constant (D) and solubility k are related by

$$P = Dk\frac{\Delta p}{l},$$

where $\Delta p/l$ is the pressure gradient across the membrane. If the values of P and of k are known one may compute the more fundamental quantity D. The values of k (24, 42) are given in Table 37. It may be noted that the solubilities are quite

comparable with the solubilities of gases in rubber membranes (p. 418), in liquids and in crystals (p. 111). Further, the differences in permeability which one encounters for gases in silica and pyrex are, one is now led to believe, governed mainly by the differences in D, which are in their turn (p. 125) governed partly by an exponential term.*

TABLE 37. *The solubilities of hydrogen and helium in silica*

System	Temp. ° C.	Solubilities (average values in c.c. at N.T.P./c.c./atm.)	
		Wüstner(24)	Williams and Ferguson(42)
H₂-SiO₂	1000	0·0103	—
	900	0·0102	—
	800	0·0109	—
	700	0·0099	—
	600	0·0082	—
	400	0·0057	0·0095 (extrapolated)
	300	0·0055	0·0099 „
He-SiO₂	500	—	0·0101 „
	450	—	0·0103 „
He-pyrex	500	—	0·0084 „

When the permeability constant is expressed as c.c./sec./ cm.²/mm. thick/atm. pressure, and the solubility as c.c./c.c. of silica/atm. pressure, the use of the equation

$$P = Dk\frac{\Delta p}{l}$$

leads to a value of D expressed as cm.² sec.$^{-1}$ These values of D are of interest for purposes of comparison with corresponding values of D obtained for liquid-liquid or gas-liquid systems; for gas-metal, and gas-rubber systems; and for ion-ionic lattice diffusion systems. This comparison will be made elsewhere (p. 426). In Table 38 the values of D are computed from the solubilities of Table 37 and the permeabilities of Tables 24–34.

---

* But where grain-boundary diffusion predominates the number of internal surfaces, which is determined by the history of the specimen, is also important.

TABLE 38. *The diffusion constants inside silica and glass in cm.^{2} sec.$^{-1}$*

Solid	Gas	Temp. °C.	Solubility taken c.c./c.c. solid	D cm.^{2} sec.$^{-1}$	Authors
SiO$_2$	He	20	0·01	0·024–0·055 × 10^{-8}	Rayleigh
SiO$_2$	He	500	0·01 (Williams and Ferguson)	0·017–0·14 × 10^{-6}	Authors of Table 24
SiO$_2$	H$_2$	500	0·01 (Williams and Ferguson)	0·006–0·011 × 10^{-6}	Authors of Table 28
SiO$_2$	H$_2$	500	0·0055 (Wüstner)	0·012–0·021 × 10^{-6}	Authors of Table 28
SiO$_2$	H$_2$	200	0·0055	0·05–0·08 × 10^{-8}	Barrer
Pyrex	He	20	0·0084	0·0045 × 10^{-8}	Rayleigh
Pyrex	He	500	0·0084 (Williams and Ferguson)	0·02 × 10^{-6}	van Voorhis

The diffusion constants of Table 38 may be written as

$$D = D_0 e^{-E/RT},$$

and then D takes the following values:

$$D^{20°C.}_{He\text{-}SiO_2} = (7\cdot9 - 3\cdot5)\,10^{-6}\,e^{-5600/RT}\,\text{cm.}^2\,\text{sec.}^{-1},$$

$$D^{500°C.}_{He\text{-}SiO_2} = (5\cdot2 - 0\cdot64)\,10^{-6}\,e^{-5600/RT}\,\text{cm.}^2\,\text{sec.}^{-1},$$

$$D^{500°C.}_{H_2\text{-}SiO_2} = (8\cdot3 - 14\cdot5)\,10^{-6}\,e^{-10100/RT}\,\text{cm.}^2\,\text{sec.}^{-1},$$

$$D^{200°C.}_{H_2\text{-}SiO_2} = (13\cdot7 - 35)\,10^{-6}\,e^{-10100/RT}\,\text{cm.}^2\,\text{sec.}^{-1},$$

$$D^{20°C.}_{He\text{-}pyrex} = 1\cdot3 \times 10^{-4}\,e^{-8700/RT}\,\text{cm.}^2\,\text{sec.}^{-1},$$

$$D^{500°C.}_{He\text{-}pyrex} = 5\cdot5 \times 10^{-6}\,e^{-8700/RT}\,\text{cm.}^2\,\text{sec.}^{-1}.$$

The result for the He-pyrex system at 20° C. studied by Rayleigh suggests that grain-boundary diffusion (see Table 23) has been taking place, with a lower energy of activation than the 8700 cal. assumed, which is the activation energy* for "lattice" diffusion. With this exception the values of D_0 are all of the same order of magnitude, and do not alter markedly with temperature, but do show random fluctuations which would conform well with the theory (p. 127) of mixed grain-boundary and lattice diffusion.

* See p. 139.

Theories of the diffusion process

Several authors (33, 27, 25) have attempted theories of the diffusion process. Urry (33) who considered flow to be a process of molecular streaming, as observed when rarefied gases pass through capillaries, is obviously incorrect for silicate glasses. The other theories (27, 25) are based upon more acceptable premises, but do not lead to any notable advance in the study of the subject. They need not therefore be discussed here.

REFERENCES

(1) Taylor, W. H. *Proc. Roy. Soc.* **145** A, 80 (1934).
(2) Barrer, R. M. *Proc. Roy. Soc.* **167** A, 392 (1938).
(3) Shishacow, N. A. *Phil. Mag.* **24**, 687 (1937).
(4) Nagelschmidt, G. *Z. Kristallogr.* **93**, 481 (1936).
(4 a) Farkas, A. Private communication.
(5) Tiselius, A. *Z. phys. Chem.* **169** A, 425 (1934).
(6) —— *Z. phys. Chem.* **174** A, 401 (1935).
(7) Hey, M. *Miner. Mag.* **24**, 99 (1935).
(8) —— *Phil. Mag.* **22**, 492 (1936).
(9) Mollwo, E. *Z. Phys.* **85**, 56 (1933).
(10) Rögener, H. *Ann. Phys., Lpz.*, **29**, 387 (1937).
(11) Mollwo, E. *Ann. Phys., Lpz.*, **29**, 394 (1937).
(12) Hilsch, R. *Ann. Phys., Lpz.*, **29**, 407 (1937).
(13) E.g. see Faraday Society Discussion, "Chemical Reactions involving Solids", pp. 883 *et seq.* (1938).
(13 a) Durau, F. and Schratz, V. *Z. phys. Chem.* **159** A, 115 (1932).
(13 b) Herbert, J. *Trans. Faraday Soc.* **26**, 118 (1930).
(13 c) Tompkins, F. C. *Trans. Faraday Soc.* **34**, 1469 (1938).
(13 d) Kraft, H. *Z. Phys.* **110**, 303 (1938).
(14) Bradley, R. *Trans. Faraday Soc.* **30**, 587 (1934).
(15) Rayleigh, Lord. *Proc. Roy. Soc.* **156** A, 350 (1936).
(16) —— *Proc. Roy. Soc.* **163** A, 377 (1937).
(17) Urry, W. *J. Amer. chem. Soc.* **55**, 3242 (1933).
(18) Watson, W. *J. chem. Soc.* **97**, 810 (1910).
(19) Villard, P. *C.R. Acad. Sci., Paris*, **130**, 1752 (1900).
(20) Berthelot, M. *C.R. Acad. Sci., Paris*, **140**, 821 (1905).
(21) Jaquerod, A. and Perrot, F. *C.R. Acad. Sci., Paris*, **139**, 789 (1904).
(22) Richardson, O. and Richardson, R. C. *Phil. Mag.* **22**, 704 (1911).
(23) Bodenstein, M. and Kranendieck, F. *Nernst Festschrift*, p. 99 (1912).
(24) Wüstner, H. *Ann. Phys., Lpz.*, **46**, 1095 (1915).
(25) Alty, T. *Phil. Mag.* **15**, 1035 (1933).

(26) Ward, A. F. *Proc. Roy. Soc.* **133** A, 506, 522 (1931).

(27) Lennard-Jones, J. E. *Trans. Faraday Soc.* **28**, 333 (1932).

(28) Barrer, R. M. *J. chem. Soc.* 378 (1934).

(29) Braaten, E. O. and Clark, G. *J. Amer. chem. Soc.* **57**, 2714 (1935).

(30) T'sai, L. S. and Hogness, T. *J. phys. Chem.* **36**, 2595 (1932).

(31) Burton, E., Braaten, E. O. and Wilhelm, J. O. *Canad. J. Res.* **21**, 497 (1933).

(32) Williams, G. A. and Ferguson, J. B. *J. Amer. chem. Soc.* **44**, 2160 (1922).

(33) Urry, W. *J. Amer. chem. Soc.* **54**, 3887 (1932).

(34) Paneth, F. and Peters, K. *Z. phys. Chem.* **1** B, 253 (1928).

(35) Smithells, C. and Ransley, C. E. *Proc. Roy. Soc.* **150** A, 172 (1935).

(36) van Voorhis, C. C. *Phys. Rev.* **23**, 557 (1924).

(37) Piutti, A. and Boggiolera, E. *R.C. Accad. Lincei* (5), **14** (1923). Also *R.C. Accad. Sci. Napoli* (3) **29**, 111 (1923).

(38) Mayer, E. *Phys. Rev.* **6**, 283 (1915).

(39) Johnson, J. and Burt, R. *J. opt. Soc. Amer.* **6**, 734 (1922).

(40) Roeser, W. *Bur. Stand. J. Res., Wash.,* **7**, 485 (1931).

(41) Taylor, N. W. and Rast, W. *J. chem. Phys.* **6**, 612 (1938).

(42) Williams, G. A. and Ferguson, J. B. *J. Amer. chem. Soc.* **46**, 635 (1924).

CHAPTER IV

GAS FLOW THROUGH METALS

INTRODUCTION

It is difficult to prepare a pure metal, for not only do metals contain traces of other metals, carbon, sulphur, or phosphorus, but they also contain combined or occluded gases—hydrogen, oxygen, nitrogen, and sulphur dioxide. These impurities exert in many instances a profound effect upon the properties of the metal. The present discussion concerns the behaviour of such gas-metal systems. Pioneer researches on hydrogen-palladium systems were made by T. Graham[1] in 1866; even earlier observations on the system hydrogen-iron were made by Cailletet[2], who in 1864 found that some of the hydrogen evolved when an iron vessel was immersed in dilute sulphuric acid was absorbed in the iron. Deville and Troost[3] first showed that hydrogen diffused through platinum, and the interesting permeability of silver towards oxygen was observed by Troost[4] in 1884. These workers have been followed by others [5, 6, 7, 8], amongst whom must be mentioned Richardson, Nicol and Parnell[9], who developed an equation for the flow of gas through a metal which is to-day the basis of interpretations of diffusion processes:

$$P = \frac{k}{l} p^{\frac{1}{2}} T^{\frac{1}{2}} e^{-b/T},$$

where P denotes the permeability constant, k and b are constants, l denotes the thickness, and p and T are respectively pressure and temperature.

It has also been found [2, 5, 7, 10, 11, 12] that hydrogen gas in nascent form can penetrate metals such as palladium, iron, or nickel at room temperature, if the metal is made the cathode during electrolysis or if the hydrogen is generated by chemical reaction at the surface. Pickling a metal in hydrogen in this

way may alter its mechanical properties to a marked degree (13), and the process of absorption is also very sensitive to traces of poisons (14). The earliest observations on this type of diffusion we owe to Bellati and Lussana (7), Cailletet (2), and Nernst and Lessing (12), but the field is one which has not been extensively studied, although the results should give information concerning interface reactions, and diffusion within the metal.

Before discussing the experimental data upon the permeability of metals to gases it will be of advantage to consider the cognate subject of gas solubility in metals. The differences in behaviour met with there may be reflected in the permeabilities (P), since the latter are defined by

$$P = -D\frac{\partial C}{\partial x},$$

where D is the diffusion constant and $\partial C/\partial x$ is the concentration gradient, defined in certain circumstances by the solubility of the gas in the metal.

THE SOLUBILITY OF GASES IN METALS

For the study of gas-metal systems one has all the apparatus and technique developed for measuring the sorption of gases by solids (15). The powerful X-ray method then gives the crystal habit of the products (16), or shows the effect the absorption has upon lattice constants (17), so that one may construct the phase diagrams for the system. Absorption equilibria have been studied for over a decade by Sieverts and his co-workers (18) and by many others, and as a result these often remarkable systems are being increasingly understood. Summaries of findings on gas-metal equilibria will be found in the books of McBain (15) and of Smithells (19), and it is not intended to give more than a résumé of the data here.

The metals which absorb common gases are summarised in Table 39. Oxides are not mentioned in the table; but apart from oxygen, hydrogen interacts most freely with metals, not as a rule to give hydrides but rather alloy systems, or solid

solutions. Solution of gases such as hydrogen, oxygen, or nitrogen occurs with dissociation, as is shown by a proportionality between the solubility (at small concentrations) and the square root of the pressure. Compound molecules, such as sulphur dioxide, ammonia, carbon dioxide, or carbon

TABLE 39. *Summary of the reactivity of metals towards gases*

Gas	Group	Metals which dissolve gas	Group	Metals which do not dissolve gas
H_2	I A	Hydrogen gives salt-like hydrides	I B	Au
	I B	Cu, Ag (slight)	II B	Zn, Cd
	II A	Hydrogen gives salt-like hydrides	III B	In, Tl
	III A	Al. Rare earths Ce, La, Nd, Pr	IV B	Ge, Sn, Pb (but give covalent hydrides)
	IV A	Ti, Zr, Hf. Th	V B	As, Sb, Bi (but give covalent hydrides)
	V A	V, Nb, Ta	VI B	Se, Te give covalent hydrides
	VI A	Cr, Mo, W	VIII	Rh
	VII A	(Mn)		
	VIII	Fe, Co, Ni, Pt, Pd		
O_2	I B	Cu, Ag		
	IV A	Zr		
	VIII	Fe, Co, (Ni)		
N_2	III A	Al (molten)	I B	Cu, Ag, Au
	IV A	Zr	II B	Cd
	V A	Ta (nitrides)	III B	Tl
	VI A	Mo (nitrides only), W (nitride)	IV B	Sn, Pb
			V B	Sb, Bi
	VII A	Mn (various nitrides)	VIII	Rh
	VIII	Fe (various nitrides)		
CO	VIII	Ni, Fe (above 1000° C.)	I B	Cu
SO_2	I B	Cu (liquid), Au (liquid)	VIII	Pt
He Ne Ar Kr Xe				Do not dissolve in any metal so far studied either when liquid or solid
CO_2	VIII	Fe	VIII	Rh, Pt

monoxide, must also dissociate before they can penetrate into the body of a metal. Temperature alters the solubility according to an exponential law, so that curves of log (solubility) versus $1/T$ are often linear, save where two alloy phases co-exist (H_2-Pd, H_2-Th, H_2-Ti), where a limiting composition is approached (H_2-Pd, -Th, -Ti, -Zr, -V), or where various

allotropic forms of the metal exist, and show different capacities to dissolve the gas (H_2-Fe).

The greatest diversity of interaction is shown by hydrogen, which reacts with metals to give three different types of products:

    (a) covalent hydrides: B_2H_6, SbH_3, SiH_4, AsH_3,

    (b) salt-like hydrides: $[Na^+][H^-]$, $[Ca^{++}][2H^-]$,

    (c) alloys: $PdH_{0.55}$.

Those systems with which experiments on hydrogen permeability have to do are alloy systems, at least over an appreciable range of compositions. The hydrogen exists in the metallic lattice most probably in an ionised or partially ionised condition.

Metals

A metallic crystal is to be regarded as a giant molecule, composed of positive nuclei and electrons, so that electrostatic forces ensure the cohesion of the whole. The electrons occupy definite energy levels, there being two electrons in each level
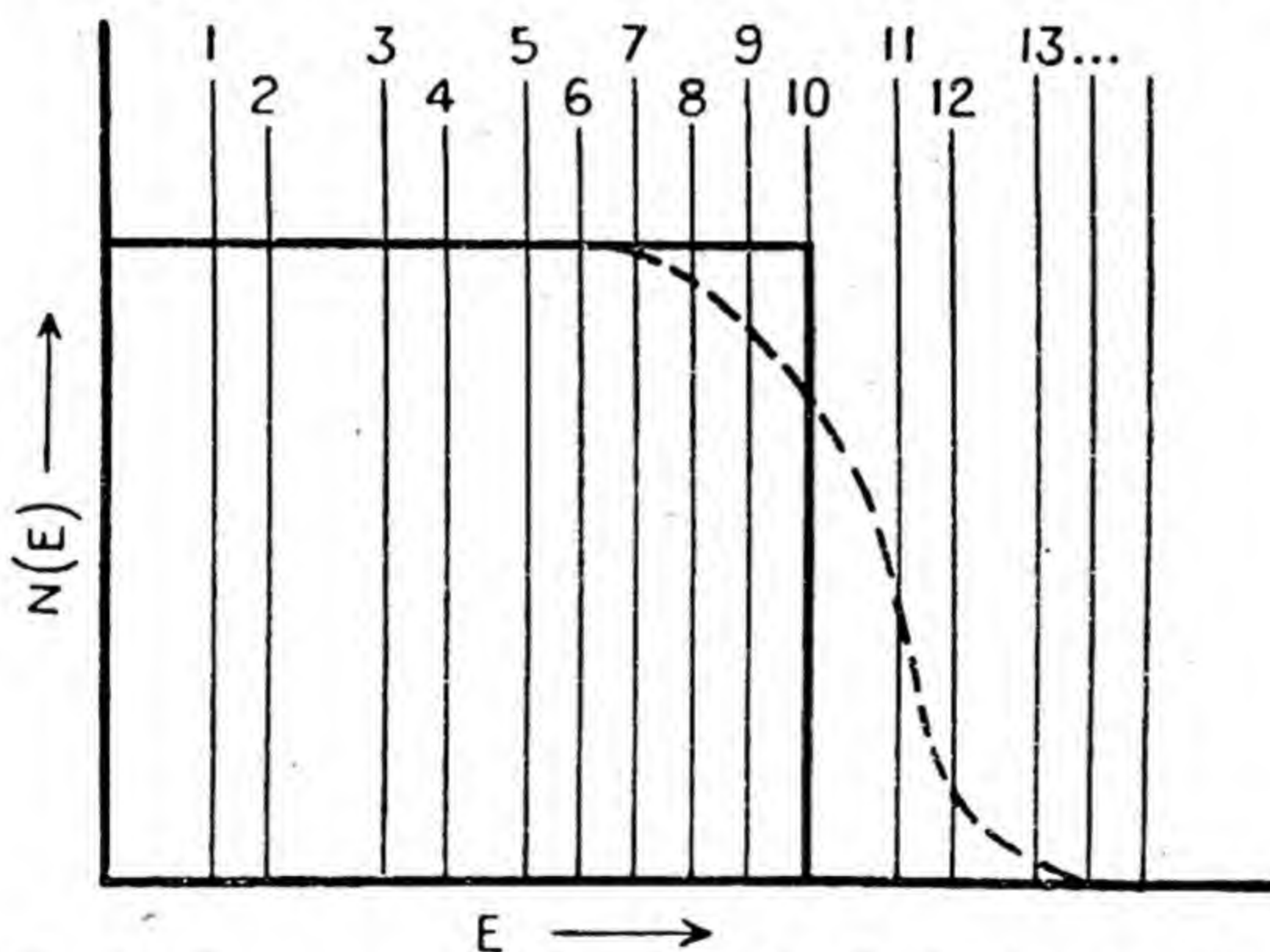
Fig. 38. Representation of electron distribution in a metal at 0 and 300° K. (after Emeleus and Anderson[20]).

at 0° K. At room temperature a few of the electrons by virtue of thermal energy are promoted to higher energy levels. In Fig. 38[20] one sees the number of electrons per level plotted against the number of levels, the full curve representing the

distribution at 0° K., and the dotted curve that at 300° K. In a metal with the electron distribution obtaining at 0° K. no electrical conductivity can occur because, since all levels are filled, the Pauli exclusion principle indicates that no nett flow of electrons may take place under any external potential, for no level can receive further electrons. There can be conductivity with the 300° K. distribution because there are some
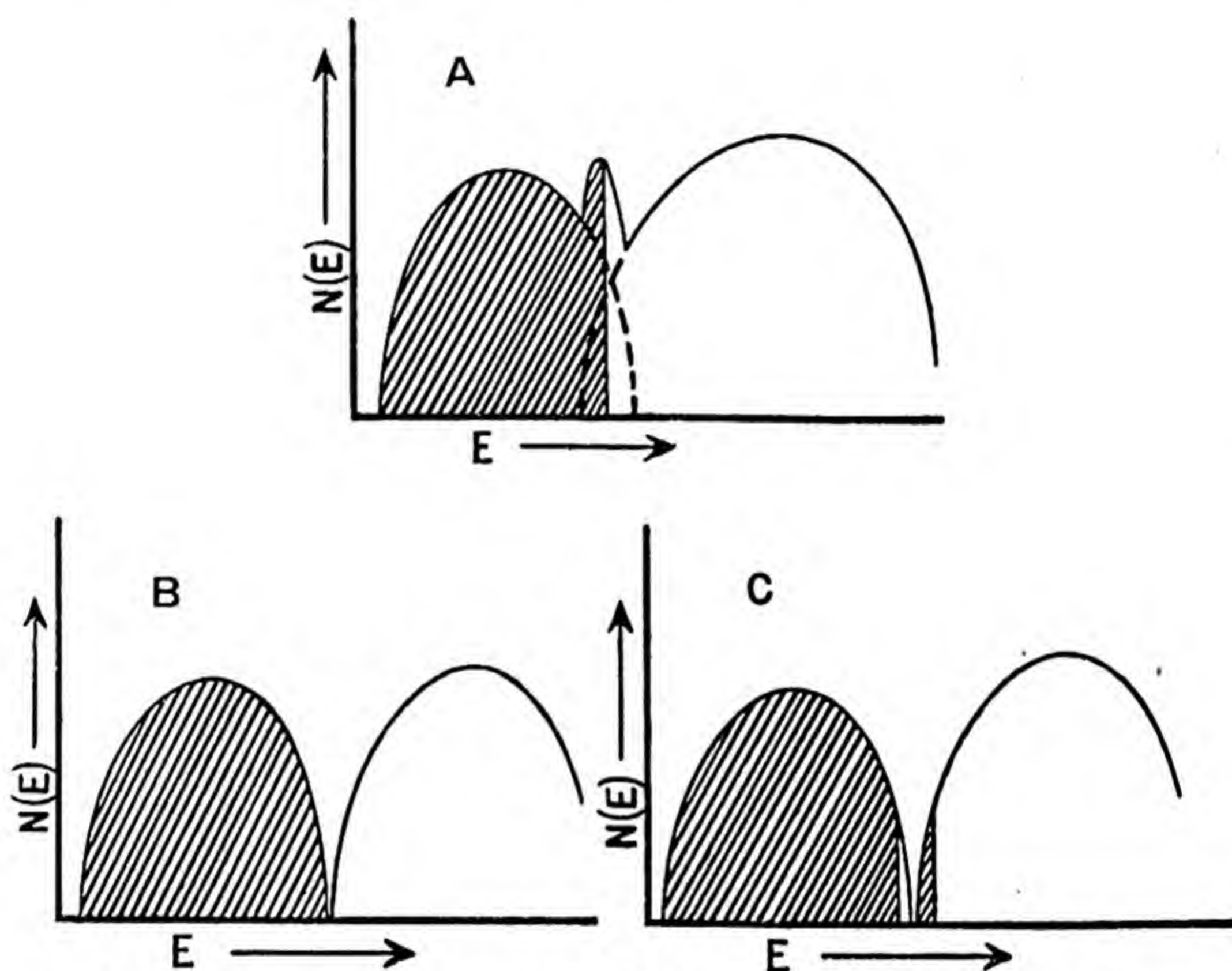
Fig. 39. Graphical representation of electron distributions in metals and semi-conductors (after Emeleus and Anderson[20]).

levels with only one electron, or no electrons. These levels may receive electrons and there may be a nett flow of electrons when a potential is applied.

The distribution curve of Fig. 38 is highly idealised. In the actual lattice the positive nuclei cause a periodic variation in the potential encountered by an electron moving through the lattice. The solution of the wave equation for such a potential distribution leads to the result that the electrons cannot assume any energies from zero to a maximum, but that there are bands or zones of permitted energies alternating with

bands of forbidden energies. If there are fewer electrons than levels in a given band, or Brillouin zone, the condition of partially filled levels and so of metallic conduction is fulfilled. Correspondingly, if two Brillouin zones overlap (Fig. 39 A) [20], and there are not enough electrons to fill both zones, metallic conduction is again observed. If the zones do not overlap but are adjacent, and one zone is full and the other empty (Fig. 39 B), the substance is a semi-conductor, for clearly the input of a small activation energy will promote electrons from the first zone to the second, and so leave incompletely filled levels in both zones, with consequent electrical conduction (Fig. 39 c). In an insulator the completely occupied zone and the unoccupied zone are so far apart that with normal activation energies no electrons are promoted, and so electrical conductivity is absent.

Hydrogen-metal systems

The nature of alloy systems of hydrogen with metals is now easily understood. The alloying hydrogen atom may provide electrons which fill the empty levels in a band, while the metal loses its para-magnetic properties [20]. An H_2-Pd alloy ceases to be para-magnetic at the composition $H_{0.55}Pd$ and then, since no more electrons can be supplied, very little more hydrogen will dissolve. Hydrogen and deuterium give the well-known isobaric curves [21] of Fig. 40, in which there is an apparent invariant region, and a hysteresis effect. This is due to the formation first of an α-alloy, and then of a β-alloy, the two alloys co-existing along the vertical lines of Fig. 40. The occurrence of two phases may be explained by supposing that, as the concentration of hydrogen atoms in the palladium lattice rises, the atoms interact with each other as well as with the lattice. When a critical interaction energy is reached, some of the atoms gather together in closer association in the palladium lattice, and so a new phase appears which is in equilibrium with the original more dilute phase. As the concentration of hydrogen in the lattice increases, the dilute phase diminishes and the concentrated phase increases in

amount, and one travels along the invariant part of the curve. When the initial dilute or α-phase is all consumed the system becomes once more univariant, and also the lattice is nearly saturated. The limiting composition is not certain but is of
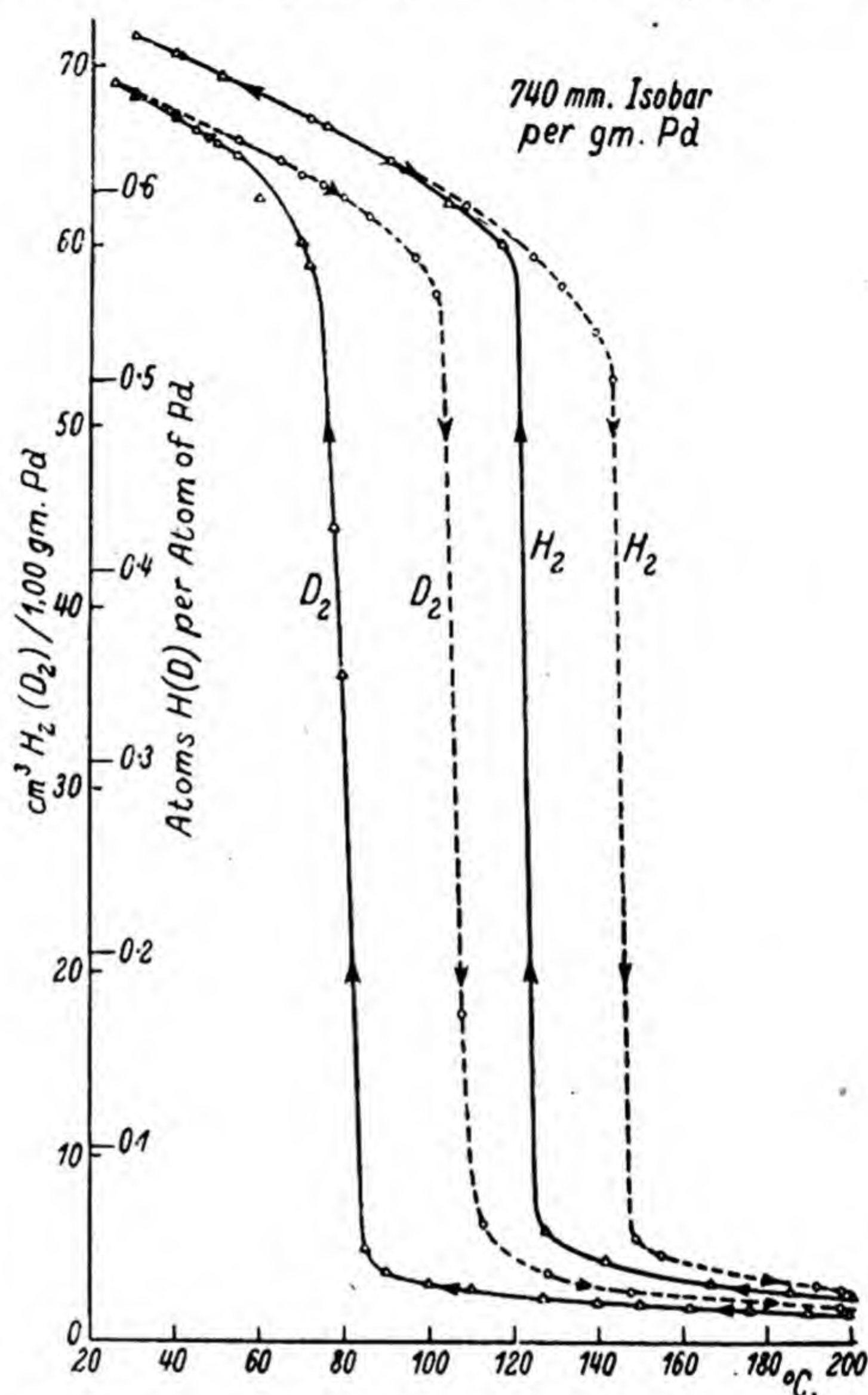
Fig. 40. The solubility of hydrogen and deuterium in palladium at atmospheric pressure.

the order $PdH_{0.55}$ to $PdH_{0.59}$. Lacher[22] analysed the solubility-pressure-temperature data for the hydrogen-palladium system and concluded that the heat of absorption of hydrogen in palladium could be expressed as

$$\Delta H_{cal./mol.} = 2040n_H + \frac{2257n_H^2}{n_s},$$

where the second term expresses the interaction energy between dissolved atoms, or protons, n_H is the number of

gram-atoms of hydrogen dissolved and n_s is the number of gram-atoms of potential energy "holes" in the palladium*. Various other hydrogen-metal systems have properties analogous to the hydrogen-palladium system, except that the interaction energy between dissolved hydrogen atoms or protons is not usually sufficient to cause the separation of two phases, at some critical composition. In Fig. 41 are given absorption isobars for metals which dissolve hydrogen[23]. It is evident from the slopes of such isobars that the solution process is strongly exothermic for metals such as V, Th, Zr,
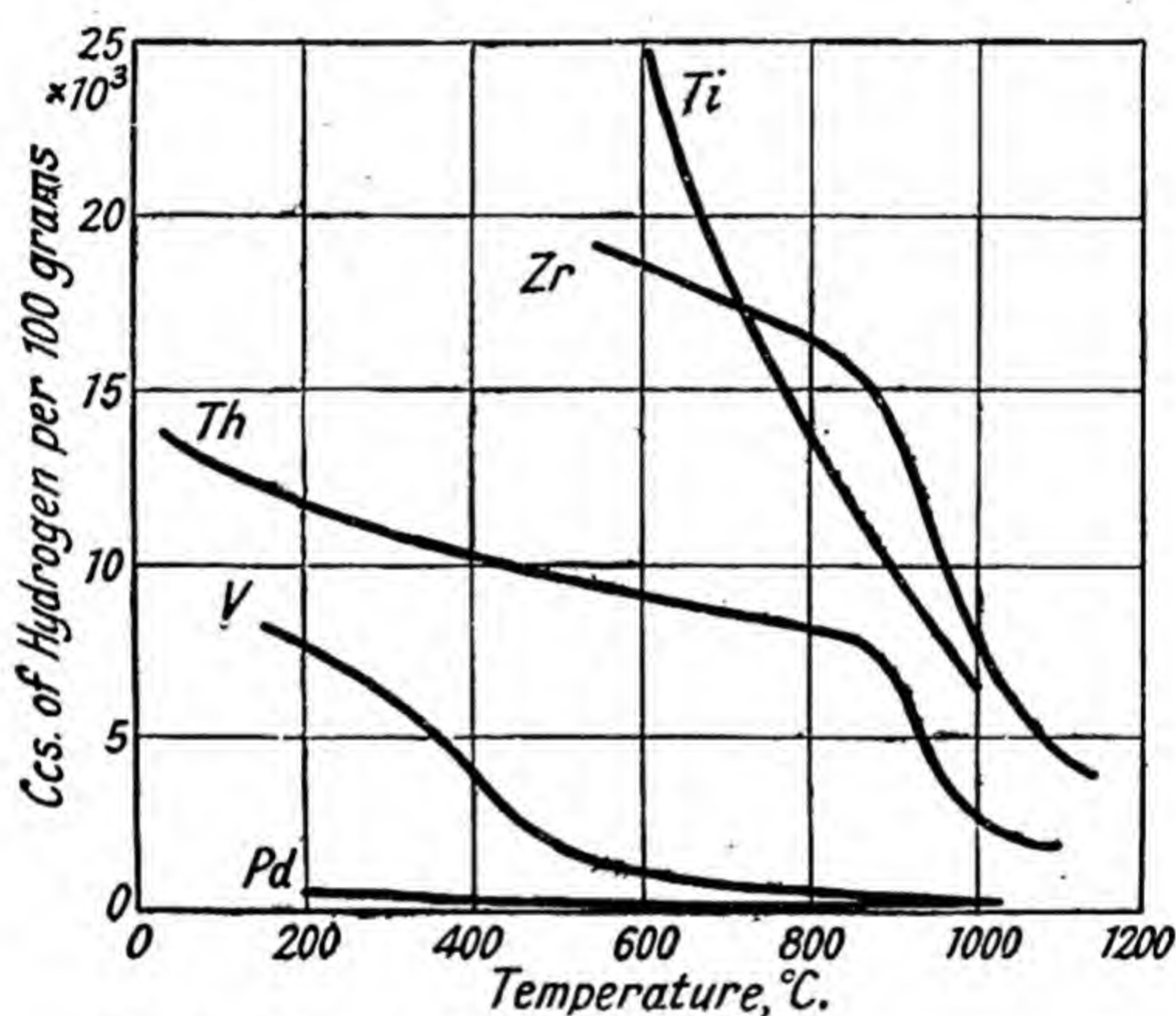
Fig. 41. Some isobars for metal hydrogen systems.

Ti, Ta, but endothermic for Cu, Fe, Co, and Ni. From the slopes of log (solubility)-$1/T$ curves[24] (Fig. 42) the heats of solution given in Table 40 have been calculated. In some of the metals, notably those in which hydrogen dissolves endothermically, there is no appreciable alteration in the lattice constants on solution of the gas in the metal. On the other hand, when hydrogen dissolves in palladium one may have at saturation 10 % expansion of the lattice. In the metals Ti, V, Zr, Th, and Ta, where great quantities of hydrogen are

* The dissolved hydrogen is supposed to occupy interstitial positions in the palladium lattice. These positions of minimum energy are referred to as potential energy "holes" in the lattice.

absorbed, the systems approach a limiting composition and have a new lattice structure. The densities and limiting compositions in the expanded states are illustrated by Table 41.
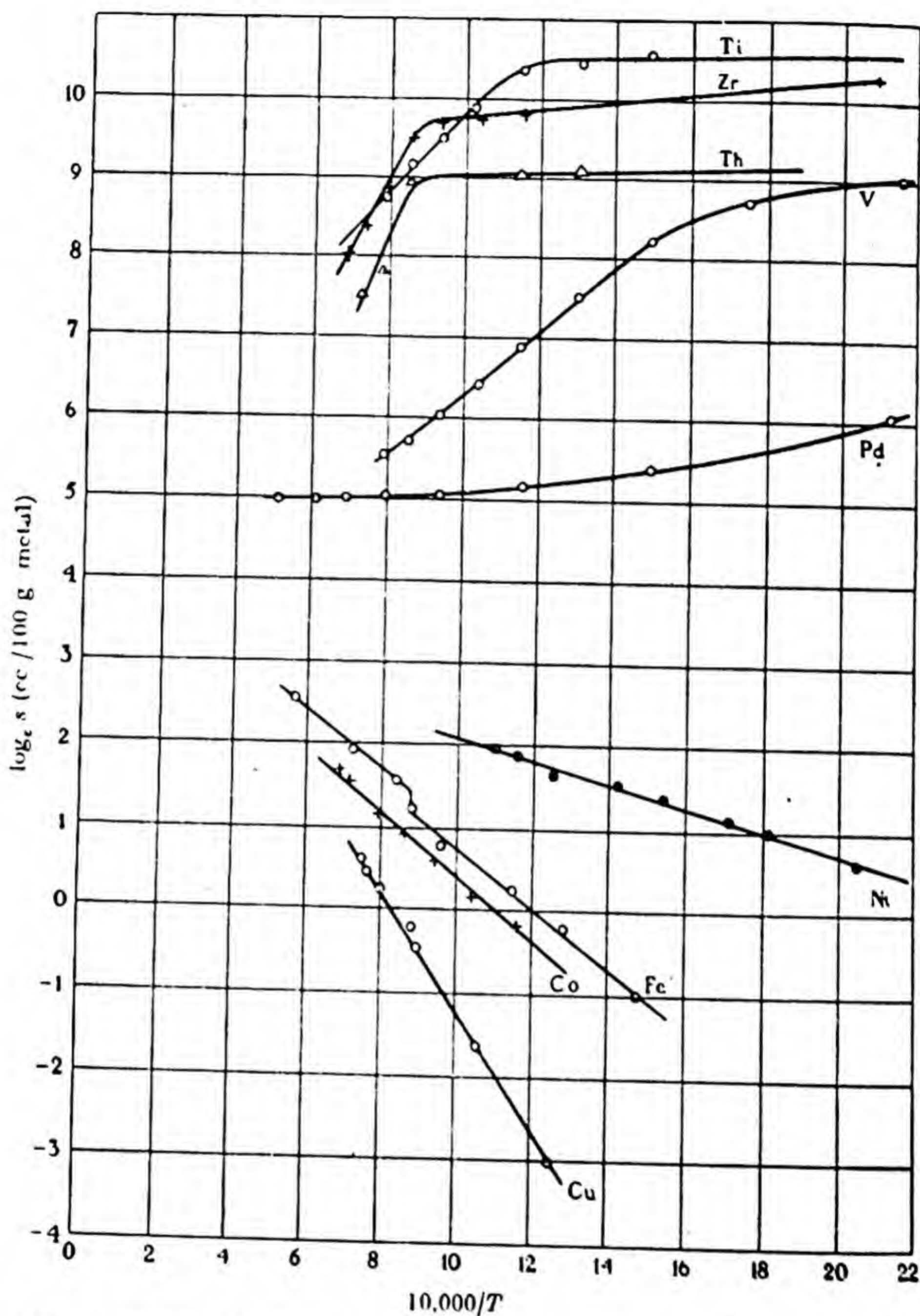
Fig. 42. Observed solubilities s of hydrogen in various metals subjected to one atmosphere pressure of H_2, shown by plotting $\log_e s$ against $10^4/T$. The solubility s is the volume of H_2 gas (reckoned in c.c. at N.T.P.) absorbed by 100 g. of metal.

The methods of statistical mechanics (24, 22) have provided an approach to the problem of gas-metal solubility. The metal can be regarded as containing a series of holes of low

potential energy distributed periodically according to the lattice structure of the metal. The hydrogen molecules in the gas phase dissociate and are absorbed into the lattice where as atoms or protons they vibrate in the holes, among which they

TABLE 40. *Heats of solution of hydrogen in metals*

Exothermic		Endothermic	
Metal	Heat (cal./mol. H_2)	Metal	Heat (cal./mol. H_2)
Ti	10,000	Cu	14,100
Zr	17,500	Co	7,300
Th	22,500	Fe	7,000
V	7,700	Ni	5,600
Pd	2,040	Al	45,500
		Pt	35,400
		Mo	3,500
		Ag	11,600

TABLE 41. *Densities and limiting compositions of some alloy systems*

Metal	Density	Limiting composition	Density	Density ratio
Ti	4·523	TiH_2	3·91	0·864
Zr	6·53	ZrH_2	5·67	0·867
Ta	16·62	TaH	15·10	0·906
V	6·11	VH	5·30	0·867

are distributed at random. Diffusion occurs by jumps from one hole to another, when a sufficient activation energy has been acquired. The partition function is then constructed for the systems

(i) H_2 molecules in the gas phase,

(ii) H atoms in the gas phase,

(iii) H atoms (or protons) in the metal lattice,

and so an expression for the equilibrium between gas molecules and absorbed atoms is obtained:

$$\nu_s \leqslant \left(\frac{p}{kT}\right)^{\frac{1}{2}} \frac{\frac{(2\pi mkT)^{\frac{3}{2}}}{h^3} \overline{w}_2 \exp\left[-\frac{\chi_s}{RT}\right]}{\left[\frac{\{2\pi(2m)kT\}^{\frac{3}{2}}}{h^3} \frac{8\pi^2 IkT}{2h^2}\right]^{\frac{1}{2}} \exp\left[\frac{\frac{1}{2}\chi_d}{kT}\right]},$$

where ν_s = concentration of dissolved atoms,

k = Boltzmann constant,

h = Planck's constant,

m = the mass of the hydrogen atom,

I = the moment of inertia of the hydrogen molecule,

$\overline{w}_2$ = the weight of the normal electronic state of the hydrogen molecule,

χ_s = the heat of solution of a hydrogen atom in the metal,

χ_d = the heat of dissociation of a hydrogen molecule.

Smithells and Fowler[24] showed that if one defines s, the solubility, as the number of c.c. of molecular hydrogen at N.T.P., dissolved in 100 g. of metal, the formula above reduced to

$$s \leqslant 10^{1\cdot21} \frac{p^{\frac{1}{2}}}{\rho_m T^{\frac{1}{4}}} e^{-(\chi_s + \frac{1}{2}\chi_d)/kT},$$

where ρ_m = the density of the metal. These formulae are applicable to solutions of hydrogen in metals such as Fe, Co, Cu and Ni. Those metals such as Ta, V, Ti, Zr, or Th, where the amount of hydrogen absorbed reaches a limiting value and is thereafter constant, can also be treated. The same methods led to the equation

$$\frac{s}{s_0 - s} = \left(\frac{p}{kT}\right)^{\frac{1}{2}} \frac{(1 - e^{-h\nu/kT})^{-3}}{\left[\frac{\{2\pi(2m)\,kT\}^{\frac{3}{2}}}{h^3} \frac{8\pi^2 I kT}{2h^2}\right]^{\frac{1}{2}}} e^{-(\chi_s + \frac{1}{2}\chi_d)/kT},$$

where s_0 denotes the saturation solubility. Inserting standard numerical values gives

$$\frac{s}{s_0 - s} = 10^{-1\cdot32} \frac{p^{\frac{1}{2}}}{T^{\frac{1}{4}}} e^{-(\chi_s + \frac{1}{2}\chi_d)/kT}.$$

Lacher[22] was able to use the statistical mechanical approach in the same way to explain the occurrence and form of the peculiar isothermals of hydrogen-palladium systems (Fig. 40). All that it was necessary to add to the previous treatment was the assumption that as the concentration of

hydrogen atoms increased they interacted with one another until at a critical concentration they formed clusters in the lattice of the palladium instead of being distributed uniformly.

Oxygen-metal systems

When definite chemical compounds are not formed it should be possible to apply statistical considerations similar to those above to other gas-metal systems. Often, however, as in the system O_2-Ag, the nature of the solution process is not
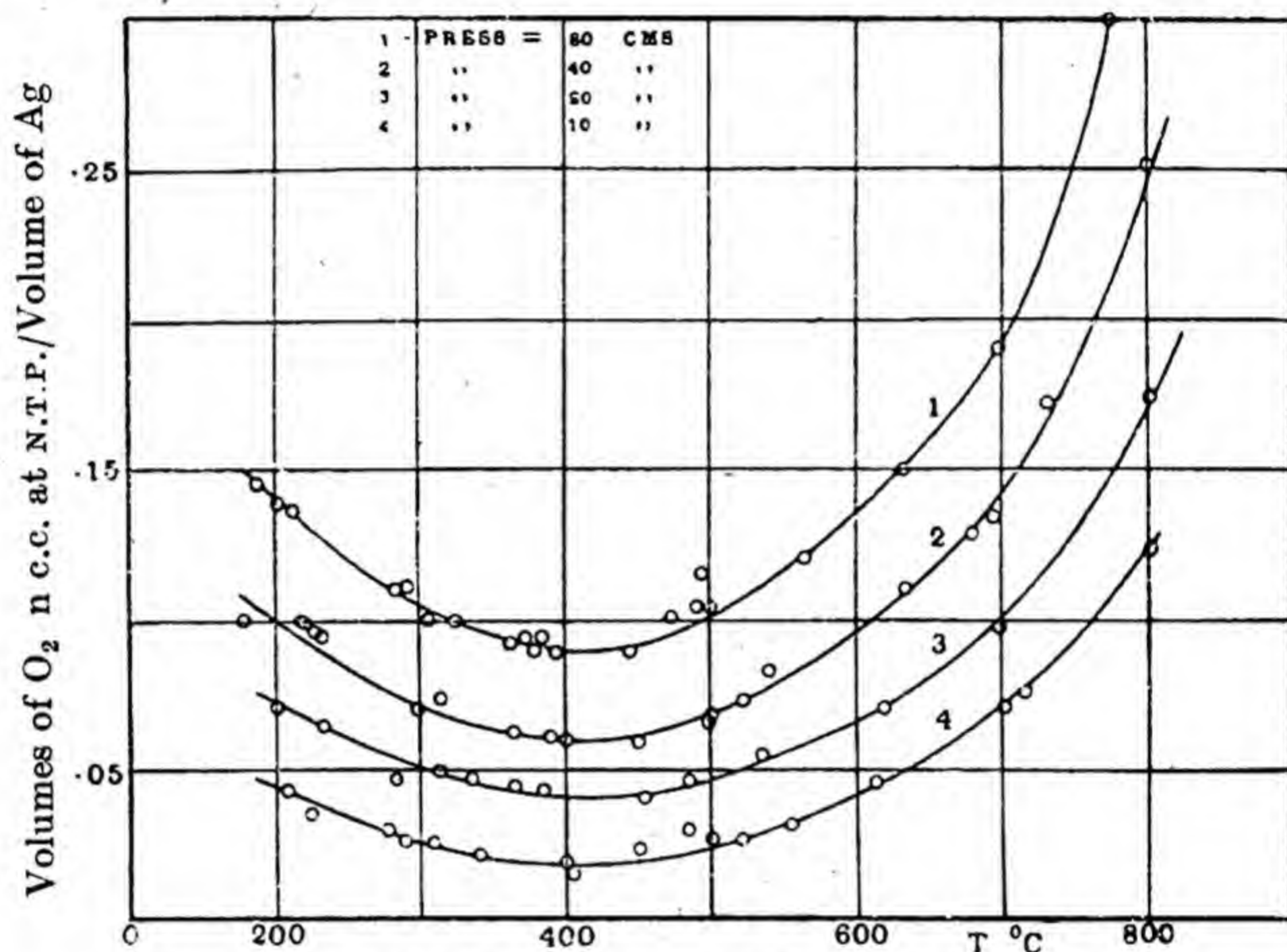
Fig. 43. The solubility of oxygen in silver.

clear (25, 26, 27). The oxygen molecule is dissociated and must be associated with the silver in at least two ways. First, an unstable oxide Ag_2O is formed, but this oxide decomposes as the temperature rises, until, above 400° C., it should under ordinary pressures disappear. However, an endothermic solubility has now set in, and so the isobaric solubility-temperature curves (Fig. 43) (26) first have a negative slope (dissociation of the oxide) and then a positive slope (endothermic solution). Other oxygen-metal systems exist where there is a solubility of oxides in each other or in the metal, or of oxygen in oxides. Here one has really to consider

compounds which do not conform exactly to the law of fixed proportions, and where there is a lattice excess of one or other component. This may occur when some lattice spaces of one component are vacant, or when the other component can occupy interstitial as well as lattice positions. Compounds
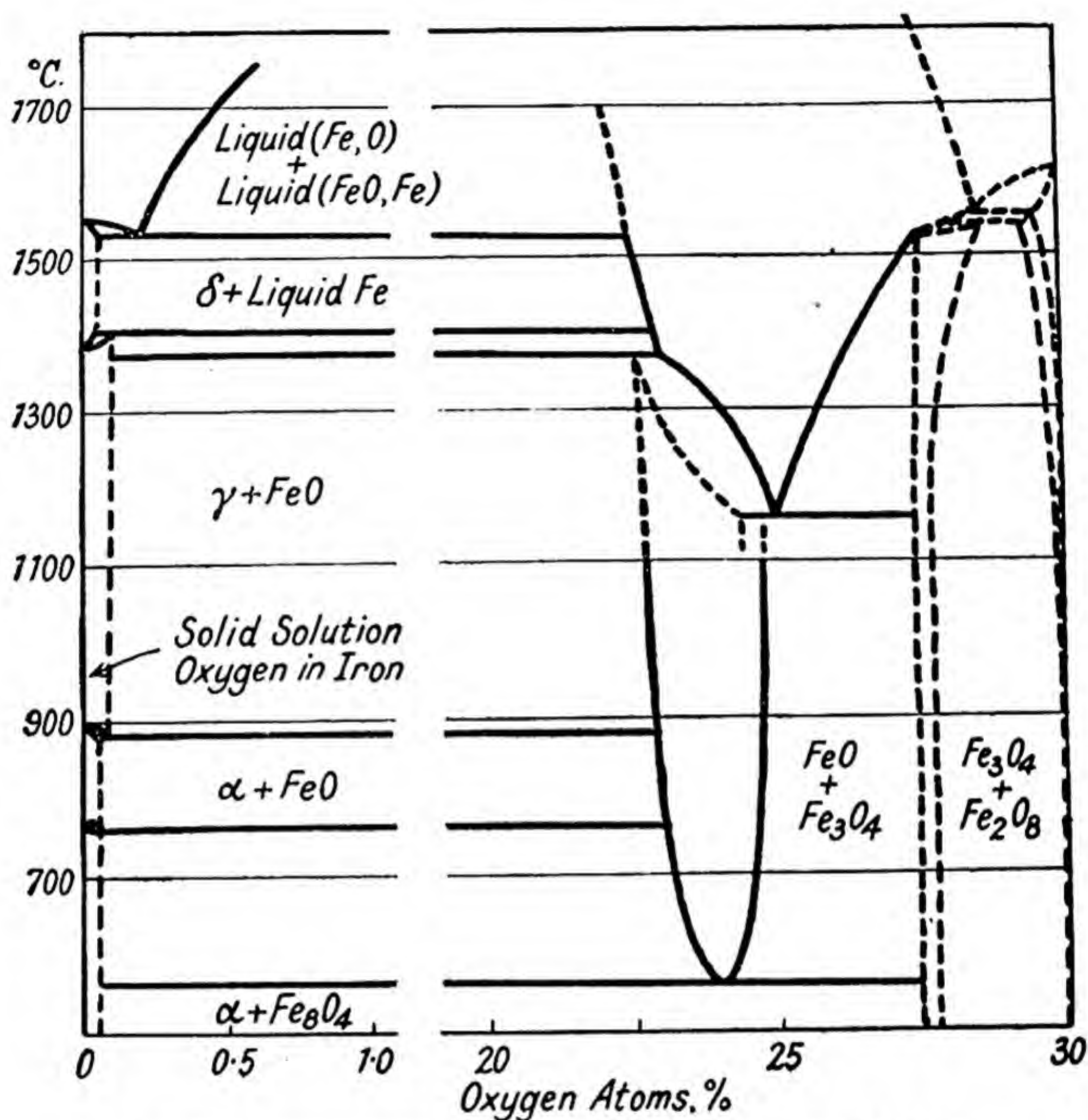
Fig. 44. Temperature-composition phase diagram for O_2-Fe.

having a variable composition are usually referred to as Berthollide compounds, and the phenomena is encountered with the following typical substances:

Oxides of Fe, Co, Ni } (the lower oxides and sulphides
Sulphides of Fe, Co, Ni } may form solid solutions with oxygen and sulphur).

Tungsten bronzes } (variability range considerable).
Spinels }

Zinc oxide (can contain excess metal).

Nickel oxide, for example, can vary in composition between $NiO_{1.000}$ and $NiO_{1.005}$.

The solubility of oxygen in metals is complicated by the formation of oxide phases, so that complex phase diagrams result. As an example, the system $Fe-O_2$ may be taken (Fig. 44)[28,29]. The temperature-composition diagram given shows that oxygen is probably more soluble in γ- than in α- or δ-iron. The solution of oxygen in molten iron occurs endothermically, since the solubility increases with rising temperature (it is 147 c.c./100 g. at the melting point and 387 c.c./100 g. at 1734° C.). The diagram illustrates the great variety of solid solutions possible, and thus indicates how iron-oxygen systems may deviate from the law of fixed proportions.

The oxygen-copper system[30] has received considerable attention, and also shows a complex temperature-composition phase diagram[31]. The solution of oxygen in metallic copper occurs endothermically, as the solubility data of Rhines and Matthewson[30] show:

Temp. ° C.	600	800	950	1050
Solubility (c.c./100 g. metal)	5.0	6.6	7.0	10.9

Other systems which have been studied are O_2-Co[32], O_2-Ni[33], and O_2-Zr[34]. One interesting feature of oxygen-metal systems is the capacity of liquid metals to dissolve large quantities of oxygen or oxides, which on cooling are frozen out, as oxide or as bubbles of oxygen.

Nitrogen-metal systems

In order for nitrogen to be absorbed by a metal it is necessary that the metal should be capable of forming a nitride. Thus, while nitrogen is not absorbed by Cu, Co, Ag, and Au, it is taken up by the metals Fe, Mo, W, Mn, Al, and Zr. A great variety of phases is observed in some of these systems. Nitrogen-molybdenum[35,36] gives the following:

α (Mo): body-centred cubic. No solid solution with nitrogen.

β (Mo$_3$N): face-centred tetragonal. Stable only above 600° C. Contains 25 % atomic nitrogen.

γ (Mo$_2$N): face-centred cubic. Stable at all temperatures, and contains 33 % atomic nitrogen.

δ (MoN): hexagonal. Contains 50 % atomic nitrogen.

Because of the use of iron catalysts for ammonia synthesis, the nitrogen-iron phase diagram is especially interesting [37,38] (Fig. 45). Other systems, such as nitrogen-manganese [39], nitrogen-aluminium [40], and nitrogen-zirconium [34], need not
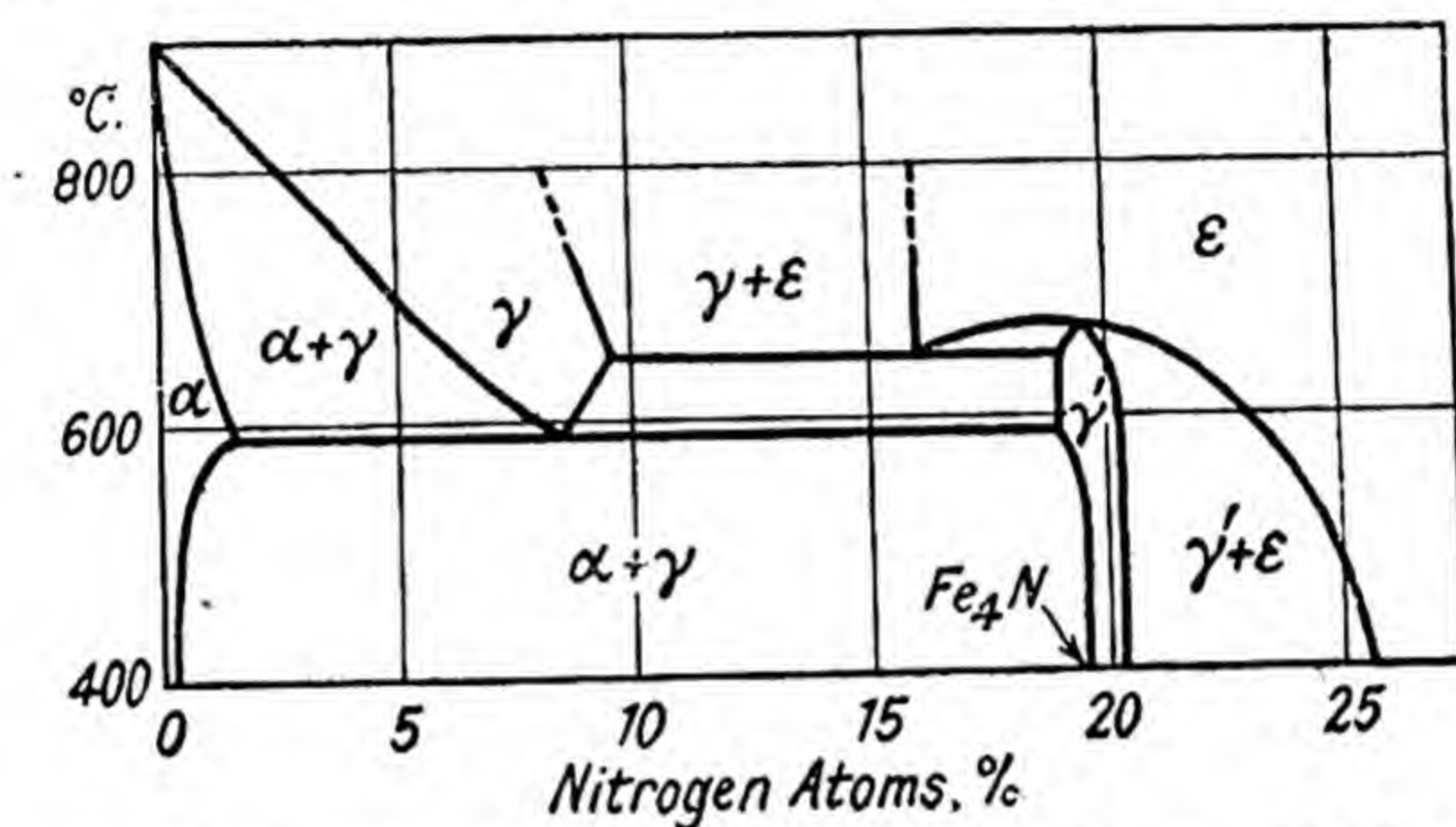
Fig. 45. Temperature-composition phase diagram of N$_2$-Fe.
α = solid solution N$_2$ in Fe, γ = solid solution N$_2$ in Fe, γ' = Fe$_4$N,
ϵ = Fe$_3$N.

be considered here, since the behaviour already described for nitrogen-molybdenum and nitrogen-iron is typical. It is interesting that nitrogen dissolves in molten aluminium to give an approximately linear plot of log (solubility) against $1/T$. This is characteristic also of solutions of oxygen in silver at high temperatures, and of solutions of sulphur dioxide in liquid copper [41,42]. In the latter case, as in the two former, the solubility is proportional to the square root of the pressure, indicating a dissociation of the sulphur dioxide molecule in solution.

THE SOLUBILITY OF GASES IN ALLOYS

The study of gas-alloy systems has been confined principally to hydrogen. One might recognise two possible classes of alloy, one compounded of two hydrogen-dissolving metals, and the

other composed of one hydrogen-dissolving metal and a second metal inert to hydrogen. The behaviour in the second of these systems is somewhat unexpected, for as the summarising data below show, instead of the hydrogen solubility diminishing steadily to a zero value as the percentage of the inert metal increases, one often finds a solubility first rising to a maximum and then falling towards zero as the percentage of the inert metal increases. When hydrogen dissolves in both metals A and B of the alloy, however, one usually finds a continuous change in solubility from 100 % A to 100 % B. The system H_2-Mo-Fe appears to be an exception:

(a) Alloys in which the gas solubility changes continuously:

$$Fe\text{-}V \ (H_2) \ [43],$$
$$Pt\text{-}Pd \ (H_2) \ [44],$$
$$Al\text{-}Cu \ (H_2) \ [44],$$
$$Ag\text{-}Au \ (O_2) \ [45].$$

(b) Alloys in which the gas solubility exhibits a maximum:

$$B\text{-}Pd \ (H_2) \ [46],$$
$$Au\text{-}Pd \ (H_2) \ [47],$$
$$Ag\text{-}Pd \ (H_2) \ [47],$$
$$Fe\text{-}Mo \ (H_2) \ [48].$$

In the following figures are given data illustrating these types of behaviour. The maxima are not always sharp as in the H_2-B-Pd system, nor are they always so well defined. The curve of log (solubility) against $1/T$ in Fe-Mo alloys, as Fig. 42 shows for many hydrogen-metal systems, is linear [49].

It would be out of place to give further details of gas-metal systems here. The purpose of this summary has been to illustrate the very interesting types of equilibria observed, so that one may have some idea of the state of combination of the gas diffusing in the solid. We have seen that hydrogen will diffuse in the form of atoms or protons, that oxygen or nitrogen diffuses after dissociation, and that oxygen-metal and nitrogen-

metal reactions lead much more frequently to the formation of new phases—oxides or nitrides—than do hydrogen-metal reactions. Thus we must think of the diffusion of oxygen or nitrogen as a handing on of the dissolved gas atom by successive decompositions of unstable oxides or nitrides. There is little evidence to show what is the condition of the diffusing particle in its transition state, but it would be anticipated that oxygen and nitrogen, being much more electro-negative than hydrogen, may move as negative ions while hydrogen may very well be considered to diffuse as protons. It has been seen that even the solution of sulphur dioxide follows dissociation of the molecule, al-
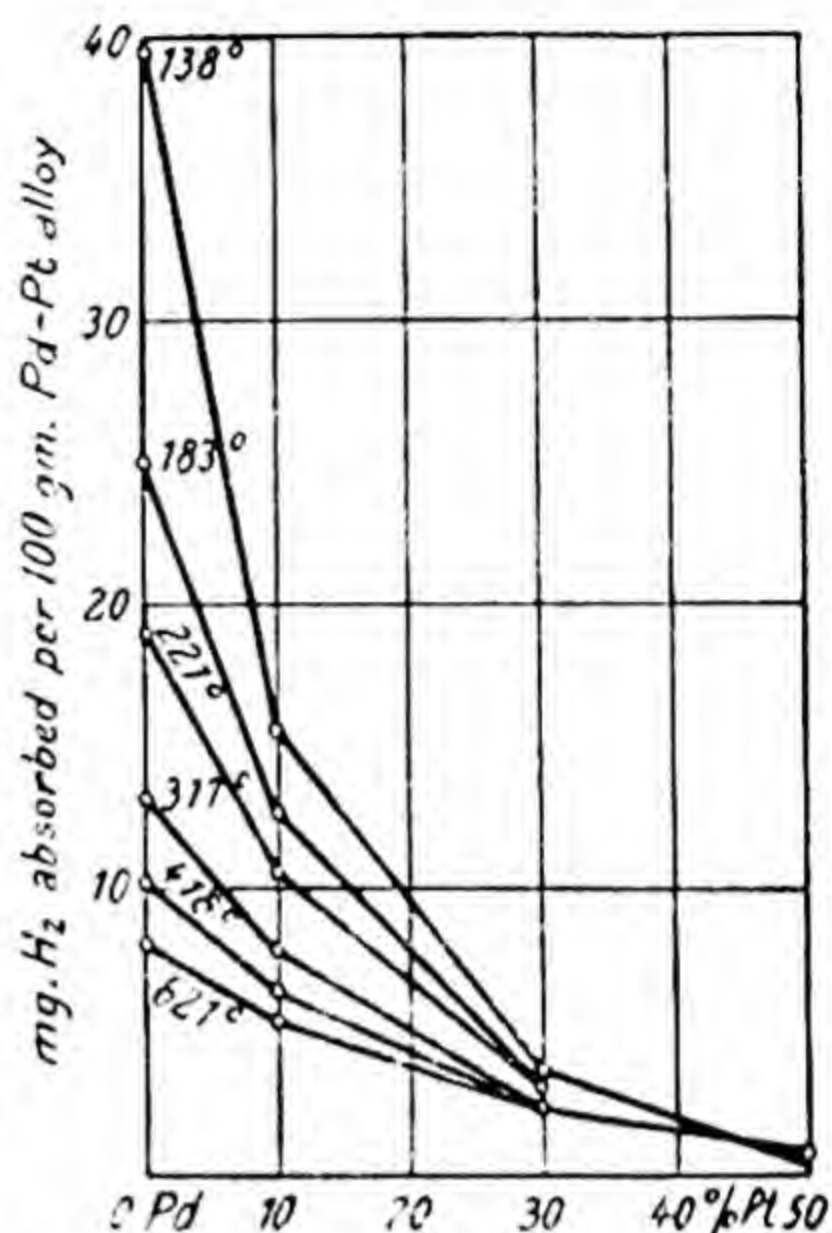
Fig. 46. The solubility of H_2 in Pt-Pd alloys.

though the nature of the fragments remains unknown. Gases such as carbon monoxide, carbon dioxide, or ammonia must
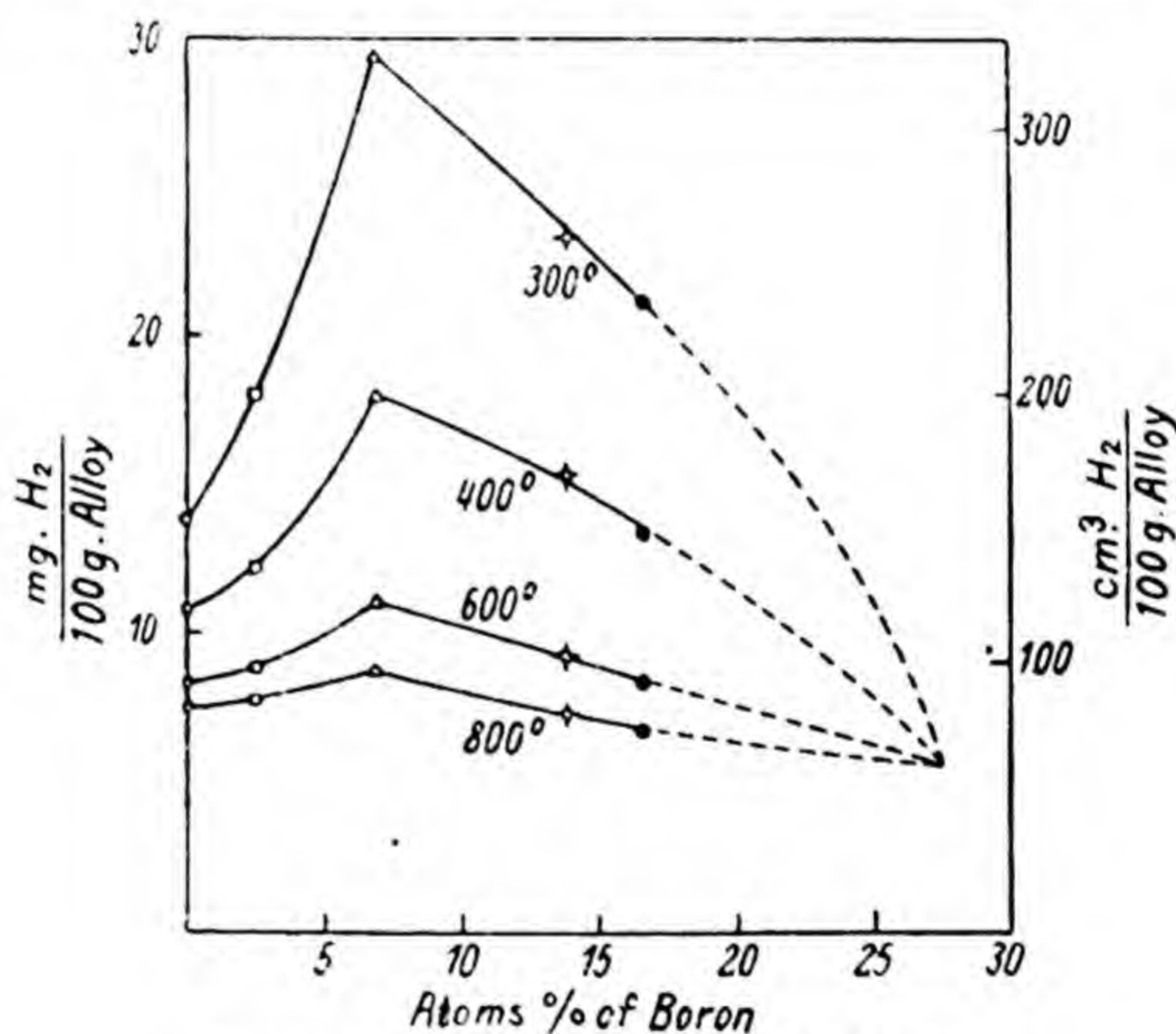
Fig. 47. Solubility of H_2 in B-Pd alloys.

in the same way undergo dissociation into their components before they can penetrate a metal. The specificity of some of

the systems is one of their most fascinating features, and a great deal of further work must be undertaken before the reactions occurring can be properly understood.

THE MEASUREMENT OF PERMEATION VELOCITIES

The usual high vacuum technique employed in studying sorption equilibria and kinetics may be used in obtaining the permeability of metals (15, 19). In addition a special problem arises, the mounting of metal membranes in a manner which will be vacuum-tight and which will permit of heating the specimen to high temperatures.

Ham (50) in an early apparatus mounted a sheet of platinum between two heavy steel tubes with flanged ends. The flanges were ground flat, and the joint put under great pressure by means of bolts passing through heavy steel rings on either side of the flange. Unless the surfaces are very smooth, or the pressure so great as to cause flow of the metal, this arrangement is not entirely vacuum-tight. In later arrangements (51) the membrane was welded across a tube by atomic hydrogen. This method is very satisfactory, but it may not always be possible to do the welding. Such systems have the advantage that effects of temperature variations along the furnace are obviated.

In other arrangements tubes of the metal may be heated in a furnace. One end of the tube is closed and the other is open to a manometer. The whole tube may be surrounded by the diffusing gas. This very simple and useful method was used by Borelius and Lindblom (52).

It is best to have the tube in the form of a bulb of large area in the centre of the furnace, with a narrow-necked tube leading from it out of the furnace. The narrow tube may then be fitted to glass by a ground joint outside the furnace. The arrangement avoids the effects of temperature inhomogeneities near the ends of the furnace. Another way of doing this requires a short tube of the permeable metal (e.g. palladium) sealed at one end by gold solder, and at the other end welded by gold solder to a less permeable metal

BD

such as platinum or nickel. If the metal is welded to platinum, the platinum may be sealed through soft glass, and the system taken up to 370° C. under vacuum for the diffusion measurements. Another variation of this arrangement is to solder (with gold or platinum solder) a plug of palladium across the mouth of a platinum tube(53), which is again sealed through soft glass. In this connection it should be remembered that copper may be brazed to soft glass, and tungsten sealed through pyrex, provided the arrangement is such that these seals need not withstand high temperatures. The pressure on the high-vacuum side may be given by mercury manometers, McLeod gauges, or Pirani gauges according to the rate at which the pressure rises on this side. At high pressures robust methods of mounting membranes across the tubes
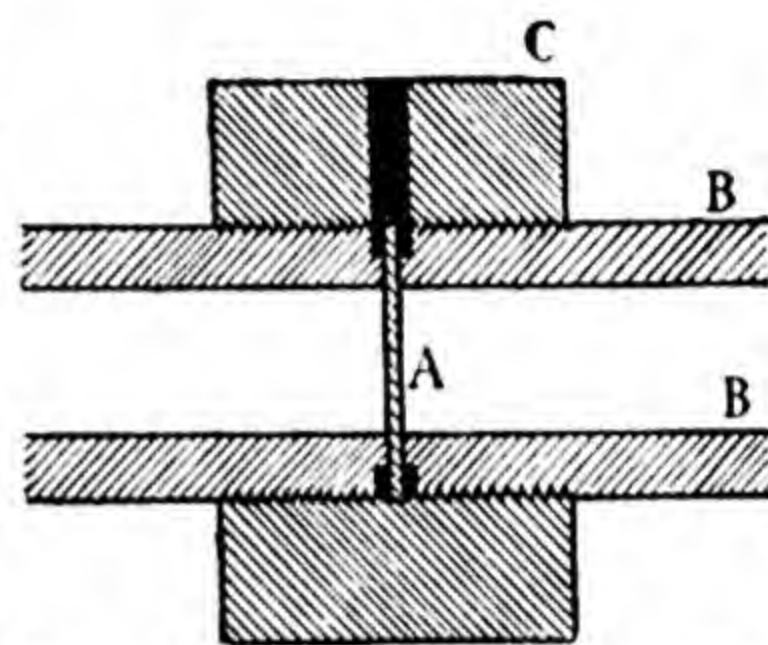
Fig. 48. Apparatus for measuring gas flow through metals at high pressures.

are necessary. A suitable arrangement is that in Fig. 48(54), used to measure permeabilities up to 112 atm. The membrane A was brazed between the faced ends of two stout-walled tubes B, the joint being heated by a small external furnace.

The apparatus required to measure the diffusion of nascent hydrogen is simpler, since permeation occurs at low temperatures. It is usual to use a hollow tube of the metal being studied, as cathode, and by a ground joint, an inseal, or by welding to another metal which is then insealed, to connect it with a manometer system. A typical apparatus of this kind is that of Borelius and Lindblom(52). If the hydrogen is generated by chemical means, the apparatus of Edwards(55) may be employed (Fig. 49), where the hydrogen diffused is measured by displacement of mercury. It would also be possible to adapt Borelius and Lindblom's apparatus to this case.

THE INFLUENCE OF TEMPERATURE UPON PERMEABILITY

The velocity of diffusion through a metal increases very rapidly as the temperature rises, as Fig. 50 illustrates for
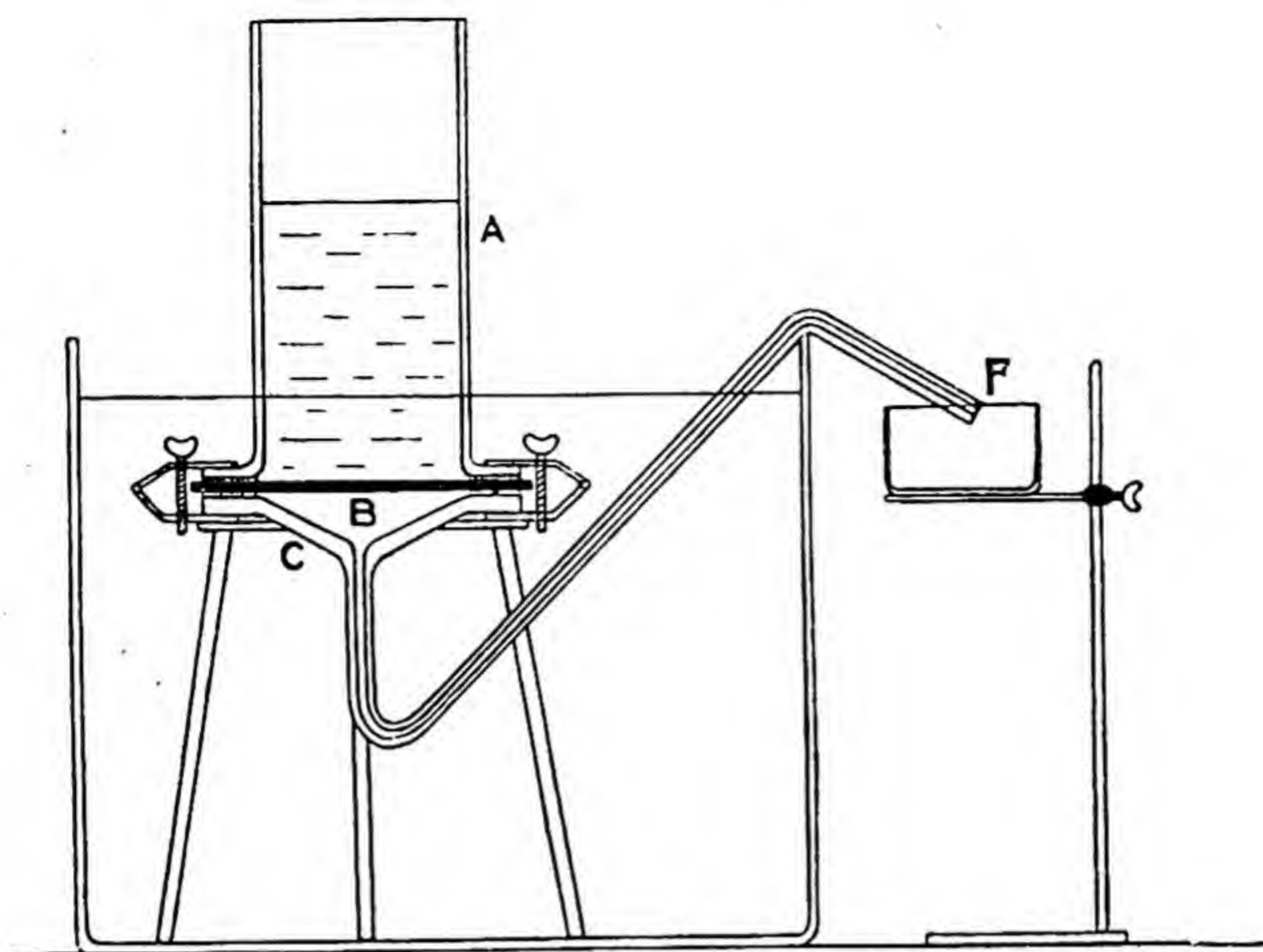
Fig. 49. Apparatus for measuring the rate of passage of nascent hydrogen through iron.

T in $^\circ$ K.
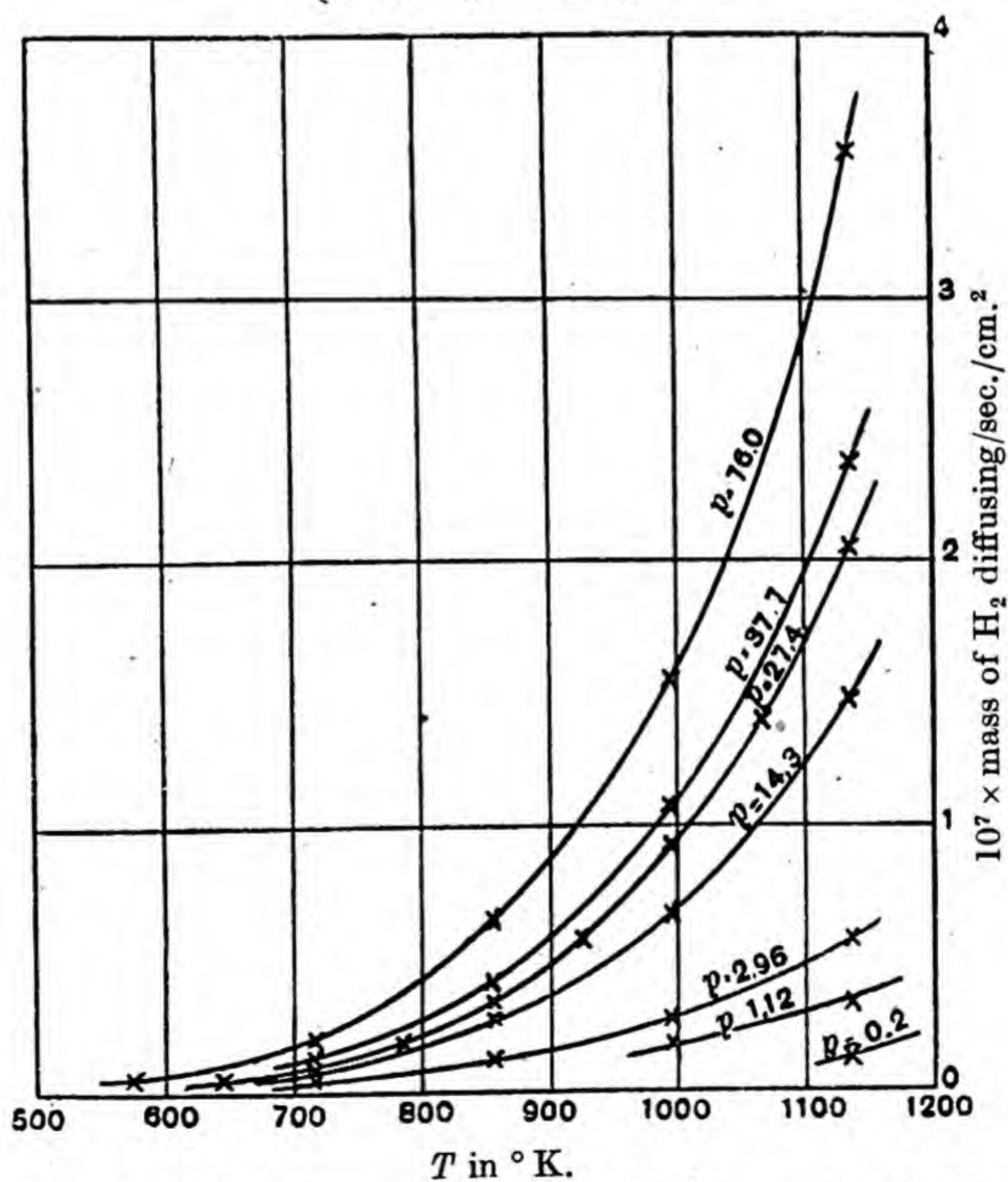
Fig. 50. The effect of temperature upon the permeation velocity of hydrogen through platinum at various pressures.

the passage of hydrogen through platinum. One notes the similarity of these curves to the exponential rise of vapour pressure with temperature, or of chemical reaction velocities with temperature. As is well known, this is due to an exponential term $e^{-\Delta H/RT}$, $e^{-E/RT}$ in the vapour-pressure equation, or expression for the velocity constant respectively; and a similar term arises in the permeability constant P:

$$P = P_0 e^{-E/RT}.$$

However, some of the earliest studies of permeation velocities expressed these velocities as

$$\text{Rate} = A T^n,$$
$$\text{Rate} = A e^{bT},$$
$$\text{Rate} = A e^{-b/T}.$$

For example, Winkelmann [8] gave for the passage of hydrogen through iron $n \sim 5$; while Johnson and Larose [56] for the diffusion of oxygen through silver gave a value of $n = 14.6$. The second of these equations has been applied to hydrogen-nickel [57] and hydrogen-palladium [58] (for the permeability); and to carbon-iron, and nitrogen-iron (for the diffusion constants) [59] with some success. There is no theoretical interpretation for these first two equations however, and the agreement is in general better when the expression $P = P_0 e^{-E/RT}$ is used, and $\log P$ plotted against $1/T$. This has been done by Smithells and Ransley [60] for most of the gas-metal systems whose permeability has been studied, and some of their diagrams are reproduced here (Figs. 51–53). They found the equation to be very satisfactory indeed, although exceptions may occur where allotropic modifications of metal exist in the temperature range considered (e.g. iron [58]), or if the diffusing gas can form two or more types of alloy or phase with the metal (H_2-Pd, N_2-Fe).

From the slopes of the curves $\log P$ against $1/T$, one may calculate the temperature coefficient in cal./atom of gas transferred. The first attempt to give a meaning to this temperature coefficient is due to Richardson, Nicol and Parnell [9], and no subsequent theories have improved greatly
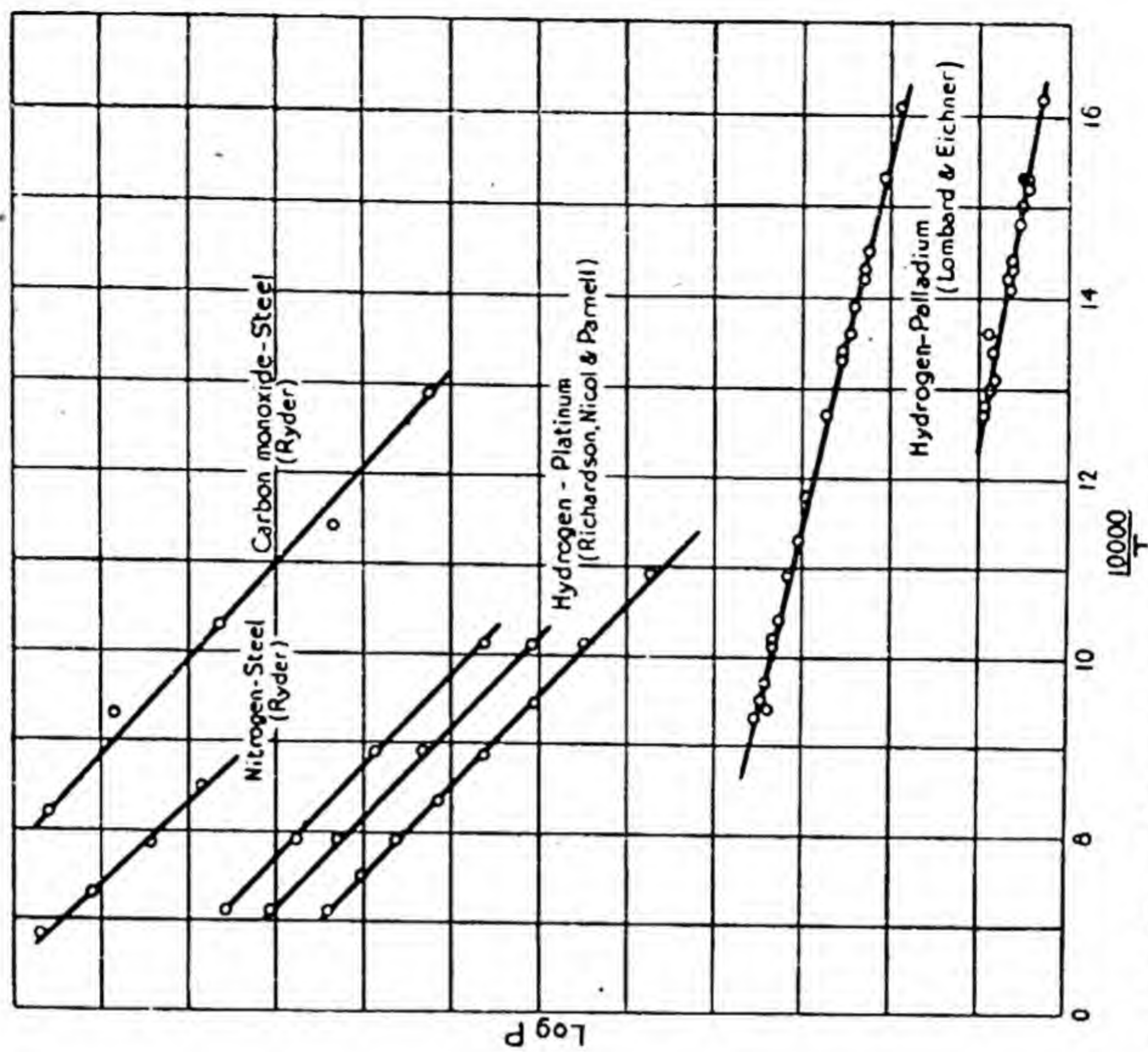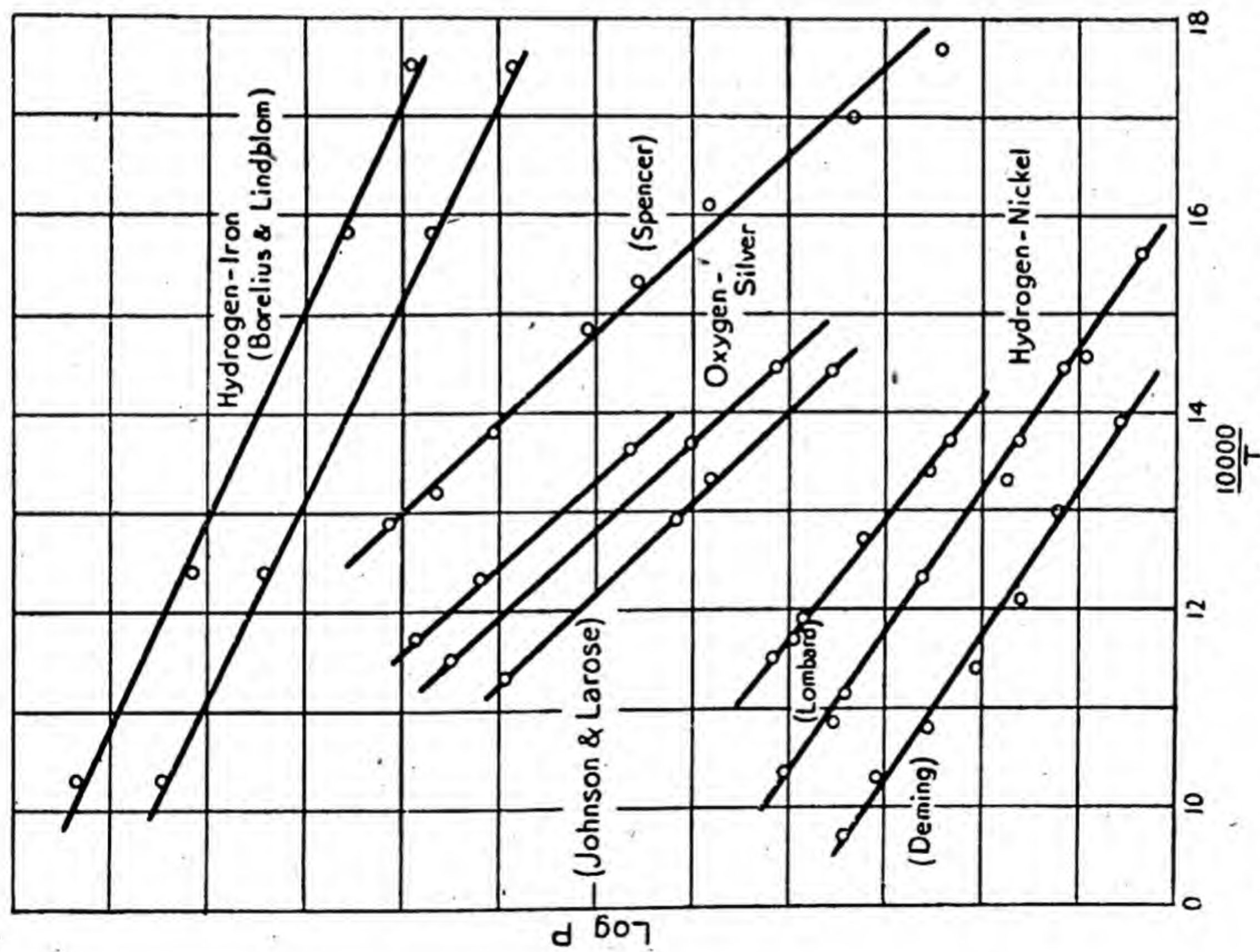
Figs. 51 and 52.   Effect of temperature on the rate of flow of gases through metals.

upon their treatment. They solved Fick's law for the special case of a gas dissociating in the medium and diffusing as atoms. In the stationary state, when $\partial^2 C / \partial x^2 = 0$, they found

$$\text{Rate of permeation} = \frac{1}{l}\frac{D}{2}\left(\frac{k_i}{s_0}\right)^{\frac{1}{2}} p^{\frac{1}{2}},$$
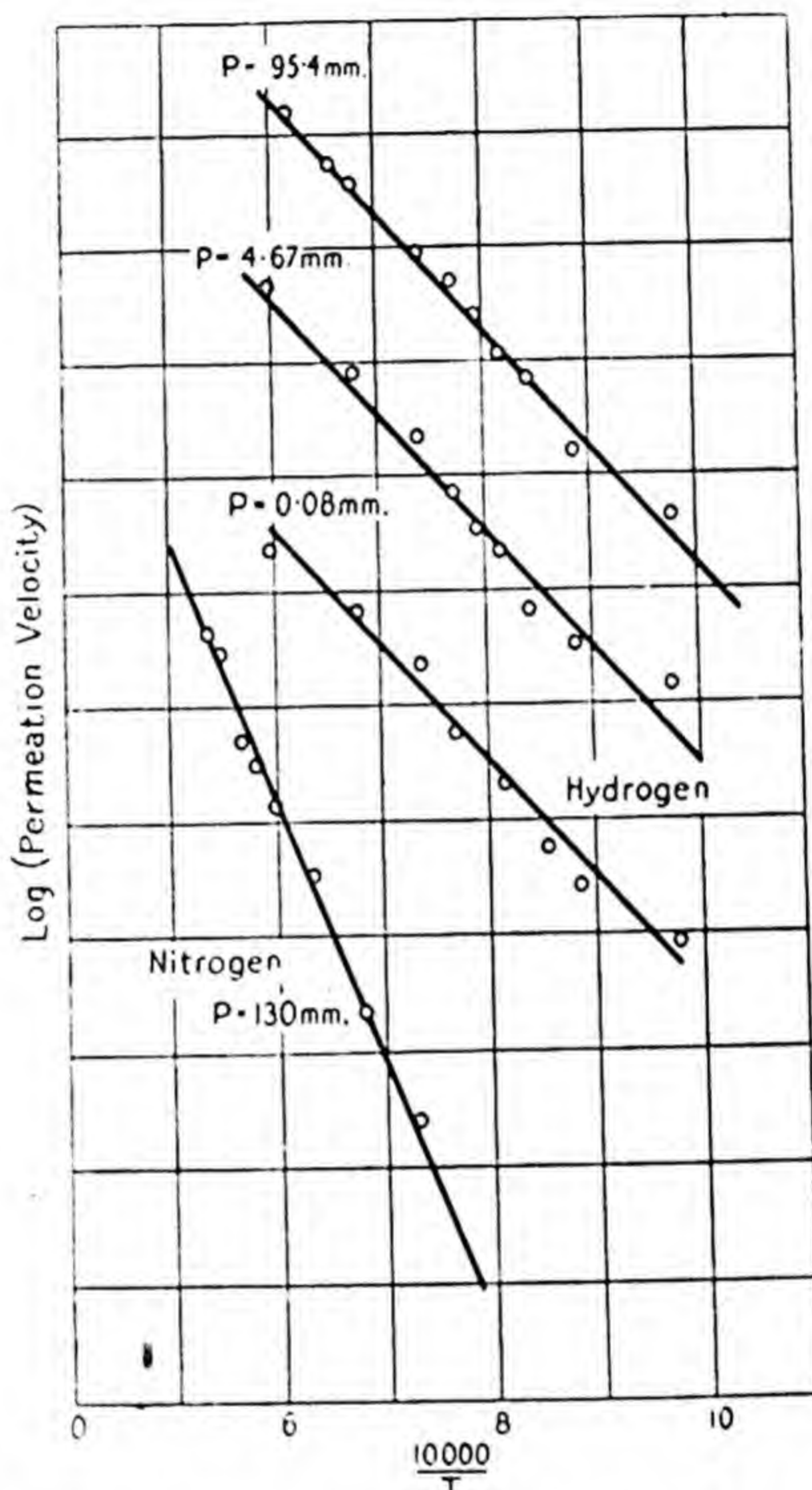
Fig. 53. Effect of temperature on the diffusion of hydrogen and nitrogen through molybdenum.

where D = the diffusion constant,

k_i = the dissociation constant of hydrogen in the metal,

s_0 = the solubility of molecular hydrogen in the metal,

p = pressure.

From the experiments they considered that

$$k_i^{\frac{1}{2}} = C T^{\frac{1}{2}} e^{-36,500/2RT},$$

where C = constant and $CD/2s_0 = 8 \cdot 59 \times 10^{-7}$; and so for the hydrogen-platinum system ·

$$Q = 6 \cdot 60 \times 10^{-9} \frac{p^{\frac{1}{2}} T^{\frac{1}{2}}}{l} e^{-36,500/2RT},$$

where Q denotes the mass of gas diffusing per sec./cm.^{2} of platinum of thickness l, from a pressure p into a vacuum. We now know of course that the heat of dissociation of hydrogen in the metal is not 36,500, because the diffusion coefficient of hydrogen atoms in a metal is itself exponentially dependent on temperature: $D = D_0 e^{-E_0/RT}$. Richardson's equation should then become

$$Q = 6 \cdot 60 \times 10^{-9} \frac{p^{\frac{1}{2}} T^{\frac{1}{2}}}{l} D_0 e^{-E_0/RT} e^{-(36,500-2E_0)/2RT},$$

and until E_0 is known one cannot find the heat of dissociation of hydrogen in platinum. The term in $T^{\frac{1}{2}}$ can as a rule be neglected in a formula such as that above, and it is usual to write $P = P_0 e^{-E/RT}$, where P denotes the permeability constant (c.c. at N.T.P. diffusing/sec./cm.^{2}/mm. thick/cm., or atmosphere, of mercury). The values of E and P_0 for a number of systems are given in Table 42. As Smithells and Ransley have pointed out, the variation in the term P_0 (10^3-fold) is small considering the variety of systems listed. Since permeability constants depend upon so many variables, this consistency is notable, and so far susceptible to no interpretation. In systems like H_2-Ni the temperature coefficient is nearly the same in all the specimens considered; but in H_2-Pd a remarkable variation in the temperature coefficient occurs, and this coefficient appears to depend upon the previous history of the specimen. In its active most permeable state, the temperature coefficient is low; but in impermeable palladium it is high. When hydrogen passes through composite metal sheets of Cu-Pd and Ni-Pd, the temperature coefficient approximates to the values for the least permeable metal (copper or nickel), while for Ni-Pt and Pt-Ni the temperature coefficient is that of the metal at the outgoing face. It should

TABLE 42. *Permeability data for gas-metal systems* $(P = P_0\, e^{-E/RT})$

System	P_0 (c.c./sec./cm.²/ mm. thick/ atm. press.)	E (cal./g. atom)	Author
H_2—Ni	—	14.600, 13,100 (below Curie point)	Post and Ham [61]
	—	13,100, 12,040 (above Curie point)	Post and Ham [61]
	$1·3 \times 10^{-2}$	15,420	Lombard [57]
	$0·85 \times 10^{-2}$	13,860	Deming and Hendricks [62]
	$1·4 \times 10^{-2}$	13,800	Borelius and Lindblom [52]
	$1·05 \times 10^{-2}$	13,400	Ham [50]
	$1·44 \times 10^{-2}$	13,260	Smithells and Ransley [60]
	—	13,400	Post and Ham [51]
H_2—Pt-Ni	—	13,400	Ham [50]
H_2—Pt	$1·41 \times 10^{-2}$	19,600	Richardson, Nicol and Parnell [9]
	$1·18 \times 10^{-2}$	18,000	Ham [50]
	$2·6 \times 10^{-1}$	19,800	Jouan [63]
H_2—Ni-Pt	—	18,000	Ham [50]
H_2—Mo	$0·93 \times 10^{-2}$	20,200	Smithells and Ransley [60]
H_2—Pd	—	5,000	Melville and Rideal [64]
	—	17,800	Melville and Rideal [64]
	$2·3 \times 10^{-1}$	4,620	Lombard, Eichner and Albert [53]
	$3·0 \times 10^{-2}$	10,500	Barrer [53]
H_2—Ni-Pd	—	14,300	Melville and Rideal [64]
H_2—Cu	$2·3 \times 10^{-3}$	16,600	Smithells and Ransley [60]
	$1·5 \times 10^{-3}$	18,700	Braaten and Clark [65]
H_2—Cu-Pd	—	13,700	Melville and Rideal [64]
	—	11,400	Melville and Rideal [64]
H_2—Fe	$1·63 \times 10^{-3}$	9,600	Smithells and Ransley [60]
	$1·60 \times 10^{-3}$	9,400	Borelius and Lindblom [52]
	$2·40 \times 10^{-3}$	11,000	Ryder [66]
	—	8,700 (below 900° C.)	Post and Ham [51]
	—	18,860 (above 900° C.)	Post and Ham [51]
H_2—Al	$3·3$–$4·2$	30,800	Smithells and Ransley [67]
O_2—Ag	$3·75 \times 10^{-2}$	22,600	Spencer [68]
	$2·06 \times 10^{-2}$	22,600	Johnson and Larose [56]
N_2—Mo	$8·3 \times 10^{-2}$	45,000	Smithells and Ransley [60]
N_2—Fe	$4·5 \times 10^{-2}$	23,800	Ryder [66]
CO—Fe	$1·3 \times 10^{-3}$	18,600	Ryder [66]

be remembered that in every case the diffusing molecule dissociates; when carbon monoxide passes through iron, for example, the carbon and oxygen diffuse separately.

The influence of pressure on the permeability of metals to gases

In this field some very thorough studies have been made for hydrogen-metal systems, especially by Lombard and Eichner[69], Smithells and Ransley[60] and Post and Ham[61]. Even for hydrogen-metal systems, however, the interpretation of the permeation rate-pressure isotherms is not clear. Studies of glass, crystal, and organic membrane permeability have shown that two possible permeation rate-pressure relationships emerge:

(i) Activated diffusion without dissociation:

$$dp/dt = kp\, e^{-b/T}.$$

(Gas diffusing in SiO_2, KBr, zeolites and organic polymers such as rubber, bakelite, ebonite, cellulose esters.)

(ii) Activated diffusion with dissociation:

$$dp/dt = kp^{\frac{1}{2}} e^{-b/T}.$$

(H_2, O_2, N_2, SO_2, CO diffusing through metals.)

It is with the second type of diffusion system we have now to do. The first type requires an open crystal structure with large interstices (e.g. zeolites); in metals the crystal form is never sufficiently open, and so one finds that inert gases cannot either dissolve in or pass through a metal. This is true of any gas which cannot in some way react specifically with the metal under consideration. One criterion of the specific interaction is the $\sqrt{p}$ law in the expression $dp/dt = kp^{\frac{1}{2}} e^{-b/T}$.

Richardson[9] deduced the first specific expression for the permeation velocity through a metal, and his expression (p. 167), $dp/dt = Ap^{\frac{1}{2}}T^{\frac{1}{2}} e^{-b_1/T}$, can be taken as the basis of the present discussion of isotherms. However, not all experiments gave an exact relationship $dp/dt = A_1\sqrt{p}$. Thus one finds, on

writing $dp/dt = A_1 p^n$, the following values of n given for hydrogen and palladium:

Schmidt (1904)[70] $n = 1$,

Holt (1915)[71] $n = 1$,

Winkelmann (1901)[8] $n = 0.7$,

Lombard and Eichner (1932)[72] $n = 0.8$, $n = 0.62$,

Lombard and Eichner (1933)[69] (i) $n = 0.58$, 0.59,

                               (ii) $n = 0.56$ (mean of a number of results).

Since Schmidt's and Holt's results are not very accurate, and could also be expressed approximately by a $\sqrt{p}$ law, one is justified in saying that the exponent is less than one, and indeed the later values show it to be very nearly one-half. Finally, Ham and Sauter[73,74] working with very pure palladium obtained many values of the exponent n between 0.535 and 0.50. They found a maximum deviation from the $\sqrt{p}$ law at $248°$ C. when $n = 0.585$. One may summarise the position by saying that there seem to be small and somewhat variable deviations from an exact $\sqrt{p}$ law, but that this law is very nearly fulfilled.

One explanation of a $\sqrt{p}$ law is, as previously indicated, that diffusion occurs as atoms. One then has the following relations:

(i) $\dfrac{C_H \text{ (solid)}}{C_H \text{ (gas)}} = k_1$, for small concentrations (Nernst distribution law).

(ii) $\dfrac{C_H^2 \text{ (gas)}}{C_{H_2} \text{ (gas)}} = k_2$ (law of mass action).

(iii) Rate of permeation, $P = -D\dfrac{dC_H \text{ (solid)}}{dx}$ (Fick's law).

From (i) and (ii)

(iv) $C_H \text{ (solid)} = k_1\sqrt{k_2}\sqrt{\{C_{H_2} \text{ (gas)}\}}$.

Then if one writes $\dfrac{dC_H}{dx} = \dfrac{{}_0C_H - {}_lC_H{}^*}{l}$ and substitutes from (iv) for C_H (solid), one finds

(v) $P = Dk_1\sqrt{k_2}\{\sqrt{({}_0C_{H_2})} - \sqrt{({}_lC_{H_2})}\}$,

---

* ${}_0C_H$ denotes the concentration of H-atoms just inside the ingoing surface ($x = 0$) and ${}_lC_H$ the concentration at the outgoing surface ($x = l$).

which gives the observed relationship if $\sqrt{(_lC_{H_2})} \ll \sqrt{(_0C_{H_2})}$, as is the case when one side of the metal is held at a near-vacuum. This preliminary treatment is, however, very much too simple. It was first noted by Borelius and Lindblom [52] that even when one side of the metal was held under a vacuum, the diffusion isotherms appeared to obey a relationship (Fig. 54)

$$P = k(\sqrt{p} - \sqrt{p_l}).$$

They therefore suggested that a threshold pressure must be reached before permeation commences—an explanation difficult to base upon theory.
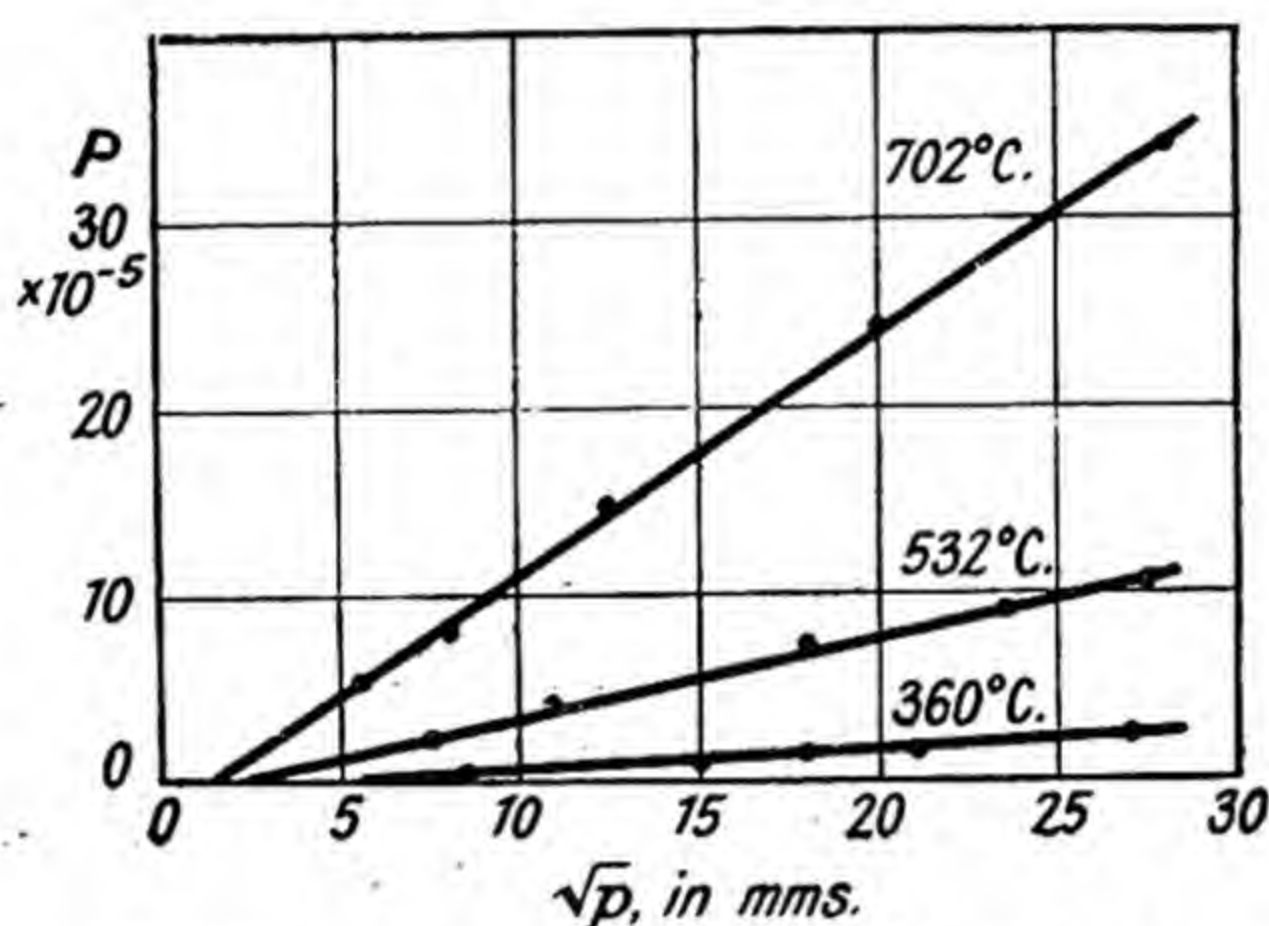
Fig. 54. Permeation rate-pressure isotherms of Borelius and Lindblom [52].

Then Smithells and Ransley [60] noted that the diffusion isotherms bent round at low pressures and thus did pass through the origin. They suggested that at low pressures the rate of permeation was proportional to the fraction of the surface covered by an adsorbed layer, θ, as well as to the square root of the pressure. Thus, at low pressures the permeability P is given by

$$P = k\theta\sqrt{p},$$

and so steadily increases until $\theta \sim 1$. Thereafter the relationship is $P = k\sqrt{p}$. Smithells and Ransley [60] plotted many of their own and other workers' permeability-pressure isotherms to illustrate their suggestion. Some of their curves are reproduced in Figs. 55 and 56. The figures show, however, as do the authors' calculations, that θ approaches unity at lower pressures the greater the temperature. That is, at high tem-

peratures the $\sqrt{p}$ law is obeyed at lower pressures. It would be necessary to suppose that adsorption was endothermic for this to be true, whereas it is well known that for these systems
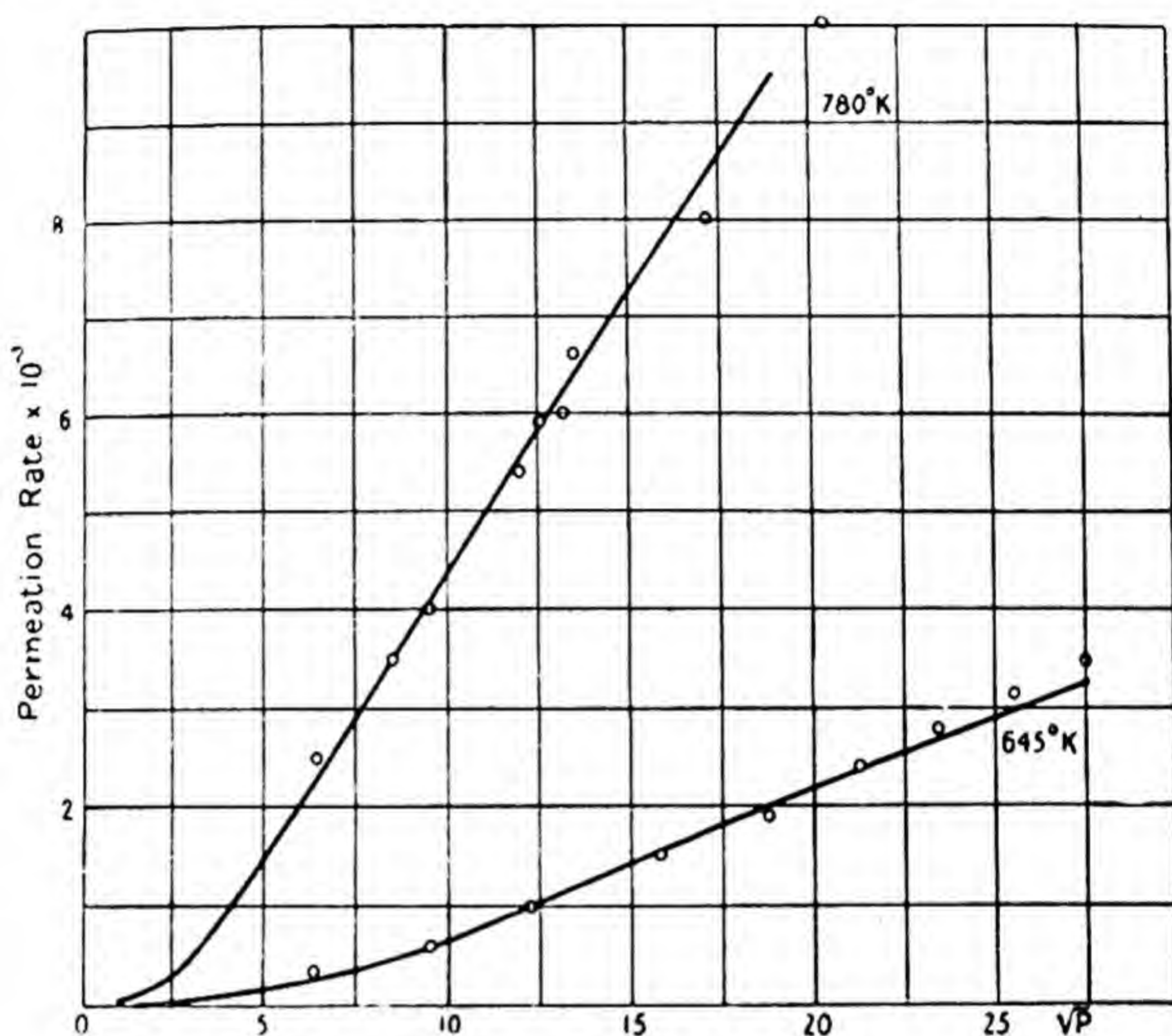
Fig. 55. Permeation rate-pressure isotherms for H_2-Pd.
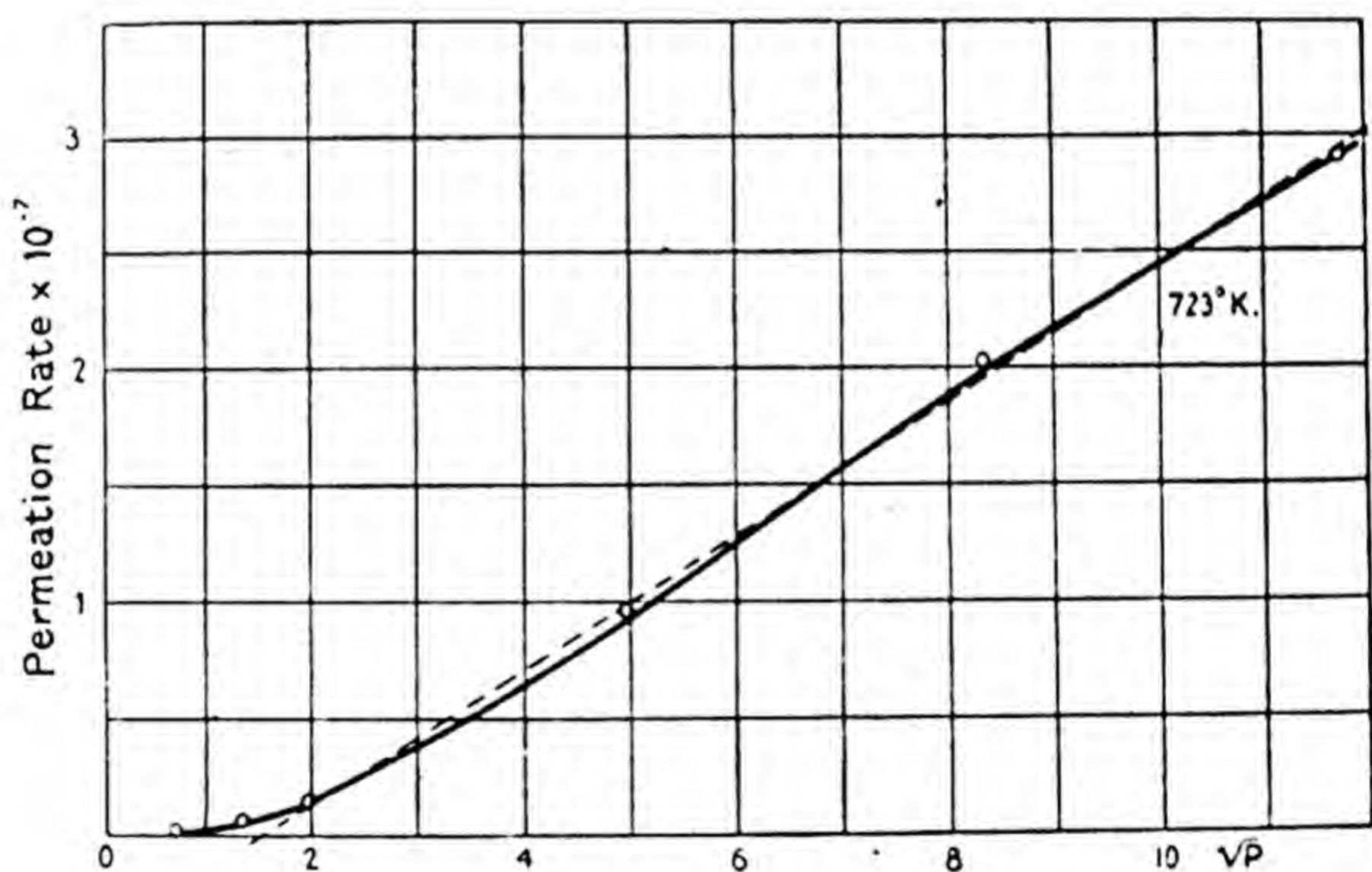
Fig. 56. Permeation rate-pressure isotherms for H_2-Cu.

adsorption occurs in atomic form with evolution of heat. The results of Borelius and Lindblom on the diffusion of hydrogen through iron at 702° C. (Fig. 54) and at 100° C. (Fig. 57) will

illustrate the seriousness of this objection. Fig. 54 shows that at 702° C. if the rate is expressed as $P = k(\sqrt{p} - \sqrt{p_t})$, p_t has a value of about 4 mm., while Fig. 57 shows that at 100° C. p_t has a value of nearly 8 atm. These, according to Smithell's theory, must give approximately the pressure needed to saturate the surface—1500 times as great a pressure at 100° as at 702° C., although adsorption occurs exothermally.
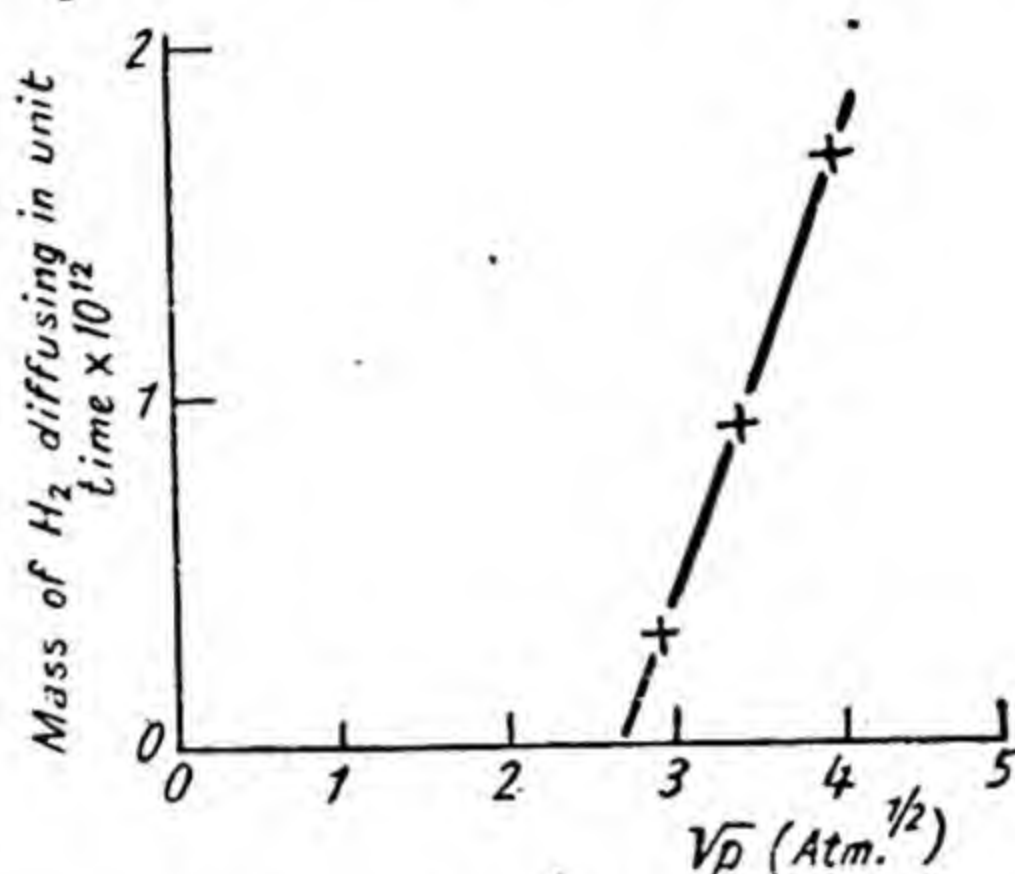
Fig. 57. H_2-Fe, the permeation velocity as a function of pressure, at 100° C.

In other ways Smithells and Ransley's theory explains the observed facts. For if

$$P = k\theta \sqrt{p} \quad \text{and} \quad \theta = \frac{k_3 \sqrt{p}}{1 + k_3 \sqrt{p}}$$

(Langmuir isotherm for sorption with dissociation), one has

$$P = k\,k_3\,p \quad \text{at low pressures,}$$

$$P = k\sqrt{p} \quad \text{at high pressures,}$$

expressions which cover the observed facts.

Another viewpoint has been developed by Ham [61] and his co-workers. These authors find that the slopes of permeation rate-pressure isotherms for hydrogen-nickel systems are not exactly 0·5, as Fig. 58 shows. The deviations from a $\sqrt{p}$ law are at a maximum near the Curie point, and are related to the purity of the specimen of nickel employed. The isotherms do not have a slope of 0·5 near the Curie point unless the nickel is thoroughly decarburised. Similarly, the isotherms for carbonyl iron [61] at 500° C. remained with an exponent well above 0·5 until the carbon was removed. The authors

considered that all deviations from the exponent of pressure of 0·5 could be attributed to volume effects—some of the diffusing substance was associated with the impurities (often carbon, and possibly nitrogen or oxygen) in atom pairs, or as ions H_2^+. They pointed out that Smithells and Ransley's materials had not been decarburised, and attributed the deviations from a $\sqrt{p}$ law to this.
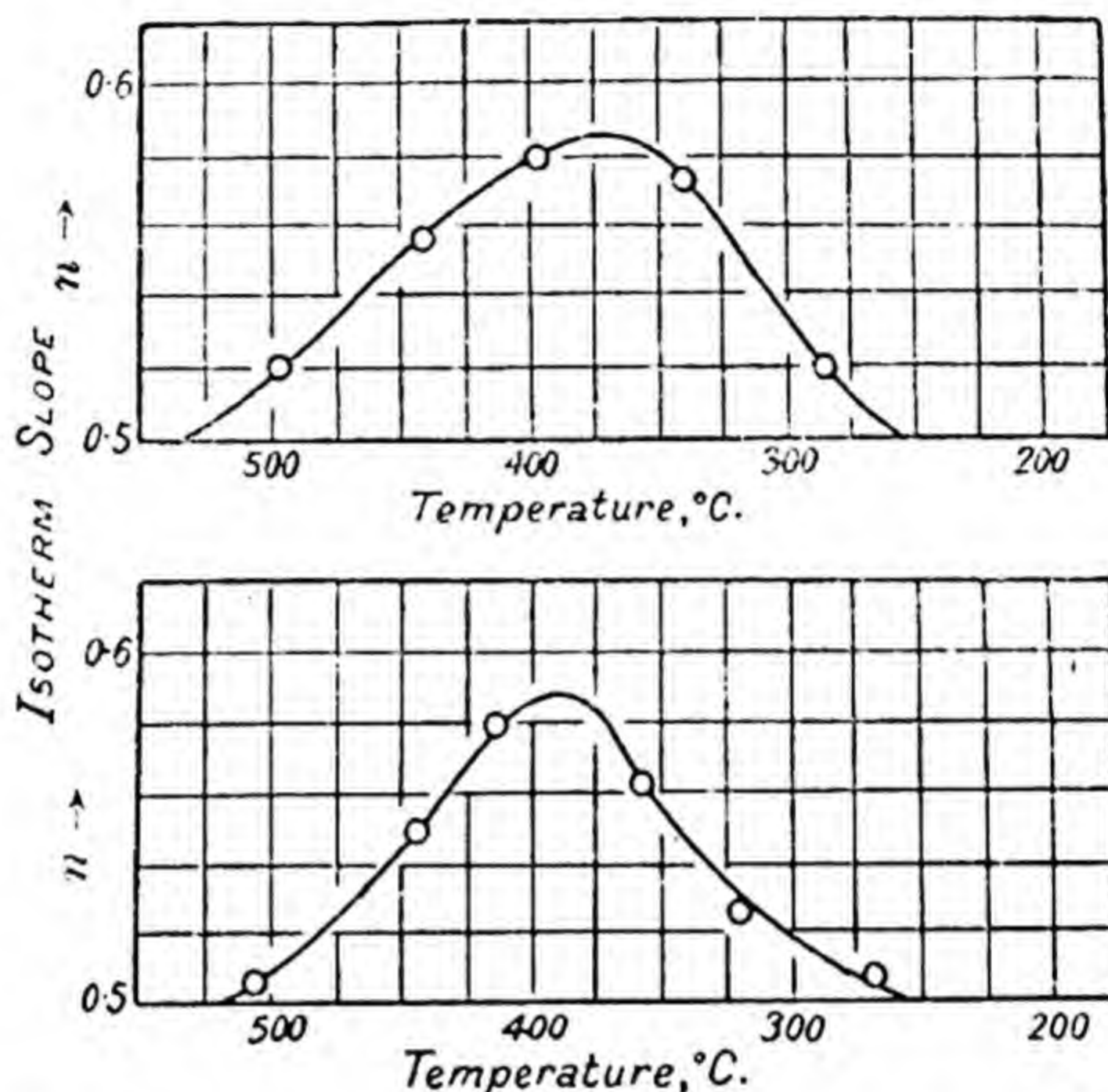
Fig. 58. Exponents n in expression permeation rate $= kp^n(H_2$-Ni$)$
for two different samples of Ni.

However, it is likely that these authors were dealing with two different phenomena. A satisfactory explanation of Figs. 54–57 may be given in terms of phase-boundary processes both at the ingoing and outgoing surfaces (53). Adopting the nomenclature of p. 170, one may suppose that the transference of an atom from both

    (i) adsorbed layer to solid at the ingoing surface,

    (ii) solid to adsorbed layer at the outgoing surface,

is comparable in speed with diffusion in the solid. Then much of the material transferred across the ingoing interface is removed by diffusion, and

$$\text{Actual } (_0C_{II}) < \text{Equilibrium } (_0C_{II}),$$

as defined by equation (i) p. 170. At the outgoing interface, the slow rate of transfer across the interface, but considerable diffusion velocity in the solid, leads to an accumulation just inside the outgoing surface:

$$\text{Actual } (_lC_H) > \text{Equilibrium } (_lC_H).$$

Thus the actual concentration gradient is smaller than the concentration gradient assumed in equation (v), p. 170. The dependence of this gradient upon the pressure is complex, but the curve of the permeation rate plotted against the pressure p must pass through the origin, because when $p = 0$ both $_0C_H$ and $_lC_H$ are zero, and therefore the permeation rate is zero. At intermediate pressures, the permeation rate depends upon a complex function of pressure (see the feet of the curves of Figs. 54–57), but as the pressure rises, or at high temperatures, experiment shows that

$$_0C_H - _lC_H = k\sqrt{p} \text{ (Figs. 54–57)}.$$

The universality of this relation must have important implications for the actual phase-boundary processes. This point will be discussed in more detail on pp. 178 *et seq.*

PERMEATION VELOCITIES AT HIGH PRESSURES

Wüstner's [75] studies upon the hydrogen permeability of silica glass (Chap. III) showed that even up to 800 atm. the permeation rate-pressure isotherm was linear:

$$\text{Rate} = k\frac{p}{l}e^{-b/T}.$$

A few comparable studies have been made upon the permeabilities of metals to oxygen and hydrogen. Smithells and Ransley [76] observed that at pressures of 112 atm. the permeation rate-pressure isotherm obeyed accurately the Richardson equation:

$$\text{Rate} = k\frac{p^{\frac{1}{2}}}{l}T^{\frac{1}{2}}e^{-b/T}.$$

Their data are shown in Fig. 59. A similar result was obtained by Lombard and Eichner [69] at pressures of 26 kg./cm.^{2} for

the H_2-Pd system, and by Borelius and Lindblom for H_2-Fe at 28 atm. The system O_2-Ni, on the other hand, gave a limiting permeation velocity at high pressures (76) (Fig. 60). In this case a visible film of oxide forms on the surface of the metal, and it is likely that in the presence of the solid oxide
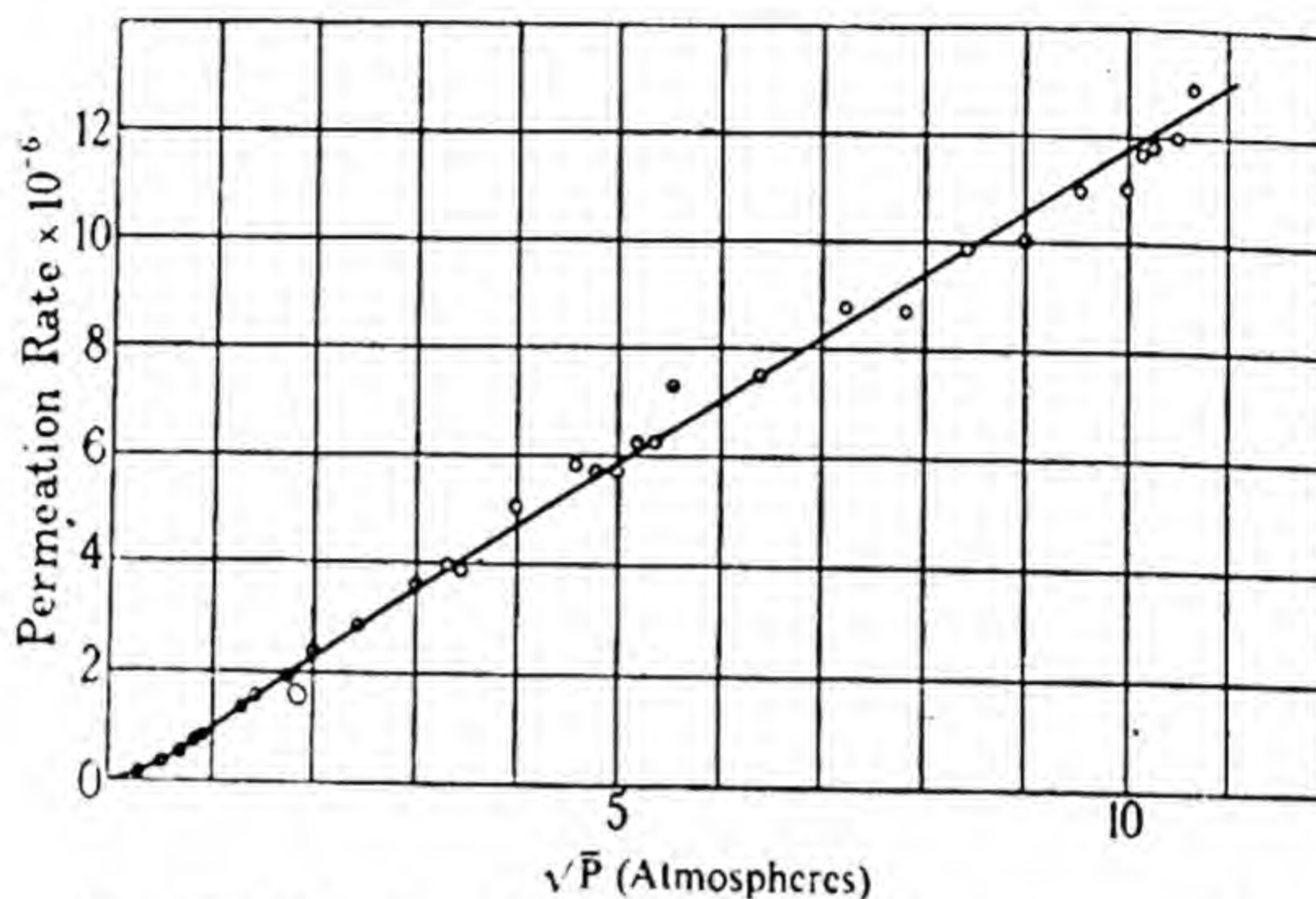
Fig. 59. Diffusion of hydrogen through nickel at 248° C.
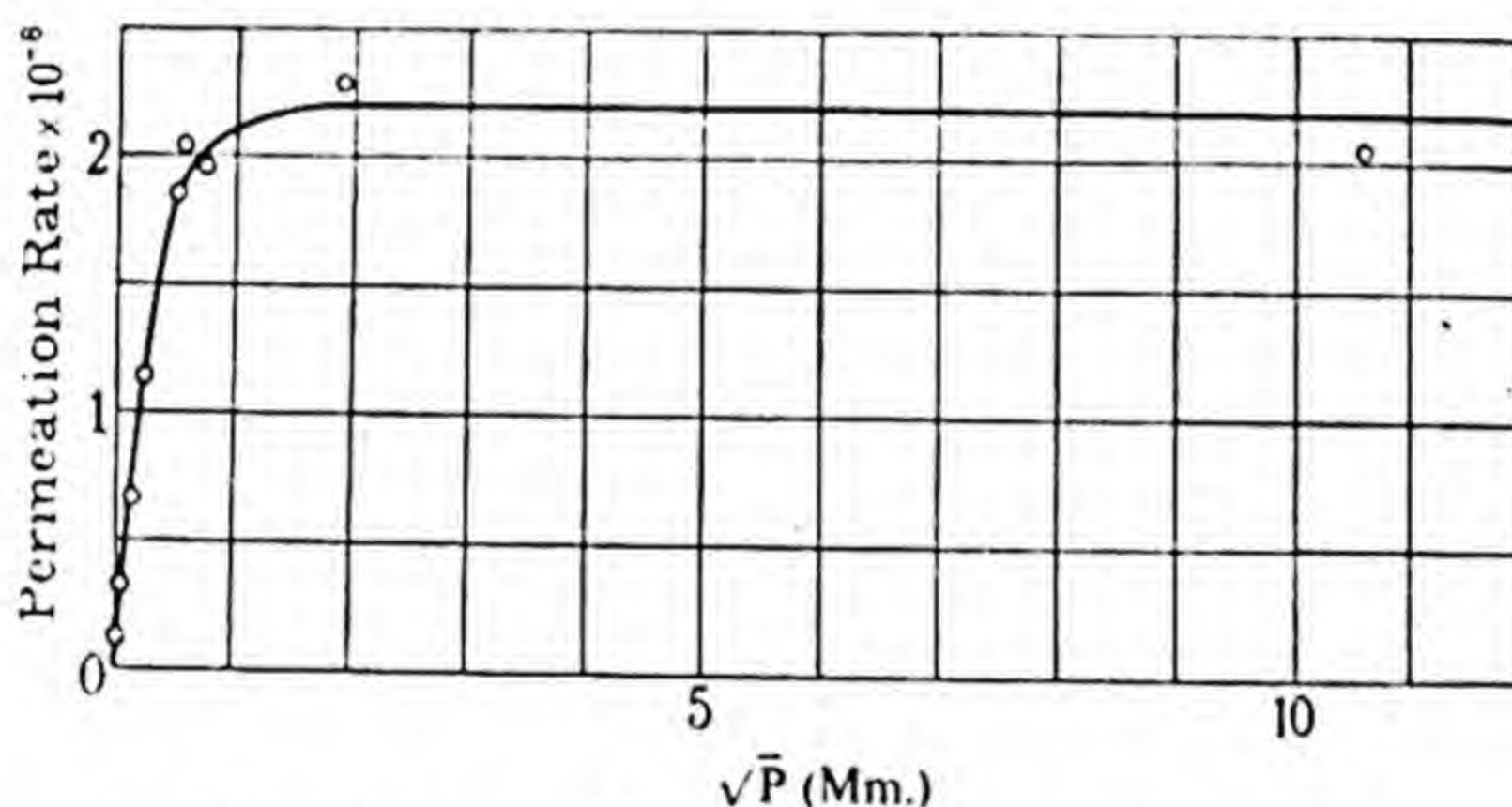
Fig. 60. Diffusion of oxygen through nickel at 900° C.

the concentration of dissolved oxide (or oxygen) in the nickel in contact with the oxide film had reached a saturation value, for this would lead to a limiting permeation rate, according to Fick's law .

$$\text{Rate of permeation} = -D\frac{C_s - C_l}{l},$$

where C_s is the saturation oxygen concentration at $x = 0$, and C_l its value at the outgoing surface $x = l$. The contrary must be

true of the systems H_2-SiO_2, H_2-Ni, H_2-Pd. The fact that many interface processes may occur in the diffusion can, as is shown subsequently (p. 182), lead to the conclusion that in the stationary state of flow concentrations within the solid may be very much less than their values in equilibrium systems.

Among the possible phase-boundary processes one might include the following: An adsorbed gas molecule or atom is driven into the solid by molecular bombardment by an activated gas molecule. Smithells and Ransley tested this possibility by introducing argon at 100 atm. into a diffusion system H_2-Ni where the hydrogen pressure on the ingoing side
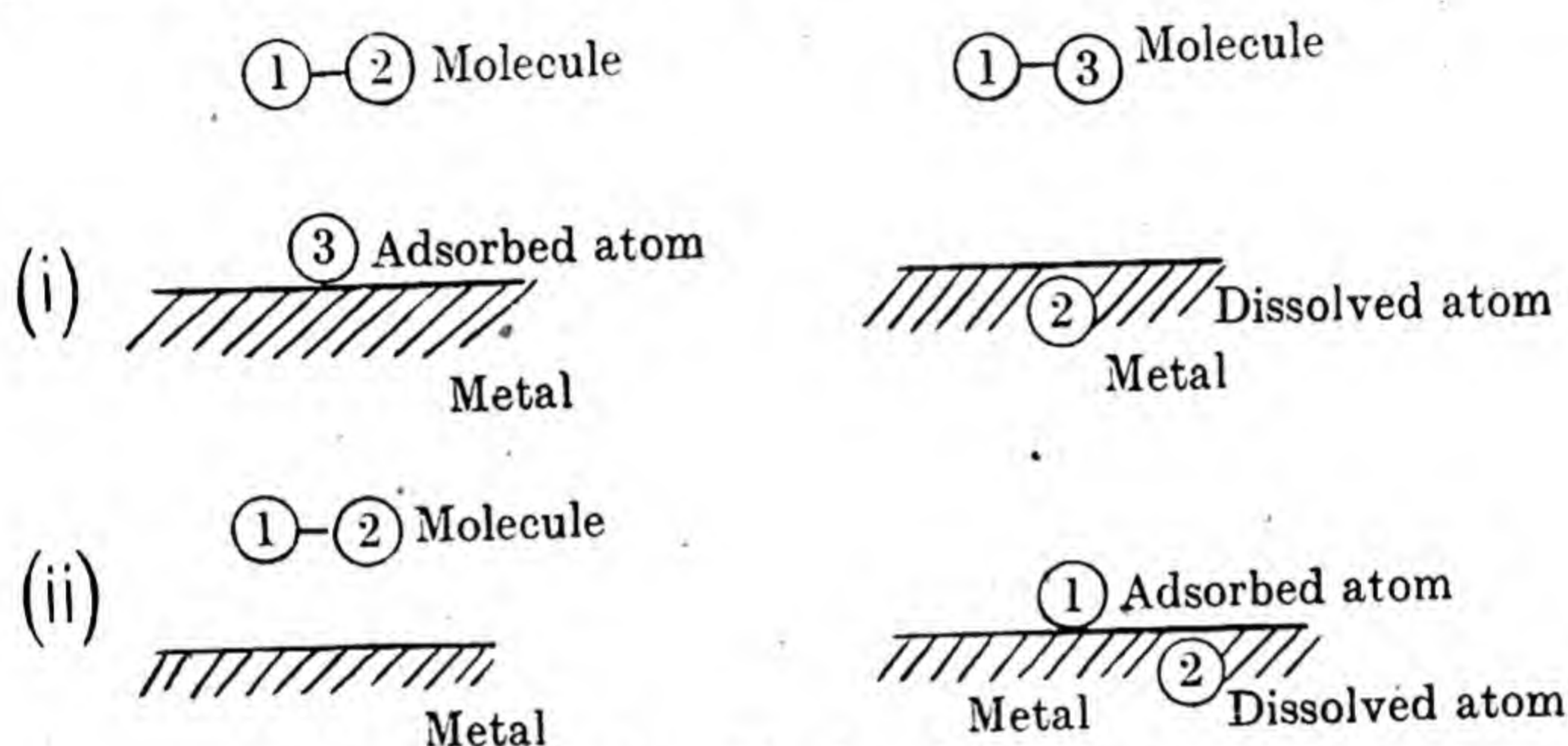
Fig. 61. Models of possible phase-boundary processes.

was 4 atm. No difference in the permeation velocity was observed, so that at least certain types of penetration process by molecular bombardment do not occur. The experiment does not eliminate the two types of penetration by bombardment represented by the diagrams above (Fig. 61). The gas molecules are supposed to be hydrogen, which are adsorbed in atomic form. To distinguish the atoms they have been numbered.

Other diffusion systems in which conditions might correspond to very high pressures indeed are met with in the passage of nascent hydrogen through metals. For example, Barrer (53) found that hydrogen supplied at a current density of 0·44 amp./cm.², by electrolysing sulphuric acid at 20° C., passed through a hollow palladium cathode 10^3-fold as rapidly as hydrogen diffused from molecular hydrogen gas through

a sample of palladium in a similar state of activity. If the phenomena encountered are essentially the same, then

$$\frac{P_{\text{elect.}}}{P_{\text{thermal}}} \sim \sqrt{\frac{p_{\text{elect.}}}{p_{\text{thermal}}}} \; ;$$

and as $p_{\text{thermal}} = 1$ cm., $p_{\text{elect.}} \sim 10^4$ atm. While in some ways the analogy may be false, there is no doubt that the pressures or concentrations of hydrogen atoms at the surface of the metal were extremely great. Similarly, Borelius and Lindblom[52] found that if hydrogen were generated electrolytically at the surface of an iron tube some of it passed through the tube and the rate of permeation P was given by

$$P = k[\sqrt{I} - \sqrt{I_t}] e^{-E/RT},$$

and was completely analogous to the expression for thermal diffusion

$$P = k_1[\sqrt{p} - \sqrt{p_t}] e^{-E/RT},$$

even the temperature coefficients E being the same. Assuming the complete analogy, Borelius and Lindblom found from their data

$$p_{\text{(atmos.)}} = 17{,}000 I_{\text{(amp./cm}^2\text{.)}}.$$

Their own experiments were conducted at current densities of up to 0·043 amp./cm.^{2} By carrying out these experiments at large current densities, it should be possible to reach a current density at which the surface layers of metal were completely saturated. The permeation velocity should then no longer increase as the current density increases. This point has been tested[53], and has important implications in the discussion on mechanisms of diffusion in the next section. It was found that only in very active palladium tubes could a limiting permeation velocity be reached (see Fig. 62).

SOME MECHANISMS FOR THE PROCESS OF FLOW

In 1935, Ham[77] proposed a specific equation for the rate of flow of gas through a metal based upon kinetic theory. Ham's equation approximates to

$$\frac{dp}{dt} = A p_0^y (1 - e^{-a/x}) \left(\frac{m}{2\pi k T} \right)^{\frac{1}{2}} e^{-b/T},$$

where A, y, a and b are constants, and $y \sim \frac{1}{2}$. It will be seen that this equation is similar in form to the Richardson equation, but since it involves a number of assumptions it need not be considered further.

Riemann [78] has suggested another variant of Richardson's equation based upon thermodynamic considerations and Fick's law. His equation took the form

$$\frac{dp}{dt} = a\frac{D}{l}(\sqrt{p_1} - \sqrt{p_2})\, T^{(\alpha - 7/4)}\, e^{\Delta H_0/2R\dot{T}}.$$

In this equation $\alpha = C_p/R$ (C_p denotes the atomic heat of dissolved gas atoms), $p_1, p_2' = $ pressures of gas at the ingoing and outgoing surfaces respectively of a plate of thickness l, and ΔH_0 is defined by $\Delta H = \Delta H_0 + (\frac{7}{2} - 2\alpha)RT$ (ΔH denotes the heat of desorption of two atoms of gas from the metal to the gas, as a molecule). But since we are dealing with an activated diffusion, D can be further written as $D = D_0 e^{-E/RT}$, where E denotes the activation energy for diffusion.

Riemann's equation, Richardson's equation (p. 167) and equation (v), p. 170 all suffer from one grave defect. It has been assumed that the concentrations just inside the solid are equilibrium concentrations, and this is only true where there are no rate-controlling phase-boundary processes. There do in fact seem to be no slow phase-boundary processes for diffusion through rubbers [79], but this is not so for diffusion through metals. Melville and Rideal [64] made the first attempt to include possible phase-boundary processes in the equation of flow. Other possible phase-boundary processes were given by Smithells and Ransley [76], Wang [80], and Barrer [81]. They regarded the following as possible:

(i) An adsorbed atom passes into the metal:

$$\text{Rate} = k_1\theta_1\left(1 - \frac{C_H}{C_s}\right)$$

(k_1 is the velocity constant of the reaction, θ_1 the fraction of the surface covered by adsorbed atoms, C_H is the concentration

of hydrogen gas just inside the metal, and C_s is the concentration of hydrogen in the metal when saturated with the gas).

(ii) A dissolved atom re-enters the surface:

$$\text{Rate} = k_2 C_H (1 - \theta_1).$$

(iii) A molecule strikes the surface and is adsorbed as atoms:

$$\text{Rate} = k_3 p_{H_2} (1 - \theta_1)^2.$$

(iv) Two adsorbed atoms evaporate as a molecule:

$$\text{Rate} = k_4 \theta_1^2.$$

(v) A molecule strikes the surface, one atom being absorbed and the other adsorbed:

$$\text{Rate} = k_5 p_{H_2} (1 - \theta_1) \left(1 - \frac{C_H}{C_s} \right).$$

(vi) An absorbed atom combines with an adsorbed atom, and evaporates as a molecule:

$$\text{Rate} = k_6 C_H \theta_1.$$

Other processes may be conceived, but they are not probable ones, and in any case the six listed above are adequate for this discussion. Smithells and Ransley, considering the first four of the preceding rate equations, deduced as a general expression for the velocity of permeation

$$\frac{dp}{dt} = A\{\sqrt{[1 + Kf(p)]} - 1\},$$

where A and K are terms involving θ, and considered that a simple form of this equation

$$\frac{dp}{dt} = A\{\sqrt{(1 + K\theta p)} - 1\}$$

agreed with their experimental findings that at low pressures dp/dt approximates to Bp, where B is a constant; and at high pressures to $C\sqrt{p}$, where C is also a constant.

Wang[80] and Barrer[81] gave equations defining the permeation velocity which included all six of the processes above.

Wang's treatment led him to conclude that the permeation velocity would increase indefinitely with pressure, according to a $\sqrt{p}$ law when p is large. This would explain Smithells and Ransley's observation that even at 100 atm. the rate of permeation of hydrogen through nickel was still proportional to the square root of the pressure. At these pressures it had previously been supposed that the surface layer would be saturated with adsorbed gas, and so the processes (i) to (iv) would give a limiting value for the permeability. Wang considered that the inclusion of (v) and (vi), however, made this no longer necessary, and so his equations indicated that some such processes as (v) and (vi) must have occurred. However, Barrer[81] pointed out that Wang reached these conclusions because the rate equations given by him and by Smithells and Ransley took no account of the approach towards saturation in the metal itself. The rate equations (i) and (v) were in fact written by them as

(i) Rate $= k_1 \theta_1$.

(v) Rate $= k_5 p(1 - \theta_1)$.

The correct equations for the permeability showed that it always reached a limiting value at infinite pressure. Barrer[82] also showed that the phase-boundary processes could result in very great concentration discontinuities at the surface of a metal, and that under these conditions, even at high pressures, the concentration just within the metal could be a fraction only of the equilibrium value found in the absence of phase-boundary processes. He advanced the view that in the expression

$$\text{Permeation rate} = D\frac{C_1 - C_2}{l},$$

the concentration C_1 just inside the ingoing surface was even at 100 atm., for the H_2-Ni system, nowhere near its saturation value, so that Wang's deduction of a $\sqrt{p}$ law is valid at these pressures. The manner in which concentration discontinuities arise is indicated on pp. 174–5.

Later[53], it was shown that for certain H_2-Pd systems $(C_1' - C_2')$ was indeed much less than its equilibrium value. This was indicated by measuring both the permeability constant and the diffusion constant (Chap. V). When gas flow occurred from a finite pressure through palladium into a vacuum the values of $(C_1' - C_2')$ were those in Table 43, for palladium samples of low permeability. On the other hand, when a palladium sample was alternately oxidised and reduced the permeability was high, and for some measurements of Lombard and his co-workers[69] the values of $(C_1 - C_2)$ approached the equilibrium ones (Table 43). Here the phase-boundary processes have

TABLE 43

T° C.	D cm.^{2}sec.$^{-1}$ $\times 10^{-5}$	P_1 (Barrer) c.c./sec./cm.^{2}/ mm./cm.Hg $\times 10^{-5}$	$(C_1 - C_2)$ (Barrer) at 1 atm. pressure c.c./c.c.Pd	P_2(extrap.) (Lombard) c.c./sec./cm.^{2}/ mm./cm.Hg $\times 10^{-3}$	$(C_1 - C_2)$ (Lombard) c.c./c.c.Pd/ atm.	$(C_1 - C_2)$ (equilibrium) c.c./c.c.Pd/ atm.
350	6·8	0·65	0·73	0·84	11·8	12·0
334	5·4	0·52	0·73	0·78	12·6	12·5
310	3·7	0·366	0·75	0·70	16·5	13·6
272	2·0	0·193	0·74	—	—	—

accelerated so much that diffusion and equilibrium solubility at the interfaces control the permeation velocity. Finally, in support of this view Barrer[53] found that the permeation rate through a very active palladium sample was independent of the current density, but that as the activity decreased it became dependent upon current density, approaching more and more nearly to the relation

$$\text{Rate} = k\sqrt{I}$$

found for inactive samples (Fig. 62).

Earlier attempts were made to fix the nature of the rate-controlling process by noting the type of kinetic expression followed[83, 84, 85]. Wagner[83] claimed to have found in an H_2-Pd system that various laws were valid under different conditions:

(i) $\dfrac{\partial C}{\partial t} = D\dfrac{\partial^2 C}{\partial x^2}$ (diffusion).

(ii) $\dfrac{\partial C}{\partial t} = k' \sqrt{p_{H_2}} - k_1 C$ (penetration of atoms into the metal).

(iii) $\dfrac{\partial C}{\partial t} = k'' p_{H_2} - k_2 C^2$ (sorption of hydrogen as molecules).

Mechanisms based upon kinetic expressions are to be accepted with some reserve.
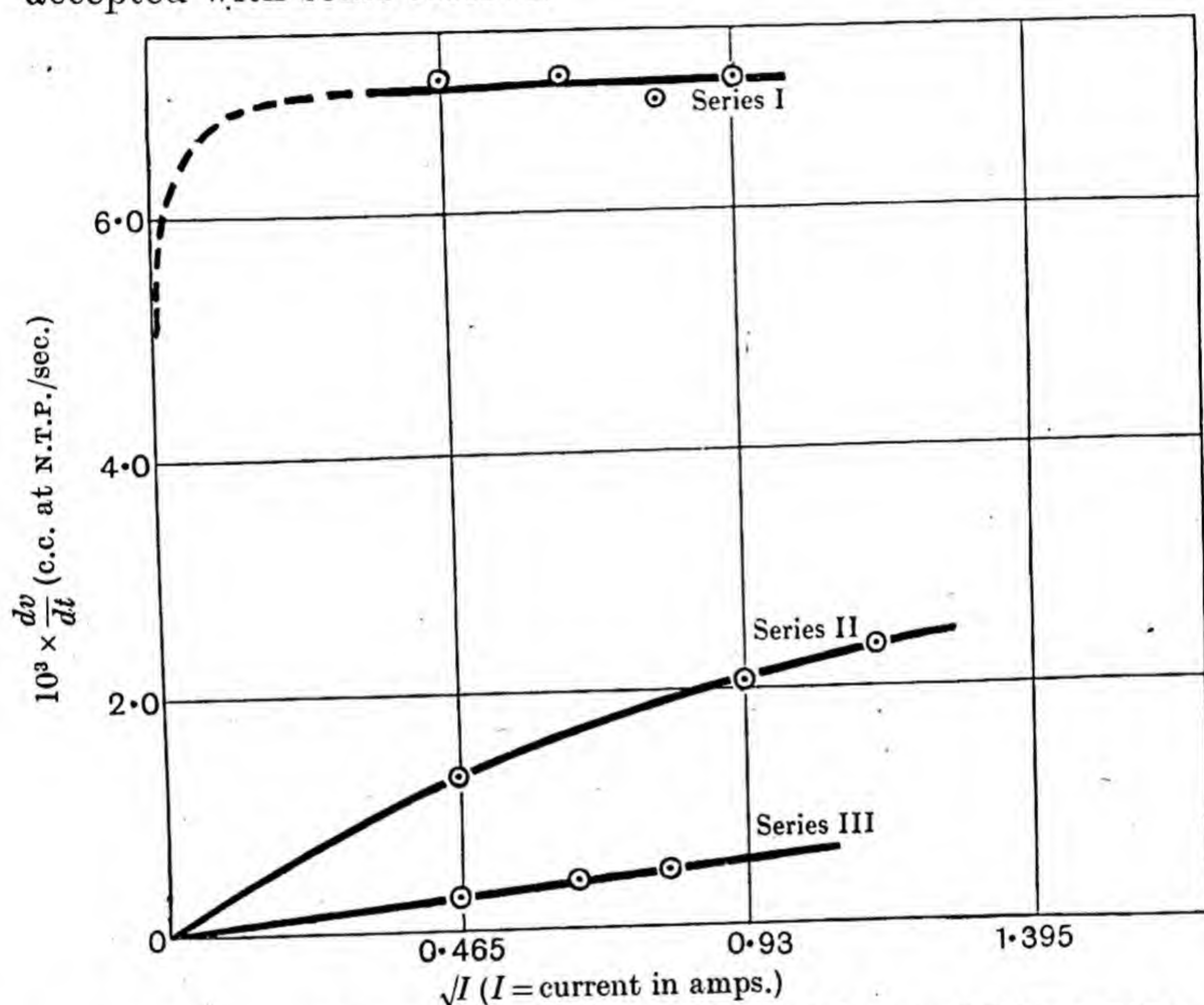
Fig. 62. Influence of current density upon diffusion of H_2 through Pd in varying stages of activity. Series I, most active; Series II, less active; Series III, still less active.

THE BEHAVIOUR OF HYDROGEN ISOTOPES IN DIFFUSION AND SOLUTION IN METALS

There are several reasons why hydrogen and deuterium should react at different velocities:

(1) They have different masses. Kinetic theory leads one to expect that on this account the reaction velocity constants should be in the ratio $\dfrac{k_{H_2}}{k_{D_2}} = \sqrt{2}$.

(2) They have different zero point energies. Hydrogen has the greater zero-point energy, and so should not need so large an additional activation energy before passing over a given energy barrier as would deuterium. The effect of these differences may be expressed by an exponential term $e^{-\Delta E/RT}$, where ΔE is a small energy increment.

(3) According to quantum theory there exists a finite probability that the atoms H or D may pass through an energy barrier without having sufficient energy to surmount it. The mass appears in a negative exponential term, and so may result in very great velocity differences, hydrogen always reacting more rapidly. It may here be said that hitherto no velocity difference has been great enough to suggest that this quantum mechanical leakage occurs[86].

In activated diffusions as in chemical reactions a component of the system passes over an energy barrier, or succession of energy barriers, in passing from its initial to its final state. Thus the same phenomena which govern the one process govern the other also. No difference in the diffusion velocities of hydrogen and deuterium is large enough for it to be necessary to assume a quantum mechanical leakage. The processes involving (1) and (2) remain to be considered. In their earliest publication on the subject, A. Farkas and L. Farkas[87] reported a permeation velocity ratio for hydrogen and deuterium which could be expressed as

$$\frac{P_{H_2}}{P_{D_2}} = e^{830/RT}.$$

Subsequently, however, Jost and Widmann[88] measured the diffusion velocity of hydrogen and deuterium inside the palladium lattice, and found

$$\frac{D_{H_2}^{302\cdot5^\circ C}}{D_{D_2}^{302\cdot5^\circ C}} = \frac{1\cdot35}{1},$$

which was nearly the value $\sqrt{2}$ indicated by simple kinetic theory. Further, Jouan[89] stated that the permeation rate ratio of hydrogen and deuterium through platinum was

constant at approximately $\sqrt{2}:1 = P_{H_2}:P_{D_2}$ from 550 to 950° C. However, a re-examination of these authors' results shows that this is by no means so, the mean ratio at a series of temperatures being:

$T°$ C.	550	650	750	850	950
P_{H_2}/P_{D_2}	1·55	1·50	1·35	1·36	1·27

These ratios conform to the expression

$$\frac{P_{H_2}}{P_{D_2}} = e^{680/RT}$$

with some accuracy. A. Farkas [90] reinvestigated the permeability of palladium to hydrogen isotopes, using the half-life of diffusion as a measure of the permeation velocity. He also used the half-life of the process of conversion at the surface of para-hydrogen to equilibrium hydrogen to measure the velocity of sorption or desorption of hydrogen at the surface. It must be remembered, however, that the solution of the diffusion equation is in the form of an infinite series of exponentials, and thus the "half-life period" does not accurately measure the velocity of diffusion* and is, moreover, a function of the thickness. Also, the conversion to the equilibrium mixture of para-hydrogen need not occur by sorption and desorption of an atomic layer of hydrogen, but may result from an exchange reaction between a molecule and an atom in the hydride layer. However, the ratios of the half-life periods for diffusion of hydrogen and deuterium depend on temperature, and are often too large for explanations involving only a factor $\sqrt{2}$. These velocity ratios depend at low temperatures in a somewhat capricious manner upon the history of the palladium specimen.

A convincing proof that an exponential factor $e^{-\Delta E/RT}$ governs the permeation rate ratio is provided by the measure-

---

* As it does for a first order reaction, where, since $C = C_0 e^{-kt}$, one has

$$\ln \frac{C_0}{C} = kt, \text{ and } kt_{\frac{1}{2}} = \ln 2$$

if $t_{\frac{1}{2}}$ denotes the half-life period of the reaction.

ments of Melville and Rideal [64] on the diffusion of the isotopes through palladium, using tubes and disks of palladium. Their data are presented in the following tables:

TABLE 44. *Area* Pd *tube* 1·51 *cm.*^{2}, *thickness* 0·1 *mm.*
Volume of system 41 *c.c.*

$T°$ C.	Gas	Quarter-life of permeation (min.)	Half-life of permeation (min.)	Three-quarter-life of permeation (min.)	Ratio H/D	ΔE (kg.cal.)
228	H	16·7	42·2	—	1·80	0·76
	D	30	79	—		
281	H	2·55	8·0	18·4	1·58	0·68
	D	4·40	12·7	29·0		
322	H	1·40	4·0	8·95	1·73	0·86
	D	2·52	6·6	15·1		
362	H	0·65	1·76	3·95	1·26	0·4
	D	0·80	2·30	4·95		

TABLE 45. *Area* Pd *disk* 0·78 *cm.*^{2}, *thickness* 0·075 *mm.*
Volume of system 44·1 *c.c.*

$T°$ C.	Gas	Half-life of permeation process (min.)	Ratio H/D	ΔE (kg.cal.)
154	H	3·30	2·42	1·04
	D	8·0		
167	H	2·31	1·90	0·90
	D	4·41		
189	H	2·15	1·75	0·83
	D	3·75		

Farkas [90], in another set of data, gave the ratios as

$T°$ C.	186	131	106	20
P_H/P_D	1·24	1·36	1·40	1·84

which conform satisfactorily to the relationship

$$P_H/P_D = 0·6e^{660/RT}.$$

Data have also been obtained [64] for composite membranes in which copper or nickel were deposited electrolytically upon palladium. The deposited films were very thin, about 10^{-3} cm.

thick, and the possibility of there being holes in the copper membrane was checked by measuring the apparent activation energy, which is different for copper and for palladium. As a measure of the permeation velocity the time required for a given pressure drop was used—a procedure which may give only an approximate measure of the actual permeation rate process. The deposition of copper films reduced the permeation rate by a large factor; the mean ΔE for the process was, for a series of measurements involving membranes Cu-Pd-Cu and Pd-Cu-Pd, 770 cal. Analogous measurements for Ni-Pd membranes gave a ΔE of 600 cal. It is interesting that the deposition of a copper layer 8.4×10^{-5} cm. thick, on one side of the palladium, gave a velocity twice that observed when a copper film 8.4×10^{-5} cm. thick was also deposited on the other side of the disk. Therefore the palladium did not appreciably affect the characteristics of the copper membranes, which alone governed the velocity of gas permeation.

Since the permeability constant depends on the diffusion constant, upon phase boundary processes and upon the solubility $\left(P = -D \dfrac{\partial C}{\partial x} \right)$, it is not possible to interpret these results in any exact way. The difference in cal./mol. of the temperature coefficients for hydrogen and deuterium may depend on the following factors:

(i) The activation energy for adsorption and for desorption.

(ii) The activation energies for penetration from the adsorbed layer into the solid, and the converse process.

(iii) The activation energy for diffusion in the metal lattice.

(iv) The heat of solution of the gas in the lattice.

Even when all phase-boundary processes occur much more rapidly than any other processes, the temperature coefficients of the permeability constants are governed by the terms (iii) and (iv) above. But one notes the general correspondence between the differences ΔE in the temperature coefficients of permeability of metals to hydrogen and deuterium, and

between differences in the temperature coefficients of a variety of heterogeneous reaction velocity constants (Table 46).

There is also an agreement in the order of magnitude of the ΔE observed in diffusion and in heterogeneous reactions, and the ΔE calculated by Sherman[95] as the difference in zero-point energy of a large number of oscillators such as

TABLE 46. *Some differences in temperature coefficients for heterogeneous processes involving* H *and* D

Reaction	$E_{(apparent)}$ cal./mol.	$\dfrac{k_H}{k_D} = e^{-\Delta E/RT}$	Author
$H_2 + 2C_{(solid)} \rightarrow 2CH_{(surface)}$ $D_2 + 2C_{(solid)} \rightarrow 2CD_{(surface)}$	$\geqslant 15,700$	$\Delta E = 700$ cal.	Barrer[91]
Tungsten $2NH_3 \xrightarrow{\text{filament}} N_2 + 3H_2$ Tungsten $2ND_3 \xrightarrow{\text{filament}} N_2 + 3D_2$	42,400	800, 790, 890, 900	Barrer[92]
Tungsten $2PH_3 \xrightarrow{\text{filament}} 2P_{(solid)} + 3H_2$ Tungsten $2PD_3 \xrightarrow{\text{filament}} 2P_{(solid)} + 3H_2$	32,200	510, 550	Barrer[92]
$H_2O + Al_4C_3 \rightarrow 4Al(OH)_3 + 3CH_4$ $D_2O + Al_4C_3 \rightarrow 4Al(OD)_3 + 3CD_4$	14,200	750	Barrer[86]
$CH_4 + 3C_{(solid)} \rightarrow 4CH_{(surface)}$ $CD_4 \rightarrow 3C_{(solid)} + 4CD_{(surface)}$	$\geqslant 26,700$	780	Barrer[91]
$H_2 + CuO \rightarrow Cu + H_2O$ $D_2 + CuO \rightarrow Cu + D_2O$	—	400	Melville and Rideal[64]
Hydrogenation of styrol (Pd-BaSO$_4$ catalyst)	—	540	Cremer and Polanyi[93]
$H_2, D_2 + \tfrac{1}{2}O_2(Ni) \rightarrow H_2O, D_2O$	—	750	Melville[94]
$H_2, D_2 + N_2O(Ni) \rightarrow H_2O, D_2O + N_2$	—	720	Melville[94]
$H_2, D_2 + C_2H_4(Ni) \rightarrow C_2H_6, C_2H_4D_2$	—	700	Melville[94]

Ni-H, Ni-D ($\Delta E = 0.7$ k.cal.) or Pt-H, Pt-D ($\Delta E = 0.5$ k.cal.). The calculations are only approximate; they assume that the metal atom behaves as though it were independent of all other lattice atoms, save only the hydrogen atom; and that the same is true of its associated hydrogen atom. They also assume that the oscillation is a simple harmonic motion.

The solubility of the isotopes in palladium has been made the subject of an experimental study by Sieverts and his co-workers [21], and shows that in an equilibrium system there are considerable solubility differences. Sieverts and Danz's [21] results are shown in Fig. 40. The higher temperature results, where Nernst's distribution law, $S = k \sqrt{p}$, may be expected to hold (S denotes the solubility and k is a constant), lead to the following solubility ratios at one atmosphere pressure:

$T°$ C.	200	220	240	260	280	300	320	340	350	400
S_D/S_H	0·60	0·63	0·64	0·67	0·68$_5$	0·68	0·67$_5$	0·71	0·71	0·74

The heat of solution per g.mol. of hydrogen dissolved is, in the range 220–350° C., 2200 cal., while the heat of solution of deuterium is 1760 cal./mol., using the ratio $S_D/S_H = e^{440/RT}$ calculated from the above data. Melville and Rideal in an analogous temperature range obtained

$$\Delta H_{H_2} = 2500 \text{ cal./mol.},$$

$$\Delta H_{H_2} - \Delta H_{D_2} = 740 \text{ cal./mol.}$$

It is then clear that interpretation of relative permeation velocities may have to take account of this large difference in solubility. In another study [37] the solubilities of hydrogen and deuterium were measured in iron, giving results of which the following are typical:

$T°$ C.	600	700	800	950	1000	1200	1350	1450
S_{H_2} (c.c./100 g. Fe)	1·8	2·4	(3·2)	5·9	6·6	9·0	(10·8)	12·6
S_{D_2} (c.c./100 g. Fe)	1·5	2·2	2·9	5·5	6·1	8·5	10·0	11·7
S_{H_2}/S_{D_2}	1·20	1·09	1·10	1·07	1·08	1·06	1·08	1·08

A theoretical study of the solubility of the isotopes in palladium [22] led to the expression

$$\Delta H_H - \Delta H_D = (\chi_0^H - \chi_0^D) - \tfrac{1}{2}(\chi_d^H - \chi_d^D) - RT^2 \frac{\partial}{\partial T} \log \frac{V(T)_H}{V(T)_D},$$

where ΔH denotes the heat of absorption of gaseous hydrogen in palladium, χ_0 is the heat of solution of a hydrogen atom in the lattice, χ_d the heat of dissociation of a hydrogen

molecule into atoms, and $V(T)$ is the partition function of a dissolved atom. The subscripts H and D refer to hydrogen and deuterium respectively. The difference in the zero-point energies of the isotopes in solution may be calculated if the vibration frequency ν is known. Assuming

$$\nu_H = 8.75 \times 10^{-12} \, \text{sec.}^{-1},$$

and that $\dfrac{\nu_D}{\nu_H} = \sqrt{\dfrac{M_H}{M_D}}$, one finds

$$\chi_0^H - \chi_0^D = -470 \, \text{cal.}$$

and

$$RT^2 \frac{\partial}{\partial T} \log \frac{V(T)_H}{V(T)_D} = +260 \, \text{cal.} \quad (T = 1200° \, \text{K.}).$$

An additional assumption in the latter calculation is that

$$V(T) = (1 - e^{-h\nu/kt})^{-3}.$$

Finally one knows, from an argument analogous to that for computing $(\chi_0^H - \chi_0^D)$, that $\frac{1}{2}(\chi_d^H - \chi_d^D) = 900 \, \text{cal.}$, and so

$$\Delta H_H - \Delta H_D = -470 + 900 + 260 = 690 \, \text{cal.}$$

Lacher found he could express Sieverts and Zapf's[21] data on the solubility of the isotopes in palladium at high temperatures as

$$\log p_H^{\frac{1}{2}} = \log \theta_H - \frac{1150}{RT} + \log 129,$$

$$\log p_D^{\frac{1}{2}} = \log \theta_D - \frac{410}{RT} + \log 104$$

(p in atmospheres; θ = fraction of saturation hydrogen content). There is then a good agreement between the experimental and calculated heat difference. Although fitting equations of the type given above to experimental data is prone to small errors, these are greater in the temperature-independent than in the temperature-dependent term.

One can thus see that many factors control the relative behaviour of the isotopes in solution, diffusion, and permeation in metals. The solubility ratio combines the effects indicated above: the diffusion constant ratio involves differences in the zero-point energies of dissolved hydrogen and deuterium

atoms in initial and transition states respectively; and the permeability constant ratio combines the effects of differing diffusion constants, and differing solubilities, or, if phase-boundary processes are also important, differences in the relative rates of reaction such as (i) to (vi) on pp. 179 and 180. One may express these different possibilities in a single potential-energy distance diagram, in which a molecule is supposed to approach a membrane, be adsorbed, penetrate into the solid, diffuse through it, emerge into the adsorption layer on the other side, and be desorbed into the gas phase from this layer. The heights of the various energy barriers may vary greatly from case to case.

The influence of phase changes upon permeability

It has been found that in the region of concentrations where two hydrogen-palladium alloys coexist (the perpendicular sections of the curves of Fig. 40) it is not possible to trace out the same isobaric curve on sorption and desorption. There is a hysteresis effect illustrated by Fig. 40. It is interesting to find in the study by Lombard, Eichner and Albert [96] that the permeability-temperature curve follows in an inverse manner the absorption isobar, there being a great increase in the permeability in the region 180–200° C. It may be that this rapid alteration in permeability marks the change from β-phase to α-phase alloy.

The same type of hysteresis loop which was noted in the absorption of hydrogen in palladium, where α- and β-phases co-exist, is observed also in the absorption of hydrogen by iron [31], where now the two phases are produced by allotropy in the metal. The permeability-temperature curve shows a break at this point (Fig. 63) [51]. Indeed, wherever a phase change occurs one may look for a variation in the permeability, so that the property of permeability may be used to determine transition points. The change in permeability of nickel towards hydrogen has similarly been used to characterise the Curie point in nickel [62].

When the phase changes are brought about by alloying two metals, one would anticipate that in the same way the permeability would vary with the composition of the alloy, and discontinuously so wherever a new phase is formed. Evidence upon these points is scanty, but the data of Baukloh and Kayser (97) indicate that discontinuities do exist in the permeability-composition curve of alloys of nickel with copper and with iron (Fig. 64).
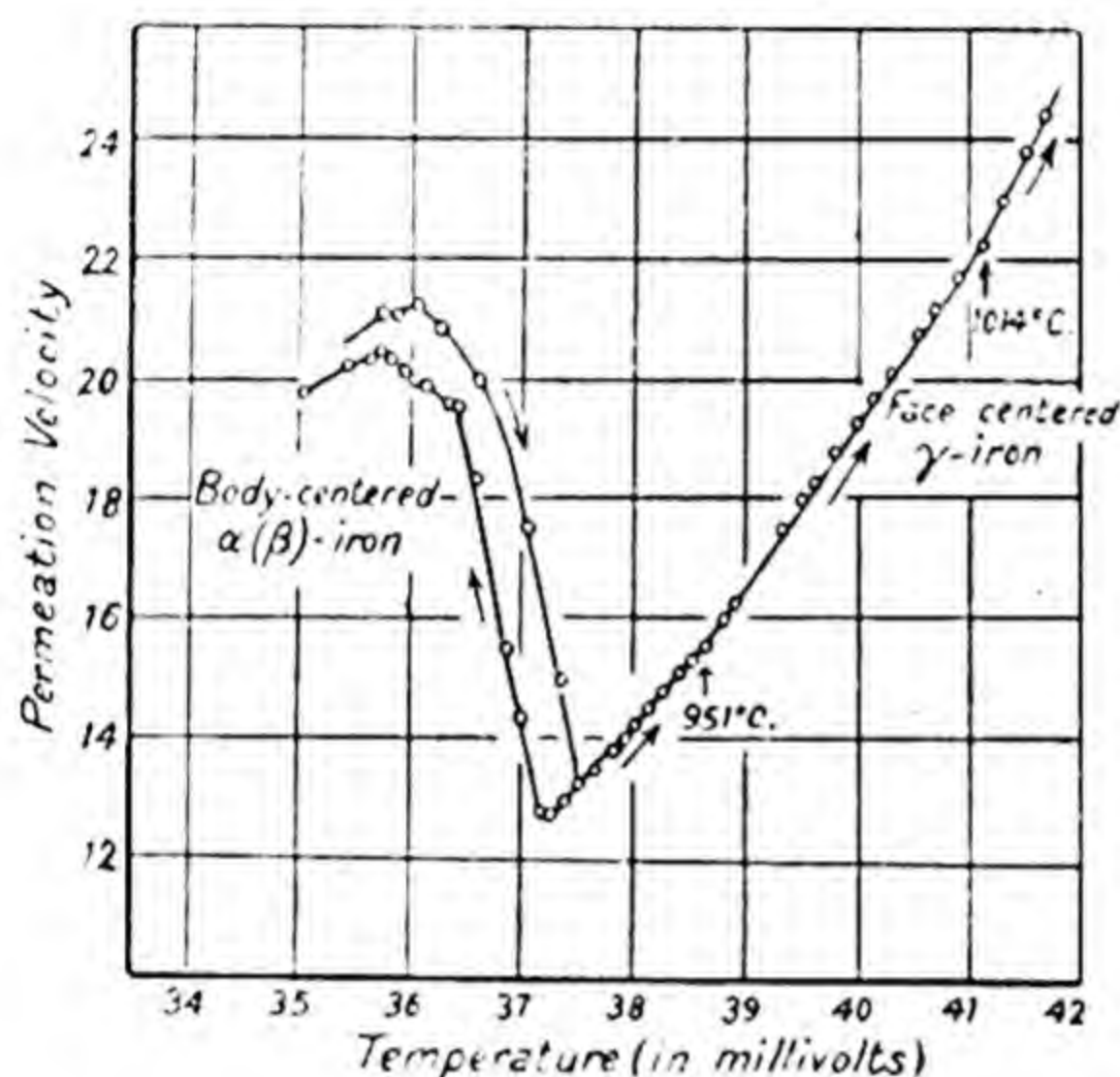
Fig. 63.
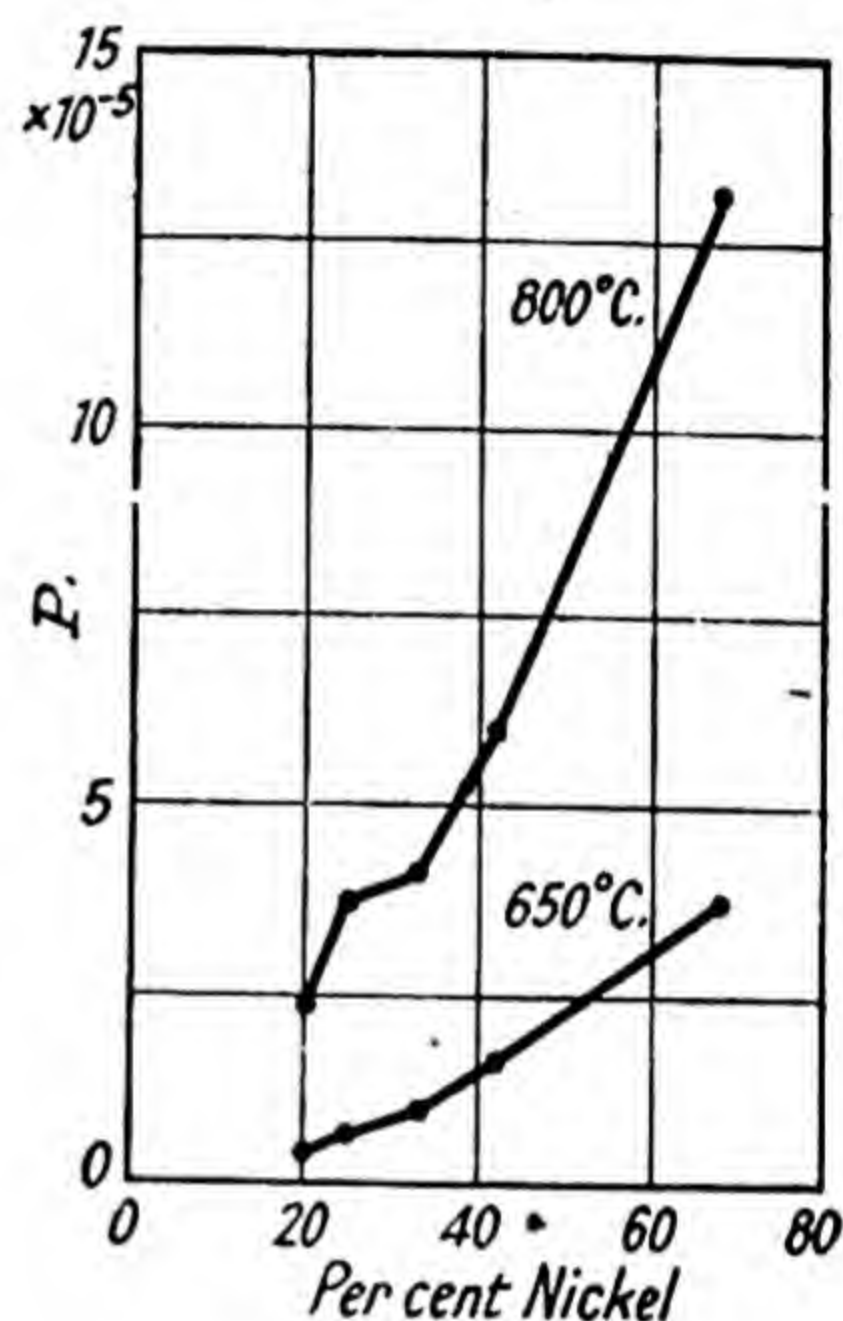
Fig. 64.

Fig. 63. The permeability curve for iron.

Fig. 64. Effect of composition upon rate of H_2-permeation through Ni-Cu alloy.

THE INFLUENCE OF PRE-TREATMENT UPON PERMEABILITY

A metallic crystal, like a salt crystal, normally consists of a mosaic of small crystallites—dendritic, block-like, or columnar. Impurities exist in part at surfaces of separation of the crystallite components, and in part in true solution. Permeability is, like diffusion, a structure sensitive property and one is accordingly likely to find permeation anisotropy in aleotropic single crystals; diminution in permeability with growth of crystallites following annealing, if grain boundary diffusion occurs; effects due to impurities in the metal; and sensitivity to the state of the metal surface, its roughness, degree of oxidation, or the extent of foreign metallic films.

The experimental difficulty of preparing and mounting metallic single crystals has so far prevented the discovery of any diffusion anisotropy in metallic systems, with few exceptions such as bismuth (Chap. VI). Effects which may be due to any of the other possibilities are more frequently encountered, and in a few instances have been systematically studied. Some of this evidence may be discussed.
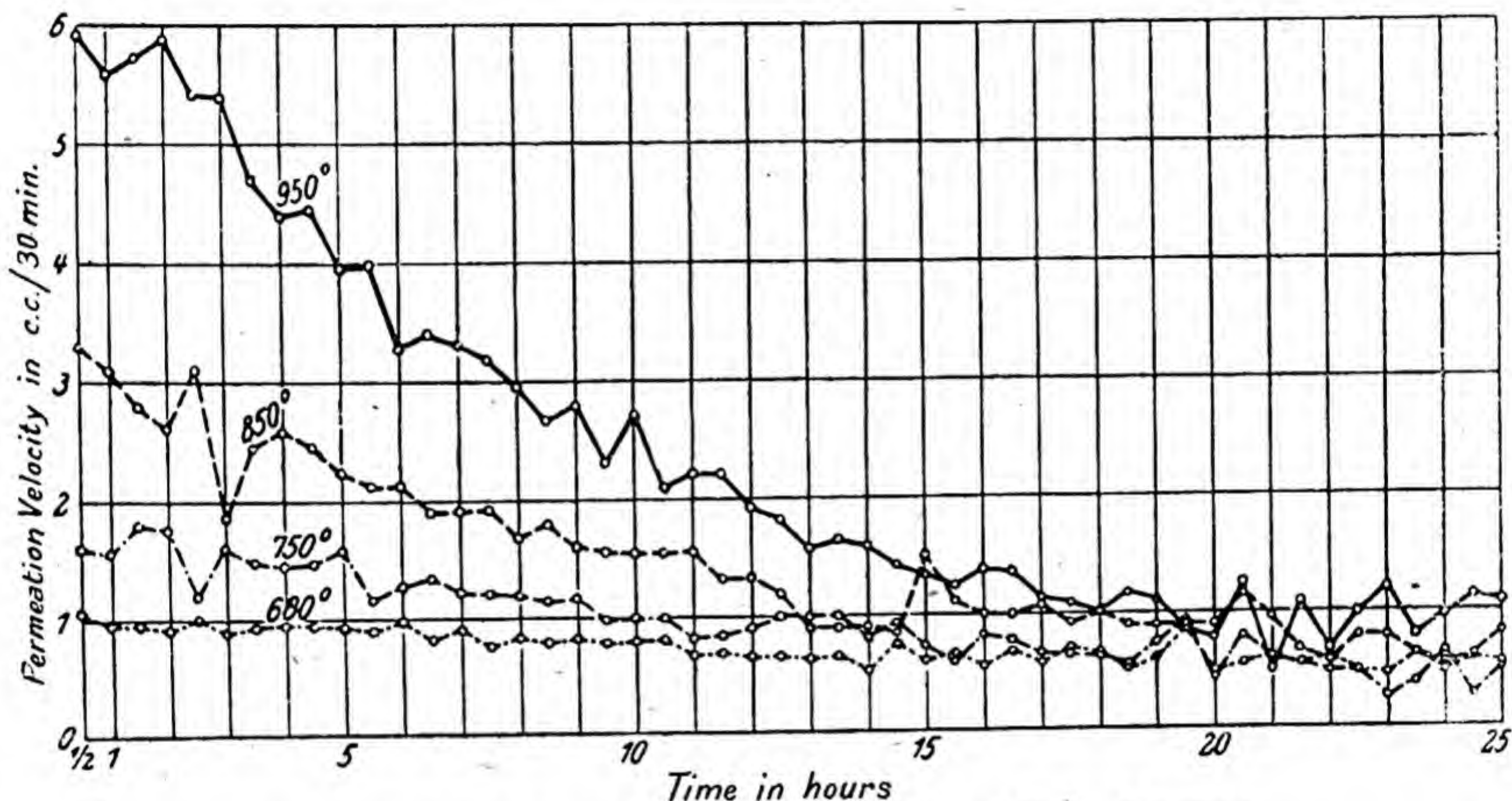
Fig. 65. H_2-permeability of nickel as a function of time of heating.

Baukloh and Kayser[97] showed that while the hydrogen permeability of nickel was not affected by prolonged heating at temperatures of 600° C. or even higher, at temperatures of 950–1050° C. a decrease in permeability followed. The influence of heating upon the metal is not the same, at a given temperature, for all samples, as their figures show. One such diagram is given in Fig. 65 and illustrates a rather extreme case, where a diminution can be observed even at 680° C. These effects could be attributed either to movements of impurities, or to recrystallisation with a diminution in the amount of grain boundary diffusion. Ham and Sauter[73, 74] also made the observation that the permeability of both palladium and iron was very much affected by the heating given the metal.

BD

13

One of the most complete investigations upon the influence of heating upon permeability has been carried out by Lombard and his co-workers(96). Their observations upon the permeability of hydrogen to palladium led them to the conclusion that it was possible to reduce the permeability of palladium 100-fold or more by heating the metal. This loss in the permeability of pure palladium towards hydrogen, which occurred progressively and the more rapidly the higher the temperature, was irreversible, and could amount almost to a total loss. By heating palladium to 500–520° C. for specified periods and then cooling it to temperatures below 450–500° C., any steady state of permeability could be attained. Heating the metal in air at 500° C., and then cooling it in air and subsequently reducing it in hydrogen at 150° C. partly if not wholly restored the permeability; but oxidising the metal at 500° C. and reducing it again at this temperature failed to increase its permeability. The authors found that a given sheet of palladium could be regenerated a number of times by oxidation and reduction, and pointed out that this behaviour recalls the preparation of metallic catalysts for hydrogenation, and focuses attention upon the state of the surface of the membrane. The loss of permeability was ascribed to a process of agglomeration of fine particles at the palladium surface, with a consequent reduction of the surface, and decrease in ease of access of hydrogen to the lattice of the palladium. This temperature of agglomeration was considered to be in the vicinity of 500° C. for pure palladium, and to be retarded by some impurities and accelerated by others. One membrane lost its diffusing power at 315° C. Experiments by Barrer(53) also revealed a great diminution in the permeability of palladium due to long heating at temperatures between 270 and 360° C., the palladium at these temperatures tending to approach a final steady state. Thus two states of permeability may be possible for palladium, one when the metal surface is activated by suitable oxidation and reduction, and one when the metal has undergone the maximum crystallisation at the surface. In the former state surface processes have their

minimum effect on the diffusion velocity; in the latter they have their maximum.

In Fig. 66 is illustrated the effect of prolonged heating upon the permeability of palladium for a number of heating and cooling cycles, with regeneration of the palladium between the cycles. In the first cycle the metal was maintained at a constant temperature, and its permeability fell steadily; in other cycles the temperature was raised or lowered and the
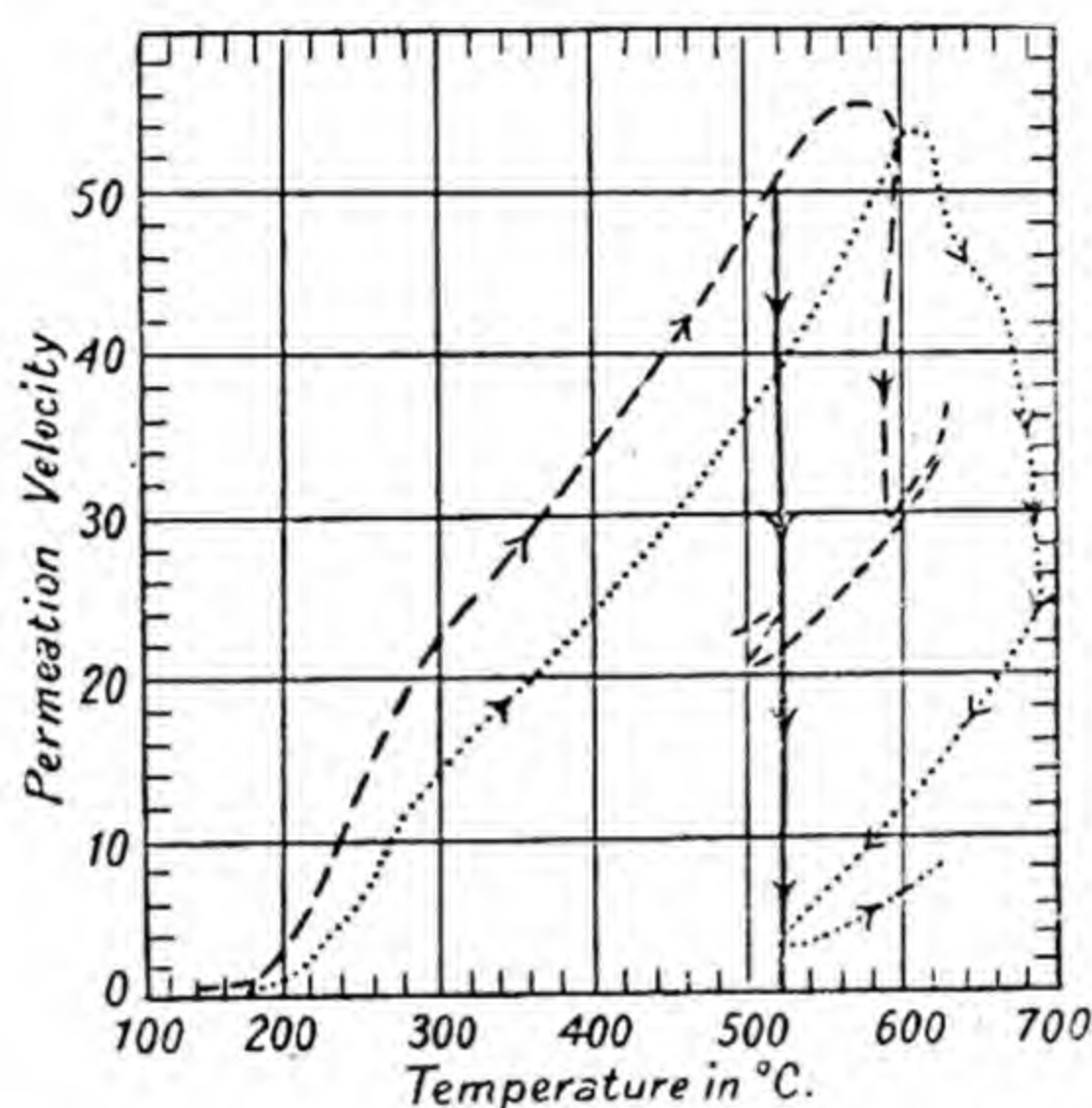
Fig. 66. Effects of heat-treatment upon the permeability of palladium (96).

permeabilities were measured simultaneously. The different permeabilities which palladium may possess have usually different temperature coefficients. This may be illustrated by Table 47.

Smithells and Ransley (67) made a study of the effects of oxidation, reduction, polishing, and etching upon the permeability of nickel and iron. Polished nickel membranes were less permeable than oxidised and reduced nickel. Etching increased the permeability of iron more than oxidation and reduction, but oxidation without adequate reduction of the iron poisoned it, and rendered it impermeable to hydrogen. Table 47a gives the data obtained. Another metal, the permeability of which is sensitive to surface treatments, is aluminium, also studied by Smithells and Ransley. The apparatus was so arranged that the aluminium could be

13-2

scratched with a steel brush without exposing it to air. Results of a number of the experiments are shown in Fig. 67. The effects are not simple; oxidation reduced the permeability; scratching the surface appeared to reduce the permeability when only the outside was abraded; but increased the permeability when the inside was abraded as well. The most

TABLE 47. *The permeabilities for a number of palladium membranes*

Sample	Permeability c.c./cm.^{2}/hr./atm.	Condition of sample
1	$20 \cdot 73 T^{\frac{1}{2}} e^{-4040/RT}$	High permeability [69]
Average for a number of samples	$8 \cdot 3 \times 10^2 e^{-4620/RT}$ $18 T^{\frac{1}{2}} e^{-3660/RT}$	High permeability [96]
3	$10 \cdot 7 \times 10^2 e^{-7500/RT}$	Inactive (by heating) [96]
4	$9 \cdot 5 \times 10^2 e^{-10500/RT}$	Inactive (by heating) [53]

TABLE 47a. *Effect of surface treatment upon permeability*

Metal	Treatment	Temp. ° K.	Pressure mm.	Permeation rate at this pressure c.c./sec./cm.^{2}/mm. thick
Ni	Polished	1023	0·042	$1 \cdot 39 \times 10^{-6}$
	Oxidised and reduced	1023	0·042	$2 \cdot 70 \times 10^{-6}$
Ni	Polished	1023	0·091	$2 \cdot 91 \times 10^{-6}$
	Oxidised and reduced	1023	0·091	$4 \cdot 23 \times 10^{-6}$
Fe	Polished	673	0·77	$0 \cdot 47 \times 10^{-7}$
	Etched	673	0·77	$4 \cdot 4 \ \times 10^{-7}$
Fe	Polished	863	0·073	$1 \cdot 28 \times 10^{-7}$
	Oxidised and reduced at 600° C.	863	0·073	$0 \cdot 76 \times 10^{-7}$
	Oxidised and reduced at 800° C.	863	0·073	$1 \cdot 54 \times 10^{-7}$

important effect was the steady diminution in permeability with the time of heating, whatever the surface condition. This phenomenon may compare with the surface changes in palladium [96], or the effect of heat treatment of nickel [97, 98, 99]. Sometimes the chemical treatment of a metal with a gas may increase its permeability to a second gas; for example, Ham

and Sauter noted that heating iron in nitrogen increased the velocity of permeation of hydrogen by 10 to 15-fold, although baking out reduced the permeability to its former value.
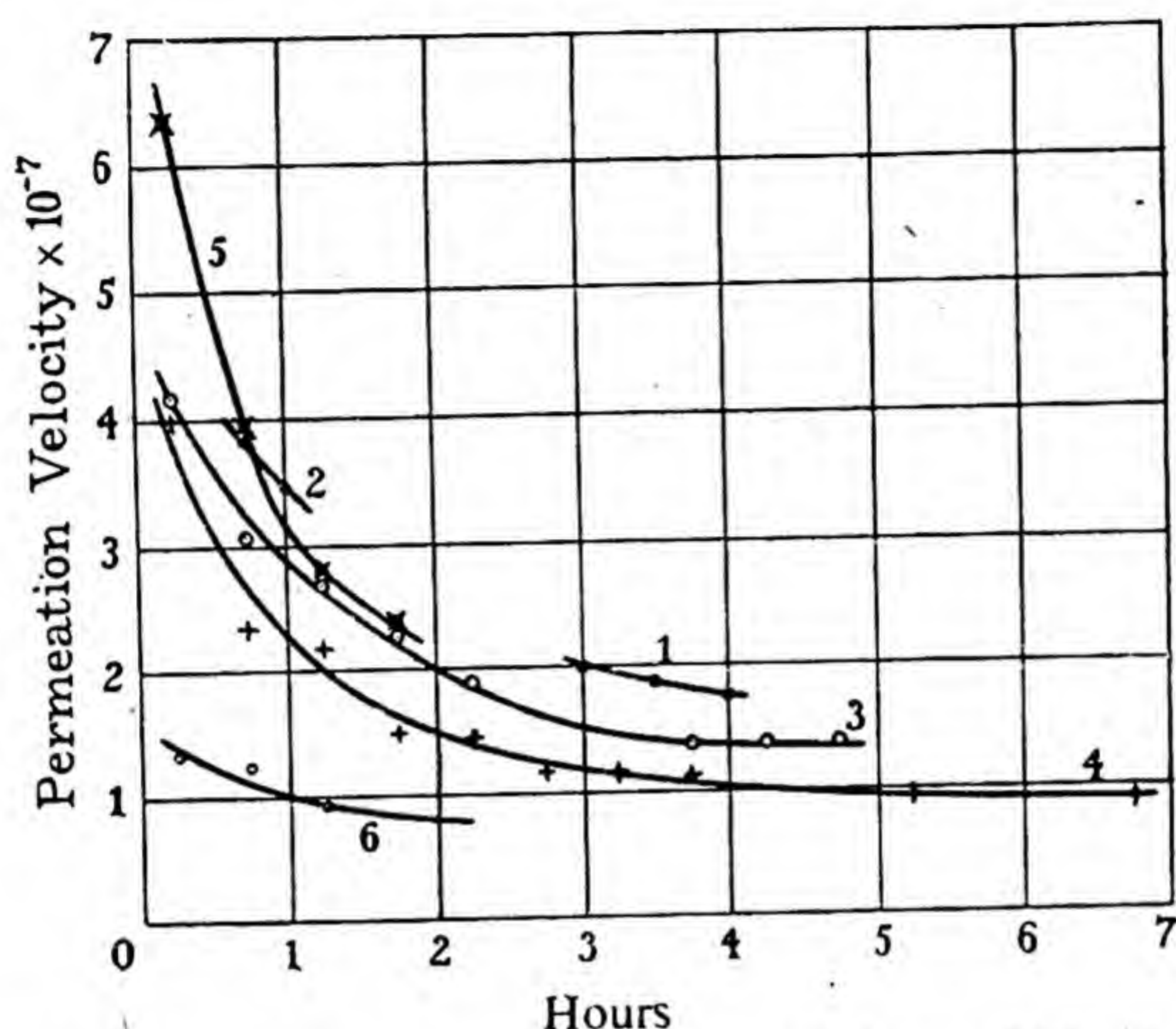
Fig. 67. Effect of surface treatment on the permeability of aluminium to H_2 at 580° C.

Run 1. Al exposed to air.
Run 2. Outer surface scratched.
Run 3. Outer surface scratched again.
Run 4. Outer surface scratched again.
Run 5. Inner and outer surfaces scratched.
Run 6. Outer surface anodically oxidised.

GRAIN-BOUNDARY AND LATTICE PERMEATION

Photo-micrographs may illustrate both the mosaic structure of metals, and a concentration of impurity between crystal blocks. If diffusion occurs mainly down these boundaries, the permeability of a metal would be governed by their number and nature. The mere fact that oxide is found concentrated in these boundaries does not, however, necessarily imply that diffusion of oxygen occurs along them, since the oxide may be formed within the lattice and then be thrown out of solution in the zones between crystallites. That grain-boundary diffusion plays an important part in diffusion processes such

as that of thorium in tungsten, of ions in microcrystalline sodium chloride, or of gases through silica glass is undoubted, and these and other examples have been considered elsewhere (Chaps. VII and III). It is not easy, however, to establish similar cases when gases diffuse through metals. It is true that great variations in permeability may be encountered with different samples of metal (e.g. H_2-Pd systems), but these differences may also be attributed to the variable influence of phase-boundary processes. The evidence available casts doubt upon the special importance of grain boundary diffusion for hydrogen-nickel [97] and hydrogen-iron systems [100] at high temperatures. In both cases it was shown that crystal size had no marked effect upon the permeability. Edwards [55] found the same permeability towards hydrogen in a single crystal plate of iron before heating it, and after heating it to refine the grain. Smithells and Ransley [l.c.] observed that a single crystal iron tube had the same permeability as a similar tube with 100 grains/mm.^{2} (Table 48). Grain boundary diffusion is

TABLE 48. *Permeability to hydrogen of iron of different grain sizes*

Temp. °C.	Pressure mm.	Permeation rate c.c./sec./cm.^{2}/mm.	
		Fine grain × 10^{-6}	Single crystal × 10^{-6}
245	140	2·4	1·2
413	140	17·6	17·1
621	140	92·8	89·5
779	140	203·0	205·0

more easily observed the lower the temperature, and thus experiments of this type should be conducted at the lowest possible temperature.

The permeability of hydrogen-iron systems has received considerable attention at low as well as at high temperatures. Ham and Rast [100] studied the permeability from 55 to 920° C. In addition to discontinuities in permeability at every

thermal critical point, they observed a hysteresis loop in the ~meability-temperature curve illustrated in Fig. 68. At . temperatures, when the diffusing atoms were supplied by .ctrolysis, Barrer (53) found that a bright steel tube was at .rst impermeable, but quickly became more and more permeable to hydrogen in successive diffusion experiments. Poulter and Uffelman (101) found that hydrogen diffused
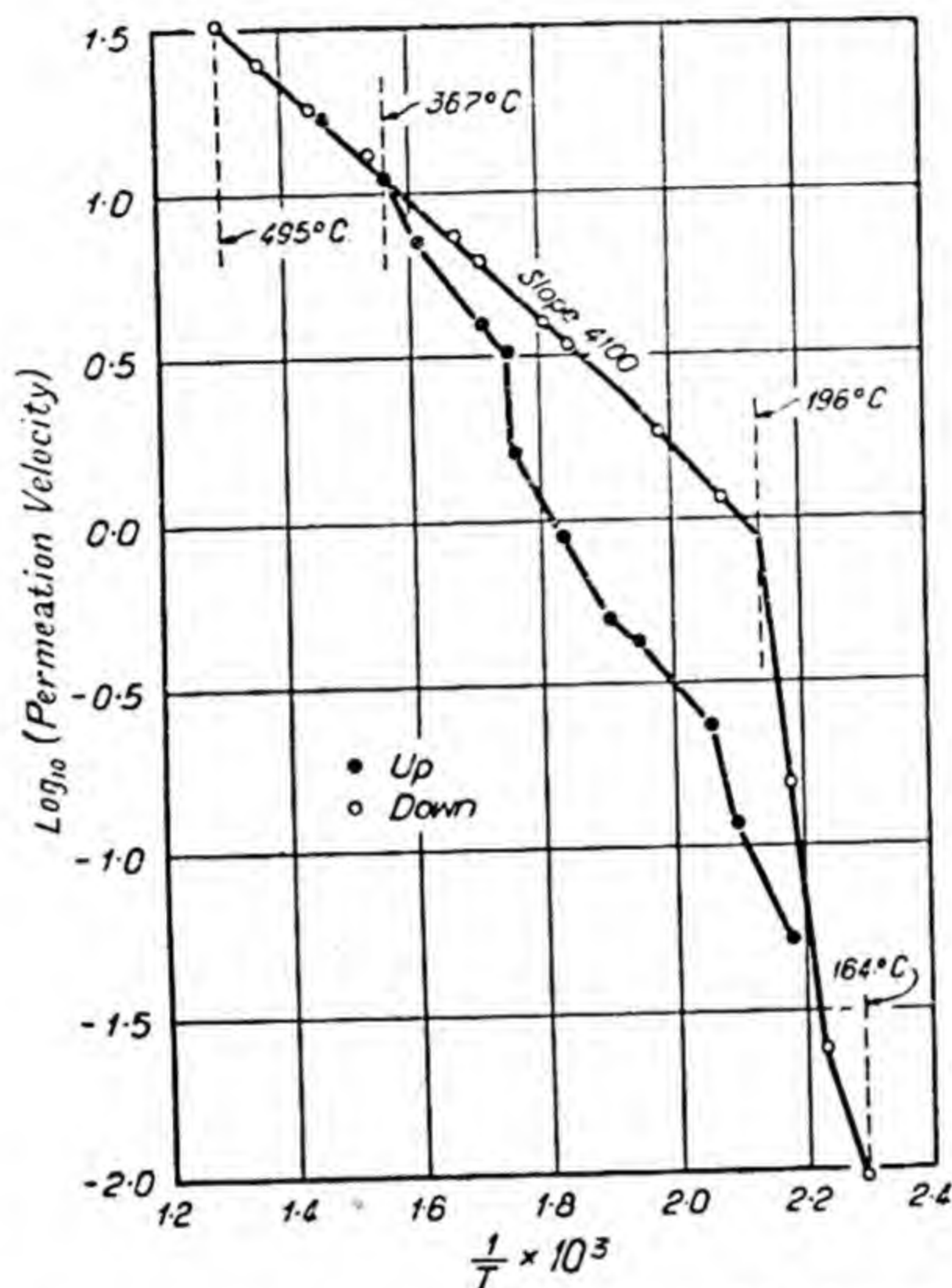
Fig. 68. The low-temperature permeability of hydrogen to iron(101), showing a typical hysteresis loop.

through iron at room temperature, but not until a pressure of 4000 atm. was applied. When the diffusion had thus been started the steel was permeable in a second run at only 100 atm. Some if not all of these observations point to an opening up of grain boundaries as diffusion proceeds. The grain structure can develop due to desorption between grains, of hydrogen which has diffused in the lattice. Thus the system may commence as one where lattice diffusion predominates (p. 198 and Table 48), and end as one where grain boundary diffusion predominates.

Not only may diffusion occur through the lattice, and probably in certain conditions down grain boundaries, but also in each crystallite preferred directions of diffusion may be encountered. Smith and Derge [102, 103] prepared palladium specimens of various grain sizes and showed that grain size did not affect the sorptive capacity. They considered, from crystallographic evidence, and from the marked influence of deformation upon the velocity of uptake, that slip planes in each crystal grain are of special importance in absorption. Etching rolled foils previously charged with hydrogen revealed that fissures had developed inclined at 45° to the direction of rolling. It was thought that the fissures were caused by preferential penetration of hydrogen along slip planes which were dilated as hydrogen diffused into the lattice.

Much more evidence of this kind is necessary before any generalisation concerning the relative importance of grain-boundary, slip-plane, or isotropic lattice diffusions may be made.

FLOW OF NASCENT HYDROGEN THROUGH METALS

Atoms of hydrogen may be generated by electrolysis or by chemical reaction at the metal surface. Some of the atoms of hydrogen thus liberated may leave the surface as molecules and others may enter the metal and diffuse through it. The possible sequence of processes is

$$2H^+ + 2\epsilon \to 2H \begin{cases} 2H_{(dissolved)} \\ H_{2\,(gas)} \end{cases}.$$
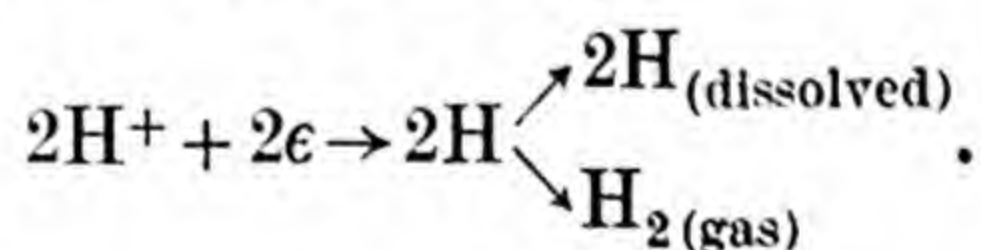
Except for the processes which liberate the atomic hydrogen, the reactions are the same as those occurring during thermal diffusion. Morris [104] showed in agreement with the scheme above that some hydrogen gas, generated by the action of citric acid on iron, diffused through it, and some was evolved (Fig. 69). The fraction diffusing was greater the more rapid the rate of corrosion of the steel (the acid strength being constant).

The possible variables in this type of diffusion include current density, temperature, the dimensions of the membranes, concentration of acid, time, and the concentration of added salts. Bodenstein [11] considered that his results on the diffusion of hydrogen through iron obeyed the relation

$$\text{Permeation velocity} = k\sqrt{I}.$$
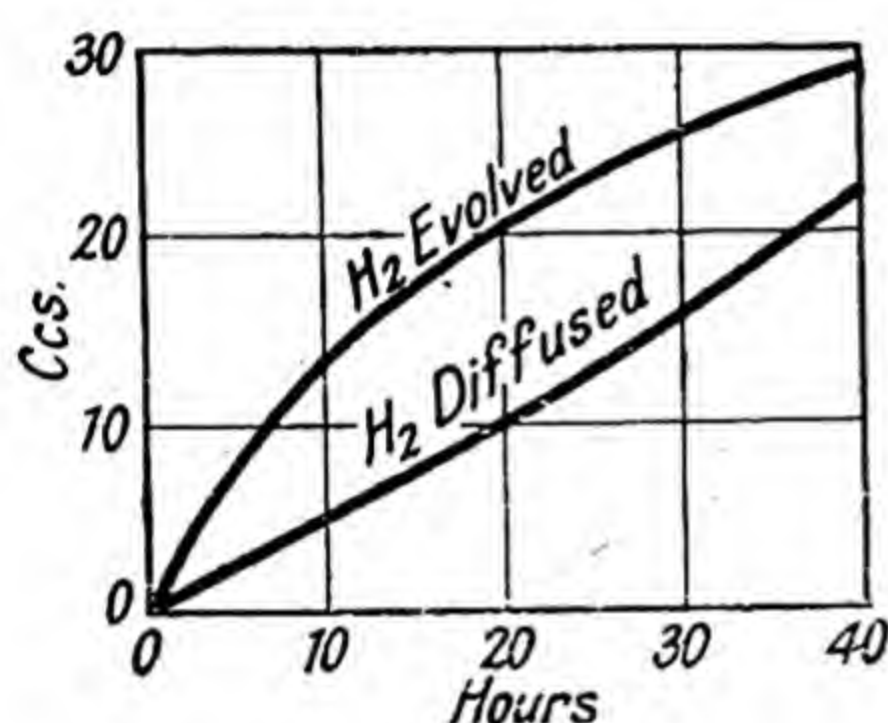
Fig. 69.
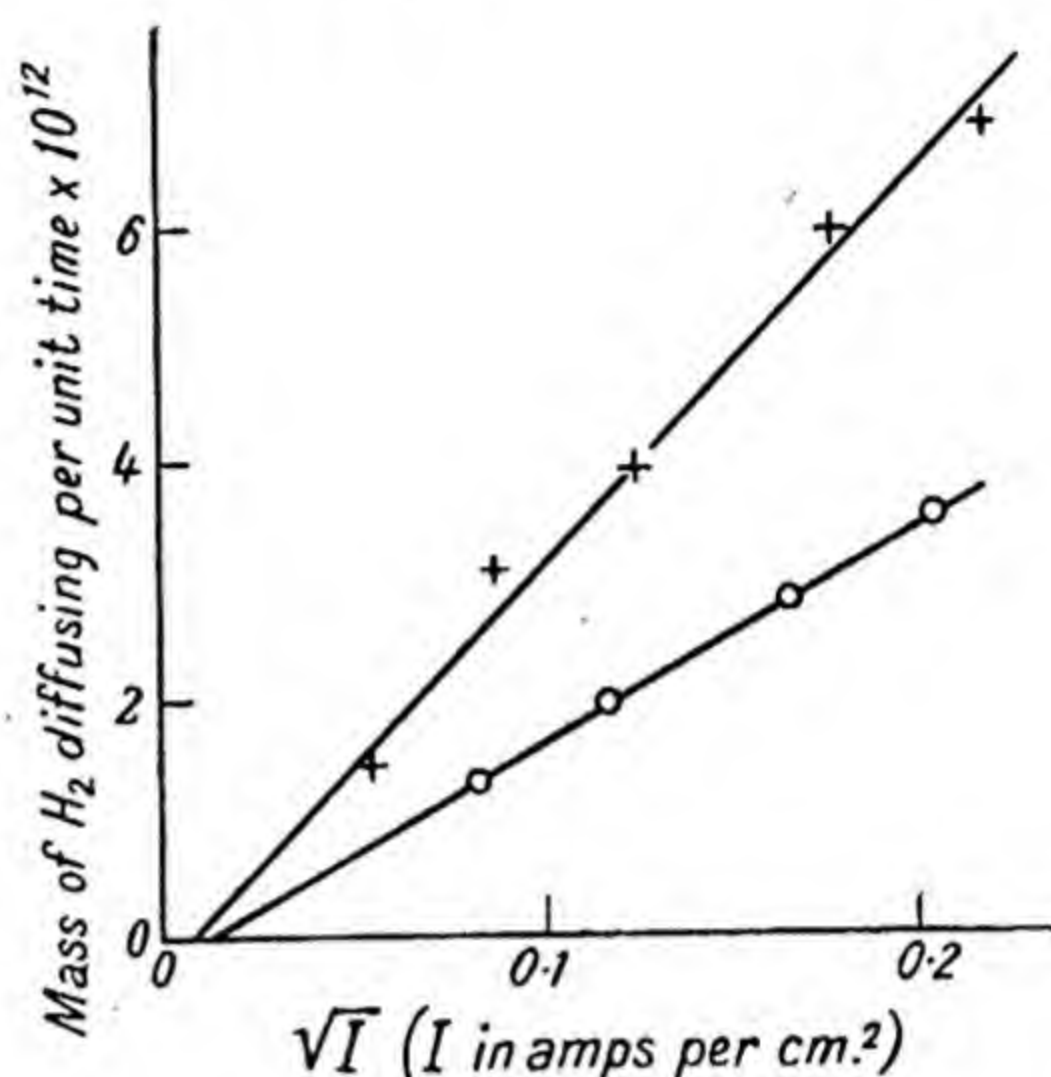
Fig. 70.

Fig. 69. Volumes of hydrogen [simultaneously evolved and diffused by the action of citric acid on fast corroding steel.

Fig. 70. The electrolytic diffusion of hydrogen through iron as a function of current density. Fe, 0·18 % C.   × = untreated.   ○ = annealed.

Borelius and Lindblom [52], however, showed that over a considerable range of current densities the relationship was

$$\text{Permeation velocity} = k(\sqrt{I} - \sqrt{I_t}),$$

where $\sqrt{I_t}$ is a constant, called the threshold current density (Fig. 70). The relation is analogous to their equation for the thermal permeation rate (p. 171):

$$\text{Permeation velocity} = k_1(\sqrt{p} - \sqrt{p_t}).$$

The explanation that the rate of permeation can be expressed as $P = k\theta\sqrt{I}$ and that the surface is not fully saturated at low-current densities is not more tenable than Smithells and Ransley's earlier explanation of the same facts for thermal diffusion (p. 171). The most satisfactory explanation is that advanced by Barrer (p. 174).

The influence of temperature upon the permeation velocity of hydrogen through iron and through palladium (53) shows that the rate of flow rises exponentially with the temperature. The slope of the curves log (permeability) against $1/T$ ($T = °$ K.) for the H_2-Fe system (Fig. 71) is the same at all current densities from 0·0075 to 0·045 amp./cm.^{2}, and is very nearly that found for the thermal permeability ($E_{elect.} = 9400$ cal./atom,
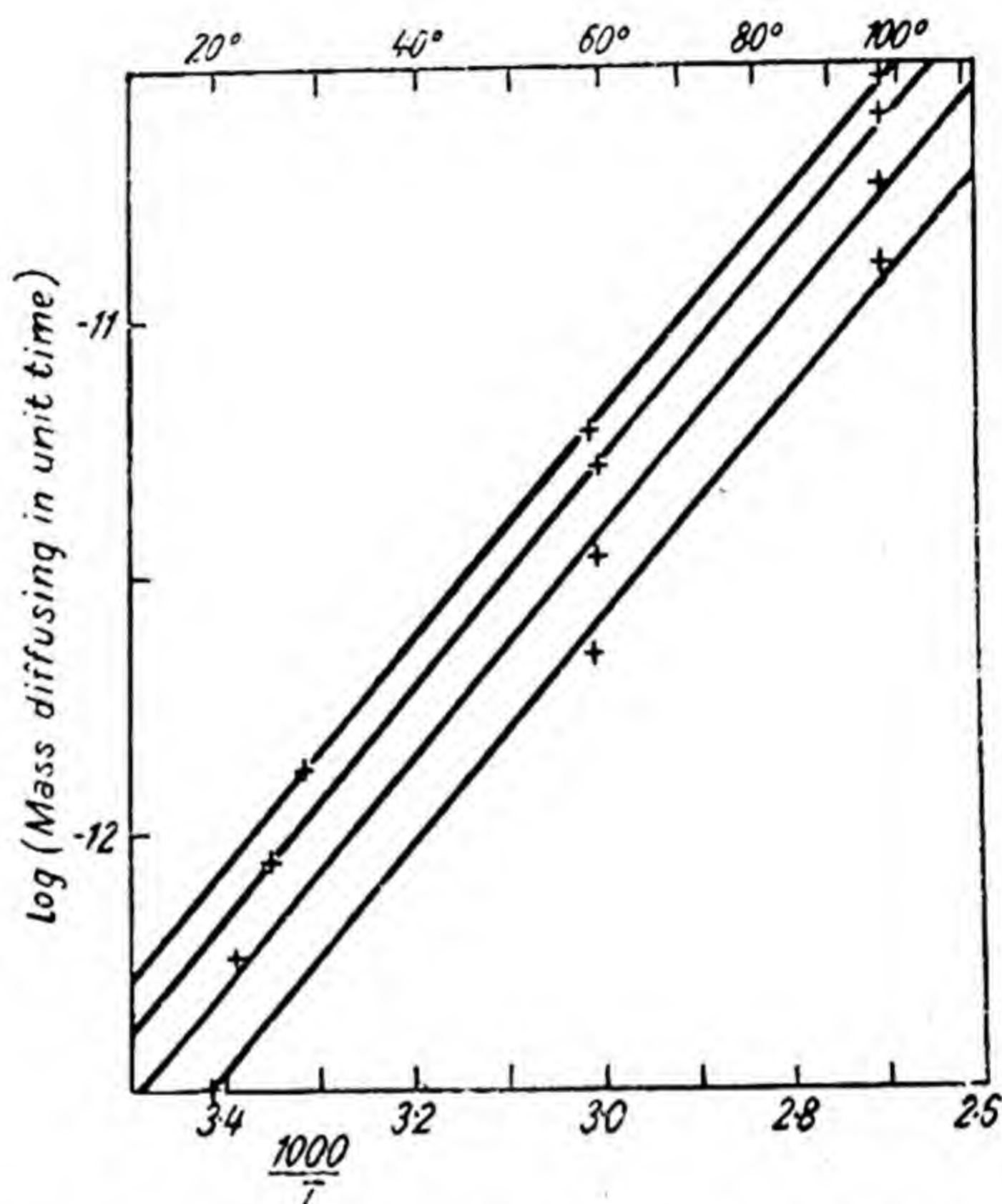
Fig. 71. Electrolytic diffusion of hydrogen through iron as a function of temperature. Curves for current densities: 0·0075 amp./cm.^{2}, 0·015 amp./cm.^{2}, 0·030 amp./cm.^{2} and 0·045 amp./cm.^{2}.

compared with $E_{thermal} = 9100$ cal./atom). This relationship and the similar dependence of the permeability upon current density and gas pressure (p. 178) led Borelius and Lindblom (52) to assume that all rate-controlling processes were the same for thermal diffusion and diffusion of nascent hydrogen.

In Edwards' (55) experiments, the gas was generated by the action of hydrochloric and sulphuric acids upon the iron membrane. In the steady state the permeation velocities

gave a linear $\log P - 1/T$ curve whose slope gives $E = 7300$ cal./atom for the data using $N\,H_2SO_4$. Barrer's[53] data for the H_2-Pd system also gave linear $\log P - 1/T$ curves, and the slopes corresponded to $E = 8500$ and 9200 cal./atom.

As Edwards' and Barrer's data show, the steady state of flow through the membrane is established slowly (Fig. 72), and the interval required depends strongly upon the temperature. During this interval the metal is absorbing a quantity of gas and setting up its steady state concentration gradient. It is
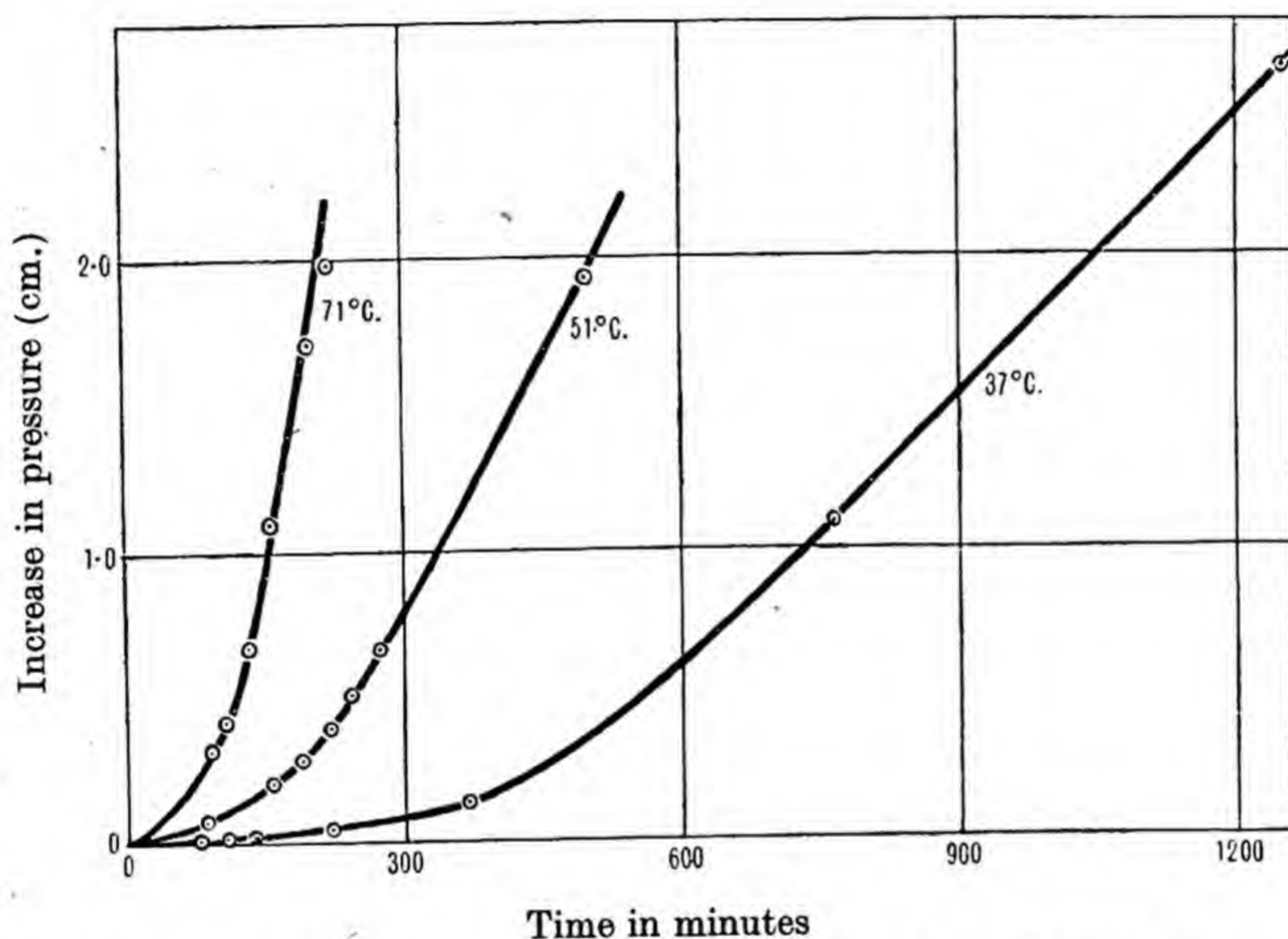
Fig. 72. Time lag in establishing steady state of flow of H_2 through a steel cathode[53].

connected therefore with the velocity of diffusion of the gas within the bulk metal, and the slower this diffusion the more slowly is the steady state approached.

Other studies of the diffusion of nascent hydrogen have given empirical relations between the rate of passage through the metal and the concentration of the acid generating the gas at the surface of the metal[55]; and for the influence of various capillary active substances[105] upon the velocity of permeation. For example, the addition of mercuric chloride caused an acceleration in the rate of permeation. This accelera-

tion in the passage of hydrogen results in a more rapid decrease in the mechanical strength of the iron [13] which is a normal consequence of "pickling" the metal in acid.

REFERENCES

(1) Graham, T. *Phil. Mag.* (4), **32**, 401 (1866); *Ann. Phys., Lpz.,* **129**, 549 (1866); *Chem. Zbl.* **38**, 129 (1867).

(2) Cailletet, L. *C.R. Acad. Sci., Paris,* **58**, 327 and 1057 (1864).

(3) Deville, H. and Troost, L. *C.R. Acad. Sci., Paris,* **56**, 977 (1863).

(4) Troost, L. *C.R. Acad. Sci., Paris,* **98**, 1427 (1884).

(5) Reynolds, O. *Proc. Manchr lit. phil. Soc.* **13**, 93 (1874).

(6) Ramsay, W. *Phil. Mag.* **38**, 206 (1894).

(7) Bellati and Lussana. *Atti. Ist. veneto,* **1**, 1173 (1890).

(8) Winkelmann, A. *Ann. Phys., Lpz.,* **6**, 104 (1901); **17**, 591 (1905); **19**, 1045 (1906).

(9) Richardson, O. *Phil. Mag.* (6), **7**, 266 (1904).
   Richardson, O., Nicol, J. and Parnell, T. *Phil. Mag.* (6), **8**, 1 (1904).

(10) Charpy, G. and Bonnerot, S. *C.R. Acad. Sci., Paris,* **154**, 592 (1912).

(11) Bodenstein, M. *Z. Elektrochem.* **28**, 517 (1922).

(12) Nernst, W. and Lessing, A. *Nachr. Ges. Wiss. Göttingen,* 146 (1902).

(13) Alexejew, D. and Polukarew, O. *Z. Elektrochem.* **32**, 248 (1926).

(14) Aten, A. and Zieren, M. *Rec. Trav. chim. Pays-Bas,* **49**, 641 (1930).

(15) *See* McBain, J. W. *Sorption of Gases by Solids,* Routledge (1932).

(16) E.g. Zr-H_2, Hägg, G. *Z. phys. Chem.* **11**, 433 (1931).

(17) E.g. Pd-H_2, Linde, J. and Borelius, G. *Ann. Phys., Lpz.,* **84**, 747 (1927).
   Krüger, F. and Gehm, G. *Ann. Phys., Lpz.,* **16**, 174 (1933).

(18) A full list of references to work of Sieverts and his co-workers up to 1930 is given in J. W. McBain, *Sorption of Gases by Solids* (1932). Other later references will be given subsequently.

(19) Smithells, C. *Gases and Metals,* Chapman and Hall (1937).

(20) Emeleus, H. and Anderson, J. *Modern Aspects of Inorganic Chemistry,* Chap. 13, Routledge (1938).

(21) Sieverts, A. and Zapf, G. *Z. phys. Chem.* **174**A, 359 (1935).
   Sieverts, A. and Danz, W. *Z. phys. Chem.* **34**B, 158 (1936).

(22) Lacher, J. *Proc. Roy. Soc.* **161**A, 525 (1937).

(23) Smithells, C. *Gases and Metals,* pp. 153 *et seq.* (1937).

(24) Smithells, C. and Fowler, R. H. *Proc. Roy. Soc.* **160**A, 38 (1937).

(25) Sieverts, A. and Hagenacker, J. *Z. phys. Chem.* **68**, 115 (1910).

(26) Steacie, E. and Johnson, F. *Proc. Roy. Soc.* **112**A, 542 (1926).

(27) Simons, J. H. *J. phys. Chem.* **36**, 652 (1933).

REFERENCES   205

(28) Mathewson, C., Spire, E. and Milligan, W. *J. Amer. Steel Treat.
       Soc.* **19**, 66 (1931).
(29) Smithells, C. *Gases and Metals*, Fig. 124.
(30) Rhines, F. and Mathewson, C. *Trans. Amer. Inst. min. (metall.)
       Engrs*, **111**, 337 (1934).
(31) Smithells, C. *Gases and Metals*, Fig. 123.
(32) Seybold, A. and Mathewson, C. *Tech. Publ. Amer. Inst. Min.
       Engrs*, **642** (1935).
(33) Merica, P. and Waltenburg, R. *Bur. Stand. Sci. Pap.* **281** (1925).
(34) de Boer, J. H. and Fast, J. *Rec. Trav. chim. Pays-Bas*, **55**, 459
       (1936).
(35) Sieverts, A. and Brüning, K. *Arch. Eisenhüttenw.* **7**, 641 (1933).
(36) Hägg, G. *Z. phys. Chem.* **7** B, 339 (1930).
(37) Sieverts, A., Zapf, G. and Moritz, H. *Z. phys. Chem.* **183** A, 33
       (1938).
       Earlier references are given in Smithells, C., *Gases and Metals*,
       p. 171.
(38) Smithells, C. *Gases and Metals*, Fig. 119.
(39) Hägg, G. *Z. phys. Chem.* **4** B, 346 (1929).
(40) Röntgen, P. and Braun, H. *Metallwirtschaft*, **11**, 459 (1932).
(41) Sieverts, A. and Krumbharr, W. *Z. phys. Chem.* **74**, 295 (1910).
(42) Smithells, C. *Gases and Metals*, Fig. 107.
(43) Kirschfeld, L. and Sieverts, A. *Z. Elektrochem.* **36**, 123 (1930).
(44) Sieverts, A. *Z. Metallkunde*, **21**, 37 (1929).
(45) Toole, F. and Johnson, F. *J. phys. Chem.* **37**, 331 (1933).
(46) Sieverts, A. and Brüning, K. *Z. phys. Chem.* **168**, 411 (1934).
(47) Sieverts, A. and Hagen, H. *Z. phys. Chem.* **174**, 247 (1935).
(48) Cf. ref. (35). See also Takei, T. and Murakami, T. *Sci. Rep.
       Tohoku Univ.* **18**, 135 (1929).
(49) Smithells, C. *Gases and Metals*, p. 186, Fig. 132.
(50) Ham, W. *J. chem. Phys.* **1**, 476 (1933).
(51) Post, C. and Ham, W. *J. chem. Phys.* **5**, 915 (1937).
(52) Borelius, G. and Lindblom, S. *Ann. Phys., Lpz.*, **82**, 201 (1927).
(53) Barrer, R. *Trans. Faraday Soc.* **36**, 1235 (1940).
(54) Smithells, C. *Gases and Metals*, p. 84 (1937).
(55) Edwards, C. *J. Iron and Steel Inst.* **110**, 9 (1924).
(56) Johnson, F. and Larose, P. *J. Amer. Chem. Soc.* **46**, 1377 (1924).
(57) Lombard, V. *C.R. Acad. Sci., Paris*, **177**, 116 (1923).
(58) Lombard, V., Eichner, C. and Albert, M. *Bull. Soc. chim. Paris*,
       4, 1276 (1937).
(59) Bramley, A. *Carnegie Schol. Mem., Iron and Steel Inst.*, **15**, 155
       (1926).
(60) Smithells, C. and Ransley, C. E. *Proc. Roy. Soc.* **150** A, 172 (1935).
(61) Post, C., and Ham, W. *J. chem. Phys.* **6**, 599 (1938).
(62) Deming, H. and Hendricks, B. *J. Amer. chem. Soc.* **45**, 2857
       (1923).
(63) Jouan, R. *J. Phys. Radium*, **7**, 101 (1936).

(64) Melville, H. and Rideal, E. *Proc. Roy. Soc.* **153**A, 89 (1936).

(65) Braaten, E. and Clark, G. *Proc. Roy. Soc.* **153**A, 504 (1936).

(66) Ryder. *Elect. (Cl.) J.* **17**, 161 (1920)

(67) Smithells, C. and Ransley, C. E. *Proc. Roy. Soc.* **152**A (1935).

(68) Spencer, L. *J. chem. Soc.* **123**, 2124 (1923).

(69) Lombard, V. and Eichner, C. *Bull. Soc. chim. Fr.* **53**, 1176 (1933).

(70) Schmidt, G. *Ann. Phys., Lpz.,* **13**, 747 (1904).

(71) Holt, A. *Proc. Roy. Soc.* **91**A, 148 (1915).

(72) Lombard, V. and Eichner, C. *Bull. Soc. chim. Fr.* **51**, 1462 (1932).

(73) Ham, W. and Sauter, J. D. *Phys. Rev.* **47**, 337 (1935).

(74) —— —— *Phys. Rev.* **47**, 645 (1935).

(75) Wüstner, H. *Ann. Phys., Lpz.,* **46**, 1095 (1915).

(76) Smithells, C. and Ransley, C. E. *Proc. Roy. Soc.* **157**A, 292 (1936).

(77) Ham, W. *Phys. Rev.* **47**, 645 (1935).

(78) Smithells, C. *Gases and Metals,* p. 90 (1937).

(79) Barrer, R. M. *Trans. Faraday Soc.* **35**, 628, 644 (1939).

(80) Wang, J. S. *Proc. Camb. phil. Soc.* **32**, 657 (1936).

(81) Barrer, R. M. *Phil. Mag.* **28**, 353 (1939).

(82) —— *Phil. Mag.* **28**, 148 (1939).

(83) Wagner, C. *Z. phys. Chem.* **159**A, 459 (1932).

(84) Engelhardt, G. and Wagner, C. *Z. phys. Chem.* **18**B, 369 (1932).

(85) Doehlemann, E. *Z. Elektrochem.* **42**, 561 (1936).

(86) Barrer, R. M. *Trans. Faraday Soc.* **32**, 486 (1936).

(87) Farkas, A. and Farkas, L. *Proc. Roy. Soc.* **144**A, 467 (1934).

(88) Jost, W. and Widmann, A. *Z. phys. Chem.* **29**B, 247 (1935).

(89) Jouan, R. *J. Phys. Radium,* **7**, 101 (1936). See Fig. 4.

(90) Farkas, A. *Trans. Faraday Soc.* **32**, 1667 (1936).

(91) Barrer, R. M. *Trans. Faraday Soc.* **32**, 482 (1936).

(92) —— *Trans. Faraday Soc.* **32**, 490 (1936).

(93) Cremer, E. and Polanyi, M. *Z. phys. Chem.* **19**B, 443 (1932).

(94) Melville, H. *J. chem. Soc.* 1243 (1934).

(95) Eyring, H. and Sherman, J. *J. chem. Phys.* **1**, 345 (1933).

(96) Lombard, V., Eichner, C. and Albert, M. *Bull. Soc. chim. Fr.* **3**, 2203 (1936).

(97) Baukloh, W. and Kayser, H. *Z. Metallk.* **26**, 157 (1934); **27**. 281 (1935).

(98) Lewkonja, G. and Baukloh, W. *Z. Metallk.* **25**, 309 (1933).

(99) Baukloh, W. and Guthmann, H. *Z. Metallk.* **28**, 34 (1936).

(100) Ham, W. and Rast, W. *Trans. Amer. Soc. Metals,* **26**, 885 (1938).

(101) Poulter, T. and Uffelman, L. *Physics,* **3**, 147 (1932).

(102) Smith, D. and Dergo, G. *Trans. Amer. electrochem. Soc.* **66**, 253 (1934).

(103) —— —— *J. Amer. chem. Soc.* **56**, 2513 (1934).

(104) Morris, T. *J. Soc. Chem. Ind.* **54**, 7 (1935).

(105) Aten, A. and Zieren, M. *Rec. Trav. chim. Pays-Bas,* **49**, 641 (1930).

CHAPTER V

DIFFUSION OF GASES AND NON-METALS IN METALS

INTRODUCTION

In the previous chapter were considered the main phenomena of gas flow through metals. It was shown there that the gas flow (P) is governed by the equation

$$P = -D\frac{dC}{dx},$$

where D is the diffusion constant, but so far we have had little to say concerning the important constant D. It has, however, been stated (Chap. IV) that the diffusion constant obeys an exponential law

$$D = D_0 e^{-E/RT}$$

analogous to the expression

$$P = P_0 e^{-E_1/RT}$$

for the permeability constant. It is not difficult to see why an energy of activation should be involved in diffusion processes in solids. The solid lattice contains atoms distributed in a periodic manner, to give the regular crystalline array. Just as when the solubility of gases in metals was discussed (Chap. IV, p. 153), one may regard the interstitial positions in the lattice as positions of minimum potential energy—potential "holes"—separated by energy barriers. The diffusing atom requires an activation energy before it may pass from one minimum of energy to another, exactly as does an atom undergoing a chemical reaction. In this way an exponential term $e^{-E/RT}$ is introduced. While the value of E in a diffusion process is a relatively easily interpreted quantity, the E_1 in the expression for the permeability is a complex quantity, which may be made up of E for diffusion processes, and phase-boundary processes, and the heat of solution (ΔH) of the gas in the metal. Thus the energy of activation for diffusion can

be related to the crystal structure and force fields, and the dimensions of the diffusing particle, but the temperature coefficient for the permeability is not easily related to these quantities.

When one examines the literature one finds that relatively few measurements have been made of the diffusion constants of gases in solids. One has to be sure that phase-boundary processes do not control the velocities of absorption, but this is not always easy to establish. Again, the mathematical analysis of the data often presents difficulties, and very frequently a number of phases co-exist which render inter-pretation even more uncertain. One has sometimes to deal with the case when the diffusion constant is a function of the concentration, necessitating the use of Fick's law in the form

$$\frac{\partial C}{\partial t} = \frac{\partial}{\partial x}\left(D\frac{\partial C}{\partial x}\right).$$

However, the mathematical handling of the data in this instance is now possible (Chap. I), and the formal treatments of Fick's law for the great proportion of the possibilities which arise have been completed.

THE MEASUREMENT OF DIFFUSION CONSTANTS IN METALS

To measure the concentration gradient in a metal, one may conveniently employ the method of Bramley (1, 2, 3, 4, 5) and his co-workers. They heated iron in a suitable gas atmosphere of which the following are examples:

CO and CO_2 (diffusion of oxygen or carbon),

CO and CH_3CN (diffusion of nitrogen or carbon),

CO and ⬡N (diffusion of nitrogen or carbon),

CO and ⬡CH_3 ⎫
⬡ ⎬ (diffusion of carbon),
CH_3⬡CH_3 ⎭

CO and paraffins (diffusion of carbon),

CO and NH_3 (diffusion of carbon or nitrogen),

N_2 and NH_3 (diffusion of nitrogen),

H_2 and PH_3 (diffusion of phosphorus),

CS_2 and $\langle\underline{\hspace{1em}}\rangle CH_3$ (diffusion of carbon and sulphur).

After the metal in the form of bars had been heated to a definite temperature for a suitable period it was removed, and successive thin layers taken off in the lathe and analysed. In this way the concentration gradient was determined and the solution of Fick's law in the form

$$C = C_0\left(1 - \frac{2}{\sqrt{\pi}}\int_0^{x/2\sqrt{(Dt)}} e^{-z^2}\,dz\right)$$

was used to evaluate D. Here C_0 is the concentration at $x = 0$, supposed constant and conditioned by the gas atmosphere. Bramley and Lord (4) showed that bars of the same steel heated for the same time and at the same temperature but in very different atmospheres gave the same distribution of carbon in all cases.

The concentration-distance curves into the metal are, however, not always of a shape to which a simple solution of the Fick law is applicable. Figs. 73 and 74 give different types of concentration-distance curve, for which the solution given above is manifestly not correct. In the former case a saturated carbon layer has established itself at the surface, and in the latter the surface has been to some extent decarburised by hydrogen present in the carburising atmosphere. An attempt has been made to treat diffusion problems of the type illustrated by Fig. 73 (6), but a complete treatment of Fig. 74 is not available. However, Bramley and his co-workers neglected the initial parts of these unusual forms of concentration distance curve, and applied the simple solution of Fick's law only to the tail of the curves. The error involved in evaluating D is therefore smaller.

In addition to this analytical method of determining the concentration gradient it should in some cases be possible to

use an X-ray method. This would reveal the presence of embedded crystals of carbide, nitride, or other compounds of the diffusing element and the metal, and the intensity of the typical pattern may be used as a measure of concentration. The method might be used where the lattice is expanded by its content of dissolved gas, for the expansion is often a
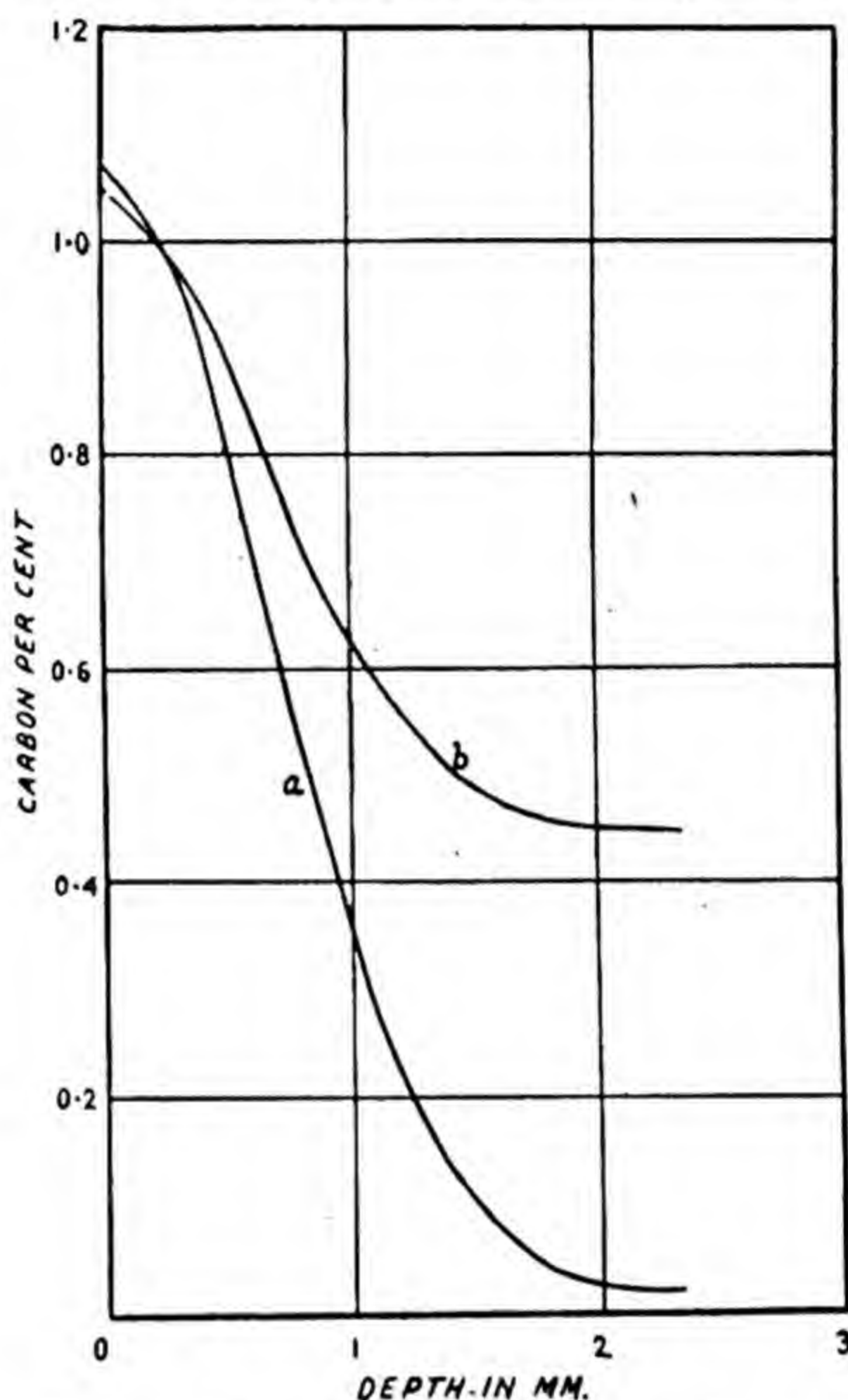
Fig. 73. Types of concentration gradient.

function of the charge of gas. The X-ray method has been employed for following the inter-diffusion of metals; it has also been used in studies (7, 8, 9, 10) of the hydrogen-palladium system in which the lattice constants both for the α- and β-phases increase with the concentration of hydrogen in the lattice (Fig. 75). However, while the method is frequently available in investigating equilibrium (11, 12, 13) systems, it is not so often employed in measuring concentration gradients.

When one does not require the concentration gradient, but simply the total quantity absorbed or desorbed, one may use
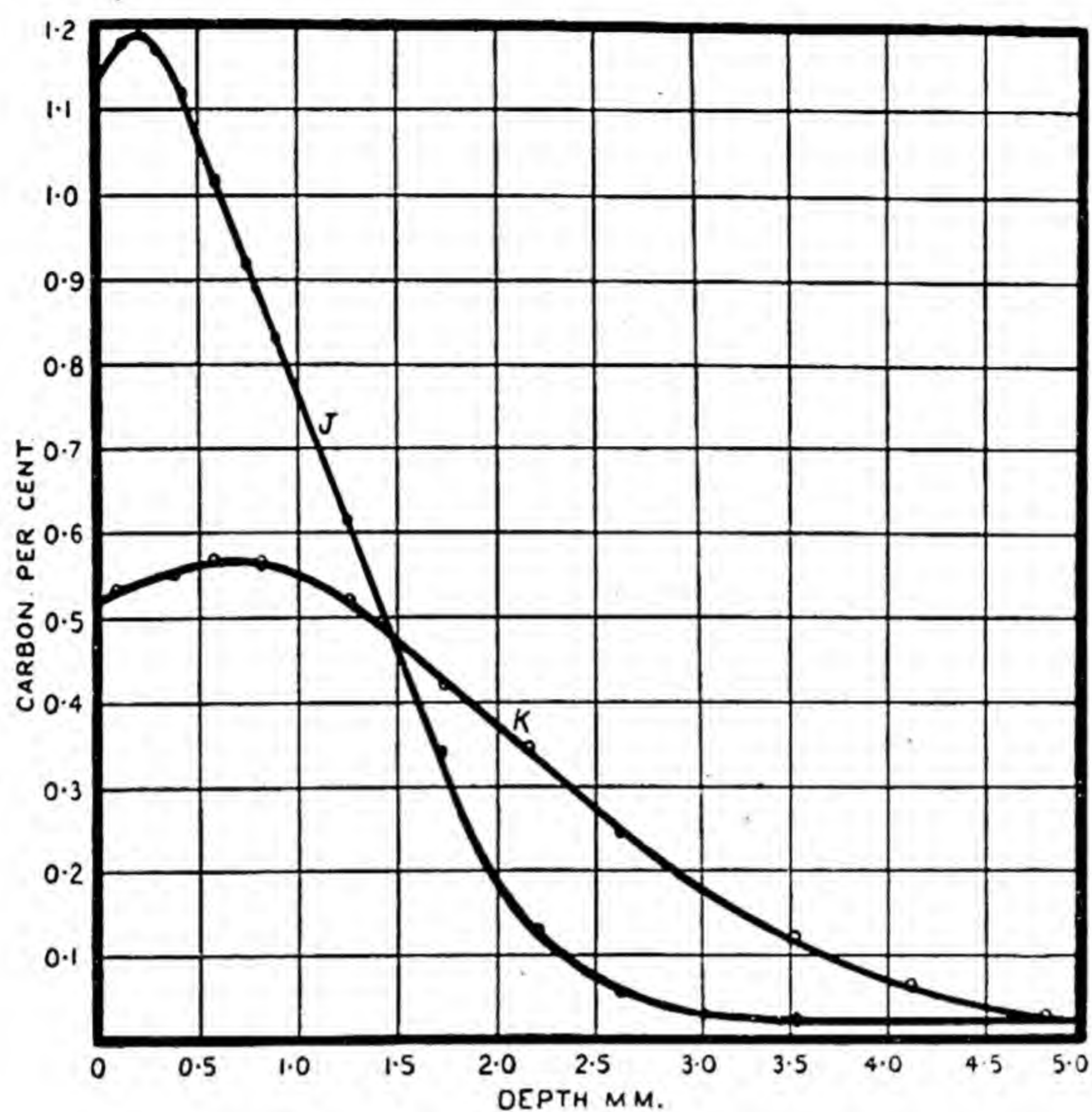
Fig. 74. Types of concentration gradient.
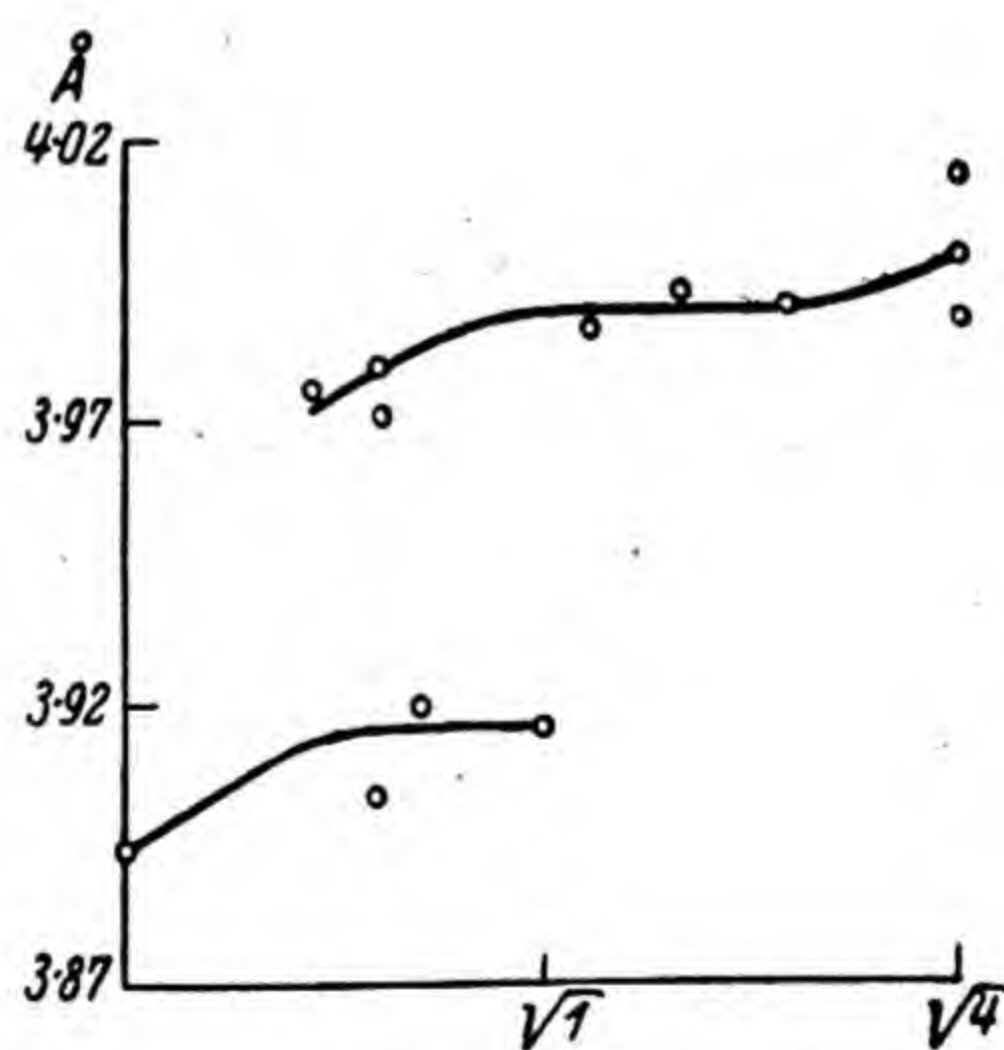
Fig. 75. Lattice constants in H_2-Pd alloys as a function of $\sqrt{p}$.

the metal in the form of a wire, and measure its electrical resistance. This method has been used for carbon-oxygen (carbon at very high temperatures is believed to dissolve oxygen [18]), and for hydrogen-palladium [14, 15]. The assumption is usually made that the change of resistance is a linear function of the charge of hydrogen. Similarly Coehn and Jürgens [16] followed the absorption of hydrogen by a large number of palladium-silver alloys by measuring their electrical resistance. It is probable that the absorption of gases by any other metal or oxide which reacts with or dissolves the gas appreciably could be followed by electrical resistance changes. As suitable systems one may give

H_2-Ta*	O_2-Cu_2O [17]
H_2-V	O_2-NiO [18]
H_2-Ti	O_2-Zr [19]
H_2-Ce, La, and certain rare earths	N_2-Zr [19]
H_2-Th	
N_2-Fe	
N_2-Mo	
N_2-Mn	

The E.M.F. produced by a palladium wire charged with hydrogen and immersed in a solution containing hydrogen ions is different from the E.M.F. given by uncharged palladium, and Coehn and Specht [21] measured the diffusion of hydrogen along a palladium wire whose centre was electrolytically charged with hydrogen, by measuring the potential at other points along the wire as a function of time. The speed of movement of a point of constant potential was related to the time by an expression

$$4Dt = x^2,$$

and from curves such as those in Fig. 76 the authors were able to measure D. The numbers of the curves relate to the point on the wire at which the potential was measured.

* Sieverts and Brüning [20] have shown that the resistivity rises in direct proportion to the quantity of hydrogen absorbed, being 30 % greater when the metal is saturated.

Another method for following the diffusion of hydrogen along filaments was devised by Coehn and Sperling (22). The centre of a palladium wire was charged with hydrogen gas, and the wire clamped under a photographic plate. The hydrogen liberated at the surface of the wire blackened the plate. As before, the movement of the black strip, by means
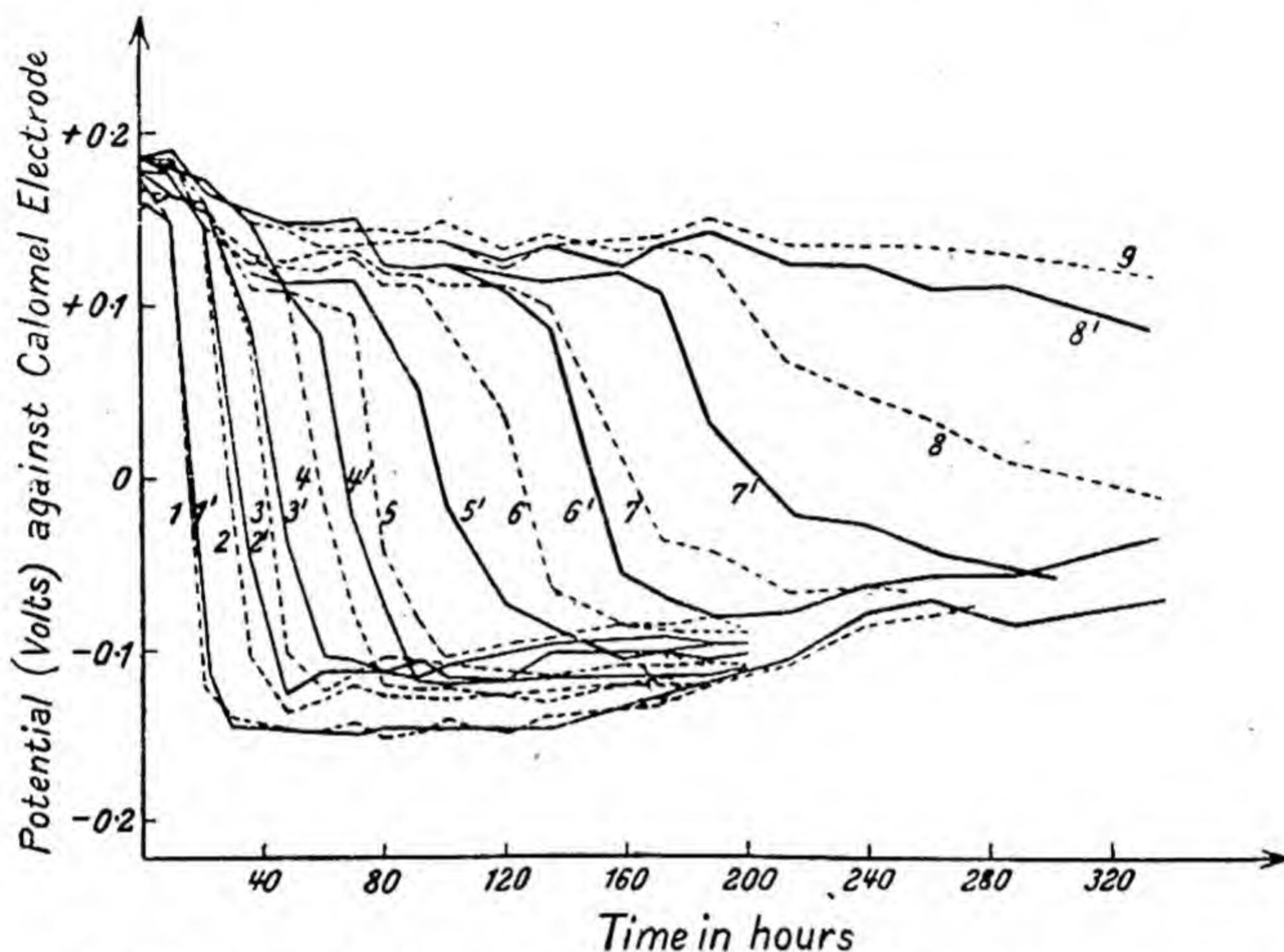
Fig. 76. Flow of hydrogen in a palladium wire followed by measuring the change of potential with time.

of the relationship $x^2 = 4Dt$ (x denotes a point of a given darkness on the plate), was used to calculate D.

The thermo-electric properties of metals are also altered when they absorb gases. If a thermocouple is made between a pure metal and a hydrogen-saturated metal, the pure metal is electronegative, and the thermal E.M.F. per $1°$ C. is (23)

Fe	0.705×10^{-7} V.,
Pt	0.223×10^{-7} V.,
Ni	1.08×10^{-7} V.,
Pd	174.5×10^{-7} V.

As the capacity of the metal for dissolving gas increases, so does the thermal E.M.F. The method ought therefore to be

applicable to the solution of hydrogen in tantalum, titanium, cerium, thorium and other metals which dissolve hydrogen in large quantities.

Euringer[24], who measured the evolution of hydrogen from nickel wires, gave a method for measuring both the solubility and the diffusion constant. The method, which should be of general applicability, was based upon the following solution of Fick's law (Chap. I):

$$C = \frac{2C_0}{r_0} \sum_{n=1}^{\infty} \frac{J_0(\alpha_n r)}{\alpha_n J_1(\alpha_n r)} e^{-D\alpha_n^2 t},$$

where α_n is the nth root of the Bessel function of zero order, and C_0 is the initial uniform concentration in a wire of radius r_0. The rate of evolution, P, of gas from the wire is

$$P = -D\left(\frac{\partial C}{\partial r}\right)_{r=r_0}$$

$$= -\frac{2C_0 D}{r_0} \sum_{}^{\infty} e^{-D\alpha_n^2 t},$$

since $\dfrac{\partial\{J_0(\alpha_n r)\}}{\partial r} = -J_1(\alpha_n r).$

The rate of evolution of gas therefore depends upon a constant $2C_0 D/r$ and an infinite series of exponentials. The shape of the curve of $\log P$ against $\log t$ does not therefore change through alterations in C_0 or D, save to undergo bodily displacement. Thus an experimental curve can be compared, for a given C_0 and D with a calculated one, upon a log-log scale of axes. When the curves are correctly ascertained, the theoretical curve may be made to coincide with the experimental one, by suitable horizontal and vertical displacements. D and C_0 are then observed as follows:

Use the suffix "e" to denote experimental, and "c" to denote values assumed in calculation. Take a point (t_c, P_c) on the log-log curve which after displacement coincides with a point (t_e, P_e). For this point the products Dt must be equal, and so the series $\sum_{n=1}^{\infty} e^{-D\alpha_n^2 t}$ are equal. Thus $D_c t_c = D_e t_e$, and

D_e is calculated. Similarly, if the exponential series are equal, one must have

$$\frac{P_e r_{0_e}}{C_{0_e} D_e} = \frac{P_c r_{0_c}}{C_{0_c} D_c}; \quad \text{or} \quad C_{0_e} = \frac{P_e r_{0_e}}{D_e} \frac{C_{0_c} D_c}{P_c r_{0_c}},$$

and so one may calculate C_{0_e}, the experimental value of C_0. One might also find the slope and intercept of the asymptotic curve

$$\log P = \log \frac{2 C_0 D}{r_0} - \frac{D \alpha_1^2 t}{2 \cdot 303},$$
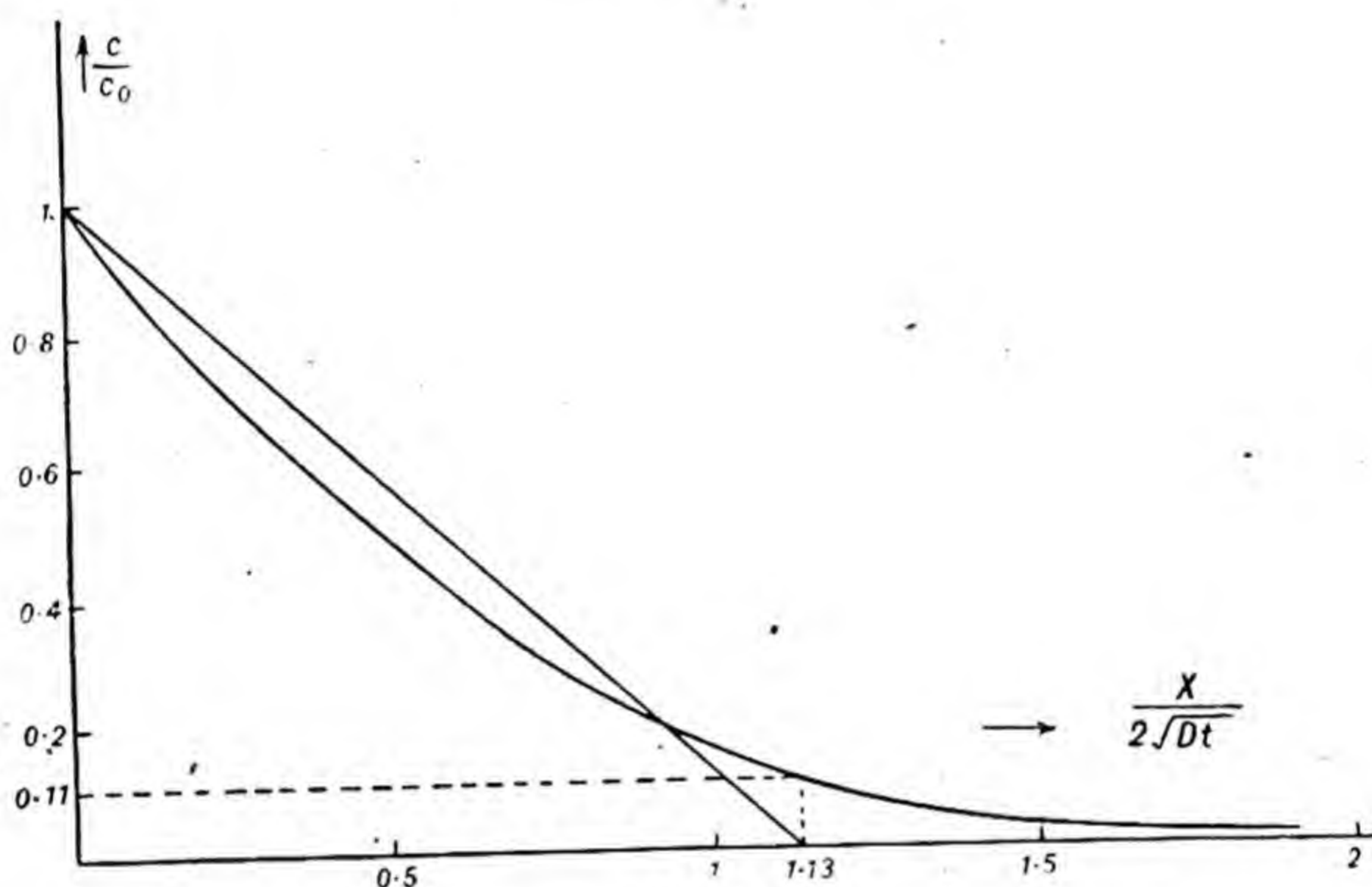
Fig. 77.

valid for large values of t, but Euringer pointed out that then changes in P may not be easy to evaluate, since they have become small. He therefore advocated the method already indicated.

Van Liempt[25] outlined a method of obtaining D approximately from the evolution of gases from wires and plates. The Fick law for diffusion into a semi-infinite sheet is

$$\frac{C}{C_0} = 1 - \frac{2}{\sqrt{\pi}} \int_0^{x/2\sqrt{(Dt)}} e^{-w^2} dw.$$

If one plots C/C_0 against $x/2\sqrt{(Dt)}$, the typical curve of Fig. 77 is obtained. The curve encloses the same area $C_0/\sqrt{\pi}$ as the

triangle of which the hypotenuse cuts the $x/2\sqrt{(Dt)}$ axis at the point $2/\sqrt{\pi} = 1\cdot13$, where $C/C_0 = 0\cdot11$. This point of intersection was called the "apparent penetration depth", a, or "apparent outgassing depth" if one is considering desorption. When the real curve is replaced by the straight line in this way, one can find simple formulae for the diffusion constant D in terms of plate thickness, d, and breadth $B(B \gg d)$ (Fig. 78). If $Q = $ gas evolved/cm. length of the plate being degassed,
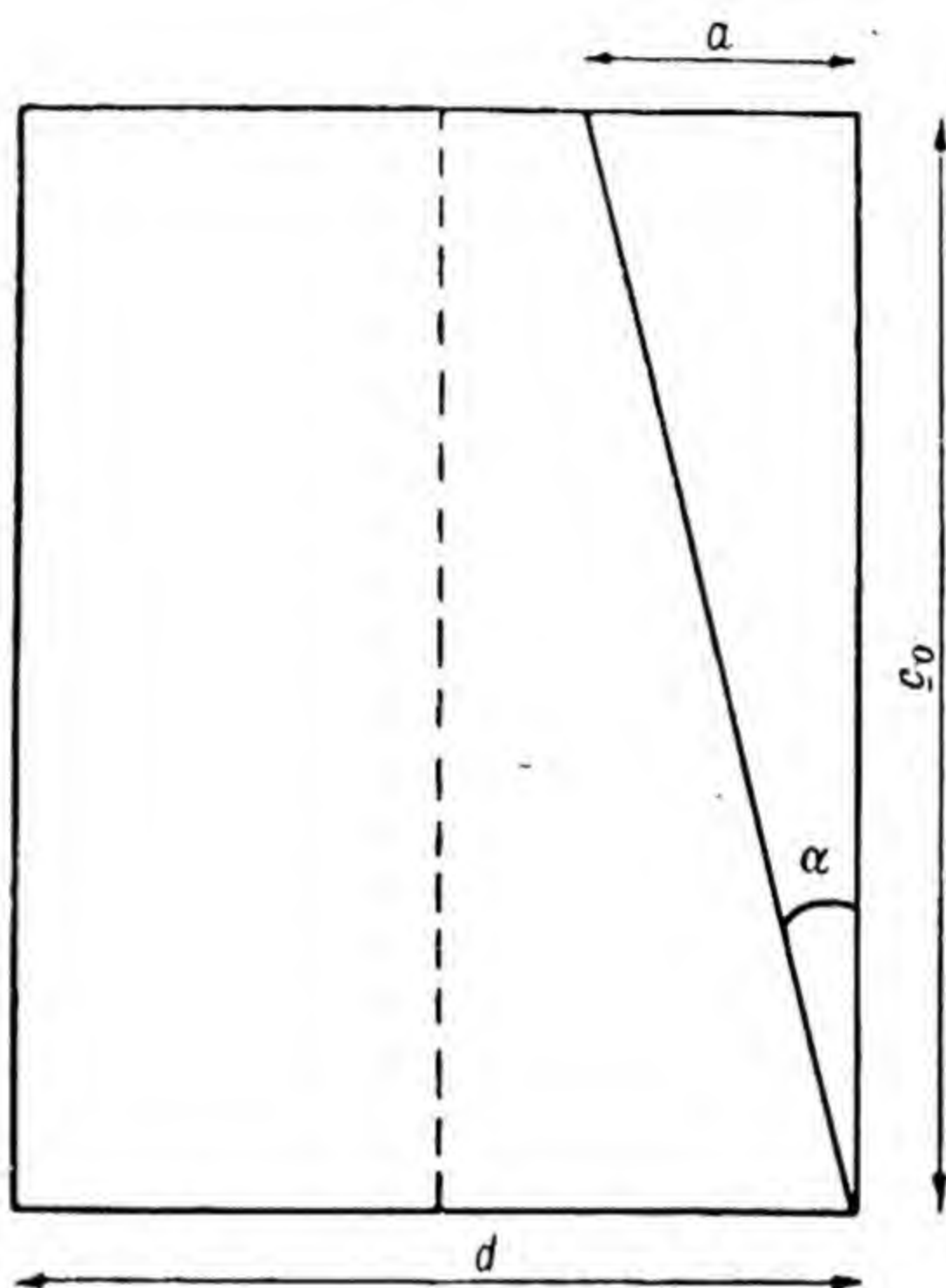
Fig. 78.

one has so long as $a \leqslant \frac{1}{2}d$ or $Q/Q_0 \leqslant 0\cdot50$: $Q = 2[\frac{1}{2}aC_0]$. The original quantity absorbed was

$$Q_0 = dC_0 B,$$

so that
$$\frac{Q}{Q_0} = \frac{a}{d} = \frac{4}{d}\sqrt{\frac{Dt}{\pi}}.$$

Other cases were given which are listed below:

(i) Degassing a plate, where $a \geqslant \frac{1}{2}d$ or $Q/Q_0 \geqslant 0\cdot50$:

$$\left(1 - \frac{Q}{Q_0}\right) = \sqrt{\left(\frac{\pi}{Dt}\right)\frac{d}{16}}.$$

(ii) Degassing a wire of radius r_0, where $Q/Q_0 < 0.67$:

$$D = 3\pi r_0^2 \left\{ \frac{3 - 2Q/Q_0 - \sqrt{(9 - 12Q/Q_0)}}{32t} \right\}.$$

(iii) Degassing a wire of radius r_0, where $Q/Q_0 > 0.67$:

$$D = \frac{\pi r_0^2}{144t(1 - Q/Q_0)^2}.$$

It must be remembered that the values of D calculated by these formulae were not exact, although all the values of D were of the correct magnitudes. Table 49 illustrates the data obtained by outgassing a nickel sheet 3 cm. wide and 0.15 mm. thick. The composition of the evolved gases was not given.

TABLE 49. *Diffusion constants by van Liempt's method*

Temp. ° C.	Time min.	Q/Q_0	D cm.^{2} sec.$^{-1}$	Mean value of D cm.^{2} sec.$^{-1}$
700	2	0.33	4×10^{-8}	
	5	0.43	1.8×10^{-8}	2.5×10^{-8}
	10	0.50	1.8×10^{-8}	
800	1	0.41	12×10^{-8}	
	2	0.52	9.9×10^{-8}	
	10	0.70	9.4×10^{-8}	10×10^{-8}
	20	0.85	8.5×10^{-8}	
900	2	0.67	2.1×10^{-7}	
	4	0.80	2.9×10^{-7}	2.5×10^{-7}

Another method, which depends upon the time-lag in setting up the stationary state of flow through a membrane, is applicable to gas flow in metals. The first treatment was given by Daynes[26], and later extended by Barrer[27, 28, 29]. The initial concentration in the plate is C_0, and at the ingoing and outgoing surfaces, C_1 and C_2 respectively. Then if one plots the pressure on the high-vacuum side against the time, the curve takes the course shown in Fig. 79, and tends to the steady state asymptotically. In the simplest case the asymptote cuts the time-axis at the point

$$L = \frac{d^2}{D} \frac{1}{C_1 - C_2} \left[\frac{C_2}{6} + \frac{C_1}{3} - \frac{C_0}{2} \right],$$

where d is the membrane thickness. If $C_2 = 0$, $C_0 = 0$,

$$L = \frac{d^2}{6D}$$

and D may readily be calculated. This formula is applicable only if interface reactions are fast compared with the diffusion process[28,29]. When the rates of the processes
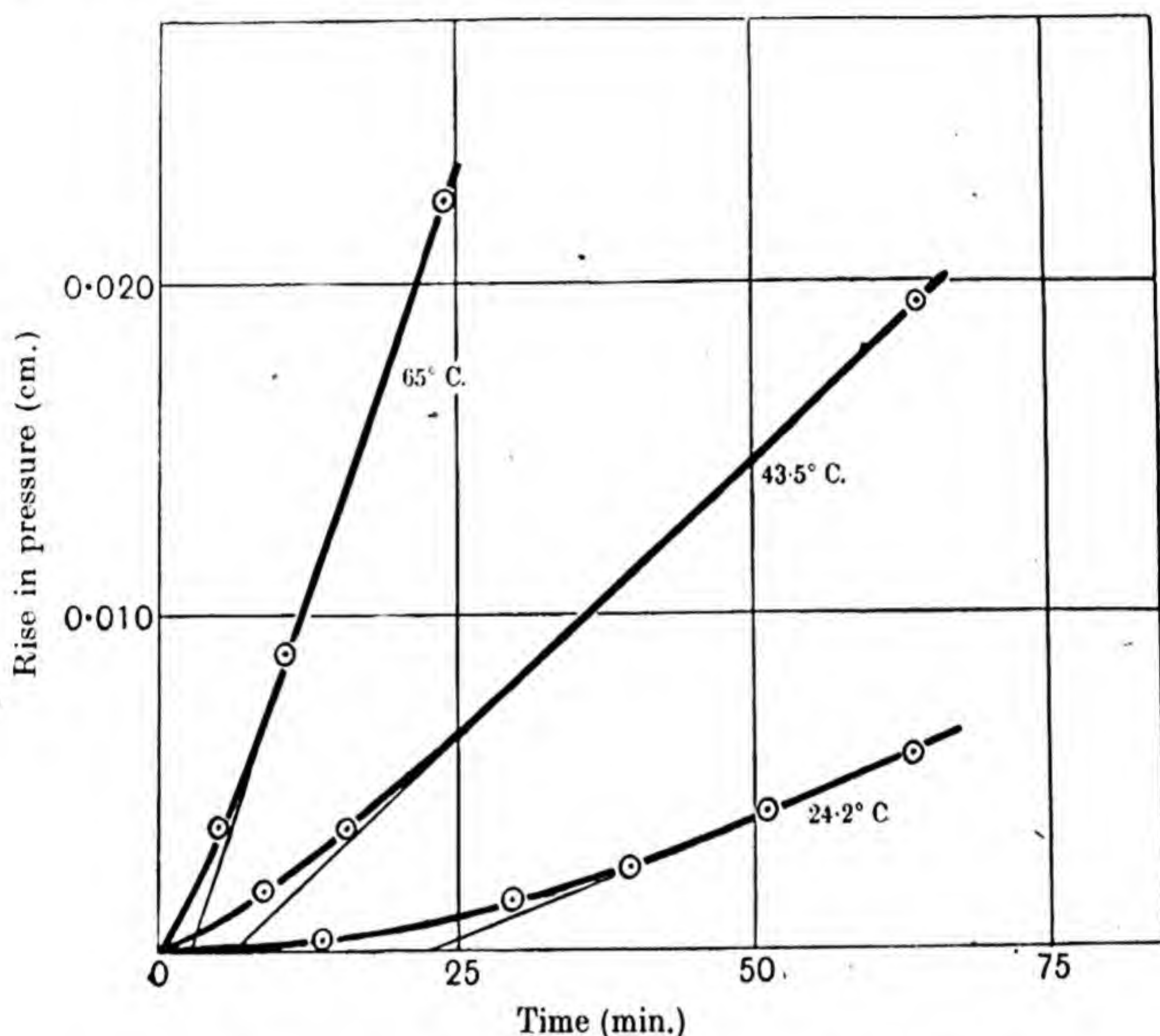
Fig. 79. Time-lag in setting up the steady state of flow of hydrogen through a palladium tube[29].

(i) passage of adsorbed atom or molecule into the metal (velocity constant k_1),

(ii) emergence of dissolved atom or molecule into the surface (velocity constant k_2)

are much smaller than D, one can see that the values of L are no longer governed by D. The value of L is a complex function of k_1 and k_2 where the process of permeation is controlled solely by these two phase-boundary reactions.

When k_1, k_2 are much greater than D, the expression for L reduces to

$$L = \frac{d^2}{6D}.$$

Thus the expression $L = d^2/6D$ gives a value of D which is more nearly equal to the real value the more the phase-boundary processes are accelerated. The method can be applied equally to the diffusion of gases through hot metals, or to the diffusion of nascent gases liberated at room temperatures by electrolysis or by chemical reaction at the metal surface.

This review of the possible ways of measuring diffusion constants in metals indicates the lines of approach which have been developed. Future work should aim at the establishment of the relative importance of phase-boundary reactions and volume diffusion; the estimation of the influence of concentration upon the diffusion "constant"; the understanding of the role of impurities and mechanical treatment; and measurements of the influence of temperature and other variables upon the diffusion constants. In this way the investigations will ultimately contribute to the problems of mobility and reaction in solids. Unfortunately there is so far a great scarcity of data.

A COMPARISON OF METHODS OF MEASURING DIFFUSION CONSTANTS

It is perhaps unfortunate that the only system for which the diffusion constant has been measured by a great many different methods is the hydrogen-palladium system, for palladium membranes have shown very capricious permeabilities (Chap IV, p. 194), and this variability seems to extend also to diffusion constants. The permeability to hydrogen of nickel membranes, on the other hand, has shown itself to be more constant, as the data of Table 42, p. 168, indicate, so that hydrogen-nickel systems might prove a better testing ground.

The published data for the diffusion constants, in the form of $\log D$ against $1/T$ curves, are shown in Fig. 80. These data are by no means concordant, and their divergences from one another may be explained in part by the difficulty of the technique employed. In part, however, differences in the properties of the palladium may be responsible, for, as Tammann and Schneider showed, the rate of absorption of hydrogen depends on the state of the metal, e.g. whether it is soft or tempered. Also one may anticipate effects due to impurities, and strongly developed grain boundaries. Duhm's[32] result ($9\cdot5 \times 10^{-5}$ cm.^{2}/sec. at room temperature) is so far away from all other published data that it has not been given in Fig. 80. The equations of the different curves in Fig. 80 are given in Table 50. The most unlikely data are in square brackets.* By drawing a straight line through the various points in Fig. 80 one may obtain a mean diffusion equation for all the different palladium samples and methods.

It is known that when a potential difference is maintained between the ends of a palladium wire charged with hydrogen, the hydrogen moves towards the negative end[21, 32]. It therefore carries a positive charge, and may move as protons. These protons are probably well screened by electrons, for their effective charge has been found to be $\frac{1}{900}$ to $\frac{1}{250}$ of its value for a free proton. Coehn and his co-workers, and also Duhm, measured the mobility of the hydrogen under an applied potential, by measuring the E.M.F. or resistance of sections of the wire after intervals of passing a current. The temperature coefficient of the mobility, U, obeyed the expression

$$U = U_0 e^{-E/RT},$$

where E was $6\cdot3$ and $4\cdot9$ k.cal. respectively by the two methods.

---

* These figures are considered doubtful not because of the value of E but of D_0. The value of D_0 is such that a different mechanism of diffusion would have to be postulated in the transition state, involving a large disturbance in the surrounding palladium lattice, and thus a large entropy of activation, or large D_0. If the diffusing particle is a proton this disturbance is most unlikely.
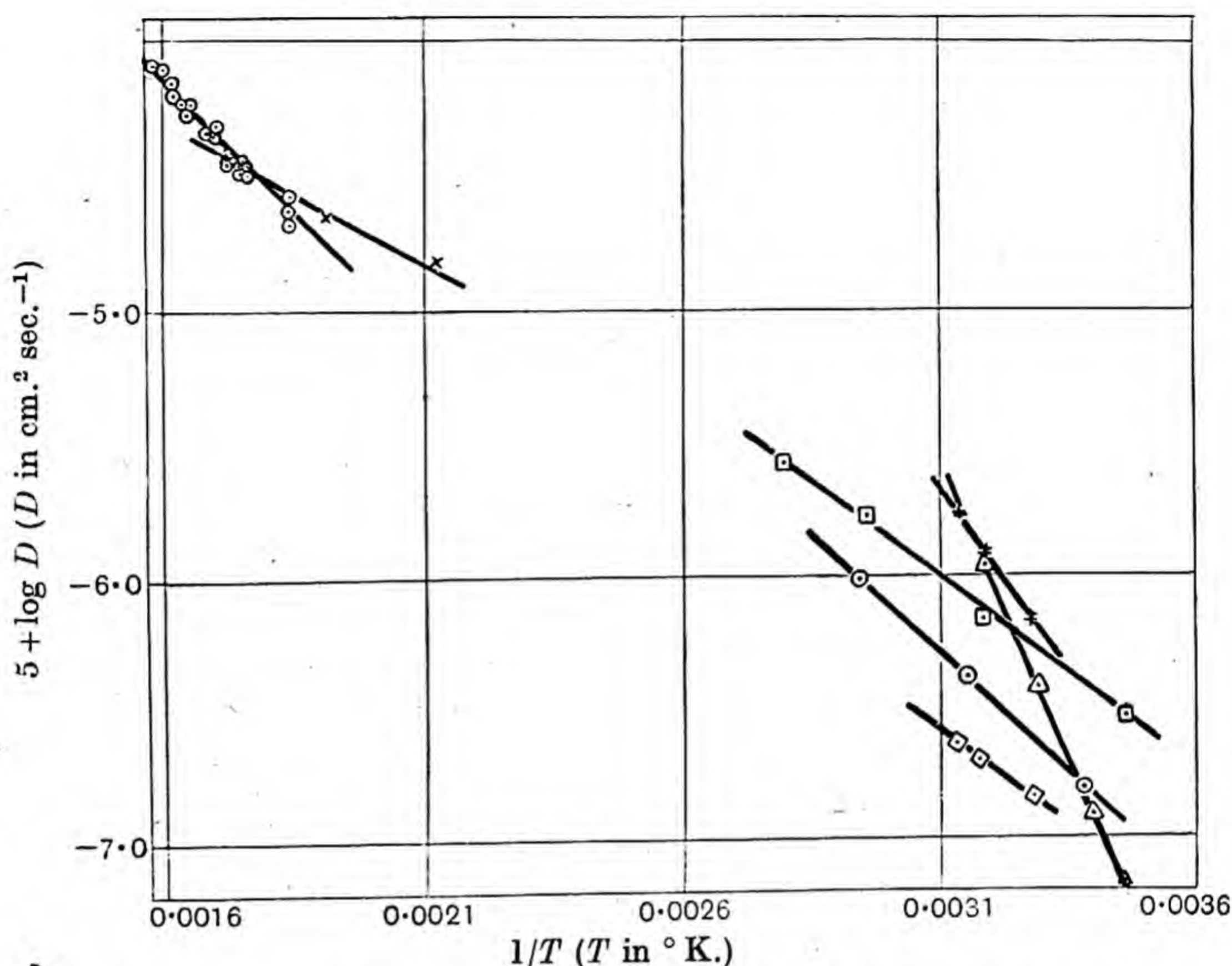
Fig. 80. Summary of data on diffusion constants of hydrogen in palladium.

⊙ = Time lag (Barrer).

× = Rate of sorption (Jost and Widmann).

▫ = Variations in E.M.F. (Coehn and Specht).

△ = Action on photographic plate (Coehn and Sperling).

* = Rate of sorption (Tammann and Schneider).

‡ = Rate of sorption (Tammann and Schneider).

TABLE 50. *The diffusion constants, D, in palladium, defined by $D = D_0 e^{-E/RT}$*

Method of measurement	Diffusion constant cm.²/sec.	Author
Time lag	$2 \cdot 5 \times 10^{-1} e^{-10100/RT}$	Barrer [29]
Rate of absorption	$5 \cdot 4 \times 10^{-3} e^{-5740/RT}$	Jost and Widmann [30]
Rate of absorption	$2 \cdot 6 \times 10^{-2} e^{-7400/RT}$*	Tammann and Schneider [31]
[Rate of absorption	$1 \cdot 07 \times 10^3 e^{-12900/RT}$†	Tammann and Schneider [31]]
E.M.F. of wire	$7 \cdot 4 \times 10^{-1} e^{-7200/RT}$	Coehn and Specht [21]
[Effect on photographic plate	$2 \cdot 5 \times 10^8 e^{-20700/RT}$	Coehn and Sperling [22]]
Mean curve from Fig. 80	$1 \cdot 5 \times 10^{-2} e^{-6800/RT}$	

* Soft.   † Tempered.

The diffusion constants of various
elements in metals

Euringer[24] employed the method described on p. 214 to interpret his results on the desorption of hydrogen from nickel. He obtained the values for $D = D_0 e^{-E/RT}$ given in Table 51. There are no data available with which to compare Euringer's measurements, since van Liempt's data (Table 49) on the outgassing of commercial nickel sheets and wires refer to a mixture of gases (H_2, CO, CO_2).

TABLE 51. *Diffusion constants* $D = D_0 e^{-E/RT}$ *of hydrogen in nickel*

Temp. °C.	D cm.^{2} sec.$^{-1}$	$D_0 e^{-E/RT}$ cm.^{2} sec.$^{-1}$	Solubility of hydrogen in nickel in c.c. at N.T.P./c.c. metal at 760 mm. pressure
165	$10 \cdot 5 \times 10^{-8}$	$2 \cdot 04 \times 10^{-3} e^{-8700/RT}$	0·192
125	$3 \cdot 4 \times 10^{-8}$		0·194
85	$1 \cdot 16 \times 10^{-8}$		0·202

Edwards'[33] measurements on the diffusion of nascent hydrogen may be interpreted by the time-lag method (p. 217) to give limiting values to the diffusion constants of hydrogen in iron. The curves of Fig. 81 show a considerable time lag in setting up the steady state permeation velocity, and by writing $D = l^2/6L$, where L is the intercept on the time axis and l the thickness of the sheet, the data of Table 52 were obtained.

Hydrogen gas may diffuse in a metallic lattice as protons, which will not greatly disturb the lattice in the act of diffusion, since the dimensions of the proton are small. When oxygen, nitrogen, phosphorus, sulphur, or carbon diffuse in solids, there will be a tendency for the diffusing particle to be negatively charged or to diffuse as an atom; its size will not therefore be less than that of the free atom, and considerable distortion may occur in solution in the lattice and in the act of diffusing.* There is therefore a tendency for compounds of these sub-

* In metals such as iron, however, the ratio $\dfrac{\text{radius of diffusing atom}}{\text{radius of iron atom}}$ is small enough for the atoms of nitrogen or carbon to exist interstitially in the iron lattice.

stances with the metal to separate out of the lattice as crystals embedded in the solid metal, or aggregated at grain boundaries (34). When elements such as sulphur diffuse in iron, the process may be regarded as the passing on of the diffusing atom by alternate dissociation and formation of sulphides,
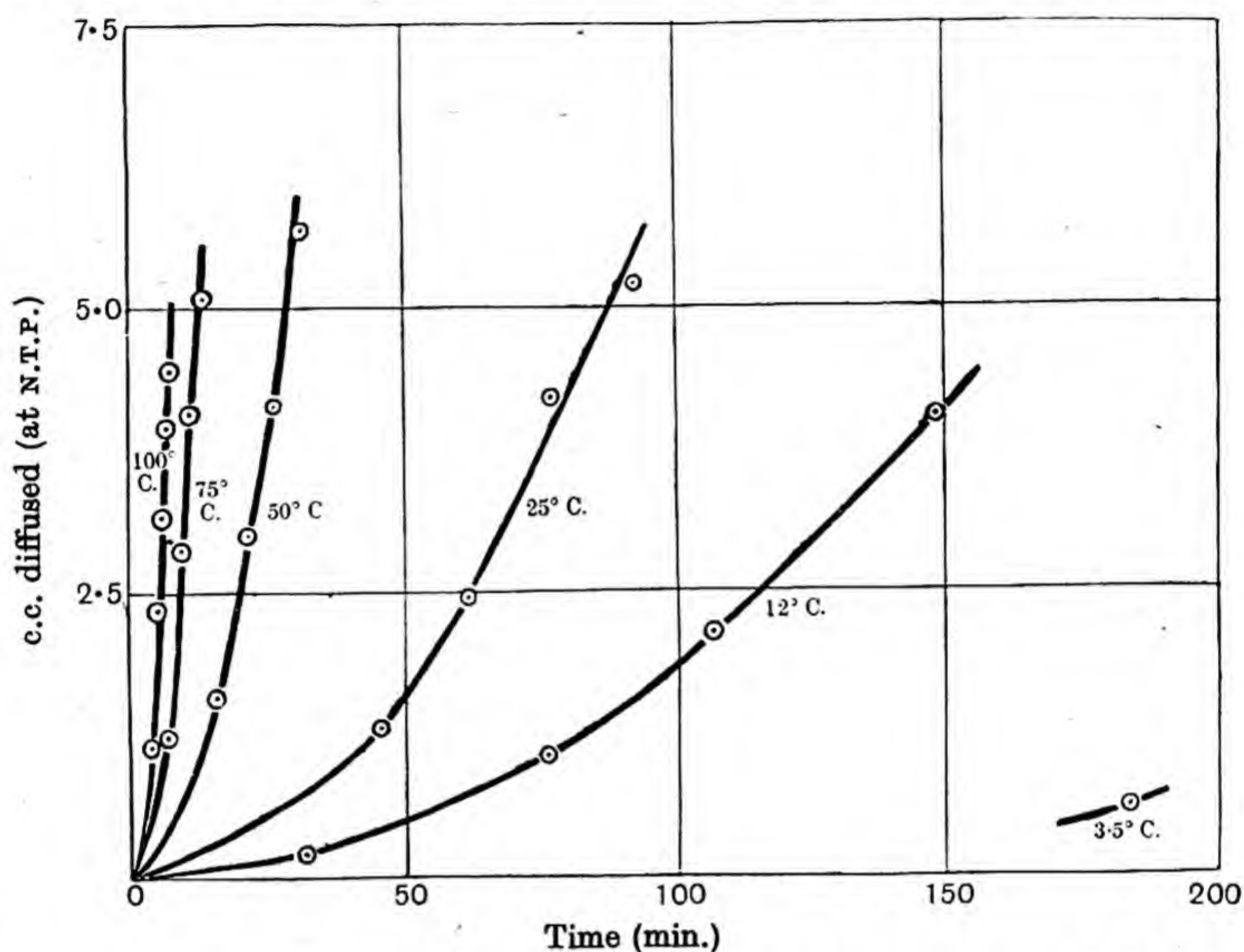
Fig. 81. Diffusion of nascent hydrogen through iron sheet (thickness 0·005 in.).

rather than as the inter-penetration of alloying metals, by place change, or as the zeolitic type of diffusion occurring when hydrogen passes into a metal as atoms or protons.

TABLE 52. *Diffusion constants of hydrogen through iron*
(H_2 *liberated by* HCl)

Temp. ° C.	Intercept L min.	$D = l^2/6L$ cm.^{2} sec.$^{-1}$	$D = D_0 e^{-E/RT}$
10	270	$1·66 \times 10^{-9}$	$1·65 \times 10^{-2} e^{-9200/RT}$
20	173	$2·59 \times 10^{-9}$	
40	67	$6·68 \times 10^{-9}$	
50	39·4	$1·14 \times 10^{-8}$	
75	15·6	$2·87 \times 10^{-8}$	
100	3·6	$1·24 \times 10^{-7}$	

TABLE 53. *Diffusion constants of carbon in iron*

Temp. °C.	Carburising mixture	$D \times 10^8$ cm.^{2} sec.$^{-1}$	Values of D (cm.^{2} sec.$^{-1}$) at 1000° C., as obtained by various authors
950	CO + xylene	7·0	$19·3 \times 10^{-7}$ [6]
	CO + toluene	9·6	$4·2, 11·2 \times 10^{-7}$ [35]
	CO + benzene	10·5	
	CO + petrol	12·0	$10·4, 12·4 \times 10^{-7}$ [36]
1000	CO + xylene	12·0	
	CO + toluene	15·0	
	CO + petrol	21·5	
1050	CO + toluene	24·0	
	CO + petrol	40·0	
1100	CO + toluene	42·0	
	CO + petrol	48·0	

The values of the diffusion constants for a number of the electro-negative elements (C, O, N, P, S) in iron are given in Tables 53 and 54. Many authors [6, 35, 36] have given figures for the diffusion constant of carbon in iron, and the diffusion has been followed by heating the metal in a variety of gaseous atmospheres [1, 2, 3, 4, 5] (p. 208, and Table 53). The diffusion constants are similar also if nitrogenous hydrocarbons replace the hydrocarbons of Table 53. In Table 54 are given the

TABLE 54. *Diffusion of various elements into steel* (D in cm.^{2} sec^{-1})

Temp. °C. ...	800	850	900	950	1000	1050	1100	1150
Diffusion system								
$D \times 10^8$ for C-Fe [1]	—	1·7	3·8	8·7	20·0	—	—	—
$D \times 10^8$ for C-Fe [1]	1·5	3·8	7·5	11·7	20·0	28	45	—
$D \times 10^8$ for N-Fe [1]	1·2	3·0	6·0	10·8	13·5	25·0	40	—
$D \times 10^{10}$ for S-Fe [5]	—	—	—	3·0	5·5	7·0	10	13
$D \times 10^9$ for P-Fe [5]	—	—	—	0·72	1·31	2·5*	—	—
$D \times 10^{10}$ for O-Fe [5]	—	—	—	—	1·0	—	—	—

* At 1040° C.

diffusion constants obtained by Bramley and his co-workers for different elements in steel at various temperatures. In considering these data it must be remembered that the diffusion constants are often very different in the presence of other

impurities in the lattice; for example, the diffusion of sulphur and phosphorus is retarded by carbon (p. 236), while the diffusion of nitrogen is accelerated by oxygen but retarded [36a] by carbon (Table 54a).

TABLE 54a. *Diffusion of N_2 in α-Fe at 550° C., as a function of the carbon content*

% C in Fe	0·01	0·06	0·54	0·82	1·40
$D \times 10^8$ cm.² sec.$^{-1}$	2·14	1·16	0·33	0·11	0·05

The data in Table 54 may be presented in the form

$$D = D_0 e^{-E/RT},$$

and the following formulae are applicable:

C-Fe: $D = 5\cdot5 \times 10^{-2} e^{-32,200/RT}$ (1); and $3\cdot5\text{--}4\cdot7 e^{-3140/RT}$ (1),

N-Fe: $D = 1\cdot07 \times 10^{-1} e^{-34,000/RT}$ (1),

S-Fe: $D = 4\cdot8 \times 10^{-6} e^{-23,400/RT}$ (5),

P-Fe: $D = 4\cdot5 \times 10^{-2} e^{-43,300/RT}$ (5).

The expressions $D = D_0 e^{-E/RT}$ are derived from data considerably less accurate for S-Fe and P-Fe than for C-Fe, N-Fe systems.

A very recent series of measurements by Wells and Mehl [36b] applied Matano's method of analysis (Chap. I, p. 47) to determine D for carbon in iron over a range of carbon concentrations of 0·1 to 1·0 % C. by weight. They found that the diffusion, which was unaffected by the grain size of the samples of iron used, followed the expression

$$D_C^{\gamma\text{-Fe}} = (0\cdot07 + 0\cdot06 \times \% \text{ C.}) \exp. \left(\frac{-32,000}{RT} \right) \text{ cm.}^2 \text{sec.}^{-1}.$$

Fig. 81a summarises all data on the diffusion of C in steel. It may be noted that the most satisfactory analysis of the experimental data is that of Wells and Mehl.

DEGASSING OF METALS

The evolution of gases from metals is a process of some technical importance. The commonest gases to be evolved are hydrogen, oxides of carbon, and nitrogen (Table 55). When
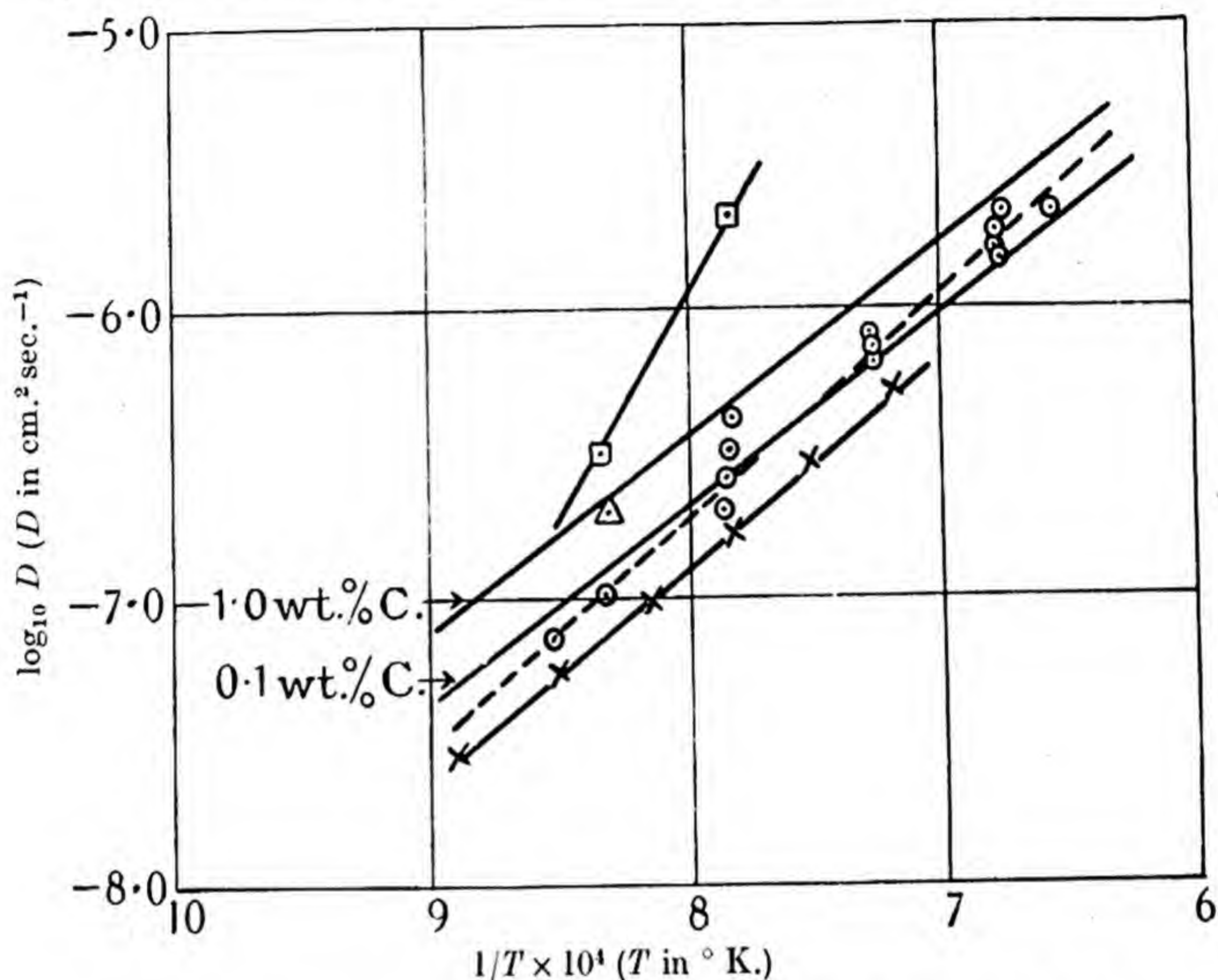
Fig. 81a. Summary of data on diffusion of carbon in iron and steel.

-□-   Tammann and Schonert (35)
———   Wells and Mehl (36b)
△   Runge (6)
.. ☉ ..   Paschke and Hauttmann (36e)
-×-   Bramley and Allen (36d)

the metalloid, graphite, for example, is degassed (37) the composition of the evolved gas alters with the period of heating, and the evolution of gas is more rapid the smaller and less perfect the component crystallites, so that charcoals more readily evolve gases than graphite. It is very difficult indeed to remove the last traces of gas from carbon, the general behaviour being that at a given temperature a state is reached where no appreciable gas evolution occurs, but as soon as the temperature is raised again a fresh burst of gas is obtained.

TABLE 55. *Gases evolved in heating metals*

Metal	Temp. °C.	Gases evolved	Remarks
Mo [38]	>1000 1000 >1200	Mainly H_2 CO, CO_2, and H_2 Oxides of carbon and N_2	Amounts of gas slight by 1760° C.
W [38]	≤2430	H_2, CO, CO_2, N_2	No further gas evolved after outgassing at 2430° C. Amounts of gas relatively small by 1760° C.
C [38]	1300 1600 1900 2110	H_2 (52%) CO (44%) CO_2 (4%) H_2 (30%) CO (48%) CO_2 (6%) N_2 (16%) H_2 (11%) CO (13%) CO_2 (5%) N_2 (71%) CO (9%) CO_2 (4%) N_2 (87%)	Graphite (tungar anode) could be freed of gas completely by prolonged heating to 2150° C.
Fe [39]		H_2, oxides of carbon, nitrogen	Guillet and Roux [39] found 30 c.c./100 g. metal
Zn [40]		Almost pure H_2 from electrode-deposited Zn	
Ni [38, 41]	 750 850 950 1050 1150	CO, H_2, and CO_2 CO_2 (12%) CO (54%) H_2 (34%) CO_2 (7·7%) CO (84·6%) H_2 (7·7%) CO_2 (5%) CO (90%) H_2 (5%) CO_2 (9·5%) CO (84·8%) H_2 (5·7%) CO_2 (11%) CO (48%) H_2 (41%)	As much as 100 c.c./100 g. Mainly CO for Mond nickel, and mainly H_2 for electrode deposited nickel Total 0·67 c.c. in 20 min. (from 100 g. metal) Total 0·39 c.c. in 20 min. Total 0·60 c.c. in 20 min. Total 0·53 c.c. in 20 min. Total 0·27 c.c. in 20 min.
Al [42, 43]		CO, H_2, CH_4	Quantities from 2 to 30 c.c./100 g. reported. Solubility of gases in aluminium small, and therefore gases evolved and retained in pinholes. Hydrogen occluded as a result of the action of water upon aluminium
Cu [43]		SO_2 (60%) CO (20%) H_2 (14%)	Total gas extracted 2 c.c./100 g.

These characteristics of graphite filaments are common to all metal filaments, and it is also usual to find that if the filament is degassed at a high temperature and cooled in vacuum to room temperature it remains free of gas at this temperature for a long period. This is the result of the high temperature coefficient of the diffusion constant. The data in Table 55 give some typical results on the degassing of metals. The composition of the evolved gases, besides depending upon the time of heating and the temperature, depends also upon the nature of the metallurgical process by which the metal has been obtained. Therefore the data in this table are by no means comprehensive, and are intended only to give some typical experiments on degassing. In addition to considering the effects of time of heating and temperature upon the gas evolution, one may also have to consider the place of origin of the gas. Eltzin and Jewlew [37] considered the gases evolved from graphite to be different in composition according as they were evolved from the "surface" of the filament, or from the "interior" of the filament,* their analysis giving:

Surface CO_2 34 %   Interior   CO   68 %
           CO   58 % N_2 32 %
           N_2 8 %

It is interesting to find nitrogen among the products evolved from graphite, for its presence as a stable compound in the lattice may mean that it replaces carbon atoms in the edges of graphite laminae, or is firmly attached to peripheral carbon atoms in the laminae.

Kinetic studies of the evolution of gases from metals have been made which indicate that the processes involved are often true diffusions. The evolution of carbon monoxide from nickel wires [41] shows that the curve log (gas evolved) against time has the typical shape associated with a diffusion process (Chap. I, Fig. 7), and from this curve the diffusion constants

* Their concept of "surface" and "interior" is however rather vague. They considered the first gases evolved to come from the surface, and subsequent gases to come from the interior.

may be calculated. The method which van Liempt [25] applied (p. 215) to measure the mean diffusion constant of gases from commercial nickel should give comparable constants, since the main gas evolved is carbon monoxide. Some of these diffusion constants are given in Table 56, from which it is evident that the two methods agree in order of magnitude only. Van Liempt also calculated "diffusion" constants for the outgassing of molybdenum wire, obtaining a mean value of $7 \cdot 6 \times 10^{-9}$ cm.^{2} sec.$^{-1}$ at 900° C.

TABLE 56. *Diffusion constants of* CO *in nickel*

Author	Form of nickel	Diffusion constant cm.^{2} sec.$^{-1}$	Temp. ° C.
Smithells and Ransley [41]	Wire	$4 \cdot 0 \times 10^{-8}$	950
		$14 \cdot 0 \times 10^{-8}$	1050
van Liempt [25]	Thin sheet	$2 \cdot 5 \times 10^{-8}$	700
		$9 \cdot 9 \times 10^{-8}$	800
		$2 \cdot 1 \times 10^{-7}$	900
(Using Smithells and Ransley's data)	Wire	Final 14×10^{-7}	1050
		Initial 91×10^{-7}	
		Mean 6×10^{-8}	950

Filaments glowed in gas atmospheres will frequently absorb the gas, by reactions which are in part chemical and in part processes of diffusion. Tantalum [44] absorbs nitrogen slowly at 1300° C. and rapidly at 1800° C.; while oxygen is taken up at 730° C. and rapidly at 1500° C. Tantalum will also decompose hydrocarbon vapours at high temperatures, the carbon diffusing into the filament (from 1700 to 2500° C.) with the formation of carbides, while evacuation at 2200° C. causes the carbon to evaporate again from the metal until only pure tantalum remains. Similarly, nitrogen [38] can be absorbed by molybdenum wire, setting up an equilibrium whose temperature variation implies a heat of 38,500 cal./mol., while the rate of establishment of the equilibrium involves an apparent activation energy of 26,600 cal. The analogous tungsten nitride could also be formed. Another type of filament-gas reaction may also be found in which the metal filament

evaporates and the condensing metal combines with or adsorbs an otherwise inert gas. In this way metal filaments may be used in the clean-up of residual gas [45].

DIFFUSION AND ABSORPTION OF GASES IN
FINELY DIVIDED METALS

When a gas is allowed to come into contact with a thoroughly outgassed finely divided metal, there may take place an instantaneous adsorption and one or more slow processes.

TABLE 57. *Some data on the sorption of gases by finely divided metals*

System	Behaviour
H_2, D_2-Cu [46]	$-78°$ C. rapid initial and slow subsequent sorption. $0°$ C. amount taken up by slow sorption increased
H_2-Cu [47]	Initial rapid sorption and slow subsequent sorption at all temperatures studied
H_2-Cu [48]	Slow process observed
H_2, D_2-Ni [49]	Two processes, fast and slow. H_2 more rapidly sorbed than D_2
H_2-Ni [50]	One and possibly two slow processes observed
H_2-Ni [51]	Slow process observed
H_2-Fe [52]	One rapid sorption process and two slow ones suggested
H_2-Fe [53]	$-190°$ C., van der Waals' sorption. Above $0°$ C. two slow processes suggested
N_2-Fe, Al_2O_3 [54] N_2-Fe, Fe-Al_2O_3, K_2O	Slow uptake of nitrogen by iron, as well as initial rapid sorption
O_2-Ag [55]	Slow uptake of oxygen by silver, as well as initial rapid sorption

The nature of the slow uptake of gas has been the cause of considerable discussion. The general similarity of the phenomena observed for a number of sorption systems is illustrated in the summarising data of Table 57. In all the cases given, at least two processes have been established. The initial rapid process is correctly associated with the van der Waals' adsorption on the surface, and it might be anticipated that the slow process was the solution of the gas in the metallic lattice, either forming an alloy (H_2) or a compound (N_2) with the metal. However, the behaviour is not necessarily

so easily explained, for not only do some authors describe two slow processes, but in a large number of studies of sorption very similar slow processes have been observed
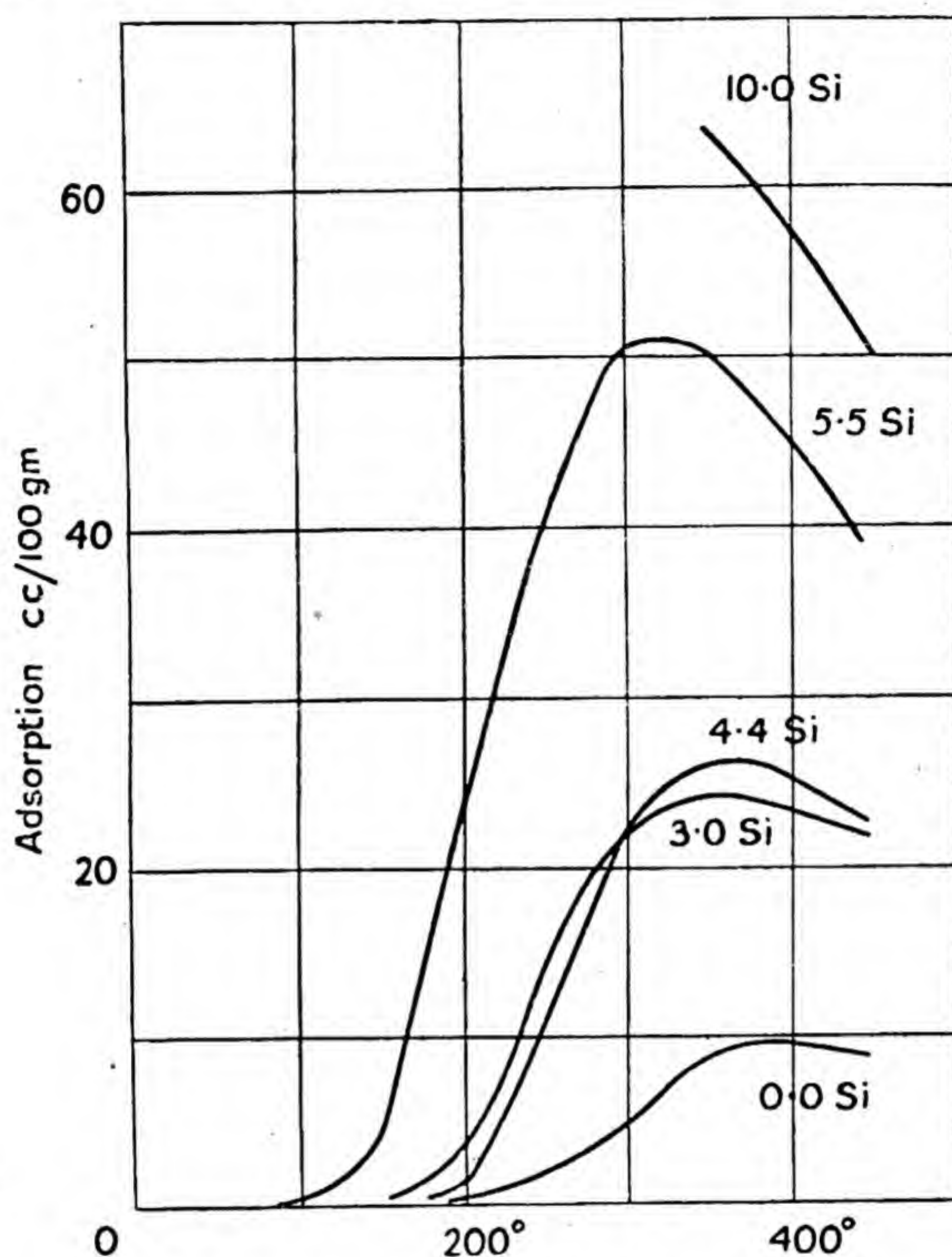
Fig. 82. Sorption of hydrogen by Mo-Si catalysts.

where solution is not probable. Among these systems are the following:

H_2, D_2-Cr_2O_3 [57, 58],

H_2-Cr_2O_3, ZnO [56],

O_2-$CuCr_2O_4$, $ZnCr_2O_4$, $CoCr_2O_4$, $NiCr_2O_4$, $BeCr_2O_4$ [59],

H_2-MoO_3, SiO_2 [60],

H_2-C (Charcoal [61], Graphite [62], and Diamond [63]),

CH_4-C [61],

C_2H_4-Ni [64].

All these systems give the characteristic high-temperature isobar illustrated in Fig. 82, in which at first the amount sorbed increases with rising temperature, and then decreases. It is considered that the rising part of the isobar denotes a non-equilibrium condition, but that the falling part is reversible for such systems as H_2-C, H_2-ZnO.Cr_2O_3. In other cases, however, no part of the curve denotes a reversible equilibrium (CH_4-C; C_2H_4-Ni). It is also a characteristic of these reversible and irreversible chemical sorptions that the velocity of sorption increases exponentially with temperature, and from this increase in sorption velocity an apparent energy of activation may be calculated, whose magnitude is that of ordinary chemical reactions or of activated diffusions. The apparent energy of activation increases with the amount of gas sorbed, and so the sorption velocity decreases strongly as the charge of gas is increased. This means that at low temperatures one will not get saturation of the available surfaces in any finite time.

Now one may compare these properties with those noted in the processes of slow sorption of gases by finely divided metals. Once more one finds high temperature isobars in which the amount sorbed at first increases with rising temperature and then decreases (Fig. 83). The decreasing part of the isobar is reversible, and the increasing part is irreversible. The velocity of sorption increases strongly as the temperature rises, and an apparent energy of activation is observed. Once again the irreversible part of the isobar may be interpreted as due to variable apparent activation energies which increase with gas charge, so that at low temperatures the velocity of sorption is so diminished that the available sorption volume is not saturated in any finite time.

It seems therefore that activated diffusion into the bulk of a metal and reversible chemical adsorption (called by H. S. Taylor[65] activated adsorption) may be similar in their observable properties. Indeed there has been considerable argument as to whether reversible chemical adsorptions may not be activated diffusions, and vice versa. The situation is

clarified by the proof that activated diffusion processes into solids (e.g. H_2-Pd (30)) can occur to give, eventually, homogeneous solutions; but that reversible chemical adsorptions which do not involve inter- or intra-lattice diffusion also occur (e.g. H_2-C (61, 62, 63)). There is no need to strain either the hypothesis of activated diffusion or of activated adsorption to include *all* the features observed in considering gas-solid
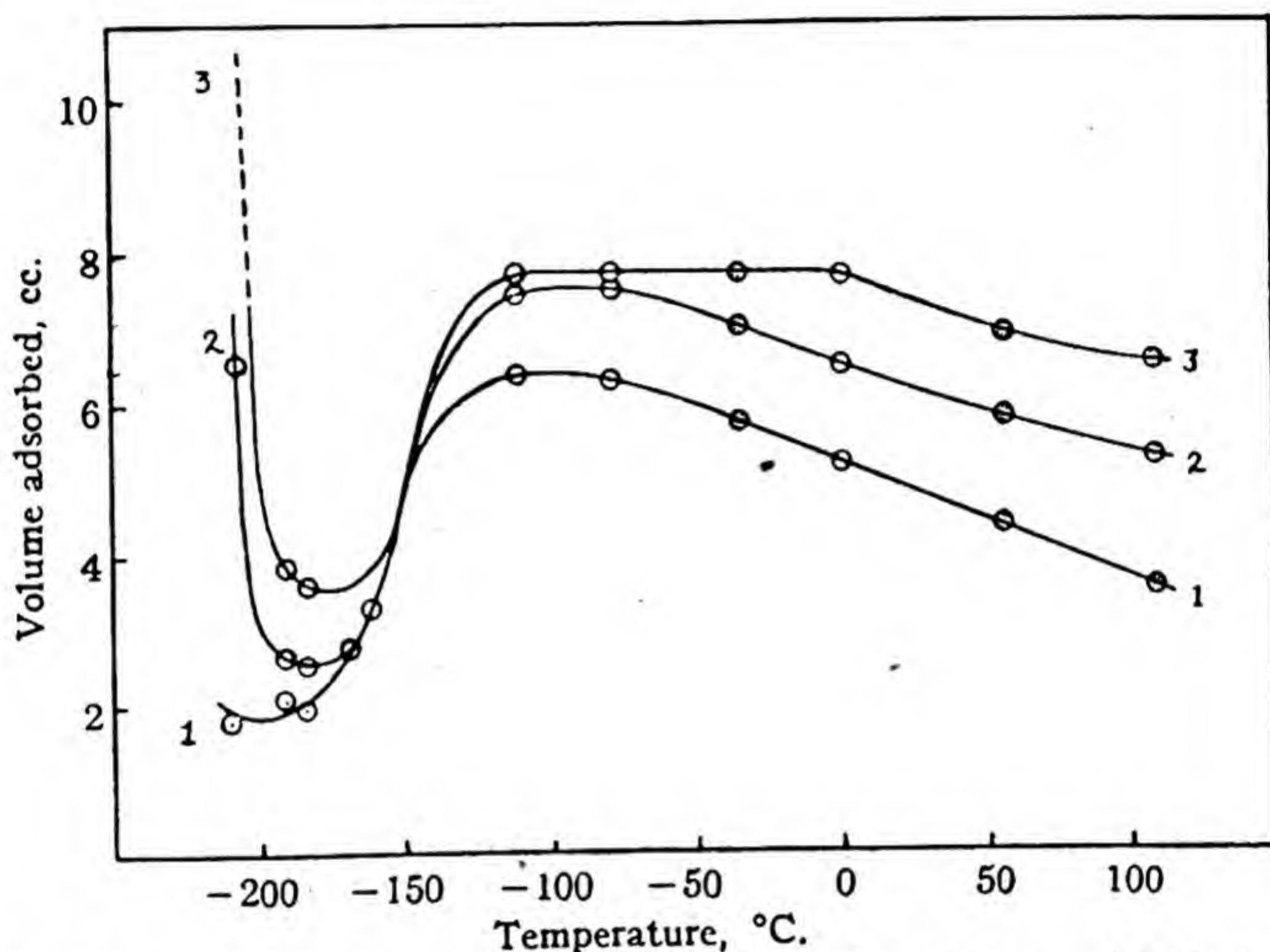
Fig. 83. Sorption isobars of hydrogen on nickel, showing low and high temperature sorption. Curve 1, 2·5 cm. pressure; curve 2, 20 cm. pressure; curve 3, 60 cm. pressure.

systems. In those cases where two slow processes of sorption of hydrogen by metals have been postulated, it may be that a slow chemical adsorption process occurs at the surface, followed by a slow absorption process by the metal. The adsorption process can be either on the metal surface itself, or as seems likely under some experimental conditions, it may be a chemical adsorption of the hydrogen by an oxide monolayer.

One of the few quantitative analyses of sorption kinetics in gas metal systems was made by Ward (47), who after heating and evacuating finely divided copper in hydrogen a number of times, concluded that he was measuring an activated diffusion

process, and analysed the data on the rate of sorption by means of Fick's law. In accordance with this law, for small values of the time, t, Ward found that Q, the quantity of hydrogen absorbed, was proportional to $\sqrt{t}$. If n_0 denotes the concentration in the adsorbed film of gas from which solution in the metal occurs, one should have, from Lennard-Jones' [66] analysis of this problem,

$$Q \propto n_0 e^{E/RT} \sqrt{t},$$

and so by plotting $\dfrac{Q}{n_0 \sqrt{t}}$ against $\dfrac{1}{T}$ one may measure the activation energy for the solution process. The figure obtained was

$$E = 14,100 \, \text{cal./g. atom},$$

which may be compared with the temperature coefficients for the permeability of copper to hydrogen of 18,700 and 16,600 cal. (Chap. IV, p. 168).

THE INFLUENCE OF IMPURITY UPON DIFFUSION CONSTANTS

It has been observed that the presence of carbon in nickel decreases the permeability of nickel towards hydrogen below 700° C., but above this temperature increases the permeability [67, 68]. Also in steel it is very important to know the effects which various possible impurities (O, N, S, P, C, Si) have upon the permeability and diffusion velocity of other elements in the steel. While few experiments have been made on the permeability, the diffusion velocity within the material has been very thoroughly studied by Bramley and his co-workers [1, 2, 3, 4, 5]. Ham and Sauter [69] showed that nitriding the surface of steel increased its hydrogen permeability 10–15 times, and that the original permeability was restored after out-gassing the metal. Bramley and his co-workers found that the nitriding of a steel rod was accelerated by the presence of small amounts of oxygen in the metal, as the following data indicate (Table 58). The nitriding process occurs

on heating in an atmosphere of ammonia, and the processes taking place may be visualised as

$$4Fe + 2NH_3 \rightarrow 2Fe_2N + 3H_2,$$

$$2Fe_2N \rightarrow 2Fe_2N \text{ (dissolved)},$$

$$Fe_2N \rightleftharpoons 2Fe + N \text{ (dissolved)}.$$
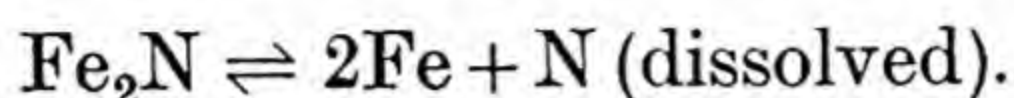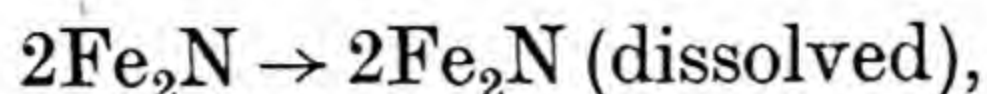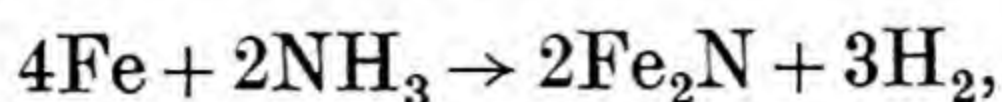
The role of the oxygen or oxide may be to fix the nitrogen atoms as oxides of nitrogen, which prevents the formation and subsequent evolution of molecular nitrogen. These two

TABLE 58. *Nitriding after various treatments, involving solution or removal of oxygen*

Condition of Fe before nitriding	Diffusion constant for $N_2 \times 10^8$
Swedish Fe, heated 200 hr. at 1050° C. in dry H_2	1·8
Swedish Fe, in original state	2·1
Swedish Fe, in original state oxidised in $CO\text{-}CO_2$ (75–25%) for 30 hr.	2·5
Armco Fe, in original state	2·6
Swedish Fe, oxidised for 100 hr. in malleabilising furnace at 1000° C.	2·9
Swedish Fe, oxidised for 200 hr. in malleabilising furnace at 1000° C.	3·5

systems (H_2 diffusing in nitrided Fe; and N_2 diffusing in oxidised Fe) are the only ones where acceleration occurs. More usually one finds a retardation, as for instance when sulphur diffuses through steel of increasing carbon content. Fig. 84 shows how the diffusion constant decreases with the percentage of carbon and is nearly inhibited by a large quantity of this element. Analogous experiments were made by heating a mixture of toluene and carbon bi-sulphide in contact with steel. The shape of the curves was attributed to a de-sulphurisation brought about by the hydrogen liberated from the toluene. However, the analysis of the deepest part of the curves led to the conclusion that the diffusion constant of the carbon was decreased by increasing the sulphur content, while the diffusion constant for sulphur was decreased by increasing the carbon content.

The last of this series of experiments was a study of the phosphorisation of steels. Phosphorisation occurred on heating the steel sample in a hydrogen-phosphine mixture, and concentration gradients of phosphorus into the metal were established. It was found on analysing the concentration-distance curves that carbon retarded the diffusion of phosphorus very strongly, and that phosphorus entering the metal swept the carbon in front of it.
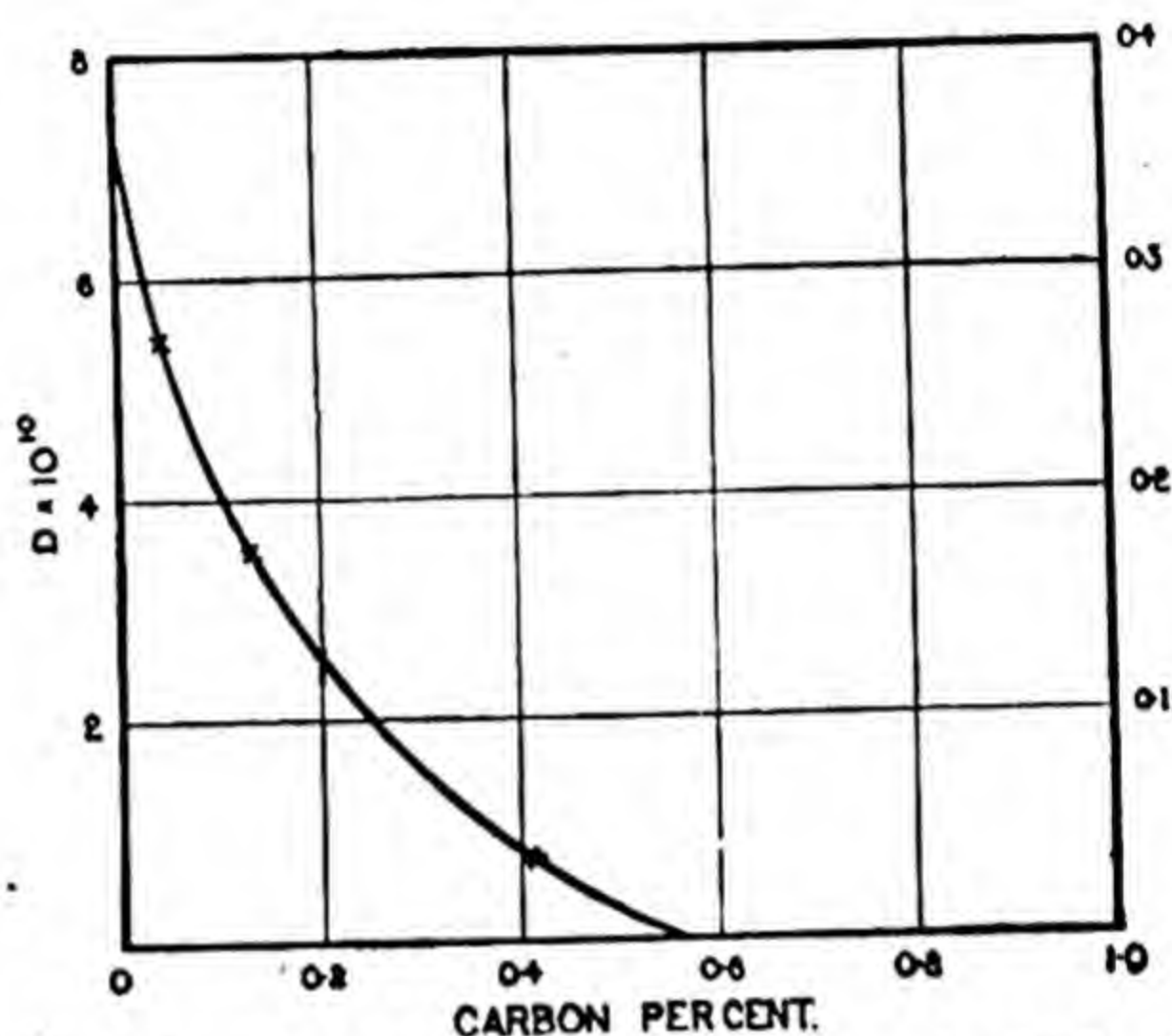
Fig. 84. The decrease in the diffusion constant of sulphur in steels as the carbon content increases.

REFERENCES

(1) Bramley, A. and Jinkings, A. *Carnegie Schol. Mem.*, Iron and Steel Institute, **15**, 17 (1926).

Bramley, A. and Beeby, G. *Carnegie Schol. Mem.*, Iron and Steel Institute, **15**, 71 (1926).

Bramley, A. and Jinkings, A. *Carnegie Schol. Mem.*, Iron and Steel Institute, **15**, 127 (1926).

Bramley, A. *Carnegie Schol. Mem.*, Iron and Steel Institute, **15**, 155 (1926).

(2) Bramley, A. and Lawton, G. *Carnegie Schol. Mem.*, Iron and Steel Institute, **15**, 35 (1927).

(3) Bramley, A. and Turner, G. *Carnegie Schol. Mem.*, Iron and Steel Institute, **17**, 23 (1928).

(4) Bramley, A. and Lord, H. *Carnegie Schol. Mem.*, Iron and Steel Institute, **18**, 1 (1929).

(5) Bramley, A., Heywood, F., Cooper, A. and Watts, J. *Trans. Faraday Soc.* **31**, 707 (1935).

(6) Runge, B. *Z. anorg. Chem.* **115**, 293 (1921).

(7) Hanawalt, J. D. *Phys. Rev.* **33**, 444 (1929).

(8) Linde, J. and Borelius, G. *Ann. Phys., Lpz.*, **84**, 747 (1927).

(9) Kruger, F. and Gehm, G. *Ann. Phys., Lpz.*, **16**, 174 (1933).

(10) Owen, E. A. and Jones, J. *Proc. phys. Soc.* **49**, 587 (1937).

(11) Hägg, G. *Z. phys. Chem.* **7**B, 339 (1930).

(12) —— *Z. phys. Chem.* **4**B, 346 (1929).

(13) Meyer, L. *Z. phys. Chem.* **17**B, 385 (1932).

(14) Wagner, C. *Z. phys. Chem.* **159**A, 459 (1932).

(15) Sieverts, A. and Hagen, H. *Z. phys. Chem.* **174**A, 247 (1935).

(16) Coehn, A. and Jürgens, H. *Z. Phys.* **71**, 179 (1931).

(17) Dunwald, H. and Wagner, C. *Z. phys. Chem.* **22**B, 212 (1933).

(18) v. Baumbach, H. and Wagner, C. *Z. phys. Chem.* **24**B, 59 (1934).

(19) de Boer, J. H. and Fast, J. *Rec. Trav. chim. Pays-Bas,* **55**, 459 (1936).

(20) Sieverts, A. and Brüning, K. *Z. phys. Chem.* **174**A, 365 (1935).

(21) Coehn, A. and Specht, W. *Z. Phys.* **62**, 1 (1930).

(22) Coehn, A. and Sperling, K. *Z. Phys.* **83**, 291 (1933).

(23) Franzini, T. *R.C. Ist. Lombardo,* [2] **66**, 105 (1933).

(24) Euringer, G. *Z. Phys.* **96**, 37 (1935).

(25) van Liempt, J. *Rec. Trav. chim. Pays-Bas,* **57**, 871 (1938).

(26) Daynes, H. *Proc. Roy. Soc.* **97**A, 286 (1920).

(27) Barrer, R. M. *Trans. Faraday Soc.* **35**, 628 (1939).

(28) —— *Phil. Mag.* **28**, 148 (1939).

(29) —— To be published.

(30) Jost, W. and Widmann, A. *Z. phys. Chem.* **29**B, 247 (1935).

(31) Tammann, G. and Schneider, J. *Z. anorg. Chem.* **172**, 43 (1928).

(32) Duhm, B. *Z. Phys.* **94**, 34 (1935).

(33) Edwards, C. A. *J. Iron and Steel Inst.* **60**, 9 (1924).

(34) Smithells, C. *Gases and Metals,* p. 173 (1937), Figs. 120, 121.

(35) Tammann, G. and Schonert, K. *Stahl u. Eisen, Düsseldorf,* **42**, 654 (1922).

(36) Calculated by Runge[6] from observations of Giolotti and co-workers.

(36*a*) Eilender, W. and Meyer, O. *Arch. Eisenhüttenw.* **4**, 343 (1931).

(36*b*) Wells, C. and Mehl, R. *Metals Technol. A.I.M.E.* 1940, Tech. Publ. No. 1180.

(36*c*) Paschke, M. and Hauttmann, A. *Arch. Eisenhütt.* **9**, 305 (1935–6).

(36*d*) Bramley, A. and Allen, K. *Engineering,* 11 March 1932.

(37) E.g. Eltzin, I. and Jewlew, A. *Phys. Z. Sowjet.* **5**, 687 (1934).

(38) Norton, A. and Marshall, F. *Trans. Amer. Inst. min. (metall.) Engrs,* Feb. 1932.

(39) Guillet, L. and Roux, A. *Rev. Métall.* **26**, 1 (1929).

(40) Röntgen, P. and Möller, H. *Metallwirtschaft,* **11**, 685 (1932). Burmeister, W. and Schloetter, M. *Metallwirtschaft,* **13**, 115 (1934).

(41) Smithells, C. and Ransley, C. J. *Proc. Roy. Soc.* **155**A, 195 (1936).

(42) Villachon, A. and Chaudron, G. *C.R. Acad. Sci., Paris,* **189**, 324 (1929).

(43) Hessenbruch, W. *Z. Metallk.* **21**, 46 (1929).

(44) Andrews, M. *J. Amer. chem. Soc.* **54**, 1845 (1932).

(45) E.g. Bryce, G. *J. chem. Soc.* p. 1513 (1936).

(46) Beebe, R., Low, G., Wildner, E. and Goldwasser, S. *J. Amer. chem. Soc.* **57**, 2527 (1935).

(47) Ward, A. F. *Proc. Roy. Soc.* **133** A, 506, 522 (1931).

(48) Leypunsky, O. *Acta phys.-chim. U.R.S.S.* **2**, 737 (1935).

(49) Magnus, A. and Sartori, G. *Z. phys. Chem.* **175** A, 329 (1936).

(50) Iijima, S. *Sci. Pap. Inst. phys. chem. Res., Tokyo*, **23**, 164 (1934).

(51) Benton, A. and White, T. *J. Amer. chem. Soc.* **52**, 2325 (1930).

(52) Harkness, R. and Emmett, P. *J. Amer. chem. Soc.* **56**, 490 (1934).

(53) Morosov, N. M. *Trans. Faraday Soc.* **31**, 659 (1935).

(54) Hammett, P. and Brunauer, S. *J. Amer. chem. Soc.* **56**, 35 (1934).

(55) E.g. Benton, A. and Elgin, J. *J. Amer. chem. Soc.* **51**, 7 (1929).

(56) Pace, J. and Taylor, H. S. *J. chem. Phys.* **2**, 573 (1934).

(57) Taylor, H. S. and Diamond, H. *J. Amer. chem. Soc.* **56**, 1821 (1934).

(58) Kohlschütter, H. *Z. phys. Chem.* **170** A, 300 (1934).

(59) Frazer, J. and Heard, L. *J. phys. Chem.* **42**, 855 (1938).

(60) Griffith, R. and Hill, S. *Proc. Roy. Soc.* **148** A, 195 (1935).
Hollings, H., Griffith, R. and Bruce, R. *Proc. Roy. Soc.* **148** A, 186 (1935).

(61) Barrer, R. *Proc. Roy. Soc.* **149** A, 231 (1935).

(62) —— *Trans. Faraday Soc.* **32**, 481 (1936).

(63) —— *J. chem. Soc.* p. 1256 (1936).

(64) Steacie, E. and Stovel, H. *J. chem. Phys.* **2**, 581 (1934).

(65) Taylor, H. S. *J. Amer. chem. Soc.* **53**, 578 (1931).
—— *Trans. Faraday Soc.* **28**, 131 (1932).

(66) Lennard-Jones, J. *Trans. Faraday Soc.* **28**, 333 (1932).

(67) Lewkonja, G. and Baukloh, W. *Z. Metallk.* **25**, 309 (1933).

(68) Baukloh, W. and Guthmann, H. *Z. Metallk.* **28**, 34 (1936).

(69) Ham, W. and Sauter, J. *Phys. Rev.* **47**, 337 (1935).

CHAPTER VI

DIFFUSION OF IONS IN IONIC CRYSTALS AND THE INTERDIFFUSION OF METALS

INTRODUCTION AND EXPERIMENTAL

The study of the interdiffusion of solids probably begins with the empirical facts of carburisation of steel, an art many centuries old. That solid metals will interdiffuse was early observed[1]; but the velocity of this interdiffusion was not realised until the quantitative measurements of Roberts-Austen[2] revealed that at 300° C. gold would diffuse through lead faster than sodium chloride would diffuse through water at 18° C. The first alloys were prepared by Faraday and Stodart[3] in 1820, by heating together mixtures of metal powders. It is interesting to find that this original method is employed today[4, 5] for the preparation of special alloys[6, 7]. One may also trace, from early studies of carburisation of steel[8, 9], and with increasing research on intermetallic diffusion, the development of nitriding, chromizing, calorizing, sherardizing, and siliconizing, and the formation of bi-metal strip and veneer metals[10, 11]. The processes of homogenisation of segregated alloys, rates of transformation in metals, and of precipitation of crystals in solids (e.g. Fe_3N in Fe), are all closely connected with processes of diffusion in solids. One may see therefore the technical importance of a knowledge of the laws governing intermetallic diffusion. The subject has not yet reached a completeness in itself or in relation to cognate topics such as the diffusion of gases in metals (Chaps. IV and V) or of ions in ionic lattices. Since the diffusion usually occurs in the lattices of the solids, it is likely to yield much information on the physics of crystals, and phenomena such as annealing, age-hardening, plasticity, recrystallisation, and order-disorder transformations in alloys.

The problem of diffusion in ionic lattices has been studied principally by the indirect method of measuring the conductivity of the crystal. Some of the earliest measurements of conductivity in solids are due to Faraday [12]. The study of conductivity in electrolytes has been developed along three main lines:

(1) The movement of ions in ionic lattices.

(2) The movement of ions in molten ionic liquids (e.g. molten $NaCl$).

(3) The movements of ions in solution.

While we are not concerned with (2) and (3), it is interesting to note that the conductivity of silver halides shows no discontinuous jump on passing from the solid to the liquid state [13, 14], although it is more usual to find discontinuities whenever a phase change occurs (KI [14], $HgCu_2I_4$ [15], HgI_2 [16]). Early measurements upon the conductivity of solid oxides [17, 18, 19] showed that the current carriers were ions, and also led to the development of the Nernst lamp, using a filament of zirconia, with thoria and rare earths. One of the earliest observations upon the increase of conductivity of microcrystalline salts under pressure was made by Graetz [20], and upon photoconductivity by Arrhenius [21], who noted that the conductivity of silver chloride and bromide was altered by light. The modern developments of the subject we owe especially to von Hevesy, Seith, Jost, Wagner, and Tubandt.

Application of the mobility of hydrogen or sodium ions in glass is made in the glass electrode, or the preparation of pure sodium by electrolysing sodium ions from molten sodium nitrate through glass. Processes of base exchange in zeolites (as in water softening by "permutit"), or even in clays, must occur in part by diffusion of ions down concentration gradients in the individual crystallites composing the mass. Zeolites contain large interstitial channels down which such a diffusion is possible.

The determination of diffusion constants in metals may be made by a number of rather special experimental techniques,

only some of which permit the whole concentration gradient to be measured. Dunn [22] followed the diffusion of zinc from α-brass by vaporising the zinc *in vacuo*, and measuring the loss in weight of the sample. This method involves the assumption that the concentration of zinc at the outgoing surface is zero and, like all methods of averaging, does not easily show whether the diffusion "constant" depends on the concentration. Another method of averaging has been employed to find the rate of diffusion of carbon and nitrogen in iron [23]. The diffusing element is removed as a gas (CO, or N_2) as soon as it reaches the surface A similar method [24] was used to measure the diffusion rate of oxygen in γ-iron, the oxygen being removed at the surface by hydrogen. If the metal is in the form of wires, the electrical conductivity may be used to give the average composition of the wire [25, 26, 27] The method has proved successful for hydrogen-palladium, carbon-tantalum, and other systems. The lattice parameter, in a few cases [28], undergoes a steady change as the concentration increases, and this change may be employed to find the mean concentration.

When it is desired to find the actual concentration gradient, one may use several methods. The first, used by Bramley and his co-workers [23] to measure diffusion coefficients in iron, is to heat the metal with the diffusing substance, and to remove and analyse chemically thin layers at that interface from which diffusion proceeded. Other methods of analysis are available besides chemical ones. The shavings may be examined by means of an X-ray camera, and variations in lattice parameter, or occurrence of known alloy phases noted, and used to establish concentration gradients. Similarly, spectroscopic analysis of the shavings by giving the position and intensity of spectral lines will allow the concentration gradients to be measured. This method was used to follow the diffusion of a number of metals in silver [29]. A micrographic method of establishing concentration gradients in Cu-Al, Mg-Al systems has also proved successful [30].

A very interesting method [31], which could be used either as

TABLE 59.* *Artificial radioactivity (after Hevesy and Paneth*(34))

Atomic no. and element	Mass numbers of isotopes bombarded	Half-life periods of radioactive products	Nature of radiations emitted
4 Be	10	10y.	(−)
9 F	17, 18, 20	1·2m., 108m., 9s.	(+), (+), (−)
11 Na	22, 24	3y., 15h.	(+), (−)
14 Si	27, 31	6·6m., 2·5h.	(+), (−)
15 P	30, 32	3m., 14·5d.	(+), (−)
16 S	31, 35	26m., 80d.	(+), (−)
18 A	41	110m.	(−)
19 K	38, 42	7·5m., 12·5h.	(+), (−)
20 Ca	39, 45	4·5m., 2·3h.	(+), (−)
21 Sc	41, 42, 43, 44, 46, 48	53m., 4·1h., 4·0h., 52h., 90d., 41h.	(+), (+), (+), (+), (−), (−)
23 V	48, 49, 50, 52	16d., 32m., 3·6h., 3·8m.	(+), (+), (−), (−)
25 Mn	?, 56, ?, ?	46m., 2·5h., 21m., 5d., 7mth.	(+), (−)
26 Fe	55, 59	8·9m., 40d.	(+), (−)
27 Co	55, ?, 58, 60	18h., 150d., 11m. ~1y.	(+ and −), (+), (−)
28 Ni	63	120m.	(−)
29 Cu	61, 62, 64, 66	3·3h., 10·5m., 12·5h., 5m.	(+), (+), (+ and −), (−)
30 Zn	63, 65	38m., 60m.	(+), (−)
31 Ga	66, 68, 70, 72	9·4h., 60m., 20m., 23h.	(+), (−), (−)
32 Ge	75, ?	20h., 30m.	(−), (−)
33 As	76, 78	26h., 65m.	(−), (−)
34 Se	79 or 81, 83	1h., 17m.	(+), (−)
35 Br	76, 80, 80, 82, 83	6·3m., 18m., 4·5h., 34h., 2·5h.	(−), (−), (−)
36 Kr	?	74m., 4·5h., 18h.	(?)
37 Rb	86, 88	18m., 18d.	(−), (−)
38 Sr	89	3h., 55d.	(−), (−)
39 Y	90	70h.	(−)
40 Zr	97	44h.	(−)

Element	Mass numbers	Half-life periods	Particle
42 Mo	?	2·5 m., 17 m., 36 h.	(−), (−), (−), (−)
44 Ru	?	40 s., 100 s., 11 h., 170 h.	
46 Pd	?	60 h., 15 m., 12 h., 3 m.	(+), (−), (−), (−), (−), (−)
47 Ag	106, 106, 108, 110, 111, 112	24·5 m., 8·2 d., 2·3 m., 22 s., 7·5 d., 8·2 h.	
48 Cd	?, 115, 117	33 m., 4·3 h., 58 h.	(+), (−), (−)
49 In	111, 112, 114, 114, 116, 116, 117	20 m., 72 s., 4·1 h., 50 d., 13 s., 54 m., 2·3 h.	(+), (−), (−), (−), (−), (−), (−)
51 Sb	120, 122, 124	16 m., 2·5 d., 60 d.	(+), (−), (−)
52 Te	?	1·1 h.	(−)
55 Cs	134	1·5 h.	(−)
56 Ba	?, 139	2·5 m., 80 m.	(?), (?)
57 La	140	1·3 d.	(−)
59 Pr	140, 142	3 m., 19 h.	(+), (−)
60 to 71 (other rare earths)	—	In nearly every case half-life periods of suitable length	—
72 Hf	181	55 d.	(−)
73 Ta	180, 182	8 h., 97 d.	(+), (−)
74 W	?	1 d.	—
75 Re	?, 188, ?, ?	20 m., 18 h., 85 h., 40 h.	(?), (−), (−)
76 Os	?	40 h.	
77 Ir	192, 192 or 194, 189, 192 or 195	2 m., 1·4 m. and 19 h., 28 m., 8·5 h.	(?), (−), (−), (−), (−)
78 Pt	197, 199	18 h. and 3·3 d., 50 m.	(−), (−)
79 Au	198, 199	2·7 d., 13 h., 4·5 d.	(−), (−), (−)
80 Hg	205, 206	41 h., 45 m.	(−), (−)
81 Tl	204, 206	5 m., 97 m.	(−), (−)
82 Pb	209	3 h.	(−)

* In the table, m. = minute, h. = hour, d. = day, mth. = month, y. = year. Also (−) denotes electron and (+) denotes positron.

16-2

an averaging method, or to determine the actual concentration gradients, from the radioactive emission of successive thin layers, is the radioactive isotope technique. The method was originally employed to determine self-diffusion constants in lead, using radium D or thorium B as indicator. Thorium B may be condensed on the metal foil or single crystal. The path of α-particles in lead is only 50μ, so that when some of the thorium B atoms have penetrated more deeply than this their radioactivity can no longer be detected, and the radioactivity of the lead sheet falls off. Instead of following]diffusion by measuring the ionisation produced by α-rays, the recoil rays accompanying emission of α-particles were measured in some cases (32), the improvement effected by this method being that recoil particles in lead have a range of only 0.5×10^{-6} cm., so that diffusion coefficients as small as 10^{-13} cm.^{2} day^{-1} can be evaluated. The α-ray and recoil-atom methods have been used also to follow the self-diffusion of bismuth using thorium C as indicator. The results obtained by the two methods are in satisfactory agreement.

The radioactive indicator method has been used in just the same way to follow the diffusion of lead ions in lead chloride and lead iodide (32). With the discovery of artificial radioactivity the method seems capable of very wide application indeed. Gold, for example, has been rendered radioactive by neutron bombardment, and then used (33) to measure the self-diffusion constant of gold in gold; and radioactive zinc has been used to measure self-diffusion in copper (33a). Some of the substances which may be rendered radioactive by bombardment with neutrons, deuterons, protons, or γ-rays, and whose half-life period seems adequately long for the duration of possible diffusion experiments, have been collected in Table 59.

In addition to the normal radioactivity of radium, thorium, polonium, and uranium, radioactivity may be induced in these elements. The cyclotron has made it possible to obtain high-energy particles in considerable concentrations, and so it may be anticipated that artificial radio elements will become increasingly accessible to research workers. It is for this reason

that the radioactive isotope method is regarded as extremely important.

The diffusion of elements from the interior to the surface of a metal will usually change its thermionic emission [35], photo-electric emission [36], or contact potential [37]. These methods have been used especially in following the grain-boundary diffusion of thorium in tungsten, and the surface migration of barium, caesium, sodium, and potassium over tungsten (Chap. VIII). Cichocki [38] demonstrated the diffusion of metals from salts through copper, silver, and gold foil by making use of the positive-ion emission. The salt was enclosed in the foil, and heated, and after an interval positive ions escaped from the outer surface.

Diffusion constants in ionic lattices are in many instances calculated from the conductivities. The actual transfer in the ionic lattices may be demonstrated by the method of Tubandt [39] who employed cells such as

$$Pt \mid AgCl \mid Ag_2S \mid Ag_2S \mid Ag_2S \mid Ag,$$
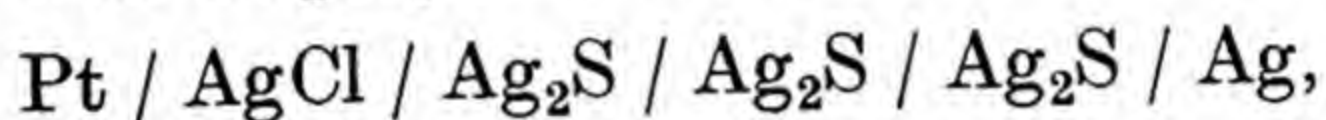
and passed a current through the cell, so that silver dissolved at the silver electrode, and was precipitated at the platinum electrode, the quantity transferred being found by weighing. If sticks of two salts are pressed together and heated they diffuse into one another, and the composition could be found by dividing the material into sections, and determining their density or chemical composition.

TYPES OF DIFFUSION GRADIENT

The diffusion gradients established on the interdiffusion of two solids may take a variety of forms. When two slabs of metal, e.g. Cu and Ni, are heated together, the simplest type of diffusion gradient which may be established is that illustrated in Fig. 85 [40]. The figure shows that the presence of a third substance may alter the shape of the concentration gradient. The form of the concentration gradient on either side of an interface is not always of this smooth form. Bramley and his co-workers [23] heated steel bars in various atmospheres from

which the elements C, N, O, S, and P diffused into the steel. The variety of shapes of concentration gradient which they obtained are illustrated in Chap. V, Figs. 73 and 74. Under certain conditions they obtained gradients with a maximum, as well
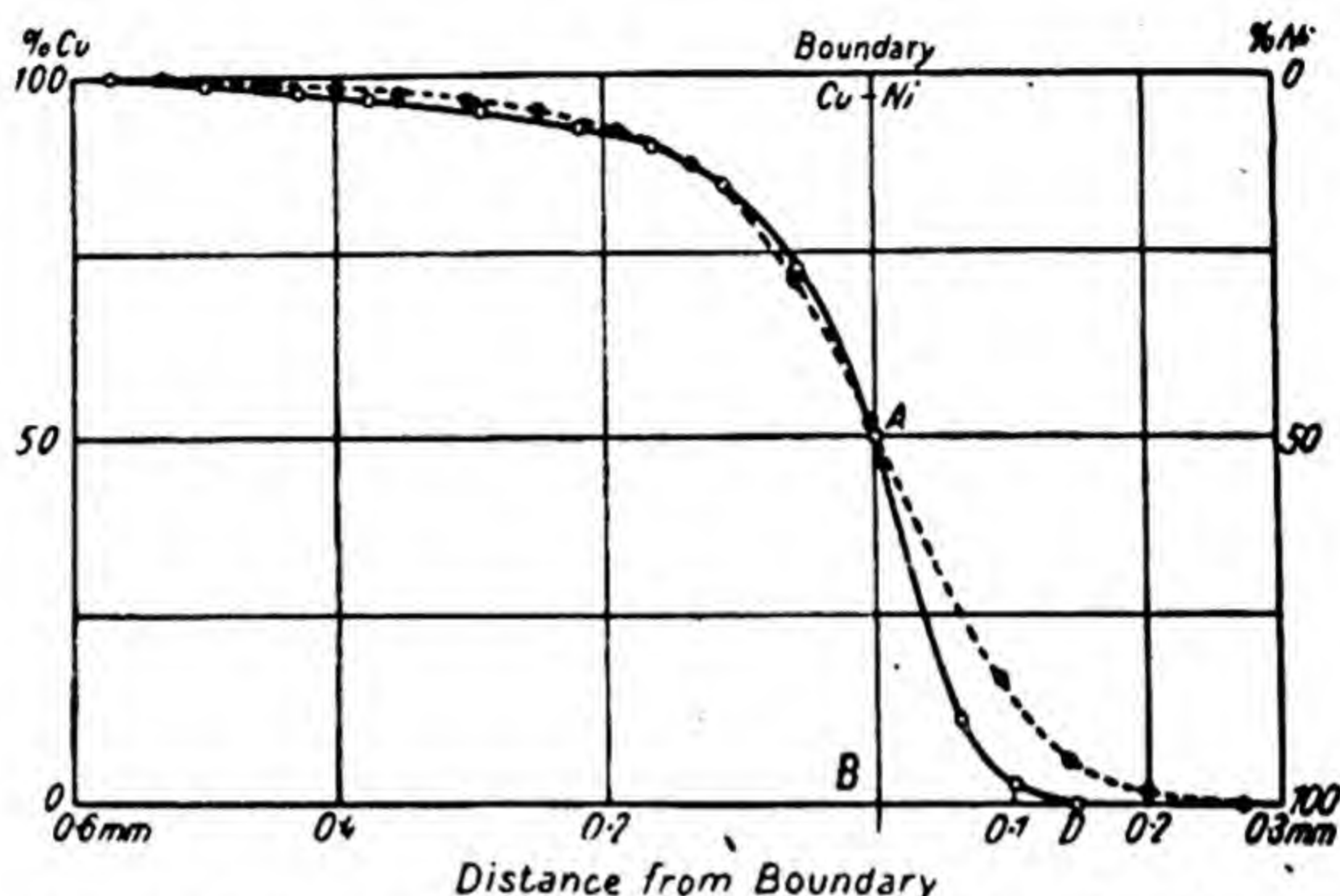
Fig. 85. Diffusion of copper into nickel (Grube and Jedelé[40]).

---- Pure Ni.
—— Ni containing Mn.
Curve after heating at 1025° C. for 120 hours.
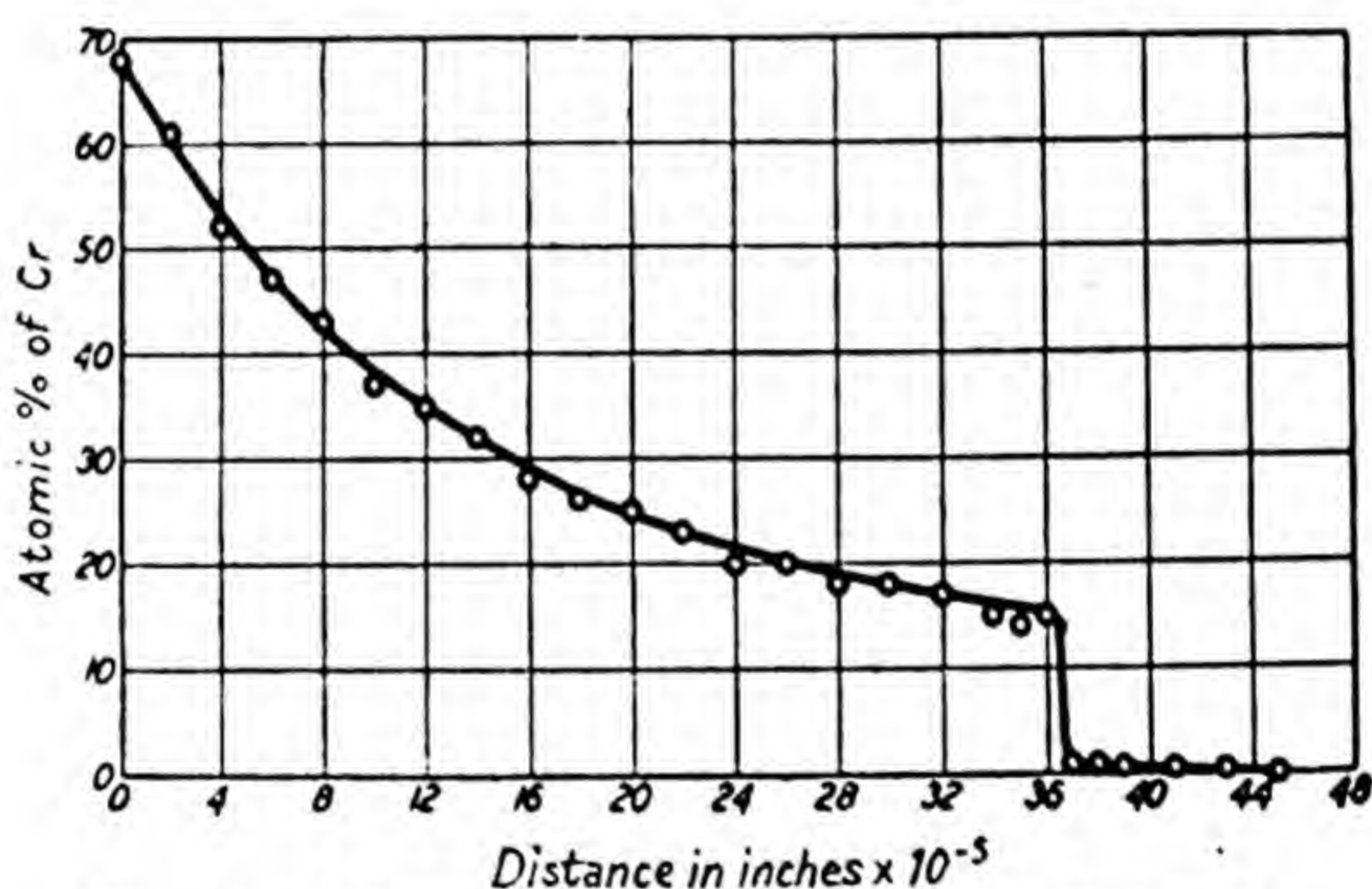
Fig. 86. Diffusion of chromium into iron (Hicks[41]).
Gradient after 96 hours at 1200° C.

as S-shaped. Obviously the analysis of such curves to give diffusion constants will be difficult. Another complicating factor arises when two phases co-exist. In this instance concentration discontinuities occur (Fig. 86)[41]. Systems in which concentration discontinuities exist may often be analysed

readily to give the diffusion constant, D. The discontinuity usually marks points of fixed concentration, and the rate at which this discontinuity progresses into the solid is therefore likely to be governed (for linear diffusion) by the law

$$x^2 = 4Dt,$$

where x denotes the distance of the discontinuity from the origin, and t is the time.

The Structure of Real Crystals

The ideal crystal consists of a perfectly ordered array of atoms, ions, or molecules in three dimensions. This ideal is difficult to attain experimentally, although in one instance at least (NaCl)[42] it appears to have been closely approached. There cannot be any ionic conductivity or atomic diffusion in a perfect lattice which conserves its ideal order in all circumstances, and the observation that conductivity and diffusion do occur is only one of a number of lines of evidence which lead to the conclusion that a real crystal is not perfectly regular under all conditions.

As a result of a large number of researches it has been established that two types of fault system may exist in crystals which may be called reversible and irreversible fault systems. The former have reproducible properties in many respects, but properties of the latter depend upon the previous history of the specimen. In particular, irreversible fault systems give rise to the "structure-sensitive" diffusion and conductivity data described in the following chapter, while reversible fault systems give rise to reproducible conductivity and diffusion phenomena. Some of the reproducible and equilibrium types of fault systems may be briefly discussed before the conductivity and diffusion data are given.

Besides defects which have been artificially introduced in crystals, other types of imperfection exist of the greatest significance for understanding ionic mobility in crystal lattices. Lattice imperfections of this kind are:

(1) Ions existing interstitially within the normal lattice. This leaves holes in the lattice, and electrolytic conduction or diffusion may proceed by jumps of the ions from one interstitial position to another; or by diffusion of the holes.

(2) Some positions in the normal lattice are vacant, although there are no interstitial ions. Again the holes may diffuse, by jumping of ions from an adjacent lattice place into the hole, leaving a second hole.

The equilibrium between holes, interstitial ions, and the normal lattice is maintained at temperatures upwards of about 100–200° below the melting-point (43, 44, 45); but at low temperatures the amount of disorder in the lattice depends upon the history of the specimen. This *non-equilibrium* distribution of points of disorder in the lattice is referred to as "irreversible gitterauflockerung"* by von Hevesy (46). It may have the most remarkable influence upon the ionic conductivity, and, with the subject of grain-boundary diffusion, is discussed later (Chap. VII). The *equilibrium* types of disorder existing in a few lattices are especially interesting when considering models for the diffusion process at high temperatures, such, for example, as that given by Frenkel (47).

Some equilibrium types of disorder in crystals

In *silver chloride* the current-carrying ion is the cation, and therefore only the cations are in disorder (Fig. 87) (48). In Fig. 87 the arrows indicate the possible processes of ionic

Ag^+	Cl^-	Ag^+	Cl^-	□	Cl^-	Ag^+	Cl^-
	$Ag^+ \longrightarrow$			↗			
Cl^-	Ag^+	Cl^-	Ag^+	Cl^-	Ag^+	Cl^-	Ag^+
Ag^+	Cl^-	Ag^+	Cl^-	Ag^+	Cl^-	Ag^+	Cl^-
						Ag^+	
Cl^-	□	Cl^-	Ag^+	Cl^-	Ag^+	Cl^-	Ag^+
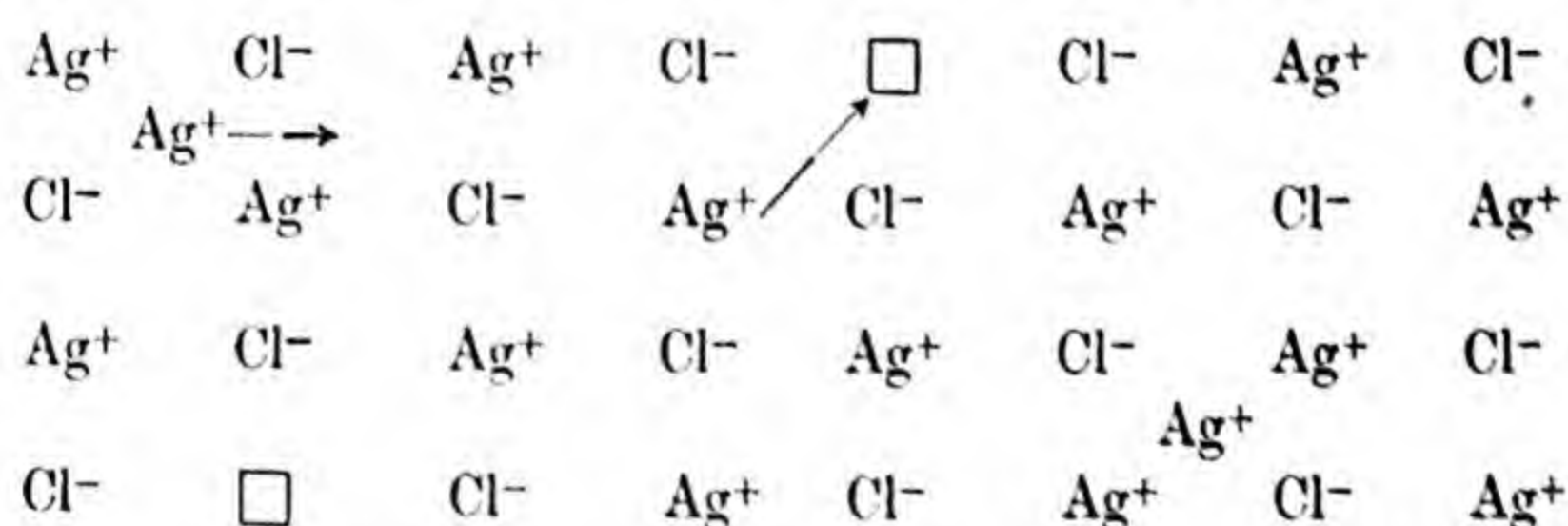
Fig. 87. Disorder in the silver chloride lattice according to Frenkel.

mobility. These are of two kinds corresponding to migrations of holes and of interstitial ions respectively. There is an energy

* Gitterauflockerung = lattice loosening.

of activation for the types of jump illustrated in Fig. 87, as well as an endothermic heat of formation of the interstitial positions. α-*silver iodide* (49), *silver mercury iodide* (50), and similar compounds give the extreme example of the disorder illustrated in Fig. 87, for they show an almost perfect anionic lattice, but a nearly random distribution of cations within it. This accounts for the observation (p. 240) that the ionic conductivity of solid and molten silver iodide are nearly the same ($\sim 1 \, \mathrm{ohm}^{-1} \mathrm{cm}.^{-1}$). Diffusion in *potassium chloride* occurs, according to Schottky, because of a disorder in both anion and cation lattices (Fig. 88) (45) which does not produce interstitial ions. The similar size of K^+ and Cl^- ions renders the
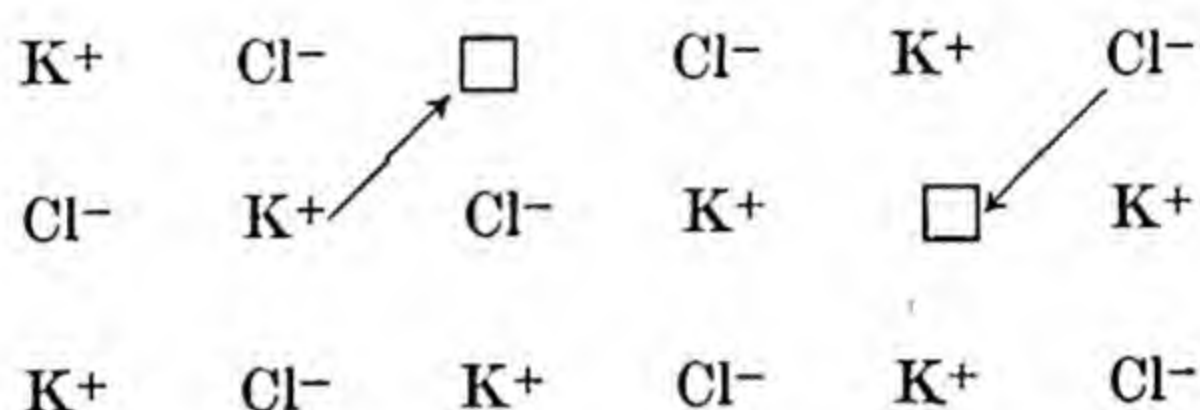
Fig. 88. Disorder in potassium chloride according to Schottky.

interstitial spaces too small to accommodate K^+ or Cl^- ions. Instead, there are equal numbers of cation and anion vacant spaces formed by movements of ions into the crystal surface where they tend to build new lattice layers.

It has been found that a number of compounds exist which do not rigidly obey the law of fixed proportions. In the spinel group of compounds, of which $MgAl_2O_4$ is the type, certain constituents of the lattice may be lost but the lattice still retains its structure. Spinel itself may undergo the continuous transition $MgAl_2O_4 \rightarrow Mg_2Al_{8/3}O_4$ (γ-alumina). The excess of one component is due either to the existence of gaps in the lattice where that component should be, or to an interstitial excess of another component. The behaviour is shown by certain oxides, sulphides and halides.

As an example of an oxide with metal excess one may take *zinc oxide* (51). At 600° C. some oxygen has been lost by dissociation, and a solid solution of zinc in zinc oxide remains in which the metal is dissociated into cations and electrons. The

higher the oxygen pressure the less the zinc ion excess, and so the smaller the conductivity. *Cadmium oxide* (51) behaves in a similar manner.

Other oxides give systems with an oxygen excess (*oxides of iron, cuprous oxide,* and *nickel oxide* (52)). Cuprous oxide, for example, takes up an excess of oxygen as O'' ions, as a result of which vacant cation sites appear in the lattice. The electrons for this process are liberated by the reaction $Cu^+ \rightarrow Cu^{++} + e$, and electronic conductivity occurs because electrons may be supplied by the electron transfer of the above reaction. The higher the oxygen pressure the more excess oxygen is dissolved in the lattice (e.g. $\sim 0\cdot 1 \%$ at $1000°$ C. and at 30 mm. Hg pressure), and so the higher the conductivity. The sizes of the ions ($O'' = 1\cdot 32$ A.; $Cu^+ = 0\cdot 96$ A.) do not allow one to arrange the excess oxygen interstitially, and so the type of disorder given in Fig. 89 (48) is postulated. X-ray studies (53) of *ferrous oxide, sulphide,* and *selenide* showed that empty cation positions similar to those in Fig. 89 may indeed exist.

$$Cu^{++} \quad Cu^+ \quad \square \quad Cu^+ \quad Cu^+ \quad Cu^+$$
$$O'' \quad O'' \quad O'' \quad O'' \quad O''$$
$$Cu^+ \quad Cu^{++} \quad Cu^+ \quad Cu^+ \quad \square \quad Cu^+$$
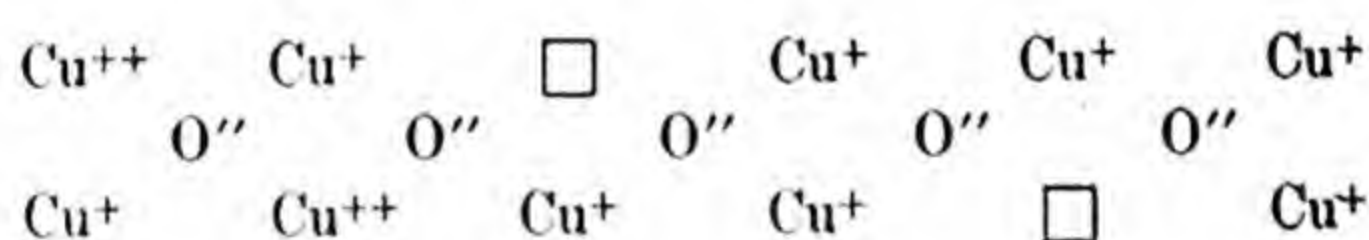
Fig. 89. Disorder in cuprous oxide with excess oxygen.

Cuprous iodide (54) and *bromide* (39) show in part an electronic conductivity due to the solution of an excess of iodine or bromine as ions, the electrons for the formation of the ions being supplied by the reaction

$$Cu^+ \rightarrow Cu^{++} + e,$$
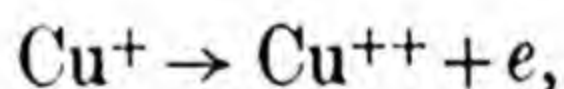
Potassium iodide if pure has a small conductivity ionic in type. The lattice may dissolve excess either of iodine or of metal, and the conductivity is then altered by the presence of iodine ions, or potassium ions:

$$\tfrac{1}{2}I_2 + e \rightarrow I^-, \quad K \rightarrow K^+ + e.$$
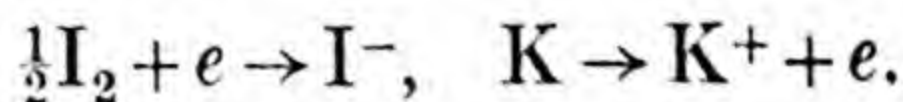
The alkali halides in general (55) can behave as solvents for small amounts of halogens, alkali metals, and even hydrogen. The solute is not always in atomic or ionic form however (Chap. III).

THE INFLUENCE OF GAS PRESSURE UPON CONDUCTIVITY

Most important from the viewpoint of lattice disorder are the observations of Wagner and his co-workers upon changes of conductivity brought about by surrounding the crystal by a gas atmosphere of its electronegative component (oxygen for oxides, or halogen for halides). These measurements were the basis of the classification of lattices, as in the previous section, into those with anion excess, cation excess, or stoichiometric cation anion ratio.

As an example of the influence of pressure we may consider O_2-Cu_2O systems which contain excess of the electronegative component oxygen. It may be supposed that Cu^+ ions release electrons, giving Cu^{++} ions, and an equivalent number of Cu^+ ions diffuse from their lattice sites. These ions and electrons react at the surface of the crystal with gaseous oxygen, producing more crystalline Cu_2O. One denotes Cu^{++} by the symbol $(e)_l$, or electron defect site; similarly $(Cu^+)_l$ is a vacant lattice site. The corresponding occupied sites are denoted by $(e)_g$, $(Cu^+)_g$. The symbols "l" and "g" mean respectively "leerstelle" or "vacant place", and "gitterplatz" or "lattice site". The reaction is then

$$O_2(gas) + 4(e)_g + 4(Cu^+)_g \rightleftharpoons 2(Cu_2O)_g + 4(e)_l + 4(Cu^+)_l.$$
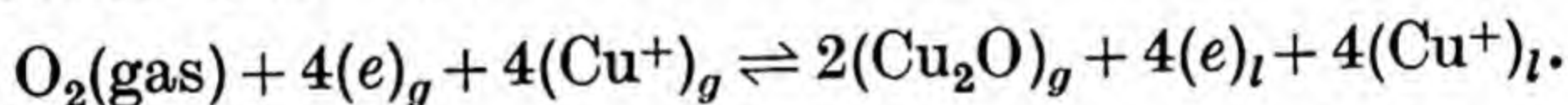
Since $(Cu_2O)_g$ is simply an array of $(O^{--})_g + 2(Cu^+)_g$, the net reaction is

$$O_2(gas) + 4(e)_g \rightleftharpoons 2(O^{--})_g + 4(e)_l + 4(Cu^+)_l.$$
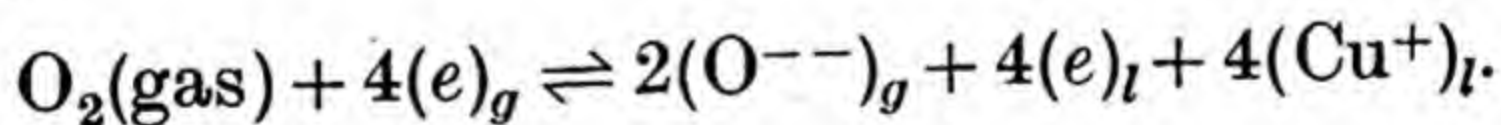
Application of the law of mass action then gives

$$\frac{(Cu^+)_l^4 (e)_l^4}{p_{O_2}} = K,$$

because $(e)_g$ and $(O^{--})_g$ are nearly constant. But $(Cu^+)_l = (e)_l$, and so

$$(e)_l = [K \cdot p_{O_2}]^{\frac{1}{8}}.$$

The conductivity, which in cuprous oxide is mainly electronic, is thus proportional to the eighth root of the pressure of oxygen. While the theory predicts an eighth root, experiment

shows an approximate seventh root dependence of conductivity on pressure (Fig. 90), a satisfactory agreement.

Table 60, after Wagner(43), gives in a simple form all the available information concerning lattice disorder and the conduction process in certain oxides and halides. The use of the table may be illustrated with reference to silver chloride:

Column 2. There are almost equal numbers of interstitial cations and vacant cation sites in the silver chloride lattice. The number of quasi free electrons or electron-defect sites is negligible.
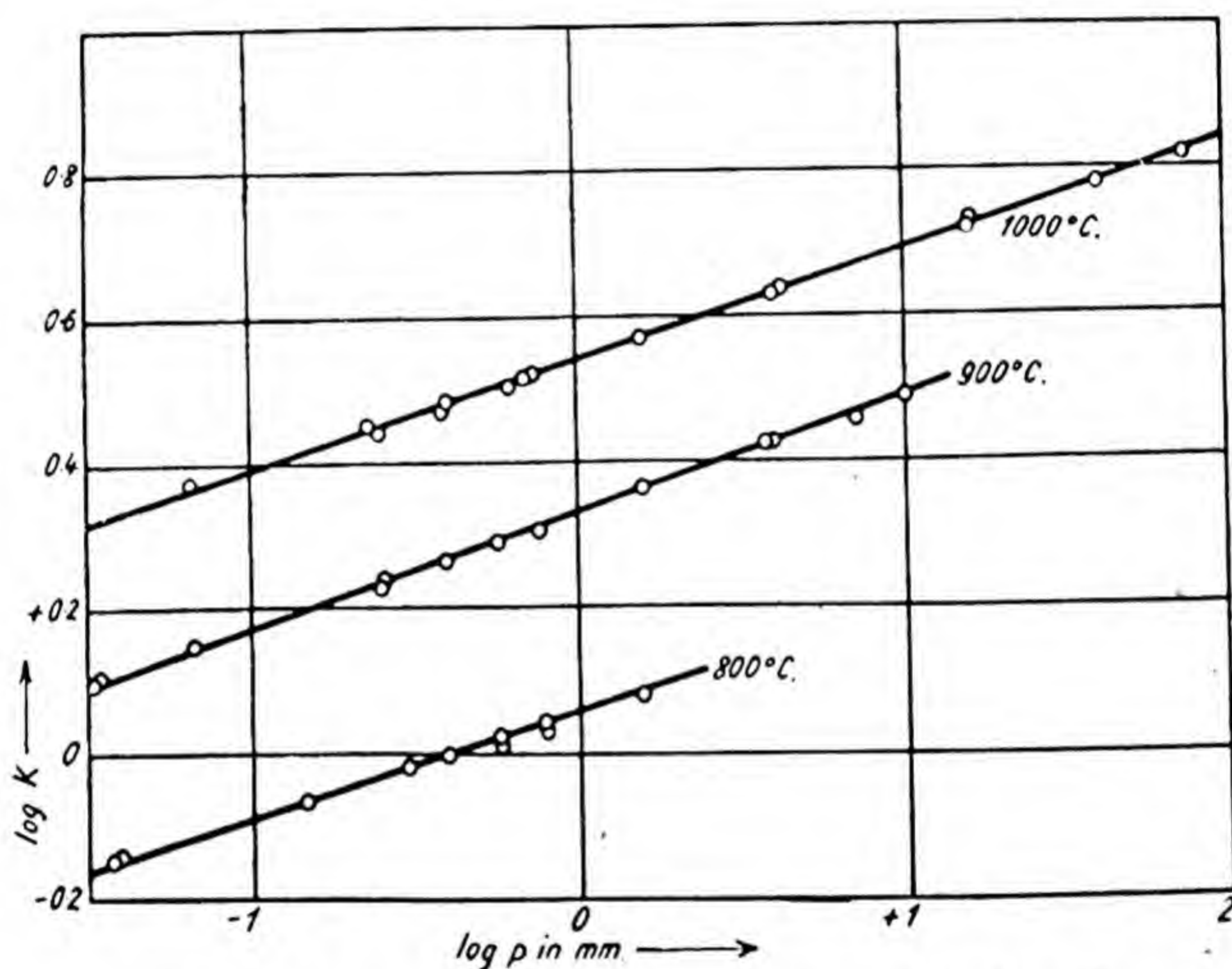
Fig. 90. The dependence of the conductivity of Cu$_2$O on the oxygen pressure. (Dunwald and Wagner(52).)

Column 4. Neither silver nor chlorine is in any appreciable excess over their stoichiometric ratio.

Columns 5, 6 and 7. Increased partial pressure of chlorine has no influence upon conduction due to cations, but may alter the electronic conductivity. Electronic conductivity (columns 2 and 9) occurs however only to a negligible extent.

Columns 8 and 9. Silver chloride is almost exclusively a cationic conductor.

TABLE 60. *Types of lattice disorder, with examples if known, and characteristics of conduction of electricity in corresponding lattices* (Wagner[43])

Number	Types of lattice* disorder possible in compound Me X	Example	Component present in excess	Influence of increasing the partial pressure of negative component on conduction due to			Transport numbers of	
				Cations	Anions	Electrons	Cations	Anions
1a	$(Me^+)_z = (e)_z$	ZnO	Me	Decreases	—	Decreases	$\ll 1$	0
b	$(X')_l = (e)_z$	?	Me	—	Decreases	Decreases	0	$\ll 1$
2a	$(X')_z = (e)_l$	?	X	—	Increases	Increases	0	$\ll 1$
b	$(Me^+)_l = (e)_l$	Cu$_2$O, NiO	X	Increases	—	Increases	$\ll 1$	0
3	$(e)_z = (e)_l$		—			None		
a	$(Me^+)_z \ll (e)_z$	?	Me	Decreases	—	None	$\ll 1$	0
b	$(X')_l \ll (e)_z$	CuO	Me	—	Decreases	None	0	$\ll 1$
c	$(X')_z \ll (e)_l$	?	X	—	Increases	None	0	$\ll 1$
d	$(Me^+)_l \ll (e)_l$	?	X	Increases	—	None	$\ll 1$	0
4a	$(Me^+)_z \cong (Me^+)_l$	?	Me	None	—	Decreases	$\cong 1$	0
b	$\left\{ \begin{array}{l} (e)_z \ll (Me^+)_l \\ (e)_l \ll (Me^+)_l \end{array} \right.$	AgCl	X	None	—	Increases	$\cong 1$	0
5a	$(X')_z \cong (X')_l$	BaCl$_2$	Me	—	None	Decreases	0	$\cong 1$
b	$\left\{ \begin{array}{l} (e)_z \ll (X')_l \\ (e)_l \ll (X')_z \end{array} \right.$	?	X	—	None	Increases	0	$\cong 1$

* "z" denotes "zwischengitter" or "interstitial"; "l" (see p. 251) denotes "leerstelle", "vacant site", or "electron defect site".

THE ENERGY OF DISORDER IN CRYSTALS

The results of the previous sections lead us to consider important types of equilibrium ionic disorder to be:

Vacant cation sites, with an equal number of interstitial ions;

Vacant anion sites, with an equal number of interstitial ions;

Equal numbers of anions and cations in interstitial positions;

Equal numbers of vacant anion and cation sites.

The first three examples are known as Frenkel disorder, and the last example as Schottky disorder. Calculations of the energies of disorder [56] are likely to be of importance if they give the absolute values of the energy of disorder from known force laws and crystal parameters; and if they show which type of disorder is most likely to be met with in different salts.

Let E denote the lattice energy, that is, the energy needed to dissociate 1 Mol. of the lattice into gaseous ions. Then E/N_0 is this energy referred to one ion pair of the lattice; it is connected with the energy E_s needed to produce a Mol. of Schottky lattice defects, and the corresponding polarisation energy, E_{pol}, released around the vacant sites, by $E = E_s + E_{pol}$. In a preliminary calculation of E one may use the force law

$$F = -\frac{dE}{dr} = \frac{A}{r^2} - \frac{B}{r^n},$$

in which the first term gives the Coulombic attractive force, and the second the repulsive force.* Born's expression for the lattice energy is then applied, and the lattice energy per ion pair in sodium chloride for example is

$$\frac{E_B}{N_0} = 1 \cdot 74 \frac{2e^2}{a} \left(1 - \frac{1}{n}\right),$$

where a denotes the lattice parameter, and e is the electronic charge. In addition, the polarisation energy involved is approximately equal to that when an ion is transferred from a medium

* The repulsive exponent n is usually given a value of 9–13.

of dielectric constant ϵ to a medium of dielectric constant unity, given for a *pair* of ions by

$$\frac{E_{\text{pol.}}}{N_0} = \frac{2e^2}{a}\left(1 - \frac{1}{\epsilon}\right).$$

Accordingly, the net energy of disorder per ion pair becomes

$$\frac{E}{N_0} = 1 \cdot 74 \frac{2e^2}{a}\left(1 - \frac{1}{n}\right) - \frac{2e^2}{a}\left(1 - \frac{1}{\epsilon}\right),$$

which is very much smaller than the lattice energy. However, it must be remembered that many approximations are involved in so simple a calculation as that above. The nature of these approximations is now indicated:

(1) The force law used in calculating the lattice energy is inadequate since it neglects contributions of van der Waals' interactions, which may become appreciable in lattices where the mass of the ions is large, or where one type of ion exists largely in interstitial positions. Thus in α-AgI, or α-Ag$_2$S, where the cations are in almost complete disorder in an anion lattice, van der Waals' forces are considerable.

(2) Interactions between induced quadrupoles also contribute to the polarisation energy.

(3) When a vacant site is formed, surrounding ions will tend to rearrange themselves slightly, and the corresponding energy term must be allowed for.

(4) A better method of expressing the repulsive potential replaces the term

$$E_{\text{rep.}} = \frac{B}{r^n}$$

by

$$E_{\text{rep.}} = be^{\frac{(r_+ + r_- - r)}{\rho}},$$

where r_+ and r_- are the radii of a positive and a negative ion, distant r from each other, and b and ρ are constants. Even this equation is inaccurate at very small separations.

(5) The crystal cannot be regarded as a continuum, as was assumed in calculating the polarisation energy, $E_{pol.}$, for one is dealing with phenomena on a molecular scale. Thus one is uncertain what value to give to ϵ and what the effects of inhomogeneity of the medium upon the polarisation energy may be.

Other refinements may be suggested (56), but enough has been said to indicate the nature of the calculation which must be made, and its difficulties. The energy of disorder may be determined experimentally, however, from conductivity data. Koch and Wagner (57) measured the conductivity of solutions such as $PbCl_2$, $CdCl_2$, in AgCl, and of pure AgCl. The addition of cadmium chloride will alter the number of vacant lattice sites in a silver chloride lattice with which it forms a homogeneous solution. For in cadmium chloride the cation to anion ratio is 1 : 2, instead of 2 : 2 for silver chloride, and there is thus one cation too few for every Cd^{++} ion in the lattice, giving one vacant site for each cadmium ion incorporated. The authors have established that the electrical conductivity of solutions of cadmium chloride in silver chloride is in the main determined by the product of concentration and mobility of the vacant sites, the concentration of interstitial ions being much smaller. But the concentration of vacant sites is equal approximately to the concentration of the cadmium chloride, and so the exact analysis of the conductivity data permits one to find the mobility of vacant sites, and by extrapolating to zero concentration of cadmium chloride to find the much smaller concentration of vacant sites in pure silver chloride, as well as their mobility. The results of this investigation appear in Table 61 (48), and from the measurements at various temperatures, by application of the van't Hoff isochore $\dfrac{\partial \ln K}{\partial T} = \dfrac{E}{RT^2}$ the following energies of disorder were found:

$$AgCl : E \sim 25{,}000 \text{ cal./ion}$$
$$AgBr : E \sim 20{,}200 \text{ cal./ion.}$$

These energies show that the mathematical treatment of

energies of disorder is correct in outline, since, as the theory indicates, the energy of disorder is much less than the lattice energy.

The question as to which of the two main types of disorder (that of Frenkel or that of Schottky) will prevail in a given system can be treated analogously by the mathematical theory. Simple geometrical considerations are, however, sufficient to show the conditions which decide the actual types of disorder.

TABLE 61. *Concentrations and mobilities of interstitial ions and vacant positions in silver halides**

Compound	Temp. ° C.	Mobility of vacant sites in Ag lattice cm./sec./v./cm.	Fraction of ions in interstitial positions = fraction of vacant spaces
AgCl	350	6.6×10^{-4}	1.5×10^{-2}
	300	4.2×10^{-4}	5.5×10^{-4}
	250	2.3×10^{-4}	2.2×10^{-4}
	210	1.5×10^{-4}	8.1×10^{-5}
AgI	300	7.6×10^{-4}	4.0×10^{-3}
	250	3.4×10^{-4}	1.8×10^{-3}
	210	2.0×10^{-4}	7.6×10^{-4}

* The concentrations are calculated assuming that the mobility of holes and interstitial ions is the same. This assumption may lead to errors in the data of Table 61.

If the ions displaced from their regular lattice sites are small compared with the interstices, they may more easily exist in interstitial positions, and Frenkel's disorder is possible. If the anions and cations are of comparable radii, the lattice must be highly distorted for ions to exist interstitially, and Schottky's disorder becomes probable.

THE INFLUENCE OF TEMPERATURE ON DIFFUSION IN METALS AND CONDUCTIVITY IN SALTS

The earliest attempts to express conductivity data for salts made use of power series in the temperature (T). Foussereau [58] represented a number of specific resistances by the expression

$$\log R = a - bT + cT^2,$$

17

where a, b, and c are constants. Rasch and Hinrichsen [59] and Konigsberger [60] independently employed the equation

$$\log K = a + b/T,$$

where K denotes the conductivity. Phipps, Lansing and Cooke [61] followed Konigsberger's suggestion that the equation was really of the form

$$\log K = - E/RT + C,$$

where E is an energy term concerned as we now know with the movement of the current-carrying ion or diffusing metal atom from one position of minimum potential energy in the lattice to another. All results are now expressed in terms of Konigsberger's formula, although sometimes two or more exponential terms are necessary when two or more ions participate in the transport of electricity. The general and very satisfactory applicability of the exponential law, both for diffusion in metals and conductivity in salts, is illustrated in Figs. 91–93. It can be seen from these figures and from Figs. 94 and 95 that one may classify diffusion and conductivity systems into three groups:

(A) Substances which conduct by transport of one ion, or where the diffusion constant, D, obeys a simple exponential law $D = D_0 e^{-E/RT}$. This is the normal and by far the most numerous group (Figs. 91 and 92).

(B) Substances in which more than one exponential term is important, according to the temperature. Thus the diffusion constants of indium and of cadmium in silver [29], and the conductivity of lead iodide [32] involve two exponentials. One may write for lead iodide:

$$K_{PbI_2} = K_{Pb^{++}} + K_{I^-} = A_1 e^{-E_1/RT} + A_2 e^{-E_2/RT},$$

because both ions carry the current. At low temperatures, one exponential predominates, and the behaviour is that of class (A). Another salt which may follow a similar law is silver chloride, for which Smekal [62] gives

$$K_{AgCl} = 0 \cdot 00015 e^{-4320/RT} + 3 \cdot 2 \times 10^5 e^{-22,120/RT}.$$
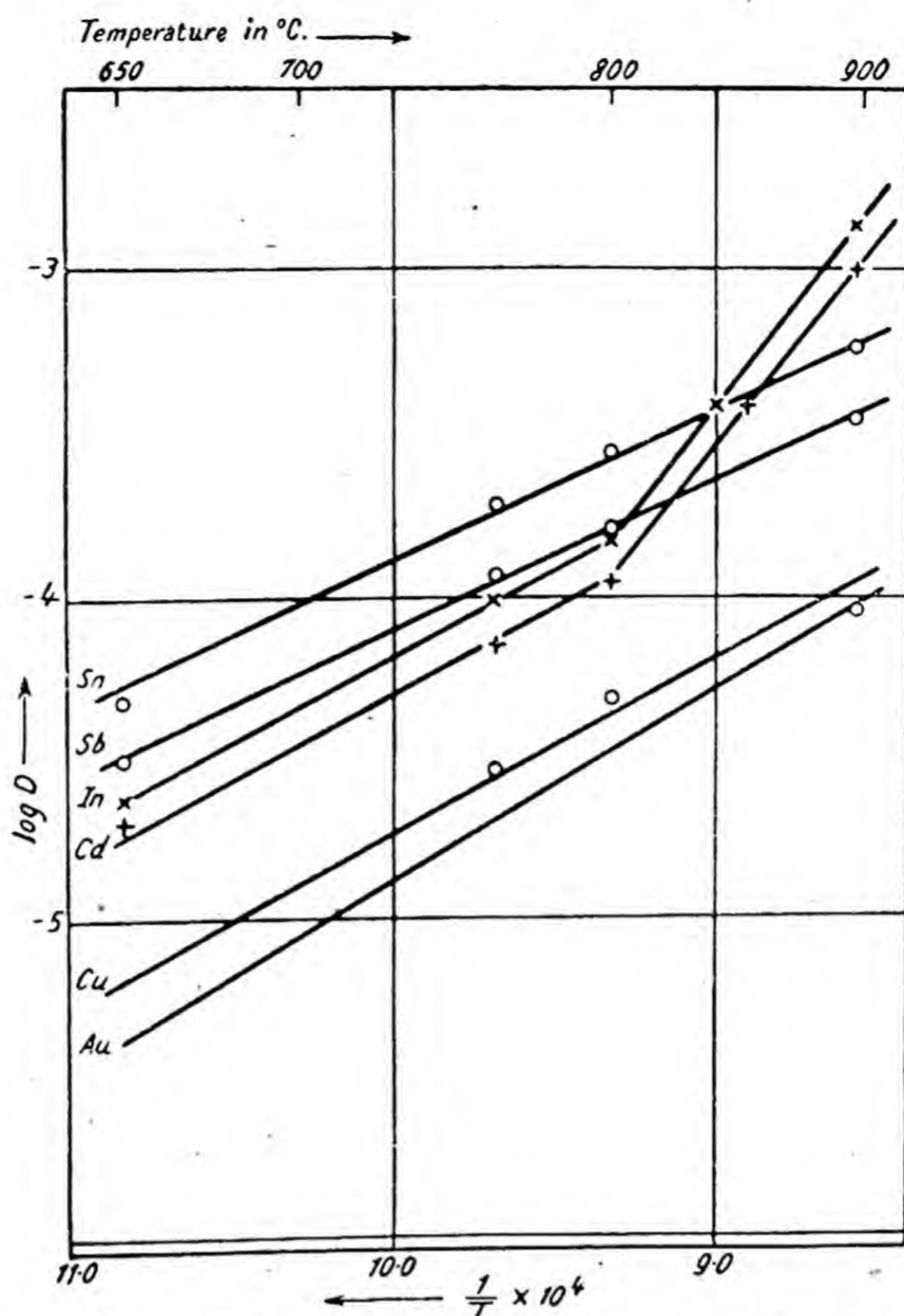
Fig. 91. The diffusion constants of various metals in silver
(Seith and Peretti[29]).
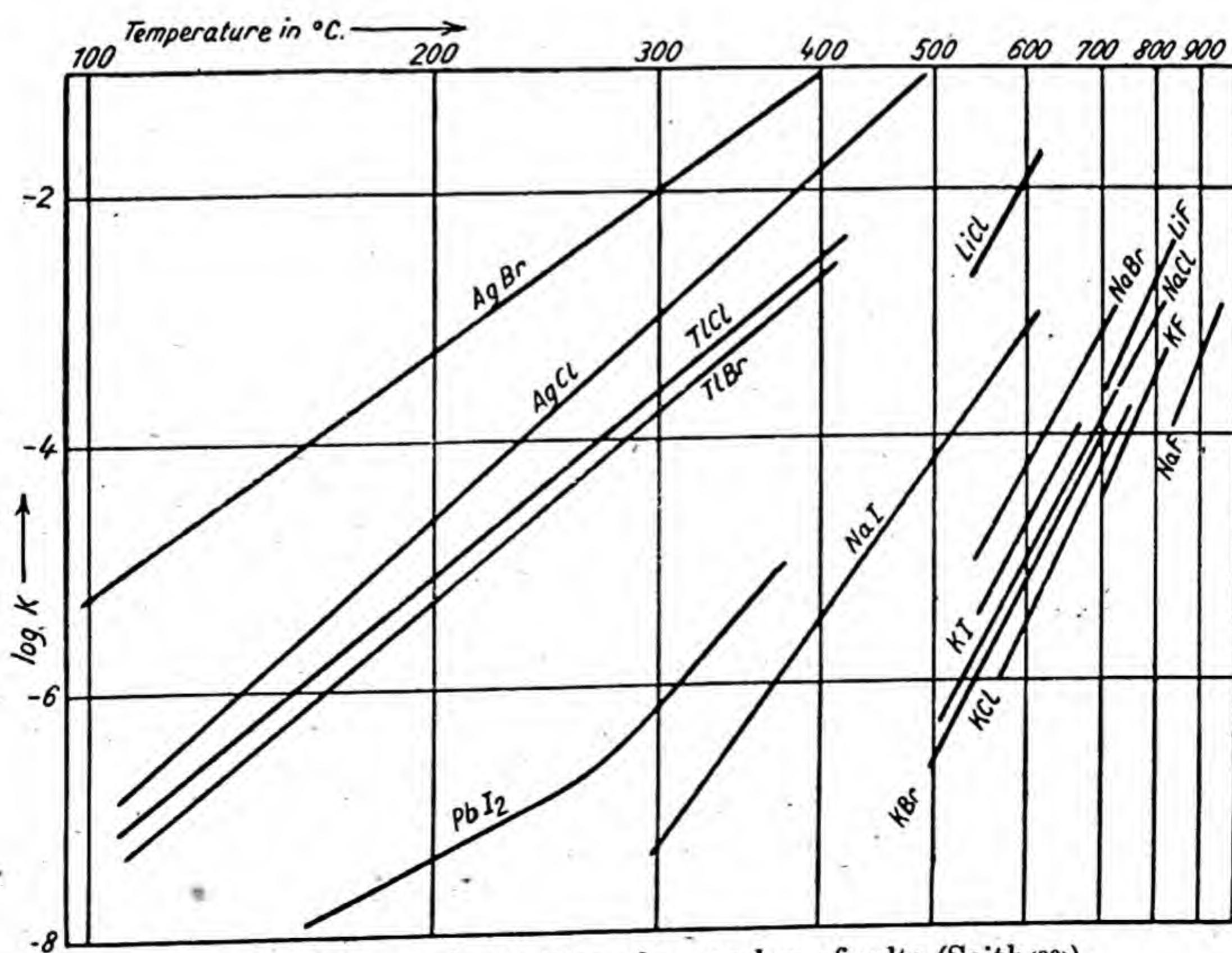
Fig. 92. The conductivities of a number of salts (Seith [39]).
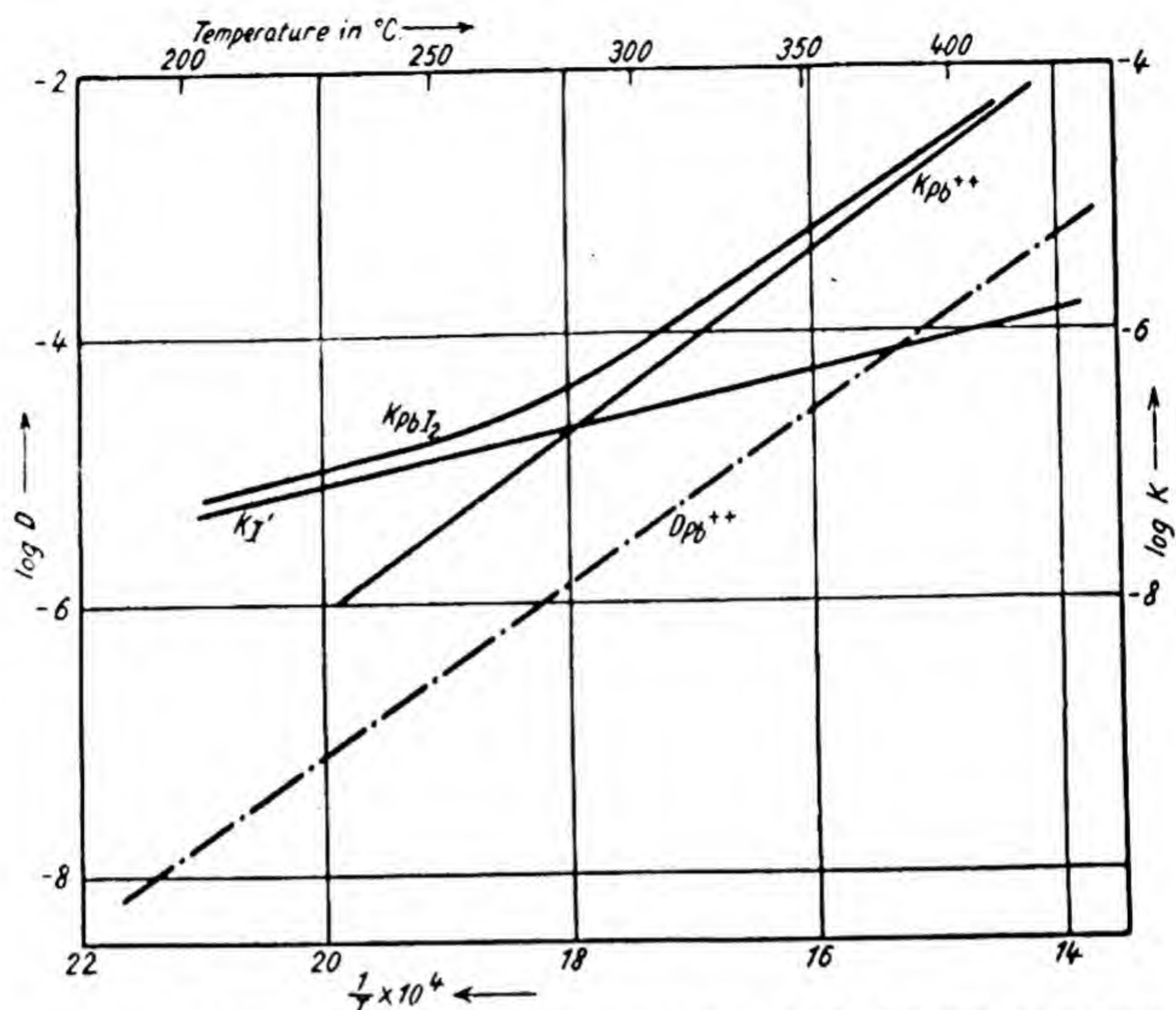
Fig. 93. The diffusion and conductivity data for lead iodide (Seith[39]).

K_{PbI_2} = conductivity of PbI_2.
$K_{I'}$ = conductivity of I' ions.
$K_{Pb^{++}}$ = conductivity of Pb'' ions.
$D_{Pb^{++}}$ = self-diffusion constant of Pb'' ions.
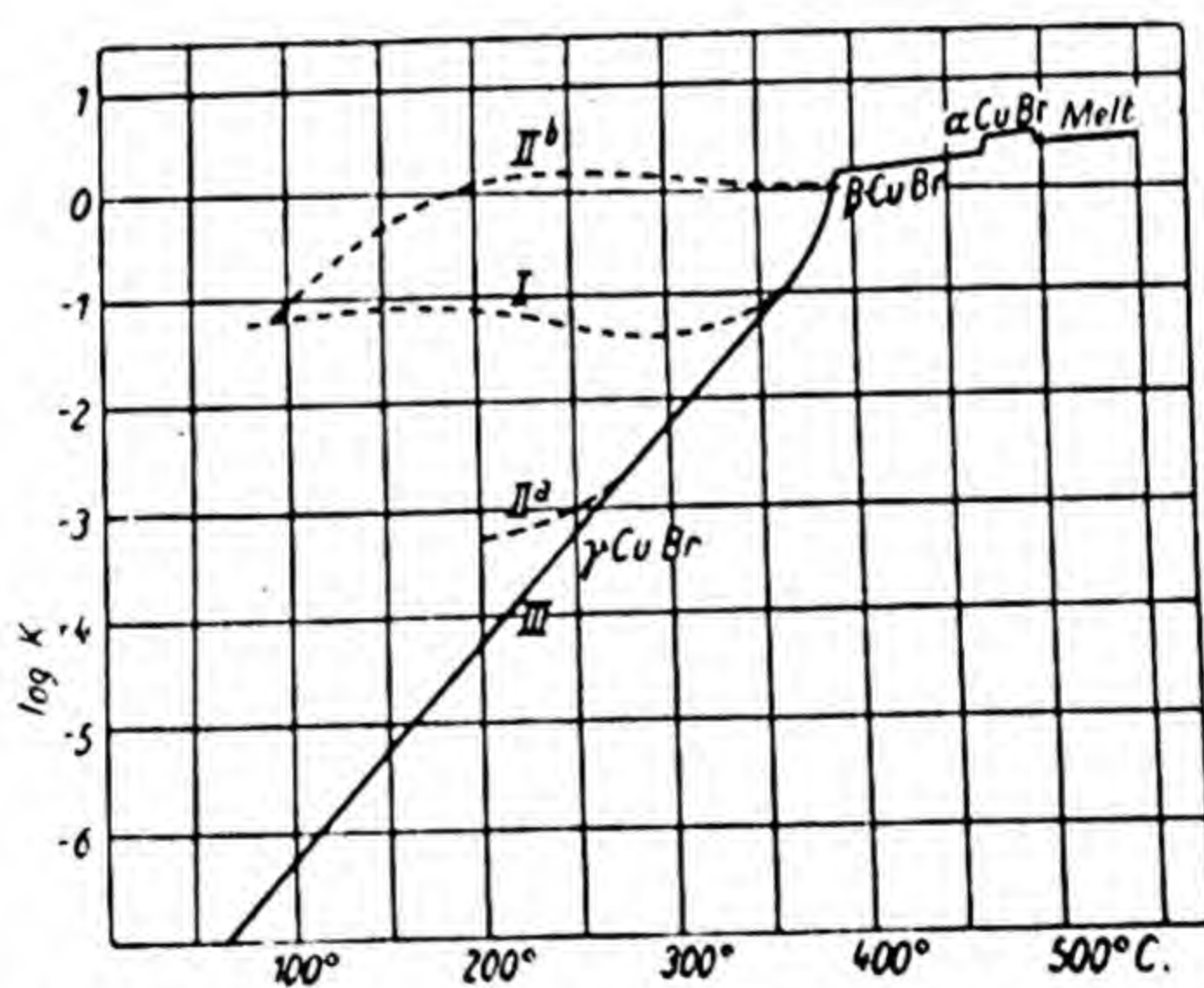
Fig. 94. The conductivity of cuprous bromide as a function of
temperature (Tubandt[39]).

Where one has a pair of mutually soluble salts the behaviour tends to be that of group (B). For example, in Table 62 [39] are given the constants for the conductivity of CuBr-AgBr mixed crystals. The conductivity may be represented by

$$K = K_{Cu^+} + K_{Ag^+} = A_{Cu^+}\, e^{-E_1/RT} + A_{Ag^+}\, e^{-E_2/RT}.$$
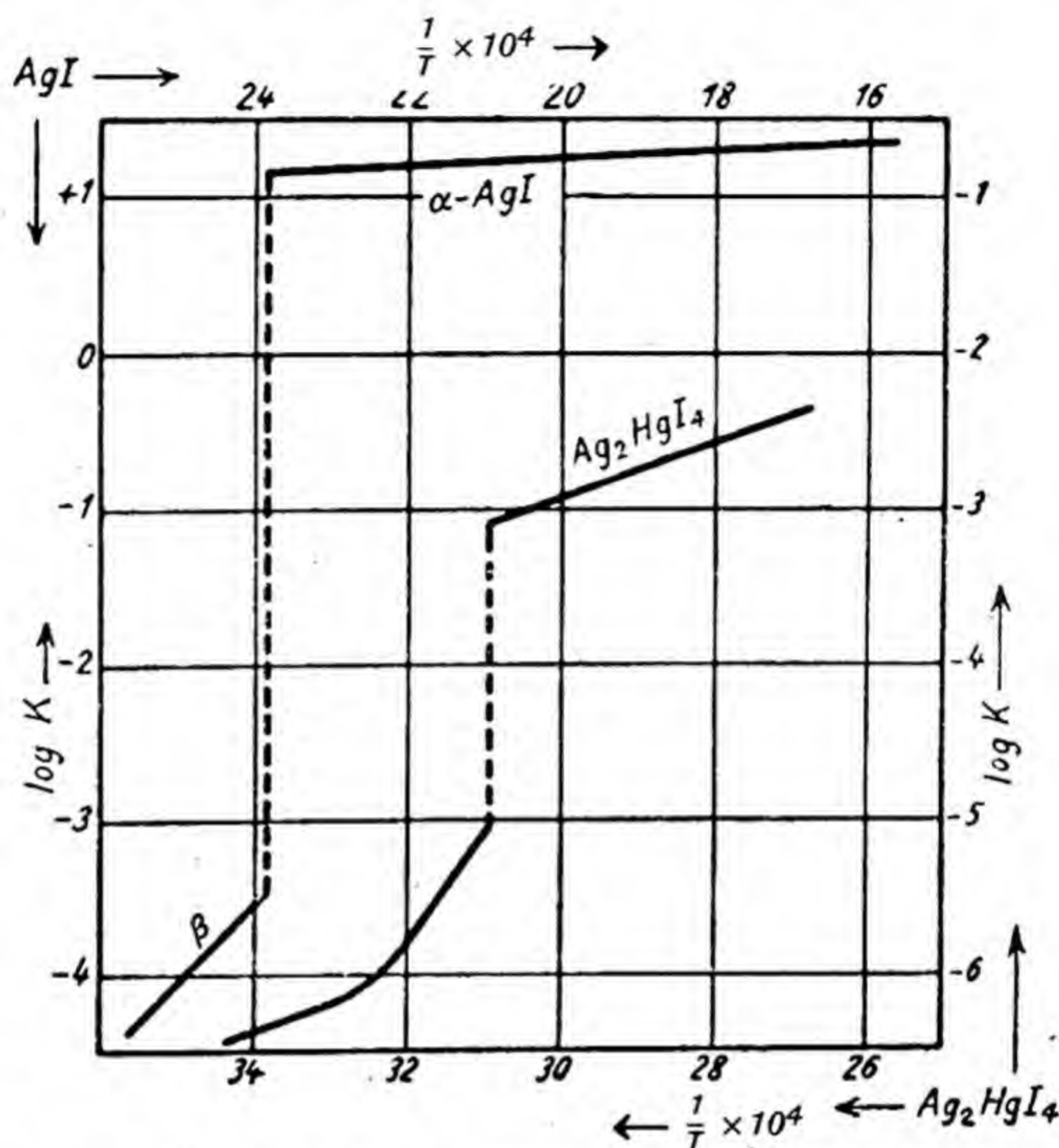
Fig. 95. Conductivity of silver iodide and silver mercury iodide (Seith [39]).

TABLE 62. *Constants in the equation*

$$K = A_{Cu^+}\, e^{-E_1/RT} + A_{Ag^+}\, e^{-E_2/RT}\ (\text{ohm}^{-1}\ \text{cm.}^{-1})$$

for the conductivity of CuBr-AgBr *mixtures*

Composition mol. % AgBr	A_{Ag^+}	E_{Ag^+} cal./ion	A_{Cu^+}	E_{Cu^+} cal./ion
100	$1\cdot5 \times 10^6$	20,600	—	—
90	1245	10,040	66	7540
80	850	8,460	7·3	3720
65	235	6,540	17·3	3960

Similar data for CuI-AgI mixed crystals are given in Table 63 [39].

The tables illustrate the loosening of the lattice by the

addition of the component having the least tightly bound conducting ion. For example, the energy term required for the migration of silver ions in CuBr-AgBr mixtures falls from 20,600 to 6540 cal. when 35 mol. % of CuBr have been added.
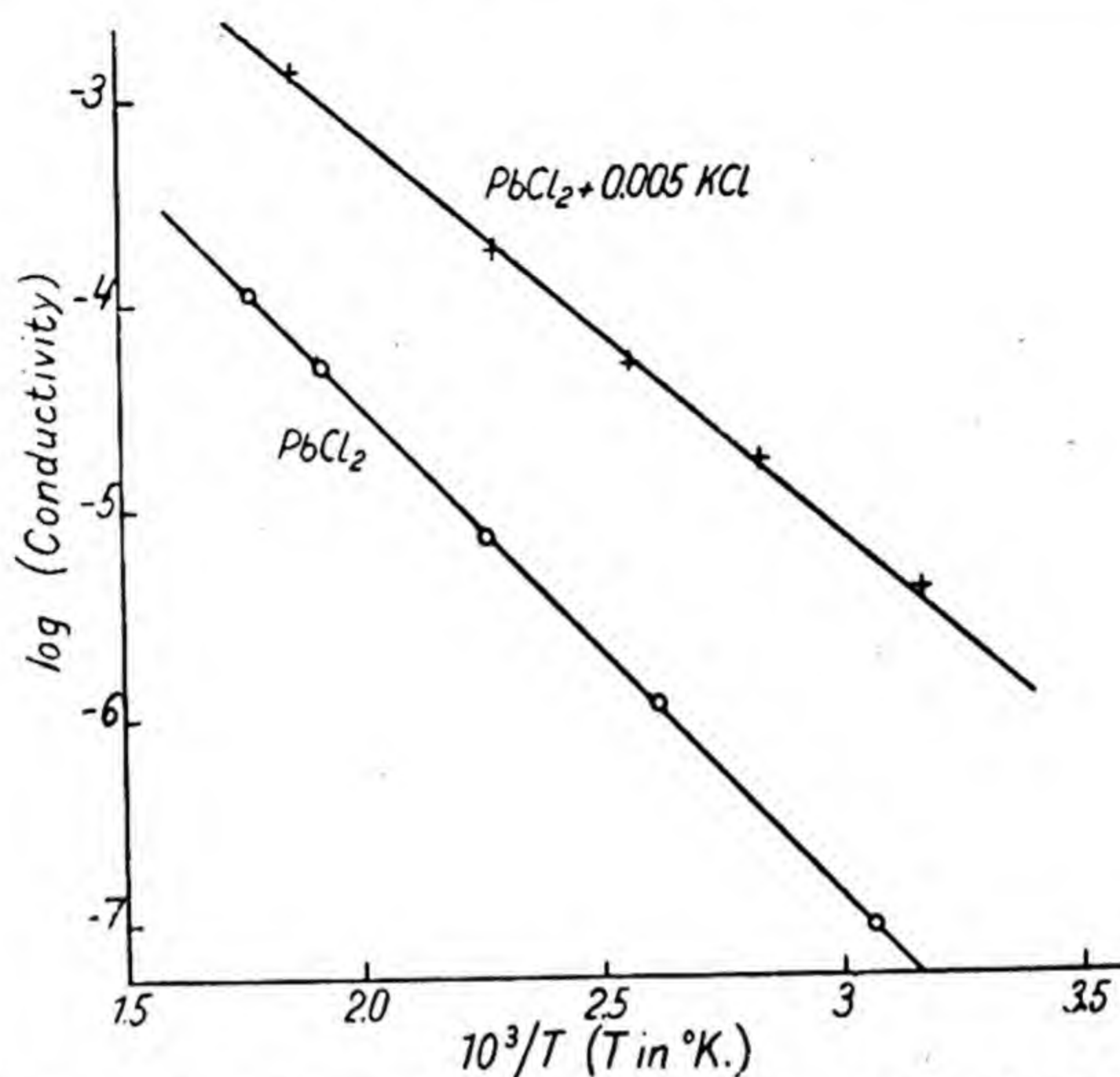
Fig. 96. The influence of potassium chloride on the conductivity of lead chloride (Gyulai[63]).

TABLE 63. *Constants in the equation*

$$K = A_{Cu^+}\, e^{-E_1/RT} + A_{Ag^+}\, e^{-E_2/RT} \; (\text{ohm}^{-1}\,\text{cm.}^{-1})$$

for the conductivity of CuI-AgI mixtures

Composition mol. % AgI	A_{Ag^+}	E_{Ag^+} cal./ion	A_{Cu^+}	E_{Cu^+} cal./ion
100	24·9	4600	—	—
95	36	5400	3·7	5400
90	26	4960	5·7	4960
70	10	3720	8	3720
50	6·3	3270	10·7	3270
30	2·8	2400	11·2	2400
0	—	—	5·5	1190

The same loosening has been effected for lead chloride by adding small amounts of potassium chloride, as Fig. 96[63] shows. It can be seen that the potassium chloride has reduced

the energy needed for rendering mobile the current-carrying ion, for the slope of the log K–$1/T$ curve is greater for $PbCl_2$ than for $PbCl_2 + 0{\cdot}005\,KCl$.

For KCl-NaCl solutions Smekal[62] proposed an equation with three exponential terms, since all three ions may act as current carriers:

$$K_{NaCl-KCl} = K_{Na^+} + K_{Cl^-} + K_{K^+}$$
$$= A_{Na^+}\, e^{-E_1/RT} + A_{Cl^-}\, e^{-E_2/RT} + A_{K^+}\, e^{-E_3/RT}.$$

(C) Some salts do not obey any simple conductivity-temperature law, as Fig. 94 illustrates in the case of cuprous bromide, and Fig. 95 for silver iodide and silver mercury iodide (Ag_2HgI_4). Each transition point shows a sharp break in the conductivity-temperature curve, and the conductivity of α-CuBr and α-AgI can actually be greater in the solid state than in the molten state. In the case of cuprous bromide one notes (Fig. 94) that in addition to the basic curve III some irreversible curves are also shown (I, IIa, IIb). This peculiarity is due to the extreme sensitivity of the conductivity of cuprous bromide to excess halogen, and to the difficulty of excluding traces of such impurities, which are sufficient to raise the conductivity by several powers of ten.

The extremely high mobility of silver ions in α-AgI and Ag_2HgI_4 has been the subject of a number of researches. The solution of their unique behaviour came from the studies of Strock[49] and Ketelaar[50] on silver iodide and silver mercury iodide respectively. Strock showed that while the anion lattice was in perfect order the cation lattice was almost completely disordered. The work of rendering the silver ions mobile is thus very small, and their conductivity high. Ketelaar found that the same property explained the conductivity-temperature curve of Ag_2HgI_4.

α-Ag_2S, α-Ag_2Se and α-Ag_2Te have also extremely high conductivities, and it was some time before the explanation of the conductivity values was forthcoming[64]. Ultimately, Wagner[65] pointed out that the conductivity of α-Ag_2S was sensitive to the sulphur-vapour pressure in the surrounding

gas phase. Therefore, just as for Cu_2O and similar oxides (p. 251), the conductivity is in part due to electrons. The electrons are supplied by reactions in the lattice such as

$$S'' \to S + 2e, \quad Se'' \to Se + 2e, \quad Te'' \to Te + 2e.$$
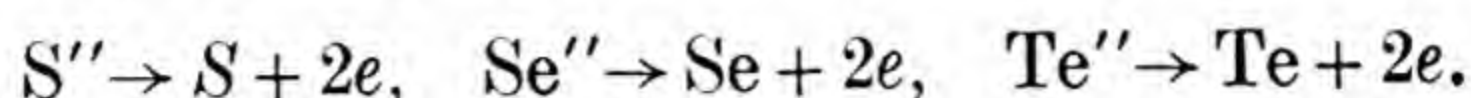
The values for the conductivity K, and the constants A and E in the formula $K = Ae^{-E/RT}$ for electrolytic conductors in which the conductivity is predominantly by one ion, are

TABLE 64. *Conductivity, and constants in the conductivity formula $K = Ae^{-E/RT}$ (Seith [39])*

Salt	Melting-point °C.	K (at the melting-point) ohm^{-1} cm.$^{-1}$	A ohm^{-1} cm.$^{-1}$	E cal./ion	E e.V.
LiF	842	$0 \cdot 6 \times 10^{-2}$	4×10^7	51,000 L.	2·20
LiCl	606	$1 \cdot 5 \times 10^{-2}$	5×10^7	38,000 L.	1·65
NaF	992	$1 \cdot 7 \times 10^{-3}$	$1 \cdot 5 \times 10^6$	52,000 L.	2·25
NaCl	800	$1 \cdot 3 \times 10^{-3}$	1×10^6	44,000 L.	1·90
NaBr	735	$1 \cdot 3 \times 10^{-3}$	1×10^6	41,200 L.	1·78
NaI	661	$4 \cdot 0 \times 10^{-3}$	$1 \cdot 5 \times 10^6$	33,000 L.	1·42
KF	846	$8 \cdot 0 \times 10^{-4}$	3×10^7	54,400 L.	2·35
KCl	768	$2 \cdot 0 \times 10^{-4}$	2×10^6	47,800 L.	2·06
KBr	728	$2 \cdot 0 \times 10^{-4}$	$1 \cdot 5 \times 10^6$	45,600 L.	1·97
KI	680	$1 \cdot 5 \times 10^{-4}$	3×10^5	41,000 L.	1·77
RbCl	717	$5 \cdot 0 \times 10^{-5}$	3×10^6	49,200 L.	2·12
RbBr	681	$3 \cdot 5 \times 10^{-5}$	$1 \cdot 8 \times 10^6$	47,000 L.	2·03
TlCl	427	$5 \cdot 0 \times 10^{-3}$	$2 \cdot 5 \times 10^3$	18,320 L.	0·79
TlBr	457	$5 \cdot 0 \times 10^{-3}$	$1 \cdot 7 \times 10^3$	18,560 L.	0·80
AgCl	455	$1 \cdot 0 \times 10^{-1}$	3×10^6	22,200 T.	0·96
AgBr	422	$6 \cdot 0 \times 10^{-1}$	3×10^6	20,600 T.	0·89
α-AgI	522	25	5·5	1,186 T.	0·05
Ag_2HgI_4	—	—	4×10^2	8,600 K.	0·37
$PbCl_2$	501	5×10^{-3}	6·6	10,960 S.	0·47
PbI_2	402	3×10^{-5}	$1 \cdot 2 \times 10^5$ (Pb^{++})	30,000 S.	1·30
			$9 \cdot 8 \times 10^{-4}$ (I$^-$)	9,360 S.	0·40

L. Lehfeldt.   T. Tubandt.   K. Ketelaar.   S. Seith.

summarised in Table 64. Lehfeldt [66] showed that the energy E in the conductivity equation $K = Ae^{-E/RT}$ depends upon the radius of the halogen ions in the lattice to a remarkable extent. His representation of this effect is given in Fig. 97. As the

anion increases in size, the energy needed to render the current-carrying ion mobile diminishes considerably. The effect is to be traced partly to the increasing polarisability of the anions with increasing radius. On the other hand, the polarising capacity of the cations increases in the order $Rb < K < Na < Li$. The polarisation energy liberated around vacant lattice sites tends to offset the work of forming the vacant site.
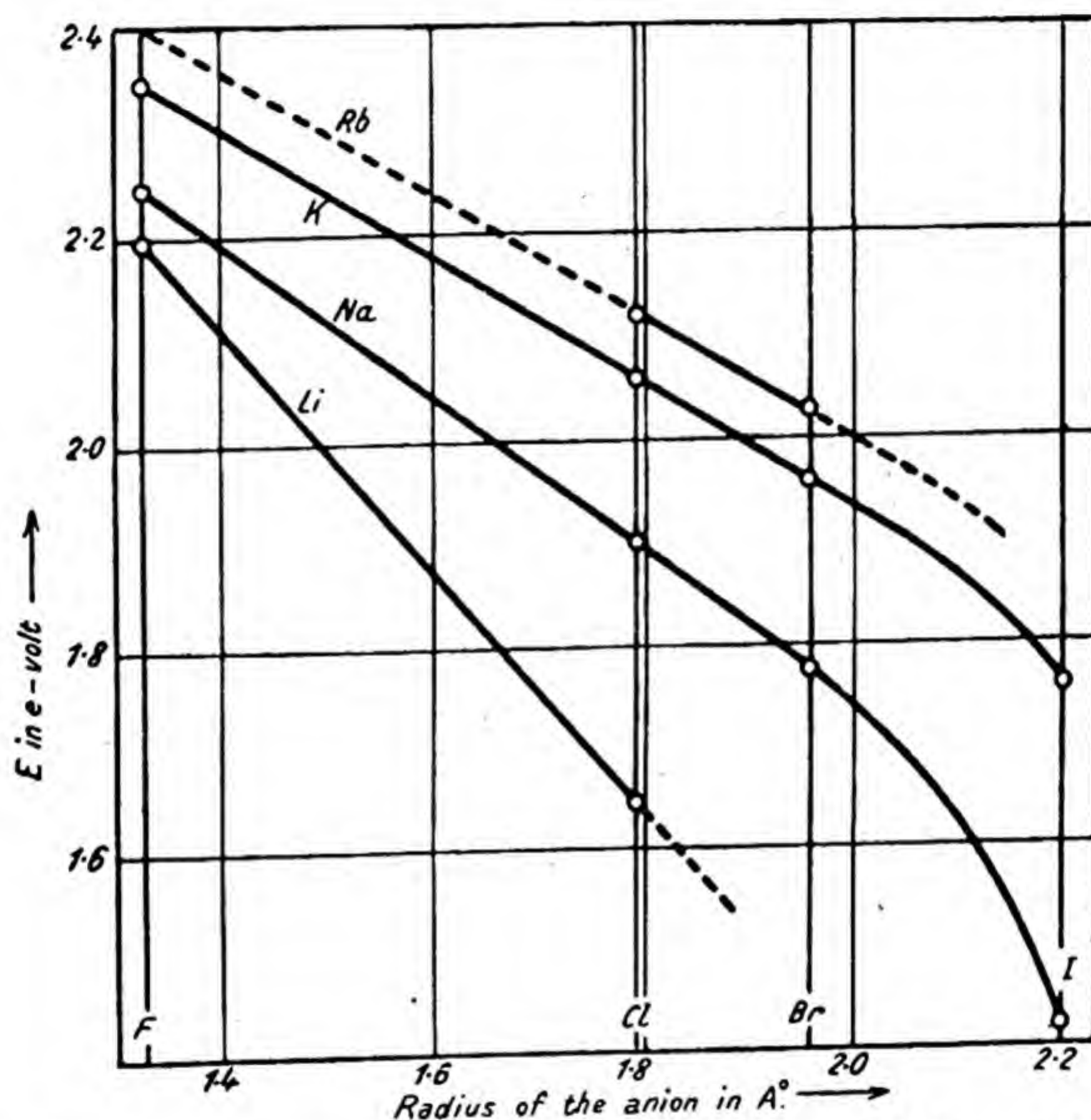
Fig. 97. Dependence of the energy E in the conductivity equation $K = Ae^{-E/RT}$ upon the anion radius (Lehfeldt[66]).

THE IDENTITY OF THE CURRENT-CARRYING IONS

The method of the radioactive indicator affords a simple means of determining whether the anion or cation is the conductor in a given salt. One has only to compare the expressions

$$K = Ae^{-E/RT}, \text{ for the conductivity } K,$$

and $$D = D_0 e^{-E/RT}, \text{ for the diffusion constant } D.$$

If the values of E are equal, the current carrier is the ion used as the indicator. An example of this method has been given elsewhere for lead iodide and lead chloride (p. 271).

The second method is the measurement of the transport number, for which the experimental technique was developed by Tubandt and his co-workers[39]. It was early discovered[67,68] that Faraday's laws were valid for the salts barium chloride and silver chloride, and thus that the current carriers are ions. Tubandt and his school carried these investigations much further by pressing salt cylinders together between metal electrodes and electrolysing the system. By weighing the cylinders and electrodes before and after electrolysis the amounts of material transported were estimated directly. However, it was shown that in many instances threads of metal formed stretching from anode to cathode, so that conduction soon became metallic. α-AgI did not behave in this manner, and it was sufficient to coat the electrodes with a protective layer of this salt to suppress the formation of metal threads. With a cell arranged as below:

$$Pt \mid \alpha\text{-AgI} \mid Ag_2S \mid Ag_2S \mid Ag_2S \mid Ag,$$
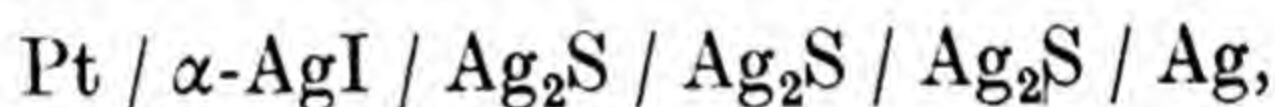
it was possible to measure the total current, the weight of silver deposited at the cathode, the weight of silver dissolved from the anode, and the loss or gain of weight of any intermediate silver sulphide cylinder. In this way it was found that the transport number of silver was unity. Nevertheless the result does *not* mean that Ag_2S is a pure cationic conductor, but only that any electrons in the silver sulphide lattice do not enter the silver iodide lattice. At the Ag_2S/AgI boundary both Ag^+ ions and electrons are liberated and removed, with formation of excess sulphur:

$$Ag_2S = S + 2e + 2Ag^+.$$
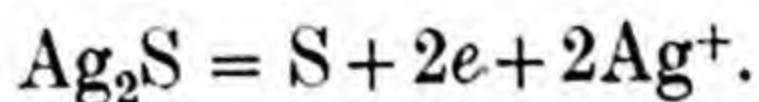
The Ag^+ ions move to the cathode, while the electrons move to the anode. Therefore in the AgI phase all the current is carried by Ag^+ ions, and the transport number measured by deposition of silver at the cathode is unity. The excess sulphur liberated at the phase boundary Ag_2S/AgI eventually reacts

with silver from the anode. Other examples of Tubandt's method do, however, speak unequivocally for cationic or anionic conductivity, especially if used in conjunction with a supplementary method such as that described in the next paragraph. The example of α-Ag_2S serves to indicate the type of difficulty encountered.

Finally, should the conductivity be sensitive to the pressure in a surrounding gas atmosphere of a component of the crystal, the investigations of Wagner and his school [51, 52, 43] have suggested that part of the conduction may be electronic (p. 251).

By the application of these methods the current-carrying ions have been identified in the instances given below. Inspection of these examples shows that in salts with ions of

Cationic conductors	Anionic conductors	Cationic and anionic conductors	Ionic and electronic conductors	Electronic
AgCl AgBr α-AgI $AgNO_3$ α-Ag_2HgI_4 (Hg^{++} and Ag^+) Alkali halides below 500° C.	PbF_2 $PbCl_2$ $PbBr_2$ BaF_2 $BaCl_2$ $BaBr_2$	PbI_2 Alkali halides near their melting-points	α- and β-Ag_2S α- and β-Ag_2Se α- and β-Ag_2Te α-CuI α-ZnO α-Cu_2O α-NiO α-FeO α-FeS etc.	Metals Fe_3O_4 PbS

different valency it is as a rule the ion of smallest valency which migrates under the applied E.M.F. The extent to which electronic and ionic conduction occur in the case of salts conducting by the two mechanisms may depend very much upon the temperature. Fig. 98 [54] shows that in α-CuI the conductivity becomes 100 % ionic at high temperatures, and 100 % electronic at low temperatures.

In the studies of the conductivity of metallic alloys (H_2-Pd, Au-Pb) it has been found that the alloying constituents may move in the lattice under the impressed E.M.F., so that the conductivity is not really completely electronic. The movements of dissolved hydrogen in palladium under an impressed

E.M.F. have been used to measure the charge on the hydrogen, and its mobility and diffusion constant (69) (Chap. V). The transference numbers of hydrogen are of course small. Seith (70) showed that if carbon is dissolved in iron it will move in an electric field towards the cathode, so that it is positively charged. The transport number for the solution Fe + 1 % C
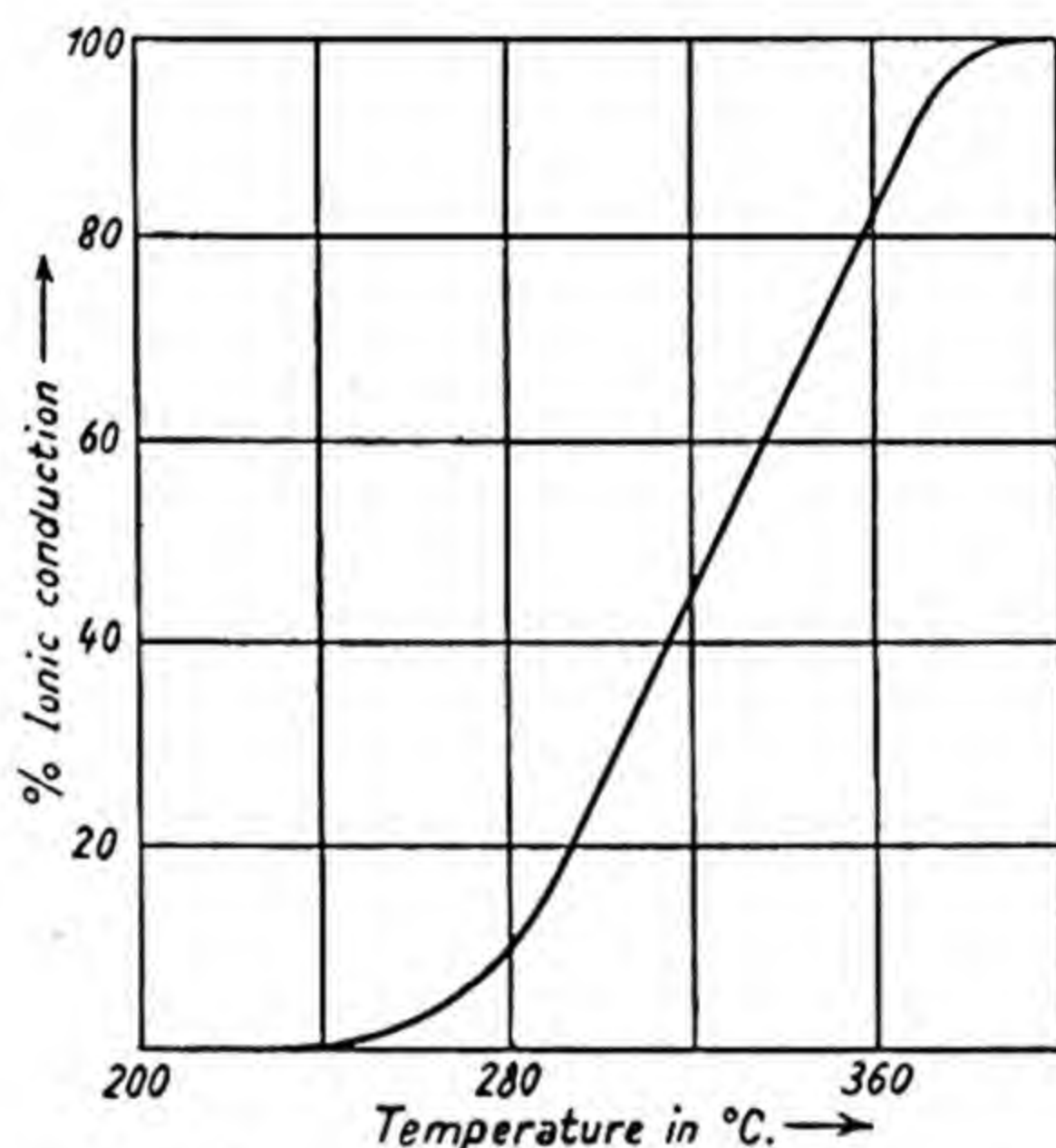
Fig. 98. The percentage of ionic conduction in α-CuI at various temperatures.

at 1000° C. was ~ 10^{-6}. The measurements were extended to alloys of gold in lead (71), and of gold in palladium or copper (72, 73), transport numbers being respectively 10^{-10} at 200° C. and 10^{-11} at 900° C. However, although ionic mobility may be demonstrated, it is of very slight importance compared with electronic conduction.

THE RELATION BETWEEN CONDUCTIVITY AND DIFFUSION CONSTANTS

Nernst (74), and later Einstein (75), found a relation between the diffusion constant in electrolytic solutions and the conductivity. The relation is

$$D = \frac{RT}{N_0} B,$$

where B denotes the steady velocity, or mobility, of the solute under unit force. Von Hevesy and his co-workers [76, 32], Braune [77], Tubandt, Reinhold and Jost [78] made use of an analogous expression in dealing with the conductivity of ionic crystals. The results justified the use of the Nernst equation at least qualitatively.

Wagner [79] made a quantitative calculation of the relationships involved, using thermodynamic and kinetic properties of the crystals. His treatment applied to mixed crystals of the type $Cu_2S + Ag_2S$, $PbCl_2 + PbBr_2$, $AgCl + AgBr$. If one denotes by Y_i the equivalent fraction of the species i of valence Z_i, then

$$Y_i = \frac{Z_i n_i}{\Sigma Z_i n_i},$$

where n_i gives the number of gram ions of the substance i in the solution. If the species "i" is cationic, the summation $\Sigma Z_i n_i$ refers only to the cations. If it is anionic, the summation refers only to anions. The concentration of the species i in equivalents/c.c. is

$$C_i = \frac{Z_i n_i}{V},$$

if V is the volume of the system. The mean velocity u_i of an ion of transport number U_i is given by

$$u_i = \frac{U_i K}{F C_i},$$

when u_i is the velocity under a gradient of 1 V./cm., F is the Faraday, and K the specific conductivity. Since a field of 1 V./cm. is equivalent to a force of $\frac{1}{300} (Z_i e)$ dynes on the ion (e denotes the electronic charge), one obtains as an expression for the mobility B_i, defined as the stationary velocity attained by the ion under a force of one dyne:

$$B_i = \frac{300 u_i}{Z_i e}.$$

If in a mixture of $Cu_2S + Ag_2S$ one denotes silver, copper,

and sulphur ions as species 1, 2, and 3 respectively, Wagner showed by considering both forced and natural diffusion that

$$D_{Ag^+} = D_1 = \frac{Z_1 B_1 (Z_2 B_2 + Z_3 B_3)}{Y_1 Z_1 B_1 + Y_2 Z_2 B_2 + Z_3 B_3} \frac{Y_2}{N_0} \frac{\partial(\mu_{Ag_2S})}{\partial Y_2},$$

$$D_{Cu^+} = D_2 = \frac{Z_2 B_2 (Z_1 B_1 + Z_3 B_3)}{Y_1 Z_1 B_1 + Y_2 Z_2 B_2 + Z_3 B_3} \frac{Y_2}{N_0} \frac{\partial(\mu_{Ag_2S})}{\partial Y_2}.$$

In these expressions, μ_{Ag_2S} denotes the chemical potential of Ag_2S, as defined by Gibbs. When the solution of Ag_2S in Cu_2S is dilute, $\dfrac{\partial \mu_{Ag_2S}}{\partial Y_2} = \dfrac{RT}{Z_2 Y_2}$, and the expressions for D_1 and D_2 are

$$D_1 = \frac{Z_1 B_1 (Z_2 B_2 + Z_3 B_3)}{Y_1 Z_1 B_1 + Y_2 Z_2 B_2 + Z_3 B_3} \frac{RT}{N_0} \frac{1}{Z_2},$$

$$D_2 = \frac{Z_2 B_2 (Z_1 B_1 + Z_3 B_3)}{Y_1 Z_1 B_1 + Y_2 Z_2 B_2 + Z_3 B_3} \frac{RT}{N_0} \frac{1}{Z_2}.$$

When the mobility of the anion is small compared with the mobility of the cations*, the terms containing B_3 may be omitted, and the equations reduce to

$$D_1 = D_2 = \frac{Z_1 B_1 B_2}{Z_1 Y_1 B_1 + Z_2 Y_2 B_2} \frac{RT}{N_0} \simeq B_2 \frac{RT}{N_0}$$

for dilute solutions of one salt in the other.

The mobility B_2 may be obtained from the transport number of the cations in the solid solution by means of the relationship

$$B_2 = \frac{300 u_2}{Z_2 e} = \frac{300}{F} \frac{U_2 K_2}{(Z_2 e) C_2}.$$

The relationship gives, in the simplest case, the connection between D and K,

$$D = \frac{RT}{N_0} \frac{300}{F} \frac{UK}{(Ze)C}.$$

---

* In a binary salt mixture, with a common non-diffusing anion, elementary considerations of electrical neutrality throughout the crystal will also show that, for natural diffusion, $-\dfrac{\partial C_1}{\partial x} = \dfrac{\partial C_2}{\partial x}$, and $D_1 \dfrac{\partial C_1}{\partial x} = -D_2 \dfrac{\partial C_2}{\partial x}$, if the cations have the same valency. Thus $D_1 = D_2$.

In this connection mention should be made of Frenkel's relation between K and D (Table 76). This is

$$K = \frac{N_1 (Ze)^2}{kT} D.$$

In this expression N_1 denotes the number of ions per unit volume, and the factor of proportionality turns out to be nearly unity. That the factor is actually small is illustrated by the expressions for the conductivity of lead iodide (Fig. 93), and for the self-diffusion constant of lead ions in lead iodide as measured by the method of the radioactive indicator. Thus

$$K_{Pb^{++}} = 1 \cdot 15 \times 10^5 \, e^{-\frac{30,000}{RT}} \text{ ohm}^{-1} \text{ cm.}^{-1},$$

$$D_{Pb^{++}} = 3 \cdot 43 \times 10^5 \, e^{-\frac{30,000}{RT}} \text{ cm.}^2 \text{day}^{-1}.$$

For lead chloride, on the other hand, only anionic conduction occurs, and the equations are

$$K_{Cl^-} = 6 \cdot 55 \, e^{-\frac{10,960}{RT}} \text{ ohm}^{-1} \text{ cm.}^{-1},$$

$$D_{Pb^{++}} = 6 \cdot 65 \times 10^5 \, e^{-\frac{36,800}{RT}} \text{ cm.}^2 \text{day}^{-1}.$$

TABLE 65. *Self-diffusion of* Ag^+ *in AgI from conductivity and diffusion measurements*

Temp. ° C.	454	500	551	594	651	701	744
$D_{(calc.)}$ cm.^{2} day^{-1}	2·14	2·68	3·32	3·86	4·60	5·25	5·85
$D_{(obs.)}$ cm.^{2} day^{-1}	1·53	2·00	2·48	2·88	3·46	3·98	4·19
α	0·71	0·75	0·75	0·75	0·75	0·76	0·72

Wagner's [79] treatment shows that the relationship

$$D = \frac{RT}{N_0} B$$

is only approximate. Tubandt, Reinhold and Jost [78] used the relation

$$D = \frac{RT}{N_0} B\alpha,$$

where α is a constant. They calculated the diffusion constant of silver in silver iodide from the conductivity, using Nernst's

equation, and compared the value so obtained with the self-diffusion constant (see below). Table 65(78) shows the value of α to be about 0·74.

DIFFUSION CONSTANTS IN METALS AND IONIC LATTICES

It has been indicated how the diffusion constant in a salt may be calculated from the ionic mobility of the current carrier (p. 268), or from the use of a radioactive isotope as an indicator (p. 244). Von Hevesy (31) considers that it will be possible to use the latter method to follow the self-diffusion of numerous metals (Table 59). The method can be extended in a few instances by using as indicators small quantities of certain salts in solid solution in a closely related salt(77, 78). For example, (78) small amounts of CuCl or NaCl were dissolved in AgCl. These mixtures are all cationic conductors in the temperature and concentration range investigated. The diffusion constants D_{Na^+} or D_{Cu^+} were measured, and also the conductivity, and transport numbers of each ion. These latter data served to calculate the ionic conductivities. The self-diffusion constant, D_{Ag^+}, was found for pure AgCl by assuming the correctness of the relation:

$$\frac{\text{Specific Ionic Mobility* of Ag}^+ \text{ in pure AgCl}}{\text{Specific Ionic Mobility of Na}^+ \text{ in mixed crystal}}$$
$$= \frac{\text{Self-diffusion Constant of Ag}^+ \text{ in pure AgCl}}{\text{Diffusion Constant of Na}^+ \text{ in same mixed crystal}}.$$

It was established that, at 238° C.,

$$D_{Na^+} = 3\cdot5 \times 10^{-6}\,\text{cm.}^2\,\text{day}^{-1},$$

where the specific mobility ratio = 25, and

$$D_{Cu^+} = 2\cdot1 \times 10^{-2}\,\text{cm.}^2\,\text{day}^{-1},$$

where the specific mobility ratio = 0·01.

Then the above relation gives for the self-diffusion constant 9×10^{-5} and $21 \times 10^{-5}\,\text{cm.}^2\,\text{day}^{-1}$ respectively. The agreement is satisfactory.

* Defined by $K_1' = \dfrac{U_1 K}{Y_1}$, where Y_1 and U_1 are the mol fraction and transport number of species 1 in a crystal of conductivity K. For pure AgCl, $K'_{Ag^+} = K$.

The results of a great many investigations are summarised in the following tables (Tables 66, 67). It will be seen that the diffusion constants in salts may roughly be divided into two groups, in one of which the energy needed to render the ions mobile is greater than 10 k.cal., and in the other it is less. In the second group of electrolytes fall those substances such as α-AgI, Ag_2HgI_4, CuBr, whose conductivity is unusually high. The Langmuir-Dushman expression (p. 298) for the diffusion constant is often used as a means of correlating the diffusion data. This equation gives for D

$$D = d^2 \frac{E}{N_0 h} e^{-E/RT},$$

where d is the lattice constant, E the activation energy for diffusion, and h is Planck's constant. The empirical nature of this equation is stressed elsewhere (p. 299), but its applicability in many cases is outstanding. In Tables 66 and 67 in the last column are given the values of E calculated from D and d. The point to be noted here is that for the salts of group II of Table 66 the equation does not hold (Smekal[62]), but that as a rule when the activation energy is large the equation is satisfactory.

Those diffusion systems which have been marked with an asterisk in Table 67 represent metal pairs which form a continuous series of mixed crystals. As a rule in such systems the value of D_0 is small, an important exception being self-diffusion processes (Pb in Pb: $D_0 = 5\cdot1$ cm.^{2}sec.$^{-1}$; Au in Au: $D_0 = 1\cdot26 \times 10^2$ cm.^{2}sec.$^{-1}$). The normal range of values of D_0 lies between 10^{-1} and 10^{-5} cm.^{2}sec.$^{-1}$. There are exceptions, however; for example, the diffusions of silicon and tin into copper give $D_0 = 1\cdot0 \times 10^4$ and $6\cdot7 \times 10^2$ cm.^{2}sec.$^{-1}$. D_0 for the self-diffusion of bismuth, in a direction perpendicular to the c-axis, reaches a value of $(1\cdot33—16\cdot3) \times 10^{45}$. It is difficult to assess the reproducibility of some of the data, since some of the diffusion processes listed are structure sensitive, but those for bismuth appear reasonably consistent (see Fig. 100). It is to be noted that the higher the

BD

18

activation energy the larger the factor D_0, although there is no simple relationship between them, and exceptions also occur. Some of these exceptions are, however, for structure-sensitive diffusions (Th-W, Mo-W) where diffusion does not occur solely through the lattice. Here the number of channels available for diffusion may be restricted to grain boundaries,

TABLE 66. *Diffusion constants of ions in salts according to the equation* $D = D_0 e^{-E/RT}$

System	D_0 cm.^{2} sec.$^{-1}$	E cal./ion	E (cal./ion) calculated by Langmuir-Dushman formula
Group I. Salts with $E > 10,000$ cal./ion			
Ag$^+$ in AgCl[46]	—	23,000	19,300
Ag$^+$ in AgBr[46]	—	19,000	21,000
Na$^+$ in NaCl[46]	—	11,800	35,000
Cl$^-$ in NaCl[46]	—	47,200	38,600
Pb^{++} in PbCl$_2$[46,80,32]	7·7	36,800	34,500
Pb^{++} in PbI$_2$[46,80,32]	4·9, 10·6	30,000	29,000
Cl$^-$ in PbCl$_2$[46,32]	—	11,000	18,000
Se″ in α-Ag$_2$S[62,81]	67 × 10^{-5}	20,040	—
Ag$^+$ in α-Cu$_2$Te[80,78]	2·4	20,860	—
Group II. Salts with $E < 10,000$ cal./ion			
I′ in PbI$_2$[46,32]	—	9,300	4,300
Ag$^+$ in α-CuI[62]	4·5 × 10^{-3}	6,760	—
Li$^+$ in α-AgI[80,62,78]	58·3 × 10^{-4}	4,570	—
Cu$^+$ in α-AgI[80,62,78]	16·3 × 10^{-5}	2,260	—
Cu$^+$ in α-Ag$_2$S[62]	46 × 10^{-5}	3,180	—
Cu$^+$ in α-Ag$_2$Se[63]	15·5 × 10^{-5}	2,940	—
Cu$^+$ in α-Ag$_2$Te[62]	3·85 × 10^{-5}	2,660	—
Ag$^+$ in α-Cu$_2$S[62,81]	32·7 × 10^{-5}	4,570	—
Ag$^+$ in α-AgI[46]	—	2,260	—

and so the factor D_0 becomes correspondingly small. On the basis of Eyring's [99] theory of diffusion (p. 302) a large value of D_0 implies a big entropy increase on passing into the activated state, or a large disturbance in the lattice in this state. The larger disturbances are usually found in self-diffusion processes, where the chemical similarity between the diffusing atom and the solvent is a maximum. One has in the large and small values of D_0 an analogy with the "fast"

TABLE 67. Diffusion constants in metals according to the equation $D = D_0 e^{-E/RT}$

System	D_0 cm.^{2} sec.$^{-1}$	E cal./atom	E (cal./atom) from Langmuir-Dushman equation
*Pb in Pb [32, 46, 80]	5·1	27,900	24,400
β-Tl in Pb [46, 80, 52]	3·7 $\times 10^{-2}$	21,000	22,400
β-Sn in Pb [46, 80, 82]	3·4 $\times 10^{-1}$	24,000	23,200
Au in Pb [46, 80, 71, 83]	4·9 $\times 10^{-1}$	13,000	13,300
Ag in Pb [80, 83]	7·5 $\times 10^{-2}$	15,200	—
Bi in Pb [80, 82]	7·7 $\times 10^{-3}$	18,600	21,900
Hg in Pb [80, 84]	3·6 $\times 10^{-1}$	19,000	—
Cd in Pb [80, 84]	~2·1 $\times 10^{-2}$	~18,000	20,000
Zn (9·58%) in Cu [80, 22]	3·2 $\times 10^{-2}$	42,000	41,000
Zn (29·08%) in Cu [80, 22]	5·8 $\times 10^{-3}$	42,000	38,000
Sn (10%) in Cu [85, 86]	—	40,200	40,000
*Au in Au [33]	1·26 $\times 10^{2}$	51,000	—
*Pd in Au [80, 87]	1·11 $\times 10^{-3}$	37,400	—
*Cu in Au [80, 87]	5·8 $\times 10^{-4}$	27,400	—
*Pt in Au [80, 87]	1·24 $\times 10^{-3}$	39,000	—
†Th in W (small grains) [85, 88]	7·5 $\times 10^{-1}$	94,000	96,700
†Th in W (large grains) [85, 88]	4·1 $\times 10^{-3}$	94,400	118,200
Th in W (volume) [35]	1·0	120,000	—
†U in W [85, 89]	1·0	100,000	100,500
†Yt in W [85, 89]	0·46	68,000	70,100
†Ce in W [85, 89]	1·0	83,000	82,700
†Zr in W [85, 89]	1·0	78,000	77,400
*†Mo in W (polycrystal) [46, 80, 90]	5 $\times 10^{-3}$	80,500	—
*Mo in W (single crystal) [46, 80, 90]	6·3 $\times 10^{-4}$	80,500	—
N$_2$ in Fe [85, 23]	1·07 $\times 10^{-1}$	34,000	38,100
C in Fe [80, 23, 91]	4·9 $\times 10^{-1}$	36,600	36,700
†C in W$_2$C [62]	—	108,000	—
Zn in (Cu + 4% Zn) [92]	1·57 $\times 10^{-3}$	34,100	—
Al in (Cu + 4% Al) [92]	6·34 $\times 10^{-2}$	40,400	—
Si in (Cu + 4% Si) [92]	1·0 $\times 10^{4}$	64,200	—
Sn in (Cu + 4% Sn) [92]	6·7 $\times 10^{2}$	54,000	—
*Cu in Ni [80, 93]	1·04 $\times 10^{-3}$	35,500	—
Cu in Ag [29, 80]	5·9 $\times 10^{-5}$	24,800	—
Sb in Ag [29, 80]	5·3 $\times 10^{-5}$	21,700	—
Sn in Ag [29, 80]	7·9 $\times 10^{-5}$	21,400	—
In in Ag [29, 80]	7·3 $\times 10^{-5}$	24,400	—
Cd in Ag [29, 80]	4·9 $\times 10^{-5}$	22,350	—
*Au in Ag [80, 94, 95]	1·1 $\times 10^{-4}$	26,600	—
	5·3 $\times 10^{-4}$	29,800	—
*Pd in Ag [80, 87]	4·16 $\times 10^{-6}$	20,200	—
Au in Ag-Au [92]	5·2 $\times 10^{-4}$	29,800	—
Ag-Pd (20% Pd) in Ag-Au [92]	7·0 $\times 10^{-6}$	20,200	—
Au-Pd in Ag-Au [92]	8·3 $\times 10^{-4}$	37,400	—
Cu in Ag-Au [92]	1·06 $\times 10^{-3}$	27,400	—
Au-Pt in Ag-Au [92]	1·28 $\times 10^{-3}$	39,000	—
†Bi in Bi ($\perp$ c-axis) [96, 80]	(1·33–16·3) $\times 10^{15}$	137,000	—
†Bi in Bi ($\parallel$ c-axis) [96, 80]	(2·2–6·5) $\times 10^{-4}$ to 6 $\times 10^{-4}$	30,000	—
Cu in Al [97]	2·3	34,900	31,400
Mg in Al [97]	1·5 $\times 10^{2}$	38,500	29,000
Cu in Cu [33a]	1·1 $\times 10^{1}$	57,200	—
Al in Cu [98]	1·2 $\times 10^{-2}$	37,500	—
Zn in Cu [98]	8 $\times 10^{-1}$	38,000	44,000
Sn in Cu [98]	1·0	45,000	—
Si in Cu [98]	5·2 $\times 10^{-2}$	39,950	—
Be in Cu [98]	4·5 $\times 10^{-5}$	27,900	—
Cd in Cu [98]	3·5 $\times 10^{-9}$	8,200	—
Zn in Cu + 20% Zn [98]	—	31,000	38,500
Al in Cu + 16% Al [98]	—	54,000	39,000

* Interdiffusing metals form a continuous series of solid solutions.

† Diffusion may show structure sensitivity (see next Chapter).

and "slow" reactions of chemical kinetics. In the former case the kinetic theory suggests accumulation of energy through many degrees of freedom, a viewpoint corresponding with a large disturbance of the lattice. A tentative explanation of the influence of chemical and physical similarity of solute and solvent upon the diffusion is advanced on p. 285.

It is also noteworthy that on the whole the activation energy for diffusion and for conductivity (Table 64) in ionic lattices is smaller than the activation energy for diffusion in metallic lattices. It is probable that this difference may be traced to the greater influence of polarisation forces in the case of salts, and to the greater density and so closer atomic packing in the case of many metals.

DIFFUSION ANISOTROPY

When diffusion occurs with different velocities along different crystallographic axes one has the phenomenon of diffusion anisotropy. It is of interest to see what examples can be found of diffusion anisotropy in salts and metals. This property has already been encountered in the sorption of gases by zeolites, heulandite (100), for example (Chap. III, p. 102), giving a very great anisotropy indeed, and being in one direction (perpendicular to the anionic laminae of this layer crystal) quite impermeable, and in two other directions easily but differently permeable. It should be noted that anisotropy in diffusion has never yet been observed in cubic crystals. One finds that diffusion of zinc into copper (101), of oxygen into copper-silicon alloys (102), and of carbon (103) or nitrogen (103) into iron, occurs with equal velocities in all directions.

Seith (82) showed that the conductivity of lead iodide could be expressed by the relation

$$K = 9 \cdot 78 \times 10^{-4} e^{-9300/RT} + 1 \cdot 15 \times 10^5 e^{-30,000/RT},$$

in which expression the first term refers to iodine ion transport and the second to the lead ion transport. The equation applied

to a compressed pellet of iodide for conductivity in the direction of the pressure, which caused the crystallites to orient themselves so that their c-axes coincided with the direction of pressure. The conductivity as shown by the following figure depends on the direction of diffusion [96] in the crystal to a very marked extent. Fig. 99 shows $\log K$ (K = conductivity) plotted against $1/T$ (T = temperature in ° K.), and the curves $2a$ and $2b$ are $\log K$–$1/T$ curves of different samples of lead iodide perpendicular to the c-axis, while 1 shows this conductivity curve parallel to the c-axis. The former curves have slopes of about 9000 cal. and the latter has a slope of 30,000 cal. One
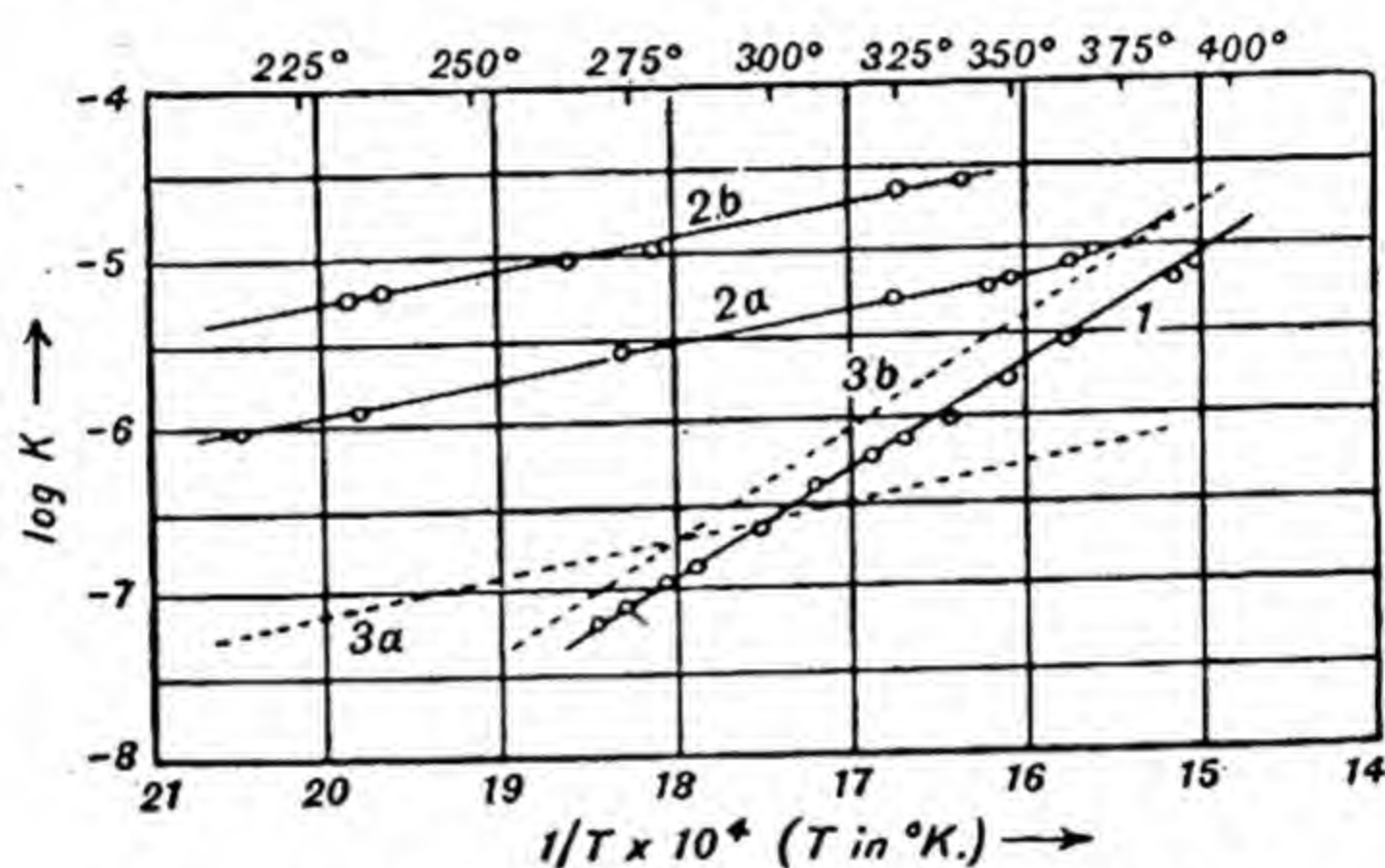
Fig. 99. Diffusion anisotropy in lead iodide.

concludes that the iodide ion carries most of the current normal to the c-axis, but the lead ion carries most of the current parallel to it. The anisotropy is several powers of ten at low temperatures, but is naturally temperature dependent, and seems to vary somewhat for different specimens. The curves $3a$ and $3b$ are plotted from the two terms of Seith's equation [32] given in this paragraph For the self-diffusion of lead ions in lead iodide the following diffusion constants were obtained (Table 68).

The table shows that diffusion anisotropy for lead ions may exist, but is slight compared with the anisotropy of the iodide ion. Like heulandite, lead iodide is a layer lattice, and it is the layer structure which is responsible for its behaviour in diffusion.

Both Warburg and Tegetmeier [104] and Joffé [105] observed

TABLE 68. *Self-diffusion of lead ions in lead iodide*
(cm.^{2} day^{-1}) (using ThB as radioactive indicator)

Number	Temp. ° C.	D (cm.^{2} day^{-1})	Remarks
1	323	$6{\cdot}14 \times 10^{-6}$	$\perp$ to c-axis
2	316	$5{\cdot}02 \times 10^{-6}$	$\perp$,,
3	306	$2{\cdot}05 \times 10^{-6}$	$\perp$,,
4	278	$5{\cdot}94 \times 10^{-7}$	$\perp$,,
5	262	$3{\cdot}31 \times 10^{-7}$	$\perp$,,
1	317	$2{\cdot}50 \times 10^{-6}$	$\parallel$,,
2	314	$2{\cdot}57 \times 10^{-6}$	$\parallel$,,
3	300	$3{\cdot}26 \times 10^{-6}$	$\parallel$,,
4	268	$2{\cdot}67 \times 10^{-7}$	$\parallel$,,

anisotropy in the conductivity of quartz. Perpendicular to the crystal axis the conductivity is 10^{4-6}-fold greater than parallel to the axis, although the temperature coefficient was the same in both directions. A third example of diffusion anisotropy is provided by bismuth [96]. Self-diffusion parallel and perpendicular to the c-axis, using ThC as radioactive indicator, gave an anisotropy of up to 10^6-fold (Fig. 100). The figure shows that parallel to the c-axis the activation energy for diffusion is 30 k.cal., but that perpendicular to it the activation energy is 137,000 cal.

Another study of the same type [106] was made of the diffusion of mercury into single crystals of cadmium or zinc. In both cases the diffusion was a maximum parallel to the basal

Fig. 100. Self-diffusion in Bi. (1) Parallel to c-axis, (2) perpendicular to c-axis (Seith[96]).

planes and a minimum perpendicular to them. On the basal planes mercury drops gave circular diffusion, while all other

planes gave ellipses with the major axis parallel to the basal plane. The ellipticity diminished as the temperature was raised. Similarly, Spiers (107) observed, during the spreading of mercury on tin, that the mercury diffused into ellipses.

THE INFLUENCE OF CONCENTRATION UPON THE DIFFUSION CONSTANTS IN ALLOYS

When silver ions move in a silver halide lattice the concentration of ions within the lattice is fixed by the number of lattice points available to silver, per unit volume. When, however, gold diffuses into lead, or lead into gold, concentration gradients of one metal into the other are established, and it is then necessary to find whether the diffusion constant D varies with the concentration, in order to interpret the data. This means that one must use not the equation $\dfrac{\partial C}{\partial t} = D\dfrac{\partial^2 C}{\partial x^2}$ but the equation $\dfrac{\partial C}{\partial t} = \dfrac{\partial}{\partial x}\left(D\dfrac{\partial C}{\partial x}\right)$ and the method of Matano (108) (Chap. I). The concentration gradients may be measured by any of the methods outlined for the normal Fick law, the most usual being by spectroscopic, X-ray, or chemical analysis of thin layers adjacent to the interface.

The application of the equation $\dfrac{\partial C}{\partial t} = \dfrac{\partial}{\partial x}\left(D\dfrac{\partial C}{\partial x}\right)$ to the copper-nickel system then gives for the variation of D with the percentage of copper the curve of Fig. 101 (108). The value of D does not alter very markedly until the copper constitutes 80 % of the alloy. Then, however, a rapid increase occurs. Fig. 102 shows similar effects of composition upon the diffusion constants in Au-Ni, Au-Pd and Au-Pt alloys. As the percentage of alloying metal increases the constants at first remain fairly steady with decreasing gold content, but after a certain threshold value a much more rapid increase is observed. Similarly, Table 69 shows the diffusion constants of a number of metals in copper at 750° C., along with other data which will be discussed later. It can be seen again that the diffusion

constants alter with changing concentration of the diffusing metal.

The diffusion of Al, Be, Cd, Si, Sn and Zn in copper was subjected to the Matano method of analysis by Rhines and Mehl[98], with the result that in every instance the diffusion constant was found to vary with concentration. In all cases the diffusion in nearly pure copper was less rapid than diffusion
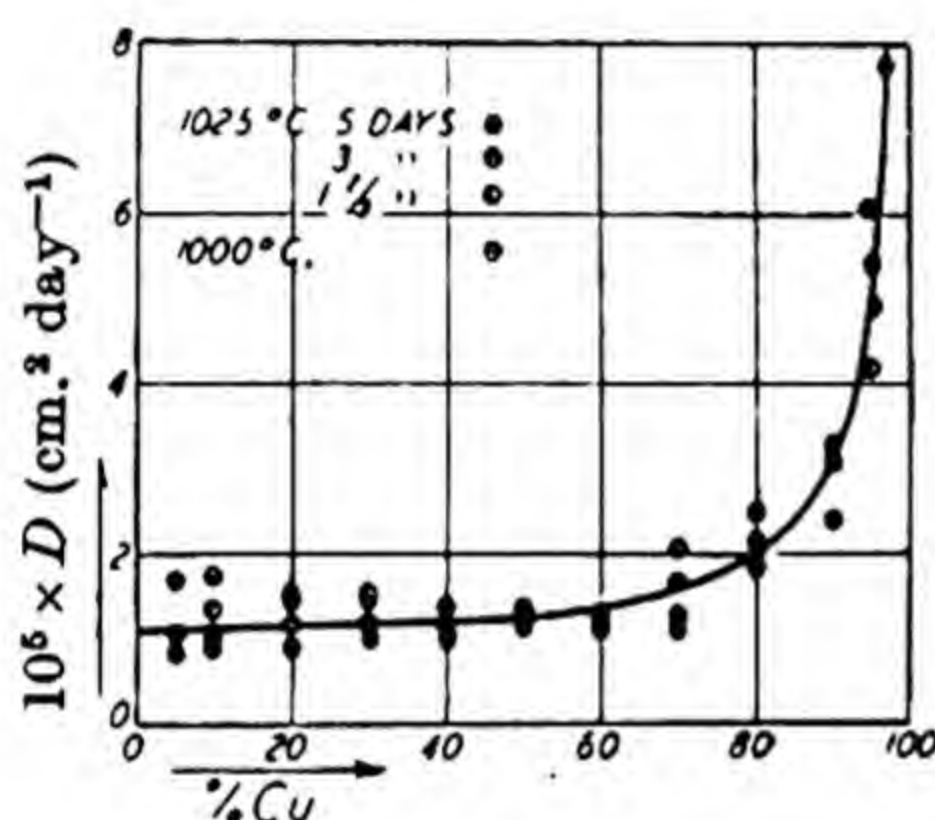
Fig. 101.
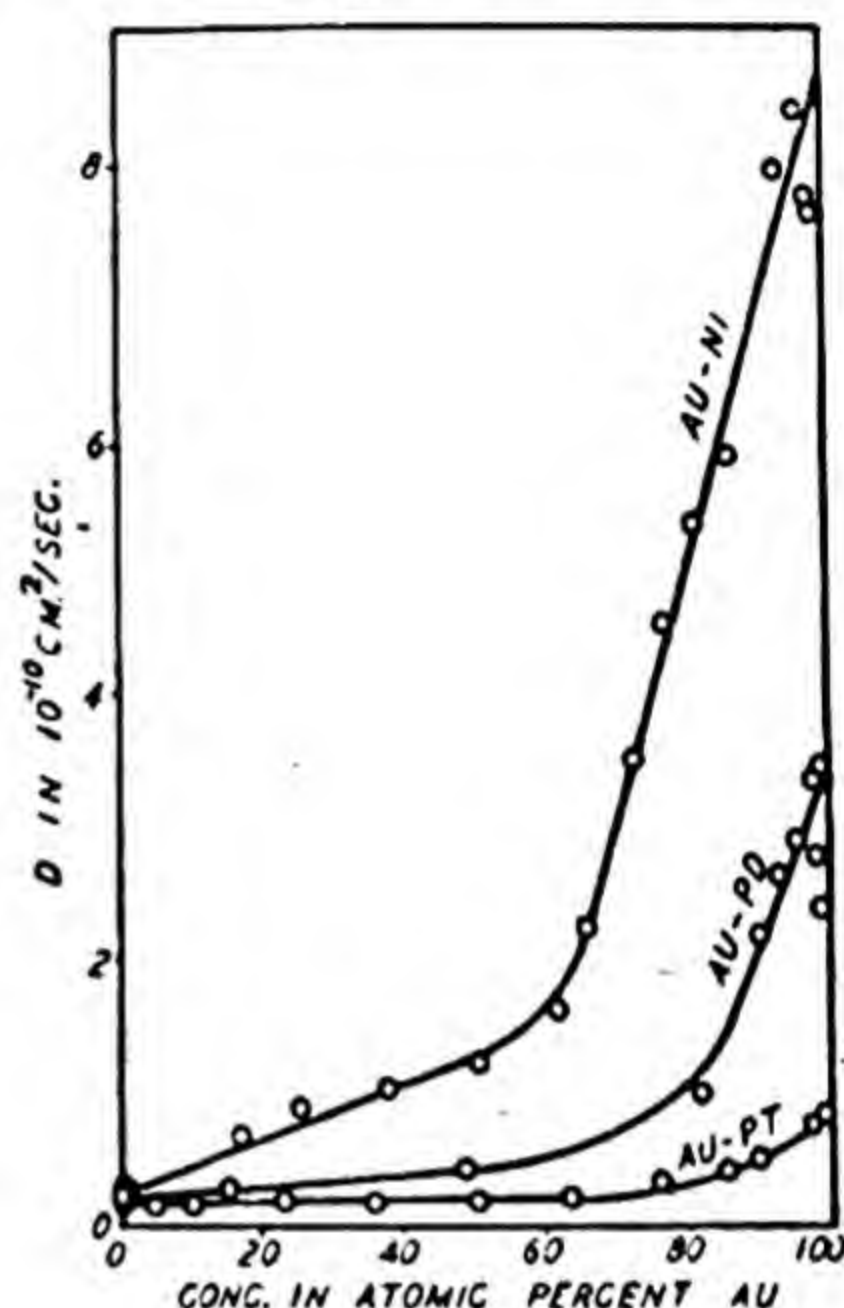
Fig. 102.

Fig. 101. The diffusion constant as a function of composition for a nickel-copper alloy (Matano[108]).

Fig. 102. The diffusion constant at 900° C. for the inter-penetration of Au and Ni, Pd and Pt as a function of composition of the Au-Ni, Au-Pd, and Au-Pt alloys (Mehl[92] after Matano[108]).

in the alloy (Fig. 103) and rose at first slowly and then rapidly with increasing amounts of the solute. It is made apparent from these data that the diffusion constant is generally concentration-dependent, and that the application of the normal Fick equation to metal-metal systems can yield only an average value of D, and may therefore lead to errors in evaluating D_0 and E in $D = D_0 e^{-E/RT}$. Many more diffusion studies, using the Matano method, are essential before the relationships between D_0 and E can be put upon a quantitative basis.

From measurements of D which have been derived by the Matano treatment of the law $\frac{\partial C}{\partial t} = \frac{\partial C}{\partial x}\left(D\frac{\partial C}{\partial x}\right)$, trends in the

TABLE 69. *The diffusion of metals in copper*

Metal composition	Zn from base 13.6% alloy			Zn from base 29.6% alloy			Al from base 17.8% alloy			Si from base 10.85% alloy			Sn from base 5.6% alloy		
	0% Zn	4% Zn	10% Zn	0% Zn	4% Zn	10% Zn	0% Al	4% Al	16% Al	0% Si	4% Si	8% Si	0% Sn	4% Sn	5% Sn
$D \times 10^{-10}$ cm.^{2} sec.$^{-1}$ at 750° C.	1·4	1·5	3·2	3·1	3·6	5·6	1·6	1·7	10·8	2·0	2·8	8·6	2·1	22·2	33·5
Activation energy, E	—	34,100	—	—	31,400	—	—	40,400	—	—	64,200	—	—	56,000	—
Crystal habit of solute	C.p.h.			C.p.h.			F.c.c.			Diam.			Tetrag.		
Solid solubility at the peritectic temperature in atomic %	32			32			16			11			75		
Atomic radii (Goldschmidt) in A.	1·374			1·374			1·40			—			1·582		
Melting-point of solute ° C.	419·4			419·4			660			1420			231·9		
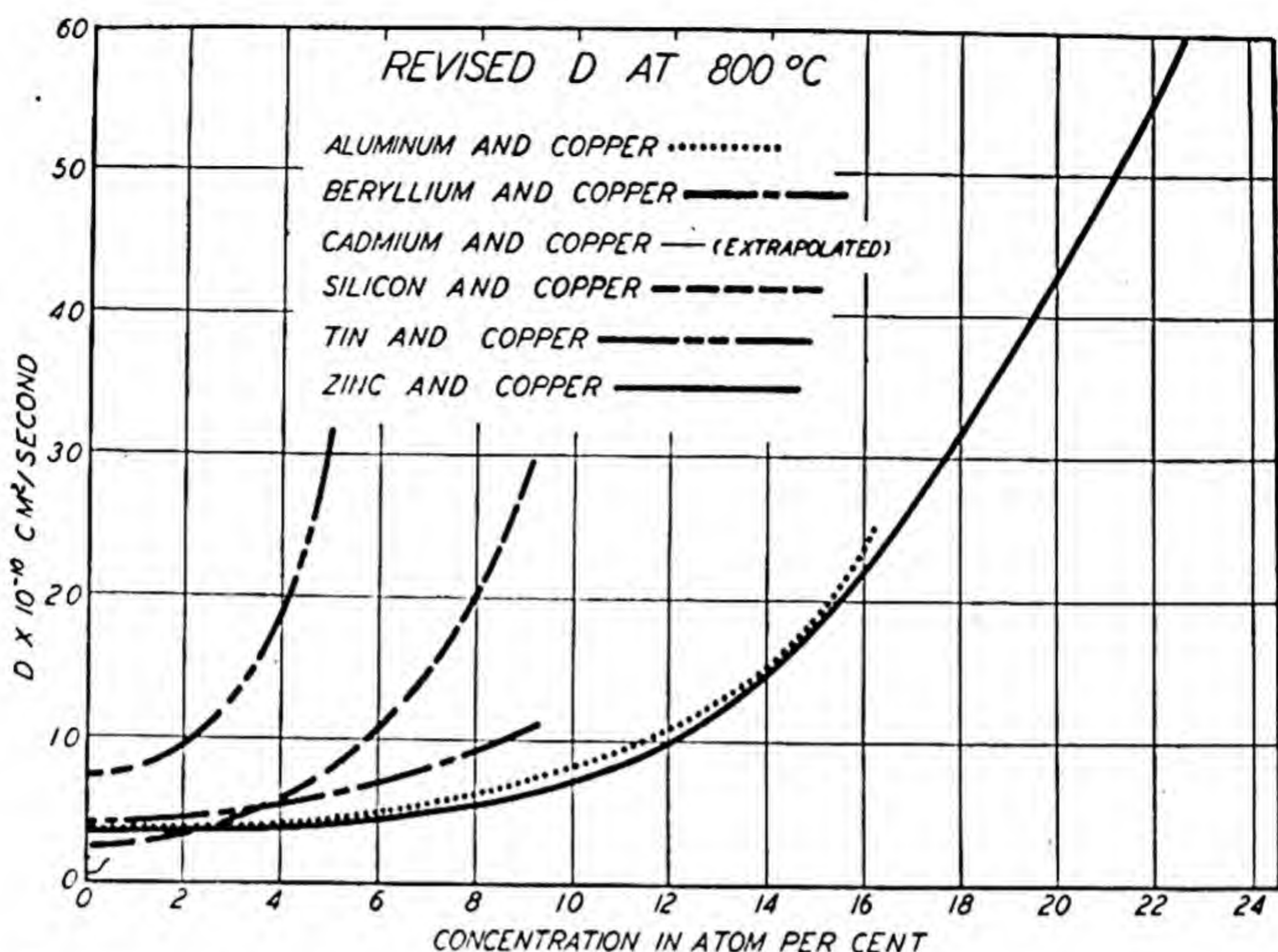
Fig. 103. Selected average diffusion coefficients interpolated to 800°C. for Cu-Al, Cu-Be, Cu-Cd, Cu-Si, Cu-Sn and Cu-Zn systems (Rhines and Mehl[98]).
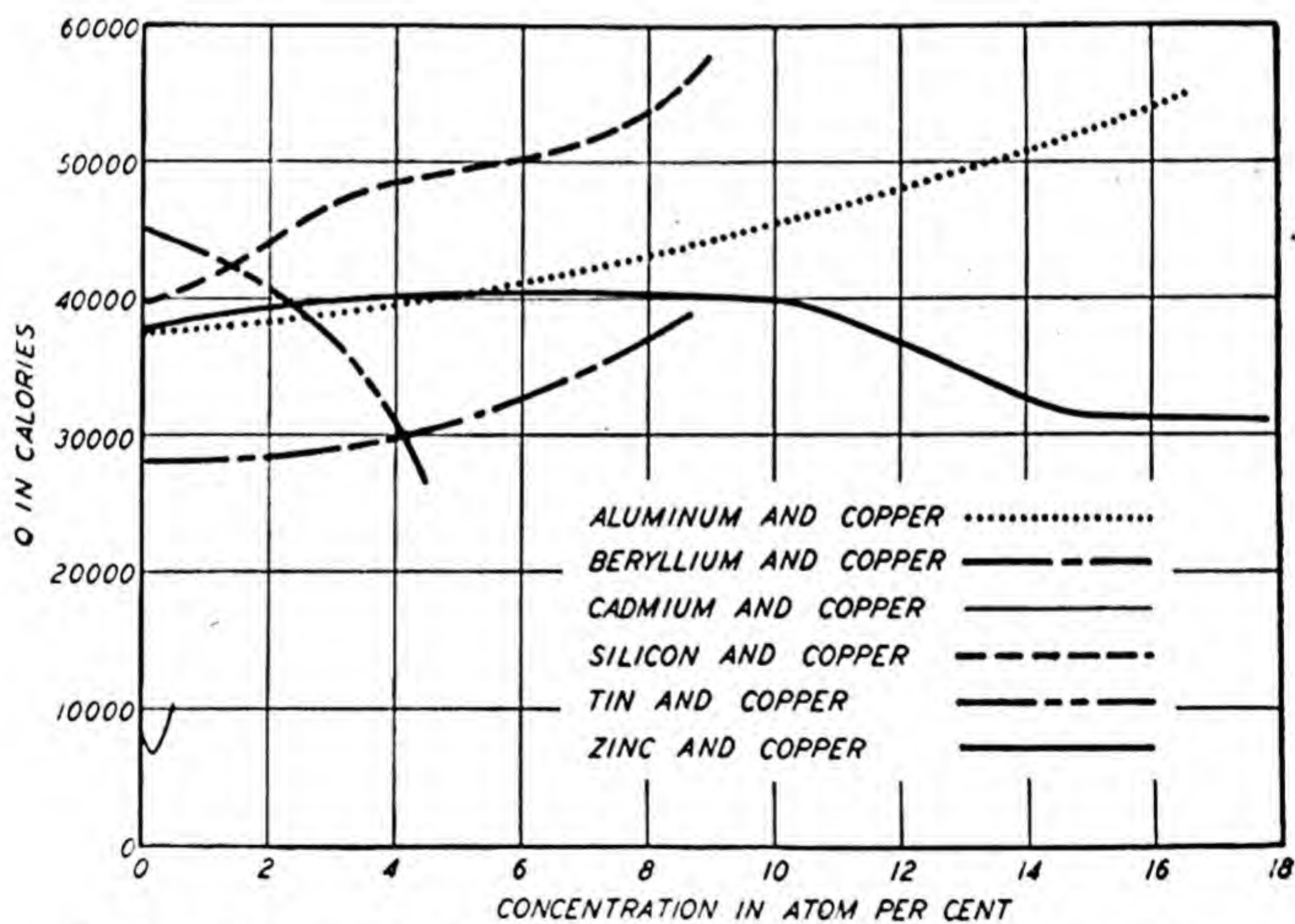
Fig. 104. Relationship between E and the concentration for the systems Cu-Al, Cu-Be, Cu-Si, Cu-Sn, Cu-Zn (Rhines and Mehl[98]).

activation energy for diffusion may also be obtained. These trends (Fig. 104) in E with concentration are usually initially slight, but may become large and rapid at higher concentrations. The data of Mehl(92) for the system Al-Cu follow an approximately linear law $E \propto$ [conc. of Al]². The values of the energy of activation for the diffusion process can be seen in Fig. 104(98) both to increase and to decrease with increasing concentration of the alloying material. In some instances, therefore, the solute is more easily loosened in the lattice by the alloying process, in others the converse is true.

SUMMARY OF FACTORS INFLUENCING DIFFUSION CONSTANTS

Some factors which influence the diffusion velocity and conductivity have already been indicated:

(a) It has been seen that, when certain types of disorder exist in a crystal lattice, an increasing partial pressure of the electronegative component may alter the conductivity (O_2 in FeO, Cu_2O, NiO, ZnO, CdO; S in FeS; Br_2 in CuBr; I in CuI).

(b) The constants D, D_0 and E in the equation

$$D = D_0 e^{-E/RT}$$

have been shown to depend very much upon the concentration of solute in the solvent metal.

(c) The importance of polarisability has been observed. The data of Table 66 showed how a high polarisability of ions in a lattice may reduce the term E in the conductivity equation $K = A e^{-E/RT}$. In polarisable salts (AgI, Ag_2S, CuBr) the activation energy E is small ($< 10,000$).

(d) Lehfeldt's diagram (Fig. 97), showing the connection between E for a series of alkali halides and the radius of the halogen ions, indicated that with increasing radius of the halide ion the energy E diminished; and with increasing radius of cation E increased. This relation may also be due in part to polarisation.

It is now interesting to see what other factors can alter diffusion constants. Tables 70, 71 and 72 give the diffusion

TABLE 70. *Diffusion of metals in lead*

Metal	Au	Ag	Cd	Bi	Tl	Sn	Pb (self-diffusion)
D cm.^{2} sec.$^{-1}$ at 285° C.	4.6×10^{-6}	9.1×10^{-8}	2×10^{-9}	4.4×10^{-10}	3.1×10^{-10}	1.6×10^{-10}	7×10^{-11}
Activation energy	13,000	15,200	18,000	18,600	21,000	24,000	28,000
Crystal habit of solute	F.c.c.	F.c.c.	C.p.h.	Rhombic	F.c.c.	Tetrag.	F.c.c.
Maximum solid solubility (atomic %)	0.05	0.12	17	35	79	29	100
Atomic radii (A.) after Goldschmidt	1.44	1.44	1.52	1.82	1.71	1.58	1.74
Melting-point of solute ° C.	1062	960	321	271	303	232	327

TABLE 71. *Diffusion of metals in silver*

Metal	Sb	Sn	In	Cd	Au	Pd
D cm.^{2} sec.$^{-1}$ at 760° C.	1.4×10^{-9}	2.3×10^{-9}	1.2×10^{-9}	9.5×10^{-10}	3.6×10^{-10}	2.4×10^{-10}
Activation energy	21,700	21,400	24,400	22,350	26,600	20,200
Crystal habit of solute	Rhombic	Tetrag	F.c., tetrag.	C.p.h.	F.c.c.	F.c.c.
Maximum solubility of solute in atomic %	5	12	19	42	100	100
Atomic radii (A.) after Goldschmidt	1.614	1.582	1.569	1.521	1.438	1.372
Melting-point of solute ° C.	630.	231.9	155	320.9	1063	1555

constants of metals in lead, in silver, and in noble metals [92]. Table 69 (p. 281) gives the same data for copper [92]. Examination of these and other data indicates the following properties of diffusion systems:

(i) The melting-point and atomic radius of the solute show no direct connection with the diffusion constant in lead and silver (Tables 70 and 71), since the trend is in opposite directions for lead and for silver.

(ii) The diffusion constant is smaller the greater the melting-point of the *solvent*.

The influence of the melting-point of the solvent upon the diffusion constant is large, and there exists in a number of instances a well-defined relationship between the energy E in the equation $D = D_0 e^{-E/RT}$ and the melting temperature:

System	Cu in Au	Cu in Ni	Mo in W
Melting-point of solvent temp. ° K.	1356	1728	3743
E/T_m	20·2	20·6	21·3

The influence of the melting-point upon the diffusion constant was the basis of attempts by Braune [94] and by van Liempt [109] to incorporate the empirical relationship of Table 76 in equations for the diffusion constant $D = D_0 e^{-E/RT}$ by writing $E = b^2(T_m/T)$, where b is a constant. These formulae will be referred to later (p. 301).

(iii) The diffusion constant depends inversely upon the solid solubility, being least for metals which form a continuous series of mixed crystals, or for self-diffusion.

The influence of solubility may be explained in the following way (cf. p. 274). When the atoms of solute and solvent are identical, the solute occupies a lattice site in the crystal without distorting the lattice. When the atoms of solute and solvent are dissimilar, the solute atom distorts the solvent lattice until in the extreme case it is thrown out of solution. The difference in degree of disorder between the normal and transition states of the solute atom before and in the act of diffusing respectively

TABLE 72. *Diffusion of metals in Ag (r = 1·642 A., melting-point 960·5° C.) and Au (r = 1·438, melting-point 1063° C.)*

Diffusion system	Au (diffusing in Ag)	Au-Ag alloy	Ag-Pd alloy 20% Pd	Au-Cu alloy 10% Cu	Ni (in Au)	Pd (in Au)	Au-Pd alloy	Pt (in Au)	Au-Pt alloy
D cm.^{2} sec.$^{-1}$ at 900° C.	$1·16 \times 10^{-9}$	$1·6 \times 10^{-8}$	$1·1 \times 10^{-9}$	$5·0 \times 10^{-9}$	$0·34 \times 10^{-10}$ Ni rich $6·0 \times 10^{-10}$ Au rich	$0·22 \times 10^{-10}$ Pd rich $2·3 \times 10^{-10}$ Au rich	$1·0 \times 10^{-10}$	$0·16 \times 10^{-10}$ Pt rich $0·61 \times 10^{-10}$ Au rich	$0·77 \times 10^{-10}$
Activation energy	29,800	26,600	20,200	—	—	—	37,400	—	39,000
Atomic radii (A.) after Goldschmidt	1·438	—	—	—	1·244	1·372	—	1·385	—
Melting-point, ° C.	1063	—	—	—	1452	1555	—	1755	—

is therefore much less when solute and solvent are dissimilar than when they are similar. The additional energy needed to loosen the lattice sufficiently for diffusion to occur is accordingly less for dissimilar than for similar atoms. At the same time the entropy of activation is greater for the similar than for the dissimilar atoms. This entropy of activation is defined by (p. 303)

$$D = D_0 e^{-E/RT}, \quad D_0 = e^{\Delta S \pm /R} \frac{kT}{h} d^2 \frac{1}{2 \cdot 72},$$
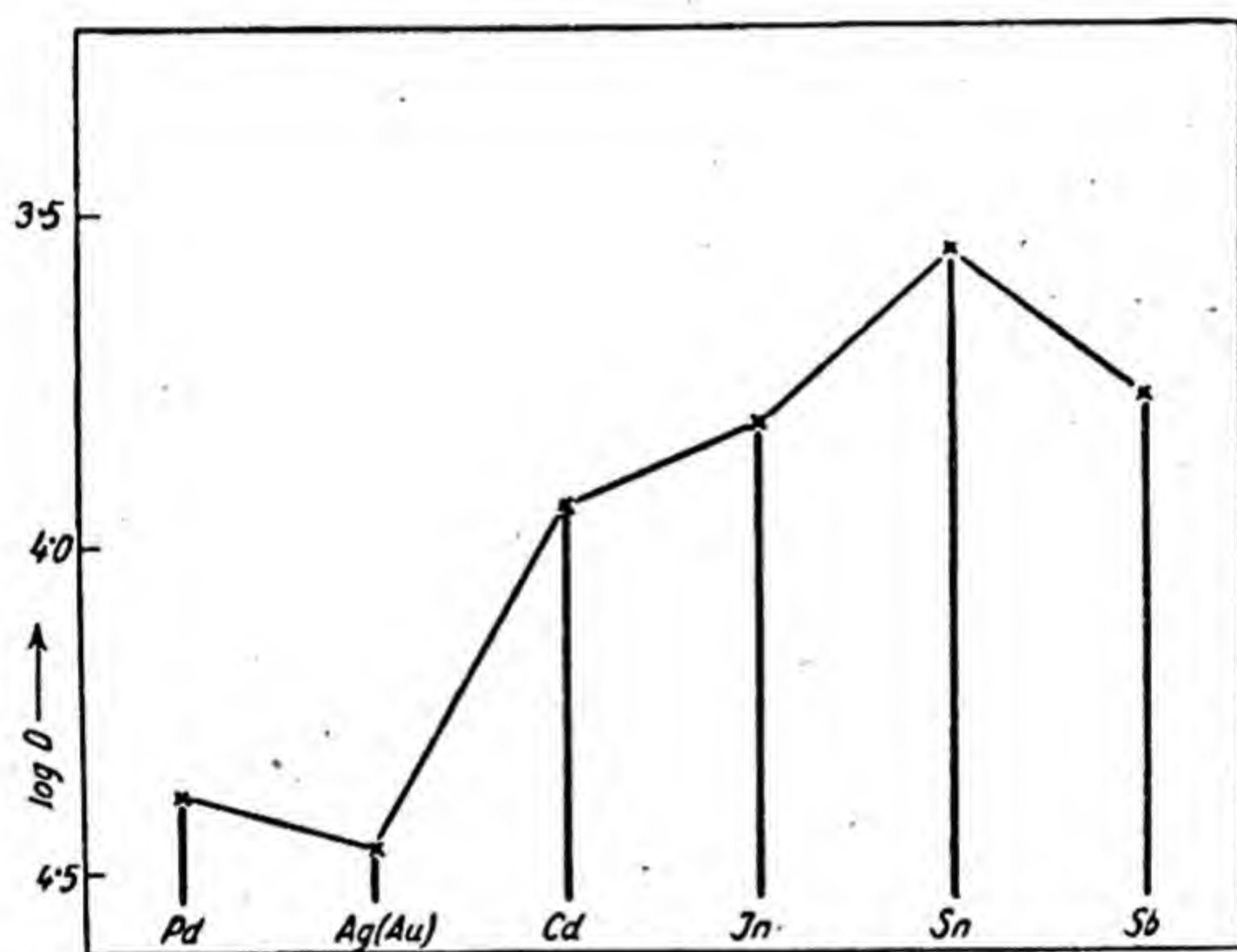
Fig. 105. Diffusion constants of metals in silver at 800° C.
(D in cm.^{2} day^{-1}.)

where d denotes the mean free path (identified normally with the lattice parameter), h is Planck's constant, and k is Boltzmann's constant. These two effects act in opposite directions, but the net result is a diminution in D with increased solid solubility.

Data giving the diffusion constants of a number of metals in lead are given in Fig. 106 [46, 92]. Here also one sees the diminishing diffusion rates with increasing solid solubility. An interesting method of representing the diffusion data in lead and in silver has been adopted by Seith and Peretti [29], and the data given (Fig. 105 [56]) illustrate in another way this dependence of the diffusion rate upon the mutual solubility. These figures also show definite trends in D with the position

of the solute and solvent in the periodic table. This position governs in part the mutual solubility of the diffusing elements.

It may be considered as surprising that so far no relationship between diffusion velocities and the atomic radii of solute and solvent has emerged. That such relationships may exist has, however, been shown by Sen [110], who demonstrated the following rule. In a pair of solids M and N the direction of most rapid diffusion is from M to N when the minimum distance of approach of atoms in N is greater than the same distance in M. The rule is illustrated by Table 73. It is thus to be anticipated that small atomic size of solvent will usually favour slow diffusion, unless the solute diffusing is of even smaller atomic radius.

Valence and polarisation effects are observed in metals as in ionic lattices, especially where zinc, cadmium, mercury, and thallium act as solvent metals. Similarly with copper, silver,
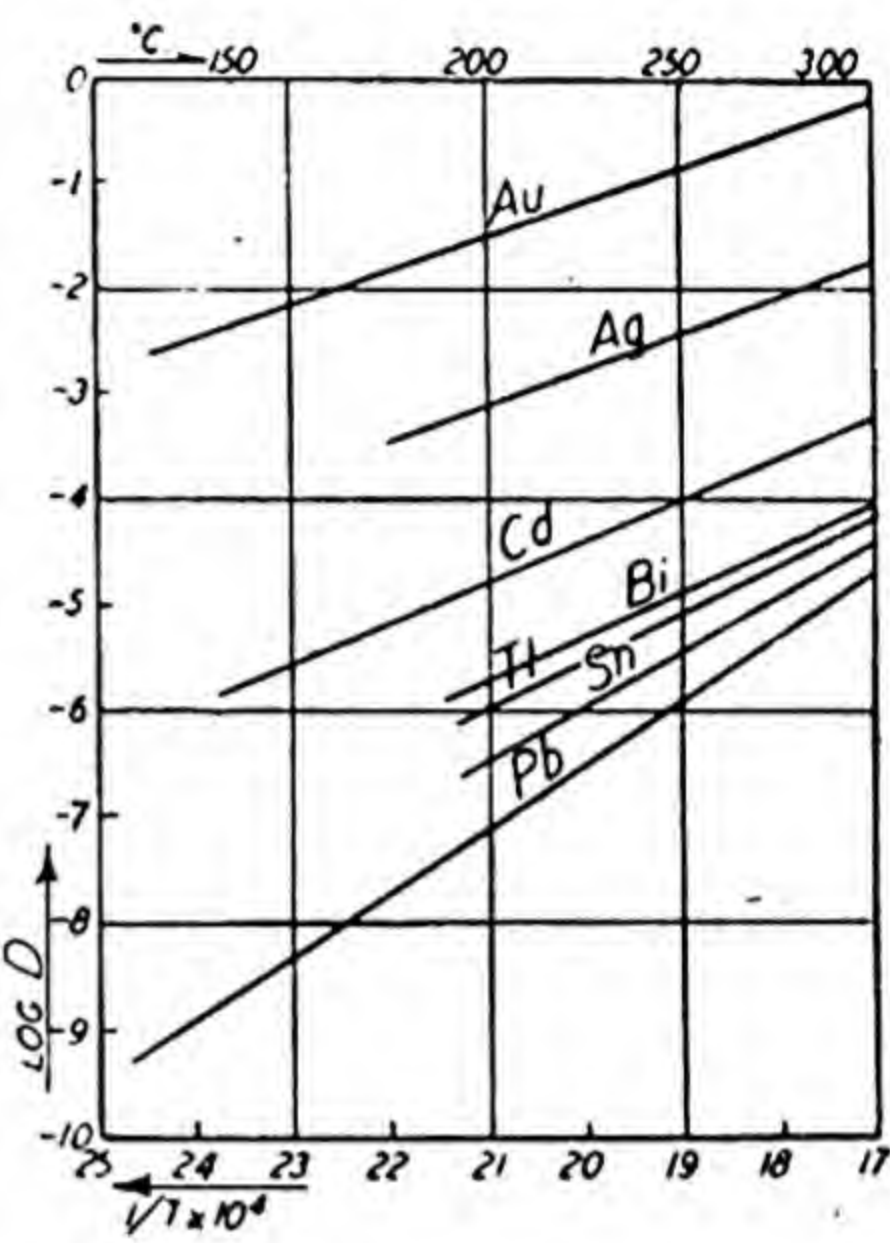
Fig. 106. Diffusion constants of various metals in lead (D in cm.^{2} sec.$^{-1}$).

TABLE 73. *Effect of atomic radius upon direction of diffusion*

System	Minimum distance of approach in cm.		Direction of diffusion
Cu-Pt	Cu : $2\cdot54 \times 10^{-8}$	Pt : $2\cdot78 \times 10^{-8}$	Copper into platinum
Cu-Zn	Cu : $2\cdot54 \times 10^{-8}$	Zn : $2\cdot67 \times 10^{-8}$	Copper into zinc
		$2\cdot92 \times 10^{-8}$	
Fe-Ag	Fe : $2\cdot54 \times 10^{-8}$	Ag : $2\cdot876 \times 10^{-8}$	Iron into silver
Au-Pb	Au: $2\cdot88 \times 10^{-8}$	Pb : $3\cdot48 \times 10^{-8}$	Gold into lead
Fe-C	Fe : $2\cdot54 \times 10^{-8}$	C : $1\cdot50 \times 10^{-8}$	Carbon into iron

gold, and some B subgroup metals with atomic radii not very favourable for solid solution, and with which valence effects occur also to a certain extent, one obtains numerous alloy phases. The metals of group 8, on the other hand, have atomic

radii favouring solid solution, so that electrovalence effects are subordinated and intermediate phases not so numerous. Although in metals ionisation and deformation are hard to measure, it has already been indicated (p. 267) that Au-Fe, Au-Pd, and C-Fe systems may be electrolysed so that there is definitely polarisation of the constituents. Frenkel's theory (47, 44) (p. 293) of ionic conductivity illustrates the great importance of polarisation forces in decreasing the energy needed to render an ion mobile in an ionic lattice. The polarisation is a maximum when the electron affinity of the cation is large, and of the anion small. In Fig. 107 we may,
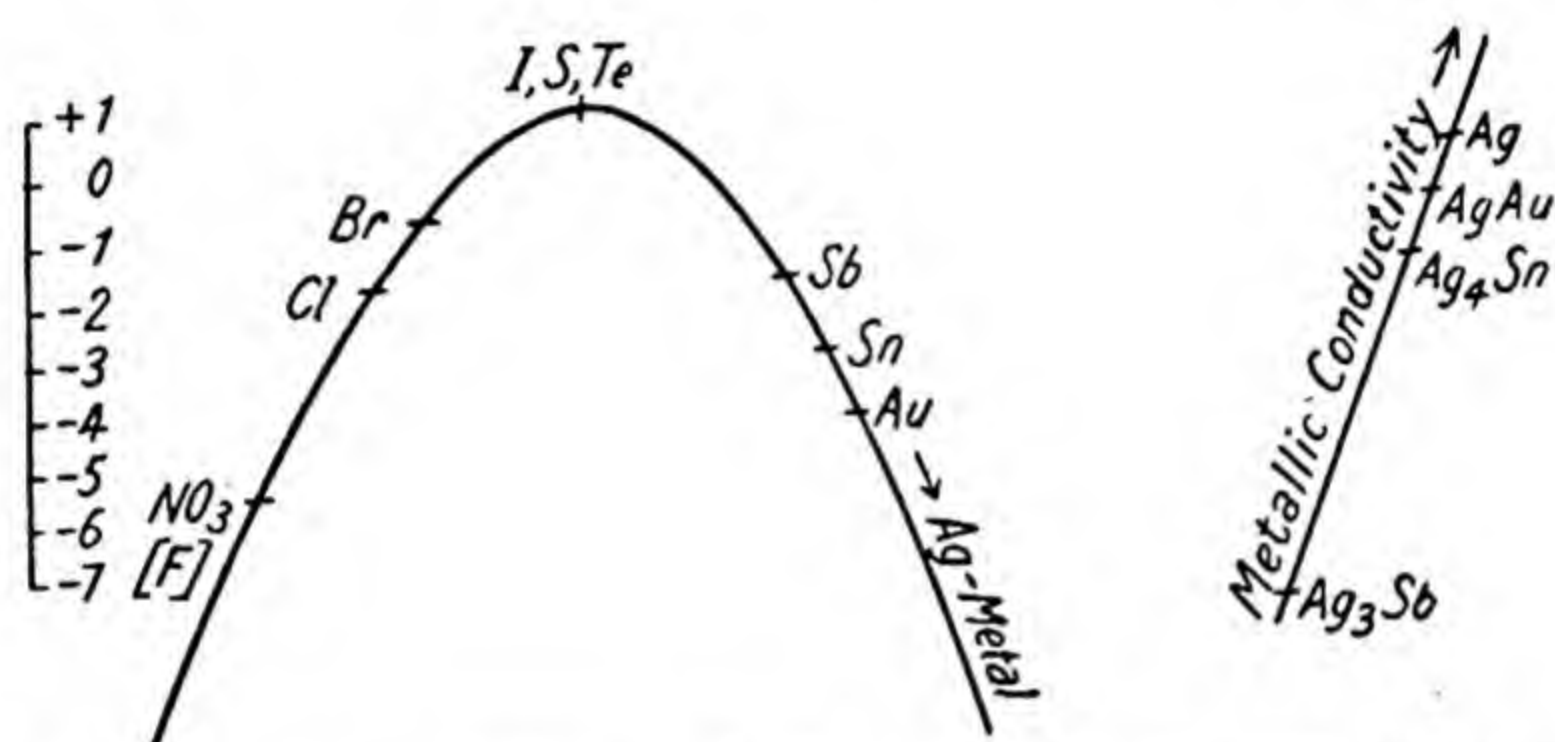
Fig. 107. The relative mobilities of silver ions in various silver compounds, arranged around a parabola. On the right is the relative electronic contribution to conductivity.

after von Hevesy (46), arrange the mobilities of silver in a series of different lattices (ionic and metallic) around a parabola. It is seen that the ionic mobility rises strongly from fluoride to telluride as the electron affinity of the anion diminishes, or its polarisability increases. On the right-hand side of the parabola it is shown that the small self-diffusion rate of silver in silver is raised by the addition of tin or antimony, while the electronic conduction is decreased. Similar considerations apply when the anion is the same and is combined with various cations.

The increased mobility of silver in a silver-antimony alloy as compared with a pure silver lattice may be considered as due to the loosening of the silver lattice by distortion due to introducing antimony. Von Hevesy (46) suggested that as a

qualitative measure of lattice loosening in ionic compounds one might employ the ratio

$$\frac{\text{Conductivity above the melting-point}}{\text{Conductivity below the melting-point}}.$$

The ratio is great in many instances, but in a few cases (α-AgI, α-CuI) it is less than unity (Table 74). As another method of comparing the relative loosening of two metallic lattices one may use the ratio

$$\frac{\text{Self-diffusion constant for first metal}}{\text{Self-diffusion constant for second metal}}.$$

This ratio for lead and gold at $326°$ C. is 26,000, and one sees that the lead lattice is loosened but the gold lattice is not at this temperature.

TABLE 74. *The ratio of conductivities above and below the melting-point*

System	Ag$^+$ in AgCl	Ag$^+$ in AgBr	Ag$^+$ in AgI	Li$^+$ in LiCl	Na$^+$ in NaCl	Na$^+$ in NaNO$_3$
Conductivity ratio above and below melting-point	16	2·5	0·5	1·0 × 10⁴	1·5 × 10⁵	1·0 × 10⁵

One of the most interesting phenomena allied to the problem of diffusion in metals is the order-disorder transformation in alloys. The terms order and disorder are being used in a different sense from that previously used when discussing vacant sites and interstitial ions in a lattice, as will be seen when the transformation is described. When a binary alloy with constituents in the ratio 1 : 1 or 1 : 3 is cooled, the melt solidifies to give a crystal. At these high temperatures all the atoms, though regularly arranged in space, are interchanged at random through the lattice. A given lattice point is as likely to be occupied by an atom of one kind as the other. As the lattice is cooled a reorganisation occurs which sets in at a fairly definite temperature, in which certain of the lattice sites tend always to be occupied by one type of atom, and

other definite sites by the second type of atom. In the alloy Cu₃Au, for example, at high temperatures Au and Cu atoms are distributed at random in the face-centred cubic lattice, while at low temperatures gold occupies cube corners and copper face centres. The transitions may be followed by resistance or X-ray measurements, and as a result of many studies[110a] it appears that the process of ordering may not reach its equilibrium state over a long interval of time at temperatures below the critical temperature of the transformation. This is because small zones of order are set up through the crystal which are out of phase with each other. The incorporation of one zone in another to give a homogeneous ordered phase is then very slow.

In any one zone undergoing the transformation disorder to order the time, τ, required for a given fraction of the transformation should be

$$\tau = Ae^{E/RT},$$

where A is a constant and E is the energy barrier which must be surmounted before the reorganisation occurs. This energy barrier must be very similar to that which occurs during diffusion, for in both cases a momentary mobility must be imparted to the atom. Owing, however, to the numerous antiphase nuclei which form through the crystal, the simple expression $\tau = Ae^{E/RT}$ is not valid [110b], for the slow coalescence of antiphase nuclei is occurring simultaneously, and one cannot measure the change in the separate nuclei independently.

MODELS FOR CONDUCTIVITY AND DIFFUSION PROCESSES IN CRYSTALS

From a number of different viewpoints expressions have been derived for conductivity or diffusion constants in crystals. A number of types of conduction may be recognised as theoretically possible, and examples of some of these are well established. It is now convenient to review some of the models for diffusion and also equations for the diffusion constant which have been derived by a number of workers.

An important type of ionic diffusion is that which occurs in zeolitic structures. In zeolites one has an anionic framework with large interstices in which exist the cations necessary for electrical neutrality. The anionic framework is sufficiently open to allow cations to pass through it, along cation channels, without any appreciable loosening of the anionic network. Thus one may often exchange one cation for another in these interstitial compounds. It is probable that the diffusion of hydrogen as atoms or ions in the metallic lattices of palladium and similar metals may also be referred to this type. This is also the mechanism by which gases flow into zeolites, or through silicate glasses and organic membranes. Von Hevesy(46) regarded the very rapid diffusion of gold into lead as zeolitic, and indeed considered that most examples of rapid diffusion in pure metals occurred by zeolitic diffusion. The process of amalgamation may perhaps be regarded as a zeolitic diffusion, accompanied simultaneously with a disintegration or reorganisation of the solvent lattice into amalgams. In order, however, for diffusion in metals to be truly zeolitic the solute atoms should be small enough to fit interstitially between the solvent atoms.* It is conceivable that a metallic lattice could be formed in which one kind of atom was freely mobile, while the other kind of atom formed a more rigid lattice framework. Such a system would compare with the anionic disorder in lattices of AgI, or Ag_2HgI_4 (p. 263).

A picture which is often given of the process of inter-diffusion of metal pairs supposes place exchange by a thermal loosening of the lattice sufficient for the molecules to pass round each other, as distinct from Frenkel's mechanism (p. 293). It has been illustrated in Fig. 108. This model has not passed uncriticised. Bernal(111), for example, considered that the activation energy needed for the loosening would be too great but that diffusion might occur by spontaneous small gliding processes along different planes. As with the Frenkel mechanism, however, the polarisation energy may consider-

* The atomic radii of gold and lead are respectively 2·88 A. and 3·48 A., probably not sufficiently different for interstitial solution.

ably diminish the energy needed to create the momentarily disorganised lattice.

On the quantitative side one may indicate the theory of volume diffusion and conductivity in ionic crystals due to Frenkel [47] and extended by Jost [44, 56]. The theory is based upon the concept of equilibrium disorder introduced in a lattice

I	II
Undisturbed lattice	Lattice momentarily loosened to permit place exchange of molecules A and B
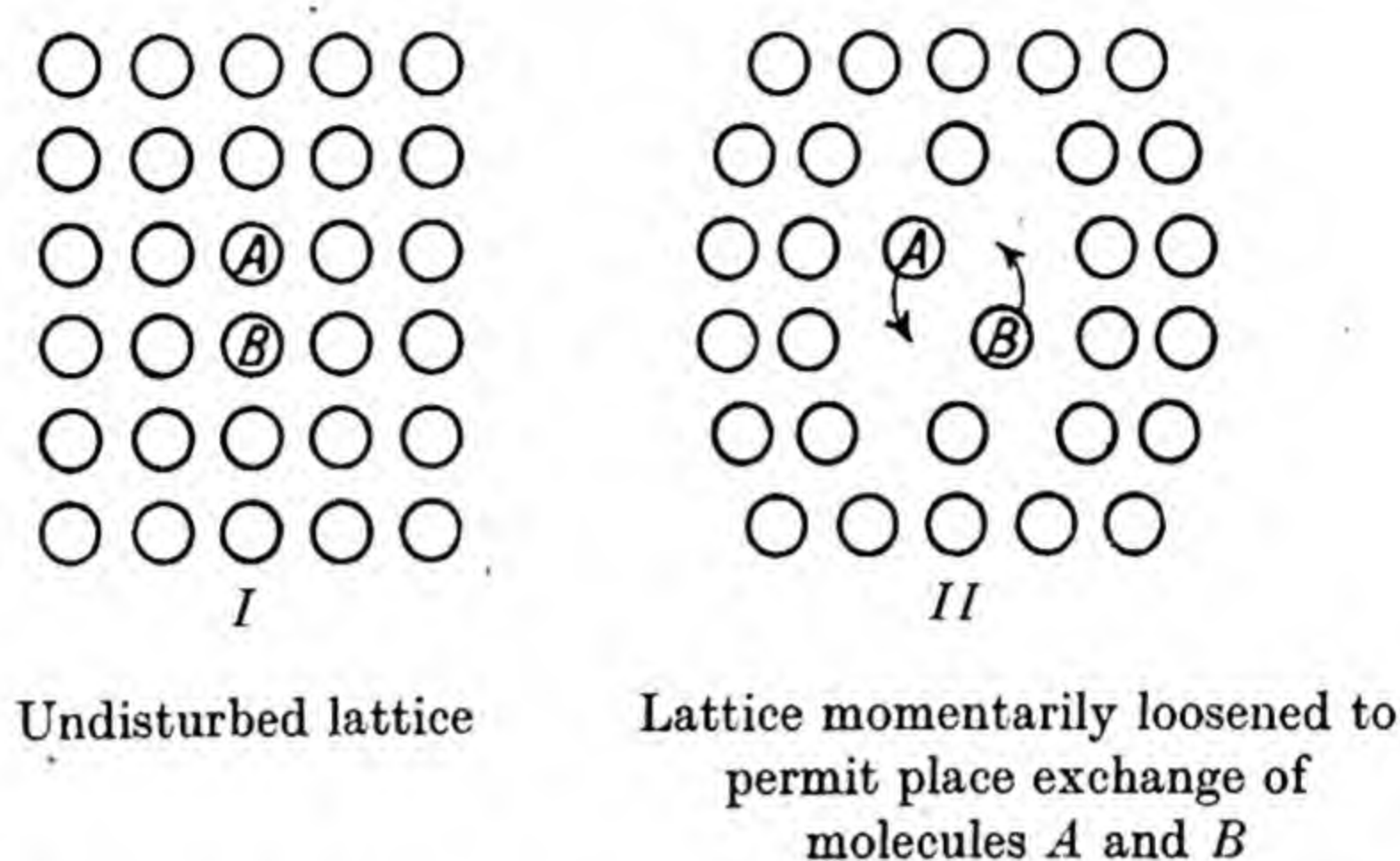
Fig. 108. A place exchange process as pictured in a crystal lattice.
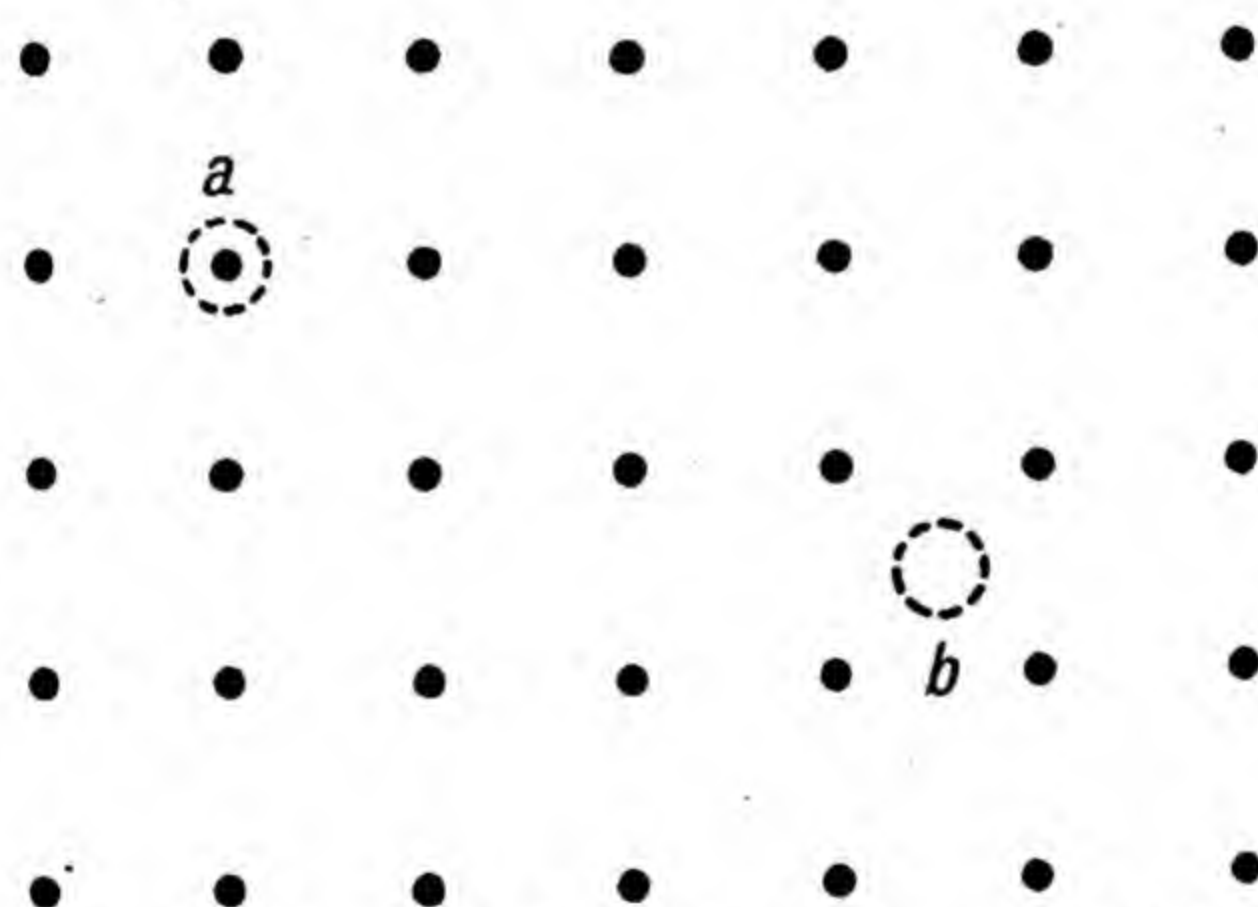
Fig. 109. Frenkel disorder in a two-dimensional lattice.

by the thermal energy (p. 248). Thus in Fig. 109 it may be supposed that the atom or ion at the position (a) has gained sufficient energy for it to migrate to the position (b), while at any temperature the average number of vacant sites and interstitial atoms or ions is constant and in equilibrium with the normal lattice. Diffusion can ensue by two mechanisms: an atom may move over a potential energy barrier E_1 into the vacant

site, giving a diffusion of the vacant sites; or an interstitial ion may move over an energy barrier to another interstitial position. When

n = the number of vacant sites/unit volume,

N = the number of lattice sites/unit volume,

E_0 = the energy needed to create a hole,

Frenkel [47], by kinetic theory, and Jost [44, 56], by statistical mechanics*, showed that $n \sim Ne^{-E_0/2RT}$. Only a fraction of these holes, or corresponding interstitial atoms, will diffuse however, because an activation energy is necessary for diffusion. Thus the number moving is proportional to $e^{-(E_0+2E_1)/2RT}$. An approximate value of D, the diffusion coefficient, can be deduced if it is assumed that there are six ions around each hole, distant d from its centre, and capable of moving with the mean thermal velocity in any one of six directions. Each of the six particles may move in a single direction (to the hole), so the six of them are equivalent to a single particle free to move in all directions. Therefore the diffusion constant for a hole is

$$D_h = \frac{1}{6}\frac{d\bar{v}}{2}e^{-E_1/RT},$$

and the diffusion constant for all the ions is

$$D = \frac{1}{6}\frac{d\bar{v}}{2}e^{-E_1/RT}\left(\frac{6n}{N}\right),$$

since $6n/N$ is the fraction of ions around the holes. Then

$$D = \frac{d\bar{v}}{2}e^{-(E_0+E_1)/2RT}.$$

In this equation $\frac{1}{2}d\bar{v} = 65\,\text{cm.}^2/\text{day}^{-1}$, when $d = 3\,\text{A.}$, and $\bar{v} = 5 \times 10^4\,\text{cm./sec.}$ The case of forced diffusion (electrical conductivity) may be obtained by using the Einstein equation:

$$D = BkT \quad (B \text{ denotes the mobility})$$

and also $\qquad\qquad K = N(Ze)^2B,$

---

* For Schottky disorder the analogous relationship is $n = \alpha Ne^{-E_0/RT}$. The exponential does not contain the factor $\frac{1}{2}$, and α may have values as high as 10^4.

where K denotes the conductivity, and N the number of ions per unit volume of valency Z, and charge Ze. Then

$$K = N(Ze)^2 \frac{d\bar{v}}{2kT} e^{-(E_0+2E_1)/2RT}.$$

The factor before the exponential has a magnitude similar to that for D, and normally one may write

$$K = (10\text{–}100)\, e^{-(E_0+2E_1)/2RT}.$$

We have now to consider how accurately this theoretical expression predicts the experimental findings. The value of $(E_0 + 2E_1)$ might, at first sight, be thought to be comparable with the lattice energy (100–200 k.cal.); whereas the experimental values are instead from 1 to 50 k.cal. The suggestion by Smekal[112] that the mobility occurs only along internal surfaces and outer surfaces leads to impossible values of the constant A in the equation

$$K = A e^{-(E_0+2E_1)/2RT}.$$

Reasonable values of the quantity $(E_0 + 2E_1)$ may, however, be computed for lattice ion movement if the polarisation properties are also considered, for it has been found that polarisability and polarising properties and conductivity are connected (cf. pp. 254 and 265)[114]. One may proceed to calculate the energy, E_0, involved in the formation of a hole, and removal of an ion to an interstitial position, in a manner analogous to that outlined on p. 254. To $\frac{1}{2}E_0$ must then be added E_1, the energy required before the hole, or the interstitial ion, can migrate. Calculations of this kind have been made by Jost[44]. He determined E_0 for NaCl by evaluating the following energy terms:

(i) Coulombic energies in normal and displaced positions.

(ii) Repulsive energy in the normal and displaced position.

(iii) Polarisation energies around the vacant site and the displaced ion.

The calculation is subject to the limitations outlined on p. 255. The next step is to find E_1, the energy of activation

for diffusion of either a vacant site or an interstitial ion. The term $\frac{1}{2}E_0 + E_1$ might then be compared with the experimental figure for $\frac{1}{2}E_0 + E_1$ obtained from conductivity data (44 k.cals.). The theory indicates a qualitative agreement with experiment.

Certain salts (e.g. α-Ag_2S; $D = 10 \times e^{-1610/T}$ cm.^{2} day^{-1}) have a very high electrolytic conductivity; $\frac{1}{2}(E_0 + 2E_1)$ is only 3220 cal. For this salt the polarisation properties reduce $\frac{1}{2}(E_0 + 2E_1)$ to a very low value. Calculation gives:

$$E_0 = \text{energy of "hole" formation} = E_{coulomb} + E_{rep.} + E_{pol.}$$
$$= (2{\cdot}31 - 0{\cdot}11 - 2{\cdot}15)\, e^2/a$$
$$= \sim 5{\cdot}7 \text{ k.cal.}$$

A similar approximate computation of E_1, the potential energy needed for migration from a displaced position, $-\frac{1}{2}, -\frac{1}{2}, -\frac{1}{2}$, to a displaced position $+\frac{1}{2}, +\frac{1}{2}, +\frac{1}{2}$ gives

$$E_1 \sim 0{\cdot}1 e^2/a \sim 10{\cdot}7 \text{ k.cal.}$$

and thus $\qquad \frac{1}{2}(E_0 + 2E_1) \sim 13{\cdot}1 \text{ k.cal.,}$

which may be compared with the experimental value 3220 cal. Qualitatively, if not quantitatively, the Frenkel theory can thus account for the exponential term.

The constant A in the equation

$$K = A e^{-(E_0 + 2E_1)/2RT},$$

to which the theory of Frenkel gives a value 2×10^1 to 2×10^2, actually takes experimental values of $10 > A > 10^6$. To explain this discrepancy three possibilities arise:

(i) By analogy with the theory of thermionic emission it may be assumed that there is a temperature coefficient to the quantity $\frac{1}{2}(E_0 + 2E_1)$, which has been neglected in the Frenkel treatment outlined.

(ii) A molecule having once acquired the energy $\frac{1}{2}(E_0 + 2E_1)$ may retain it while describing a mean free path far greater than corresponds to a single displacement.

(iii) The activation energy may be stored through many degrees of freedom (p. 300).

Braunbek [115] developed an analogous expression for the conductivity of an ionic solid. Using sodium chloride as his model lattice, he assumed a simple linear vibration of sodium ions, while the chlorine ions were supposed to remain fixed. Each sodium ion was situated in the mid-point of an octahedron of chlorine ions, and the sodium ion on acquiring sufficient energy could move from the centre of its octahedron through the mid-point of one of its faces, and enter a new vacant octahedron whose central sodium has diffused away by a similar process. The probability of occurrence of such a process during a vibration was calculated, and from this the self-diffusion constant, and the conductivity K:

$$K = \frac{2e^2 N_0}{3\tau d(8\cdot3)\,E} \exp\left(-E/RT\right),$$

where e = electronic charge,

$d = 5\cdot63 \times 10^{-8}$ cm.,

τ = the vibration period, $\sim 2\cdot1 \times 10^{-13}$ sec.

The quantity E was regarded as comparable with the energy of melting of the lattice. This equation should however also contain the ratio $\dfrac{n}{N} = \dfrac{\text{No. of vacant Na}^+ \text{ ion sites}}{\text{Total No. of Na}^+ \text{ ion sites}}$, which gives the probability that the second octahedron will be empty to receive the migrating Na$^+$ ion. The agreement with v. Seelen's [116] data is thus probably fortuitous.

Cichocki [117] derived an expression for the self-diffusion constant in ionic or metallic lattices. He used a body-centred cubic lattice as his model, and then endeavoured to calculate the probability that a given atom would have the requisite energy and direction of vibration to move to a new position, at a time at which the atoms surrounding that position have the energy and direction of vibration to make an adequate interstice for it. His theory is interesting as an attempt to allow for correct timing in the diffusion. An analogous treatment by Dorn and Harder [118], in which the crystal is regarded as a periodic system of energy wells, is less satisfactory. It is

not possible to assume constant potential energy walls about the hole in which the solute atom resides. Sometimes it may be almost impossible for the atom to escape in a given direction, and sometimes it may readily be able to do so. The height of the surrounding energy barriers fluctuates with time according to the differences in phase of vibrations in surrounding atoms in the lattice. Cichocki's formula, which allows for this, is nevertheless open to the same objection as Braunbek's (p. 297).

Langmuir and Dushman [119] proposed a semi-empirical equation for diffusion in cubic lattices, which has proved a useful guide to the behaviour of diffusion processes in ionic and metallic lattices (Tables 66 and 67). It was derived by considering the lattice as composed of layers of atoms in planes a distance d apart, where d denotes the interionic or interatomic distance. It was assumed that d was also the mean free path of a diffusing ion or atom. The number of atoms per unit area is then d^2, and the chance that an atom will leave this area in unit time is kd^2. By analogy with an early expression for the reaction velocity constant [120], Langmuir and Dushman wrote $k = \nu e^{-h\nu/kT}$, and $D = \dfrac{E}{N_0 h} d^2 e^{-E/RT}$, where ν is the vibration frequency of the solid, $N_0 h\nu = E$, and h denotes Planck's constant, and the other terms have their usual significance. The Langmuir-Dushman equation is to be regarded as empirical, the frequency ν being fictitious, as. the following correct derivation of the diffusion constant shows. Suppose two salts which form solid solutions of cubic symmetry are interdiffusing, salt A passing in the $+x$ direction. Draw planes at x and $x + d$ (Fig. 110), where d is the mean free path of an activated molecule, and also at $x - \frac{1}{2}d$ and $x + \frac{3}{2}d$, normal to the x-co-ordinate. All salt A ions in the region $x - \frac{1}{2}d$ to $x + \frac{1}{2}d$ can if they acquire the necessary activation energy with suitable direction ($+x$) pass the intermediate plane $x + \frac{1}{2}d$. The chance that an activated ion will move in the $+x$ direction is one-sixth the chance it will move in any direction and this latter chance is assumed equal to the probability of activation, $\nu_0 e^{-E/RT}$, where $\nu_0 = $ the vibration frequency in the lattice = the

number of vibrational collisions/second. The total number of ions of the salt A moving/sec./unit area in the $+x$ direction across the plane $x + \frac{1}{2}d$ is thus $\frac{1}{6}dCv_0 e^{-E/RT}$; while the number moving in the $-x$ direction is $\frac{1}{6}d\left(C - d\dfrac{\partial C}{\partial x}\right)v_0 e^{-E/RT}$. Thus the nett flow across the plane $x + \frac{1}{2}d$ per second per unit area in the $+x$ direction is $\frac{1}{6}d^2 \dfrac{\partial C}{\partial x} v_0 e^{-E/RT}$, which also equals $D\dfrac{\partial C}{\partial x}$.
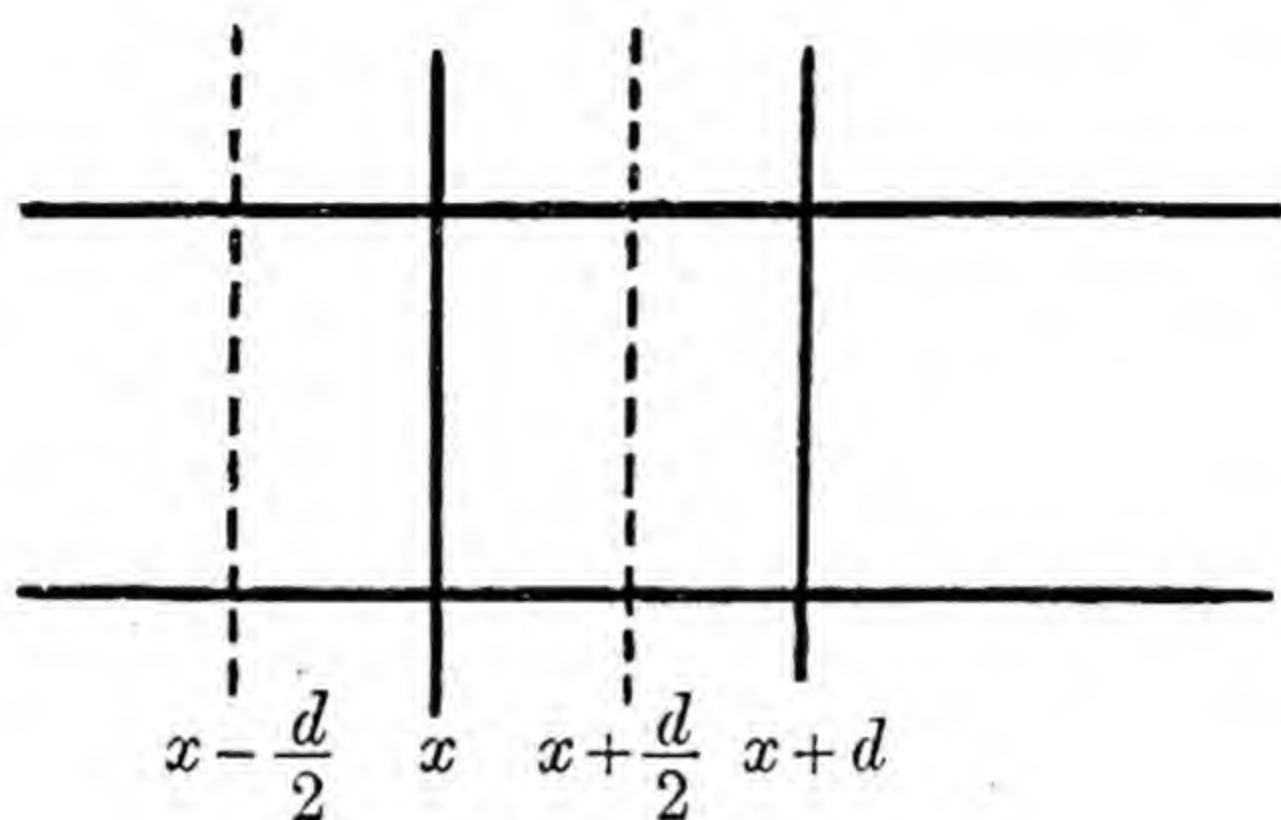
Fig. 110.

Thus

$$D = \tfrac{1}{6}d^2 v_0 e^{-E/RT} \qquad \text{(kinetic theory deduction),}$$

$$D = d^2 \frac{E}{N_0 h} e^{-E/RT} \qquad \text{(Langmuir-Dushman empirical expression),}$$

so that if there were any correspondence $E/N_0 h = \frac{1}{6}v_0$; but since $v = E/N_0 h$, and as E can be even greater than 90,000 cal./mol., v_0 must if derived from the Langmuir-Dushman expression correspond in such a case to an energy of 540,000 cal. Clearly no physical significance can then be attributed to the term $E/N_0 h$ in the Langmuir-Dushman expression. When not one but two degrees of freedom are included for the storing of the activation energy, the rate R at which the ions are activated becomes

$$R = v_0 \frac{E}{RT} e^{-E/RT}$$

with $\qquad D = \tfrac{1}{6}d^2 \frac{E}{RT} v_0 e^{-E/RT},$

which is Bradley's expression [121]. When n degrees of freedom

are included the appropriate expressions are those of Wheeler [122]*

$$R = \nu_0 \left(\frac{E}{RT} \right)^{(n-1)} \frac{1}{(n-1)!} e^{-E/RT},$$

and

$$D = \tfrac{1}{6} d^2 \left(\frac{E}{RT} \right)^{n-1} \frac{1}{(n-1)!} \nu_0 e^{-E/RT}.$$

Langmuir and Dushman's empirical relationship

$$D = d^2 \frac{E}{N_0 h} e^{-E/RT}$$

has been used fairly extensively as a guide to the behaviour of diffusion systems, perhaps unfortunately, since there has been a tendency to read a physical significance into the values of d thus computed. These happen in many cases to be of the order of magnitude of the inter-crystalline distances. In general a better agreement is found from the Langmuir-Dushman equation, between $D_{calc.}$ and $D_{obs.}$, using for d the crystal parameters, when the systems have a high activation energy for diffusion, and this may perhaps be regarded as evidence that activation energies are then stored in only one or two degrees of freedom. However this may be, many systems of diffusing metal pairs obey Langmuir and Dushman's formula with some precision, as Table 67 shows. Agreement is much poorer for those ionic solids for which low activation energies are observed. The self-diffusion of lead may be cited as

an example of diffusion obeying the equation $D = \dfrac{E}{N_0 h} d^2 e^{-E/RT}$

with precision. Fig. 111 [16] shows experimental and calculated curves of $\log D$ versus $1/T$, in which the experimental curve (1) gives an E value of 27,900 cal. When d is taken as the shortest distance between two neighbours, 4·94 A., the whole $\log D$–$1/T$ curve is fixed by a single experimental point and in the figure is given by curve (2). When d is 8·5 A.

---

* These three formulae apply in their present form to zeolitic diffusion in dilute solution, or to place exchange diffusion. In concentrated zeolitic solution the ratio $\dfrac{\text{No. of vacant interstices}}{\text{Total No. of interstices}}$ must be included. For diffusion by Frenkel or Schottky mechanisms the ratio $\dfrac{n}{N}$ (p. 303, footnote) must be included.

(the unit cube diagonal) the agreement is a little better and the $\log D$–$1/T$ curve is given by (3) in the figure. For this system the Langmuir-Dushman empirical equation is remarkably satisfactory, and a single diffusion constant would suffice, using crystallographic data, to map out the whole course of the $\log D$–$1/T$ curve.

$$1/T \times 10^4.$$
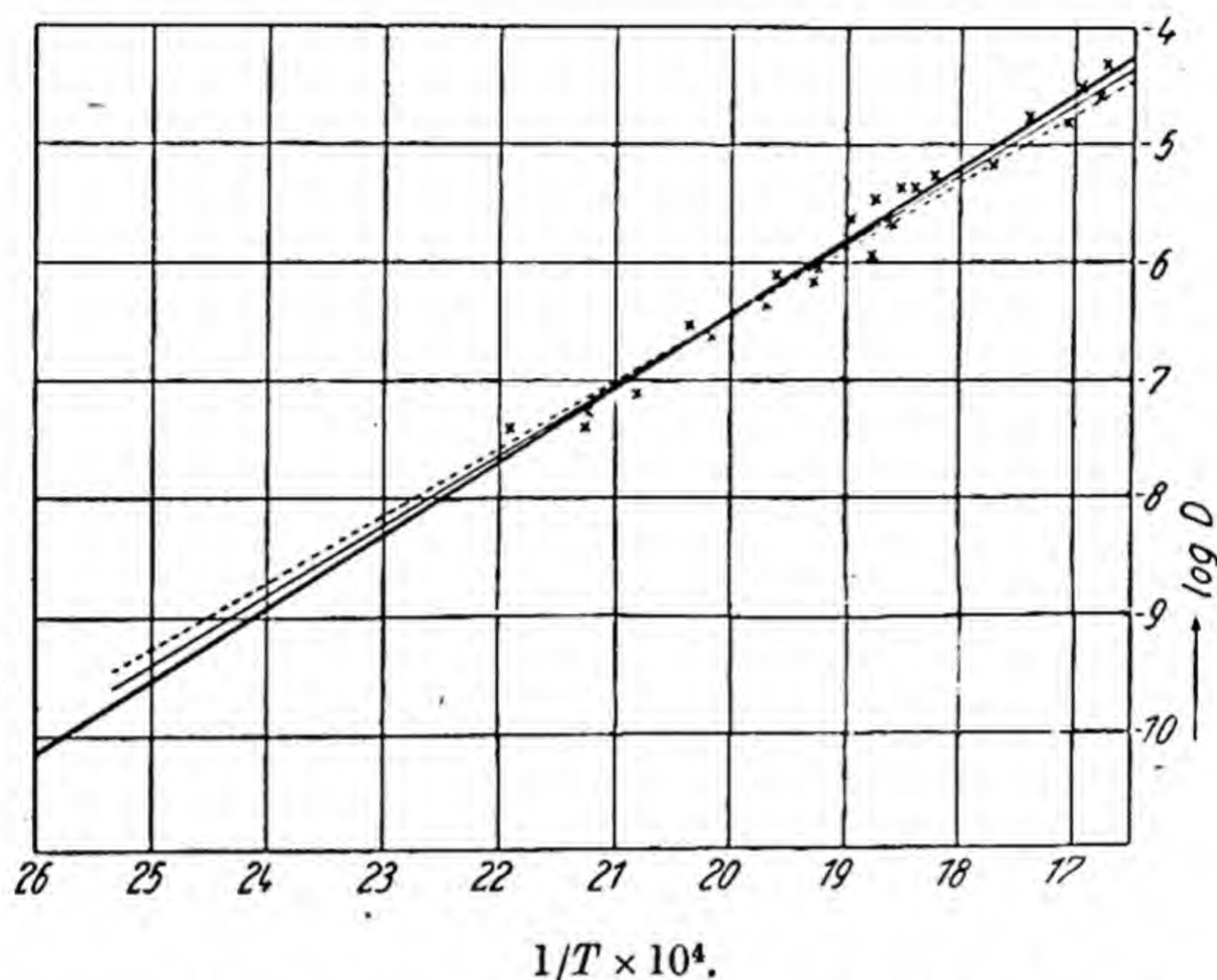
(1) ———— Experimentally found curve, $E = 27{,}900$ cal./atom.
(2) · · · · · · Calculated using $d =$ shortest distance between Pb atoms, and $E = 25{,}500$ cal./atom.
(3) ———— Calculated using $d = \sqrt{3} \times$ shortest distance between Pb atoms, and $E = 26{,}700$ cal./atom.

Fig. 111. Self-diffusion in Pb calculated from $D = \dfrac{E}{N_0 h} d^2 e^{-E/RT}$ calculated from a single experimental diffusion constant and the distance between neighbouring atoms (d).

The formulae of Braune (94) and of van Liempt (109) recognise the dependence of the velocity of diffusion upon the melting-point by introducing in the exponential term the equality

$$\frac{E}{RT} = 3b^2 \frac{T_m}{T} \quad \text{or} \quad \frac{E}{R} = 3b^2 T_m,$$

wherein T_m is the melting-point. In these equations the constant b depends upon the atomic size, and polarisation properties of the lattice. The usual value of b^2 is about 2, and for lattices of very different melting-points such as lead, silver,

and tungsten respectively (Table 75) the values of b^2 are as 1 : 2 : 1, while the absolute melting-points are as 1 : 3 : 10 (see also p. 285).

Eyring[99] in 1936 showed how the transition state theory of reaction velocity could be applied to viscosity, plasticity, and diffusion. This treatment has been applied especially to liquids, and to organic polymers, but it should be still more applicable to the problem of diffusion in crystals. The ion or atom in a body-centred cubic lattice, for example, may diffuse through the centre of any one of six faces, over a potential energy barrier, to a neighbouring vacant site or interstitial position. The velocity constant for passing over a potential energy barrier is

$$k' = \alpha \frac{F_a^*}{F_n} \frac{kT}{h} e^{-E_0/RT}.$$

In this expression

α = the probability that a system having once crossed the top of the energy barrier will not recross it in the reverse direction before losing its activation energy.

TABLE 75. *The dependence of the self-diffusion constant upon the melting-point*

Metal	Melting-point ° C.	$D_{18° C.}$ in cm.^{2} day^{-1}
Pb	327	$2 \cdot 2 \times 10^{-15}$
Ag	961	$9 \cdot 6 \times 10^{-20}$
W	3400	$4 \cdot 3 \times 10^{-59}$

F_n = the partition function for the normal state of the system.

E_0 = the energy of activation for the transition from the initial to the final state.

F_a^* = the partition function for the activated state, excluding the partition function for the co-ordinate in which the transition occurs. This latter partition function gives the frequency term kT/h (k = the Boltzmann constant; h = Planck's constant).

If it is now supposed that there is a concentration gradient $\partial C/\partial x$ in the $+x$ direction, and that the distance between two

successive minima of potential energy in this direction is d, one finds the concentration C at one minimum and $C + d(\partial C/\partial x)$ at the next. The number of ions or atoms passing in the $+x$ direction is thus $N_0 dk'C$, and in the reverse direction it is $N_0 dk'\left(C + d\dfrac{\partial C}{\partial x}\right)$. The excess flow in the $-x$ direction is thus

$$N_0 d^2 k' \frac{dC}{dx} = N_0 D \frac{dC}{dx},$$

where N_0 is Avogadro's number. Finally*,

$$D = d^2 k' = d^2 \alpha \frac{F_a^*}{F_n} \frac{kT}{h} e^{-E_0/RT}.$$

In the simplest cases $F_a^*/F_n \sim (1 - e^{-h\nu/kT})$, and tends to unity for large ν (ν is the vibration frequency of the atom or ion in the lattice). If the equation is to apply to diffusion processes in solids for which the Langmuir-Dushman equation also holds, one may write $E = RT + E_0$ and so

$$d^2 \frac{E}{N_0 h} = 2 \cdot 72 d^2 \alpha \frac{kT}{h} \frac{F_a^*}{F_n}; \quad \text{i.e. } \alpha \frac{F_a^*}{F_n} = \frac{E}{RT} \frac{1}{2 \cdot 72}.$$

For the self-diffusion of lead at 230°C, this relationship becomes

$$\alpha \frac{F_a^*}{F_n} \simeq 10.$$

There is so far no analysis of factors determining the ratio $\dfrac{F_a^*}{F_n}$ for diffusion by place exchange or other mechanisms. In some instances, the considerations of the footnote below may have to be allowed for.

Eyring and Wynne-Jones [99] have extended Eyring's equation for the diffusion constant by introducing the entropy of activation $\Delta S^{\pm}$, and the heat of activation $\Delta H^{\pm}$. The diffusion constant is now given by

$$D = D_0 e^{-E/RT} = e^{\Delta S^{\pm}/R}\left(\frac{kT}{h}\right) d^2 e^{-\Delta H^{\pm}/RT}.$$

---

* For Frenkel or Schottky disorder a term

$$\frac{n}{N} = \frac{\text{No of interstitial ions, or vacant sites}}{\text{Total No. of potentially diffusible ions}}$$

should be included (p. 294). In dilute zeolitic solution, or in place exchange diffusion (Fig. 108), no such term arises. The latter may be the mechanism of interdiffusion of many metal pairs. (See p. 297, and footnote, p. 300.)

It is then seen that the temperature independent factor D_0 is related to the entropy of activation by the expression

$$D_0 = e^{\Delta S^{\pm}/R}\left(\frac{kT}{h}\right)d^2\frac{1}{2\cdot72}.$$

Therefore a large D_0 implies a large entropy of activation, or a considerable loss of order in the lattice on passing from the initial to the transition state. This is particularly noticeable for self-diffusion constants.

These formulae based upon different conceptions of the diffusion process are collected in Table 76. It can here be seen what physical quantities have been correlated with the diffusion or conduction process. The process of diffusion is the necessary preliminary to many metallurgical and chemical processes involving solids. In addition, mechanisms of self-diffusion and diffusion are of absorbing interest as a study in themselves. Yet the very variety of the attempts which have been made to obtain satisfactory models for diffusion, and the limited application of so many of them, demonstrate how little progress has been made towards a comprehensive treatment. This is rather surprising when one considers the present knowledge of the crystalline state. Three main viewpoints have been advanced: the theory of equilibrium disorder in ionic and metallic lattices; the carrying over of kinetic theory, and of gaseous reaction kinetics to solid phases; and the application of statistical mechanics to diffusing systems.

On the experimental side much more numerous and more accurate data are required. It will be necessary to know with exactitude how D, D_0 and E in the expression $D = D_0 e^{-E/RT}$ vary with composition in alloy systems. Many more self-diffusion coefficients obtained by the radioactive indicator method are required. The connections between polarisation, atomic radius and density, position in the periodic table, alloy formation, melting-point, and degree of lattice loosening must be placed upon a more quantitative basis than the present data permit. When these properties have been correlated among themselves, and with existing X-ray data on crystal structure, it should be possible to understand more clearly phenomena of diffusion in metallic and non-metallic lattices.

TABLE 76. *Expressions for the diffusion constant and the ionic conductivity in crystals*

System	Formula	Author
Ion-ionic lattice metal atom, metallic lattice	$D = \dfrac{d\bar{v}}{2} e^{-(E_0 + 2E_1)/RT}$, d = mean free path E_0 = energy of hole formation E_1 = energy for diffusion of ion or atom into hole $\bar{v}$ = mean thermal velocity of diffusing atom or ion $K = \dfrac{N(Ze)^2}{kT} D$ K = conductivity Z = valence e = electronic charge N = number of ions per unit volume	Frenkel[47], Jost[44] Frenkel[47], Jost[44]
Ion-ionic lattice (sodium chloride)	$K = \dfrac{2e^2 N_0}{3\tau(8\cdot3)\,dE} e^{-E/RT}$ E = activation energy for ion transfer τ = vibration period, $\sim 2 \times 10^{-13}$ sec.	Braunbek[115]
Ionic or metallic lattice (self-diffusion)	$D = 2\cdot43 \times 10^3 \dfrac{M_1}{V} \sqrt{\dfrac{T_m}{M_1}} e^{-(E_1+E)/RT}$ M_1 = atomic or molecular weight V = atomic or molecular volume T_m = melting-point E_1 = energy needed to form interstitial hole E = energy needed to bring atom to interstitial position	Cichocki[117]
Ionic or metallic lattice	$D = \dfrac{E}{N_0 h} d^2 e^{-E/RT}$ $D = \dfrac{8}{3\pi} \nu d^2 e^{-3b^2} \dfrac{T_m}{T}$ ν = vibration frequency of lattice b is a constant	Langmuir and Dushman[119] van Liempt[109]
Ionic or metallic lattice	$D = \dfrac{1}{6}\left(\dfrac{E}{RT}\right) \nu d^2 e^{-E/RT}$ $D = \dfrac{1}{6}\left(\dfrac{E}{RT}\right)^{(f-1)} \dfrac{\nu d^2}{(f-1)!} e^{-E/RT}$ f = the number of degrees of freedom involved in the diffusion process $f = 2$ in Bradley's equation	Bradley[121] Wheeler[122]
Ionic or metallic lattice	$D = \dfrac{kT}{h}\left(\alpha \dfrac{F_a^*}{F_n}\right) d^2 e^{-E/RT}$ F_a^*/F_n = ratio of partition functions transition and normal states respectively (excluding for former the partition function for co-ordinate of diffusion process) α = transmission coefficient, i.e. probability that system having reached transition state will pass over the energy barrier to a new state	Eyring[99]
Ionic or metallic lattice	$D = e^{\Delta S^{\pm}/R}\left(\dfrac{kT}{h}\right) d^2 e^{-\Delta H^{\pm}/RT}$ $D_0 = e^{\Delta S^{\pm}/R}\left(\dfrac{kT}{h}\right) d^2 \dfrac{1}{2\cdot72}$ $\Delta S^{\pm}$, $\Delta H^{\pm}$ denote respectively entropy and heat of activation	Eyring and Wynne-Jones[99]

306

REFERENCES

(1) Spring, W. *Z. phys. Chem.* **15**, 65 (1894).

(2) Roberts-Austen, W. *Philos. Trans.* **187** A, p. 393 (1896).

(3) Faraday, M. and Stodart. *Quart. J. Sci.* **9**, 319 (1820). *Experimental Researches in Chemistry*, p. 57 (1859).

(4) Masing, G. *Z. anorg. Chem.* **62**, 265 (1909).

(5) Masing, G. and Overlach, H. *Wiss. Veröff. Siemens-Konz.* **9**, ii, 331 (1930).

(6) Diergarten, H. *Metal Progress*, p. 64, Jan. 1936.

(7) Mehl, R. *Trans. Amer. Inst. min. (metall.) Engrs*, **122**, 11 (1936).

(8) Arnold, J. and M'William, A. *J. Iron and Steel Inst.* **56**, 85 (1899).

(9) Giolotti, F. and Tavanti, G. *Gazz. chim. ital.* **39**, ii, 386 (1909).

(10) Rawdon, H. *Protective Metal Coatings*, New York, Chem. Cat. Co. (1928).

(11) Grimshaw, L. *Trans. Amer. Inst. min. (metall.) Engrs*, **120**, 363 (1936).

(12) Faraday, M. *Philos. Trans.* **23**, 507 (1833).

(13) Wiedmann, E. *Ann. Phys., Lpz.*, **154**, 318 (1875).

(14) Kohlrausch, W. *Ann. Phys., Lpz.*, **17**, 642 (1882).

(15) Thomson, S. P. *Nature, Lond.*, **24**, 469 (1881).

(16) Beetz, W. *Ann. Phys., Lpz.*, **92**, 452 (1854).

(17) Reynolds, O. Diss. Göttingen, 1902.

(18) Nernst, W. *Z. Elektrochem.* **6**, 41 (1899).

(19) Bose, E. *Ann. Phys., Lpz.*, **9**, 164 (1902).

(20) Graetz, L. *Ann. Phys., Lpz.*, **29**, 314 (1886).

(21) Arrhenius, S. *S.B. Akad. Wiss. Wien*, **96**, 831 (1887).

(22) Dunn, J. *J. chem. Soc.* **129**, 2973 (1926); *J. Soc. Chem. Ind., Lond.*, **46**, 109 (1927).

(23) Bramley, A. *Carnegie Schol. Mem.*, Iron and Steel Inst., **15**, 155 (1926).

Bramley, A. and Beeby, G. *Carnegie Schol. Mem.*, Iron and Steel Inst., **15**, 71 (1926).

Bramley, A. and Jinkings, A. *Carnegie Schol. Mem.*, Iron and Steel Inst., **15**, 17, 127 (1926).

Bramley, A. and Lawton, G. *Carnegie Schol. Mem.*, Iron and Steel Inst., **16**, 35 (1927).

Bramley, A. and Heywood, F. *Carnegie Schol. Mem.*, Iron and Steel Inst., **17**, 67 (1928).

Bramley, A. and Turner, G. *Carnegie Schol. Mem.*, Iron and Steel Inst., **17**, 23 (1928).

Bramley, A. and Lord, H. *Carnegie Schol. Mem.*, Iron and Steel Inst., **18**, 1 (1929).

Bramley, A., Heywood, F., Cooper, A. and Watts, J. *Trans. Faraday Soc.* **31**, 707 (1935).

(24) Brower, T., Larsen, B. and Shenk, W. *Trans. Amer. Inst. min. (metall.) Engrs*, **113**, 61 (1934).

(25) Van Arkel, A. *Metallwirtschaft*, **7**, 656 (1928).

(26) Bruni, G. and Meneghini, D. *Int. Zeit. Metallog.* **2**, 26 (1912).

(27) Tanaka, S. and Matano, C. *Mem. Coll. Sci. Kyoto*, **14**A, 59 (1931).

(28) Linde, J. and Borelius, G. *Ann. Phys., Lpz.*, **84**, 747 (1927).
Kruger, F. and Gehm, G. *Ann. Phys., Lpz.*, **16**, 174 (1933).

29) Seith, W. and Peretti, E. *Z. Elektrochem.* **42**, 570 (1936).

(30) Brick, M. and Philips, A. *Trans. Amer. Inst. min. (metall.) Engrs*, **124**, 331 (1937).

(31) v. Hevesy, G. *Trans. Faraday. Soc.* **34**, 841 (1938).
v. Hevesy, G. and Paneth, F. *Z. anorg. Chem.* **82**, 323 (1913).
Groh, J. and v. Hevesy, G. *Ann. Phys., Lpz.*, **63**, 85 (1920).
v. Hevesy, G. and Obrutscheva, A. *Nature, Lond.*, **115**, 674 (1925).

(32) v. Hevesy, G. and Seith, W. *Z. Phys.* **56**, 790 (1929).
—— —— *Z. Phys.* **57**, 869 (1929).
v. Hevesy, G., Seith, W. and Keil, A. *Z. Phys.* **79**, 197 (1932).

(33) McKay, H. *Trans. Faraday Soc.* **34**, 845 (1938).

(33a) Steigman, J., Shockley, W. and Nix, F. *Phys. Rev.* **56**, 13 (1939).

(34) v. Hevesy, G. and Paneth, F. *Manual of Radioactivity*, Oxford, 1938.

(35) Langmuir, I. *J. Franklin Inst.* **217**, 543 (1934).

(36) Bosworth, R. C. *Proc. Roy. Soc.* **150**A, 58 (1935).

(37) —— *Proc. Camb. Phil. Soc.* **34**, 262 (1938).

(38) Cichocki, J. *Ann. de Physique*, **20**, 478 (1933).

(39) Tubandt, C. *Z. Elektrochem.* **39**, 500 (1933).
Tubandt, C., Eggert, S. and Schibbe, G. *Z. anorg. Chem.* **1**, 117 (1921).
Seith, W. *Z. Elektrochem.* **42**, 635 (1936).
Tubandt, C., Reinhold, H. and Liebold, G. *Z. anorg. Chem.* **197**, 225 (1931).

(40) Grube, G. and Jedele, A. *Z. Elektrochem.* **38**, 799 (1932).

(41) Hicks, L. *Trans. Amer. Inst. min. (metall.) Engrs*, **113**, 163 (1934).

(42) Renninger, M. *Z. Kristallogr.* **89**, 344 (1934).

(43) Wagner, C. and Schottky, W. *Z. phys. Chem.* **11**B, 163 (1930).
Wagner, C. *Z. phys. Chem.* p. 177 (1931) (Bodenstein Festband).
—— *Z. phys. Chem.* **22**B, 181 (1933).

(44) Jost, W. *J. chem. Phys.* **1**, 466 (1933); *Z. phys. Chem*, **169**A, 129 (1934).

(45) Schottky, W. *Z. phys. Chem.* **29**B, 335 (1935).

(46) v. Hevesy, G. *Handbuch der Phys.* **13**, 286 (1928); *Z. Elektrochem.* **39**, 490 (1933).

(47) Frenkel, J. *Z. Phys.* **35**, 652 (1926).

(48) Wagner, C. *Trans. Faraday Soc.* **34**, 851 (1938).

(49) Strock, L. *Z. phys. Chem.* **25**B, 441 (1934); **31**B, 132 (1935). Rahlfs, P. *Z. phys. Chem.* **31**B, 157 (1935).

(50) Ketelaar, J. *Z. phys. Chem.* **26**B, 327 (1934); **30**, 53 (1935); *Z. Kristallogr.* **87**, 436 (1934).

(51) Baumbach, H. and Wagner, C. *Z. phys. Chem.* **22**B, 199 (1933).

(52) Dünwald, H. and Wagner, C. *Z. phys. Chem.* **22**B, 212 (1933).

(53) Jette, G. and Foote, F. *J. chem. Phys.* **1**, 29 (1933). Hägg, G. and Sucksdorff, J. *Z. phys. Chem.* **22**B, 444 (1933). Hägg, G. and Kindström, A. L. *Z. phys. Chem.* **22**B, 453 (1933).

(54) Seith, W. *Z. Elektrochem.* **42**, 635 (1936).

(55) Hilsch, R. and Pohl, R. W. *Z. Phys.* **108**, 55 (1937). —— —— *Z. Phys.* **57**, 145 (1929); **59**, 812 (1930). Rögener, H. *Ann. Phys., Lpz.*, **29**, 387 (1937). Mollwo, E. *Ann. Phys., Lpz.*, **29**, 394 (1937). Hilsch, R. *Ann. Phys., Lpz.*, **29**, 407 (1937).

(56) Jost, W. *Trans. Faraday Soc.* **34**, 861 (1938). —— *Diffusion ü. Chem. Reakt. im festen Stoffen*, Dresden (1937). Jost, W. and Nehlep, G. *Z. phys. Chem.* **32**B, 1 (1936).

(57) Koch, E. and Wagner, C. *Z. phys. Chem.* **38**B, 295 (1937).

(58) Foussereau. *Ann. Chim. (Phys.)*, **5**, 241, 317 (1885).

(59) Rasch, E. and Hinrichsen, F. *Z. Elektrochem.* **14**, 41 (1908).

(60) Konigsberger, J. *Phys. Z.* **8**, 883 (1907).

(61) Phipps, T., Lansing, W. and Cooke, T. *J. Amer. Chem. Soc.* **48**, 112 (1926).

(62) Smekal, A. *Handbuch der Phys.* **24**, ii, 880 (1933).

(63) Gyulai, Z. *Z. Phys.* **67**, 812 (1931). Jost, W. *Diffusion ü. Chem. Reakt. im festen Stoffen*, p. 130, Dresden (1937).

(64) Tubandt, C., Eggert, S. and Schibbe, G. *Z. anorg. Chem.* **117**, 1 (1921). Klaiber, F. *Ann. Phys., Lpz.*, (5), **3**, 229 (1929). Baedeker, K. *Ann. Phys., Lpz.*, **22**, 749 (1907). Tubandt, C. and Reinhold, H. *Z. phys. Chem.*, Bedenstein. Festband, p. 874 (1931). Jost, W. *Z. phys. Chem.* **16**B, 129 (1932).

(65) Tubandt, C. and Reinhold, H. *Z. Elektrochem.* **37**, 589 (1931). Wagner, C. *Z. phys. Chem.* **21**B, 42 (1933).

(66) Lehfeldt, W. *Z. Phys.* **85**, 717 (1933).

(67) Haber, F. and Tolloczko, St. *Z. anorg. Chem.* **41**, 407 (1904).

(68) Bruni, G. and Scarpa, G. *R.C. Accad. Lincei*, **22**, 438 (1913).

(69) Coehn, A. and Sperling, K. *Z. Phys.* **83**, 291 (1933). Coehn, A. and Specht, W. *Z. Phys.* **62**, 1 (1930).

(70) Seith, W. and Kubaschewski, O. *Z. Elektrochem.* **41**, 551 (1935).

(71) Seith, W. and Etzold, H. *Z. Elektrochem.* **40**, 829 (1934).

(72) Jost, W. *Z. angew. Chem.* **45**, 544 (1932).
Jost, W. and Linke, R. *Z. phys. Chem.* **29** B, 127 (1935).

(73) Nehlep, G., Jost, W. and Linke, R. *Z. Elektrochem.* **42**, 150 (1936).

(74) Nernst, W. *Z. phys. Chem.* **2**, 613 (1888).

(75) Einstein, A. *Ann. Phys., Lpz.*, (4), **17**, 549 (1905).

(76) v. Hevesy, G. *S.B. Akad. Wiss. Wien*, **129**, 549 (1920); *Z. phys. Chem.* **127**, 401 (1927).

(77) Braune, H. *Z. Elektrochem.* **31**, 576 (1925).

(78) Tubandt, C., Reinhold, H. and Jost, W. *Z. anorg. Chem.* **177**, 253 (1928); *Z. phys. Chem.* **129** A, 69 (1927).

(79) Wagner, C. *Z. phys. Chem.* **11** B, 139 (1931).

(80) Jost, W. *Diffusion ü. Chem. Reakt. im festen Stoffen*, p. 132, Dresden (1937).

(81) Braune, H. and Kahn, O. *Z. phys. Chem.* **112** A, 270 (1924).

(82) v. Hevesy, G. and Seith, W. *Z. Elektrochem.* **37**, 528 (1931).

(83) Seith, W. and Keil, A. *Z. phys. Chem.* **22** B, 350 (1933).

(84) Seith, W., Hofer, E. and Etzold, H. *Z. Elektrochem.* **40**, 322 (1934).

(85) Mehl, R. *Trans. Amer. Inst. min. (metall.) Engrs*, **122**, 21 (1936), collected from various sources.

(86) Matano, C. *Jap. J. Phys.* **9**, 41 (1934).

(87) Jost, W. *Z. phys. Chem.* **21** B, 158 (1933).

(88) Fonda, G., Young, A. and Walker, A. *Physics*, **4**, 1 (1933).

(89) Dushman, S., Dennison, D. and Reynolds, N. *Phys. Rev.* **29** 903 (1927).

(90) van Liempt, J. A. *Rec. Trav. chim. Pays-Bas*, **51**, 114 (1932).

(91) Paschke, M. and Hauttmann, A. *Arch. Eisenhüttenw.* **9**, 305 (1935).

(92) Mehl, R. F. *J. appl. Phys.* **8**, 174 (1937).

(93) Matano, C. *Mem. Coll. Sci. Kyoto*, **15**, 351 (1932).

(94) Braune, H. *Z. phys. Chem.* **110**, 147 (1924) (above 750° C.).

(95) Jost, W. *Z. phys. Chem.* **9** B, 73 (1930) (between 200 and 600° C.).

(96) Seith, W. *Z. Elektrochem.* **39**, 538 (1933).

(97) Brick, M. and Philips, A. *Trans. Amer. Inst. min. (metall.) Engrs*, **124**, 331 (1937).

(98) Rhines, F. N. and Mehl, R. *Trans. Amer. Inst. min. (metall.) Engrs*, **128**, 185 (1938).

(99) Eyring, H. *J. chem. Phys.* **4**, 283 (1936).
Eyring, H. and Wynne-Jones, W. *J. chem. Phys.* **3**, 492 (1935).

(100) Tiselius, A. *Z. phys. Chem.* **169** A, 425 (1934).

(101) Elam, C. *J. Inst. Metals*, **43**, 217 (1930).

(102) Smith, C. *Min. and Metall.* **13**, 481 (1932).

(103) Wells, C. Metals Res. Lab., Carnegie Inst. Tech. unpublished research.

(104) Warburg, E. and Tegetmeier, F. *Ann. Phys., Lpz.*, **32**, 442 (1887)

(105) Joffé, A. *Ann. Phys., Lpz.*, **72**, 495 (1923).

(106) Bugahow, W. and Breschnewa, N. *Tech. Phys. U.S.S.R.*, **2**, 435 (1935).

Bugahow, W. and Rybalko, F. *Tech. Phys. U.S.S.R.* **2**, 617 (1935).

(107) Spiers, F. *Phil. Mag.* **15**, 1048 (1933).

(108) Matano, C. *Jap. J. Phys.* **8**, 109 (1933); *Proc. Phys. Math. Soc. Japan*, **15**, 405 (1933).

(109) van Liempt, J. *Z. Phys.* **96**, 534 (1935).

(110) Sen, B. *C.R. Acad. Sci., Paris*, **199**, 1189 (1934).

(110a) Borelius, G. *Proc. Phys. Soc.* Extra Part, **49**, 77 (1937).

Bragg, W., Sykes, C. and Bradley, A. *Proc. Phys. Soc.* Extra Part, **49**, 96 (1937).

(110b) Sykes, C. and Evans, H. *J. Inst. Metals*, **58**, 255 (1936).

(111) Bernal, J. D. *Int. Conf. on Phys.* **2**, 119 (1934).

(112) Smekal, A. *Phys. Z.* **26**, 707 (1925).

(113) Jost, W. *Z. phys. Chem.* **6**B, 88, 210 (1929); *Z. phys. Chem.* **7**B, 234 (1930).

Joffé, A. *Z. Phys.* **62**, 730 (1930).

(114) Fajans, K. *Fortschr. Phys. Wiss.* **5**, 294 (1926).

Reis, A. *Z. Phys.* **44**, 353 (1927).

(115) Braunbek, W. *Z. Phys.* **44**, 684 (1927); **38**, 549 (1926).

(116) v. Seelen, D. *Z. Phys.* **29**, 125 (1924).

(117) Cichocki, J. *J. Phys. Radium*, **7**, 420 (1936).

(118) Dorn, J. and Harder, O. *Trans. Amer. Inst. min. (metall.) Engrs*, **128**, 156 (1938).

(119) Langmuir, I. and Dushman, S. *Phys. Rev.* **20**, 113 (1922).

(120) Polanyi, M. and Wigner, E. *Z. phys. Chem.* **139**A, 439 (1928).

(121) Bradley, R. S. *Trans. Faraday Soc.* **33**, 1185 (1937).

(122) Wheeler, C. *Trans. Nat. Inst. Sci. India*, **1**, 333 (1938).

CHAPTER VII

STRUCTURE-SENSITIVE DIFFUSION

TYPES OF IRREVERSIBLE FAULT IN REAL CRYSTALS

It is usual to classify diffusion processes into volume, grain-boundary, and surface diffusions. While the preceding and following chapters show that the problems of volume and surface diffusion have been attacked in a fairly adequate manner, the data with which the present chapter has to deal are much more fragmentary. Jost, Wagner, Frenkel, and Schottky [1] have developed the theory of disorder in equilibrium with order in crystals. It transpires from theory and experiment that the transitions

$$\text{Order} \rightleftharpoons \text{Disorder}$$

occur in both directions with an energy of activation, and that the change from left to right is an endothermic process. As with chemical reactions which proceed with an energy of activation, by suddenly chilling the system the high temperature equilibrium is frozen, and a non-reversible low temperature system results. The degree of disorder in a crystal increases with increasing temperature, so that the disordered crystal chilled suddenly should have more interstitial ions and vacant lattice sites than it would possess in its equilibrium state, and should show an increased ionic conductivity. Annealing, provided cracks and grain boundaries did not occur, should diminish the conductivity to a basic value.

A second kind of structure-sensitive diffusion is also possible. The crystal, whether metallic or ionic, consists of a mosaic of small blocks,* separated by grain boundaries, or submicroscopic flaws. It is well known that diffusion on an external surface (Chap. VIII) proceeds more easily than volume diffusion. By an analogy, which will later be supported by experimental data, one may suppose that diffusion along

---

* The evidence for this point of view is presented in the next section.

these "internal surfaces" will occur more readily than volume diffusion. The velocity of diffusion is largely governed by the exponential term in the equation $D = D_0 e^{-E/RT}$, so that if

$$E_{surface} < E_{grain\ boundary} < E_{lattice},$$

the velocity of grain-boundary diffusion may exceed that of lattice diffusion even though the number of paths available for lattice diffusion is much greater than the number of paths available for grain-boundary diffusion.

A third type of structure-sensitive diffusion process is to be attributed to impurities in the lattice. These may be incorporated during the growth of the crystal due to accidental impurity of the mother liquor, or of the vapour. They may also be introduced intentionally, as when alkali-halide lattices are heated in alkali-metal vapours, halogen vapours, or mixed gas atmospheres of hydrogen and alkali metal. Wagner[2] and his co-workers introduced excess of one component by heating the crystal in an atmosphere of its electronegative component (O_2 for CdO, ZnO, NiO, Cu_2O; S for FeS; Br_2 for CuBr; I_2 for CuI). It is not difficult to recognise the irreversible low-temperature diffusion processes resulting from this type of disorder because of the sensitivity of the high-temperature conductivity to gas pressure. In the high-temperature region there exists an equilibrium

Gaseous component $\rightleftharpoons$ Component in excess in the lattice,

which Wagner[1] used to study the different kinds of equilibrium disorder occurring at high temperatures in crystals. When a crystal with an equilibrium excess of one component is chilled to low temperatures, irreversible conductivity and diffusion properties result (cf. Fig. 94, Chap. VI).

When the conductivity cannot be attributed to excess of one component, i.e. when the conductivity is not sensitive to changes in partial pressure of a surrounding gas atmosphere of that component, and yet irreversible conductivity or diffusion phenomena are observed, the behaviour may be attributed either to grain-boundary diffusion, or to lattice disorder, frozen by rapid cooling of the high-temperature

equilibrium state of disorder. To determine to which type of fault the structure sensitivity is due requires that one should know a great deal concerning the properties of the crystal. The ways in which these properties have led one to envisage different lattice imperfections may now be briefly reviewed.

NON-EQUILIBRIUM DISORDER IN CRYSTALS

Some properties of crystals depend upon the previous history of the specimen, while others are insensitive to all treatments. On this basis a classification [3] of crystal properties may be made (Table 77). The structure sensitivity of some of these

TABLE 77. *Classification of crystal properties*

Property	Insensitive	Semi-sensitive	Sensitive
Character	Additive, contribution of anomalous parts of smaller order of magnitude than that of normal parts	Additive, but contribution of anomalous parts of same order as that of normal parts	Selective
Examples	Specific gravity, specific heat, refractive index, X-ray interference, elastic properties	Electrical conductivity in ionic crystals, diffusion, X-ray extinction, vibration damping	Tensile strength, plasticity, dielectric strength, magnetisation curve of ferromagnetic substances

properties has been related to various types of imperfection, distributed over the surface and in the interior in a random manner.

The most obvious imperfections in crystals are cracks on and within the crystal surface. It is sometimes possible to see the cracks with the eye, or under a microscope, especially after suitable etching. Examination reveals that the surface consists of blocks, or grains (Fig. 112) [4], whose interfaces extend into the solid as cracks. Cracks of this size result from thermal and mechanical treatments of the crystal, and also according to Smekal [5] as a result of strains due to primary flaws in the crystal. The primary flaws are considered by Smekal to be due to occluded impurity, or to too rapid rates

of growth of the crystal which leave gaps or local variations
in orientation. It is also possible that they result from ex-
tension of the very shallow surface cracks which Lennard-
Jones and Dent [6] consider to occur as a result of unbalanced
forces at the crystal surface, which cause a lateral contraction
of the surface. The reality of contraction due to surface tension
is demonstrated by the experiments on the electrical con-
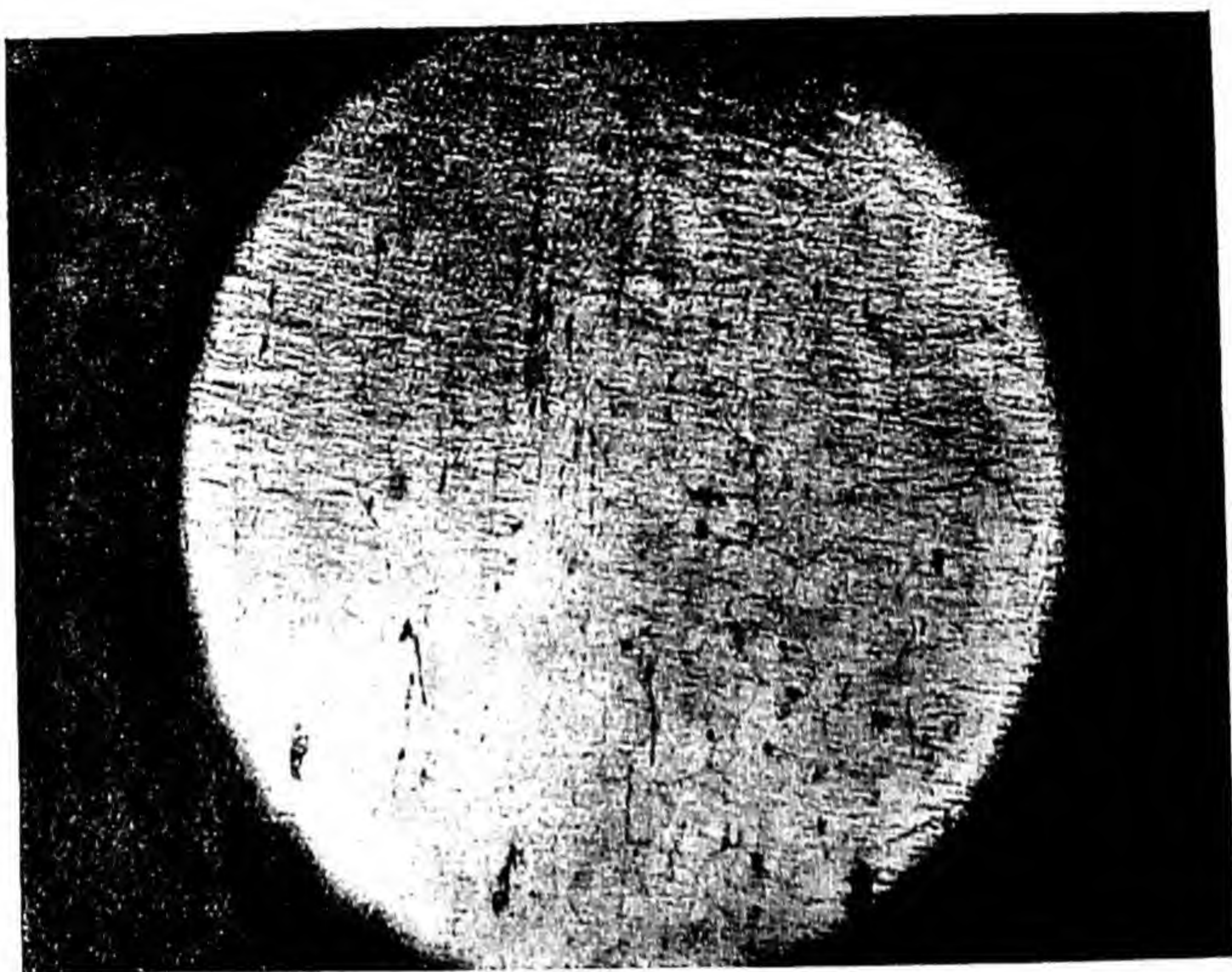
Fig. 112. Appearance of bright platinum surfaces (× 100),
showing crystallites, furrows and grain boundaries.

ductivity of thin films mentioned in the following chapter [7].
Due to the break up of evaporated films on surfaces, under
surface tension forces, the resistance rises after a time interval.

The presence of cracks and grain boundaries is revealed by
a number of additional experiments. Poulter and Wilson [8]
found that water, ether, and alcohol would penetrate into glass
or quartz for considerable distances when a pressure of
15,000 atm. was maintained for a quarter of an hour. If the
pressure was released quickly, the glass was shattered, due to
expansion of the diffused liquid in the grain boundaries. The
measurements suggested also an upper limit to the thickness

of the crack, since larger molecules such as oil, or glycerine,* caused no analogous shattering. Similarly, the diffusion of hydrogen through iron which can be made to occur at pressures of 9000–4000 (9, 10) atm., at room temperature, while in part a true lattice diffusion, also opens up grain boundaries, so that it is possible to force mercury and oil through the metal after diffusing hydrogen through it. These cracks in the iron were not visible to the naked eye.
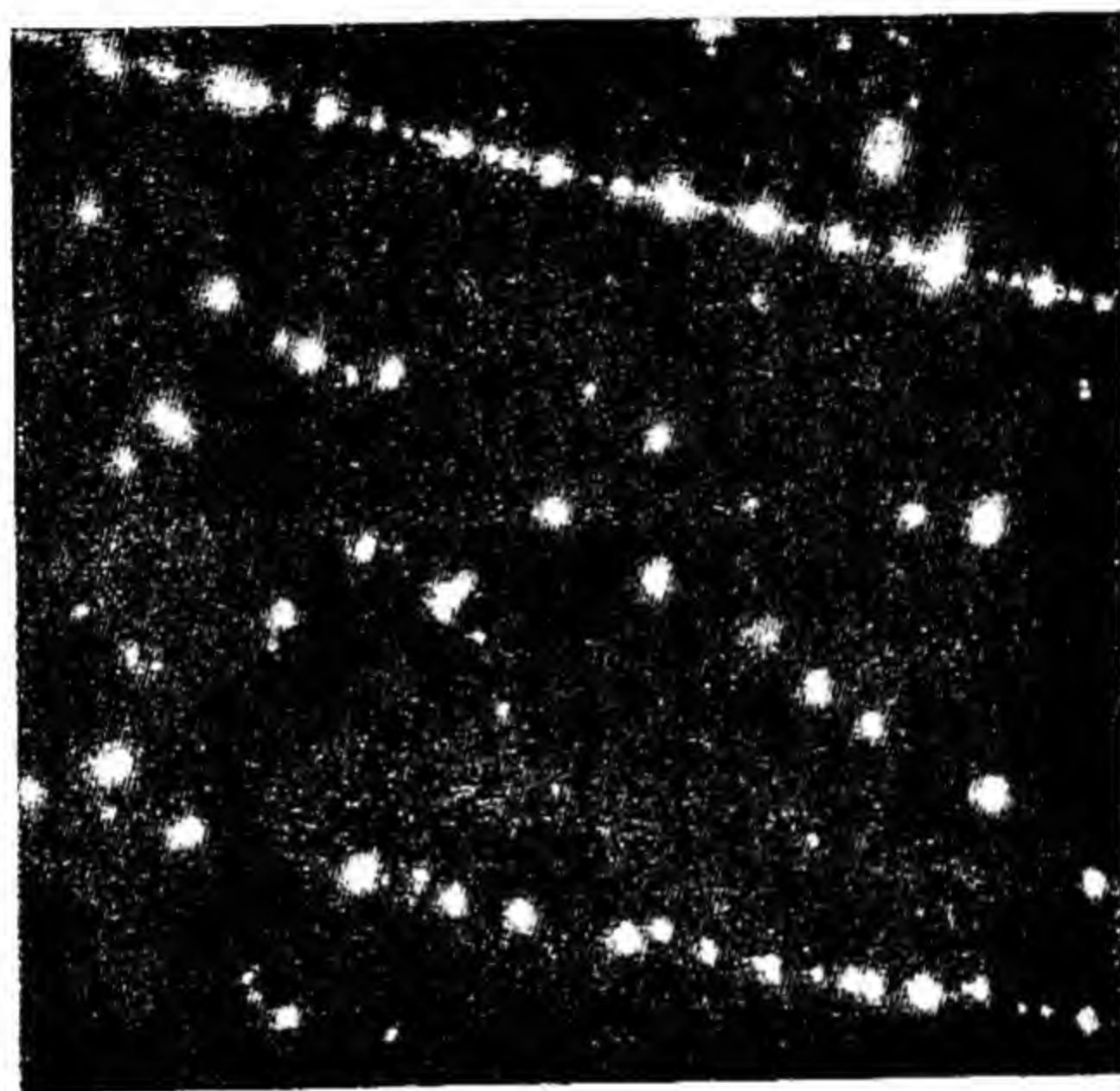
Fig. 113. Particles on SiO_2 glass, under strong grazing illumination (× 850).

The presence of cracks, especially at the surface, governs the tensile strength of crystals(11). If a specimen of rock-salt is dipped in hot water the tensile strength rises by 20-fold. Etching glass or silica fibres in hydrofluoric acid increases the tensile strength 5-fold. Some vapours sorbed on silica fibres diminish their tensile strength (water, 3-fold; alcohol, 3-fold; benzene, 2-fold). These effects may be explained as penetration of cracks by the sorbed liquid, increasing the bonding between grains or blocks in the solid rock-salt when water is sorbed, but diminishing it in glass, or silica, possibly due to hydration and swelling of silica powder down the grain boundaries and cracks, so thrusting the grains apart. Evidence of surface

* It is to be noted, however, that these larger molecules are not spherical.

cracks was adduced from experiments on the condensation of metallic atoms on diamond and silica surfaces(12). The metal atoms aggregated in lines along the surface (Fig. 113), and these lines were thought to trace out the course of surface cracks. Also the tensile strength of glass fibres is often found to increase as their diameter is diminished. This may be explained by supposing that cracks exist in the fibre, but that the probability of finding a sound fibre is greater the less its diameter, because the surface or volume of the fibre, in which the cracks exist, is in this way also diminished.

The continuation of cracks throughout the crystal results in a mosaic structure of the crystals. The existence of these secondary flaws through crystals of rock-salt may be demonstrated by heating sodium chloride in sodium vapour(13). Some vapour is absorbed and the crystal becomes coloured. Aggregation of the dissolved sodium occurs, under suitable conditions, along faults in the crystal, and the course of these faults may be traced by examination using the ultramicroscope. Aggregations of sodium of four kinds have been found (Fig. 114)(14), corresponding to tree-like, spheroidal, striated, and nearly homogeneous distributions of the metal.

When a crystal is placed on an X-ray goniometer and rotated in the X-ray beam, the intensity of reflection rises to a maximum and then falls away. The more ideal the crystal the sharper is this "sweep curve". Calculations have been made of the angular breadth of the "sweep curve" for an ideal crystal, which show that only a few seconds of arc will cover the whole breadth of the curve. Analogous calculations for a mosaic crystal indicated a much greater angular breadth of the "sweep curve", which may amount in extreme cases to several degrees. In Table 78(15) are illustrated the observed breadths of sweep curves at their points of half intensity; and also values of the "integrated reflection" defined as

$$\rho = \frac{(\text{Total reflected energy for uniform velocity of rotation}) \times (\text{velocity of rotation})}{\text{Intensity of incident radiation}}.$$

It is seen that Renninger's[15] artificial rock-salt crystal represents as near an approach to the ideal crystal as can be obtained, as far as the mosaic structure type of fault is concerned.

There has been discussion as to the size and distribution of the Smekal blocks in a mosaic crystal. Zwicky[18] suggested that a lattice is subdivided into a periodic block structure with definite spacings, basing his theory in part upon the appearance
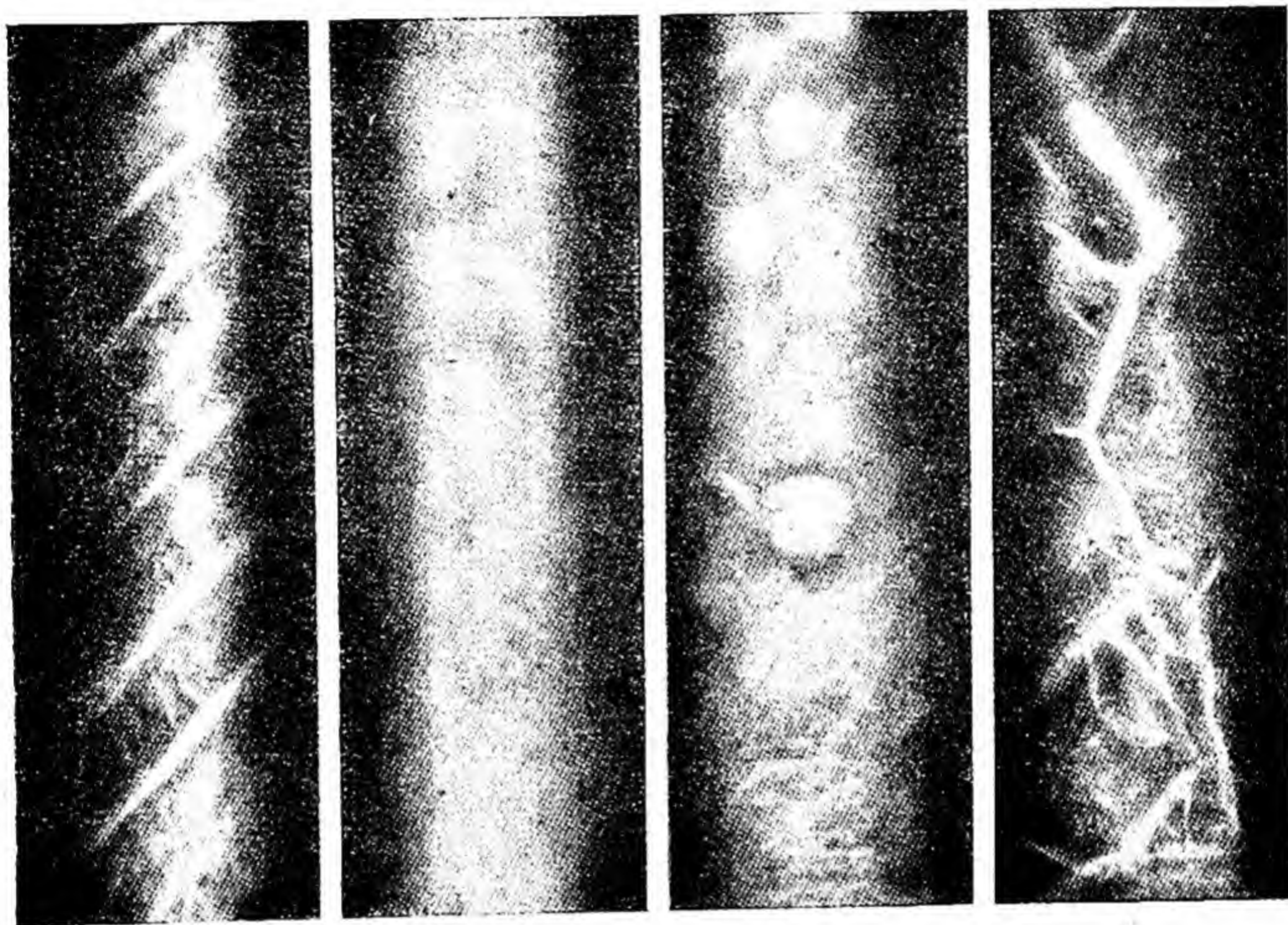
Fig. 114. Types of crystal fault in rock-salt, revealed by aggregation of absorbed sodium, and examination in Tyndall light[14].

of regular triangular etch pits on bismuth[19], and on the persistence of structure in liquids near their melting-points. He made calculations which purported to show that a crystal with such a super-lattice would be more stable than a crystal without the super-lattice. Since the calculations are not correct[20], and the evidence from the etch pits on bismuth does not necessarily imply a super-lattice of Zwicky type, his view may be discarded in favour of that of Smekal. The latter considered that any real crystal tends to become an a-periodic mosaic of blocks. The boundaries of the blocks grow from

primary flaws, or from mechanical and thermal treatment, and penetrate through the mass. Since diffusion processes down these systems of faults obey a law

$$D = D_0 e^{-E/RT},$$

where E is greater than the corresponding energy term for a surface diffusion (p. 312), it may be concluded that the Smekal cracks can be of molecular dimensions, so that the crystal force fields on either side of the crack overlap.

TABLE 78

Crystal (NaCl)	Half-breadth of sweep curve (200 face) sec.	Integrated reflection × 10⁶			
		200	400	600	
Natural crystal, polished cleavage	900	270	45	16	
Natural crystal, untouched cleavage	40 to 50	102·5	26·3	9·8	For CuKα radiation and NaCl
Artificial untouched cleavage, Renninger[15]	7·1	47·8	10·5	4·6	
Calculated for ideal crystal:					
Darwin[16]	4·2	45·0	12·1	6·9	
Prins[17]	4·9	41·0	9·9	5·1	

It must be remembered that in addition to the subdivision of the crystal into Smekal blocks, each block may have its own glide planes and that glide planes may act as regions for further break-up of the crystal block, or for preferential diffusion into the block. Palladium, after sorption of hydrogen, shows not only a block structure, but also a herring-bone pattern on the surface of each grain or block [21, 22] which has been attributed to preferential penetration of hydrogen down slip planes.

The manner in which a mosaic crystal may grow from a melt is shown by Buerger's [23] studies on dendritic crystals. A needle-like crystal first forms, the crystal branches into other needles, these yet again into more needles, and so all the space is quickly occupied by the dendritic mosaic crystal. Typical

dendritic mosaics of bismuth are illustrated in Fig. 115. Dendritic mosaics can be grown from solution, where once again the peculiar lineage structure may be recognised. Also galena and quartz may show tree-like markings and boundaries, while haematite crystals may be grown which are a mosaic of plates, laid down in a direction approximately normal to the direction of growth. Buerger considers that a complete range of structures is possible from dendritic mosaics, parallel crystal intergrowths, crystals with multiple terminations, or block structure, to crystals which, like certain specimens of gypsum

Fig. 115. A dendritic surface of rapidly cooled bismuth (× 2).

and calcite, show no imperfections under optical or X-ray examination. This lineage theory of crystal growth allows one to visualise readily how mosaics of various kinds may be formed.

The non-equilibrium disorder which is due to interstitial ions and vacant lattice sites, obtained by heating the crystal to high temperatures and then chilling it quickly, can be revealed by the absorption spectrum, if the concentration of the disordered points is large enough. It is generally necessary to incorporate impurities, however, to obtain an adequate concentration of interstitial ions or vacant sites for spectroscopic examination. For example, the blue crystal obtained by heating an alkali halide in alkali metal vapour gives a new absorption band[13] (Fig. 116). The breadth of the band, H, at

its point of half-intensity allows the concentration of colour centres, or F-centres, as they are called, to be estimated (cf. Chap. III) by the equation

$$N = 1\cdot31 \times 10^{17}\frac{\mu}{(\mu^2+2)^2}K_{max.}H,$$

where $K_{max.}$ denotes the absorption coefficient at the peak of the absorption curve, and μ is the refractive index for light having the wave-length of the absorption maximum. The number of colour centres/c.c. (N) is 10^{15}–10^{17} with the sodium vapour pressures normally employed. The F-centres are considered to be due to electrons occupying vacant chlorine-ion sites in the lattice [24]. They may be electrolysed out of the
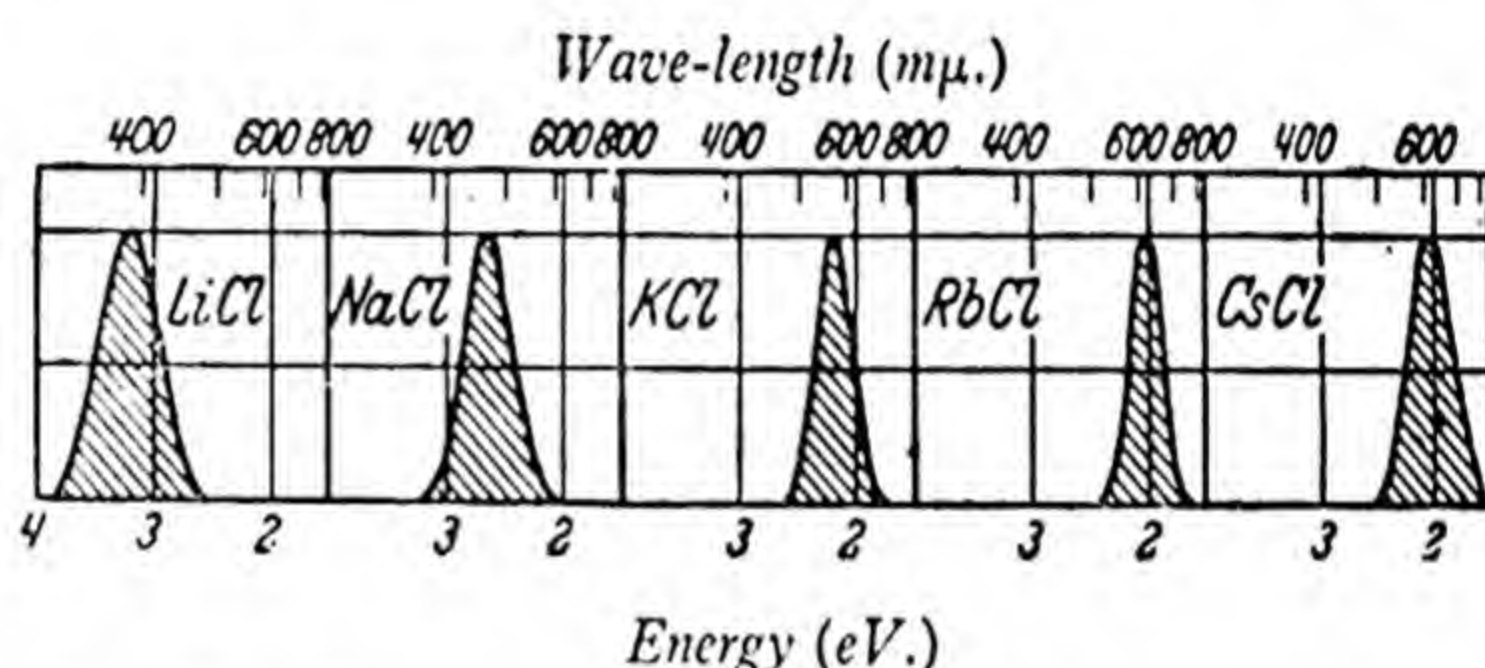
Fig. 116. Absorption bands of colour centres in solution in alkali halides at 10° C. (Pohl[13]).

crystal, and move towards the anode giving a sharp colour boundary in the crystal [13]. Irradiation with blue light causes the nature of the absorption band to change, and a new type of colour centre appears, the F'-centre, regarded by Mott [25] as consisting of two electrons in a vacant lattice site. Irradiation with infra-red light, or heating, causes the reverse change into F-centres to occur, so that a photo-equilibrium can result:

$$F\text{-centres} \underset{\text{infra-red radiation or heat}}{\overset{\text{blue light}}{\rightleftarrows}} F'\text{-centres}$$
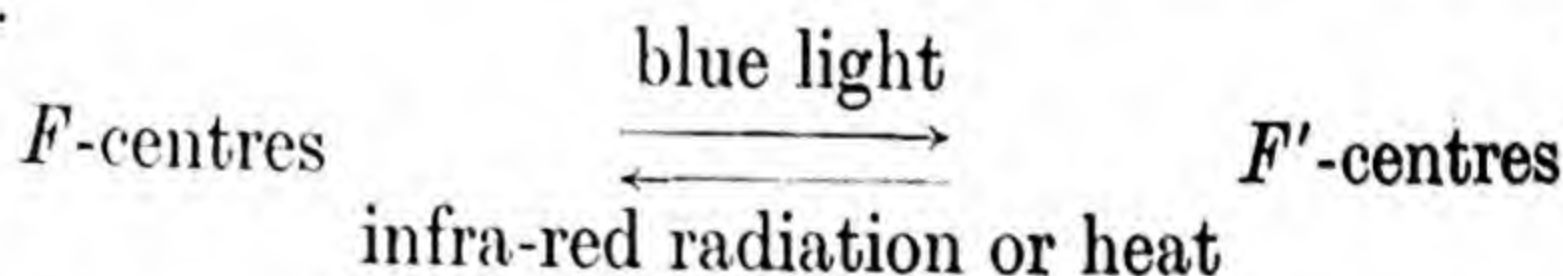
Heating a crystal of alkali halide containing dissolved alkali metal in hydrogen discharges the colour of the crystal and causes the absorption spectrum to change [13]. A new peak occurs in the ultra-violet. These centres, which are usually designated as U-centres, are in a reversible equilibrium with

F-centres, into which they may be transformed by heat or by ultra-violet light. U-centres consist of alkali-hydride (13) that has been formed in the lattice, and dissociates on heating or irradiation as follows:

$$KH \rightleftharpoons K^+ + H + e.$$
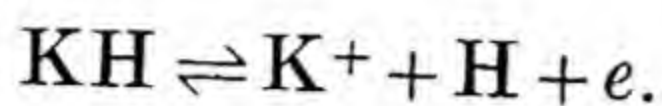
The electron occupies a vacant chlorine-ion site and constitutes an F-centre.

These centres of disorder may contribute to the conductivity, under the influence of light and of heat.

STRUCTURE-SENSITIVE CONDUCTIVITY PROCESSES

Conductivity data may be employed to demonstrate the properties of structure-sensitive diffusion in crystals. It is often found that the conductivity-temperature curve of ionic crystals divides itself into two sections, a reversible high-temperature curve, obeying a law

$$K = Ae^{-E/RT},$$

and families of low-temperature curves obeying analogous laws

$$K_1 = A_1 e^{-E_1/RT} \quad (E_1 < E).$$

The positions of the low-temperature curves depend upon the treatment accorded the specimen and are therefore structure sensitive. The high-temperature curve is obtained for all specimens of a given crystal, and is structure insensitive (27) (Fig. 117). When crystals of sodium chloride were heated for periods of 10 hr. at a series of temperatures, the conductivity rose as the temperature of heating rose, corresponding to an increased number of faults and flaws resulting from the pre-heating (Fig. 118). Smekal (26) expressed the results of Figs. 117 and 118 for the conductivity (in ohm^{-1} cm.$^{-1}$) by the expression

$$K = \underbrace{A_1 e^{-10,300/T}}_{\text{Structure sensitive}} + \underbrace{1 \cdot 4 \times 10^6 e^{-23,000/T} + \underbrace{3 \cdot 6 \times 10^6 e^{-25,700/T}}_{\text{Anion conductivity}}}$$

Structure sensitive | Anion conductivity

Cation conductivity

showing that the slopes of the structure-sensitive conductivity curves were all nearly the same, but the temperature independent factor altered very markedly.

BD 21

Single crystals of sodium nitrate (27), because of the smaller internal surface, show a lower conductivity than the poly-crystalline mass solidified from the melt. If a powdered salt is put under pressure, the coherent block, composed of a mosaic
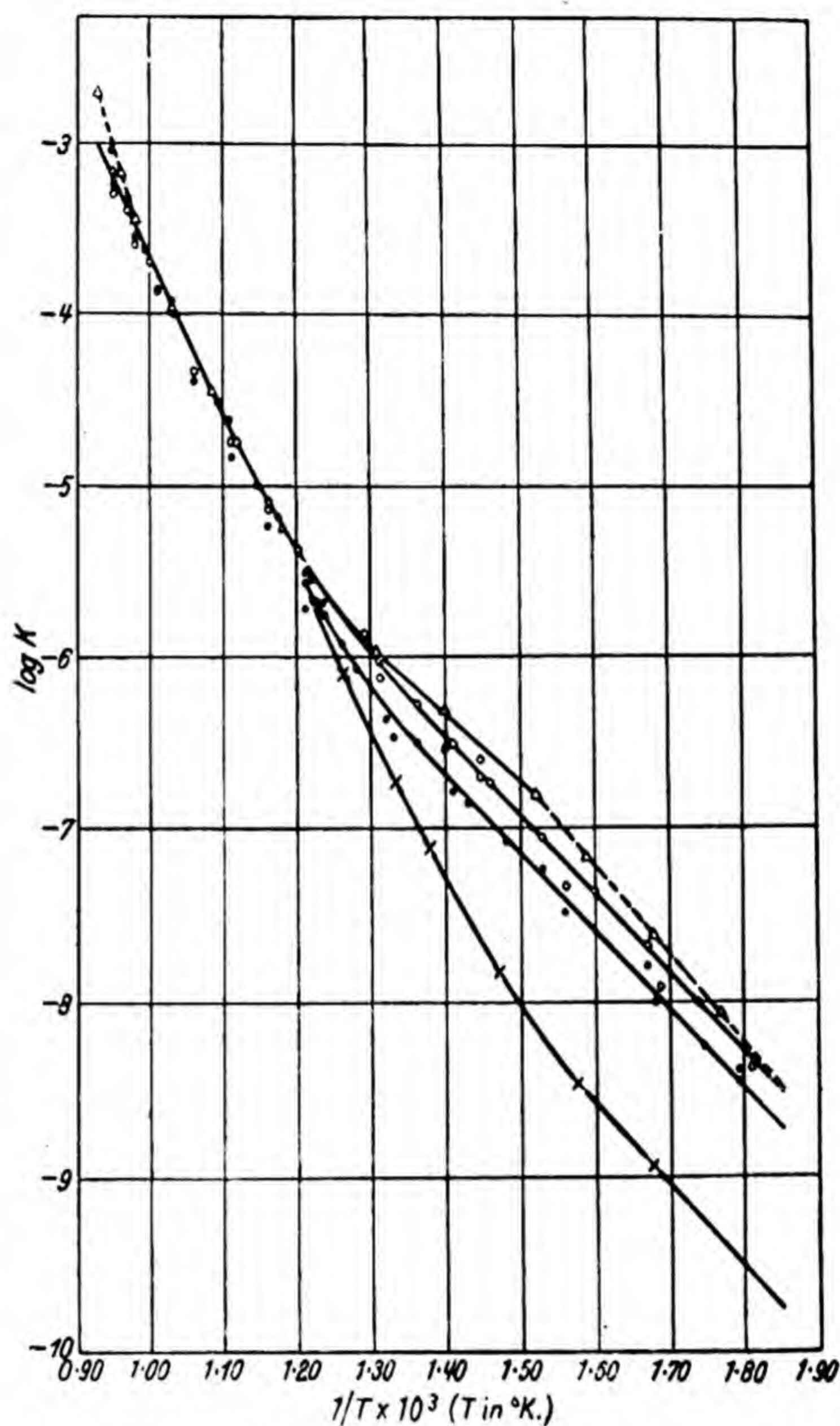
Fig. 117. The conductivity of various NaCl crystals. (The lowest curve is for a single crystal.)

of small crystallites, shows a higher conductivity than a single crystal (28). Quartz sand when mixed with the crystals of sodium nitrate (62 % SiO_2), by increasing the number of grains and diminishing their size, was observed to double the con-ductivity (29). Rock-salt crystals, prepared by crystallisation from aqueous solution, possessed at 90° C. a conductivity

100-fold smaller than that of a rock-salt polycrystalline mosaic prepared from a melt (30). These observations lead to the conclusion that internal surfaces are of great importance in conductivity measurements.
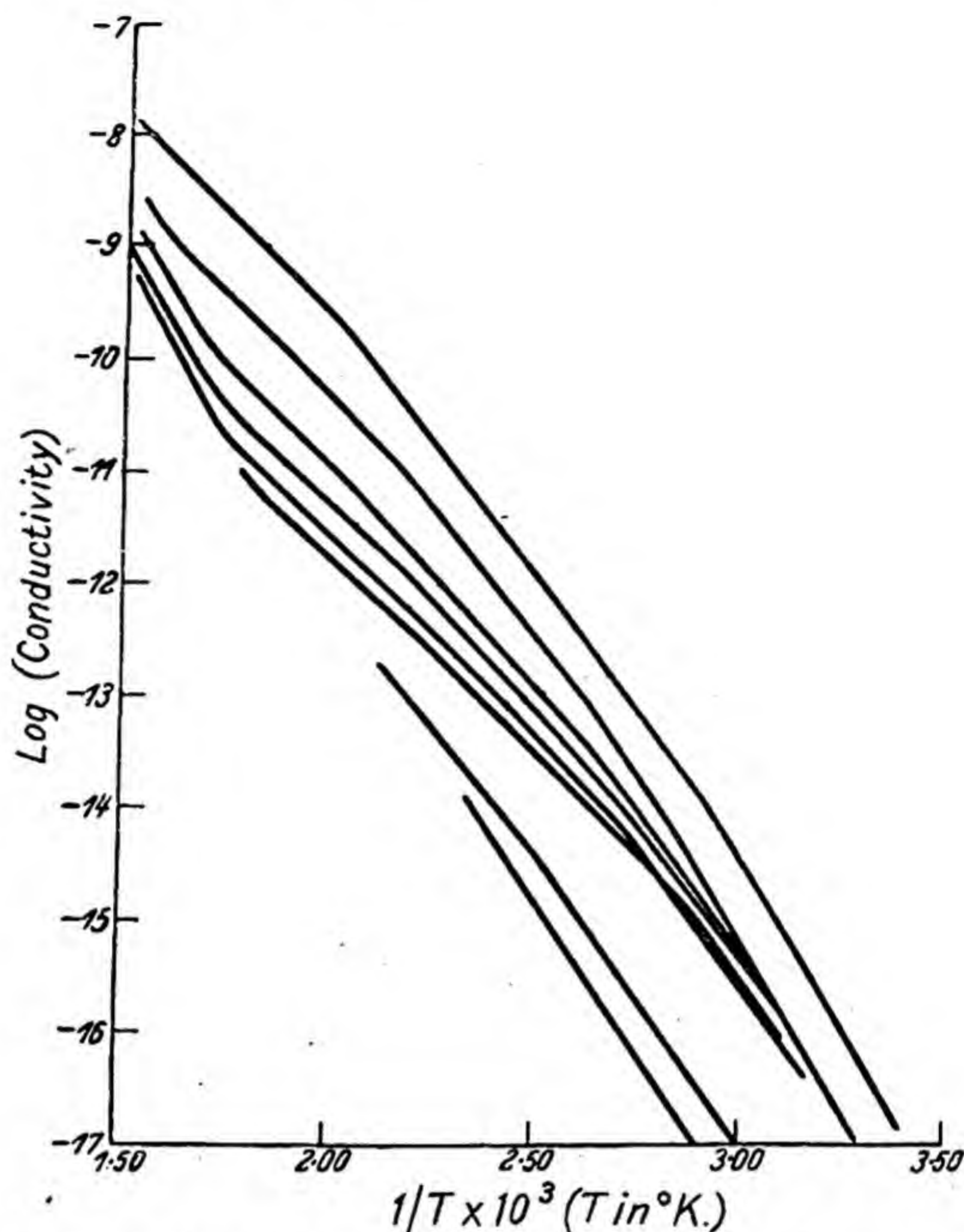
Fig. 118. Rock-salt crystals, heated for 10 hr. at a series of temperatures, show an increasing conductivity. After 10 hr. at 160° C. (the lowest curve), rising to 200, 300, 400, 500, 600, 700, 780 (the highest curve).

Another kind of experiment which has thrown light upon the nature of structure-sensitive conductivity requires the addition of small quantities of impurity to the crystal lattice. As early as 1897 (31) it was noted that the addition of sodium chloride to lead chloride caused an increase in the conductivity of the latter. One of the most remarkable examples of this phenomenon was given by Ketzer (32), who by adding 0·001 % of rock-salt to lead chloride raised the conductivity of the lead chloride 50-fold. Gyulai (33) repeated these experiments, adding

21-2

small amounts of potassium chloride, and showing that in the equation

$$K = Ae^{-E/RT},$$

both A and E altered (Table 79). Lehfeldt[34] reversed the procedure of Gyulai, and added small amounts of copper and lead salts to potassium chloride, obtaining as usual an increase in the conductivity of the solvent salt. Since the slope of the curves log (conductivity) against $1/T$ (T in ° K.) are almost

TABLE 79. *The effect of adding* KCl *to* PbCl$_2$ *(Gyulai)* *on the constants of the equation* $K = Ae^{-E/RT}$

PbCl$_2$ melted in Cl$_2$ gas		PbCl$_2$ + 0·005% KCl melted in Cl$_2$ gas	
A	E	A	E
1·41	10,620	4·36	8680
1·65	10,860	6·88	9000
1·29	11,000	4·04	8720
1·08	10,840	9·02	9360
PbCl$_2$ melted in N$_2$ gas		PbCl$_2$ + 0·005% KCl melted in N$_2$ gas	
A	E	A	E
5·12	10,920	4·78	4400
6·55	11,070	Sublimed	
6·29	10,860		Seith[35]
1·43	11,700	Crystallised from solution	

the same, the change in the conductivity is due to an increase in the factor A in the equation $K = Ae^{-E/RT}$. In general, however, the effects encountered are in part due to a loosening of the lattice (see Table 79, KCl in PbCl$_2$), when the impurity is added, and in part to a decrease in the size of constituent crystal grains. A loosening of the lattice suggests an increase in the number of interstitial ions and vacant sites, and this viewpoint is supported by Lehfeldt's[34] observation that long-continued electrolysis will free some crystals of impurity (e.g. of PbCl$_2$ in KCl[34]). On the other hand, Tubandt and Reinhold[36] found no redistribution of solute and solvent by electrolysis for NaCl or KCl in PbCl$_2$, so

that this experiment supports the viewpoint that the solute here enhances the conductivity solely by increasing the number of crystal grains in a given mass of crystal.

When a current is passed through a crystal, the resistance in the low-temperature structure-sensitive conductivity region rises rapidly, as a counter-electromotive force is set up. This
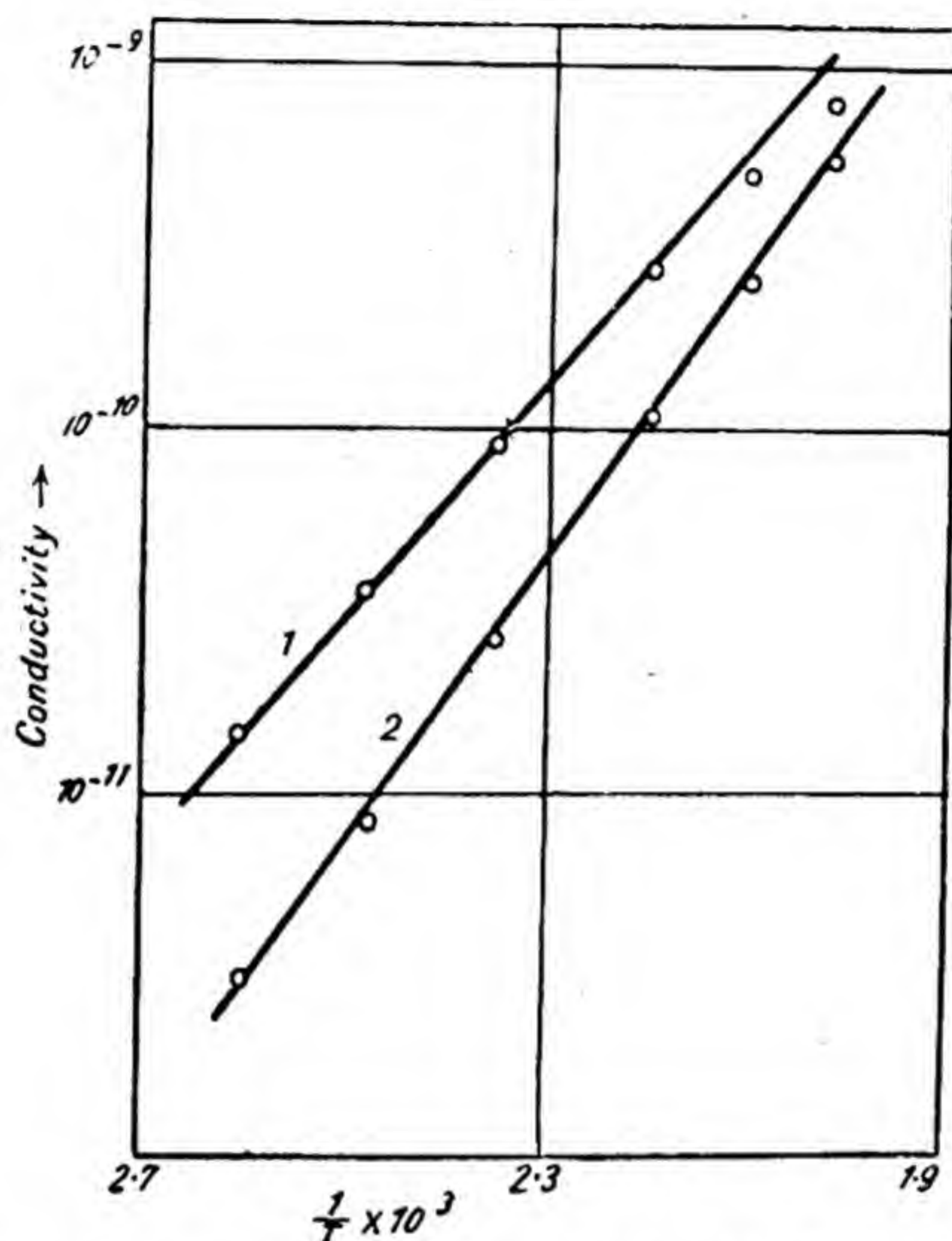
Fig. 119. The two conductivities for rock-salt. (1) True conductivity, (2) conductivity after space-charge redistribution (Beran and Quittner[37]).

counter-electromotive force is not always due, however, to polarisation at the electrodes, but to a redistribution of charges in the body of the crystal[28, 37]. The experiments therefore suggest that interstitial ions exist in the crystal which are not in reversible equilibrium with the lattice. Both the initial, or true, conductivity of the crystal, and the conductivity after the redistribution of space charge in the crystal, conform to the well-known exponential equation $K = Ae^{-E/RT}$ (Fig. 119), the values of E being respectively 7510 and 9600 cal./ion.

Mechanical deformation will create centres of disarray in a crystal[38] which result in a momentary increase in con-

ductivity. When a rock-salt crystal was put under a series of pressures rising by steps from 20 to 700 kg./cm.², each successive step caused a momentary increase in the conductivity, while releasing the pressure resulted in no new effect. When the pressure was again applied there was no further conductivity jump until the previous maximum pressure was exceeded, when a momentary increase in conductivity appeared once more. The jump in the conductivity was shown by Stepanow [39] to be an increase in the true conductivity rather than a decrease in the counter-electromotive force due to polarisation. It was later found that a crystal, if put under pressure and then annealed, would give a conductivity jump when it was subjected to a second compression, even when this compression did not exceed the initial load. The suggestion by Joffé [40] that these phenomena result not from an increase in the number of centres of disorder, but from a displacement of the charge in the crystal was contradicted by Gyulai [41].

The experiments reviewed show the multiplicity of effects which can influence the non-reversible disorder of crystals and, so the conductivity or diffusion. The conductivity depends upon the few mobile ions in the crystalline mass which are perhaps 10^{-4} or less of the total number of ions [42]. The energy for loosening these ions is considered by Smekal to be only 0·4 of the energy for loosening a lattice ion. This estimate may be compared with the values given in Chap. VIII, p. 363, for the ratio of the activation energy for volume and surface diffusion, which may vary from 0·2 to 0·5. The latter is the ratio for the thorium-tungsten system, the former for caesium on tungsten.

STRUCTURE-SENSITIVE DIFFUSION PROCESSES

Structure-sensitive diffusion in metallic systems is of fairly common occurrence. The self-diffusion of bismuth, while strongly anisotropic, is to a certain extent dependent upon the bismuth crystal [43] employed:

$$D (\| \text{ to } 111 \text{ plane}) = (1 \cdot 33 - 16 \cdot 3) \times 10^{45} e^{-137,000/RT} \text{ cm.}^2 \text{ sec.}^{-1},$$

$$D (\perp \text{ to } 111 \text{ plane}) = (2 \cdot 22 - 6 \cdot 5) \times 10^{-4} e^{-30,000/RT} \text{ cm.}^2 \text{ sec.}^{-1}.$$

The variation in the above equations for D is in the temperature independent factor, D_0, but only a small range of values of D_0 is found. Bugahow and Rybalko [44] made a study of the diffusion of zinc and copper in brass in which they found that the diffusion constants increased when one passed from single crystals to polycrystalline masses because the diffusion constant depended on grain size. On passing from a single crystal to a polycrystalline mass, both E and D_0 (in the equation $D = D_0 e^{-E/RT}$) changed; but in all polycrystalline samples the E values were the same and only the values of D_0 altered. It has proved possible to measure changes in the state of tungsten surfaces very readily by following the thermionic emission, which is extremely sensitive to adsorbed films. Molybdenum or tungsten filaments are used containing a certain amount of thorium (in the intergranular boundaries).* By flashing the filaments at very high temperatures the surface may be momentarily freed of thorium; and if the filaments are then kept at some lower temperature (2050° K. is usual for tungsten), the thorium diffuses slowly from inner to outer surfaces and the process may be followed by measuring the thermionic emission. It was found that the rate at which this diffusion outwards occurred depended on the size of the crystallites which comprised the filaments [45, 46] (Fig. 120), the extreme variation in D being in the instance cited 300 : 1. It is to be noted, however, that the slopes of the three lines of Fig. 120 are all the same—the activation energy

* The solubility of thorium in a tungsten lattice is negligible.

does not depend on grain size. By mechanical treatment of a tungsten single crystal[46] it was possible to increase the diffusion rate without appreciably changing other properties. This phenomenon can be contrasted with the behaviour of the malleable metal lead in which mechanical working caused no change in the self-diffusion co-
efficient[47].

Gehrts[48] showed that the therm-
ionic activation of tungsten and molybdenum filaments, by diffu-
sion of thorium from inside to the surface, obeyed the law

$$\theta = 1 - Ce^{-(D/r^2)\alpha_1^2 t} = 1 - Ce^{-kt},$$

where $\alpha_1 = 2\cdot406$ (the first root of the Bessel function of zero order),

θ = the fraction of the surface covered by thorium after flash-
ing,

D = the diffusion constant,

Fig. 120. Diffusion of thorium in tungsten crystallites of various sizes[46].
A. Particle diameter $5\cdot3\mu$;
B. Particle diameter $7\cdot3\mu$;
C. Particle diameter 3000μ.

r = the radius of the crystallites composing the filament.

C = a constant.

From the data of Fonda, Young and Walker[46] he calculated the intergranular diffusion constant at $2050°$ K. to be

$$D = 0\cdot5 \times 10^{-10} \text{ cm.}^2 \text{sec.}^{-1}.$$

Langmuir's[49] data gave

$$D = 1\cdot1 \times 10^{-10} \text{ cm.}^2 \text{ sec.}^{-1} \text{ at } 2055° \text{ K.}$$

Mehl[50] gave for the volume diffusion of thorium in tungsten the equation

$$D = 1\cdot00e^{-120,000/RT} \text{ cm.}^2 \text{ sec.}^{-1},$$

and for grain-boundary diffusion

$$D = 0\cdot74e^{-94,000/RT} \text{ cm.}^2 \text{ sec.}^{-1}.$$

Some numerical values of D_0 and E, showing the influence of grain size, are given below:

TABLE 80. *Constants in the equation* $D = D_0 e^{-E/RT}$
for a grain-boundary diffusion

System	Particle radius in μ	E cal./atom	D_0 cm.^{2} sec.$^{-1}$
Th in W	3000	94,400	$3 \cdot 0 \times 10^{-3}$
	7·3	95,600	$4 \cdot 8 \times 10^{-1}$
	5·3	93,600	$7 \cdot 9 \times 10^{-1}$
	—	94,600	$8 \cdot 4 \times 10^{-1}$

The diffusion of a number of elements through tungsten has been followed by the thermionic emission method [51]. None of the films formed at the tungsten surface is as stable as a thorium film, but the results are analogous. They demonstrate that a large energy of activation is necessary for diffusion, and that the velocity of diffusion depends upon the grain size of the tungsten. The diffusion data for these metals are collected in Table 81. Since the values for D and D_0 are dependent upon

TABLE 81. *The constants* D, D_0 *and* E *in the equation*
$D = D_0 e^{-E/RT}$ *for diffusion in particular samples of tungsten*

Diffusing metal	$D \times 10^{11}$ cm.^{2} sec.$^{-1}$ at 2000° K.	D_0 cm.^{2} sec.$^{-1}$	E cal./atom	Atomic weight
U	1·3	1·0	100,000	238·5
Th	5·9	0·75	94,000	232
Ce	95	1·0	83,000	140·3
Zr	324	1·0	78,000	91
Yt	1820	0·46	62,000	89
C in W_2C [56]	—	—	~108,000	12
C in single W crystal at 2460° K. [55, 56]	5×10^4	—	72,000	12

the grain size, they are not to be taken as more than a measure of these constants for particular specimens of tungsten. The diffusion of carbon in tungsten [52] was followed by measuring the conductivity of the wire whose surface was maintained saturated with carbon. The conductivity fell linearly with its carbon content until at the composition W_2C it

was only 7 % of that of pure tungsten. Further diffusion in the carbide W_2C resulted in the formation of WC. The process was reversible, when the surface carbon was removed by evaporation, or with oxygen as carbon monoxide. The diffusion constants in tungsten were those in Table 82, when a constant concentration at the surface of 0·002 % of carbon was

TABLE 82. *Diffusion of carbon in tungsten*

(*a*) for 7 mil. pure W

$D \times 10^7$ cm.^{2} sec.$^{-1}$	5	10
T C.	2185	2355

(*b*) for 4 mil. W, 0·5 % ThO_2

$D \times 10^7$ cm.^{2} sec.$^{-1}$	1·6	4·8	7·8	18
T C.	2070	2188	2300	2400

assumed at all temperatures. Zwikker's[53] data on the same system emphasise the influence of grain boundaries, since he found values of the diffusion constant varying in the ratio 30 : 1 at 1970° K. for different tungsten specimens.

Van Liempt[54] made a study of the diffusion of molybdenum in tungsten single crystals* and polycrystals, and found once again a dependence upon the size of the individual crystallites. His data for the two cases may be expressed by

(*a*) "Single crystal": $D = 1\cdot6 \times 10^{-3} e^{-80,000/RT}$,

(*b*) Polycrystalline mass: $D = 2 \times 10^{-2} e^{-80,000/RT}$.

The energy of activation is the same in the "single crystal" and the polycrystalline mass, but the temperature independent factor is different.

Preferential penetration down grain boundaries may sometimes be shown by taking microphotographs of the crystal in which diffusion has occurred[50]. Fig. 121 gives a cross-section of a bi-crystal of brass, stained so that the preferential loss of zinc from the grain boundary is very clearly indicated.

* Since E was the same for the supposed single crystal and for the polycrystal, and as diffusion occurred down grain boundaries for the latter, it may be inferred that grain boundary diffusion occurred also in the former, which did not therefore remain a single crystal.

It might be thought that all metals showing well-defined grain boundaries would show preferential penetration down those boundaries, but the photographic evidence is often very decisively against such an hypothesis. The photographs show that carburising and nitriding of iron or the penetration of zinc into a copper bi-crystal do not occur preferentially down the grain boundaries. It is therefore rather remarkable that evaporation of zinc from brass can occur preferentially
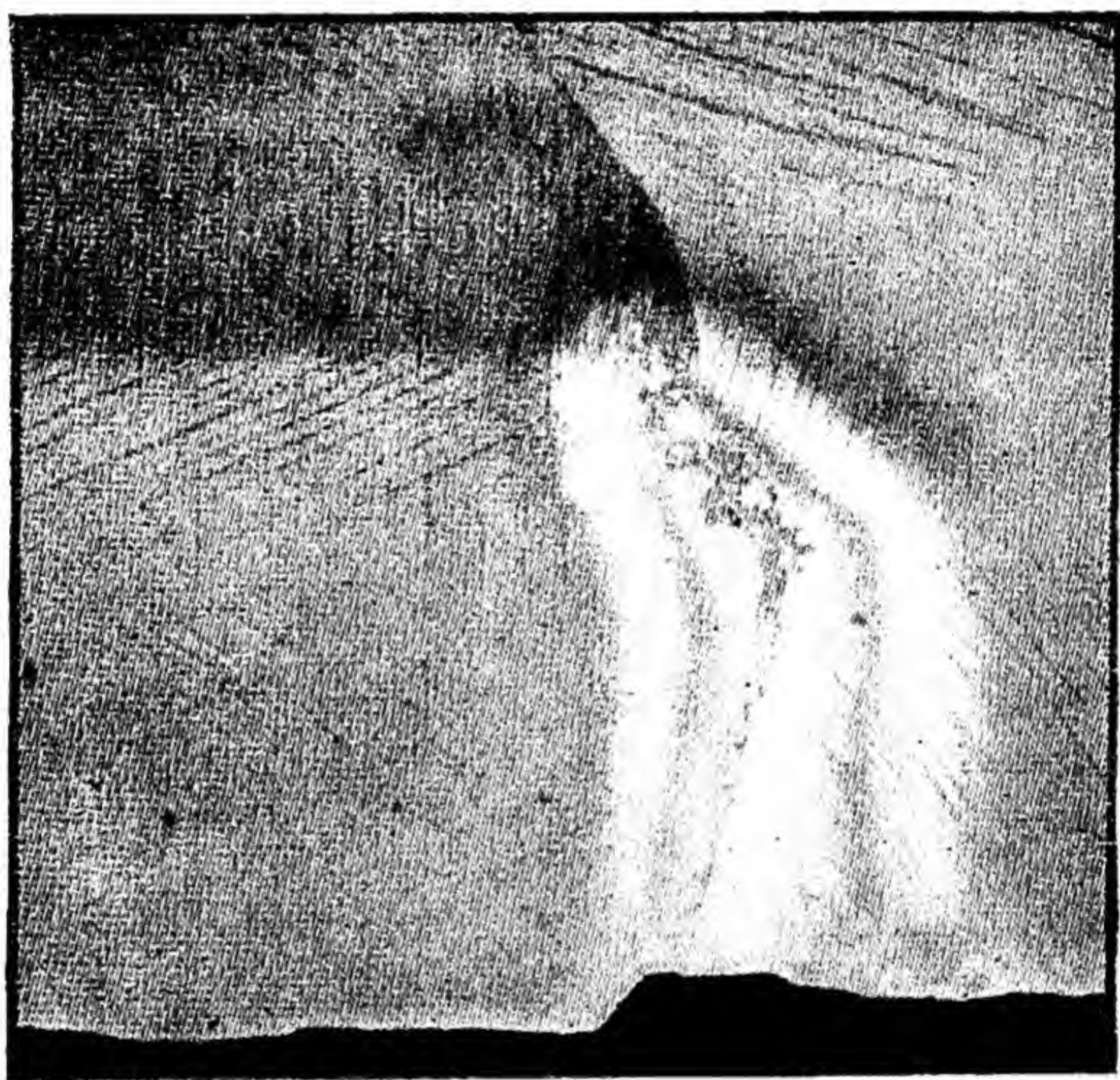
Fig. 121. Bi-crystal of brass held for 1 hour at 790° C. in vacuum. The loss of Zn has occurred around the grain boundary.

down a grain boundary (Fig. 121), and that Bugahow and Rybalko (44) found that both zinc and copper diffuse in brass more rapidly when grain boundaries are present (p. 327). It is also noteworthy that structure-sensitive diffusion processes in metals occur most often when the metals are hard, and have a high melting-point. The diffusion of metals in lead for example (melting-point 327° C.) is always a true lattice diffusion, while in tungsten one finds predominantly a grain-boundary diffusion. The malleability of lead makes it capable of being deformed without actually breaking the crystals into

small crystallites, while the effect of mechanical working upon any hard single crystal is to cause it to change into a poly-crystalline mass.

It has been observed in a number of studies of the oxidation rate of metals[55] that, after sintering the oxide film, further oxidation of the metal obeys a law

$$x^2 = kt + C,$$

where x denotes the thickness of the oxide film, and k and C are constants. The form of the above equation suggests that
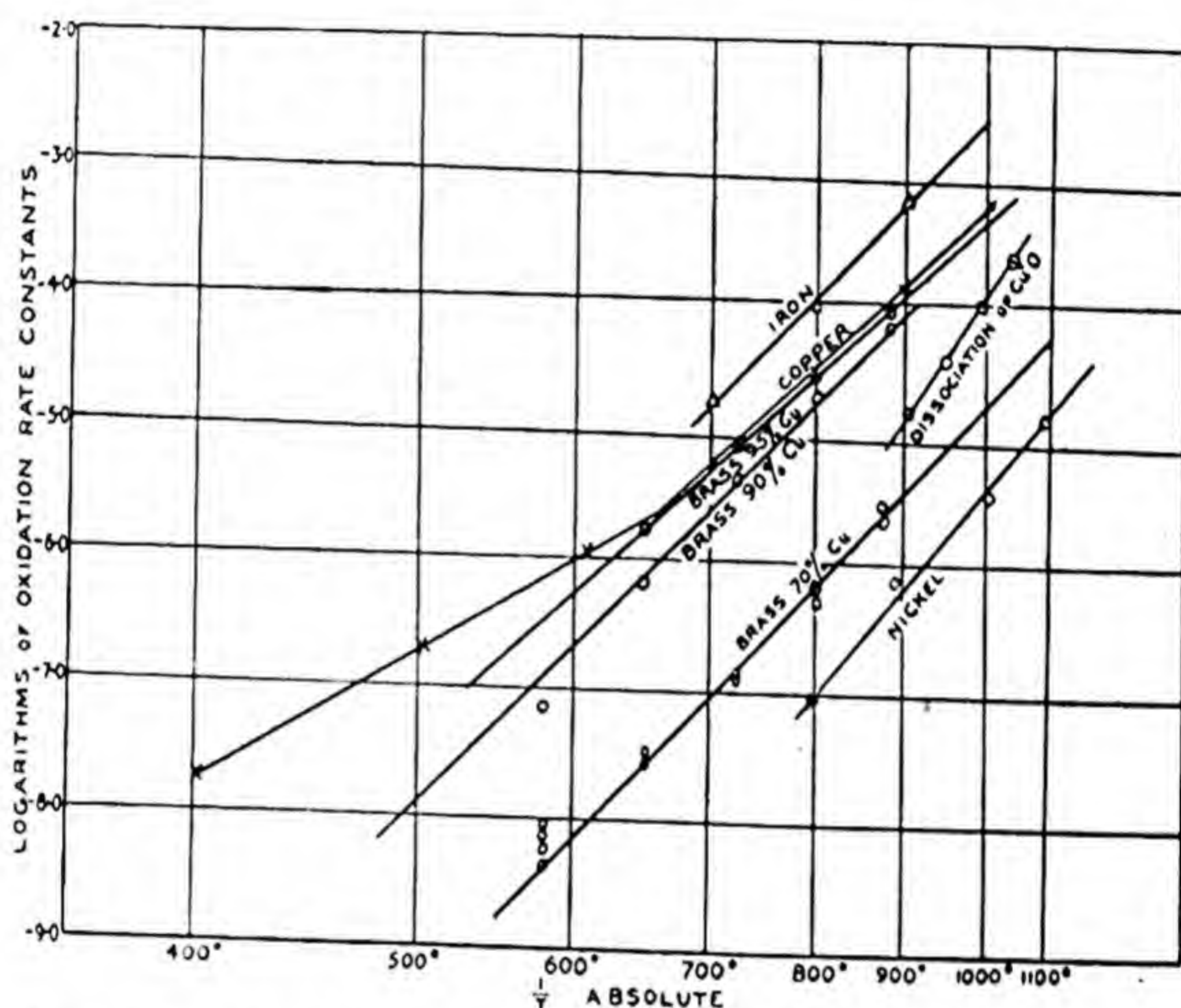
Fig. 122. The velocity constant for oxidation of some metals as a function of temperature (Dunn)[55].

oxygen attacks the underlying metal by diffusion of oxygen or of metal ions and electrons through the intervening oxide layer. The constant k obeys the usual exponential formula $k = k_0 e^{-E/RT}$ (Fig. 122), and on the hypothesis of diffusion as a rate-controlling factor the slopes of these $\log k$–$1/T$ curves give the activation energies for diffusion. It is noted that a break occurs in the oxidation velocity of copper at about 660° C., although the corresponding curves for the samples of brass are linear down to 580° C. Wilkins and Rideal[56] suggested that the break in the curve for copper was due to

TABLE 83. *Systems which may show structure-sensitive diffusion*

Process	Examples	Remarks	Author
Gas in solid	$O_2\text{-}Cu_2O$ H_2, He, Ne, N_2, Ar, $O_2\text{-}SiO_2$ } He-pyrex Air-porcelain $H_2\text{-}Fe$	$D = D_0' e^{-9500/RT} + D_0 e^{-16000/RT}$ $D = \Sigma D_0' e^{-E_1/RT} + D_0 e^{-E_2/RT}$ Chap. III	Dunn[55], Wilkins[56] Barrer[57] Urry[59] Roeser[63] Poulter and Uffelman[10]
Ion in ionic lattice	Inorganic salts (e.g. $NaNO_3$, KCl, NaCl)	Electrical conductivity increased by cold work, and by pressure. Pressed powders, or rapidly cooled melts, have conductivities much greater than single crystals	Seith[35], Hevesy[45], Gyulai[38], Lehfeldt[34] and many others[39,42,29,30]
Metal in metallic lattice	Th in W C in W	See Fig. 120 Ten to thirty times as fast in imperfect crystal as in vapour-grown single crystal	Gehrts[48], Langmuir[49], Fonda, Young and Walker[46] and others[46], Andrews[52], Zwikker[53]
	Ce, Th, U, Fe, Yt in W	Diffusion rate increases as grain size decreases	Dushman, Dennison and Reynolds[51], Giess and van Liempt[64]
	Mo in W	Ten times as fast at 1600° K. in polycrystal as in single crystal	Van Liempt[54]
	Self-diffusion in Bi	Increased by cold work; decreased by annealing	Seith[43] and others[45]
	Zn in α-brass	Diffusion 40-fold faster in polycrystal than in single crystal	Bugahow and Rybalko[44]
	Cu in γ-Fe Cr from Cr-Ni to pure Cr Cu from duralumin to pure Al	Preferential penetration along grain boundaries	Cf. Mehl[50], Sakharova[65]
	Cu in zinc	Diffusion six times as rapid in polycrystalline mass as in single crystal	Cf. Mehl[50], Sakharova[65]

a low-temperature grain-boundary diffusion through cuprous oxide merging into a high-temperature lattice diffusion.

When gases (He, H_2, Ar, N_2, O_2) diffuse through silica glass, one sometimes gets a continual change in slope of log (permeation rate)$-1/T$ curves at low temperatures ((57, 58, 59); see also Table 23 and Chap. III), thought to be due to grain-boundary diffusion.

Diffusion through metals may pass from being predominantly lattice diffusion to grain-boundary diffusion by the action of the diffusing gas upon the metal. Steel becomes brittle when exposed to the continued action of hydrogen. Similar observations upon brittleness created in metals by diffusion have been collected by McBain (60). Copper became brittle and fissured after diffusion experiments (61), and the diffusion rate increased rapidly even at constant temperatures and pressure, suggesting that grain boundaries have developed, and even become macroscopic channels. Similarly palladium in hydrogen becomes disintegrated to a considerable extent, developing a thready structure, with longitudinal fissures (62).

One may conclude this chapter by giving in Table 83 a list of those systems in which grain-boundary diffusion can play an important part. There are undoubtedly many others which have not been studied, or have been inadequately studied, and a number of properties of structure-sensitive diffusion not yet revealed.

REFERENCES

(1) Chapter VI, pp. 247 *et seq.*, also 292 *et seq.*

 Wagner, C. and Schottky, W. *Z. phys. Chem.* **11 B**, 163 (1930).

 Frenkel. J. *Z. Phys.* **35**, 652 (1926).

 Jost, W. *J. chem. Phys.* **1**, 466 (1933); *Z. phys. Chem.* **169 A**, 129 (1934).

 Wagner, C. *Z. phys. Chem.* **22 B**, 181 (1933).

(2) Baumbach, H. and Wagner, C. *Z. phys. Chem.* **22 B**, 199 (1933).

 Dunwald, H. and Wagner, C. *Z. phys. Chem.* **22 B**, 212 (1933).

(3) Orowan, E. *Int. Conf. Phys.* **2**, 81 (1934).

(4) McBain, J. W. *Sorption of Gases by Solids*, p. 279. Routledge (1932).

(5) Smekal, A. *Int. Conf. Phys.* **2**, 93 (1934).

(6) Lennard-Jones, J. E. and Dent, B. *Proc. Roy. Soc.* **121** A, 247 (1928).

(7) Lovell, A. *Proc. Roy. Soc.* **166** A, 270 (1938).
Appleyard, E. *Proc. Phys. Soc.* **49**, 118 (1937) (extra part).

(8) Poulter, T. and Wilson, R. *Phys. Rev.* **40**, 877 (1932).

(9) Bridgman, P. *Rec. Trav. chim. Pays-Bas*, **42**, 568 (1923); *Proc. Amer. Acad. Arts Sci.* **59**, 173 (1924).

(10) Poulter, T. and Uffelman, L. *Physics*, **3**, 147 (1932).

(11) Joffé, A. *Int. Conf. Phys.* **2**, 77 (1934).

(12) Andrade, E. *Int. Conf. Phys.* **2**, 112 (1934).
Andrade, E. and Martindale, J. *Philos. Trans.* **235**, 69 (1935).

(13) Hilsch, R. and Pohl, R. *Trans. Faraday Soc.* **34**, 883 (1938), where numerous other references may be found. Also Pohl, R. *Proc. Phys. Soc.* **49**, 1 (1937) (extra part).

(14) Smekal, A. *Handbuch d. Phys.* **24/2**, 835. Berlin: Julius Springer (1933).

(15) Renninger, M. *Z. Kristallogr.* **89**, 344 (1934).

(16) Darwin, C. G. *Phil. Mag.* **27**, 315, 675 (1914).

(17) Prins, I. *Z. Phys.* **63**, 477 (1930).

(18) Zwicky, F. *Rev. Mod. Phys.* **6**, 193 (1934).

(19) Goetz, A. *Int. Conf. Phys.* **2**, 62 (1934); *Z. Kristallogr.* Sonderheft, 1934.

(20) Orowan, E. *Z. Phys.* **79**, 573 (1932); **89**, 774 (1934).

(21) Smith, D. and Derge, G. *Trans. Amer. Electrochem. Soc.* **66**, 253 (1934); *J. Amer. chem. Soc.* **56**, 2513 (1934).

(22) Barrer, R. M. To be published.

(23) Buerger, M. J. *Z. Kristallogr.* **89**, 195 (1934).

(24) de Boer, J. H. *Rec. Trav. chim. Pays-Bas*, **56**, 301 (1937).

(25) Mott, N. F. *Trans. Faraday Soc.* **34**, 822 (1938).

(26) Smekal, A. *Handbuch d. Phys.* **24/2**, 883 (1933).

(27) v. Hevesy, G. *Z. phys. Chem.* **101**, 337 (1922).

(28) Tammann, G. and Veszi, G. *Zeit. anorg. Chem.* **150**, 355 (1926).
v. Seelen, D. *Z. Phys.* **29**, 125 (1924).

(29) Goethals, C. *Rec. Trav. chim. Pays-Bas*, **49**, 357 (1930).

(30) Smekal, A. (with Quittner, F.). *Z. Phys.* **55**, 298 (1929).

(31) Fritsch, C. *Ann. Phys., Lpz.*, **60**, 300 (1897).

(32) Ketzer, R. *Z. Elektrochem.* **26**, 77 (1920).
Le Blanc, M. *Z. Elektrochem.* **18**, 549 (1912).

(33) Gyulai, Z. *Z. Phys.* **67**, 812 (1931).

(34) Lehfeldt, W. *Z. Phys.* **85**, 717 (1933).

(35) Seith, W. *Z. Phys.* **56**, 802 (1929).

(36) Tubandt, C. and Reinhold, H. *Z. Elektrochem.* **29**, 313 (1923).

(37) Beran, O. and Quittner, F. *Z. Phys.* **64**, 760 (1930).
Wenderowitsch, A. and Drisina, R. *Z. Phys.* **98**, 108 (1936).

(38) Gyulai, Z. and Hartley, D. *Z. Phys.* **51**, 378 (1928).

(39) Stepanow, A. *Z. Phys.* **81**, 560 (1933).

(40) Joffé, A. *Z. Phys.* **62**, 730 (1930).

(41) Gyulai, Z. *Z. Phys.* **78**, 630 (1932).
(42) Smekal, A. *Z. Techn. Phys.* **8**, 561 (1927).
(43) Seith, W. *Z. Elektrochem.* **39**, 538 (1933).
(44) Bugahow, W. and Rybalko, F. *Tech. Phys. U.S.S.R.* **2**, 617 (1935).
(45) v. Hevesy, G. *Z. Elektrochem.* **39**, 490 (1933).
(46) Fonda, G., Young, A. and Walker, A. *Physics*, **4**, 1 (1933).
(47) v. Hevesy, G., Seith, W. and Keil, A. *Z. Phys.* **79**, 197 (1932).
Seith, W. and Keil, A. *Z. Metallk.* **25**, 104 (1933).
(48) Gehrts, A. *Z. Techn. Phys.* **15**, 456 (1934).
(49) Langmuir, I. *Phys. Rev.* **22**, 357 (1923).
(50) Mehl, R. *Trans. Amer. Inst. min. (metall.) Engrs*, **122**, 11 (1936); *J. Appl. Phys.* **8**, 174 (1937).
(51) Dushman, S., Dennison, D. and Reynolds, N. *Phys. Rev.* **29**, 903 (1927).
(52) Andrews, M. *J. phys. Chem.* **27**, 270 (1923).
Andrews, M. and Dushman, S. *J. phys. Chem.* **29**, 462 (1925).
(53) Zwikker, C. *Physica*, **7**, 189 (1927).
(54) v. Liempt, J. *Rec. Trav. chim. Pays-Bas*, **51**, 117 (1932).
(55) Feitknecht, W. *Z. Elekrochem.* **35**, 142 (1929).
Pilling, N. and Bedworth, R. *J. Inst. Met.* **29**, 529 (1923).
Dunn, J. *Proc. Roy. Soc.* **111** A, 203, 210 (1926).
(56) Wilkins, F. and Rideal, E. K. *Proc. Roy. Soc.* **128** A, 394 (1930).
(57) Barrer, R. M. *J. chem. Soc.* p. 378 (1934).
(58) Burton, F., Braaten, E. and Wilhelm, J. *Canad. J. Res.* **8**, 463 (1933).
(59) Urry, W. *J. Amer. chem. Soc.* **54**, 3887 (1932).
(60) McBain, J. W. *Sorption of Gases by Solids*, p. 264 (1932).
(61) Deming, H. and Hendricks, B. *J. Amer. chem. Soc.* **45**, 2857 (1923).
Hendricks, B. and Ralston, R. *J. Amer. chem. Soc.* **51**, 3278 (1929).
(62) Graham, T. *J. chem. Soc.* Series II, **7**, 419 (1869); *Proc. Roy. Soc.* **17**, 212, 500 (1869); *Chemical and Physical Researches*, p. 269 (1876).
(63) Roeser, W. *Bur. Stand. J. Res., Wash.*, **7**, 485 (1931).
(64) Giess, W. and v. Liempt, J. *Z. anorg. Chem.* **168**, 107 (1927).
(65) Sakharova, M. *Tzvetnuie Metallui (Non-Ferrous Metals)*, No. 4 (1932).

CHAPTER VIII

MIGRATION IN THE SURFACE LAYER OF SOLIDS

INTRODUCTION

Since molecules, ions and atoms can move in solid lattices (as when ammonia is sorbed by natrolite, or two metals or salts interdiffuse), it is not difficult to visualise a similar migration of particles along external surfaces. Grain-boundary diffusion occurs more readily than lattice diffusion (for example, the activation energies are 90 and 120 k.cal. respectively for thorium diffusing in tungsten[1]), so that surface migration might be expected to occur more readily still. The main lines of experiment which have led to the present knowledge of surface migration are:

(1) The study of the growth and dissolution of single crystals.

(2) Phenomena of condensation and aggregation of continuous films on solid surfaces.

(3) Examination of stable monolayer or multi-layer systems by photoelectric and thermionic methods.

Much of the early evidence of the reality of surface migration came from the first source, and this more or less classical evidence may now be reviewed.

EVIDENCE OF MOBILITY FROM GROWTH AND DISSOLUTION OF CRYSTALS

Volmer and Estermann[2], when studying the rate of growth of mercury crystals at $-63°$ C. from mercury vapour at $-10°$ C., noted a remarkably rapid rate of growth of thin hexagonal crystals in the directions of the plane of the hexagon. The linear growth of a hexagon was 3×10^{-2} cm./min., which was 1000-fold greater than could be explained by the kinetic

theory. This growth must occur either by surface migration, or because impacting molecules entered the lattice and expanded it laterally. Volmer and Adhikari (3) then pointed out that surface mobility was implied in certain phenomena of crystal growth from melts. Crystal needles often project above the surface of the melt, and the needle can only form in this way if lateral diffusion of ions on its surface takes place.

Even more definite evidence was forthcoming in a number of studies with benzophenone (3, 4) and with phthalic anhydride, coumarin, salol and diphenylamine (5). In the earliest experiments (3) with benzophenone a succession of mercury drops was allowed to brush a long crystal of the organic solid which was slowly worn away. Not only was benzophenone removed at the point of contact of the mercury, but also for some distance away. In a later series of experiments (4) a stream of mercury brushed the edge of a glass plate on which was benzophenone 0·1–1 mm. away from this edge. The benzophenone was removed by the mercury although it was untouched by it. Moll's (5) experiments were made by depositing a very thin film on glass, the edge of which was rinsed by dropping mercury. The films were shown to diminish in thickness by noting changes in the interference colours observed with transmitted light. Moll could find no evidence of mobility with paraffin and cetyl alcohol.

Richter and Volmer (6) attempted to measure the diffusion rates of benzophenone over a mica surface as a function of temperature. The quantity of benzophenone in units of 10^{-8} g. moving per hour over 1 cm.^{2} of mica increased as the temperature rose, although the sorption decreased. Thus the diffusion has a large temperature coefficient which suggests that it is an activated process.

An interesting new method for studying the growth of crystals from solution, which suggests that lateral migration occurs, has been developed by Berg (6a). Two plane glass plates form a wedge, so that transmitted light will give interference colours. The crystallising solution is placed in the wedge, and lateral growth of a sodium chlorate crystal takes place.

Concentration gradients caused distortion of the interference bands, which Berg succeeded in interpreting in terms of the concentration gradients established. The concentration distribution was not uniform, being greatest at the edges of a square plate of sodium chlorate. Thus the highest rate of flow occurs at the middle of each edge, and to explain the continued production of plane faces it was argued that a mobile surface film must have formed.

EVIDENCE OF MOBILITY FROM THE CONDENSATION AND AGGREGATION OF METAL FILMS

The structure of condensed films

There can be two types of film on solids, those which are stable in monolayers and those which tend to aggregate into three-dimensional structures. The conditions for stability of monolayers or aggregates are similar to those governing the stability of films at liquid surface, which either give stable monolayers (e.g. fatty acids with long chains on water) or gather into lenses (paraffin, or ethylene dibromide on water). The monolayer is stable if the spreading occasions a nett decrease in free energy, when the various interfacial free energies are considered. Another necessary condition for the reorganisation of a film is surface or bulk mobility.

There are a great number of metal films which are thermo-dynamically unstable in this sense. Such films can only be maintained as glassy deposits if the temperature is so low that no migration can occur. The predilection which various sputtered or evaporated metallic deposits have for aggregation into micro- or macro-crystals is illustrated by the collection of observations in Table 84. The evidence from X-ray, electron diffraction, and optical experiments reveals that the three-dimensional crystalline state is very readily formed. One notes also that a rise in temperature can cause an orientation of crystallites to agree with that of the underlying solid lattice. Sometimes alloy systems may occur, evidencing mobility and interdiffusion of atoms, or certain crystal parameters may be

22-2

derived from those of the underlying solid, i.e. the micro-crystal may continue the pattern of its substrate. In a great many of the systems studied, of which those in the table are only a few (17), the crystal grains grow very rapidly as the temperature is raised, due to more rapid migrations of atoms. Such a crystallisation of silver, for example, has been observed from $250°$ C. (18) to $- 173°$ C. (19).

TABLE 84. *Some observations (obtained by X-ray and electron-diffraction methods) on crystalline structure developed in thin metal films*

Nature of systems	Observed properties	Authors
Mirrors of Ni, Fe, Cd, Hg deposited from the vapour on cold surfaces	Crystallites. Parameters same as for metal in bulk. Heating causes growth of crystallites	Gen, Zelmanov and Schalnikow (7)
Various thin eva-porated films	Crystalline. Regular orientation of crystal grains to match orientation of substrate	Kirschner (8)
Sputtered Pt	Crystalline. Sometimes with lattice planes parallel to surface, sometimes irregularly deposited crystallites	Thomson, Stuart and Murison (9)
Ag on Au	Crystalline. Same orientation as underlying solid. Parameters as for bulk silver	Farnsworth (10)
Ag evaporated on to cold Cu and Au	Crystals on Au, "amorphous" on Cu	Deubner (11)
Sputtered films on quartz	Crystals, with orientation paral-lel to quartz base; heat treat-ment increases grain size	Swamy (12)
Evaporated Bi films	Crystals. Orientation of 111 plane parallel to base	Lane (13)
Au, Ni, Co, Cu, Cr, Pd and Ag films on rock-salt	Above characteristic tempera-ture, mosaic of small crystallites, similarly oriented on crystalline base	Brück (14)
Al on Pt	Crystalline, thick and thin films. Some thin films show para-meters corresponding to the Pt base	Finch and Quarrell (15)
Very thin films Pt, Pd, Ag on Cu and Ag	Films formed of crystalline alloy	Natta (16)

While the true criterion of film stability is that the free energy of film formation should be greater than the free energy of crystallite formation, another approximate criterion is also useful. It is usually noted that if the heat of condensation of

a metal as a monolayer upon a substrate (ΔH_1) is much less than its heat of condensation on itself (ΔH_2), the metal fails to form a stable monolayer on the substrate, while if ΔH_1 is greater than ΔH_2, the monolayer is stable. This relationship is illustrated for some unstable films in Table 85. On the other

TABLE 85. *A comparison of heats of condensation in uniform layers on a foreign substrate (ΔH_1), and heats of condensation of the metal on itself (ΔH_2)*

Author	System	ΔH_1 k.cal./atom	ΔH_2 k.cal./atom
Estermann [20]	Cd-glass	3·5	28
	Cd-Cu	3·0	28
	Cd-Ag	5·0	28
	Hg-Ag	2·5	18·5
Cockcroft [21]	Cd-Cu } Cd-Ag	5·7	28

hand, the following metal-substrate systems give large heats of sorption (ΔH_1), and form relatively stable monolayer systems:

Cs-W [22],   Na-OW [26],

Cs-glass [23],   K-OW [27],

Th-W [24],   Cs-WO_3 [28],

Tl, In, Ga-W [25],   Cs-Cs_2O [29].

It is systems belonging to the second group which have provided a great deal of quantitative information on surface diffusion. The group will be considered later, and one may now discuss the behaviour of unstable films.

Some properties of unstable films

The essential instability of some metal film-solid systems may be shared by films of organic and inorganic solids, which crystallise readily. The observations on metal films are, however, more numerous, and their behaviour has been studied on surfaces of metals, mica, quartz, and diamond.

When silver was evaporated on to polished quartz [30] in amounts corresponding to less than a monolayer, optical

examination showed that the film was not homogeneous but consisted of small crystalline islands. Aggregation into these islands could only occur by migration over the quartz surface. Similarly, when a cadmium atom beam was directed on to a cadmium-sensitised copper surface(21), and a wire was placed in the path of the beam, the shadow thrown by the wire on the surface had a diffuse edge. This phenomenon was attributed to the creeping of cadmium atoms along the underlying surface. The same observation(31) was made when the cadmium beam was replaced by a mercury atom beam.

Surface mobility can explain the experiments of Ditchburn(32) on the deposition by sputtering of cadmium films on glass and metal surfaces. He found that when the cadmium particles were directed on to the surfaces through fine slits, no deposit could be observed if the width of the slit was below 5×10^{-2} mm., a phenomenon which he attributed to a loss by surface diffusion of particles which could not be sufficiently rapidly replaced by condensation.

An investigation of processes of aggregation(18) of thin films of silver and gold led to definite conclusions concerning the mobility of atoms on surfaces. The films were initially about fifty atomic layers thick, and were heated to various temperatures before optical examination. It was found that after heating at temperatures from 250 to 280° C. the thin silver films had gathered into small spherulites (Fig. 123), at 300° C. more spherulites formed, while at 345° C. the size of the particle increased, and a crystalline outline began to show (Fig. 124). At 500° C. a crop of small crystallites appeared in hitherto optically empty areas. It was concluded that the most freely mobile part of the film was the surface layer, which for a silver layer on a silver film (of 50 layers) was mobile at temperatures 700° C. below the melting-point of the metal. This observation suggests an activation energy for migration of the surface layer of atoms of a clean metal very much smaller than the latent heat of evaporation, or of the activation energy for the self-diffusion constant of silver. Gold films showed their first gathering into spherulites at 400° C. The nature of the

spherulites is not quite clear, but they were supposed to consist of an aggregate of uniaxial crystalline fibres radiating
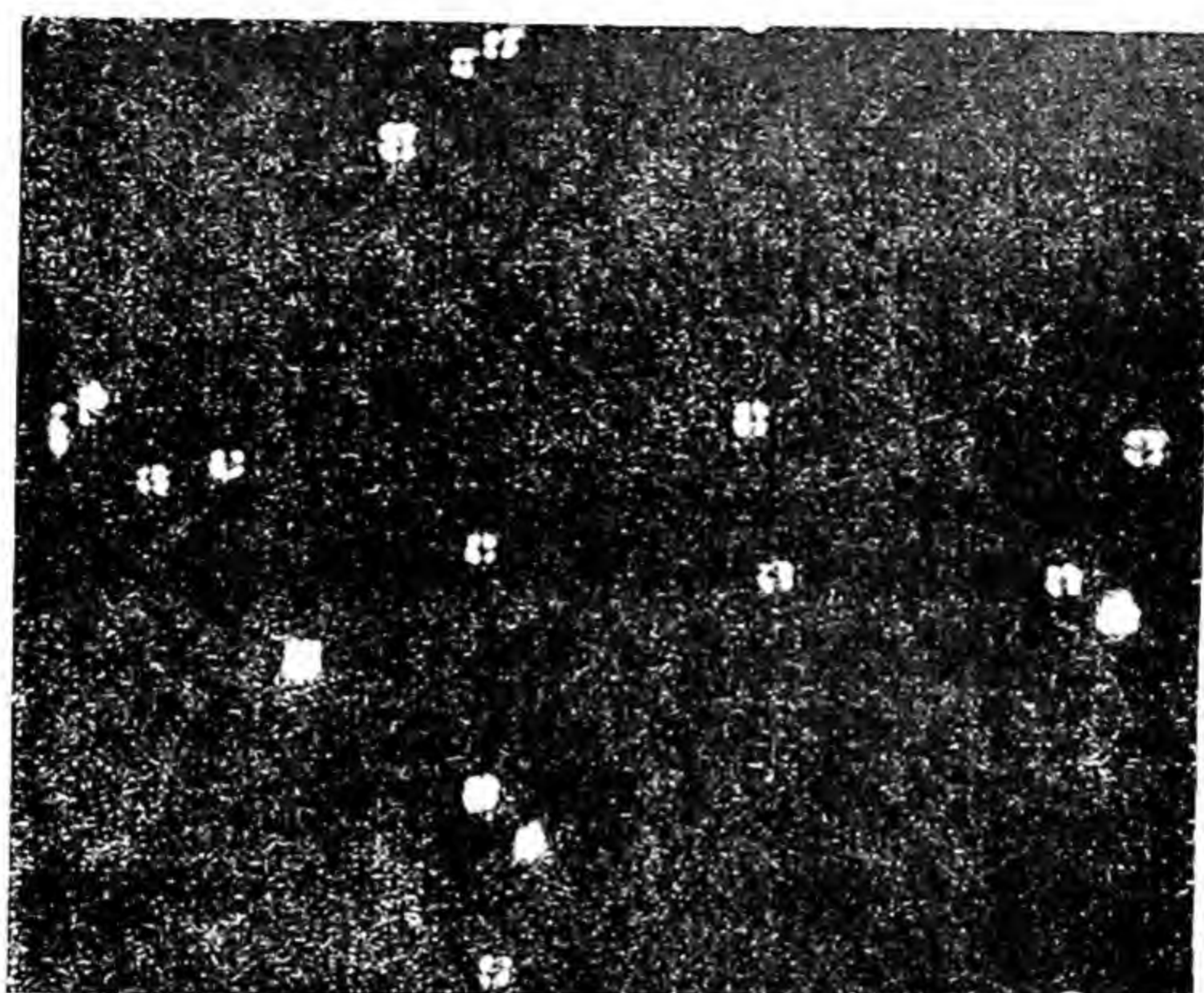
Fig. 123. Ag-particles, about 1μ across, which developed on heating an Ag-film 50 atoms thick to 280°C. (Magnification 1000.)
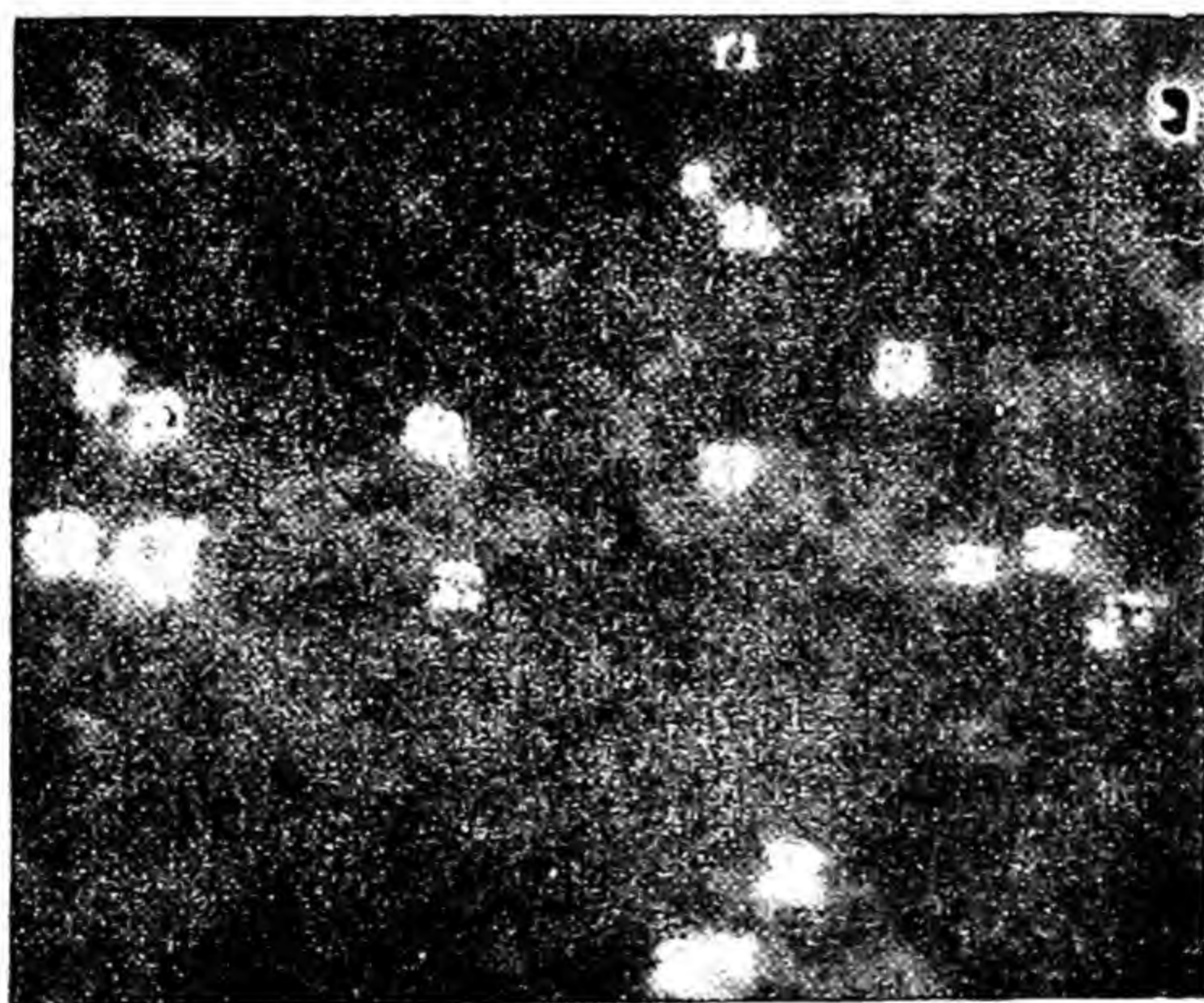
Fig. 124. Ag-particles showing their additional growth when the Ag-film was heated to 345°C. for 2 hr. (Magnification 1000.)

from a centre. Evidence of lateral diffusion is supplied by measurements of the electrical conductivity of thin films[23]. When an alkali metal is deposited upon thoroughly outgassed

pyrex at low temperatures (90° K.), a measurable conductivity is observed when the deposit is only 10 % of a monolayer. The conductivity rises as the deposit is increased, but when the deposition is stopped, the conductivity diminishes again. However, at a certain critical thickness the conductivity rises rapidly from 10^{-3} to 10^{-7} of that of the metal in bulk to a figure of the same order (e.g. Hg on pyrex, Fig. 125). In all cases, large irreversible changes in the conductivity may be effected by warming. Zahn and Kramer [33] attempted to explain the high resistivity of very thin films by assuming that a glass-like non-conducting deposit of metal is formed, but Tammann [34] has adversely criticised this suggestion. An amorphous state seems improbable in view of the numerous studies (Table 84) which indicate a crystalline form developed by aggregation even in films of high resistivity, and with films of very small "nominal thickness".*

The probable explanation of the resistivity changes of thin films can be given in terms of surface tension forces, and of lateral mobility. That a film of nominal thickness 10 % of a monolayer can conduct, suggests aggregation into rays of atoms, or islands of atoms, which touch other aggregates, and so provide a few bridges for conduction. The increase in resistivity of films on ageing, at 64–90° K., has been ascribed to a cracking of the film under surface tension forces, to give a discrete film. The disrupted film aggregates into spherulites or crystallites, especially if warmed, by processes of surface migration. As the deposition continues, there comes a time when crystallites, developing under surface tension forces, lateral migration, and bombardment of the crystallite surfaces by the impinging atomic stream, begin to touch one another more and more frequently, so that the conductivity, at a certain critical "nominal thickness", rises rapidly to a value very nearly that for the metal in bulk. Fig. 125 shows the family of curves of nominal thickness against resistivity

---

* By "nominal thickness" is meant the thickness calculated from the time of deposition of a calibrated atom stream, neglecting all subsequent aggregation, and supposing the deposit to be uniform.
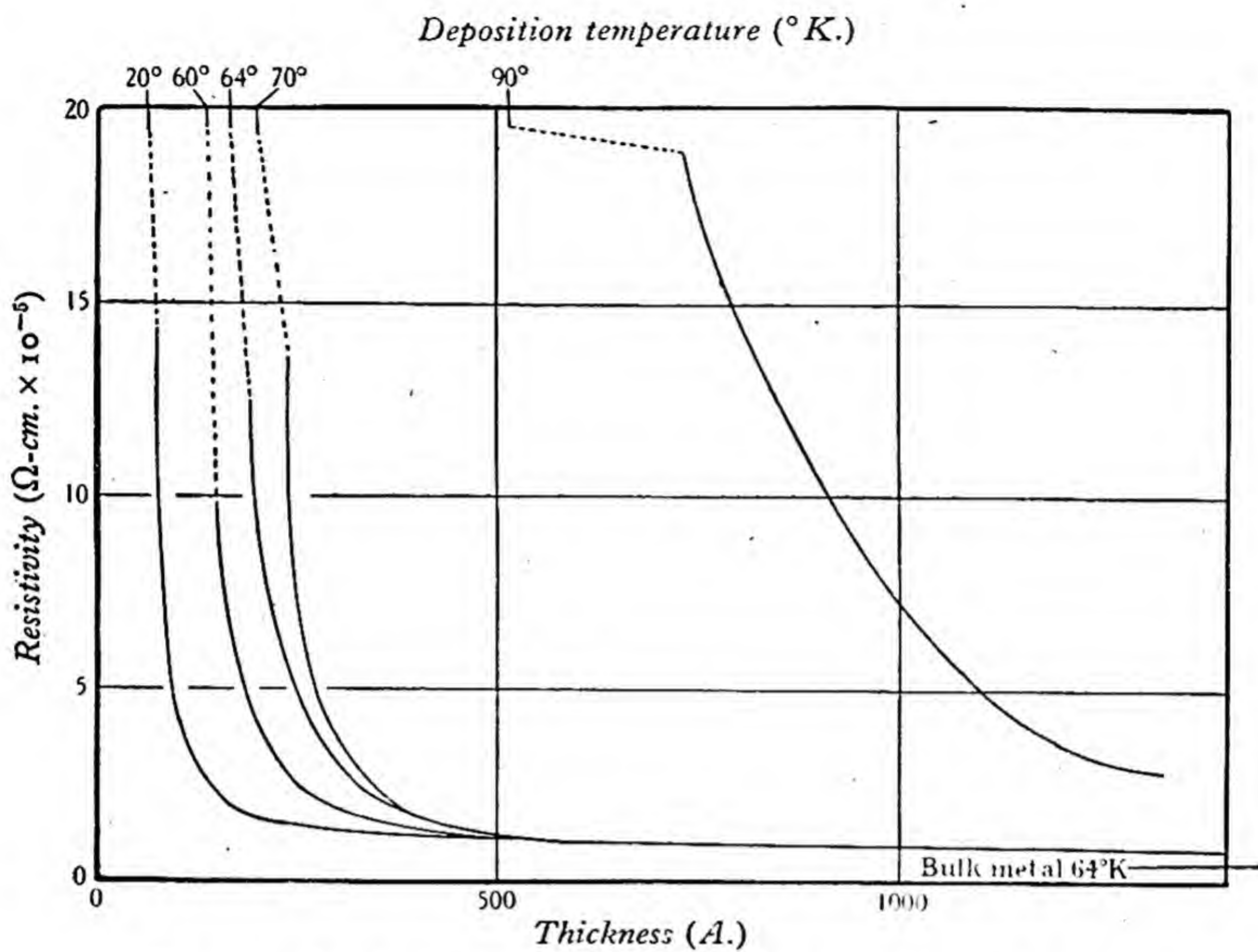
Fig. 125. The change in resistivity at a critical nominal film
thickness for mercury on pyrex.
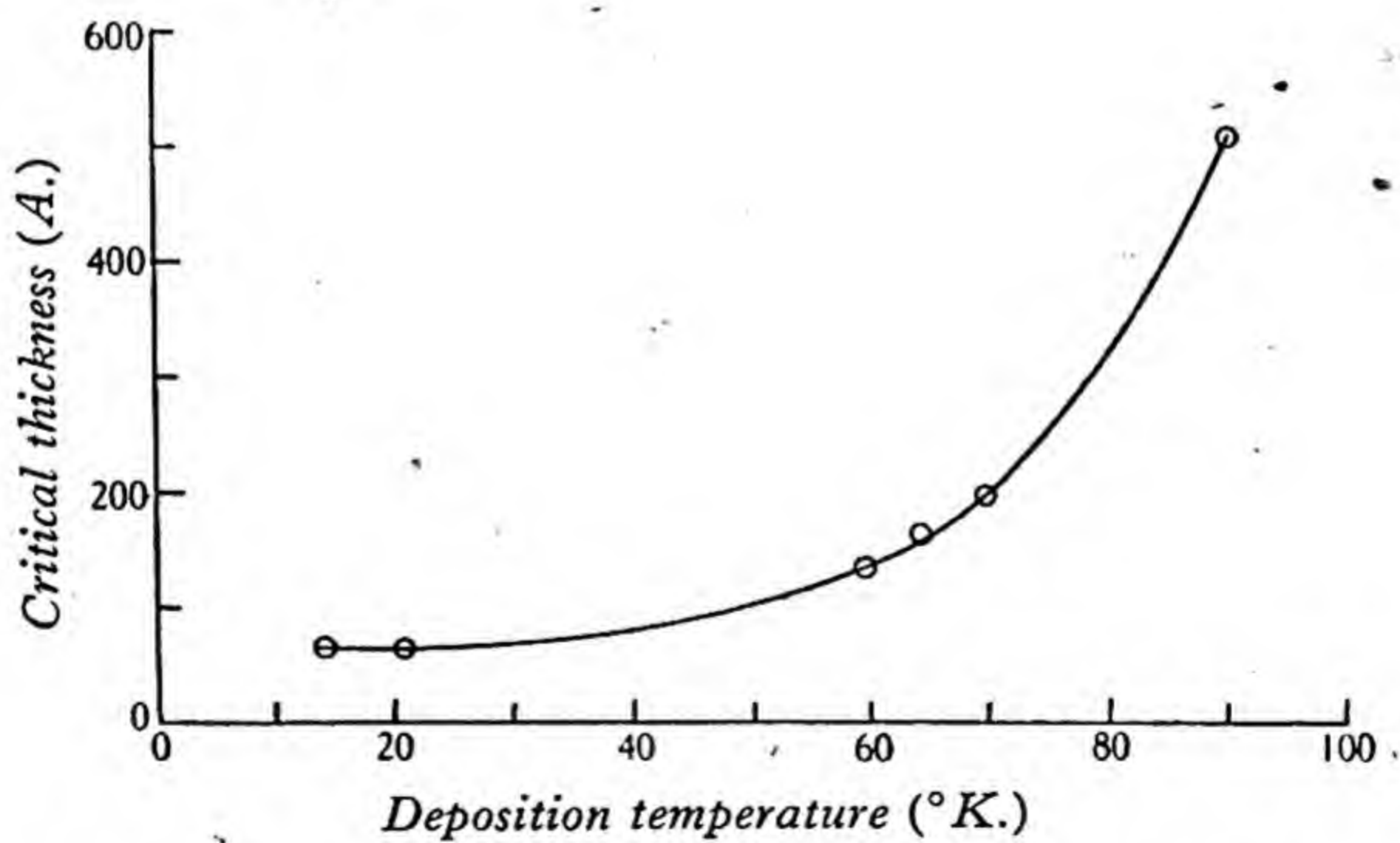
Fig. 126. The critical nominal-thickness as a function of
temperature for mercury films on pyrex.

for mercury deposited on pyrex, while Fig. 126 shows the critical thickness at which the large decrease in resistivity indicated in Fig. 125 occurs, as a function of the temperature of deposition. This critical thickness depends on temperature, and increases in the same direction with temperature as crystallite size.

Unfortunately, most of the evidence of surface mobility inferred from these experiments is qualitative only, and while with development of the theory of the processes of deformation and surface migration in the films one may hope that figures such as those above may give quantitative information concerning surface diffusion, one must at present obtain this information from the study of types of film which give stable monolayers. It is, however, possible to make an estimate of the activation energies for diffusion in a number of these systems, if the heat of sorption is known. In cases where the energy of activation for migration has been measured [35, 36] or calculated [37, 38] it has been found to be one-third to one-sixth of the heat of vaporisation. Accordingly, for the systems given in Table 85 the activation energies for migration of cadmium on glass, copper, or silver, or of mercury on silver, are from 500 to 1500 cal./atom, and mobility must persist to very low temperatures. Applying the same rule to the alkali metals, the activation energy for diffusion in the surface layer should be about 5000 cal./atom. Andrade's [18] data (p. 342) on multi-atomic silver and gold films show that the surface layer migrates at temperatures about 700° C. below the melting-point, so that this surface layer is again very mobile.

In a multi-atomic film it would be natural to assume a different mobility in the layer next the solid substrate, a layer in the middle of the film, and a layer on the surface of the film. The evidence of the previous paragraph suggests that this is true for the surface and interior. The interpretation placed by Dixit on his results [39] on the orientation of crystalline aggregates, was that the layer next the substrate may also be very mobile. By assuming that this layer on heating to moderate temperatures could assume the properties of a two-dimensional

gas, Dixit was able to show how the orientation of crystallites occurred to conform to the pattern of the substrate. It is interesting that when zinc is deposited on molybdenum the film aggregates into crystallites already orientated at 10° C.

If there are N_S adatoms/cm.^{2} of surface, and each adatom requires an activation energy E to become mobile, the number N_A which is mobile is given by

$$\frac{N_A}{N_S - N_A} = \frac{f_A}{f_S} e^{-E/RT},$$

where f_A and f_S are the partition functions for the mobile and immobile atoms. The fraction $N_A/(N_S - N_A)$ approaches unity at high temperatures, and the system behaves as a two-dimensional gas. At low temperatures $N_A/(N_S - N_A)$ tends to zero, and one has an immobile film. Since mercury still aggregates on pyrex at 20° K., according to Appleyard and Lovell's [23] electrical conductivity measurements (p. 344), mercury-on-pyrex must have a very small value of E. It is interesting that mercury shows a high mobility on a crystal of mercury at $-63°$ C. (p. 337) and a very small sorption heat on silver (Table 85). The activation energy for diffusion of mercury on the surface of tin, as an amalgam (p. 369), was only 1920 cal./atom, and occurred rapidly at room temperatures.

MEASUREMENTS OF SURFACE MIGRATION IN SOME STABLE FILMS

Properties of stable films

When atoms of barium, caesium, potassium, thorium or similar metals are deposited on a surface of metallic tungsten, stable·films may be built up varying in nominal thickness from a fraction of a monolayer to many monolayers. The new composite surface has contact potentials and thermionic or photoelectric work functions different from those of the clean metal. The movements of atoms in these films can therefore be followed by the variation in the thermionic or photoelectric currents, i, which alter as the fraction θ of the surface covered alters. It is important to find how the current i depends on θ.

The thermionic emission from the clean surface is given by the Richardson equation

$$i_0 = A T^2 e^{-b/T},$$

in which $b \times R$ is the energy needed (in cal./g.ion of electrons) to remove an electron from the metal into free space. Since this work function enters as an exponent, small changes in $b \times R$ cause large changes in i. At $1500°$ K., the value of i for a tungsten surface covered by a monolayer of thorium is 10^5 times the value for clean tungsten (40). To determine the connection between θ and i, Langmuir (40) originally supposed that the change in contact potential, V, was proportional to the electric moment $N\mu$ per unit area, where N is the number of sorbed atoms and μ is the electric moment per atom. He assumed that μ did not depend on N, and therefore that

$$V = k\theta,$$

and that the work function for a clean surface becomes for the composite surface

$$b \times R + k_1 \theta,$$

where k_1 may be either positive or negative. If i_0 denotes the current from a clean surface, and i_θ the current from the surface when a fraction θ is covered, one has

$$\ln i_0 = \ln A T^2 - \frac{b}{T},$$

$$\ln i_\theta = \ln A T^2 - \frac{(b \times R + k_1 \theta)}{RT}.$$

Similarly, if i_m is the maximum electron emission, supposed to occur at or near $\theta = 1$, a similar pair of equations may be written, and by combining the four, one obtains

$$\theta' = \frac{\log_{10}(i_0/i_{\theta'})}{\log_{10}(i_0/i_m)}.$$

In this expression θ' would be the fraction of the surface covered if the following assumptions held:

(1) that μ does not depend on N,

(2) that maximum emission occurs at $\theta = 1$.

Langmuir showed that for caesium-on-tungsten i_m occurs when $\theta = 0.67$, so that the second assumption is not always true, while Becker[41] found for barium-on-tungsten that Langmuir's relation was better replaced by

$$\frac{\log_{10}(i_\theta/i_0)}{\log_{10}(i_m/i_0)} = [1.1(1 - e^{-2.0\theta})] \quad (0 < \theta < 0.85).$$

This type of deviation may be attributed to the variations in μ with θ or N, so that the first assumption need be true only for dilute films.

Becker and Brattain[24] condensed thorium at a constant rate upon a tungsten strip, and measured the growth of $\log i$ as a function of time t. If the time needed to build up a film showing maximum electron emission is t_m, the following relationship holds:

$$f = \frac{t}{t_m} = \frac{\theta}{\theta_m}.$$

$\theta_m = 1$ if maximum emission occurs when the surface is just covered with a monolayer. When $\log i/i_m$ was plotted against f, the curve of Fig. 127 was found, which up to θ_m may be expressed by $\log_{10} i/i_0 = a(1 - e^{-cf})$, for $1 > f > 0$, and where $a = 6.54$ and $c = 2.38$. This curve may be regarded as typical of the variation of $\log i/i_0$ with θ or f for most stable alkali, or alkali earth, metal films. The thermionic emission rises to a maximum and then falls asymptotically to its value for the metal in bulk. For thorium-on-tungsten the relation between Langmuir's θ' and Becker and Brattain's f is

$$\theta' = 1.135(1 - e^{2.38f}).$$

One thus sees that to measure θ from $\log i$ one must first measure $\log i/i_0$ as a function of $f = t/t_m = \theta/\theta_m$, and then evaluate θ_m by allowing atoms to fall at a known rate on to a known area of tungsten surface, or alternatively by measuring the integrated positive ion current when the total deposit is evaporated in ionic form[42]. The specific surface of tungsten may with some measure of certainty be taken as $1.4 \times$ the geometrical area. The surface, which is made up of crystal

faces somewhat tilted from the horizontal, thus consists of an intersecting pattern of the surfaces of tungsten crystallites. Unit area of a crystal contains 1.425×10^{14} tungsten atoms and it is thought that adatoms occupy the surface so that the ratio

$$\frac{\text{Number of surface tungsten atoms}}{\text{Number of surface adatoms}}$$
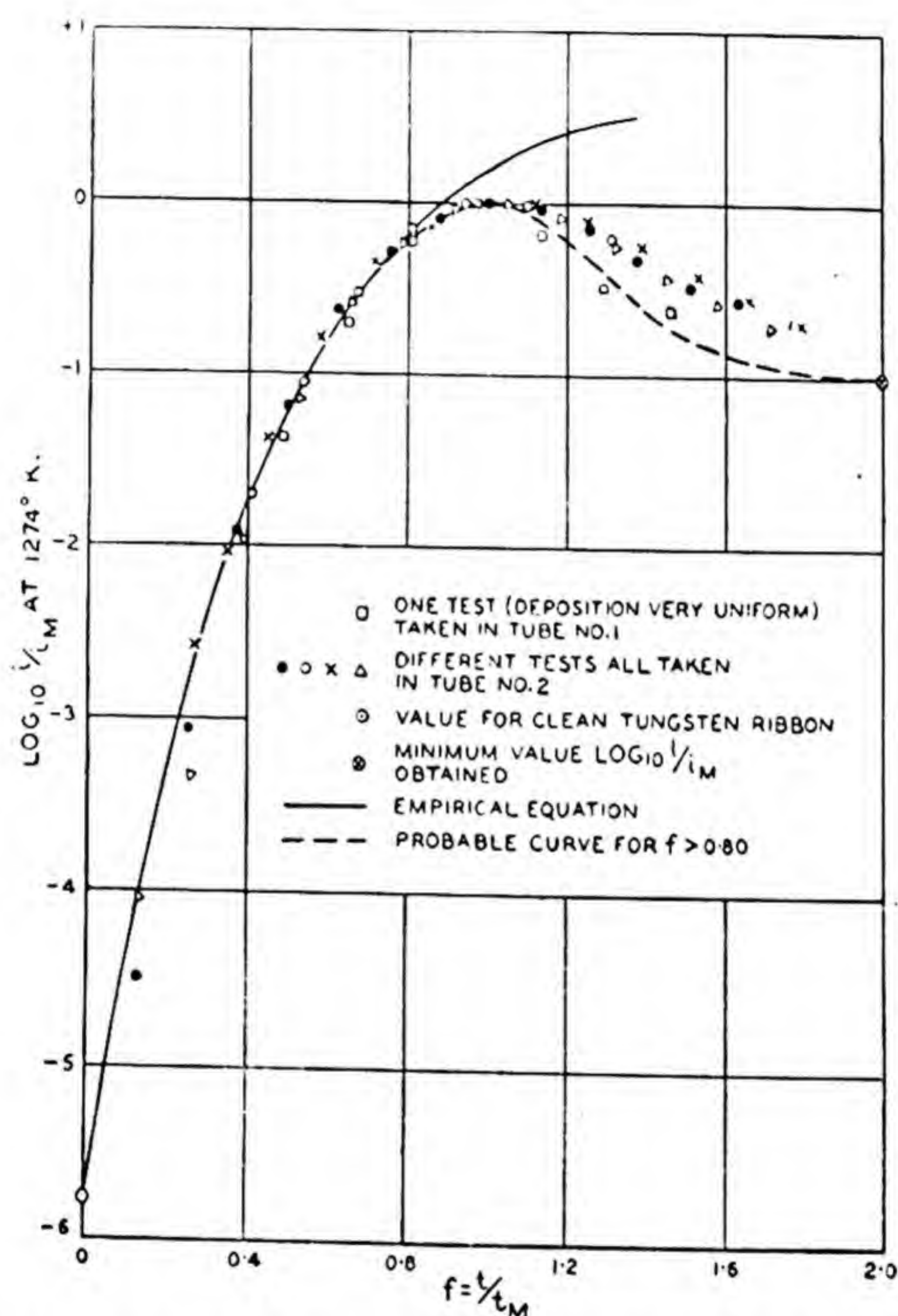
Fig. 127. The thermionic activity of a tungsten ribbon versus the time of deposition from thorium wire.

is an integer. For example, the integer for thorium on tungsten is two (22), and for caesium on tungsten is four (42).

To bring the filament into a condition suitable for thermionic and photoelectric studies of films, it must be flashed at 2800° K. in order to remove a tenaciously held monolayer of oxygen (43, 44). Tungstic oxide itself distils off the surface at

a much lower temperature, and $2200°$ K. is sufficient for its removal[26]. Thus one may prepare clean tungsten surfaces, and surfaces of W-O, both of which lend themselves admirably to migration experiments.

Methods used in measurements of surface diffusion

A group of methods depending on thermionic or photoelectric properties has been worked out for the measurement of surface migration rates. These methods and the way the data are analysed will now be discussed, taking in order thermionic and photoelectric studies.

A. *Surface diffusion by measurement of thermionic emission.*

(i) The movements of caesium, barium, and thorium in films on tungsten[24, 45] have been followed by evaporating the metal so as to give a uniform deposit on a tungsten strip, suitably pre-treated (p. 350). From calibration curves giving $\log i/i_m$ as a function of θ, or $f = \theta/\theta_m$ (Fig. 127), the movements of a deposited film down concentration gradients may be followed as a function of time. If all the film is originally on one side only of the strip, the growth of $\log i/i_m$ on the bare side and the decay of $\log i/i_m$ on the side where the film was deposited give a mean value of f or θ as a function of time on each side. The strip, after the deposition of a film where $2 > f > 0$, is raised to a temperature where migration but not evaporation proceeds. To interpret the data it is necessary to idealise the process of diffusion by assuming that the diffusion constant D is not dependent upon the concentration. One may then write

$$\frac{\partial f}{\partial t} = D\left(\frac{\partial^2 f}{\partial x^2} + \frac{\partial^2 f}{\partial y^2}\right)$$

in place of
$$\frac{\partial f}{\partial t} = \frac{\partial}{\partial x}\left(D\frac{\partial f}{\partial x}\right) + \frac{\partial}{\partial y}\left(D\frac{\partial f}{\partial y}\right).$$

Take the y-axis to be parallel to the tungsten ribbon and in the middle of its front face, so that $\partial f/\partial t = 0 = D(\partial^2 f/\partial y^2)$ in the y-direction, since the strip is very long. Let x be any distance normal to the y-axis in the surface of the ribbon,

whose width is w, so that the mid-point of the back face is then at $x = w$. The boundary conditions are:

(1) at $t = 0$: $f = f_0$ for $x = \frac{1}{2}w$ to $-\frac{1}{2}w$, $f = 0$ for $x = \frac{1}{2}w$ to w, and $-\frac{1}{2}w$ to $-w$;

(2) for all values of t, $\dfrac{\partial f}{\partial x} = 0$ at $x = 0$ and $x = w$.

The solution of the Fick law is then

$$f = \tfrac{1}{2}f_0 + \frac{2f_0}{\pi} \sum_{m=1}^{m=\infty} \left(\frac{1}{m} e^{-m^2 D\pi^2 t/w^2} \cos\frac{m\pi x}{w} \sin\tfrac{1}{2}m\pi \right),$$

and since the series converges rapidly one may compute f for any value of x and t. Brattain and Becker, for thorium on tungsten, computed f as a function of x, and of t (for $x = 0$ and $x = \frac{1}{2}w$), when the time t was expressed in units of $w^2/D\pi^2$. Then from the experimental $\log i$ versus f curve, and the computed f versus x curve, they found $\log i$ as a function of x, and finally by graphical integration $\log i$ was found as a function of t for the whole front surface of the ribbon. Next values of $w^2/D\pi^2$ were chosen until the calculated $\log i$ versus t curve fitted the experimental one.

(ii) Langmuir and Taylor [46] followed the movement of caesium along a tungsten wire by depositing a uniform film along the wire, and removing caesium from the central portion. They then measured the amount which flowed in from the ends by evaporating it, once again only from the central part of the filament, as a measured positive ion current. To carry out these measurements three metal cylinders were arranged along the length of the wire in series, the wire passing axially through them, parallel to their length. The caesium was deposited with the cylinders at $+22$ V. The caesium from the wire in the central cylinder was withdrawn as positive ions by altering the potential of the cylinder to -44 V., after which the potential was again returned to $+22$ V., and the wire held at a temperature suitably high for migration without evaporation. Finally the total caesium that had moved into the centre was estimated, as positive ion current, by again altering the

potential of the central cylinder and flashing. From this quantity of caesium the authors evaluated the diffusion constant.

(iii) Another method due to Langmuir and Taylor[46] is based on the discovery that caesium films on tungsten may exist as two phases, α and β, in equilibrium. From the condensed α-phase caesium escapes as atoms, and from the β-phase as ions, both rates being equal in the equilibrium condition to the rates of arrival from the gas. At a given temperature there is only one critical pressure, p_0, of caesium vapour at which the two phases can coexist. When p_0 is altered to p_1, one phase must disappear, and the phase boundary moves along the wire with a velocity v. The resulting surface migration is balanced by differences in the rates of evaporation (ν_a and ν_p for atoms and ions) and of condensation, μ_1. ν_a and ν_p are functions of T and θ, and μ_1 of θ and the vapour pressure of caesium. If $\nu = (\nu_a + \nu_p)$, as ordinate, is plotted against N, the number of atoms/cm.^{2}, as abscissa, the curve rises from $N = 0$ to $N = 7 \times 10^{12}$, falls from $N = 7 \times 10^{12}$ to $N = 43 \times 10^{12}$ and rises when $N > 43 \times 10^{12}$, inversely as the p-v curve of an imperfect gas. The curve $(\nu - \mu)$ versus N behaves similarly and intersects the N-axis at three points, thus enclosing two areas A_1 and A_2. The condition for the stationary phase boundary[46,47] is $A_1 = A_2$, while if μ becomes μ_1, the velocity v of the movement of the phase boundary along the wire is

$$v = (D/2A)^{\frac{1}{2}} (\mu_1 - \mu),$$

when D is regarded as independent of N and very small. The experiments did indeed suggest that at equilibrium $A_1 = A_2$ and that v was proportional to $(\mu_1 - \mu)$, thus giving a value of $D = 6 \times 10^{-4}$ cm.^{2} sec.$^{-1}$ at 967° K., where $N = 7\cdot3 \times 10^{13}$.

B. *By the measurement of photoelectric emission.*

That the photoelectric effect could be used to follow surface migration was first suggested by work of Ives[48], but the subsequent developments of the method and technique were

23

B D

carried out by various workers (26, 27, 28). The method has provided some detailed information concerning the forces governing the diffusions. It has one great advantage over the previous thermionic method, in which one measures only the integrated current over the whole filament. The photoelectric method, on the other hand, permits one to measure the actual concentration gradients along the surface, and their change with time, since a small well-defined spot of light may be made to traverse the surface on which the film is deposited.

(i) Bosworth deposited a small patch of sodium (26) or potassium(27) on the centre of a tungsten strip, and by traversing the patch with a spot of light measured the concentrations and concentration gradients as a function of time. Three methods were used to interpret the data, based on solutions of the diffusion equation and on a calibration curve giving $\log i$ as a function of N. The strip of tungsten, which had been out-gassed at a temperature sufficient to leave the oxygen monolayer but to remove oxides of tungsten (26), absorbed the sodium or potassium, a portion of which reappeared on the surface when the strip was heated to a suitably high temperature. The alkali metal thus migrated over the surface of crystallites and then between grain boundaries down into the tungsten. The capacity of tungsten to absorb the alkali metal was limited, and when the limit was reached the deposit of alkali metal simply spread over the surface to give a uniform layer and Fick's law could be applied only to the centre of the deposit. This spreading took 1 or 2 hr. at 300° K., or 5–10 sec. at 800° K. The families of curves of Fig. 128 show the processes of absorption of sodium in sodium-free tungsten.

The family of concentration-time-distance curves in Fig. 128 corresponds very nearly to the solution of the diffusion equation (26) when C_0 is the amount of substance per unit area at time $t = 0$, concentrated at the zero plane, and when diffusion occurs in the direction $+x$, inwards down inter-crystalline surfaces (Chap. I, p. 44). The diffusion

constant for this process is denoted by Δ, and the solution at $x = 0$ is

$$C_{x=0} = \frac{C_0}{\sqrt{(\pi \Delta t)}}.$$
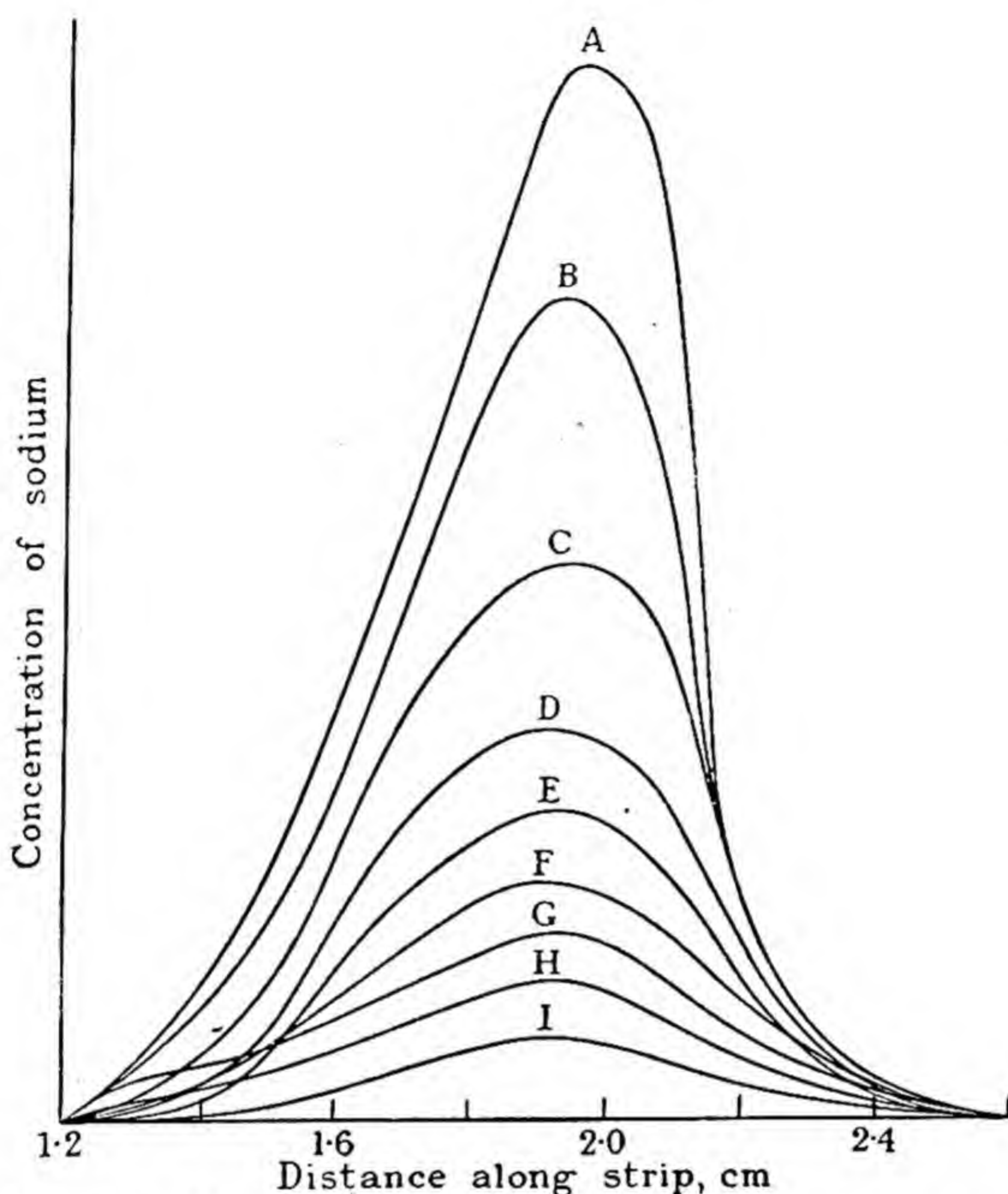
Fig. 128. The absorption of sodium by a sodium-free tungsten strip.

A.	5 mins.	
B.	10 ,,	
C.	20 ,,	at 295° K.
D.	40 ,,	
E.	60 ,,	

F.	1 min.	
G.	3 mins.	
H.	5 ,,	at 415° K.
I.	11 ,,	

Accordingly $1/C^2$ should be a linear function of t, as indeed was found to be the case (Fig. 129). The curves do not always pass through the origin because there is an uncertainty in fixing the time of the beginning of the experiment.

(ii) The analysis of the data in which the diffusion laws could be applied only to the central part of the curves [27]

23-2

(p. 367) was carried out by employing the operational notation of Heaviside, with $p = d/dt$; $\nabla^2 = d^2/dx^2$, in the case of one dimensional diffusion.
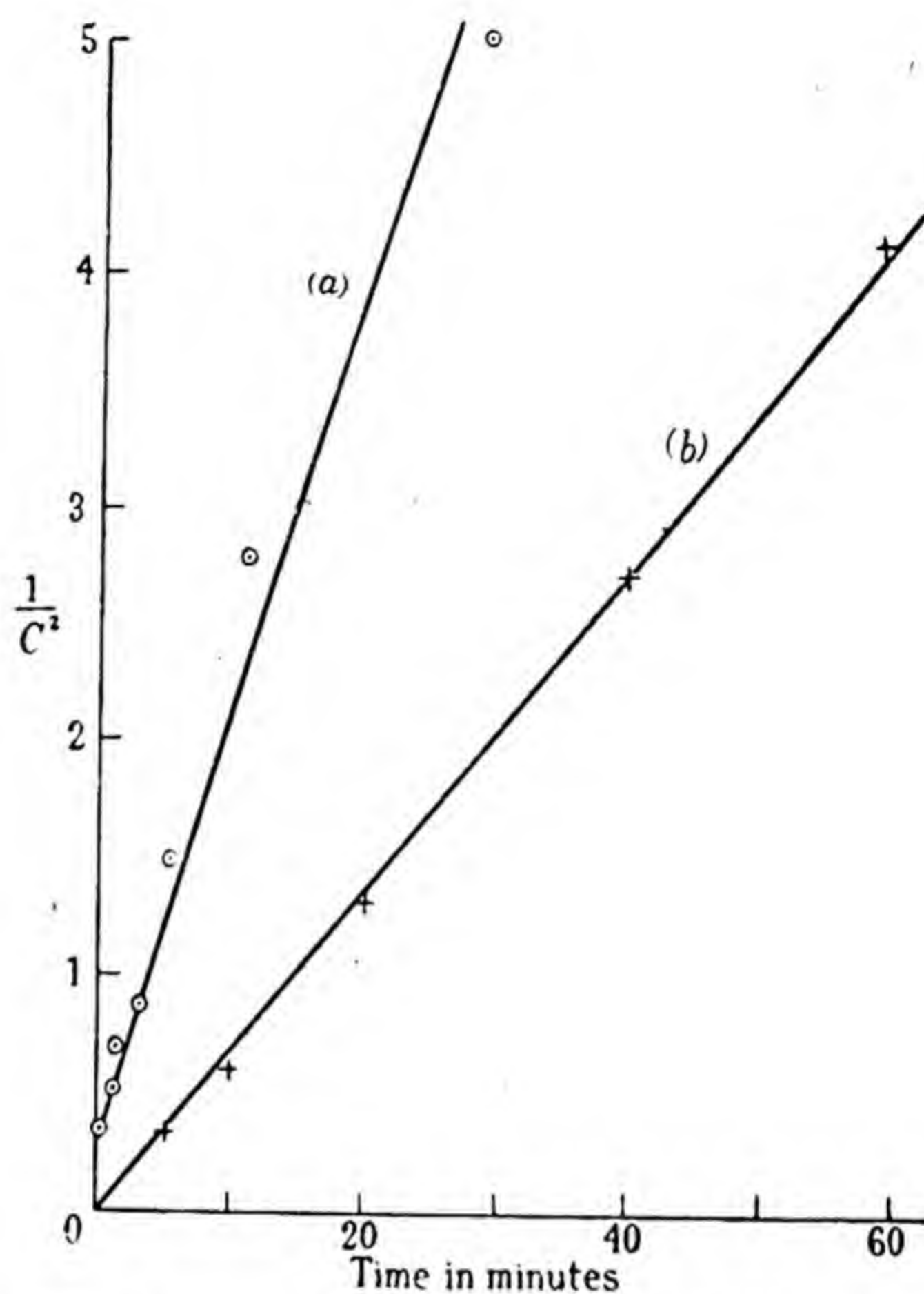
Fig. 129. The concentration of sodium at the peak of the curves of Fig. 128, as a function of time.

Curve (a) 415° K. Slope $= 0.022$.
Curve (b) 293° K. Slope $= 0.00067$.

Then, since $C_0 = f(x)$ only,

$$pC - pC_0 = D\nabla^2 C,$$

or

$$C = \frac{pC_0}{p - D\nabla^2},$$

and thus

$$C = e^{Dt\nabla^2}C_0 \quad (49)$$

or

$$C = C_0 + Dt\nabla^2 C_0 + \frac{D^2 t^2}{2!}\nabla^4 C_0 + \dots + \frac{D^n t^n}{n!}\nabla^{2n} C_0.$$

The total amount of sodium which has diffused from within

two ordinates a and b of concentration-distance curves such as shown in Fig. 128 is then

$$\int_a^b (C - C_0)\, dx = Dt\left\{\left(\frac{dC_0}{dx}\right)_a - \left(\frac{dC_0}{dx}\right)_b\right\}$$

$$+ \tfrac{1}{2}D^2 t^2\left\{\left(\frac{d^3C_0}{dx^3}\right)_a - \left(\frac{d^3C_0}{dx^3}\right)_b\right\} + \ldots.$$

If the derivatives of higher order than d^3/dx^3 are neglected and the ordinates a and b are chosen so that d^3C_0/dx^3 is zero, the expression reduces to

$$\int_a^b (C - C_0)\, dx = Dt\left[\overline{\left(\frac{dC_0}{dx}\right)_a - \left(\frac{dC_0}{dx}\right)_b}\right],$$

where the bar implies an average value of dC/dx over the time interval t. This method suffers from one weakness—the assumption that the derivatives of C_0 form a rapidly converging series. It gave values of $D = D_0 e^{-E/RT}$ and of E which were, however, in fair agreement with those obtained by the previous method.

(iii) A third method of analysis of data obtained by using the photoelectric exploration of the surface with a spot of light depends on the setting up of an equilibrium state of film concentrations along a wire with a temperature gradient. In this gradient the cooler parts of the wire are more densely covered than the hotter parts. At equilibrium,

$$\frac{dC}{dt} = 0 = \frac{d}{dx}\left(D\frac{dC}{dx}\right)$$

or

$$\frac{dC}{dx}\frac{dD}{dx} + D\frac{d^2C}{dx^2} = 0.$$

Also, since $D = D_0 e^{-b/T}$,

$$\frac{dD}{dx} = -bD\frac{d}{dx}\left(\frac{1}{T}\right),$$

giving by substitution in the first expression

$$b = \frac{E}{R} = \frac{d/dx[\log_e(dC/dx)]}{d/dx(1/T)} \text{ degrees.}$$

The values of (dC/dx) were measured photoelectrically, and of T as a function of x with an optical pyrometer. The results obtained by this method were comparable with those obtained by the other two methods.

(iv) A further method of obtaining the activation energy E, which was independent of the amounts of metal deposited, or of the thickness of the substrate into which diffusion occurred, was employed by Frank [28]. He used the simple Fick law $\frac{1}{D}\frac{\partial C}{\partial t} = \frac{\partial^2 C}{\partial x^2}$, and so neglected the variations of D with C. The method consisted in measuring the relative beam intensities n_1 and n_2 for which deposition-time curves taken at temperatures T_1 and T_2 coincide. Under these conditions

$$D_1/D_2 = n_1/n_2,$$

so that one may readily compute E. The Fick law is to be solved for the conditions:

(1) At $t = 0$, inside the substrate $C = 0$ for all x.

(2) At the surface $x = 0$, the concentration depends on time t as determined by the deposition curve: $C_{x=0} = f(t)$. Also, the total deposit is given by

$$\int_0^d C(x, t)\, dx = nt,$$

where d is the thickness of the substrate into which the film diffuses. At the temperatures T_1 and T_2 one may then write

(1)	(2)
$\dfrac{1}{D_1}\dfrac{\partial C_1}{\partial t} = \dfrac{\partial^2 C_1}{\partial x^2},$	$\dfrac{1}{D_2}\dfrac{\partial C_2}{\partial t} = \dfrac{\partial^2 C_2}{\partial x^2},$
$C_1(x, 0) = 0,$	$C_2(x, 0) = 0,$
$\int_0^d C_1(x, t)\, dx = n_1 t,$	$\int_0^d C_2(x, t)\, dx = n_2 t.$

Each solution of the equations (1) can be transformed into

a solution of the equations (2) by simply reducing the time scale. If $\alpha\tau = t$, by substitution in (2) one obtains

$$\frac{1}{\alpha D_2}\frac{\partial C_2}{\partial \tau} = \frac{\partial^2 C_2}{\partial x^2},$$

$$C_2(x, 0) = 0,$$

$$\int_0^d C_2(x, \alpha\tau)\,dx = \alpha n_2\tau,$$

and the two sets of equations are equivalent if

$$\alpha = D_1/D_2 = n_1/n_2.$$

The methods based upon the thermionic and photoelectric properties of surfaces form an interesting study in themselves. The sequel will show that the surface diffusion constant D is not independent of the surface concentration, and this fact constitutes the major objection to these analyses. Only by using the Fick law in the form

$$\frac{\partial C}{\partial t} = \frac{\partial}{\partial x}\left(D\frac{\partial C}{\partial x}\right)$$

can one allow for variations in D with C. This law cannot be satisfactorily applied by using thermionic methods, which give only integrated effects over the filament. The photo-electric method, however, is potentially capable of application to measure D as a function of C. If, by using the method A (ii) of Taylor and Langmuir (p. 352), the central part of a tungsten filament were cleared of caesium, for example, and the caesium from the sides then diffused inwards to the centre, the actual concentration gradients could be measured by a photoelectric exploration of the wire with a spot of light. The concentration-distance curves can then be submitted to Matano's analysis (Chap. I, p. 47) of the equation

$$\frac{\partial C}{\partial t} = \frac{\partial}{\partial x}\left(D\frac{\partial C}{\partial x}\right),$$

to give D as a function of C. No such experiment has yet been made, and until this has been done the surface diffusion data must suffer in accuracy, although the main properties of surface flow are reasonably well established.

Migration in films of caesium on tungsten

The composite surface Cs-W has been the subject of numerous studies (35, 45, 46). Tungsten after ageing at 2800° K. provides a surface, homogeneous save for about 0·5 %, on which a caesium monolayer is completed when N, the number of atoms per cm.^{2}, is $3·56 \times 10^{14}$, an atom density giving a ratio caesium : tungsten $= 1 : 4$ on the surface. The sorption heat of caesium on the inhomogeneous 0·5 % of the surface is 80 k.cal., compared with $\Delta H = 63·5$ k.cal. for dilute films on the rest of the surface. All the properties of the Cs-W surface—rates of evaporation of atoms, ions, and electrons, heats of sorption, velocities and activation energies of migration—depend very strongly upon the fraction of the surface covered. The electron emission reaches its maximum at $\theta = 0·67$ of a monolayer.

The migration of caesium on the surface of tungsten was first observed by Becker (45). It is interesting to compare values of the surface diffusion constant D obtained by different methods. By the method which depends on freeing the centre of the filament from caesium (p. 352), Langmuir and Taylor (35, 46) found values of D in cm.^{2} sec.$^{-1}$ at $N = 2·73 \times 10^{13}$ atoms/cm.^{2} and at temperatures of 654, 702, 746 and 812° K. which conformed to the equation

$$\log_{10} D = -0·70 - 3060/T. \tag{1}$$

The method depending upon the movement of the phase boundary between the dense and dilute surface phases (which can coexist at appropriate temperatures and pressures of caesium (p. 353)) gave a value of D of 6×10^{-4} cm.^{2} sec.$^{-1}$ when $N = 7·3 \times 10^{13}$ at $T = 967°$ K., whilst the extrapolation of equation (1) gives $D = 1·1 \times 10^{-4}$ cm.^{2} sec.$^{-1}$ at 967° K. and with $N = 2·73 \times 10^{13}$. The discrepancy may be due to the variation in D with surface concentration (p. 372) for when $N = 2·73 \times 10^{13}$ and $1·74 \times 10^{13}$ respectively the first method gives $D_{812° K.} = 3·4 \times 10^{-5}$ and $1·4 \times 10^{-5}$ cm.^{2} sec.$^{-1}$.

As the surface concentration of caesium increases the heat of sorption diminishes, being about 41,000 cal./atom when a

monolayer is nearly completed. The formation of multilayers results in a further decrease in the heat of sorption, until the film assumes the properties of caesium in bulk, for which the heat of condensation is 18,240 cal./atom. The activation energy for migration in the first layer, when $N = 2 \cdot 73 \times 10^{13}$, is about 20 % of the heat of sorption, so that if the same ratio exists in a multi-atomic film, or for the surface of the metal in bulk, the energy of activation would be 4600 cal./atom [35]. Using this assumption, Taylor and Langmuir calculated the values of D_1 and D_2, the diffusion constants in a monolayer, and in the surface layer of a thick deposit, respectively (Table 86). The diffusion constant D_2 is greater than the average diffusion constant in liquids at room temperature, and the assumed activation energy (4·6 k.cal.) compares with the energy of activation of 5·3 k.cal. when D_2O diffuses into H_2O [50]. One

TABLE 86. *Surface diffusion constants for caesium in a mono-layer, and in the surface layer of a thick deposit, of caesium on tungsten*

Temp. °K.	D_1 (cm.² sec.⁻¹)	D_2 (cm.² sec.⁻¹)
300	$1 \cdot 2 \times 10^{-11}$	0·00034
400	$4 \cdot 3 \times 10^{-9}$	0·00134
500	$1 \cdot 5 \times 10^{-7}$	0·0022
600	$1 \cdot 6 \times 10^{-6}$	0·0027
700	$8 \quad \times 10^{-6}$	0·0032

may thus regard the surface layer of a thick caesium deposit as being in a condition not very different from that of a liquid. On the other hand, the mobility of the caesium in the first layer is 10^6-fold less at room temperature than the mobility in a liquid, and does not approach the mobility of a liquid until a temperature of 700–800° K. is reached.

Migration of thorium on tungsten

Thorium-coated tungsten filaments have a high thermionic emissivity and, like caesium-coated tungsten filaments, have been widely studied [45, 24, 1, 22]. It is possible to prepare filaments of tungsten with thoria incorporated, and it is with

thoriated filaments of this type that much of the available information has been obtained. These studies have considerably extended knowledge of the grain-boundary diffusion processes already discussed (Chap. VII, p. 327), and will now be considered in relation to surface mobility.

Quantitative measurements on the surface diffusion constant are somewhat scanty, the most complete analysis being that of Brattain and Becker (24), who followed the diffusion of thorium evaporated on to tungsten from the covered to the uncovered side of the tungsten strip, by measuring the changes in thermionic emission with time. The theory of their method has been described earlier (p. 351).
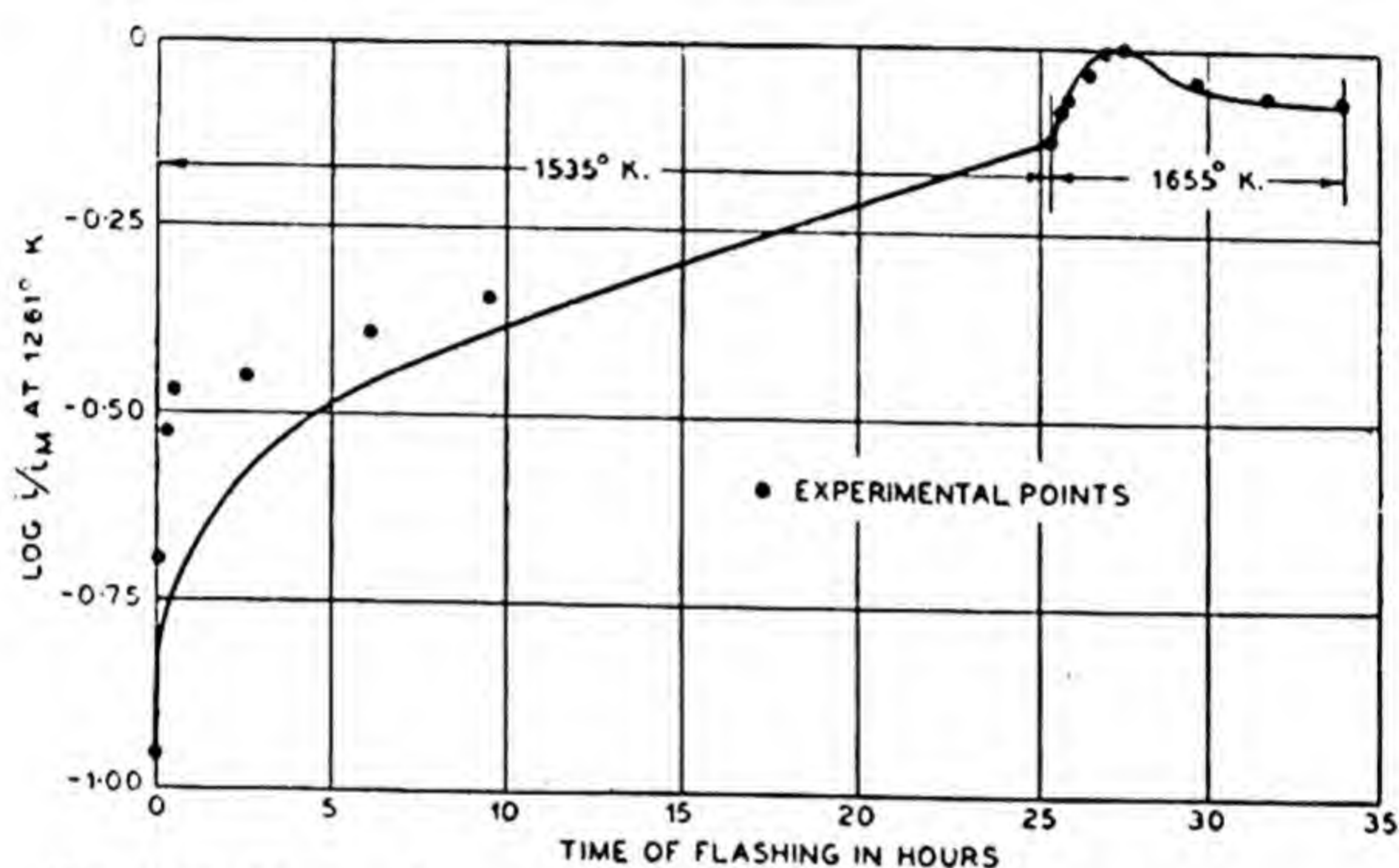
Fig. 130. Comparison of experimental and calculated migration curves for front side of ribbon.

At the start of the migration experiment $f = \theta/\theta_m$ (p. 349) was 1·77. The strip was then flashed at 1535 or at 1655° K., and its thermionic emission measured periodically at a lower temperature of 1261° K. Fig. 130 shows the observed values of $\log i/i_m$ plotted against time after flashing at 1535 and at 1655° K. In the same figure the full curve has been calculated according to the equation (p. 352):

$$f = \frac{f_0}{2} + \frac{2f_0}{\pi} \sum_{m=1}^{m=\infty} \left(\frac{1}{m} e^{-m^2\pi^2 Dt/w^2} \cos\frac{m\pi x}{w} \sin\frac{m\pi}{2} \right).$$

Very clearly the experimental and theoretical curves are a poor fit, and lack of agreement must be ascribed to the

variation in D with f (p. 371). Since the initial value of f was 1·77 on the front and zero on the back of the tungsten strip, the final value on back and front was $f = 0.885$, as was verified by the thermionic emission. Brattain and Becker made a rough calculation of the energy of activation, E, for thorium over tungsten, arriving at $E = 110$ k.cal./atom, but this value cannot be accurate since f was not the same at both the temperatures used (1535 and 1655° K.). The values of D (in cm.^{2} sec^{-1}) were

at 1535° K. $\qquad D = 1.84 \times 10^{-9}$,

at 1655° K. $\qquad D = 2.44 \times 10^{-8}$,

but perhaps half this variation had its origin in the different f values at which the observations were made. Using the Dushman-Langmuir equation $D = (E/N_0 h) d^2 e^{-E/RT}$ as an empirical guide (Chap. VI, p. 298), one finds agreement between the observed and calculated values of D at 1655° K., when $E = 66.4$ k.cal./atom. This is a much more likely value than 110 k.cal./atom, since it gives a satisfactory sequence with the expressions for lattice and slip-plane diffusion already given (Chap. VII, p. 328), as the following set of equations demonstrates:

Volume diffusion: $\qquad \log_{10} D = 0.0 - 26,200/T$.

Grain-boundary diffusion: $\log_{10} D = -0.13 - 19,700/T$.

Surface diffusion: $\qquad \log_{10} D = -0.33 - 14,500/T$.

The extent to which D varies as the surface concentration of the thorium is increased will be discussed later when the spreading pressure in films is considered (p. 372). At the moment it will be sufficient to comment that when

$\theta = 0, \qquad D/D_0 = 1$,

$\theta = 0.49, \quad D/D_0 = 11.3$,

$\theta = 0.98, \quad D/D_0 = 99.5$, if $D_0 = D$ at $\theta = 0$,

according to the calculations of Langmuir [22].

The mobility of sodium on tungsten-oxygen surfaces

Bosworth (26) using the three photoelectric methods described on pp. 353–9 measured the migration of sodium over and into tungsten which had been out-gassed at 2200° K. and therefore retained a monolayer of oxygen. These methods were:

(i) The rate of diminution of sodium concentration at the centre of an island of sodium deposited on sodium free tungsten, by one dimensional migration into the tungsten.

(ii) The rate of diminution of sodium concentration in an island of sodium deposited on sodium-saturated tungsten, using Heaviside's solution of the diffusion equation, in terms of $\partial C/\partial x$ and $\partial^2 C/\partial x^2$, etc.

(iii) The equilibrium distribution of sodium over the surface of a strip, with a temperature gradient along it.

It is noteworthy that the values of $D = D_0 e^{-E/RT}$ or of E obtained by the three methods, treated as one-dimensional diffusions, were in moderate agreement, although the diffusion processes must have varied among themselves. For instance, in (i) the diffusion is of sodium *into* the body of the tungsten, and in (ii) and (iii) is a spreading *over* the surface. The inference would be that in the strip of tungsten used the impedance to migration down grain boundaries is comparable to the impedance to migration over the surface. This is not true of the analogous thorium-tungsten systems where Langmuir's interpretation of available data gave

$$E_{\text{grain boundary}} = 90 \cdot 0 \text{ k.cal./atom,}$$

and
$$E_{\text{surface}} = 66 \cdot 4 \text{ k.cal./atom.}$$

Typical values of E computed by the method (i) for a number of experiments between 290 and 455° K. are:

6950; 6260; 5800; 5330; 6730; and 5800 cal./atom,

the mean of these data being 6260 cal./atom. The values obtained for E vary considerably with temperature, being as low as 3200 cal. between 76 and 200° K., and as high as

8600 cal./atom between 400 to 550° K. The variation in E with temperature could be regarded as a specific heat effect—the specific heat of the sodium in the mobile state being less than that in the immobile state. Finally, it should be observed that the data take no account of the variation of D with θ.

As soon as the body of the tungsten was fully charged with sodium, the spreading of sodium over the surface could be observed at room temperatures. Using the method (ii), and choosing two ordinates, a and b, such that d^3C_0/dx^3 is zero where they cut the C_0, one has

$$\int_a^b (C_0 - C)\,dx = Dt\overline{\left[\left(\frac{dC}{dx}\right)_a - \left(\frac{dC}{dx}\right)_b\right]}.$$

Then one may read off values of dC/dx from the graph, and find $\int_a^b (C_0 - C)\,dx$ graphically, and so compute D. The results are indicated by the following set of data:

	$t = 32$ min.	$t = 27$ min.	$t = 60$ min.
$\left(\dfrac{dC}{dx}\right)_a$	79	39	60
$\left(\dfrac{dC}{dx}\right)_b$	$. - 62$	$- 31$	$- 55$
$\displaystyle\int_{1\cdot85}^{2\cdot15} (C_0 - C)\,dx$	$2\cdot22$	$0\cdot68$	$2\cdot90$
$D_{293^\circ\,\mathrm{K}.}$	$0\cdot8 \times 10^{-5}$	$0\cdot6 \times 10^{-5}$	$0\cdot7 \times 10^{-5}$

For this set of data the surface concentration was $2\cdot1 \times 10^{15}$ atoms/cm.^{2}

In the manner outlined, and for initial concentrations ranging from $2\cdot8 \times 10^{15}$ to $6\cdot6 \times 10^{15}$ atoms/cm.^{2} of apparent surface a mean value of $D_{293^\circ\,\mathrm{K}.} = 0\cdot8 \times 10^{-5}$ cm.^{2} sec.$^{-1}$ was computed. It was, however, noted that the larger the value of the surface concentration, the greater was D. The values of D at a number of temperatures are given in Table 87. From the data of this table one may plot the curve $\log D/T^{\frac{1}{2}}$ against $1/T$ and from the slope of this curve compute the activation energy for diffusion as $5\cdot5$ k.cal./atom.

Method (iii), depending on the equilibrium distribution of sodium along the strip when a temperature gradient existed along it, gave values of E varying from 7·4 to 4·4 k.cal./atom, and which were therefore similar to the values of the activation energy obtained by the other methods.

TABLE 87. *Diffusion constants D for the migration of sodium into and over tungsten with a monolayer of oxygen*

Temp. ° K.	$10^5 \times D$ in cm.^{2} sec.$^{-1}$
293	0·8
350	3·2
375	6·0
410	13
420	20
430	30
450	34
500	50
520	77
555	128
620	200
690	270
740	310
800	330

The mobility of potassium on tungsten-oxygen surfaces

The same photoelectric methods were applied by Bosworth (27) to this system as he had earlier used in the analogous sodium-oxygen-tungsten surface films (l.c.). The behaviour of the two systems was closely analogous. As for sodium, the first effect observed was a uniform fading out of the photo-emission, corresponding to an absorption of the potassium film by the potassium-free tungsten. Then when the tungsten was filled with potassium, the potassium deposit spread over the surface, by a process analogous to two-dimensional evaporation rather than as a true diffusion, save in the central part of the original island of potassium.

The application of the method (i) of the previous section led to a value of the activation energy of 6960 cal./atom—a similar value to that observed for sodium, but as with the

sodium-tungsten system this figure depended upon the surface concentration. Method (ii) of the previous section employs the relation

$$\int_a^b (C_0 - C)\, dx = \left[\left(\frac{dC_0}{dx} \right)_a - \left(\frac{dC_0}{dx} \right)_b \right] Dt,$$

where the ordinates a and b are so chosen that d^3C_0/dx^3 is zero in a concentration-distance curve (Fig. 128). The values of D obtained were, for very dilute films:

Temp.° K.	480	510	590	710	780
D cm^2. sec.$^{-1}$	0.57×10^{-5}	1.4×10^{-5}	10×10^{-5}	140×10^{-5}	280×10^{-5}

When the curve $\log D$ versus $1/T$ was plotted, the activation energy was found to be 15,300 cal./atom. Table 88 shows that the slope of the $\log D$ versus $1/T$ curves changes as the surface concentration grows, and the numerical values of E are given for various values of surface concentration in this table.

TABLE 88. *The variation in activation energy E with N,
the number of atoms/cm.^{2}*

$N \times 10^{-14}$ atoms/cm.^{2}	E cal./atom
[0]	[16,700]
0·06	16,000
0·12	15,500
0·24	14,600
0·48	13,700
0·60	13,200
1·2	12,100
1·5	10,900
2·4	8,100
3·0	7,700
4·8	6,750

Mobility of caesium on tungstic oxide

Frank [28] measured the changes in photoelectric emissivity of tungstic oxide (p. 358), as caesium in measured quantity was deposited, and then allowed to diffuse away. He found that at high temperatures the deposit decayed more slowly, but this result was due in some way to the caesium which had collected below the surface by migration, during the deposition, or in earlier experiments.

THE MIGRATION OF OTHER FILM-FORMING SUBSTANCES

The method of Brattain and Becker (p. 351) has been used to show that migration of barium and caesium can occur. When barium (or caesium) was deposited on one side of the tungsten strip, which was then raised to 1000° K., the thermionic emissions from the front and back slowly became equal. The value of $f = \theta/\theta_m$ on the front was initially 0·80, while after the flashing at 1000° K., the final value of f on both back and front was 0·4.

Becker[51] remarked that while most of the results described relate to electropositive films, they should also apply to electronegative ones, such as oxygen, save that here the electron emission is decreased as the quantity of oxygen sorbed is increased. An experiment suggested that oxygen migrated very rapidly at 1400° K. These statements would merit further study, since the great readiness with which tungsten chemisorbs oxygen from the surroundings may vitiate many results.

In a study of the properties of indium, thallium and gallium films on tungsten oxide, Powell and Mercer[25] observed that, at temperatures 200° C. below the temperature of evaporation of ions, there was a gradual decay with time in the positive ion current (tested by momentarily raising the temperature of the system). These effects may be understood by assuming a migration into the oxide or over its surface. Similar observations[29] were made on a $Cs-Fe_2O_3$ system, in which it was shown that the photoelectric current decayed with time, and that an inward or lateral spreading of caesium in the oxide was a possible explanation.*

Köller[29] deposited caesium on a silver surface, to give a multimolecular layer, and then exposed the composite surface to the action of oxygen. Simultaneous observations of the photoelectric properties of the $Cs-Cs_2O-Ag$ surface showed that as fast as caesium oxide was formed it was covered by a polyatomic layer by processes of readjustment by diffusion in

---

* In this case the contamination of the metal by gas, or its re-evaporation, were not positively excluded, so that the evidence is not conclusive.

the film, so that the photoelectric properties remained almost unaltered until nearly all the caesium was used up.

Two other methods of obtaining information concerning surface migration are worthy of mention. The first is the method of the radioactive indicator. If polonium is deposited on a silver foil, at one end only, and the temperature is raised to 300° C., a creeping of the polonium along the silver could be noted, the velocity of which increased as the temperature was raised (52). No volume diffusion of polonium through the foil took place up to 500° C., an interesting commentary upon the relative ease with which surface and volume diffusion occur.

The second method is one which may have some general applicability to amalgams. It consists in measuring the rate at which mercury will spread over metal surfaces. Spiers (53) found that a drop of mercury spreads over tin foil in circular or elliptical areas in which, when diffusion has ceased, there is a uniform mercury content (11·8 % Hg). There is thus a concentration discontinuity from 11·8 % to 0 % mercury at the edge of the area, and the edge may be easily observed. Alty and Clark (54) made quantitative measurements on rates of spreading, which they found to be sensitive to the pretreatment of the surface and the nature of the medium (water, oil, or air) in contact with it. The surface diffusion was much more rapid than the volume diffusion, for after a surface diffusion of several centimetres the mercury had penetrated into a tin block by a fraction of a millimetre only.

The spreading of mercury up the surface of tin rods dipping into the mercury was a one-dimensional diffusion which was assumed to obey the following conditions:

(i)
$$\frac{\partial n}{\partial t} = D\frac{\partial^2 n}{\partial x^2},$$

where n is the number of mercury atoms/cm.^{2} at time t and height x above the surface of the liquid mercury.

(ii) $n = 0$ at $t = 0$ and $x > 0$, $n = n_0$ at $x = 0$ for all t.

This gives as the solution of (i)

$$n = n_0 \operatorname{erf}\left(\frac{x}{2\sqrt{(Dt)}}\right) \quad \text{(Chap. I)},$$

and since at the upper edge according to Spiers $n = n_1$ for all t where n_1 corresponds to 11·8 % of mercury, the progress of this boundary is given by

$$n_1 = n_0 \operatorname{erf}\left(\frac{x}{2\sqrt{(Dt)}}\right).$$

Thus

$$\frac{n_1}{n_0} = \operatorname{erf}\left(\frac{x}{2\sqrt{(Dt)}}\right) = \text{constant},$$

and so

$$\frac{x}{2\sqrt{(Dt)}} = \text{constant}, \; C.$$

Accordingly $D = x^2/4C^2 t$ and x^2 is a linear function of t. From the slopes of $x^2 - t$ curves at various temperatures, an activation energy for surface diffusion of 1920 cal./atom was calculated.

A COMPARISON OF THE DATA

The numerical values of the diffusion constants are compared at a few selected temperatures for some of the systems showing surface and intergranular diffusion, in the data following:

Temp. ° K. =	500	550	600	650	700	800
Na-OW $D_{\text{cm}^2./\text{sec.}}$ =	59×10^{-5}	102×10^{-5}	177×10^{-5}	232×10^{-5}	278×10^{-5}	330×10^{-5}
			All for $\theta \simeq 1$			
K-OW $D_{\text{cm}^2./\text{sec.}}$ =	$1\cdot1 \times 10^{-5}$	$4\cdot6 \times 10^{-5}$	19×10^{-5}	66×10^{-5}	126×10^{-5}	340×10^{-5}
			All for $\theta \simeq 0$			
Cs-W $D_{\text{cm}^2./\text{sec.}}$ =	$0\cdot015 \times 10^{-5}$	$0\cdot055 \times 10^{-5}$	$0\cdot16 \times 10^{-5}$	$0\cdot4 \times 10^{-5}$	$0\cdot85 \times 10^{-5}$	$3\cdot0 \times 10^{-5}$
			All for $\theta \simeq 0$			
Th-W $D_{\text{cm}^2./\text{sec.}}$ =	$1\cdot84 \times 10^{-9}$ at 1535° K. for $\theta \simeq 1$					

The data show considerable differences, those in the **Na-OW** system comparing with data calculated by **Langmuir**[1, 22] for a surface of caesium metal:

Temp. ° K. =	500	600	700
Cs-Cs$_{\text{metal}}$ $D_{\text{cm}^2./\text{sec.}}$ =	220×10^{-5}	270×10^{-5}	320×10^{-5}

Again the potassium in the K-OW system at low temperatures is much less mobile than in the Na-OW system, as corresponds to the difference in θ ($\simeq 0$, and $\simeq 1$ respectively); but the mobility of the potassium passes that of the sodium at 800° K.

TABLE 89. *The variation in heat of sorption with surface concentration and valence*

System	N (atoms/cm.^{2}) $f = \theta/\theta_m$, or θ	ΔH cal./atom	Reference
Cs-W	$N \simeq 0$	65,100	Taylor and
	$N = 2\cdot73 \times 10^{14}$ ($f = 1$, $\theta = 0\cdot67$)	44,500	Langmuir[35]
	$N = 3\cdot56 \times 10^{14}$ ($\theta = 1$)	40,800	
Na-OW	$N \simeq 0$, $f \simeq 0$	32,000	Bosworth[26]
	$f = 0\cdot2$	28,500	
	$f = 0\cdot4$	27,000	
	$f = 0\cdot6$	23,000	
	$f = 1\cdot0$	17,000	
Th-W	$N = 0\cdot87 \times 10^{14}$	178,000	Langmuir[1,22]
	$N = 2\cdot5 \times 10^{14}$	174,000	
	$N \doteq 5\cdot0 \times 10^{14}$	172,000	

So great is the effect of surface concentration upon mobility, however, that errors in estimating the concentration could cause the observed trends. Monovalent metals are more mobile than bivalent metals and bivalent metals than tetravalent metals. Thus mobility in alkali metal monolayers on tungsten can be observed at 300° K.; barium migrates measurably only at 1000° K.; and thorium at 1500° K. The trend shown in E, both in respect to surface concentration and valency, is reflected in corresponding trends in the heats of sorption ΔH (Table 89).

THE VARIATION IN THE DIFFUSION CONSTANTS WITH SURFACE CONCENTRATION

The cause of the increase in D or decrease in E, as the surface concentration increases, is considered to be a powerful lateral interaction of the dipoles of moment μ, formed by each adatom and its electrical image. The lateral repulsion between two such dipole systems whose centres are a distance r apart is given by

$$\text{Force} = (3/2)\,\mu^2/r^4.$$

Langmuir[42] considered a metallic surface covered with adatoms at a surface concentration N, which interacted with the force given above. He was then able to show that such an array of dipoles, if the short range forces of repulsion were also considered (so that no two adatoms can simultaneously occupy the same site), would obey the equation

$$F = NkT/(1-\theta) + 3\cdot34 N^{\frac{3}{2}}\mu^2 + 1\cdot53 \times 10^{-5} N^2 T^{\frac{1}{3}}\mu^{\frac{4}{3}} I.$$

Here I is an integral whose numerical value can be obtained from values of μ, N, and θ, and is never greater than $0\cdot89$, and F is the spreading force in dynes/cm.

Where these repulsive forces operate in a system in which there is a concentration gradient, there is a nett force operating in the direction of the concentration gradient, a force which rises rapidly with surface concentration. Thus Langmuir was able to show that the force which operates on a given adatom, due to the concentration gradient, was

$$\text{Force} = 2\left(\frac{dN}{dx}\right)\left[\frac{F - NkT}{N^2}\right].$$

This means that the height of the energy barriers for an atom moving in the direction of increasing N is greater than that for an atom moving in the opposite direction, and leads to the expression

$$D = D_0\left[\frac{2F}{NkT} - 1\right],$$

where D_0 is the diffusion constant when $N \simeq 0$. This analysis, originally made for caesium films[42], was applied also to thorium[22] films, both on tungsten. Values of F and D/D_0 are given below for a number of values of θ, for Th-W systems:

TABLE 90. *Effect of the spreading force F upon diffusion constants*

θ	0·00	0·05	0·1	0·2	0·3	0·4
F (dynes cm.$^{-1}$)	0·0	7·7	16·8	39·0	65·6	96·1
D/D_0 (Th-W)	1·0	1·25	1·46	1·85	2·20	2·25
θ	0·5	0·7	0·9	1·0	1·2	1·4
F (dynes cm.$^{-1}$)	132	226	377	502	1069	9630
D/D_0 (Th-W)	2·86	3·71	5·13	6·35	12·0	99·5

An analysis of the spreading forces for sodium on oxygen-tungsten was made by Bosworth[55]. There is a relation between the spreading force F and the vapour pressure, p, obtained from Gibb's equation:

$$F = 2 \cdot 303 kT \int N d \log p.$$

Bosworth then found the experimental connection between $\theta / \theta_m = f$ and p to be

$$\log p = \log f + 0 \cdot 71 - 1 \cdot 6f - \frac{7000 - 3200f}{T},$$

so that by inserting this value of $\log p$ in the first equation, and using numerical values, one finds

$$F = 0 \cdot 037 T \cdot f + 140 f^2 (1 - 0 \cdot 0004 T) \text{ dynes/cm.,}$$

since $F = 0$ when $f = 0$.

Topping[56] deduced the relationship $F'' = 4 \cdot 51 \mu^2 N^{\frac{3}{2}}$ for the electrical force between an array of dipoles. His equation was equated to the second term in the right-hand side of the above equation for F in terms of f. The first term is considered as due to Gibbsian thermal pressure, F'. The observed values of the spreading forces due to dipole interaction and those calculated from the Topping equation are given in Table 91, in which a quite reasonable agreement is found.

TABLE 91. *Values of spreading force due to dipole repulsion from experimental data and from Topping's equation, for the system* Na-OW

f	$F'' = 140 f^2 \times$ $(1 - 0 \cdot 0004 T)$ (dynes cm.$^{-1}$), when T is small	$F'' = 4 \cdot 51 \mu^2 N^{\frac{3}{2}}$ (degrees cm.$^{-1}$)
0·02	0·06	0·15
0·1	1·4	3·6
0·2	5·6	13·0
0·4	22·0	42·0
0·8	90·0	110·0
1·0	140·0	150·0

A somewhat different method of evaluating the spreading force is based upon the variation in the energy of activation, E, with N. If the value of E at $N = 0$ is E_0, one may write

$$F = (E_0 - E) N . 1 \cdot 58 \times 10^{-12} \, \text{dynes cm.}^{-1}.$$

Bosworth's[27] data on K-OW lead to the following values of F:

$N \times 10^{14}$ atoms/cm.^{2}	0·06	0·12	0·24	0·48	0·60	1·2	1·5	2·4	3·0	4·8
F (dynes/cm.)	0·23	0·96	3·5	10·0	14·3	38	60	142	187	322

The recorded values of F are for a range of surface concentrations comparable with those in Table 91 for Na-OW.

PHASE CHANGES IN STABLE MONOLAYERS

The equation of state of a gas shows that under suitable conditions gaseous and condensed states may coexist. When hydrogen gas dissolves in palladium, dilute and condensed phases may exist in equilibrium [57], or when a film of myristic, palmitic, or similar fatty acids is spread upon water, compressed and expanded states can occur together at suitable temperature or pH of the underlying liquid [58]. It is therefore interesting to inquire whether two phases can occur on stable monolayers on tungsten.

Using the idea of thermal and electrostatic spreading pressures developed in the previous section, one may write:

F = thermal spreading force + electrostatic spreading force

$$= \frac{kT}{A - A_0} + 4 \cdot 51 \mu^2 N^{\frac{3}{2}},$$

where A and A_0 denote the areas occupied per adatom in a film of surface concentration N ($N = 1/A$), and at saturation ($N = N_0 = 1/A_0$) respectively. When $A_0 = 11 \cdot 7$ A.^{2} one may employ the values of the electrostatic spreading pressure in Table 91, and so plot F–A curves for the Na-OW system. Below 700° K. the curves obtained resemble those for a condensible gas, so that the spreading forces calculated from experiment should lead to the formation of two phases. Probably the two phases of caesium on tungsten detected

by Langmuir and Taylor[46,35,47] were of this kind (p. 353).
Langmuir[47] attempted a kinetic analysis of conditions
favouring equilibrium between two such phases.

The phases discussed here are coexistent in a monolayer.
Their constitution therefore differs from that of films of
cadmium or mercury on glass (pp. 341 *et seq.*), where mono-
layer systems rearrange themselves into three-dimensional
aggregates. An exact analysis, employing statistical mechanics,
of conditions yielding a two-dimensional condensed phase
or a three-dimensional aggregate would be of importance.
Preliminary studies of the behaviour of double layer films
have been made by Cernuschi[59] and by Dube[60].

CALCULATION OF THE SURFACE DIFFUSION CONSTANT

The surface diffusion constant has been calculated by
several authors[37,61,35,62]. Lennard-Jones's theory[37] was
used by Ward[63] to interpret the slow sorption of hydrogen
by copper.

The most recent expression[61] takes the form

$$D = \frac{\alpha \bar{v}^2 \tau^2}{\tau + \tau^*}.$$

In this expression α denotes a constant ($\frac{1}{2}$ or $\frac{1}{4}$), $\bar{v}$ denotes the
average velocity of an adsorbed atom for the period τ during
which it is activated and τ^* is the time between successive
activations. The attempt to calculate τ and τ^* has been made
for two cases:

(1) When the activation energy is received by atomic
vibrations from the underlying solid[64]. It was concluded
that, when $RT \leqslant E$, τ was of the order 10^{-12} sec., and nearly
independent of temperature.

(2) When the activation energy is received by collisions
between metallic electrons from the adsorbent, and the
adatom[65]. It was again found that τ was approximately
10^{-12} sec., and nearly independent of the temperature. Since
metallic electrons may have as much as 50 k.cal. of energy,

and there may be 10^{15} collisions/second with the adatom, it is evident that an ample reservoir of energy is available, and that strongly bound adatoms may be activated.

The corresponding values of τ^* are of course strongly dependent on temperature, since they contain the Boltzmann factor $e^{-E/RT}$. It can also be shown [61] that

$$\frac{\tau^*}{\tau} = \frac{F^*}{F},$$

where F^* and F are the partition functions of migrating and vibrating states respectively. Thus

$$D = \alpha \bar{v}^2 \tau \frac{F}{F + F^*}.$$

These equations may as an example be applied to a simple type of potential energy field. The field is supposed to consist of cylindrical potential energy holes separated from each other by walls of height E_0 occupying a fraction ϕ of the whole surface, whose area is A. Then

$$F = A\left(\frac{2\pi m k T}{h^2}\right) e^{-E_0/RT},$$

$$F^* = A\phi\left(\frac{2\pi m k T}{h^2}\right)(1 - e^{-E_0/RT}),$$

and

$$D = \frac{\alpha \bar{v}^2 \tau}{(1 - \phi) + \phi e^{E_0/RT}}.$$

This when $E_0 \geqslant RT$ reduces to

$$D = \frac{\alpha \bar{v}^2 \tau e^{-E_0/RT}}{\phi},$$

and if $E_0 \leqslant RT$ to

$$D = \frac{\alpha \bar{v}^2 \tau}{1 + \phi(E_0/RT)}.$$

Finally, when E_0 tends to zero, $D = \alpha \bar{v}^2 \tau$, where τ is the interval between successive collisions in a two-dimensional gas. In this case simple theories give to α the value $\frac{1}{2}$. Applications of the theory to the diffusion of sodium on oxygen-tungsten surfaces [26] led to a mean free path in the activated state of $\sim 10^{-7}$ cm.

Applications of Surface Mobility in Physico-Chemical Theory

Assuming that certain adsorbed films are mobile, gas laws such as

$$\left[F+\frac{a}{A^2}\right][A-A_0] = RT$$

may be proposed, by analogy with three-dimensional equations of state. Here F denotes the surface pressure, A the area per molecule, and A_0 the area per molecule at saturation. If F is proportional to p, the gas pressure, and A to $1/x$, when x denotes the amount adsorbed, an adsorption isotherm may be derived rather like Langmuir's isotherm. A_0, like the "co-volume" in van der Waals's equation, may depend on temperature, and so explain the experimentally observed variation in the saturation value of the sorption with temperature. Langmuir's original isotherm could not do this. Similarly, the swelling of charcoals when they sorb vapours[66] may be explained as a penetration due to two-dimensional pressure which thrusts apart the interpenetrating graphitic flakes. Maxted's[67] studies of the catalytic homogeneity of certain surfaces could be reconciled with Taylor's[68] theory of active points if it is assumed that a migration of the reacting atoms, or atoms of the catalyst poison, could take place over the surface.

Various workers[69,70,71] have reported that when atom streams of cadmium, mercury, or similar metals are directed on to cooled surfaces, there is a critical stream density for each temperature below which aggregation into three-dimensional micro-crystals cannot occur. The application of an equation

$$\left(F+\frac{a}{A^2}\right)(A-A_0) = RT$$

to the sorbed atoms, which gives condensed phases, analogously to van der Waals's equation of state, has been used to explain the critical stream density and temperature. On this view the three-dimensional aggregate must build on the top of a

relatively immobile condensed phase in two dimensions, but not on the mobile gaseous phase. One should note, however, that the critical conditions are not sharply defined (72) so that aggregates may form over a range of stream densities of the impinging beam of atoms. This is illustrated in Fig. 131.
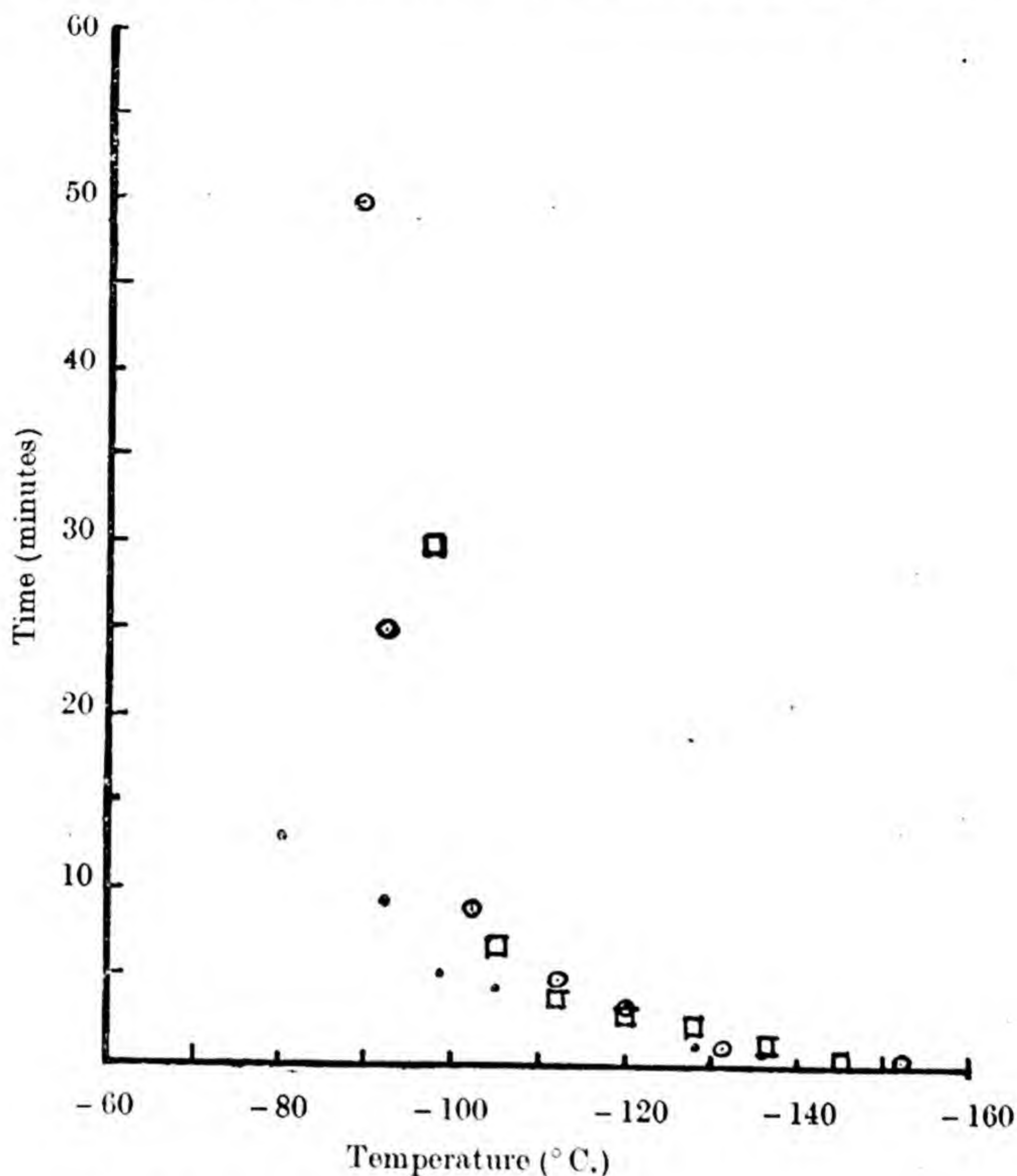
Fig. 131. Critical condensation phenomena for cadmium.
⊡, on glass; ⊙, on sulphur; O, on naphthalene.

An interesting application of the theory was made by Devonshire (73) in an attempt to explain the anomalous diffraction of helium beams at crystal surfaces observed by Frisch and Stern (74). It was found that at suitable angles of incidence impinging helium atoms need not be reflected from the surface, but could move along it in a mobile state for some distance before being emitted. It could also be shown that

when helium is sorbed on crystal surfaces (e.g. LiF), the zero point energy of the helium is so large that it can always pass over the energy barriers produced by the periodicity of the crystal surface, and so would be in the state of a two-dimensional gas even at $0°K$.

Calculations of the energy periodicity of the crystal surface for argon on KCl were made by Lennard-Jones and Dent [37]. Similar calculations were made by Barrer [38] for sorption on the basal planes of graphite. These calculations showed that gases would be mobile at quite low temperatures, in the case of hydrogen even at liquid air temperatures. More detailed calculations of the same kind were made by Orr [36], on argon-KCl, and argon-CsI systems, allowing for van der Waals's, repulsive, and electrostatic energies. In the case of KCl, the energy periodicity gave the following data for the fractional number of atoms rendered mobile:

Temp. °K.	10	20	40	60	80
$\dfrac{\text{Number mobile}}{\text{Total number adsorbed}}$	0·000012	0·0017	0·0306	0·0933	0·1667

On CsI the energy periodicity of the surface was far more marked, and there was a strong preferential adsorption above the centres of lattice cells of layers of caesium or iodine ions.

REFERENCES

(1) E.g. Langmuir, I. *J. Franklin Inst.* **217**, 543 (1934).
(2) Volmer, M. and Estermann, J. *Z. Phys.* **7**, 13 (1921).
(3) Volmer, M. and Adhikari, G. *Z. Phys.* **35**, 170 (1925).
(4) —— —— *Z. phys. Chem.* **119**, 46 (1926).
(5) Moll, F. *Z. phys. Chem.* **136**, 183 (1928).
(6) Richter, M. Diss. T.H., Berlin, 1931.
   Volmer, M. *Trans. Faraday Soc.* **28**, 359 (1932).
(6a) Berg, W. *Proc. Roy. Soc.* **164**A, 79 (1938).
(7) Gen, M., Zelmanov, I. and Schalnikow, A. *Phys. Z. Sowjet.* **4**, 825 (1933).
(8) Kirschner, F. *Z. Phys.* **76**, 576 (1932).
(9) Thomson, G. P., Stuart, N. and Murison, C. A. *Proc. phys. Soc.* **45**, 381 (1933).
(10) Farnsworth, H. E. *Phys. Rev.* **42**, 588 (1932); **43**, 900 (1933); **47**, 331 (1935).
(11) Deubner, A. *Naturwissenschaften*, **23**, 557 (1935).

(12) Swamy, R. S. *Proc. phys. Soc.* **46**, 739 (1934).

(13) Lane, C. T. *Nature, Lond.,* **130**, 999 (1932).

(14) Brück, L. *Ann. Phys., Lpz.,* **26**, 233 (1936).

(15) Finch, G. and Quarrell, A. G. *Nature, Lond.,* **131**, 877 (1933); *Proc. Roy. Soc.* **141**A, 398 (1933).

(16) Natta, G. *Naturwissenschaften,* **23**, 527 (1935).

(17) *See* Lange, H., *Kolloidzschr.* **78**; 109, 231 (1937) for a review.

(18) E.g. Andrade, E. *Trans. Faraday Soc.* **31**, 1157 (1935). Liepus, T. *Glastechn. Ber.* **13**, 270 (1935).

(19) Hass, G. *Naturwissenschaften,* **25**, 232 (1937).

(20) Estermann, J. *Z. phys. Chem.* **106**, 403 (1923).

(21) Cockcroft, J. *Proc. Roy. Soc.* **119**A, 293 (1928).

(22) E.g. Langmuir, I. *Acta Phys.-chim.* **1**, 371 (1934).

(23) Appleyard, E. *Proc. phys. Soc.* **49**, 118 (1937); *Discussion on Conductivity Electricity in Solids.*

Appleyard, E. and Lovell, A. *Proc. Roy. Soc.* **158**A, 718 (1937). Lovell, A. *Proc. Roy. Soc.* **157**A, 311 (1936); **166**A, 270 (1938).

(24) Brattain, W. and Becker, J. A. *Phys. Rev.* **43**, 428 (1933).

(25) Powell, C. F. and Mercer, R. L. *Philos. Trans.* **235**A, 101 (1935–36).

(26) Bosworth, R. C. *Proc. Roy. Soc.* **150**A, 58 (1935).

(27) —— *Proc. Roy. Soc.* **154**A, 112 (1936).

(28) Frank, L. *Trans. Faraday Soc.* **32**, 1402 (1936).

(29) Köller, L. *Phys. Rev.* **36**, 1643 (1930).

(30) Estermann, J. *Z. Phys.* **33**, 320 (1925).

(31) Knauer, F. and Stern, O. *Z. Phys.* **39**, 774 (1926).

(32) Ditchburn, R. *Proc. Camb. phil. Soc.* **29**, 131 (1933).

(33) Zahn, H. and Kramer, J. *Z. Phys.* **86**, 413 (1933). Kramer, J. *Ann. Phys., Lpz.,* **19**, 37 (1934).

(34) Tammann, G. *Ann. Phys., Lpz.,* **22**, 73 (1935).

(35) Taylor, J. B. and Langmuir, I. *Phys. Rev.* **44**, 423 (1933).

(36) Orr, W. J. C. *Trans. Faraday Soc.* **35**, 1247 (1939).

(37) E.g. Lennard-Jones, J. E. *Trans. Faraday Soc.* **28**, 333 (1932).

(38) Barrer, R. M. *Proc. Roy. Soc.* **161**A, 476 (1937).

(39) Dixit, K. R. *Phil. Mag.* **16**, 1049 (1933).

(40) Langmuir, I. *Phys. Rev.* **22**, 357 (1923).

(41) Becker, J. A. *Phys. Rev.* **33**, 1082 (Abstract) (1929).

(42) Langmuir, I. *J. Amer. chem. Soc.* **54**, 1252 (1932). *See also* Langmuir, I. and Kingdon, K. H. *Proc. Roy. Soc.* **107**A, 61 (1925).

(43) Langmuir, I. *J. Amer. chem. Soc.* **35**, 105 (1913).

(44) Roberts, J. K. *Proc. Roy. Soc.* **152**A, 445 (1935). Langmuir, I. and Villars, D. *J. Amer. chem. Soc.* **53**, 495 (1931).

(45) Becker, J. A. *Trans. Amer. electrochem. Soc.* **55**, 153 (1929); *Phys. Rev.* **28**, 341 (1926); *Phys. Rev.* **34**, 1323 (1929).

(46) Langmuir, I. and Taylor, J. B. *Phys. Rev.* **40**, 463 (1932).

(47) Langmuir, I. *J. chem. Phys.* **1**, 3 (1933).

(48) Ives, H. *Astrophys. J.* **60**, 4 (1924).

Ives, H. and Olpin, A. *Phys. Rev.* **34**, 117 (1929).

(49) Jeffreys, H. *Camb. Math. Tracts*, No. 23, 10 (1927).

(50) Orr, W. J. C. and Butler, J. *J. chem. Soc.* p. 1273 (1935).

(51) Becker, J. A. *Trans. Faraday Soc.* **28**, 148 (1932).

(52) Schwartz, K. *Z. phys. Chem.* **168**A, 241 (1934).

(53) Spiers, F. *Phil. Mag.* **15**, 1048 (1933).

(54) Alty, T. and Clark, A. *Trans. Faraday Soc.* **31**, 648 (1935).

(55) Bosworth, R. C. *Proc. Roy. Soc.* **162**A, 32 (1937).

(56) Topping, J. *Proc. Roy. Soc.* **114**A, 67 (1927).

(57) Lacher, J. *Proc. Roy. Soc.* **161**A, 525 (1937).

(58) Rideal, E. K. *Surface Chemistry*, chap. III (1930).

(59) Cernuschi, F. *Proc. Camb. phil. Soc.* **34**, 392 (1938).

(60) Dube, G. *Proc. Camb. phil. Soc.* **34**, 587 (1938).

(61) Lennard-Jones, J. E. *Proc. phys. Soc.* **49**, 140 (1937); *Discussion on Conduction of Electricity in Solids*.

(62) Alty, T. *Phil. Mag.* **15**, 1035 (1933).

(63) Ward, A. F. *Proc. Roy. Soc.* **133**A, 506 (1931).

(64) Lennard-Jones, J. E. and Strachan, C. *Proc. Roy. Soc.* **150**A, 442 (1935).

(65) Lennard-Jones, J. E. and Goodwin, E. *Proc. Roy. Soc.* **163**A, 101 (1937).

(66) E.g. Bangham, D. and Fakhoury, N. *J. chem. Soc.* p. 1324 (1931).

(67) Maxted, E. B. and co-workers. *J. chem. Soc.* p. 502 (1933); pp. 26, 672 (1934); pp. 393, 1190 (1935).

(68) E.g. Taylor, H. S. *Trans. Faraday Soc.* **28**, 247 (1932).

(69) Knudsen, M. *Ann. Phys., Lpz.*, **50**, 472 (1916).

(70) Wood, R. W. *Phil. Mag.* **30**, 300 (1915); **32**, 364 (1916).

(71) Semenoff, N. *Z. phys. Chem.* **7**B, 471 (1930).

(72) Chariton, J., Semenoff, N. and Schalnikow, A. *Trans. Faraday Soc.* **28**, 169 (1932).

(73) Devonshire, A. *Proc. Roy. Soc.* **156**A, 37 (1937).

(74) Frisch, R. and Stern, O. *Z. Phys.* **84**, 430 (1933).

CHAPTER IX

PERMEATION, SOLUTION AND DIFFUSION OF GASES IN ORGANIC SOLIDS

PERMEABILITY SPECTRUM

Membrane-forming organic solids include waxes, fats, rubbers, proteins and protein derivatives, cellulose and cellulose derivatives, resins and alkyl sulphide polymers. Many synthetic polymers have valuable properties of plasticity, rigidity or elasticity. One finds every type of gas flow through them, and a diversity of permeabilities which receives a number of practical applications. In technological journals there are numerous studies of gas flow through rubbers (especially helium, air and hydrogen); of the flow of water, air and carbon dioxide through fruit and food wrappings and cartons; and of air and water through gutta percha and paragutta insulators, leathers, and paint and varnish films. On the theoretical side these polymers provide material for the study of diffusion kinetics, and of various types of gas flow in solids, such as activated diffusion, molecular flow, streamline flow, or orifice flow. Of special interest are transition regions between one type of flow and another, as yet little studied.

The process of diffusion in polymers may conveniently be discussed in two parts: first, the flow of gases and not easily condensible vapours (CO_2, SO_2, NH_3) in organic solids; and second, the flow of water and organic liquids and vapours through the membranes. This is because, as the sequel will show, gas diffusion obeys the simple law

$$\frac{\partial C}{\partial t} = D \frac{\partial^2 C}{\partial x^2}$$

fairly rigorously, while vapour diffusion does not usually do so.

It is possible to arrange the permeabilities of organic membranes to air, for example, in a permeability spectrum[1] as indicated in Fig. 132.

The permeabilities in Fig. 132 are expressed in c.c./sec./ cm.^{2}/cm. of Hg pressure and are therefore not absolute, since thickness (which may vary from several millimetres to a fraction of a millimetre) has not been included. Generally a given type of membrane will give somewhat different permeabilities for different specimens. Thus we have border-line cases such as vegetable parchment listed in sections B and C; or cellulose compounds most of which could be grouped in section A as well as section B, according to the variable degrees of permeability which may be encountered.

A	B Includes semi-papers	C Includes papers, fibre-boards and leather		D Textile fabrics
Balloon fabrics Cellophane Regenerated cellulose Rubbers Neoprene Polysulphides Resins Lacquers Paints	Cellulose nitrate Cellulose acetate Cellulose esters Glassine Vegetable parchment Asphalt saturated paper	Filter paper Blotting paper Insulating board Newsprint paper Antique book paper Lined straw board Super-calendered book paper	Tagboard Bond paper Railroad board Solid binders board Pressboard Vegetable parchment Leathers	

-8   -7   -6   -5   -4   -3   -2   -1   0   1   2   3   4

log (permeability)

Fig. 132. Showing the logarithm of the permeability towards air of groups of organic membranes.

The experimental problem involved differs according to the section being studied. For section A, for example, where very small permeabilities are being encountered, various types of diffusion apparatus have been described, all of which have as their object the making and maintaining of gastight junctions between the membrane and the gas chambers in contact with its ingoing and outgoing surfaces. Dewar [2] in one form of cell fastened his rubber membranes by tying and then waxing. Daynes [3] found that, with glycerine lubricant between the flanges of the two chambers and the surfaces of the rubber membranes, the joints were satisfactorily airtight. Schumacher

and Ferguson [4] described a mercury sealed cell (Fig. 133) which they considered suitable for any membrane. Rayleigh [5] used membranes supported between funnels clamped together and waxed along the flanges to prevent lateral diffusion.

It is usual in these systems, in which diffusion occurs from the high-pressure side into a vacuum, to support the membrane with a metal gauze, or another rigid porous support, in order to prevent distortion of the membrane. Other types of cell have been employed (Edwards and Pickering [6]), in which the total pressure on either side was kept the same, or nearly the same, but on one side was hydrogen, whose permeability was to be studied, and on the other was air. The hydrogen diffusing into the air stream was estimated by means of a Rayleigh interferometer. These types of apparatus exemplify the two methods of measuring permeability, i.e. diffusion into vacuum, with manometric estimation of the diffusing gas, and diffusion
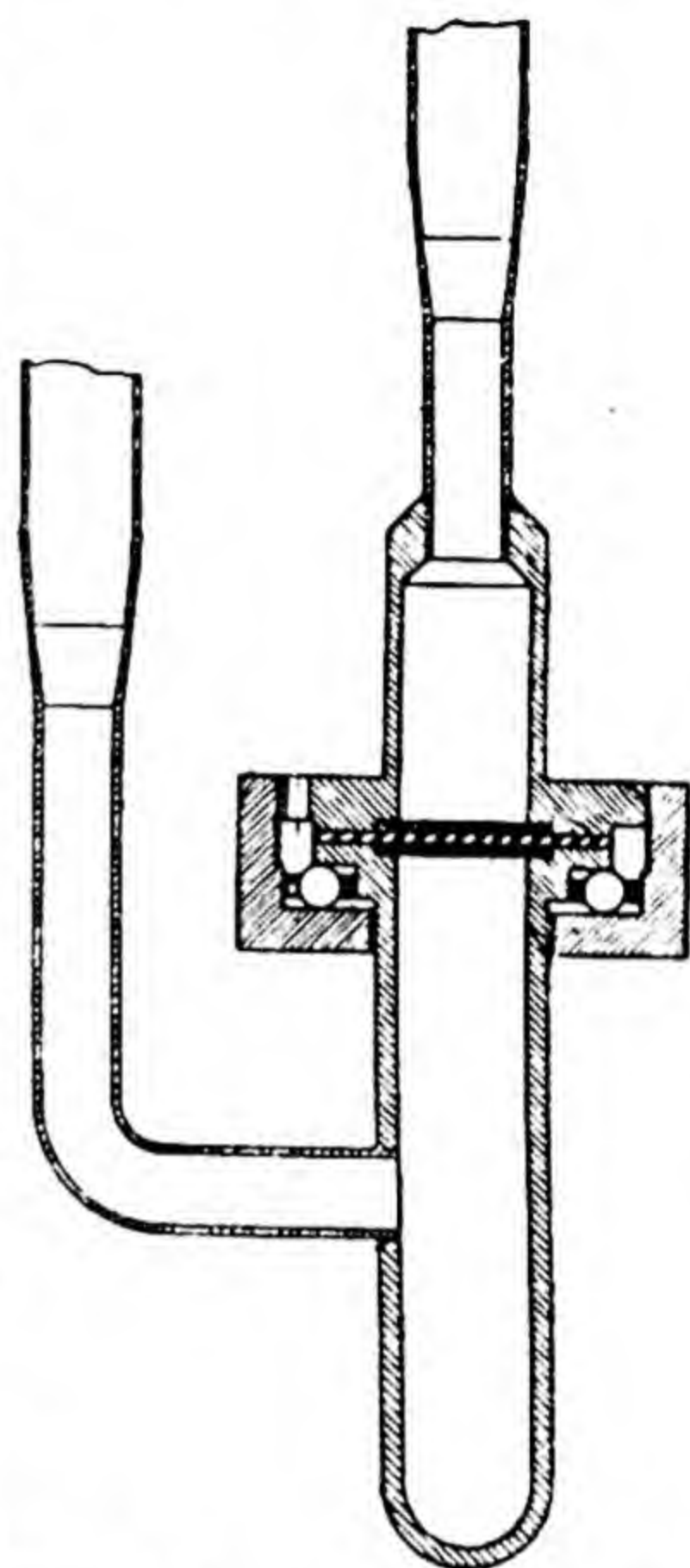
Fig. 133. Schumacher and Ferguson's diffusion cell.

into an air stream, with interferometric gas analysis.

The diffusion cells used in studying section A can readily be used to study section B of the permeability chart (Fig. 132). Similarly the apparatus for section C may be extended in its application to section B.

Apparatus has been developed in the Bureau of Standards (F. Carson [1]; also [7]) for measuring the permeability of papers, fibreboards, and leathers (section C of Fig. 132). Instruments have also been described [8] for measuring permeabilities of fabrics and textiles, of even smaller impedance to air flow. Fig. 134 illustrates the permeameter of Schiefer and Best [9]. The fabric pressure gauge is inclined at a slope of 1 in 10, which allows the difference in pressure between the chamber A and

the atmosphere to be measured to $\frac{1}{200}$ inch. The difference in pressure between the chambers A and B is registered by the air orifice gauge, and gives at once the rate of flow of gas through the calibrated air orifice, and hence through the fabric. Air is drawn from the atmosphere through the fabric and air orifice by a suction fan.

The instruments mentioned cover the groups A–D of the permeability spectrum (Fig. 132); and so cover a 10^{12}-fold variation in air permeability shown by organic membranes.
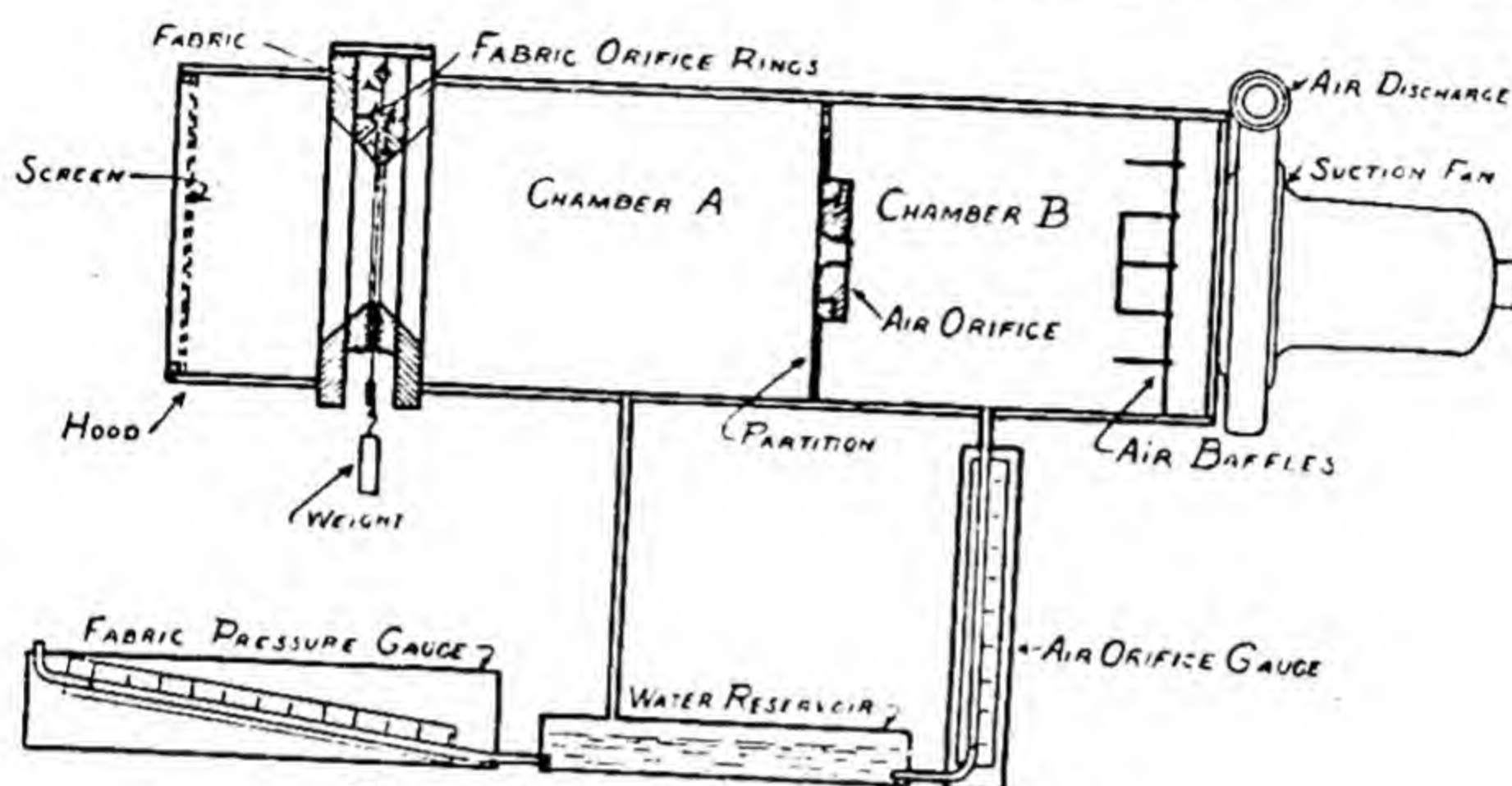
Fig. 134. Permeameter for textiles.

STRUCTURES OF MEMBRANE-FORMING SUBSTANCES

Considerable progress has been made towards understanding the chemical and physical structures of many of the polymers or condensation polymers whose permeability will be discussed. One method of attack, which has been purely chemical, has been to investigate the stages in which the polymer can be synthesised or broken down. It is found that one may have polymerisation or condensation polymerisation into chains, plates, or three-dimensional networks. The family of linear or chain polymers is a large one including

Natural and synthetic rubbers,
Certain proteins, e.g. silk, wool,
Cellulose and cellulose esters,
Fusible and soluble resins, e.g. novolaks,
Polyesters, -amides, and -anhydrides,
Polysulphides.

BD

Among platy substances one may include such naturally occurring inorganic condensation polymers as

Mica, Stilbite and heulandite,

whose structures have been considered elsewhere (Chap. III, pp. 93 and 95), and which cannot yet be synthesised. Platy polymers among organic highly polymerised substances seem to be rare, since graphite can hardly be regarded as a polymer. The three-dimensional networks include polymers and condensation polymers such as

Poly-*p*-divinyl benzene,
Styrene-*p*-divinyl benzene interpolymer,
Bakelites and similar infusible insoluble resins,
Certain urea formaldehyde resins.
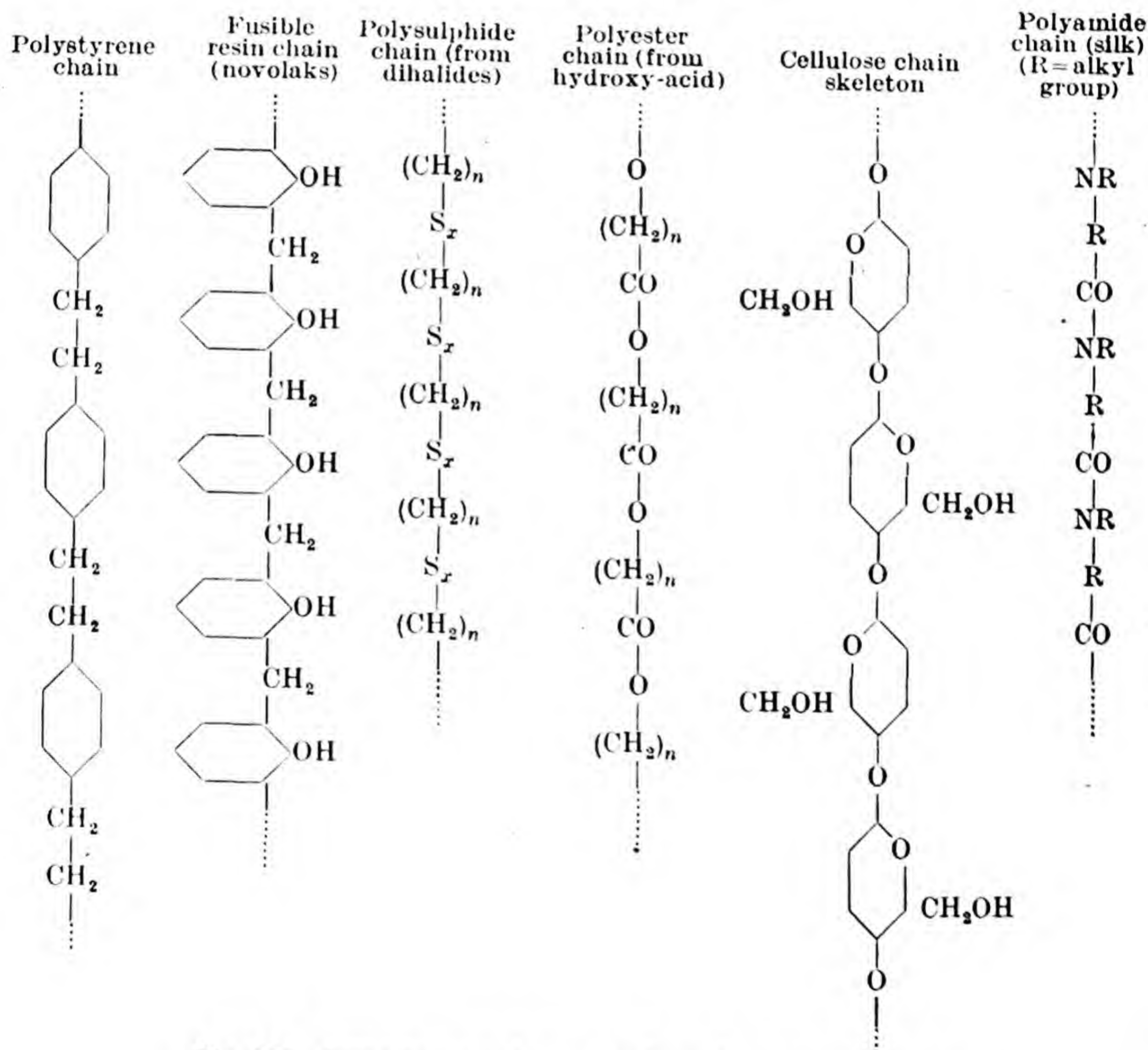
Fig. 135. Some linear polymers and condensation polymers.

In Figs. 135 and 136 are illustrated diagrammatically the manner in which certain linear and three-dimensional polymers are built up. These diagrams have of course nothing to say concerning the spatial relationships of the various chains with
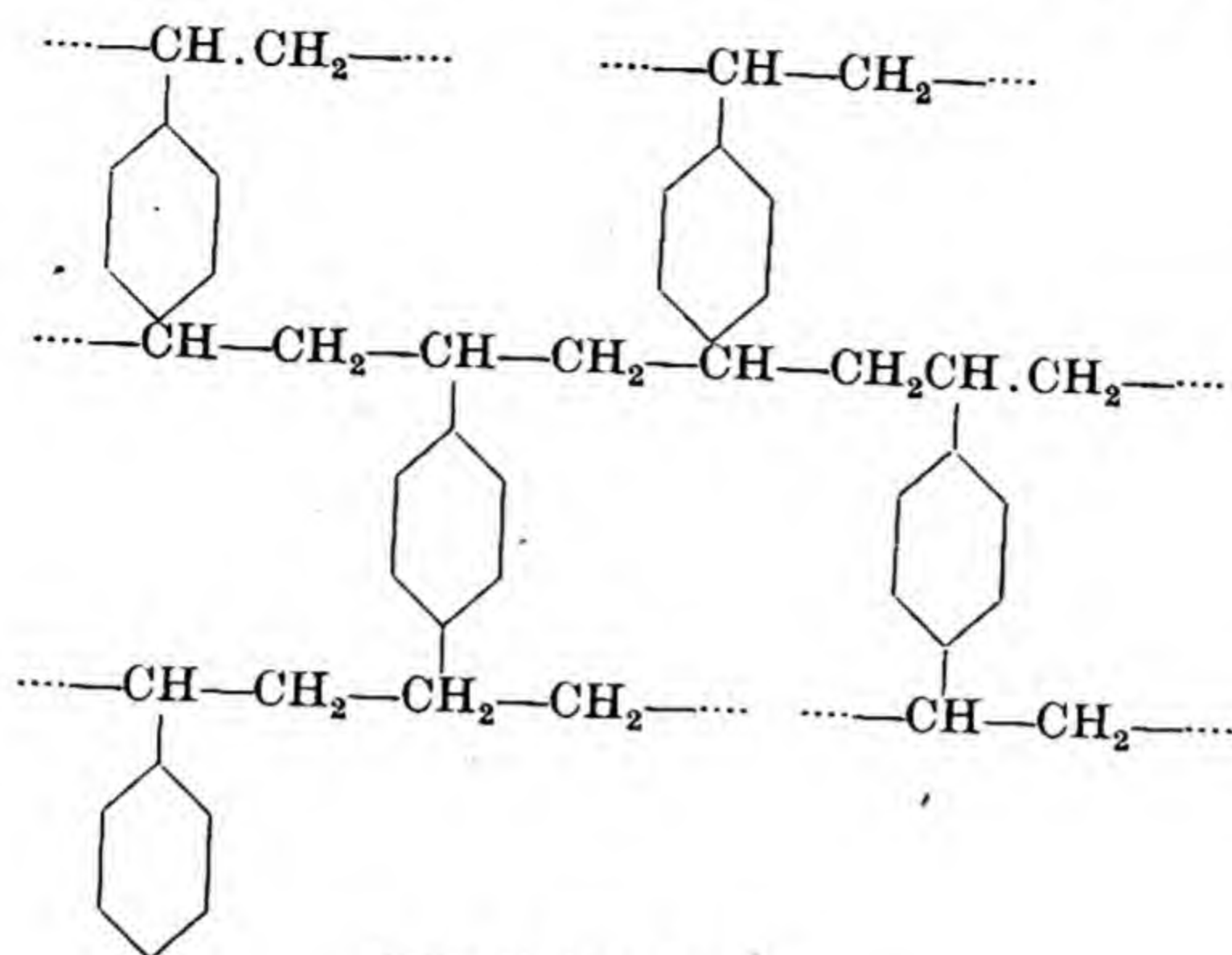
Poly-divinyl benzene
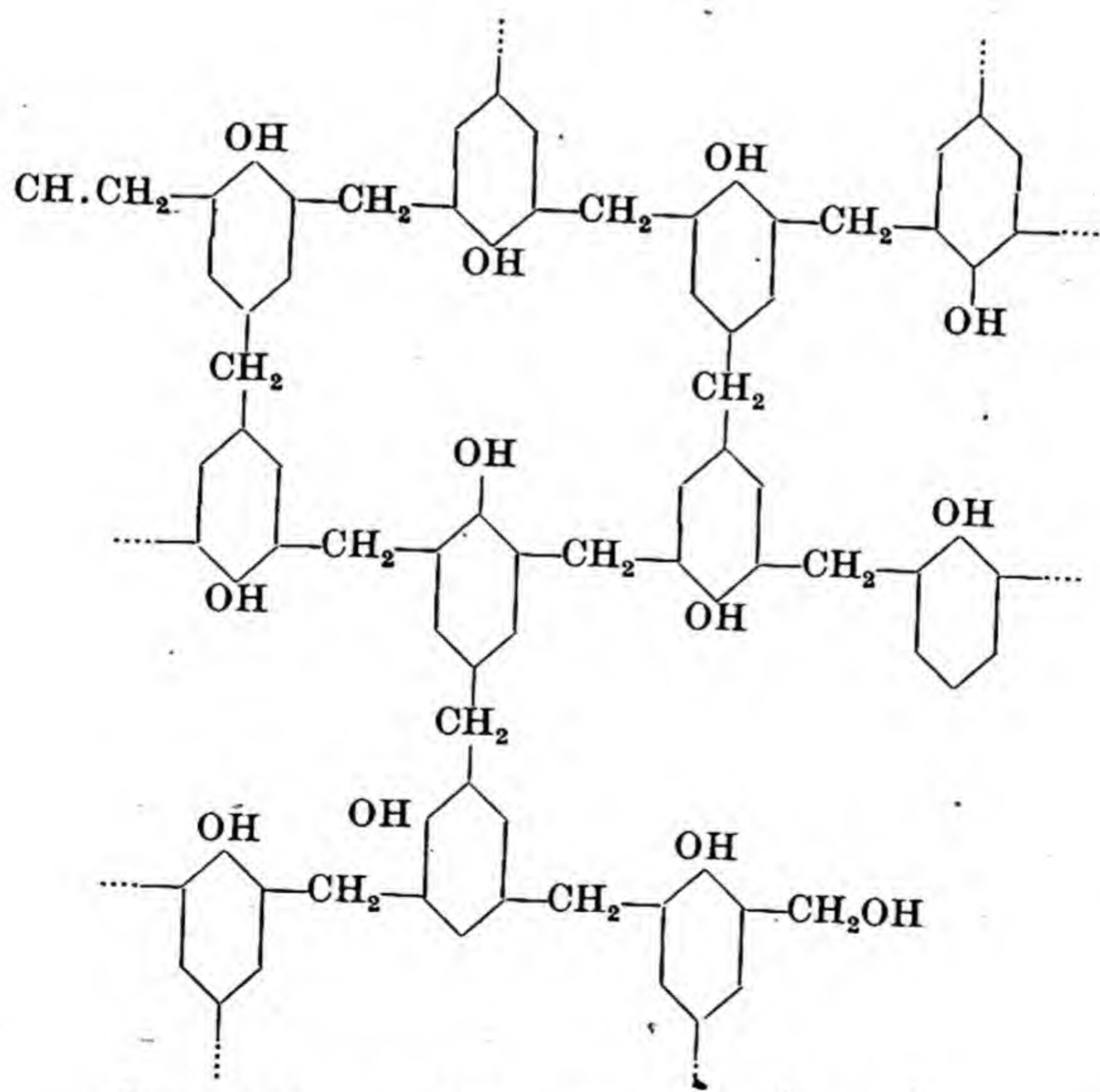
Possible structure for bakelite (infusible resin)

Fig. 136. Some three-dimensional networks.

25-2

one another, for the elucidation of which one must employ the X-ray method.

From the X-ray diffraction patterns of the polymers one can very often decide the spatial arrangement of the whole macro-molecule. The unit cell of cellulose is indicated in Fig. 137. When cellulose is nitrated (10) it is found that the glucose rings of Fig. 137 still lie in the same parallel planes and that the dimensions along the chain are nearly unaltered. Normal to the length of the chain, however, there is a big increase in the distance between the chains (in the ratio 1·7 to 1) accompanying the nitration. Similarly, when cellulose is esterified the distance between the chains grows as the aliphatic side chains become longer (11). This is reflected in a progressive lowering of the melting-point, as shown in Table 92, the interaction between chains becoming progressively less.
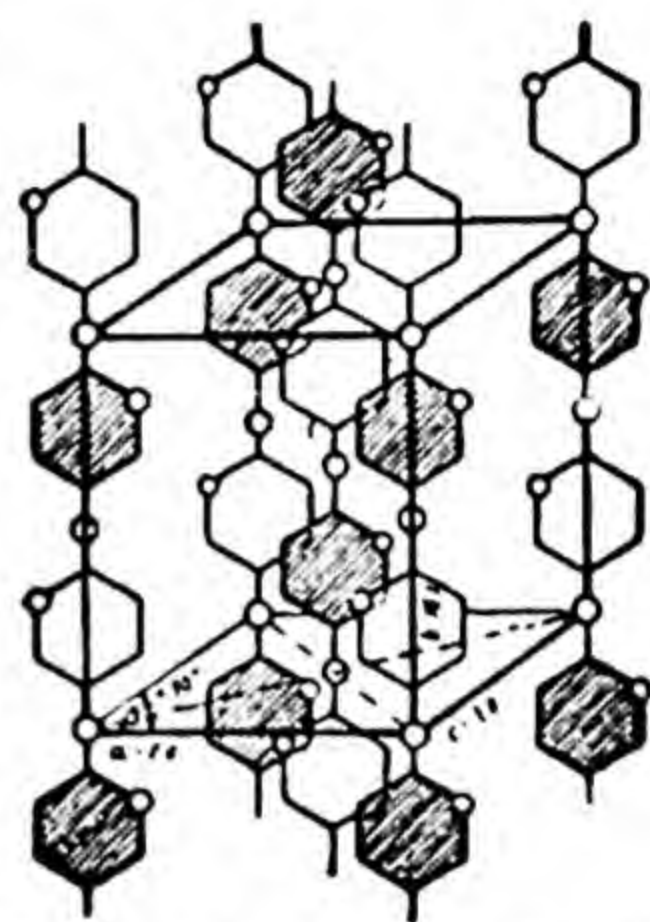
Fig. 137. The unit cell of cellulose (12).

TABLE 92. *The physical properties of some cellulose esters*

Ester	Specific weight	Melting-point (° C.) (13)	Tensile strength (14) (kg./mm.²)
Acetate	1·377	245	9–12
Propionate	1·268	239	6–7
Butyrate	1·178	183	5–6
Valerate	1·178	160	4–5
Capronate	1·110	87	2–5

The structure of certain fibrous proteins (wool and silk) has also been studied by the X-ray method, Fig. 138 giving Astbury's (15) model for part of the unit cell in wool. Usually the proteins become denatured when one attempts to dehydrate them, a fact which has prevented successful elucidation of protein structure in many instances, although in a recent study it was found that there is a great deal of crystalline order in certain highly hydrated proteins (16).

The structures of cellulose, hair, wool, and silk are plainly

fibrous ones, and the tensile strengths might be expected to be those of chemical bonds, if the chains were continuous throughout the length of the fibre. These chain strengths may be calculated (17), and it appears that the tensile strengths are not of the anticipated magnitude. This, with other evidence, leads one to the micellar view of the structure in such fibres. According to this theory, bundles of molecular threads are supposed to compose a block, and the aggregate of a number
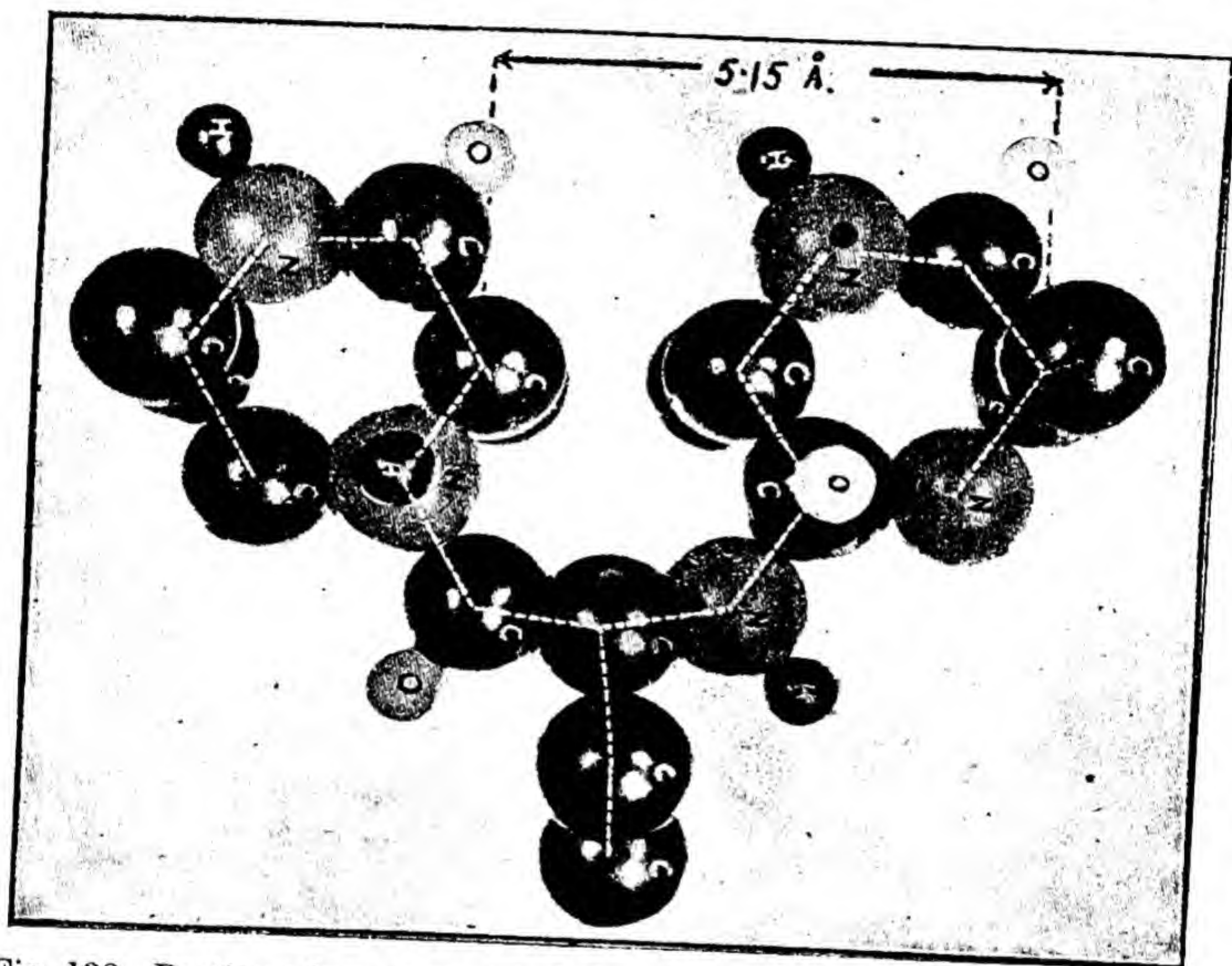
Fig. 138. Portion of space model of the structure of wool or human hair (12).

of such blocks or micelles then builds up the visible thread. The micellar theory of solids has been extended to include rubbers, most organic highly polymerised substances, and inorganic crystals. Thus one might *a priori* expect inter- and intracellular diffusion processes in organic solids analogous to grain-boundary and intracrystalline diffusion in silica glass (Chap. III, p. 125) or copper oxide (Chap. VII, p. 332). There are two types of micro-crystalline structure possible in organic polymers (18, 19, 20, 21, 22, 23) illustrated by Figs. 139 and 140.

Fig. 139 shows the discontinuous or block structure for rigid membranes such as cellulose or inorganic solids; while Fig. 140 gives a model for elastic long-chain polymers such as rubbers. The arrangement of chains is lattice-like, but the chains may be too far from or too near to neighbouring chains, and so the structure tends to be that of disorder. But in Fig. 140 ordered regions may be distinguished (marked by thicker lines), although they are not the self-contained units of Fig. 139. Stretching rubber by putting the carbon chains under tension tends to increase the degree of order by drawing them into
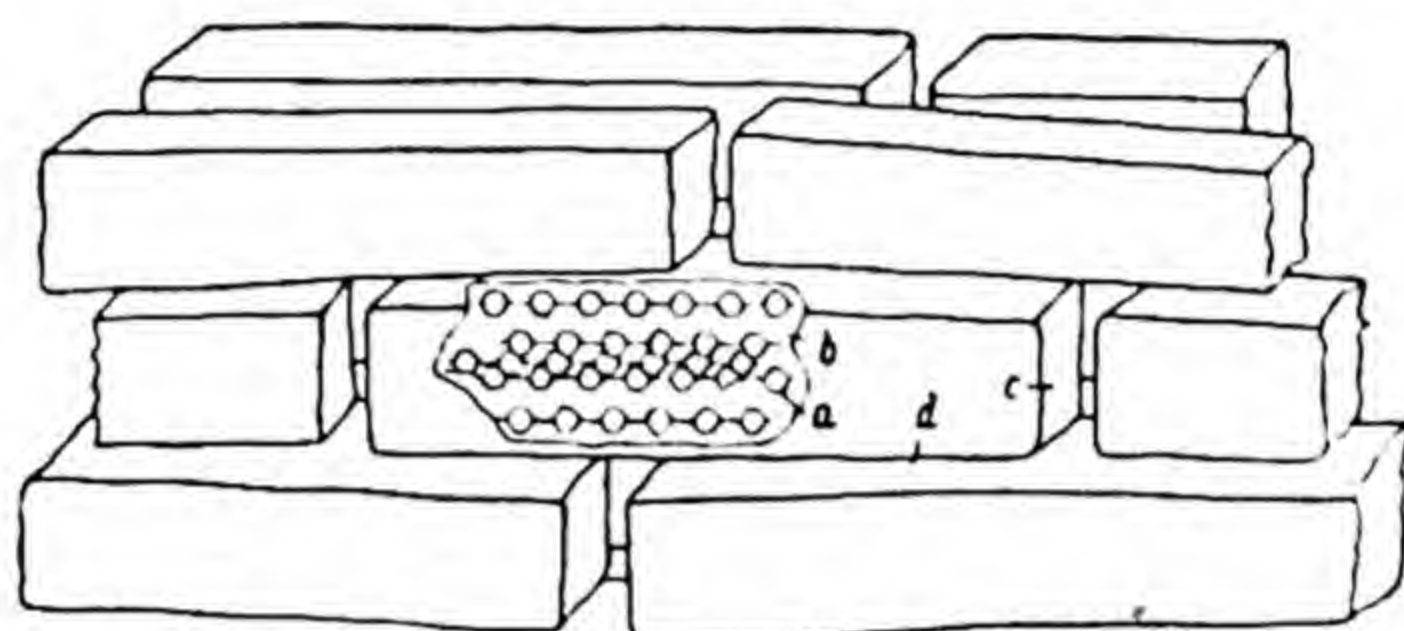
Fig. 139. Discontinuous micellar structure postulated for cellulose[23]. a, Hauptvalenzketten; b, intramicellar regions; c, intermicellar holes; d, intermicellar long spaces.

Fig. 140. Continuous micellar structure postulated for rubber[23].

alignment. The stretched rubber is then crystalline, with eight parallel isoprene residues per unit cell, although there is still some doubt as to their exact relative positions[18,24].

Staudinger[25,26,27] characterised the chain length of linear polymers by the effect upon them of suitable solvents. The characteristic behaviour was

(1) *Chain-length* 50–250 A. *Mol. wt.* ≯ 10,000. Such colloids, which dispersed easily to give true solutions, were called "hemicolloids".

(2) *Chain-length* 250–2500 A. These colloids dispersed after swelling to give highly viscous solutions. They were described as "mesocolloids".

(3) *Chain-length* > 2500 A. Polymers of this chain length dispersed only after very intense swelling to give solutions of anomalous viscosity even at great dilutions. Staudinger called these polymers "eucolloids".

The solubility may also be used to determine whether cross-linking of polymer chains to a three-dimensional network has occurred. A network cannot actually disperse, although it may undergo intense swelling. Polystyrene is a linear polymer, and therefore soluble; but when a small amount of *p*-divinyl benzene is added, the interpolymer, due to cross-linking of the polystyrene chains by *p*-divinyl benzene bridges, becomes insoluble (27).

PERMEABILITY CONSTANTS OF GROUPS A AND B OF FIG. 132

In 1866 Graham (28) studied the diffusion of gases through rubber. He regarded the permeation process as solution, diffusion and re-evaporation of the diffusing gas, a viewpoint which in essential details is held to-day. Wroblewski (29) in 1879 considered that Fick's laws of diffusion applied. This was later verified by experiment in many instances. Wroblewski also made some of the earliest measurements of the solubility of gases in rubber; and his work in this field was followed by that of Hüfner (30) and Reychler (31). Kanata (32) extended the study of membrane permeability from rubbers to celluloid and gelatin. As the importance of the permeability of leathers, balloon fabrics, packaging materials and textiles was realised, more and more studies of membrane permeability were made. The literature is so scattered in technological journals that no previous attempts have been made to give a comprehensive survey of the available data from a theoretical standpoint.

Attention has been directed in Chap. II to the possibility of defining various permeability constants. The permeability constant used in the present chapter has the dimensions

$l^3 \times t \times m^{-1}$, and denotes c.c. of gas at 1 atm. pressure and a standard temperature (293 or 273° K.) passing per second through a membrane 1 cm.^{2} in area, 1 mm. or 1 cm. thick, when the pressure difference is 1 cm. of mercury or 1 atm. When only comparative data are being considered, the original units may have been retained. The data presented in Tables 94–99 represent some of the more trustworthy of the published data, and are suitable for reference material.

TABLE 93. *The chemical nature of rubber-like membranes used in Table* 94

Name	Main constituent	Formulae of simple or polymerised molecules
Rubber (vulcanised)	Polyisoprene, cross-linked by sulphur	$CH_2{=}C{-}CH{=}CH_2$ $\vert$ CH_3
Rubber (unvulcanised)	Polyisoprene	
"Neoprene" (vulcanised commercial)	Polychloroprene, cross-linked by sulphur	$CH_2{=}C{-}CH{=}CH_2$ $\vert$ Cl
"Neoprene" (unvulcanised commercial)	Polychloroprene	"
Polychloroprene (pure)	—	"
"Vulcaplas"	Polysulphide	$\cdots\cdots{-}R{-}S{-}S{-}R{-}S$ ${-}S{-}R{-}S{-}S{-}R{-}\cdots\cdots$
Butadiene-methyl-methacrylate inter-polymer	—	$CH_2{=}C{-}CH{=}CH_2,$ $\vert$ CH_3 $CH_2{=}C{-}COOCH_3$ $\vert$ CH_3
Butadiene-acrylo-nitrile interpolymer	—	$CH_2{=}C{-}CH{=}CH_2,$ $\vert$ CH_3 $CH_2{=}CH{-}CN$
Butadiene-styrene interpolymer	—	$CH_2{=}C{-}CH{=}CH_2,$ $\vert$ CH_3 $C_6H_5{-}CH{=}CH_2$
Ethylene polymer	Ethylene	$\cdots\cdots{-}CH_2{-}CH_2{-}CH_2$ ${-}CH_2{-}CH_2{-}\cdots\cdots$

In Table 94 are given permeability constants for the rubber-like polymers of Table 93. The data summarised may be taken as typical of rubber-like membranes. There are minor variations only in permeability towards a given gas over the whole group, with the exception of the polysulphide rubbers,

which are much less permeable ($\sim$ 100-fold) than the hydro-carbon rubbers. Small amounts of cross-linking of the polymer chains by sulphur cause no appreciable changes in the permeability of neoprene or natural rubber.

The question of the effect on the permeability of cross-linking of polymer chains by sulphur or oxygen still remains uncertain. Edwards and Pickering[6] studied the influence of ageing and of vulcanisation of rubber upon its permeability, using as membranes rubber-coated balloon fabrics. It was observed:

(1) That ageing of the rubber was accompanied by a characteristic decrease in permeability, and usually by a decrease in the free sulphur.

(2) In a series of experiments where the percentage of combined sulphur varied from 0·3 to 2·5, no change in permeability was found; but in a second series where the combined sulphur varied from 1·5 to 10 % a decrease in permeability occurred. In each case the acetone extract—which gives a measure of resinification and oxidation—was about the same.

As the amount of combined sulphur is further increased, the rubber becomes dark and hard and finally forms a compound with 32 % of combined sulphur. This polymer of high sulphur content is called ebonite, and it will be seen on referring to Table 96 that the permeability of ebonite to helium is about $\frac{1}{3}$ of the permeability of rubbers; to hydrogen it is about $\frac{1}{40}$; and to nitrogen $\leqslant \frac{1}{2000}$. Thus the increased rigidity has caused the permeability to become less, and much more selective.

The impermeability[33,34] of polysulphide rubbers may be of technical importance. The permeability of polysulphide rubbers of the two following types[35] has been the subject of investigation by Sager[34]:

$$\cdots\!-\!R\!-\!S\!-\!S\!-\!R\!-\!S\!-\!S\!-\!R\!-\!\cdots$$

$$\cdots\!-\!R\!-\!\underset{\overset{\|}{S}}{S}\!-\!\underset{\overset{\|}{S}}{S}\!-\!R\!-\!\underset{\overset{\|}{S}}{S}\!-\!\underset{\overset{\|}{S}}{S}\!-\!R\!-\!\cdots$$
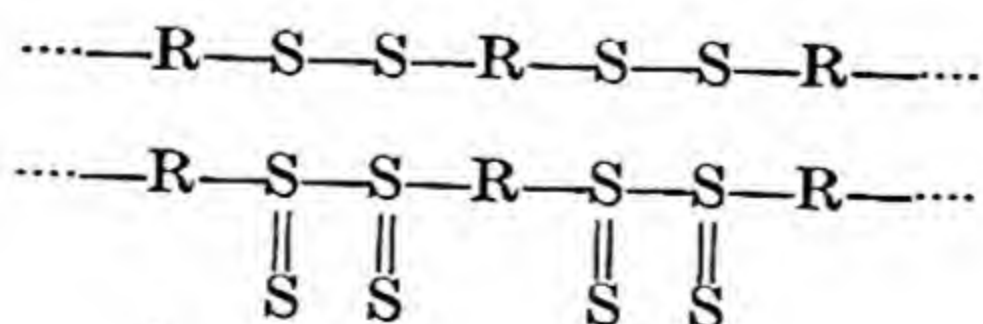
TABLE 94. *Permeability constants, P, for rubber-like polymers*[33]
(c.c. at 293° K./sec./cm.²/mm. thick/cm. Hg pressure)

System		Temp. ° C.	$P \times 10^6$
He-"neoprene" (vulcanised and with fillers)		0	0·0022
		30·4	0·0078
		41·5	0·0158
		57·0	0·035
		73·0	0·048
		101·3	0·094
He-"neoprene" (raw, unvulcanised)	I	21·6	0·0039
		37·6	0·0116
			(material softening)
	II	18·8	0·0023
		34·0	0·0055
			(material softening)
	III	0	0·0006
		18·8	0·0025
		24·6	0·0036
He-rubber (2% S, 5 min. vulcanised)		19·2	0·0051
		30·8	0·0078
		42·8	0·0116
		57·0	0·0179
		62·5	0·0195
		79·2	0·0300
He-rubber (2% S, 45 min. vulcanised)		19·5	0·0086
He-"vulcaplas"		50·0	0·000174
		59·0	0·000342
		68·5	0·00045
He-polyethylene rubber		17·0	0·0067
		22·6	0·0082
		30·8	0·0115
		38·5	0·0184
H₂-neoprene (vulcanised commercial)		17·5	0·0085
		18·2	0·0090
		26·9	0·0128
		34·6	0·0201
		44·4	0·0302
		52·0	0·0370
		63·7	0·0534
H₂-butadiene-acrylonitrile interpolymer		0	0·0032
		20·0	0·0085
		29·0	0·0128
		41·5	0·0200
		50·2	0·0315
		65·3	0·055
		78·1	0·075
H₂-butadiene-methyl-methacrylate interpolymer		20	0·023
H₂-polyethylene rubber		56	0·053
		37·2	0·021
		34·8	0·019
		22·6	0·011

TABLE 94 (*continued*)

System	Temp. °C.	$P \times 10^6$
H_2-polystyrene-butadiene polymer	I 19·9	0·0084
	II 21·0	0·0112
H_2-chloroprene polymer (pure)	31·8	0·0049
	39·7	0·0086
	41·3	0·0088
	49·9	0·0116
	58·7	0·0179
	69·5	0·0214
	73·5	0·0411
N_2-"neoprene"	27·1	0·00137
	35·4	0·0023
	44·1	0·0032
	54·1	0·0058
	65·4	0·0106
	84·7	0·0222
N_2-butadiene-acrylonitrile interpolymer	20·0	0·00061
	38·1	0·0019
	48·5	0·0029
	59·5	0·0048
	70·5	0·0070
	78·6	0·0178
N_2-butadiene-methyl-methacrylate interpolymer	21·2	0·0028
	44·6	0·0057
	54·0	0·0087
	61·9	0·0132
	77·0	0·023
N_2-polystyrene-butadiene interpolymer	20·0	0·0029
	35·5	0·0057
	50·0	0·0102
	64·2	0·0161
A-"neoprene"	36·1	0·0068
	52·2	0·0144
	61·8	0·0224
	73·7	0·0311
	86·2	0·0655
A-butadiene-methyl-methacrylate interpolymer	20·0	0·0059
	30·8	0·0111
	39·2	0·0162
	51·8	0·027
	62·3	0·0395
A-polystyrene-butadiene polymer	I 19·5	0·0109
	30·3	0·0195
	40·7	0·0287
	51·2	0·041
	64·6	0·074
	II 64·0	0·036

Sager found that the rubber with four sulphur atoms per primary molecule was the less permeable of the two, but in agreement with Table 94 both were much less permeable than polyisoprene rubber (Table 95). Barrer[35a] extended his work on rubber-like polymers to rigid or inelastic membranes of

TABLE 95. *Hydrogen permeability of polysulphide* and polyisoprene rubbers at room temperature*

(*P* in c.c. at N.T.P./cm.^{2}/mm. thick/cm. Hg pressure)

P (polyisoprene rubber) $\times 10^7$	P (for polydisulphide rubber) $\times 10^7$	P (for polytetrasulphide rubber) $\times 10^7$
Sample 1 0·46	Sample 1 0·028	Sample 1 0·010
Sample 2 0·53	Sample 2 0·031	Sample 2 0·015
Sample 3 0·54	Sample 3 0·041	Sample 3 0·018
	Sample 4 0·034	Sample 4 0·020
	Sample 5 0·033	Sample 5 0·017

bakelite, ebonite and cellophane (Table 96). For these membranes the permeability is considerably smaller than that of elastic membranes, with the exception of vulcaplas or polyethylene sulphide rubbers. This result is true for rigid membranes of inorganic (SiO_2, B_2O_3, glass) as well as of organic substances (Table 97). Not only are rigid membranes usually less permeable, but they are also more selective in preventing the diffusion of inert gases of high molecular weight (N_2, O_2, A), while allowing light gases (He, H_2, Ne) to diffuse (Chap. III).

Sager[36] measured the hydrogen permeability of a large number of film-forming substances supported on a closely woven cotton fabric. The membranes included

Inelastic:

Regenerated cellulose

Polyvinyl alcohol
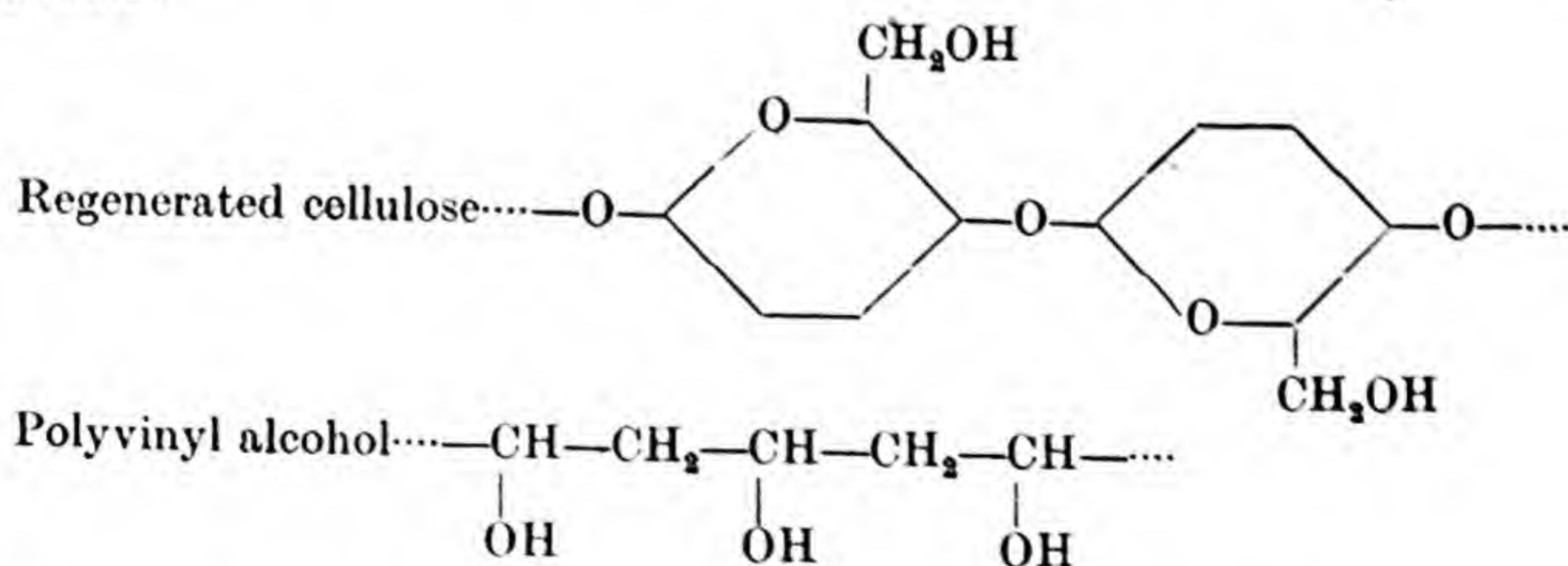
* Prepared from 2, 2′-dichlorethyl sulphide and sodium polysulphide.

'Cellulose esters····—O—⟨ring with CH$_2$OR⟩—O—⟨ring⟩—O—····

Polyvinyl alcohol acetate····—CH—CH$_2$—CH—CH$_2$—CH——····
　　　　　　　　　　　　O.CO.CH$_3$　O.CO.CH$_3$　O.CO.CH$_3$

Polyvinyl acetal····—CH—CH$_2$—CH—CH$_2$—CH—CH$_2$—CH—····
　　　　　　　　　O—C$_2$H$_4$—O　　　　O—C$_2$H$_4$—O

Polyhydric alcohol-polybasic acid resin
　　HO.OC—R—CO—OCH$_2$—CH$_2$—O—CO—R—COOCH$_2$-CH$_2$—····

Elastic:

Polychloroprene rubber (Table 93)
Polyethylene sulphide rubber····—(CH$_2$)S$_X$(CH$_2$)$_2$S$_X$(CH$_2$)$_2$S$_X$——····
Polyisoprene rubber (Table 93)

TABLE 96. *The permeability, P, of organic membranes of various kinds to gases*

System	Temp. ° C.	$P \times 10^6$ c.c. at 293° K./sec./cm.^{2}/ mm. thick/cm. Hg
H$_2$-bakelite	75·5	0·00052
	57·0	0·00035
	45·0	0·00026
	34·2	0·000164
	20·0	0·000095
N$_2$-bakelite	75·0	0·00027
	56·6	0·000115
	47·2	0·000083
	37·5	0·000048
	36·1	0·000047
	20·0	0·0000095
	18·0	0·0000085
He-ebonite	82·5	0·0072
	67·0	0·0047
	54·5	0·00305
	43·7	0·00255
	17·0	0·00105
H$_2$-ebonite	83·0	0·00192
	67·0	0·00141
	49·0	0·00091
	34·0	0·00045
N$_2$-ebonite	67·2	0·000025
He-cellophane	85·0	0·00050
	74·0	0·00035
	52·5	0·00012

Table 31. Hydrogen permeabilities of film-forming materials (after Sager[36])

Material	Solvent	$10^6 \times$ permeation rate (c.c./cm.²/sec./atm. at 25° C.)	Weight (g./cm.²)	$10^7 \times$ permeability const. $P \times$ density D (P in c.c. at N.T.P./cm.²/sec./cm. thick/atm. at 25° C.)
Regenerated cellulose sheet (cellophane)				
Polyvinyl alcohol	Water	0·12	0·0051	0·0059
Polyvinyl alcohol	Water	0·12	0·0068	0·0079
Polyvinyl acetal	Ethanol	0·23	0·0064	0·015
Polyvinyl acetal	Ethanol	0·81	0·0098	0·030
Polyvinyl acetal	Ethanol	0·46	0·0088	0·041
Polyhydric alcohol-polybasic acid resins:				
Ethylene glycol citrate	Ethanol	0·12	0·0109	0·0126
Diethylene glycol citrate	Ethanol	0·12	0·0119	0·0138
Glycerol phthalate		0·23	0·0122	0·028
Ethylene glycol phthalate		0·35	0·0125	0·044
Diethylene glycol phthalate	Ethyl acetate (10%) and acetone (90%)	0·58	0·0105	0·061
Glycerol succinate		1·16	0·0081	0·094
Diethylene glycol succinate		1·04	0·0109	0·114
Glycerol sebacate		1·28	0·0112	0·143
Diethylene glycol sebacate		1·86	0·0102	0·190
Polyvinyl cellulose esters:				
Polyvinyl acetate (high viscosity)	Ethanol	5·5	0·0092	0·51
Polyvinyl acetate (high viscosity)	Ethanol	3·6	0·0098	0·35
Polyvinyl acetate (low viscosity)	Ethanol	11·6	0·0095	1·10
Polyvinyl acetate (low viscosity)	Ethanol	15·1	0·0098	1·48
Cellulose nitrate	Mixture 2	8·6	0·0122	1·05
Cellulose nitrate	Mixture 2	11·0	0·0112	1·22
Cellulose acetate	Mixture 1	17·4	0·0078	1·36
Cellulose acetate	Mixture 1	24·4	0·0061	1·49
Cellulose acetostearate	Benzol	19·7	0·0092	1·81
Rubber substitutes:				
Polyethylene sulphide (Thiokol A)		0·23	0·0322	0·074
Polyethylene sulphide (Thiokol A)		0·58	0·0176	0·101
Polychloroprene (Duprene)	Toluol	6·85	0·0122	0·84
Ether-soluble rubber		10·8	0·0095	1·03
Smoked sheet rubber		22	0·0067	1·47
Smoked sheet rubber		25·6	0·0057	1·46

Solvent mixture 1: ethylene dichloride 60%, ethyl alcohol 10%, methyl cellosolve 10%, cellosolve acetate 5%, ethyl acetate 15%.
Solvent mixture 2: toluol 20%, ethyl alcohol 60%, ethyl acetate 10%, cellosolve 10%.

Sager's data do not give a strict comparison or measure of the permeabilities, since it was not possible to obtain films of identical thickness, nor were the actual thicknesses stated. The permeation rate defined as c.c./cm.^{2}/sec./atm. at 25° C. is not an absolute measure of permeability. If, however, one uses the quantity

Permeation rate × weight of film per unit area,

one has a good approximation to comparable and absolute data, since variations in density are less important. The true permeability constant P (in c.c. at N.T.P./cm.^{2}/sec./cm, thick/atm. at 25° C.) is given by the relation

$$P = \frac{\text{Permeation rate} \times \text{weight of film in g. per sq. cm.}}{\text{Density of film (g. per unit volume)}}.$$

It will then be remembered that the units of Tables 94 and 97 are different (cm. thickness for mm. thickness, and atm. for cm. pressure), and that the constant P of Table 94 must be multiplied by 7·6 to compare with the constant P of Table 97. The second column of the table gives the solvent used in forming the film on the cotton weave support.

Sager [36] considered that the data showed that permeability was governed by the chemical nature of the films. The films included crystalline, fibrous and amorphous substances, and the degree of polymerisation varied over a wide range, but no simple connection could be observed between permeability and crystalline structure or degree of polymerisation. This aspect of the permeability requires examination of a limited number of chemically different film types and a controlled degree of polymerisation. There is, however, a general correspondence between the hydrogen permeability in a given chemical type, and the hydrogen solubility in analogous unpolymerised molecules. The permeability of materials rich in hydroxyl groups (cellophane, cellulose, polyvinyl alcohol, and hygroscopic resins) is very low, corresponding to the small solubility of hydrogen in glycerol or water. As soon as ester groups are introduced (polyvinyl and cellulose esters), the

permeability towards hydrogen increases, to parallel the higher solubility of hydrogen in esters. Similarly, the hydrogen solubility in liquid hydrocarbons is considerable and so one finds a large permeability of rubber to hydrogen. Hydrogen is very sparingly soluble in carbon disulphide; therefore it should diffuse with difficulty through polysulphide rubbers. This analogy should not be carried too far, since the permeability is conditioned both by the solubility of the gas and by its diffusion constant within the polymer.

De Boer and Fast (37) studied the hydrogen permeability of a number of derivatives of cellulose. The permeability constants at 0° C. (c.c. at N.T.P./sec./cm.²/mm. thick/cm. Hg) were:

Regenerated cellulose	$P \times 10^7 = 0.000047$
Triacetyl cellulose	$P \times 10^7 = 0.0140$
Nitro-cellulose	$P \times 10^7 = 0.0092$
Celluloid	$P \times 10^7 = 0.0164$

These permeability constants are consistent with those in Table 97, and emphasise again the small permeability of cellulose and its derivatives. From the data of Table 98 one may construct a table showing the range of permeabilities to hydrogen of different chemical types of polymer.

TABLE 98. *Range in relative permeability in various polymers*

Type of substance	Relative permeability towards hydrogen at 20° C.
Rubbers (natural and synthetic)	1.0–0.6
Polyvinyl and cellulose esters	1.8–0.2
Polyhydric alcohol-polybasic acid resins	$(1.9–1.3) \times 10^{-1}$
Polysulphide resins (Thiokol A)	$(1.0–0.7) \times 10^{-1}$
Polysulphide rubbers	$(6.3–3.1) \times 10^{-2}$
Cellophane, polyvinyl alcohol and acetal, and regenerated cellulose	$(8.0–0.05) \times 10^{-2}$

There is a 10^3-fold variation among the permeability constants, the rubbers being among the most permeable of the membranes.

TABLE 99. *Relative permeabilities of membranes*(33) (*hydrogen permeability as standard*)

Membrane	Gas							
	H_2	He	Ar	N_2	O_2	CO	CO_2	NH_3
Rubber (vulcanised), 25° C.	1·00	0·62	—	0·16	0·44	—	2·88	8·00
Rubber (unvulcanised), 20° C.	1·00	0·30	0·19	0·11	0·35	0·16	2·50	—
"Neoprene" (vulcanised), 20° C.	1·00	0·61	0·29	0·10	—	—	—	—
Chloroprene polymer, 20° C.	1·00	0·22	—	—	—	—	—	—
Butadiene-acrylonitrile interpolymer, 20° C.	1·00	—	—	0·08	—	—	—	—
Butadiene-methyl-methacrylate interpolymer, 20° C.	1·00	—	0·26	0·11	—	—	—	—
Butadiene-polystyrene interpolymer, 20° C.	1·00	—	0·95	0·27	—	—	—	—
Ethylene polymer, 20° C.	1·00	0·75	—	—	—	—	—	—
Polysulphide rubbers (at room temperature): "Vulcaplas"	—	0·0026	—	—	—	—	—	—
Sager's disulphide polymer	0·066	—	—	—	—	—	—	—
Sager's tetrasulphide polymer	0·033	—	—	—	—	—	—	—

(*P* for H_2-neoprene as standard)
(Sager's value of P_{H_2}-rubber as standard)

Another interesting comparison can be made by considering the relative permeabilities in a given membrane of a series of gases. The relative permeation velocities bear no simple relation to the molecular weights of the diffusing gases. The ratio of the permeation velocities (6, 28, 38, 2) for CO_2 and H_2 prove to be almost independent of the sample of polyisoprene rubber employed, since for nine samples the average ratio of P_{CO_2}/P_{H_2} was 2·76, and the extreme variations were from 3·03 to 2·48. The permeation rate ratios for each of a series of gases in rubbers of different chemical types are found to show minor variations only (Table 99).

TABLE 100. *Relative permeation velocities in membranes*
(O_2 as standard)

Gas	Membrane		
	Celluloid	Rubber	Gelatin
H_2	2·47	2·86	1·00
O_2	1·00	1·00	1·00
CO_2	8·98	9·06	4·13
SO_2	—	25·0	31·9
NH_3	61·6	36·0	95·2

The same absence of any connection of relative velocities with molecular weights (as required in effusion or molecular streaming) is found when gases diffuse through widely differing membranes such as celluloid, rubber and gelatin (32) (Table 100). Once more rather striking regularities in relative velocities are revealed, although irregularities and specific effects are beginning to creep in.

The variables in permeation through membranes
of groups A and B

The pressure, area of membrane, thickness of membrane, and the temperature are the possible variables in the permeation kinetics. If (as is shown later, p. 413) Henry's law, $S = kp$, applies to the solubility S of gas in the polymer substance, and the Fick law $\dfrac{\partial C}{\partial t} = D \dfrac{\partial^2 C}{\partial x^2}$ applies to the diffusion process,

within the material, in the steady state of flow, one would find that the permeation rate was proportional to the pressure difference, the area of the membrane, and inversely to the thickness of the membrane.

The pressure difference

In the steady state the velocity of diffusion for a given constituent of a gas mixture is proportional to the difference in pressure of that constituent between the ingoing and outgoing
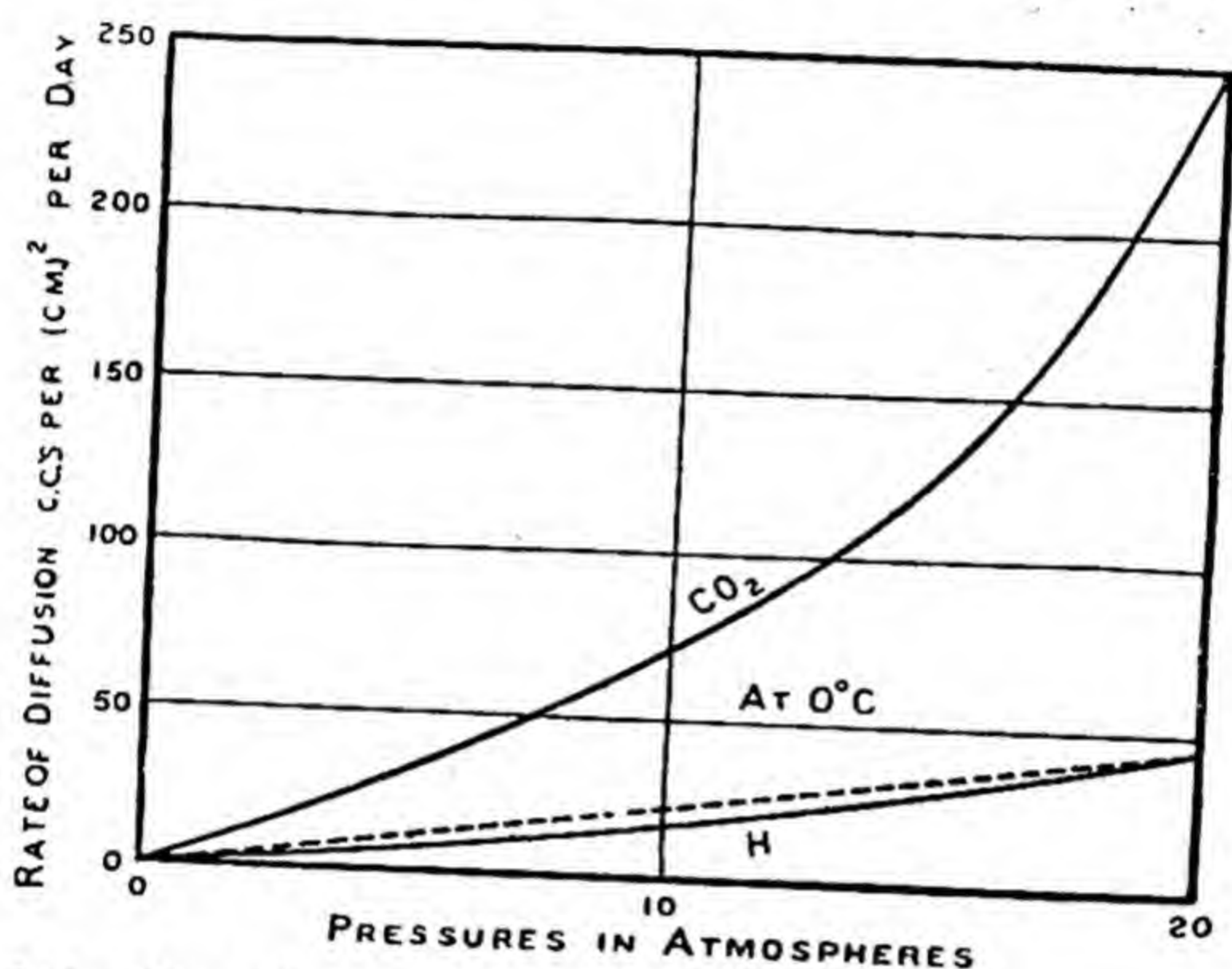
Fig. 141. The effect of high pressure upon permeation rates.

surfaces of the membrane [33, 37, 6, 39, 40]. This law holds for pressures which are not too great [2], and is a characteristic of non-specific types of activated diffusion (see Chap. III). The velocity of diffusion is the same when hydrogen diffuses into a vacuum or into an atmosphere of air [41]. Similarly, when a mixture of oxygen and nitrogen diffuses into hydrogen, the rate of permeation of each gas is practically unaltered by the presence of the other gases [41]. At high partial pressure differences [2] (up to many atmospheres) the rates of diffusion through pure rubber both for hydrogen and carbon dioxide increased with pressure, the increases being shown in Fig. 141. The departure from linearity does not appear, in the case of hydrogen at any rate, to be due to breakdown of the perfect

26-2

gas laws at these pressures, since Wüstner (see Chap. III) found linear permeation rate-pressure curves for hydrogen and silica up to 800 atm. Rather the effect might be ascribed to an influence of pressure upon the membrane itself (compression or distension) and suggests that deformation can modify permeabilities.
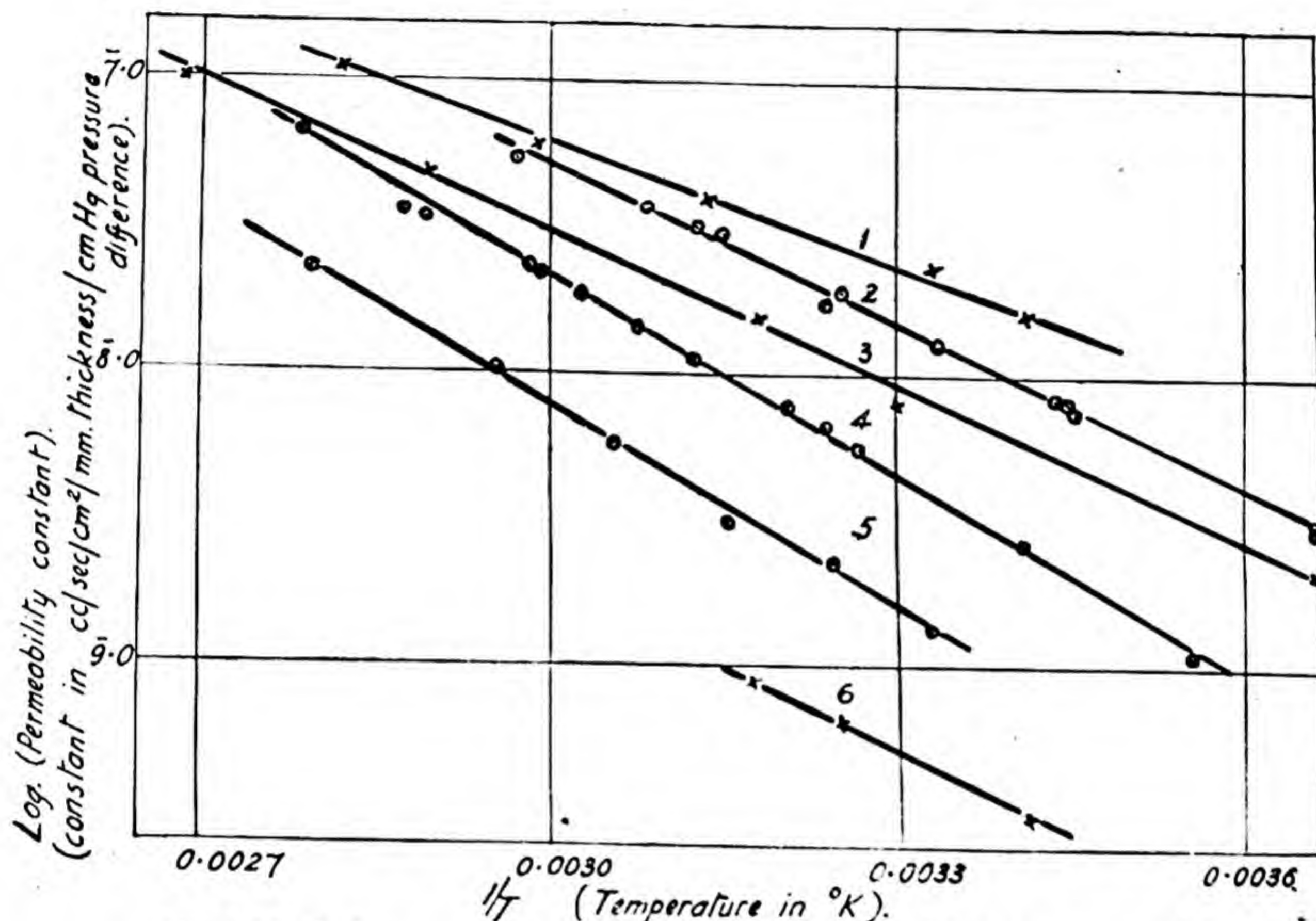
Fig. 142. Influence of temperature upon the permeability constants of elastic polymer-gas systems.

Curve 1. He-vulcanised rubber
Curve 2. H₂-vulcanised neoprene.
Curve 3. He-vulcanised neoprene.
Curve 4. Argon-vulcanised neoprene.
Curve 5. N₂-vulcanised neoprene.
Curve 6. He-vulcaplas (polysulphide rubber).

The thickness of the membrane

In the steady state of diffusion the velocity of diffusion is inversely proportional to the thickness of the membrane. This is shown by the results of Edwards and Pickering (6) who allowed hydrogen to diffuse through rubber membranes of varying thickness, and plotted the reciprocal of the per-

meability (called the impedance) against the thickness. Their graph was linear.

The influence of temperature

The most interesting relationships were revealed by the study of the influence of temperature on the permeation rate. It was found by Shakespear[40] that the temperature coefficient of the permeation rate was the same for all differences in
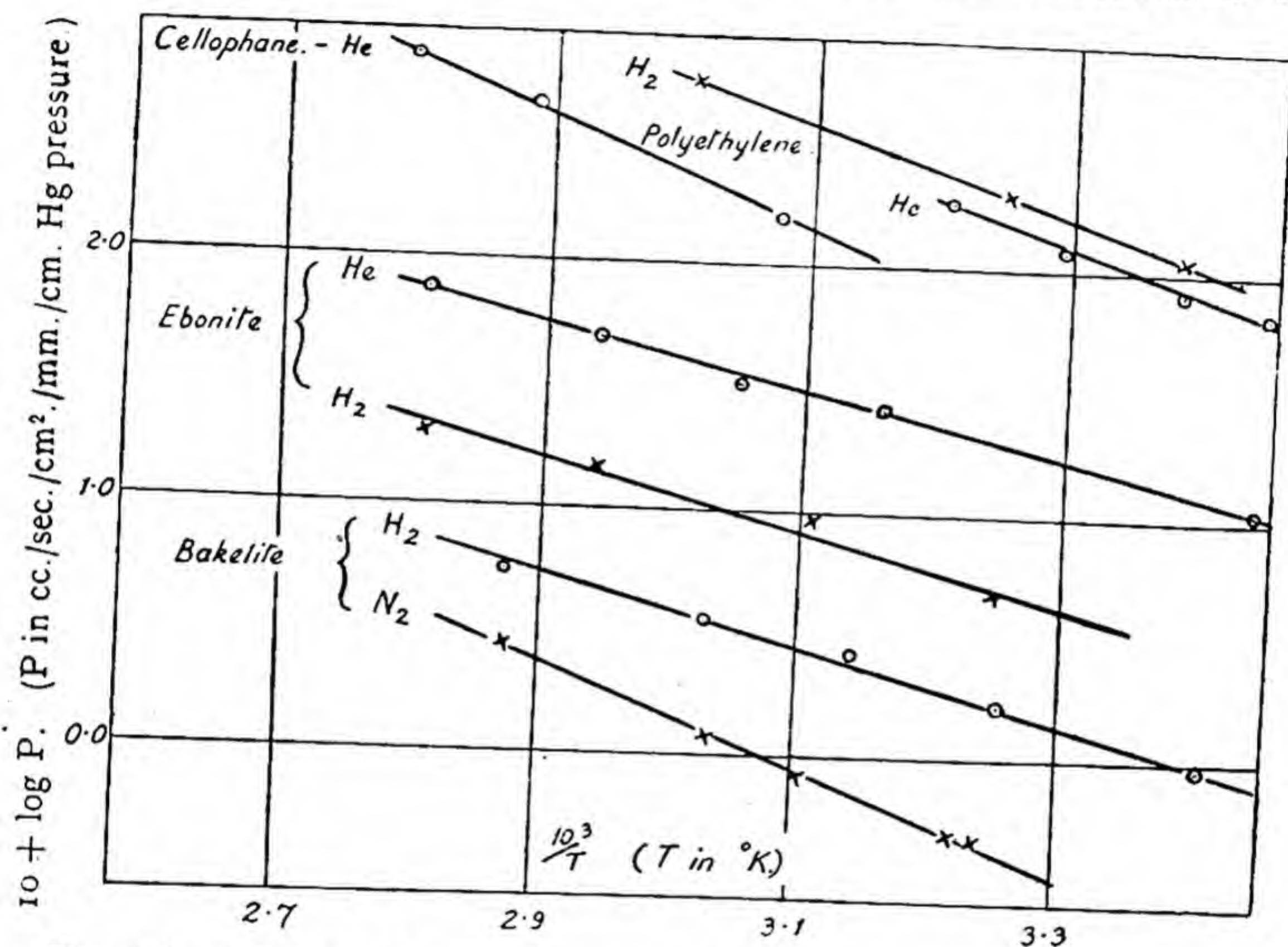
Fig. 143. Influence of temperature upon the permeability constants of inelastic polymer-gas systems.

partial pressure, and all thicknesses of membrane. Graham[28] long ago showed that the temperature coefficient was abnormally large. This is also clear from the data of Edwards and Pickering[6], Taylor, Herrmann and Kemp[42], and Dewar[2].

It may be shown that the permeabilities conform to the equation

$$P = P_0 e^{-E/RT},$$

a relationship first pointed out by Barrer[43]. The exponential temperature coefficient is shown in Figs. 142 and 143[33, 43],

for elastic and for inelastic membranes. The temperature coefficients of the permeability constant in cal./mol. of gas are collected in Table 101. It is interesting to find that these coefficients are not very different for the impermeable inelastic membranes and the permeable elastic membranes. The main differences in the permeability must therefore come from the temperature independent factor, P_0, in the equation

$$P = P_0 e^{-E/RT}.$$

As Table 101 shows, P_0 is very much smaller for cellulose and its derivatives than for elastic polymers. The difference in P_0 for rubbers and for cellulose must be due partly to the larger solubility of hydrogen in rubber. It is then possible that in cellulose, because of the low solubility, diffusion is predominantly of grain-boundary type, while in rubber it can occur readily inside the micelles composing the colloid.

THE AIR PERMEABILITY OF GROUP C OF FIG. 132

Previously we have considered coherent membranes without pin-holes or capillary channels. Most papers, fibreboards, and leathers have capillaries down which streamline (44) or Knudsen (45, 46) flow may occur, or pin-holes which may act as orifices for orifice flow (47) or effusion (48) (Chap. II). Stream-line flow conforms to the equation

$$v_1 p_1 = v_2 p_2 = \frac{\pi r^4}{16 l \eta} (p_1^2 - p_2^2) = \frac{k}{\eta} \Delta p \frac{2 p_1 - \Delta p}{2},$$

where v_1 = the volume flowing per unit time into the tube at pressure p_1,

v_2 = the volume flowing per unit time into the tube at pressure p_2,

$\Delta p = p_1 - p_2$,

η = the viscosity of the gas,

l = the length of the pore, of radius r.

TABLE 101. *Temperature coefficients, E, of permeability constants (33, 35a) in cal./mol.*

	E (cal./mol.)							
	He	H_2	N_2	Ar	O_2	CO	CO_2	H_2O
Elastic membrane:								
Rubber (vulcanised)	6,300, 6,400	6000, 6500	—	—	—	—	7600	2800
Rubber (unvulcanised)	7,800	9500	—	—	—	—	—	—
"Neoprene" (vulcanised)	8,800	8300	10,500	10,700	8200	9500	9600	—
Butadiene-acrylonitrile inter-polymer	—	8200	9,800	—	—	—	—	—
Butadiene-methyl-methacrylate interpolymer	—	—	—	—	—	—	—	—
Butadiene-polystyrene inter-polymer	—	—	9,500	8,850	—	—	—	—
Chloroprene polymer	—	8300	—	—	—	—	—	—
Ethylene polymer	7,700	8050	7,900	7,900	—	—	—	—
Inelastic membrane:								
Bakelite	—	5100	—	—	—	—	—	—
Ebonite	5,900	6500	10,500	—	—	—	—	—
Cellophane	10,100	—	—	—	—	—	—	—
Celluloid	—	5600	—	—	—	—	—	—
Nitrocellulose	—	5700	—	—	—	—	—	—
Triacetyl cellulose	—	7500	—	—	—	—	—	—
Regenerated cellulose	—	7600	—	—	—	—	—	—

H_2-celluloid: $P_0 = 4.4 \times 10^{-5}$.

H_2-nitrocellulose: $P_0 = 3.2 \times 10^{-5}$.

H_2-triacetyl cellulose: $P_0 = 142 \times 10^{-5}$.

H_2-regenerated cellulose: $P_0 = 0.59 \times 10^{-5}$.

H_2-neoprene: $P_0 = 2240 \times 10^{-5}$.

H_2-butadiene acrylonitrile interpolymer: $P_0 = 1020 \times 10^{-5}$.

For orifice flow to occur the capillary must be short enough to act as a jet or nozzle. Under these conditions the equation of flow becomes

$$\frac{v_1}{\Delta p} = \text{constant} \sqrt{T} \frac{\sqrt{\left(\frac{p_1 - \Delta p}{p_1}\right)^{10/7} - \left(\frac{p_1 - \Delta p}{p_1}\right)^{12/7}}}{\Delta p}.$$

The constant depends upon the area of the nozzle, and not its length.

The properties of streamline and orifice flow are summarised in Table 102 (49), and can easily be verified by reference to the equations of flow. The very complete series of experiments by

TABLE 102. *Characteristics of high-pressure gas flows*

Poiseuille capillary flow	Orifice flow
$v/\Delta p$ is constant for low values of Δp	$v/\Delta p$ decreases as Δp increases.
$v/\Delta p$ is proportional to the reciprocal of length (or membrane thickness)	$v/\Delta p$ is independent of the length (or membrane thickness)
The rate of flow decreases slightly as the temperature increases, because the viscosity of the gas increases as T increases	The rate of flow increases slowly with temperature
v, for small constant values of Δp, is independent of p_1	v, for constant values of Δp, increases slowly as p_1 decreases

Carson (49) has tested these features for numerous papers. For the thinnest tissues the behaviour with respect to Δp suggested that flow might be intermediate between streamline and orifice flow. Within the uncertainties of using different samples an inverse proportionality existed between the permeation velocity and the thickness, while a small change in temperature had a negligible influence upon the rate of flow. The results are on the whole more in conformity with Poiseuille flow than with orifice flow. The effect of altering the absolute pressure p_1, for a constant Δp, however, was not in accord with either theory, and was attributed by the author to elastic deformations of the membrane under pressure. In addition, an approximate proportionality between area and diffusion

rate was observed, and it was shown that the relative humidity of the air bore no simple relationship to the permeation velocity. In order for Poiseuille flow to occur in these membranes, the length of the capillaries must be much greater than their diameter. It is therefore probable that the actual thickness of the membranes is less than the length of the capillaries.

In Table 103 Carson's [49] data have been converted to absolute permeabilities, and show the range of permeability constants covered by the paper section of group C of Fig. 132.

TABLE 103. *The air permeabilities of some membranes*

Kind of material	Permeability c.c./sec./cm.^{2}/cm. Hg/mm. thickness
Insulating board	36·5
Filter paper	3·51
Blotting paper	1·51
Newsprint paper	0·047
Antique book board	0·0298
Lined strawboard	0·0177
Supercalendered book paper	0·0059
Tagboard	0·0102
Bond paper	0·00141
Railroad board	0·00116
Solid binders board	0·000465
Press board	0·0000714
Vegetable parchment	0·0000018

It is necessary to add that other types of flow than that of Poiseuille (e.g. molecular streaming, or even activated diffusion) may be occurring in the case of the least permeable membranes cited. The sorting out of flow processes is not yet at all complete.

Leathers

The air permeability of leather shows the same wide variations that were observed for papers and fibreboards, and some of the associated phenomena have been ascribed to Poiseuille flow [50, 51]. The leather may be regarded as a network of capillaries joining larger cavities within the material. These cavities and capillaries are not constant in size. Thus while in

TABLE 104

A. Sole leathers

Type of leather	Thickness cm.	Permeability × 10² c.c./sec./cm.²/mm. thick/cm. Hg	
		G* → F	F → G
English bend	0·608	9·10	7·30
	0·438	5·76	5·40
	0·490	7·40	7·80
	0·420	4·65	4·74
	0·390	4·06	3·29
Waterproofed English bend	0·536	4·76	5·34
	0·415	1·63	1·50
French bend	0·350	4·42	4·14
	0·370	1·42	1·32
	0·420	1·97	2·21
	0·382	1·85	1·85
	0·624	3·94	4·08

B. Upper leathers

Type of leather	Thickness cm.	G* → F	F → G
Box calf	0·140	15·7	11·1
	0·130	14·2	7·55
	0·120	20·7	17·65
Gorse calf	0·195	13·0	6·04
	0·160	11·0	6·00
	0·210	28·2	24·60
Willow calf	0·095	7·0	2·95
	0·130	28·3	22·6
	0·130	15·9	8·52
Glacé kid	0·060	0·734	0·360
	0·070	1·78	1·24
	0·050	1·22	0·60
Heavy chrome tanned upper	0·312	4·05	2·47
	0·310	2·78	0·485
	0·280	1·21	0·422
	0·320	7·42	4·36
Heavy vegetable tanned upper (stuffed)	0·240	0·0128	0·00413
	0·252	0·0176	0·0176
	0·240	0·00428	0·00418
	0·230	0·00845	0·0128
Russia calf (vegetable tanned)	0·220	59·5	62·5
	0·160	37·9	38·5
	0·180	62·8	65·1
Patent leather	0·125	0	0
	0·090	0	0
	0·120	0	0

* G denotes "grain side"; F denotes "flesh side."

certain cases the rate of flow through the leather was proportional to the pressure difference (51), in others the constant of proportionality changed with pressure, or with the treatment given the membrane (50). Sometimes the rate of flow from the flesh to the grain side is different from that in the converse direction (52) (see Table 104).

In Table 104 are given some absolute permeabilities for a number of leathers, calculated from data given by Edwards (50).

Bergmann and Ludewig's (51) figures for sole leather agree, when converted to similar units, with those found by Edwards in range and order of magnitude. Wilson and Lines (53) made a study of the air and water permeability of leather in which they found a parallelism between these permeabilities when the leather contained neatsfoot oil, or was finished with collodion or casein.

Membranes in series

When the leather membranes are placed in contact (51), and the permeabilities of the separate membranes are P_1 and P_2, it was found that the resultant permeability, P, was within 6 % given by

$$\frac{1}{P} = \frac{1}{P_1} + \frac{1}{P_2}.$$

The reciprocal of the permeability is called the impedance, so that the above expression means that the impedance is additive. The same property has been observed for gas-rubber diffusion systems (3).

THE SOLUTION AND DIFFUSION OF GASES IN ELASTIC POLYMERS

The passage of a gas through a membrane is governed by the equation $P = -D(\partial C/\partial x)$, where D is the diffusion constant, and $\partial C/\partial x$ the concentration gradient. When the permeability P is known, and the solubility, the diffusion constant may be

calculated. Two methods have been successfully employed to measure D:

(1) The solubility has been measured directly, and then the permeability constant. Use of the Fick law in the form

$$\bullet \quad P = D\frac{C_1 - C_2}{l}$$

(l denotes the thickness, and C_1 and C_2 are the concentrations at the ingoing and the outgoing faces respectively) then allows the evaluation of D. For measuring the solubility the same methods may be employed as in studies of sorption equilibria(54), and any sensitive apparatus described for that purpose could be employed.

(2) Another method may be used which allows one to measure P, D, and the solubility, in one experiment. This method was introduced by Daynes(3) and developed by Barrer(33, 55, 56). It will be seen, by referring to Chap. I, p. 18, that if one has a membrane with dissolved gas initially at a concentration C_0 throughout, and with constant concentrations C_1 and C_2 at the faces $x = 0$ and $x = l$ respectively, the rate of flow of gas through the membrane takes some time to settle down to a steady state. If one plots the rate of increase of concentration on the low pressure side against time, the C-t curve approaches asymptotically a line which intersects the t-axis at the point

$$L = \frac{l^2}{D}\frac{1}{C_1 - C_2}\left[\frac{C_1}{6} + \frac{C_2}{3} - \frac{C_0}{2}\right],$$

provided the increase in concentration is small. When C_0 is zero, the intercept is

$$L = \frac{l^2}{D}\frac{1}{C_1 - C_2}\left[\frac{C_1}{6} + \frac{C_2}{6}\right];$$

and when both C_0 and C_2 are negligible compared with C_1, the intercept is $L = l^2/6D$. Thus by a single experiment which follows both non-stationary and stationary states of flow one

measures P and D, and then calculates the solubility, C_1. The equations

$$L = \frac{l^2}{6D},$$

$$P = D\frac{C_1}{l} \text{ (Fick's law),}$$

$$C_1 = kp \text{ (Henry's law),}$$
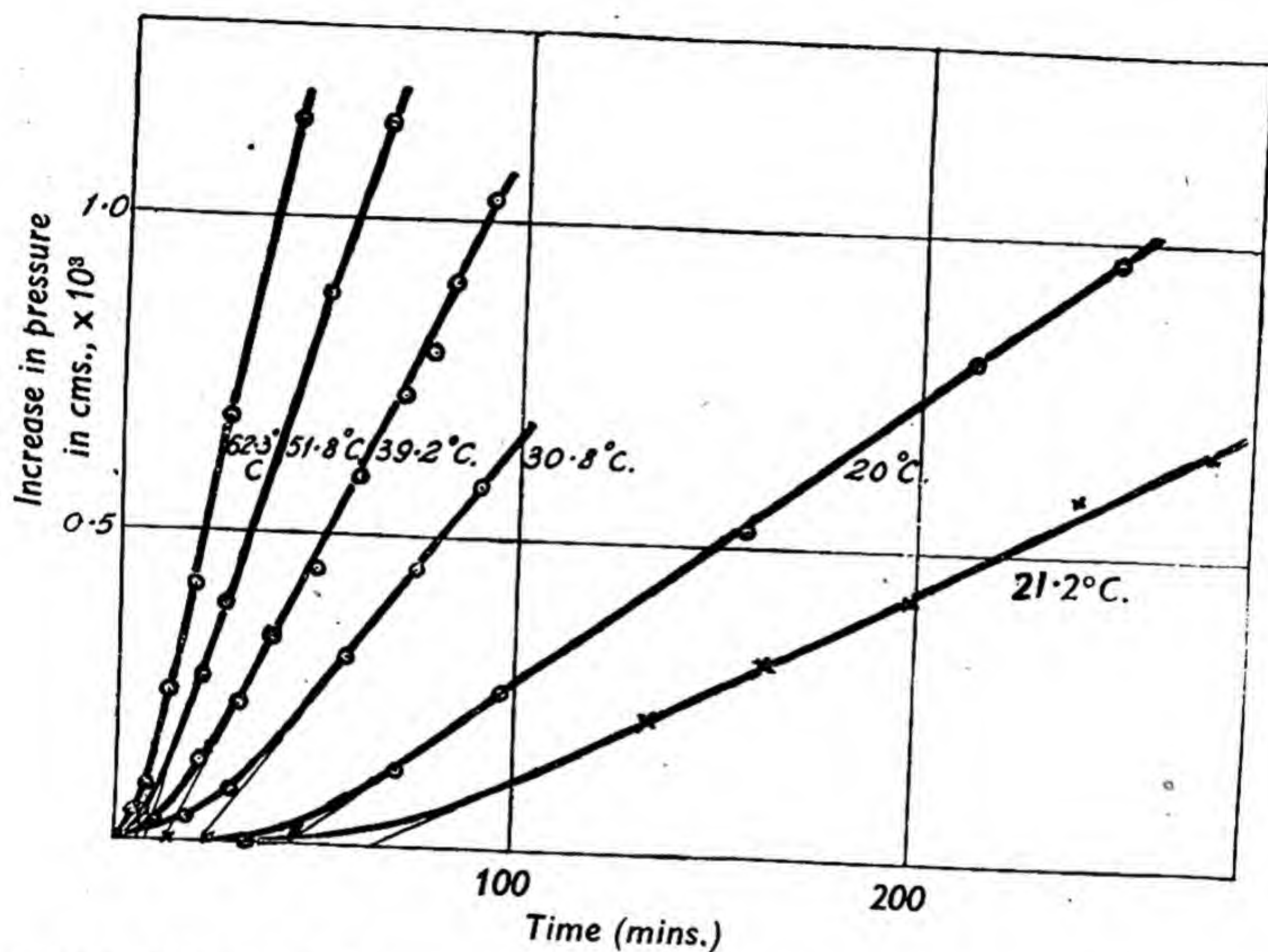
Fig. 144. The time lag in setting up a steady state of flow: ⊙, argon in butadiene-methyl-methacrylate interpolymer; ×, nitrogen in butadiene-methyl-methacrylate interpolymer.

give also the relation

$$PL = \frac{klp}{6}.$$

The predictions of all these expressions were verified by Daynes [3]. The intercepts L were, for membranes about 1 mm. thick, suitably large for evaluating D, as Fig. 144 [33] indicates. Most early measurements of solubility employed the static method [1]. Wroblewski [29] found that Henry's law was obeyed: $C_1 = kp$. The temperature dependence of the solu-

bility does not agree with some more recent data (p. 418) for hydrogen and air, although the actual solubilities are similar. Hüfner (30) found that rubber will sorb its own volume of carbon dioxide at room temperature, but could not measure the absorption of hydrogen, oxygen, or nitrogen. Reychler (31) found that rubber sorbed 1·06 vol. of CO_2 at 18° C., and 26 vol. of SO_2. The most complete and satisfactory measurements of solubility by the static method were made by Venable and Fuwa (57). They showed that Henry's law was obeyed for
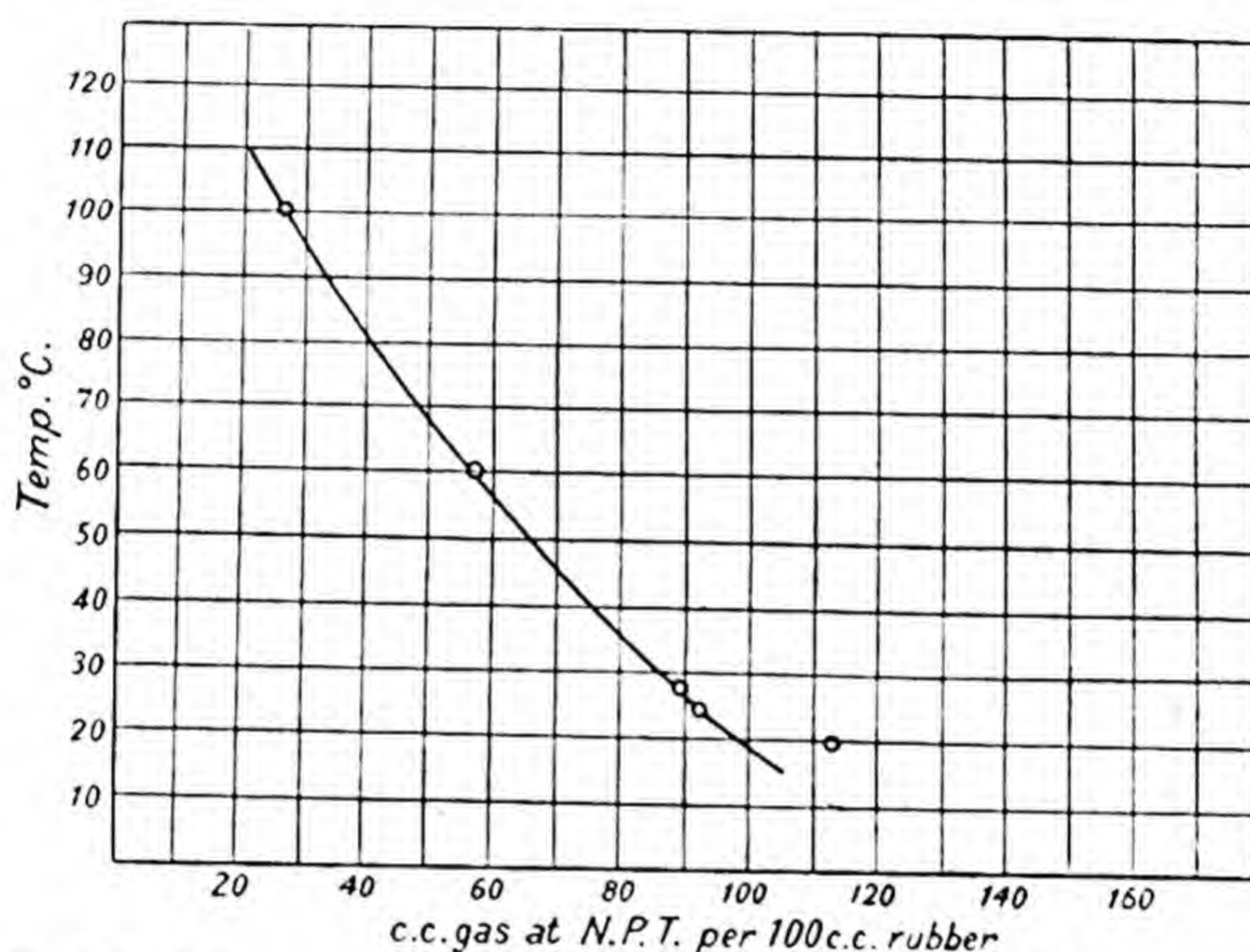
Fig. 145. The influence of temperature upon the solubility of CO_2 in rubber.

CO_2-rubber systems, and also that the solubility of ethylene and carbon dioxide decreased with temperature (Fig. 145). The data plotted as log (solubility) against $1/T$ give exothermal heats of solution of 3300 for CO_2 and 2700 for ethylene. Venable and Fuwa also showed that adsorption was not important in determining the amount of gas taken up, since the observed uptake was not altered by increasing the total rubber surface.

Tammann and Bochow (58) measured the solubility of hydrogen in a number of rubbers and at pressures as high as 1150 kgm./cm.² Even at these pressures Henry's law was approximately valid, and the solubilities extrapolated to

1 atm. pressure were of the same order as the solubilities given in Tables 106 and 107. When the pressure on such a hydrogen-filled rubber was released, the rubber swelled to several times its original volume.

Oxygen may dissolve in rubber in two ways. Physical solution can be followed by chemical reaction. Chemical reaction occurs autocatalytically[59], and as resinification proceeds the rubber becomes first tacky, and ultimately hard and brittle. When the surface area is small the rate of reaction with oxygen may depend upon the extent of the surface, but as the surface is increased diffusion becomes no longer a rate controlling step, and the reaction velocity is independent of the surface area.

The most complete and satisfactory data on solubility and diffusion in rubbers have been obtained by the second method of p. 412, depending on the time lag in setting up the stationary

TABLE 105. *A comparison of absorption coefficients measured by the methods (1) and (2) of p. 412*

Gas	$k_{21°C.}$ (c.c. at N.T.P./c.c. rubber) by sorption method (Venable and Fuwa)	$k_{17°C.}$ (c.c. at N.T.P./c.c. rubber) by non-stationary flow method (Daynes)
H_2	<0.01	0.040
O_2	0.073	0.091
NH_3	9.30	41.0
CO_2	0.99	0.86
Air	0.045	0.043

state. Where comparison is possible, the solubility constants k (from $C = kp$) agree well when obtained by the two methods (Table 105). Agreement is not good for ammonia which, however, approaches its equilibrium sorption value very slowly. The agreement for the other gases provides support for the assumption made in the time lag method that the concentrations just inside the ingoing and outgoing surfaces of rubber are governed by Henry's law, $C = kp$.

Barrer[33] used the flow method (2) to measure P, D, and k.

It was found that the intercepts L and the permeabilities obeyed the relationships

$$L = L_0 e^{E/RT} \quad \text{(Fig. 146)},$$
$$P = P_0 e^{-E_1/RT} \quad \text{(Figs. 142, 143)}.$$

Thus since

$$L = \frac{l^2}{6D},$$

one finds

$$D = D_0 e^{-E/RT},$$
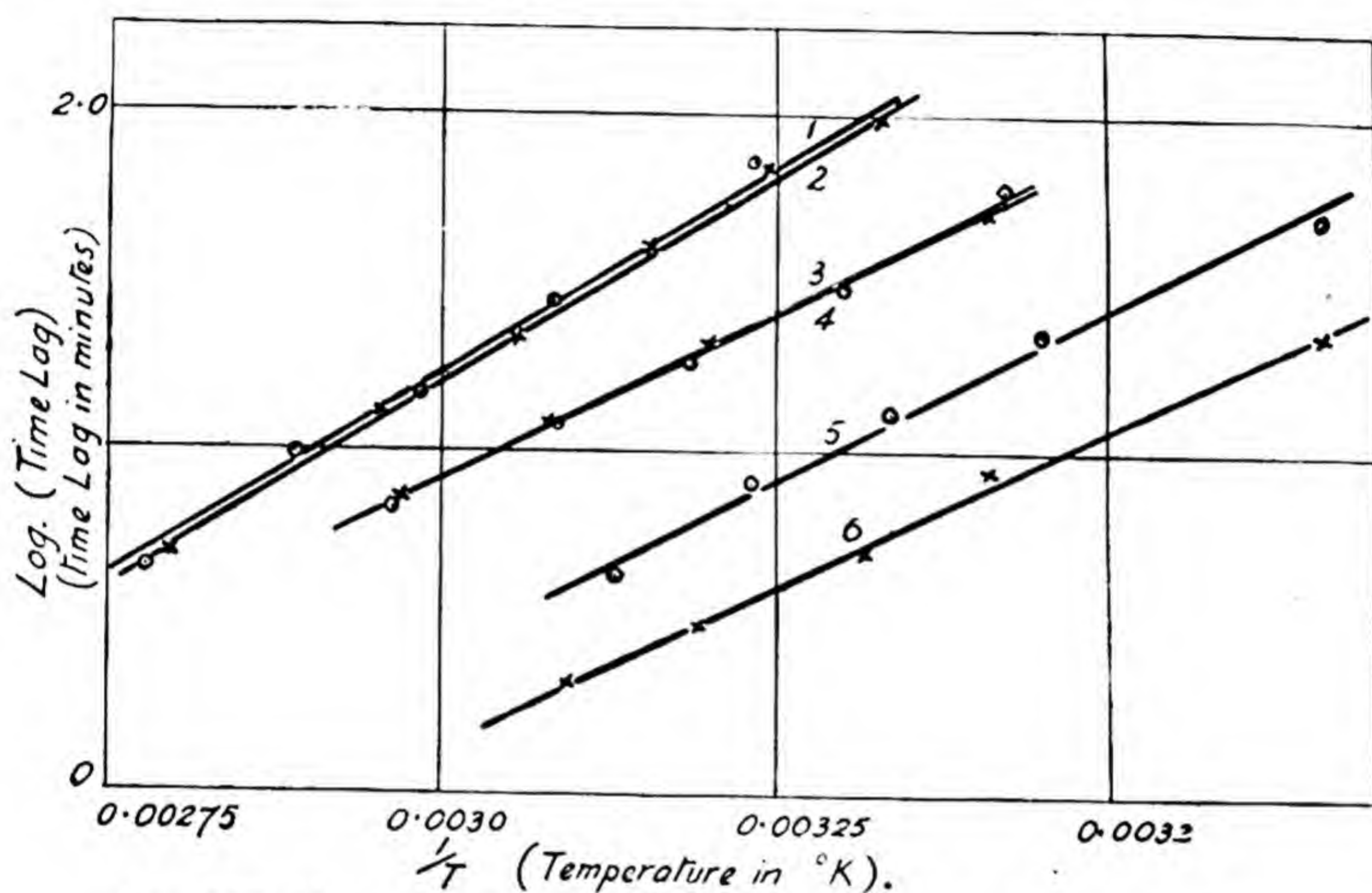
Fig. 146. Curves showing that log (L) is a linear function of $1/T$ [33].

Curve 1. A-neoprene.
Curve 2. N_2-neoprene.
Curve 3. N_2-styrene-butadiene interpolymer.
Curve 4. A-styrene-butadiene interpolymer.
Curve 5. H_2-neoprene.
Curve 6. H_2-butadiene-acrylonitrile interpolymer.

so that diffusion in polymers is activated. From the Fick law

$$P = D\frac{\Delta p}{l} k$$

one obtains

$$k = k_0 e^{(E-E_1)/RT} = k_0 e^{\Delta H/RT},$$

where ΔH denotes the heat of solution. Although activated diffusion occurs in the polymers, it is non-specific, since any gas of suitably small molecular dimensions will diffuse.* It

* And also large molecules which distend the rubber as they diffuse.

differs from the diffusion of gases in metals, which is specific to certain gases and certain metals with which the gas can react chemically (N_2-Fe), or form an alloy (H_2-Pd).

In Tables 106–108 are given data on the solubility and the diffusion constants of gases in polymers. The heats of solution

TABLE 106. *Solubility, permeability and diffusion constants in vulcanised rubber at 25° C. (calculated from data of Daynes[3] and Edwards and Pickering[6])*

Gas	Solubility c.c. at N.T.P./c.c. rubber/atm. pressure	Permeability constant (25° C.) c.c. at N.T.P./ sec./cm.^{2} mm./cm. Hg	Diffusion constant (25° C.) cm.^{2} sec.$^{-1}$
H_2	0·040		
O_2	0·070	$0·045 \times 10^{-6}$	$0·85 \times 10^{-5}$
N_2	0·035	$0·020 \times 10^{-6}$	$0·21 \times 10^{-5}$
CO_2	0·90	$0·0071 \times 10^{-6}$	$0·15 \times 10^{-5}$
		$0·132 \times 10^{-6}$	$0·11 \times 10^{-5}$

in Table 107 are not as accurate as the actual solubilities, since the latter decrease only very slowly as the temperature rises. It is also to be noted that the solubility of argon is greater in all cases than that of nitrogen, which accounts in part for the higher permeability of rubbers to argon (Tables 107 and 94).

The solution of gases in rubbers occurs exothermally even in constant volume systems [33, 60], with the possible exceptions of helium and hydrogen. This must be contrasted with the endothermic heats of solution of many gases in organic liquids [61]. The solubility constant k for a perfect gas is related to the standard free energy of solution, ΔG_0:

$$\Delta G_0 = -RT \ln k.$$

But since

$$\Delta G = \Delta H - T\Delta S,$$

one may calculate both the free energy and entropy of the solution process [33]. The solubility constant of gases in organic liquids is practically the same as the solubility constant in organic polymers, and therefore the difference in the heats of solution is due to the entropy term. When comparable entropy

BD

TABLE 107. *Solubilities of gases in organic polymers*

Polymer	Gas	Temp. °C.	Solubility k (c.c./c.c. rubber/ atm.)	$\log_{10} k = \log k_0 - \dfrac{\Delta H}{2\cdot30 RT}$
"Neoprene" (vulcanised)	H_2	0·0 17·0 27·0 36·1 46·5	0·065 0·051 0·053 0·051 0·050	$\log_{10} k = -1\cdot97 + \dfrac{970}{4\cdot60 T}$
"Neoprene" (vulcanised)	A	36·1 52·2 61·8 73·7 86·2	0·155 0·141 0·117 0·106 0·102	$\log_{10} k = -1\cdot86 + \dfrac{1630}{4\cdot60 T}$
"Neoprene" (vulcanised)	N_2	27·1 36·4 44·1 54·1 65·4 84·7	0·054 0·050 0·047 0·044 0·040 0·038	$\log_{10} k = -2\cdot28 + \dfrac{1400}{4\cdot60 T}$
Chloroprene polymer	H_2	31·8 41·3 49·9 60·8 69·5 73·5	0·115 0·103 0·097 0·090 0·083 0·082	$\log_{10} k = -2\cdot09 + \dfrac{1600}{4\cdot60 T}$
Butadiene-acrylo-nitrile inter-polymer	N_2	17·0 38·1 48·5 59·5 70·5	0·063 0·050 0·048 0·040 0·038	$\log_{10} k = -2\cdot44 + \dfrac{1700}{4\cdot60 T}$
Butadiene-acrylo-nitrile inter-polymer	H_2	0 20 29 41·5 50·2	0·040 0·037 0·036 0·033 0·036	$\log_{10} k = -1\cdot80 + \dfrac{500}{4\cdot60 T}$
Butadiene-methyl-methacrylate interpolymer	N_2	39·5 55·0 66·0 78·0	0·084 0·075 0·071 0·060	$\log_{10} k = -2\cdot45 + \dfrac{2000}{4\cdot60 T}$
Butadiene-methyl-methacrylate interpolymer	A	20·0 30·8 39·2 51·8 52·3	0·134 0·125 0·112 0·110 0·099	$\log_{10} k = -1\cdot95 + \dfrac{1450}{4\cdot60 T}$
Butadiene-styrene interpolymer (sample I)	N_2 (A	20·0 35·5 50·0 64·2 64·0	0·094 0·086 0·082 0·080 0·168)	$\log_{10} k = -1\cdot87 + \dfrac{1000}{4\cdot60 T}$
Butadiene-styrene interpolymer (sample II)	A (N_2	19·5 30·3 40·7 51·2 64·6 64·6	0·218 0·210 0·196 0·186 0·170 0·101)	$\log_{10} k = -1\cdot63 + \dfrac{1100}{4\cdot60 T}$

data are obtained for liquids (62) and polymers (33), it appears that there is a larger entropy decrease by 4 or 5 units for the process

Gas dissolving in polymer

than for the process

Gas dissolving in liquid.

This observation must be interpreted by supposing that more restrictions are imposed upon the movement of the gas molecules in the polymer than in the liquid. This shows itself in a higher energy of activation (about 10 k.cal.) needed for diffusion in polymers (Table 108) than for diffusion in liquids (3–5 k.cal.).

The activation energy for diffusions in rubbers is as large for helium and for hydrogen as the corresponding energies in rigid inorganic membranes of silica glass (Chap. III). The energy of activation rises as the molecular weight of the diffusing molecule increases, although the increases in the energy with molecular weight are very much smaller than those found in rigid membranes of silica glass. The influence of molecular weight upon the activation energy can be illustrated by reference to published data upon gas-silica (62a), gas-heulandite (63), gas-cellulose (35a, 37), and gas-neoprene (33) diffusion systems (Table 109).

One feature which has to be explained is the magnitude of the activation energy in rubbers, since the internal elasticity on a molecular scale might be expected to reduce the energy barrier involved in migration. When one calculates the energy needed to cause a gas atom to pass through an elastic two-dimensional crystal, it can be shown (33) that the potential energy barrier becomes very small indeed with only minor elastic displacements of the components of the two-dimensional lattice. Barrer advanced the theory that the major part of the energy of activation was the energy needed to create "holes" in the three-dimensional rubber network.* The energy

* The theory of holes in the rubber substance agrees with the model of a rubber polymer given in Fig. 140.

TABLE 108. Diffusion constants in polymers
$$(D = D_0 e^{-E/RT} \ cm.^2 \ sec.^{-1})$$

System	Temp. °C.	D cm.² sec.⁻¹ × 10⁵	D_0 cm.² sec.⁻¹	E cal./mol.
H_2-"neoprene" (vulcanised)	0	0·037	9·0	9,250
	17	0·103		
	27	0·180		
	36·1	0·297		
	46·5	0·481		
A-"neoprene" (vulcanised)	36·1	0·033	54·6	11,700
	52·2	0·078		
	61·8	0·145		
	73·7	0·253		
	86·2	0·484		
N_2-"neoprene" (vulcanised)	27·1	0·019	79	11,900
	35·4	0·034		
	44·1	0·055		
	54·1	0·096		
	65·4	0·180		
	84·7	0·450		
H_2-chloroprene polymer	31·8	0·33	39·4	9,900
	41·3	0·56		
	49·9	0·91		
	60·8	1·44		
	69·5	2·1		
	73·5	2·4		
H_2-butadiene-acrylo-nitrile interpolymer	0	0·061	54·4	8,700
	20·0	0·177		
	29·0	0·27		
	41·5	0·46		
	50·2	0·66		
N_2-butadiene-acrylo-nitrile interpolymer	17	0·0066	28·1	11,500
	38·1	0·029		
	48·5	0·044		
	59·5	0·088		
	70·5	0·14		
N_2-butadiene-methyl-methacrylate interpolymer (sample I)	39·5	0·041	38	11,500
	55·0	0·092		
	66·0	0·16		
	78·0	0·29		
A-butadiene-methyl-methacrylate interpolymer (sample II)	20	0·034	15·1	10,300
	30·8	0·062		
	39·2	0·112		
	51·8	0·186		
	62·3	0·309		
A-butadiene-styrene interpolymer (sample I)	19·5	0·038	1·84	9,000
	30·3	0·068		
	40·7	0·111		
	51·2	0·175		
	64·6	0·304		
N_2-butadiene-styrene interpolymer (sample II)	20·0	0·0237	0·93	8,900
	35·5	0·0506		
	50·0	0·095		
	64·2	0·153		

of hole formation would then consist of the van der Waals's energy of cohesion absorbed when a number of cohering $> CH_2$ groups in adjacent hydrocarbon chains were separated. The fluctuations of thermal energy in the rubber micelle would always be sufficient to maintain a certain number of these holes in the rubber substance, because of the existence of which the rubber can dissolve gases. There must then be a drift of dissolved gas in the direction of decreasing concentration gradient, by way of these holes. The energy absorbed in producing a hole large enough to accommodate a helium atom is a little less than the energy needed to produce a hole large enough to accommodate the bigger argon atom, and so $E_{argon} > E_{helium}$.

TABLE 109. *The influence of molecular weight upon the activation energy for diffusion in membranes*

	E (neoprene) cal./mol.	E* (SiO₂ glass) cal./mol.	E (heulandite) cal./mol.	E* (cellulose compounds) cal./mol.
He	8,000	5,600	—	—
H₂	9,250	10,000	—	7600 to 5600
N₂	11,900	26,000	—	
A	11,700	32,000	—	—
H₂O	6,900 (in rubber)	—	5400 (⊥ 201 face)	—

* These values of E are approximate since they include the small temperature coefficient of solubility.

It was also suggested that plastic deformation of a rubber under stress was due to the same causes. Sections of hydrocarbon chain become separated from other chains by thermal agitation, and under the shearing force become somewhat displaced before coming together again. The temperature coefficient for the viscosity of rubber has been given as 10,000 cal. (64), in agreement with the values 8700–11,900 cal./mol. observed (Table 108) when gases diffuse through rubbers. Permanent displacements of the hydrocarbon chains relatively to one another are only possible, however, if the chains are not strongly cross-linked by sulphur or oxygen bonds.

MODELS FOR DIFFUSION IN RUBBER

A number of formulae have been derived for D, the diffusion constant, based upon various models of the diffusion process. The formulae all depend upon the premise of a medium in which the diffusing particle is vibrating, and moving to successive positions of equilibrium when a sufficient activation energy has been acquired by the system particle-medium. The most general expression based upon kinetic theory (Chap. VI) is

$$D = \frac{1}{6} \frac{\nu}{(n-1)!} \left(\frac{E}{RT} \right)^{(n-1)} d^2 e^{-E/RT} \quad \text{(Wheeler)} \quad (65).$$

Here ν = the vibration frequency of the diffusing particle in the medium,

n = the number of degrees of freedom in which the activation energy E is stored,

d = the mean free path of the diffusing particle in the activated state.

When $n = 2$,

$$D = \tfrac{1}{6}\nu \frac{E}{RT} d^2 e^{-E/RT} \quad \text{(Bradley)} \quad (66),$$

and if $n = 1$,

$$D = \tfrac{1}{6}\nu d^2 e^{-E/RT}.$$

The transition state theory of reaction velocities may be applied to diffusion systems, the expression for D being (67):

$$D = \frac{kT}{h} \frac{F_a^*}{F_n} d^2 e^{-E/RT},$$

where F_n, F_a^* denote the partition functions of the system particle-medium in the normal and activated states respectively, excluding from the latter the partition function for the co-ordinate in which diffusion occurs.

In Table 108 the diffusion constants have been expressed by the formula $D = D_0 e^{-E/RT}$, and the values of D_0 may be used to calculate values of the mean free path, d (Table 110).

For all formulae involving a few degrees of freedom only Table 110 shows that the mean free paths are very much larger than one would expect. In Table 110 are given for comparison the mean free paths in some liquid-liquid diffusion systems in which it can be seen that the mean free paths are of normal molecular magnitudes (excepting water which usually shows anomalous properties).

An explanation of this behaviour of gas-polymer diffusion systems, compatible with the diffusion process as pictured previously (p. 421) and involving only a small mean free path of the diffusing particle, is that the activation energy is distributed through many degrees of freedom in the particle-medium system. Such a distribution of energy is needed for hole formation in the polymer. Thus one has in these systems an analogy with "fast" chemical reactions (for example, the unimolecular decomposition of large organic molecules). The numbers of degrees of freedom needed to give values of d of molecular magnitude are given in Table 111.

Eyring's formula (67) relating the diffusion constant D and the velocity constant for passing over an energy barrier, k, is

$$D = kd^2,$$

where d as before denotes the mean free path in the activated state. If the formula of Wynne-Jones and Eyring (68) for a reaction velocity constant is used, one has

$$k = e^{-\Delta H^{\pm}/RT} e^{\Delta S^{\pm}/R} \frac{kT}{h}$$

or

$$D = D_0 e^{-E/RT} = e^{-\Delta H^{\pm}/RT} e^{\Delta S^{\pm}/R} \left(\frac{kT}{h}\right) d^2 = e^{-E_0/RT} \frac{F_a^*}{F_n} \frac{kT}{h} d^2,$$

so that

$$D_0 = e^{\Delta S^{\pm}/R} \left(\frac{kT}{h}\right) d^2 \left(\frac{1}{2 \cdot 72}\right),$$

where $E = E_0 - RT$ and E_0 and $\Delta H^{\pm}$ are identified. When a value of d of 5×10^{-8} cm. is assumed, the entropies of activation are those of Table 111. A value of $d = 10 \times 10^{-8}$ cm. would reduce all these entropies by 2·76 units. The large increase in

TABLE 110. *Mean free paths calculated using various formulae for D and assuming $\nu = 2\cdot5 \times 10^{12}$ sec.$^{-1}$*

System	D_0 (cm.^{2} sec.$^{-1}$)	E (cal./mol.)	$D_0 = \frac{1}{6}\nu d^2$ $d = 1160$ A.	$D_0 = \frac{1}{6}\frac{\nu}{2\cdot72}\left(\frac{E}{RT}\right)d^2$ $d = 480$ A.	$D_0 = 2\cdot72\frac{kT}{h}\frac{F^*}{F_n}d^2$ $d\sqrt{\frac{F^*}{F_n}} = 182$ A.
H$_2$-butadiene-acrylonitrile polymer	56	8,700			
N$_2$-butadiene-acrylonitrile polymer	28	11,500	820	316	130
H$_2$-neoprene	9·4	9,250	476	204	74
A-neoprene	55	11,700	1150	410	185
N$_2$-neoprene	78	11,900	1370	490	215
N$_2$-butadiene-methyl-methacrylate interpolymer	37	11,500	946	350	150
H$_2$O in D$_2$O	0·197	5,300	69	36	11
C$_6$H$_5$OH in CH$_3$OH	$3\cdot4 \times 10^{-3}$	3,150	9·1	6·9	1·4
C$_6$H$_5$OH in C$_6$H$_6$	$3\cdot16 \times 10^{-3}$	3,080	8·7	6·9	1·4
S-C$_2$H$_2$Br$_4$ in S-C$_2$H$_2$Cl$_4$	$1\cdot68 \times 10^{-3}$	3,365	6·4	5·0	1·0
Br$_2$ in CS$_2$	$0\cdot43 \times 10^{-3}$	1,540	3·2	3·4	0·4

$\Delta S^{\pm}$ if it were all due to the diffusing molecule would correspond to more than its entropy of solution[33]. Thus the medium itself must share in the entropy change, and so both kinetic theory and transition state theory lead to the same viewpoint: that the activation energy is shared in part or

TABLE 111. *Degrees of freedom in acquiring energy of activation for diffusion from Wheeler's equation, and the entropy of activation from Wynne-Jones and Eyring's equation*

Diffusion system	D_0 cm.^{2} sec.$^{-1}$	E cal./mol.	$d^* \times 10^8$ cm.	n	$\Delta S^{\pm}$ (entropy units)
H_2-butadiene-acrylo-nitrile interpolymer	56	8,700	24	14	17·8
N_2-butadiene-acrylo-nitrile interpolymer	28	11,500	9·1	12	16·4
H_2-neoprene	9·4	9,250	6·9	14	14·2
A-neoprene	55	11,700	3·2	13	17·7
N_2-neoprene	78	11,900	3·7	13	18·4
N_2-butadiene-methyl-methacrylate inter-polymer	37	11,500	3·3	12	16·9

* d is calculated from the equation

$$d^2 = D_0 e^{(n-1)} \frac{6(n-1)!}{\nu} \left(\frac{RT}{E_{obs.} + (n-1)RT} \right)^{(n-1)}, \text{ where } \nu = 2\cdot5 \times 10^{12}.$$

wholly in various degrees of freedom of the polymer or polymer-solute system, a viewpoint already implied in the "hole" theory of solution and diffusion in elastic polymers (p. 421).

Since
$$D_0 = e^{\Delta S^{\pm}/R} \frac{kT}{h} d^2 \frac{1}{2\cdot72},$$

it is seen that $\log D_0$ is proportional to $\Delta S^{\pm}$. Barrer[33] collected the available diffusion data for a variety of systems, and plotted the number of diffusion systems having D_0 within certain limits against $\log D_0$. The frequency curve of Fig. 147 was obtained, in which the full curve represents the periodicity curve for all diffusion systems, and the dotted curves for special types of system. It can be seen that the entropy

of activation for gas-elastic polymer diffusion systems is greater than of liquid-liquid or gas- and solid-solid diffusion systems. The peak of the periodicity curve for liquid-liquid systems lies between the peaks for the curves for rubber and solid diffusion systems. The solid diffusion systems cover the
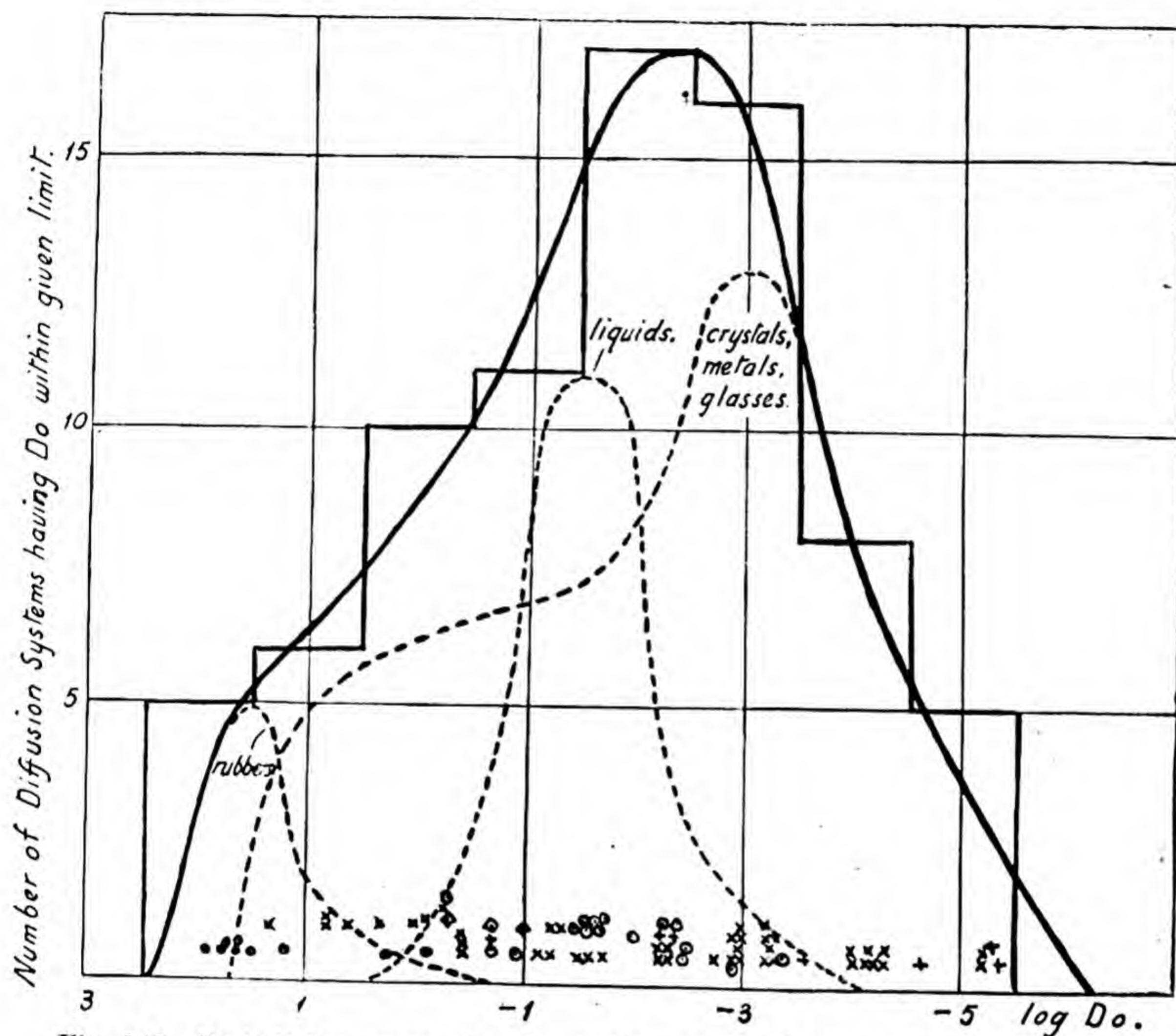
Fig. 147. Periodicity curve for D_0 in $D = D_0 e^{E/RT}$ for activated diffusions. O Rubbers; × crystals and metals; + glasses; ⊙ liquids; ⊡ surface diffusions.

greatest range in values of D_0 (10^7-fold). This may be because the greatest variety of structures occurs in crystals, metals, and glasses, involving special mechanisms of diffusion. Rubbers, and liquids, approximate to two single types, in which structural singularities are missing, so that narrow bands in the periodicity curve cover the observed range of values of D_0.

The values of D_0 and k_0 in the expressions

$$D = D_0 e^{-E/RT},$$

$$k = k_0 e^{-E/RT}$$

have been related by the relation (p. 423)

$$D_0 = k_0 d^2.$$

This equation permits a comparison of unimolecular reactions and activated diffusions. The distribution curve corresponding to Fig. 147 for unimolecular reactions[69] has its peak at $k_0 = 10^{13-14}$, and a spread of 10^{13}-fold. The corresponding curve for bimolecular reactions[70] has a peak at $k_0 = 10^{11}$ (litres $\times$ g. mol.$^{-1}$ $\times$ sec.$^{-1}$) and a spread of 10^{16}-fold. If a value of $d = 2 \cdot 1 \times 10^{-8}$ cm. is assumed, the maxima in Fig. 147 occur at

$k_0 = 3 \times 10^{16}$ sec.$^{-1}$ for rubbers,

$k_0 = 3 \times 10^{13}$ sec.$^{-1}$ for liquids,

$k_0 = 1 \times 10^{12}$ sec.$^{-1}$ for crystals and glasses.

One thus notes the similarity in activated diffusions and in unimolecular reactions.

REFERENCES

(1) Carson, F. *Bur. Stand. J. Res., Wash.*, **12**, 567 (1934).
(2) Dewar, J. *Proc. Roy. Instn*, **21**, 813 (1914–16).
(3) Daynes, H. *Proc. Roy. Soc.* **97**A, 286 (1920).
(4) Schumacher, E. and Ferguson, L. *J. Amer. chem. Soc.* **49**, 427 (1927).
(5) Rayleigh, Lord. *Proc. Roy. Soc.* **156**A, 350 (1936).
(6) Edwards, J. and Pickering, S. *Sci. Pap. U.S. Bur. Stand.* **16**, 327 (1920).
(7) E.g. Benton, A. F. *Industr. Engng Chem.* **11**, 623 (1919).
Buckingham, E. *Tech. Pap. Bur. Stand.* **14** (T 183) (1920).
Doughty, R., Seborg, C. and Baird, P. *Tech. Ass. Papers*, **15**, 287 (1932).
Emanueli, L. *Paper Tr. J.* **85** (TS 98) (1927).
Gallagher, F. *Paper*, **33**, 5 (1924).
(8) E.g. Barr, G. *J. Text. Inst.* **23**, 206 (1932).
Marsh, M. *J. Text. Inst.* **22** (T 56) (1931).
(9) Schiefer, H. and Best, A. *Bur. Stand. J. Res., Wash.*, **6**, 51 (1931).

(10) Mathieu, M. *La Nitration de la Cellulose, Actualités Scientifiques,* No. 316. Paris, 1936.

(11) Trillat, J. J. *C.R. Acad. Sci., Paris,* **197**, 1616 (1933).

(12) McBain, J. W. *Sorption of Gases and Vapours by Solids,* Figs. 110 and 111. Routledge, 1932.

(13) Sheppard, S. E. and Newsome, P. T. *J. phys. Chem.* **39**, 143 (1935).

(14) Hagedorn, M. and Moeller, P. *Veröff. ZentLab. Anilin. photogr. Abt.* **1**, 144 (1930).

(15) Astbury, W. and Woods, H. *Nature, Lond.,* **126**, 913, Fig. 1 (1930).

(16) Bernal, J., Fankuchen, I. and Perutz, M. *Nature, Lond.,* **141**, 523 (1938).

(17) E.g. de Boer, J. H. *Trans. Faraday Soc.* **32**, 10 (1936).

(18) Mark, H. and Meyer, K. *Der Aufbau der Hochpolymeren Organischen Naturstoffe.* Leipzig, 1930.

(19) Meyer, K. *Kolloidzschr.* **53**, 8 (1930).

(20) Siefriz, W. *Protoplasma,* **21**, 129 (1934).

(21) Frey-Wyssling, A. *Protoplasma,* **25**, 262 (1936).

(22) Guth, E. and Rogowin, S. *S.B. Akad. Wiss. Wien,* 11a, **145**, 531 (1936).

(23) Clews, C. B. and Schosberger, F. *Proc. Roy. Soc.* **164**A, 491 (1938).

(24) Sauter, E. *Z. phys. Chem.* **36**B, 405, 427 (1937).

(25) Staudinger, H. *Ber. dtsch. Chem. Ges.* **62**B, 2893 (1929).

(26) Staudinger, H. and Husemann, E. *Ber. dtsch. Chem. Ges.* **68**B, 1691 (1935).

(27) Staudinger, H., Heuer, W. and Husemann, E. *Trans. Faraday Soc.* **32**, 323 (1936).

(28) Graham, T. *Phil. Mag.* **32**, 401 (1866).

(29) Wroblewski, S. *Ann. Phys., Lpz.,* **8**, 29 (1879).

(30) Hüfner, G. *Ann. Phys., Lpz.,* **34**, 1 (1888).

(31) Reychler, A. *J. Chim. phys.* **8**, 617 (1910).

(32) Kanata, K. *Bull. Chem. Soc. Japan,* **3**, 183 (1928).

(33) Barrer, R. *Trans. Faraday Soc.* **35**, 628, 644 (1939).

(34) Sager, T. P. *Bur. Stand. Res., Wash.,* **19**, 181 (1937).

(35) Martin, S. and Patrick, J. *Industr. Engng Chem.* **28**, 1144 (1936).

(35a) Barrer, R. *Trans. Faraday Soc.* **36**, 644 (1940).

(36) Sager, T. P. *Bur. Stand. J. Res., Wash.,* **13**, 879 (1934).

(37) de Boer, J. H. and Fast, J. *Rec. Trav. chim. Pays-Bas,* **57**, 317 (1938).

(38) Kayser, H. *Ann. Phys., Lpz.,* **43**, 544 (1891).

(39) Barr, G. *Tech. Rep. Adv. Comm. Aero., Lond.* (ref. by H. Daynes (3)).

(40) Shakespear, G. Unpublished (ref. by H. Daynes (3)).

(41) Shakespear, G., Daynes, H. and Lambourn. *A brief account of some Experiments on the Permeability of Balloon Fabrics to Air.* Adv. Comm. for Aeronautics (ref. by H. Daynes (3)).

(42) Taylor, R., Herrmann, D. and Kemp, A. *Industr. Engng Chem.* **28**, 1255 (1936).

(43) Barrer, R. M. *Nature, Lond.*, **140**, 107 (1937); *Trans. Faraday Soc.* **34**, 849 (1938).

(44) Meyer, O. *Ann. Phys., Lpz.*, **127**, 253 (1866).

(45) E.g. Knudsen, M. *Ann. Phys., Lpz.*, **41**, 289 (1913).

(46) Clausing, P. *Ann. Phys., Lpz.*, **7**, 489, 569 (1930).

(47) E.g. Buckingham, E. *Tech. Pap. Bur. Stand.* T 183 (1920–21).

(48) E.g. Thomson, W. *Sci. Papers*, **2**, 681, 711. Cambridge, 1890.

(49) Carson, F. *Bur. Stand. J. Res., Wash.*, **12**, 587 (1934).

(50) Edwards, R. *J. Soc. Leath. Tr. Chem.* **14**, 392 (1930).

(51) Bergmann, M. and Ludewig, S. *J. Soc. Leath. Tr. Chem.* **13**, 279 (1929).

(52) Bergmann, M. *J. Soc. Leath. Tr. Chem.* **12**, 170 (1928).

(53) Wilson, J. and Lines, G. *Industr. Engng Chem.* **17**, 570 (1925).

(54) McBain, J. W. *The Sorption of Gases and Vapours by Solids.* Routledge, 1932.

(55) Barrer, R. M. *Phil. Mag.* **28**, 148 (1939).

(56) —— *Trans. Faraday Soc.* **36**, 1235 (1940).

(57) Venable, C. and Fuwa, T. *Industr. Engng Chem.* **14**, 139 (1922).

(58) Tammann, G. and Bochow, K. *Z. anorg. Chem.* **168**, 263 (1928).

(59) Kohman, G. *J. phys. Chem.* **33**, 226 (1929).

(60) Bekkedahl, N. *Bur. Stand. J. Res., Wash.*, **13**, 411 (1934).

(61) Horiuti, J. *Sci. Pap. Inst. phys. chem. Res., Tokyo*, **17**, 125 (1931). Lannung, A. *J. Amer. chem. Soc.* **52**, 68 (1930).

(62) Bell, R. P. *Trans. Faraday Soc.* **33**, 496 (1937).

(62a) Barrer, R. M. *J. chem. Soc.* p. 378 (1934).

(63) Tiselius, A. *Z. phys. Chem.* **169**A, 425 (1934).

(64) Ewell, R. H. *J. appl. Phys.* **9**, 252 (1938).

(65) Wheeler, T. S. *Trans. Nat. Inst. Sci. India*, **1**, 333 (1938).

(66) Bradley, R. S. *Trans. Faraday Soc.* **33**, 1185 (1937).

(67) Eyring, H. *J. chem. Phys.* **4**, 283 (1936).

(68) Wynne-Jones, W. F. and Eyring, H. *J. chem. Phys.* **3**, 492 (1935).

(69) Polanyi, M. and Wigner, E. *Z. phys. Chem.* **139**A, 439 (1928).

(70) Moelwyn-Hughes, E. A. *Kinetics of Reactions in Solutions*, chap. IV, p. 439 (1933).

CHAPTER X

PERMEATION OF VAPOURS THROUGH, AND DIFFUSION IN, ORGANIC SOLIDS

Diffusion of simple gases in many organic solids obeys Fick's laws and may therefore be regarded as showing the ideal behaviour. The diffusion of vapours, however, only approximately follows these laws, which then become limiting conditions only. It is these non-ideal systems which now remain to be discussed.

WATER-ORGANIC MEMBRANE DIFFUSION SYSTEMS

The most numerous researches have been carried out upon water-membrane systems, for which a summarising paper by Carson (1) has outlined the main methods of measurement. To prevent lateral diffusion of water through the edges of the specimen, or between it and its supports, various devices have been adopted. The edges have been moulded in wax, or compressed with a mixture of beeswax and resin. Shellac, petrolatum, and rubber have been used for the same purpose; or the cell may be mercury sealed. Films of lacquers and paints may be made by painting the lacquer on suitable surfaces, such as amalgamated tin-plate (2), and then peeling off the dried membrane.

A great number of the measurements on permeability have been made upon the complex membranes of Table 112, in which the chemical nature of the membranes is briefly indicated. Most of the membranes sorb water freely. Natural rubber, one of the least hydrophilic of these substances, may if exposed to water vary from a non-swelling non-sorbing medium to complete dispersion in the water, according to the carbohydrate and protein content (3). Nearly all cellulose or protein-containing substances swell and sorb water strongly (4), and the accompanying sorption is then influenced by tempera-

ture[5], vapour pressure, and markedly by saline[6,7] substances. This has led to the suggestion that sorption and swelling represent a tendency of water to equalise the salt concentrations inside or outside the membrane[8]. In so far as the permeability must depend on the concentration gradients of water within the material, the water permeability will depend upon the various factors which influence sorption processes.

TABLE 112

Membrane	Chemical constituents
Technical rubber and its derivatives (gutta-percha, paragutta, insulating compounds)	Rubber hydrocarbon (polyisoprene). Sulphur Resins Fillers Carbohydrates } present as impurity Protein Salts
Paints, varnishes, lacquers	Synthetic resins (phenol formaldehydes, glycerol phthalates, glycol sebacates, etc.) Nitrocellulose and cellulose esters Drying oils Paraffin, aromatic and terpene hydrocarbons Alcohols and esters $PbCO_3$, Al, or C black
Leathers	Natural protein membranes Tannins Oils Salts Solids such as Cr_2O_3, Al_2O_3, Fe_2O_3
Papers	Carbohydrates (cellulose, lignin) Sizing agents (alum) Protein
Textiles	Carbohydrates (cellulose, lignin) Proteins Dyes Mordants

On the basis of chemical composition one may construct a permeability spectrum for water (Fig. 148). The permeabilities cover a 10^6-fold range and may arbitrarily be regarded as comprising four main groups. In constructing the permeability chart the permeability constant was derived for a thickness of 1 mm., wherever possible. Unfortunately, in many references the thickness was not given. The range of permeabilities

(10^6-fold) is 10^6-fold less than the range of air permeabilities previously given (p. 383). A number of permeability data will be given later (p. 440) and the comparison with air or hydrogen permeabilities made in more detail (p. 443).

Wax Rubber	Rubber Asphalt	Moisture-proofed or waxed fibre-board, cellulose, papers, waxed glassine Paints, varnishes, lacquers Cellulose acetate	Paints, varnishes, lacquers Cellulose acetate Cellulose ethers · Cellulose nitrates Parchments, glassine Leathers Cellulose	Cellulose Textiles Metal gauzes Leathers Open cells
−7	−6	−5 −4	−3	−2
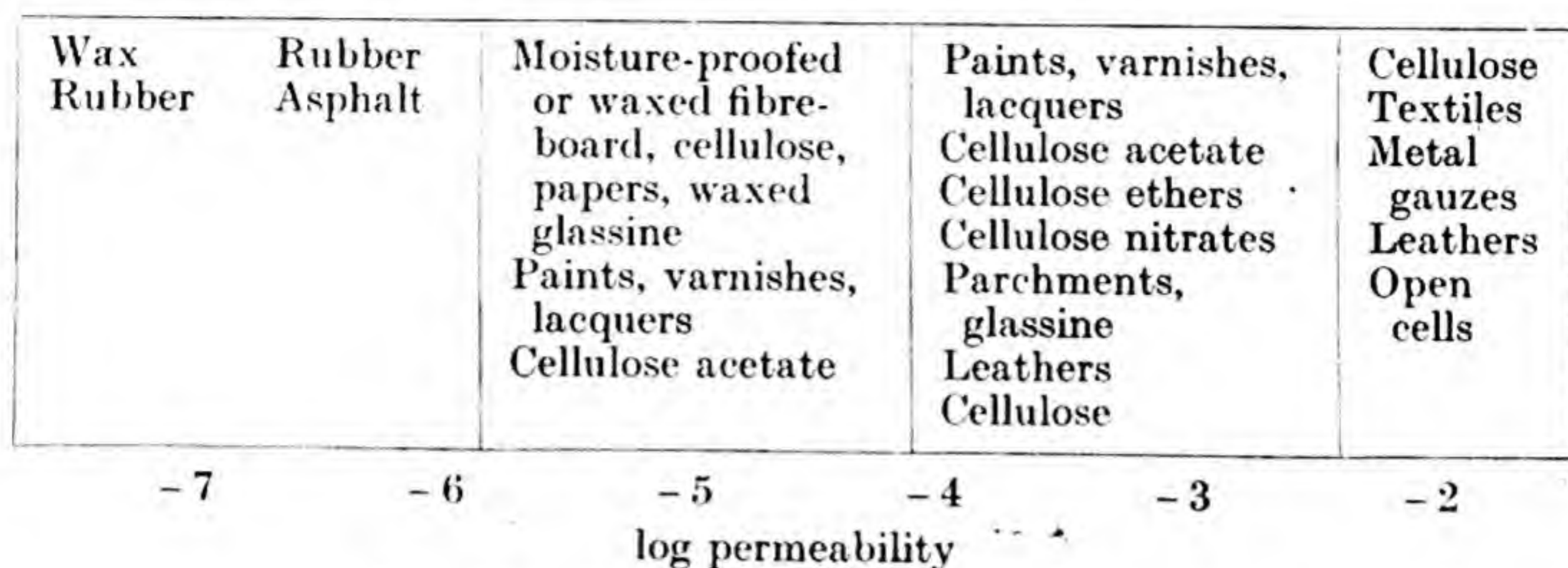
log permeability

Fig. 148. A water-permeability spectrum.
(Permeability in c.c./sec./cm.²/cm. Hg.)

Dependence of permeability upon thickness and vapour-pressure difference

Membranes which sorb little water (e.g. purified polystyrene [9]) behave at low relative vapour pressure as indicated by Fick's law, and the permeation velocity is proportional to $1/l$ (l denotes the membrane thickness). However, Fig. 149 indicates that at high humidities the permeation velocity constant rises with increasing thickness. Certain paint and varnish films [10, 11] also obeyed the law $p \propto 1/l$; but in other cases marked divergences arise [12, 13].

Similarly a number of researches [14, 15, 16, 17, 18, 19, 20] at low humidity showed that the permeation velocity was proportional to the vapour-pressure difference. The more hygroscopic the substance, however, the lower is the humidity above which this relationship breaks down. Pure rubbers and waxes sorb little water, and the permeability "constants" calculated from Fick's law are little affected by variations of humidity at the surfaces of the membrane. Many rubbers, however, contain hydrophilic impurity and sorption occurs freely. Figs. 150 [6] and 151 [9] show that the permeation rate and the sorption isotherms follow similar courses.

Cellulose and cellulose compounds are more hydrophilic than rubbers, and departures from the relation Permeation velocity ∝ Vapour pressure difference quickly appear.   In
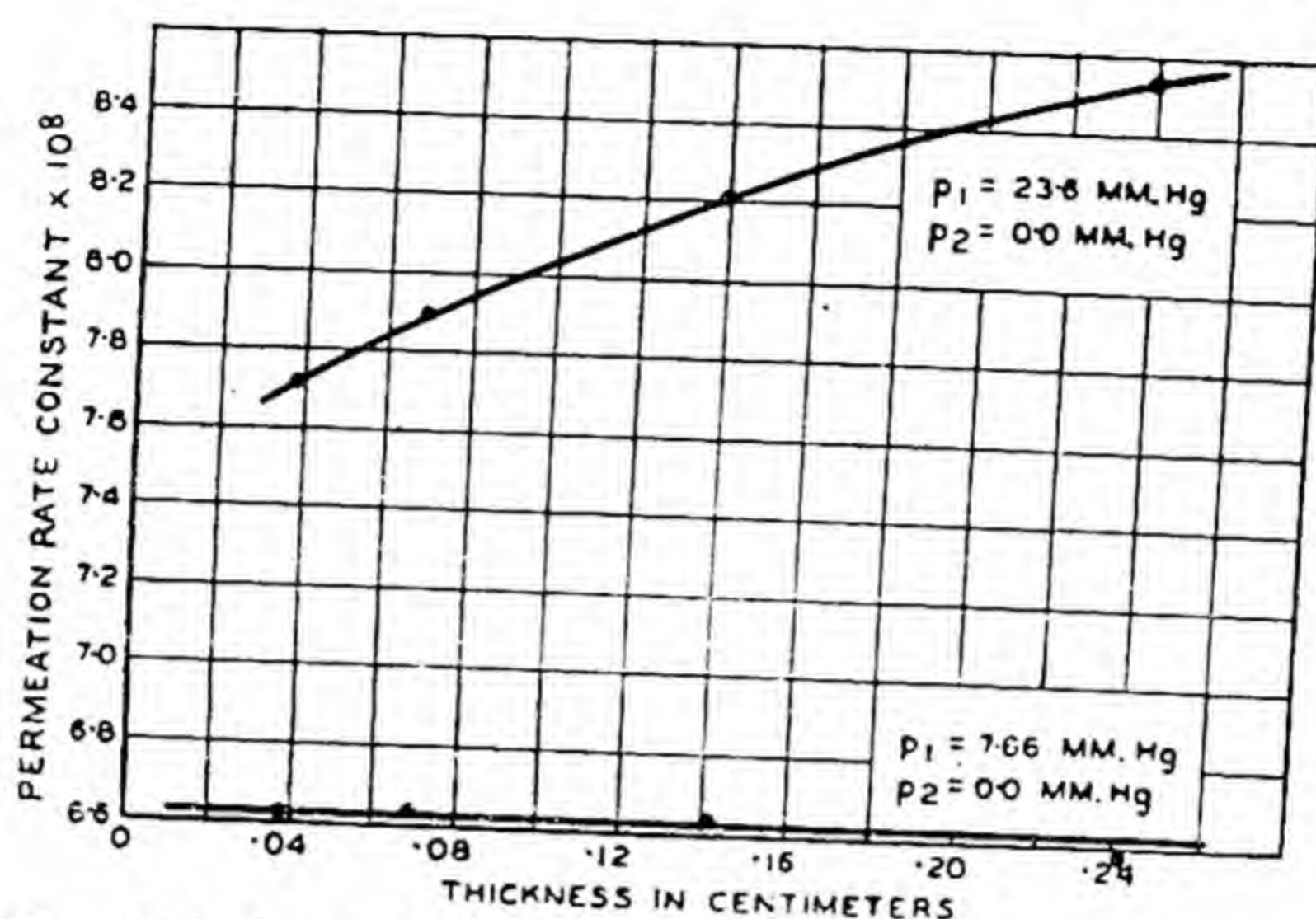
Fig. 149. Permeation rate constants at high and low humidities as a function of thickness[9].
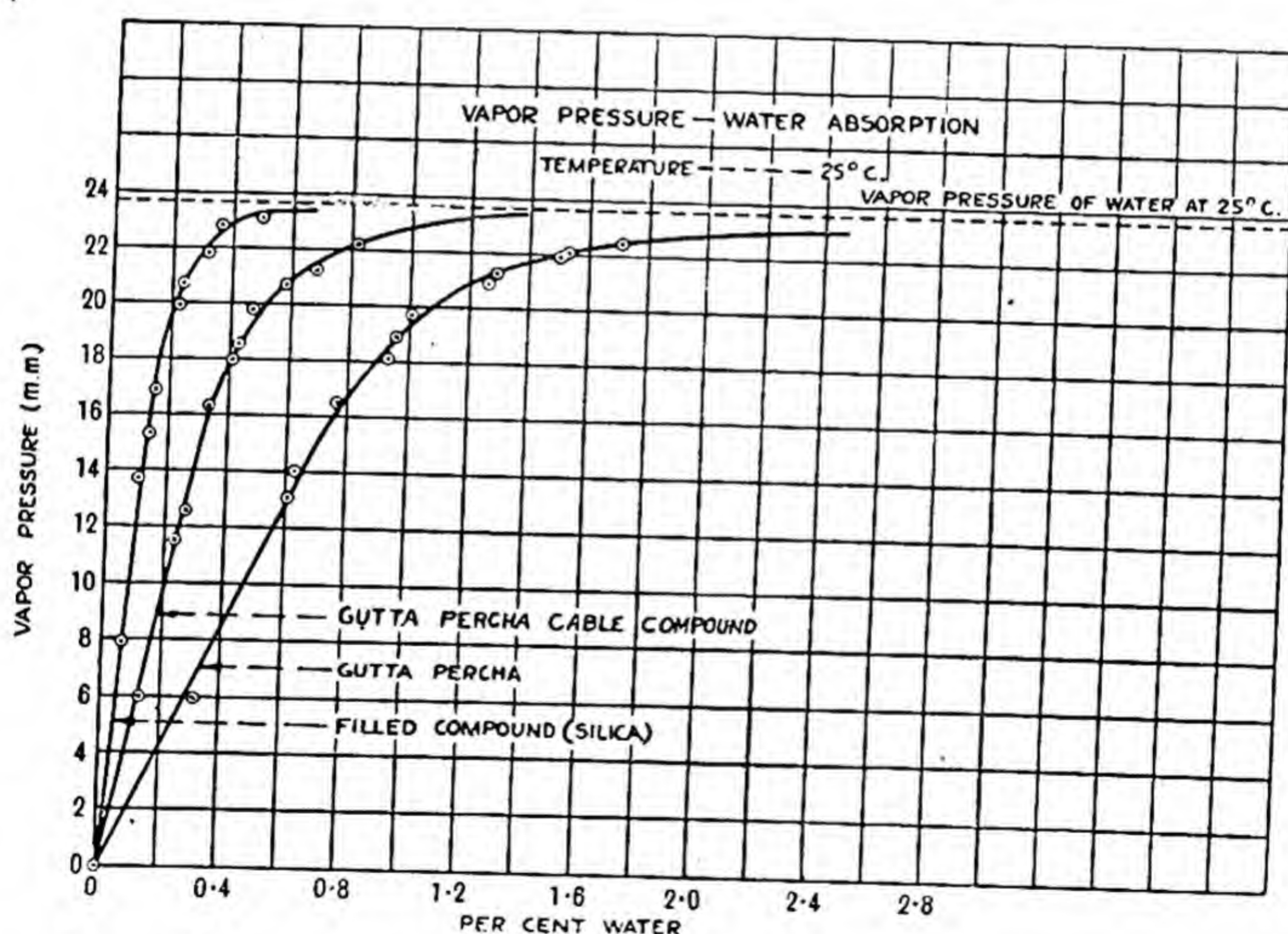
Fig. 150. Absorption of water vapour by gutta percha at 25° C. [6].

membranes made of resins, paints, and varnishes, the permeation velocity again follows roughly the sorption isothermal[16] (Fig. 152). Leathers show a very great range in their water

BD

28

and air permeability, but again on the whole conform to the general principle of increased permeability "constants" at high humidity.
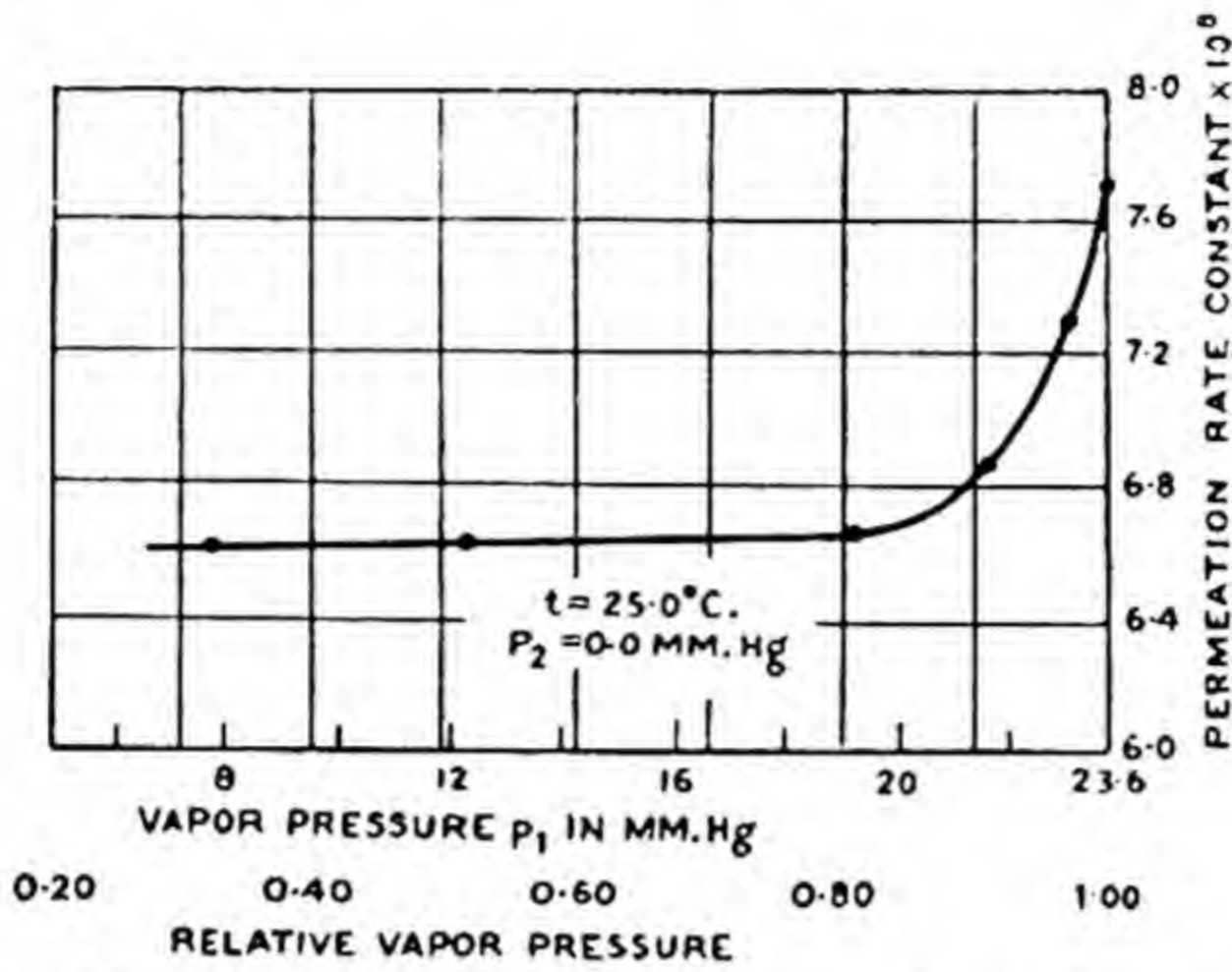
Fig. 151. Permeation rate constant as a function
of vapour pressure for rubber[9].
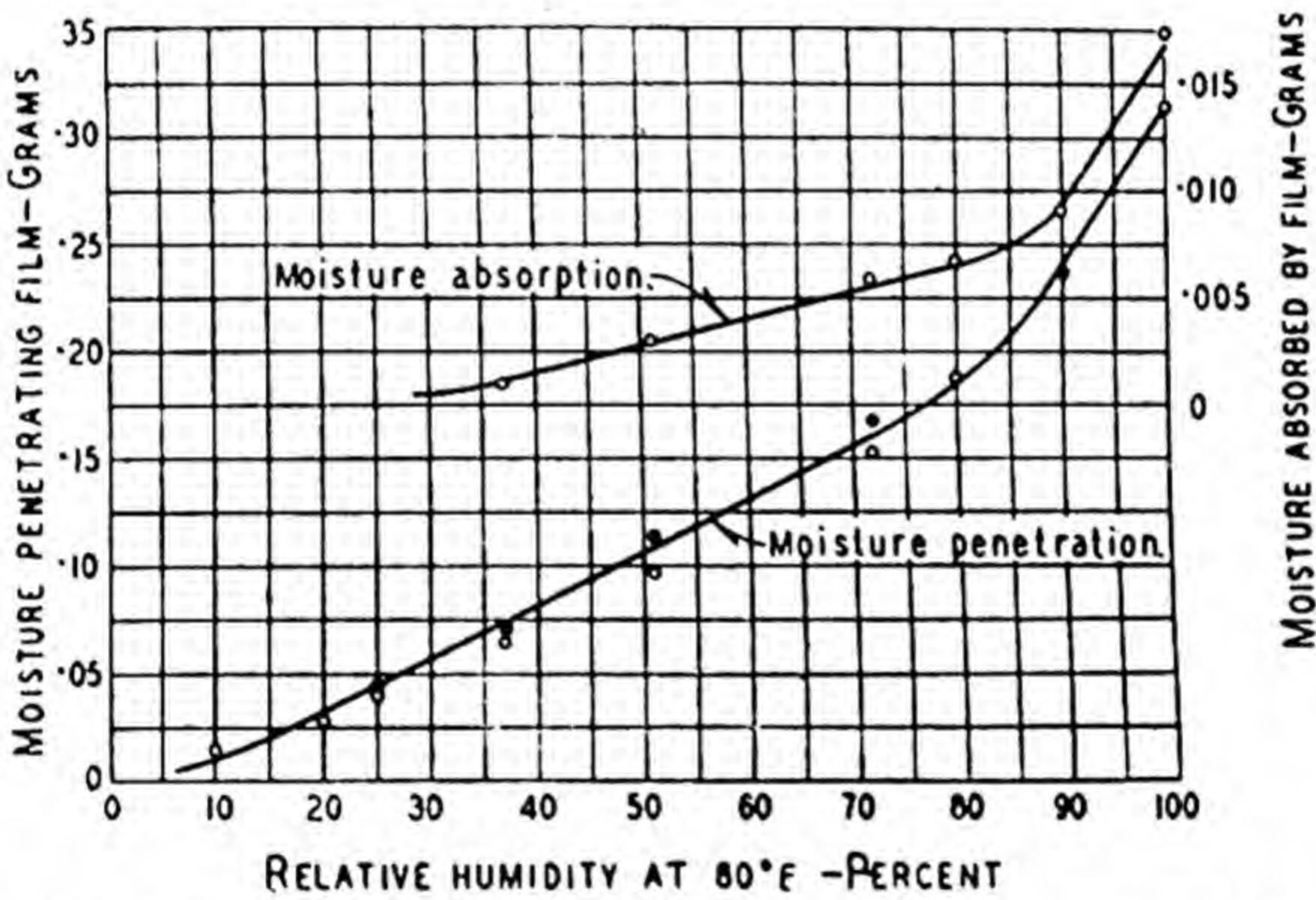
Fig. 152. The influence of varying the water-vapour pressure upon the quantity
sorbed and upon the permeation velocity through aluminium paints[16].

The concentration gradients established in rubber
during permeation

In the steady state, if the Fick law were valid, linear gradients would be established. By using thin laminae[9] of rubber joined in series, one can determine the actual concentration gradients existing in the membranes. That there is not a linear gradient at high relative humidities is shown by Fig. 153, in

which one sees an actual concentration gradient for soft vulcanised rubber under diffusion equilibrium. The dotted curve gives the concentration gradient calculated from the concentration-pressure isothermals of Lowry and Kohman (6). The two curves lie close together and indicate that while Henry's law holds at low pressure, an abnormal sorption occurs at higher humidities.
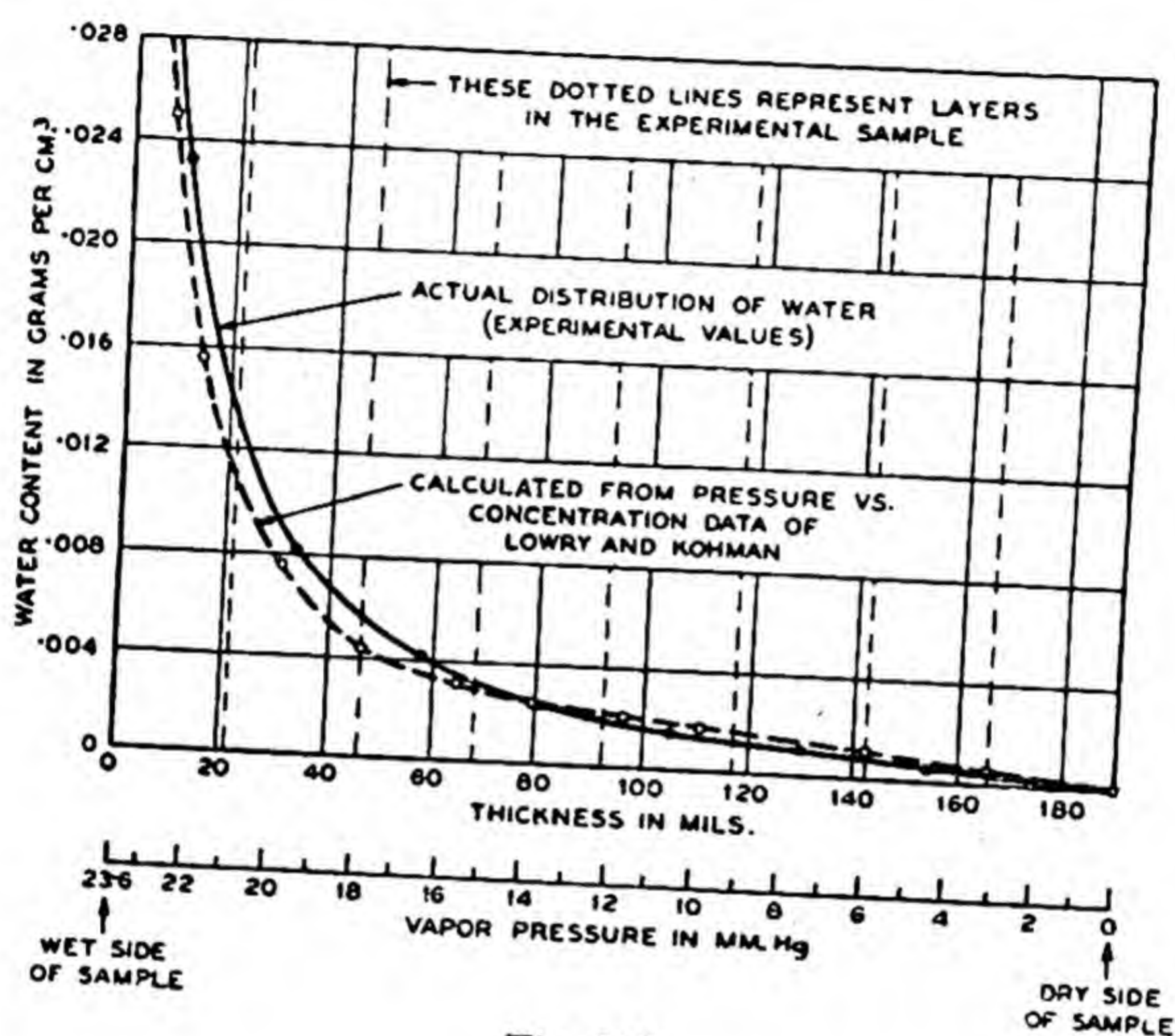
Fig. 153.

The influence of temperature upon the permeability constants

The data of previous sections indicates that at low humidities one may use the linear Fick law* as an approximation which breaks down as the humidity increases. The influence of temperature upon permeability constants is two-fold. There is first the effect upon the diffusion constant and secondly the effect upon the absorption coefficient, k. Sometimes in colloidal systems the coefficient k increases with temperature even when

* $P = D(C_1 - C_2)/l = Dk(p_1 - p_2)/l$, where k denotes the absorption coefficient, and the other symbols have their usual significance.

28-2

sorption is exothermal, due to irreversible changes in the colloid. The data on the influence of temperature upon permeability constants may be summarised as follows:

Impermeable membranes	Permeable membranes
Rubbers, silk, and rubber-like polymers[9] gave permeability constants which increased with temperature, often exponentially Gelatin latex gas-cell fabrics[2] gave permeability constants increasing rapidly with temperature Synthetic resins gave permeability constants increasing exponentially with temperature	Cellulose and cellulose compounds gave permeability constants which did not depend on temperature in many cases[14,15,16,18,19,22] The permeability constants for porous leathers did not depend on temperature[10] Paint films[16] containing aluminium gave permeability constants not appreciably depending on temperature

A rule which was found valid in rubber-gas diffusion systems again emerges, that the permeability constants of the least permeable membranes are highly sensitive to temperature changes, but that in porous membranes the constants are independent, or slightly dependent upon, temperature.

Some data giving permeability constants and permeation rates at different temperatures are presented in Tables 113 and 114, for systems with high temperature coefficients, and negligible coefficients respectively. For a number of resin, and rubber, membranes the curves of $\log P$ (P = permeability constant) against $1/T$ are linear, and from the slopes one may evaluate E in the equation $P = P_0 e^{-E/RT}$. Some of these values of E are collected in Table 115; their values are on an average somewhat smaller than E values for the permeability of gas-rubber systems. Diffusion of water in rubber is activated (p. 445); and it seems that diffusion is also activated in the resin membranes of Table 115.

Miscellaneous effects in permeation rate studies

Soluble salts, either in the membrane or in the solution in contact with the membrane, alter the amount of water absorbed, and therefore the concentration gradients and velocities of permeation. The addition of salts to water in

TABLE 113. *The influence of temperature upon permeability constants for water diffusion* [9]

Substance	Temp. °C.	Permeability constant $\times 10^8$ g./cm.^{2}/cm./ hr./mm. Hg
Polystyrene	21·1	4·0
	35·0	4·5
Varnished silk	30·0	3·4
	35·0	4·7
Vulcanised rubber	0·0	5·0
	21·0	6·9
	25·0	7·3
	35·0	8·5

TABLE 114. *The influence of temperature upon permeation rate through leather* [20]

Temp. °C.	Permeation rates mg. H_2O/24 hr./1·267 cm.^{2}		Ratio of rates
	Through leather	Through air space	
5	71	98	0·72
20	192	286	0·67
25	236	360	0·66
30	328	505	0·65
35	430	660	0·65
40	560	863	0·65
45	765	1214	0·63

TABLE 115. *Values of E in* $P = P_0 e^{E/RT}$ *(E in cal./mol.)*

Composition of membrane		E
Non-volatile	Volatile (solvents)	
Bakelite and glyceryl phthalate [2]	Butyl alcohol and hydrocarbons	8200
Cellulose nitrate, glycol sebacate, glyceryl phthalate [2]	Esters, alcohols and aromatic hydrocarbons	4700
Bakelite, China-wood oil, castor oil and linseed oil [2]	Butyl alcohol, turpentine, dipentine, mineral spirits	7500
,,	,,	5800
,,	,,	6200
Glyceryl phthalate [2]	Aliphatic and terpene hydrocarbons	6400
,,	,,	4300
Rubber [9]	—	2800

which leather was immersed decreased the amounts of water sorbed[7] in the order:

$$SO_4'' > citrate > acetate > Cl' > NO_3' > CNS',$$

and
$$Na^+ > K^+ > Li^+.$$
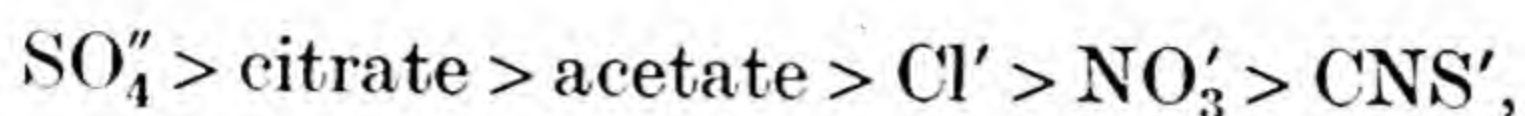
It was similarly established[21] that salt solutions decreased the permeation rates. The leather was almost impermeable at sodium chloride concentrations of 2·5 normal.

Coatings and fillers also influence permeability. Waxing diminished the permeability of celluloses, cellulose compounds, and synthetic resins[2]. Collodion and casein coatings decreased the air and water permeabilities of leather[20]. Sager[23] found that carbon black incorporated in polysulphide rubbers increased their permeability to hydrogen. On the other hand[11], the water permeability of paint films was diminished by incorporating aluminium.

Sometimes irreversible sorption effects arise. For example, the permeability of a certain rubber sample was twice as great in contact with liquid water as when saturated vapour was in contact with the membrane[24]. Occasionally, diffusion does not occur so readily in one direction as in the converse direction[20].

THE PERMEABILITY CONSTANTS TO WATER OF VARIOUS MEMBRANES

Based on the tables of Carson[1], Table 116 provides numerical values of the permeability constants, in c.c./sec./cm.²/cm. Hg, and per mm. thick, when the thickness has been given. The final column of Table 116 states whether or not the thickness was known. The values of the permeability constants are not strictly comparable unless this is so, especially since the thickness of paper and of cellulosic membranes, paint films, or varnish films will usually be less than 1 mm. There are, however, sufficient references for which thicknesses were given to permit comparisons to be made. Taking Levey's[28] value for paper (29×10^{-6} c.c./sec./cm.²/mm. thick/cm. of Hg) as an index

figure, one finds values of the permeability of the same order
or less for cellulose ethers and esters, or regenerated cellulose.
It is noteworthy that certain textiles offer a resistance to the
flow of water vapour comparable with that for cellulosic com-
pounds. Moisture-proofed and waxed cellulosic substances are
about one hundred times as impermeable (when comparable in
thickness) as paper; and the paint, varnish and lacquer films
vary from one five-hundredth to one-quarter of Levey's value
for paper. Wax is more than one thousand times less permeable,
as are certain members of the rubber group. The permeability
is greater the more hydrophilic the membrane substance. One
notes the extremely low permeability of the rubber-like
polymer polyethylene tetrasulphide, only four times the
permeability of wax, and four hundred times less permeable
than paper. The synthetic hydrocarbon polymers, such as
polystyrene, show permeabilities between those of soft
vulcanised and of hard rubber, the permeability of the latter
being one-quarter that of the former.

It has already been observed (p. 432) that the range of
values of 10^6-fold for water permeability is much less than the
corresponding range of values for air of 10^{12}-fold. At one end
of the permeability spectrum of Fig. 148, that of the least
permeable substances in Table 116, the water permeability
is 10- to 1000-fold greater than the air permeability. Similarly,
for some members of the cellulosic group (e.g. ordinary re-
generated cellulose) the water permeability is 10^3-fold greater
than the air permeability. The hydrogen permeability, like the
air permeability, is smaller than that for water, there being
a 30–100-fold difference for rubber, chloroprene, and poly-
ethylene sulphide; but a 3000–1500-fold difference for the
cellulosic substances cellophane and cellulose acetate. Once
more it is the rule that like is more permeable to like. Hydrogen
by analogy with its solubility in hydrocarbons should dissolve
more freely in rubber, and water less freely. Typical data
are collected in Table 117. On the other hand, at the high
permeability end of the spectrum (the leathers and textiles)
the air permeability may be 10–1000 times greater for

TABLE 116. *Water vapour permeabilities in c.c./sec./cm.²/cm. Hg/mm. thick; and in c.c./sec./cm.²/cm. Hg when the thickness is not stated*

Type of membrane	$10^6 \times$ permeability	Reference	Experimental details			
			Moisture gradient	Temp. °C	Pressure difference mm. Hg	Thickness given or not
Wax	0·021	Taylor, Herrmann and Kemp[9]	W-A-S-A-0h	21 to 25	6 to 24	Yes
Rubber group:						
Polyethylene sulphide	0·076	Taylor, Herrmann and Kemp[9]	W-A-S-A-0h	21 to 25	6 to 24	Yes
Polystyrene	1·26-1·50	Taylor, Herrmann and Kemp[9]	W-A-S-A-0h	21 to 25	6 to 24	Yes
Balata	0·58-0·63	Taylor, Herrmann and Kemp[9]	W-A-S-A-0h	21 to 25	6 to 24	Yes
Hard rubber	0·52	Taylor, Herrmann and Kemp[9]	W-A-S-A-0h	21 to 25	6 to 24	Yes
Gutta-percha	0·50-0·52	Taylor, Herrmann and Kemp[9]	W-A-S-A-0h	21 to 25	6 to 24	Yes
Paragutta	0·60-0·67	Taylor, Herrmann and Kemp[9]	W-A-S-A-0h	21 to 25	6 to 24	Yes
Vulcanised chloroprene-polymer	0·91	Taylor, Herrmann and Kemp[9]	W-A-S-A-0h	21 to 25	6 to 24	Yes
Soft rubber	2·3-2·7	Taylor, Herrmann and Kemp[9]	W-A-S-A-0h	21 to 25	6 to 24	Yes
Various rubbers	0·09	Edwards and Pickering[27]	W-A-S-A-P₂O₅	25	23·8	Yes
	0·014-1·4	Schumacher and Ferguson[10]	W-V-S-V-P₂O₅	25	23·8	Yes
	0·29	Levey[28]	W-A-S-50h	21	9·3	Yes
	3·45	Abrams and Chilson[14]	W-A-S-50h	21	9·3	Yes
Moisture-proofed group:						
Asphalt	0·40	Taylor, Herrmann and Kemp[9]	W-A-S-A-0h	21 to 25	6 to 24	Yes
Regenerated moisture-proofed cellulose	0·864-5·75	Church and Scroggie[15]	W-A-S-1h	40	53	No
Regenerated moisture-proofed cellulose (including cellophane)	2·9	Birdseye[29]	W-A-S-A-CaCl₂	38	50·6	No
	2·9	Hyden[30]	W-A-S-A-H₂SO₄	38	49·2	No
	2·9	Fabel[31]	W-A-S-A-CaCl₂	30	32	No
	2·9-8·6	Tressler and Evers[32]	W-A-S-50h	−14, 21	9·3	No
	10	Abrams and Brabender[33]	W-A-S-50h	21	9·3	No
	14·4	Abrams and Chilson[14]	W-A-S-50h	21	9·3	No
	23	Staedel[18]	W-A-S-65h	20	6·1	No
Moisture-proofed fibreboard	2·9	Abrams and Brabender[33]	W-A-S-50h	21	9·3	No
	2·9	Tressler and Evers[32]	W-A-S-50h	−14, 21	9·3	No
	2·9	Harvey[34]	W-A-S-A-CaCl₂	25	23·8	No

See foot of Table, p. 442, for key to column four.

TABLE 116 (*continued*)

Type of membrane	$10^6 \times$ permeability	Reference	Experimental details			
			Moisture gradient	Temp. °C	Pressure difference mm.Hg	Thickness given or not
Moisture-proofed group:						
Waxed paper	0·58–1730	Thomas and Reboulet [35]	100h-S-A-CaCl₂	30	31·9	No
	3·45–62·3	Birdseye [29]	W-A-S-A-CaCl₂	38	50·6	No
	3·60–202	Hyden [30]	W-A-S-A-H₂SO₄	38	49·2	No
	14·4	Tressler and Evers [32]	W-A-S-50h	−14, 21	9·3	No
	21·6–260	Abrams and Chilson [14]	W-A-S-50h	21	9·3	No
	23–244	Abrams and Brabender [33]	W-A-S-50h	21	9·3	No
Waxed glassine	4·9–105	Birdseye [29]	W-A-S-A-CaCl₂	38	50·6	No
Miscellaneous water-proofed papers	1·15–115	Tressler and Evers [32]	W-A-S-50h	−14, 21	9·3	No
	576	Staedel [19]	W-A-S-65h	20	6·1	No
Synthetic resins group:						
Aluminium paints	0·068–2·12	Wray and van Vorst [12]	95h-S-A-Al₂O₃	27	25·4	Yes
	0·076–2·9	Edwards and Wray [16]	95h-S-A-Al₂O₃	27	25	Yes
Varnishes, lacquers, aircraft finishes	10·1–374	Hunt and Lansing [17]	95h-S-A-Al₂O₃	27	25	No
	0·26–9·4	Kline [2]	W-A-S-65h	21 to 38	6 to 14	Yes
Cellulose and cellulose compound group:						
Plasticised cellulose acetate	0·41	Taylor, Herrmann and Kemp [9]	W-A-S-A-0h	21 to 25	6 to 24	Yes
Cellulose acetate	0·58–28·8	Tressler and Evers [32]	W-A-S-50h	−14, 21	9·3	No
	54	Taylor, Herrmann and Kemp [9]	W-A-S-A-0h	21 to 25	6 to 24	Yes
	317	Abrams and Brabender [33]	W-A-S-50h	21	9·3	No.
	634	Abrams and Chilson [14]	W-A-S-50h	21	9·3	No.
	24·5	Levey [28]	W-A-S-50h	21	9·3	No
Cellulose nitrate	8·1–4·5	Wosnessenski and Dubnikow [13]	High h-S-Low h	20	9·3	Yes
	20–86·3	Wing [11]	W-S-A-CaCl₂	20	14·9	Yes
	5·4	Levey [28]	W-A-S-50h	40	55·4	No
	4·5	Wosnessenski and Dubnikow [13]	High h-S-Low h	21	9·3	Yes
Cellulose ethers	3·6	Taylor, Herrmann and Kemp [9]	W-A-S-A-0h	20	17·6	Yes
	7·2–15·1	Levey [28]	W-A-S-50h	21. to 25	6 to 24	Yes
				21	9·3	Yes

TABLE 116 (continued)

Type of membrane	$10^6 \times$ permeability	Reference	Experimental details			
			Moisture gradient	Temp. °C.	Pressure difference mm. Hg	Thickness given or not
Cellulose and cellulose compound group:						
Regenerated cellulose	546	Birdseye[22]	W-A-S-A-CaCl₂	38	50·6	No
	560	Church and Scroggie[15]	W-A-S-1h	40	5·3	No
	965	Abrams and Chilson[14]	W-A-S-50h	21	9·3	No
	33	Levey[25]	W-A-S-50h	21	9·3	No
	1655	Gregory[36]	W-A-S-50h	21	9·3	Yes
	3240	Staedel[18]	W-A-S-63h	38, 21	37	No
	5190	Trillat and Matricon[37]	W-A-S-65h	20	6·1	No
Paper	1050	Abrams and Chilson[14]	100h-S-V-0h	20	17·5	No
	1070	Abrams and Brabender[33]	W-A-S-50h	21	9·3	No
	29	Levey[28]	W-A-S-50h	21	9·3	No
Vegetable parchment	1800–3600	Staedel[18]	W-A-S-65h	20	6·1	Yes
	25	Levey[28]	W-A-S-50h	21	9·3	No
Glassine	360	Birdseye[29]	W-A-S-A-CaCl₂	38	50·6	Yes
	23·4	Levey[28]	W-A-S-50h	21	9·3	No
	504	Fabel[31]	W-A-S-A-CaCl₂	30	32	Yes
	680	Abrams and Chilson[14]	W-A-S-50h	21	9·3	No
	806	Abrams and Brabender[33]	W-A-S-50h	21	9·3	No
Various membranes:						
Leather	14·4	Edwards[38]	High h-S-Low h	15 to 21	6 to 17	No
	72–1440	Wilson and Lines[20]	W-A-S-A-H₂SO₄	5 to 45	0 to 72	No
Textile fabrics	45·3	Levey[28]	W-A-S-50h	21	9·3	Yes
	1080–1510	Sale and Hedrick[39]	W-A-S-65h	38, 21	37	No
	1440	Barr[40]	W-A-S-Warm air	35	37	No
	1650–1870	Gregory[36]	W-A-S-63h	38, 21	37	No
Copper gauze	1730	Gregory[36]	W-A-S-63h	38, 21	37	No
Open cell	3140–19,700	Abrams and Chilson[14]	—	—	—	No
	3620	Levey[28]	—	—	—	—
	4840	Gregory[36]	—	—	—	—

The key to column four is:

W = water surface. A = air space. V = evacuated space.
S = specimen.

leathers, and even 10^5-fold greater for textiles, than the water permeability.

TABLE 117. *A comparison of some hydrogen and water permeabilities of membranes*

Membrane	10^6 × approximate* hydrogen permeability at 25° C. (c.c./cm.²/ sec./mm./cm. of Hg)	10^6 × water permeability (c.c./cm.²/sec./ mm./cm. of Hg)
Cellophane† Cellulose acetate Polyethylene sulphide Polychloroprene Rubbers	0·00008 0·018 0·001 0·011 0·019 (smoked sheet rubber) 0·019 (ether soluble rubber)	0·12–0·24 at 38° C. 54·0 at 25° C. 0·076 at 21·1° C. 0·91 at 21·1° C. 0·52 at 25° C. (hard rubber) 2·3–2·7 at 25° C. (soft vulcanised rubber)

* In computing the hydrogen permeability a density of unity had to be assumed, since Sager's[41] original paper did not give his film densities, needed to compute the actual thickness of his membranes.

† Cellophane according to Hyden[30] is manufactured in thicknesses of 0·025–0·05 mm. His permeabilities, for which the membrane thickness was not stated, have been computed on this basis.

SORPTION KINETICS IN ORGANIC SOLIDS

Fick's linear law
$$P = -D\frac{\partial C}{\partial x}$$

has been shown to be a limiting law only, for vapour-membrane diffusion systems. This is also true of the law $\frac{\partial C}{\partial t} = D\frac{\partial^2 C}{\partial x^2}$ when applied to systems which swell during sorption of vapours, and give sigmoid isotherms. Such isotherms are given by cotton[43], wool[44], leather[41], or wood[45]. More generalised laws such as

$$\frac{\partial C}{\partial t} = \frac{\partial}{\partial x}\left(D\frac{\partial C}{\partial x}\right)$$

(see also p. 47) should be used in such systems. However, it has been customary to employ the simpler law, and to use slabs of leather[42], rubber[2], bakelite[48] or cellulose deri-

vatives [46] in computing the diffusion constants D. A suitable solution is then

$$\frac{Q}{Q_\infty} = 1 - \frac{8}{\pi^2}(e^{-\theta} + \tfrac{1}{9}e^{-9\theta} + \tfrac{1}{25}e^{-25\theta} + \ldots),$$

where $\theta = \pi^2 Dt/4l^2$, l = the thickness of the slab, and Q, Q_∞ denote the amounts sorbed at time t and at equilibrium respectively.

When water is sorbed by rigid non-swelling membranes of bakelite, the solution given above holds with some accuracy [48].
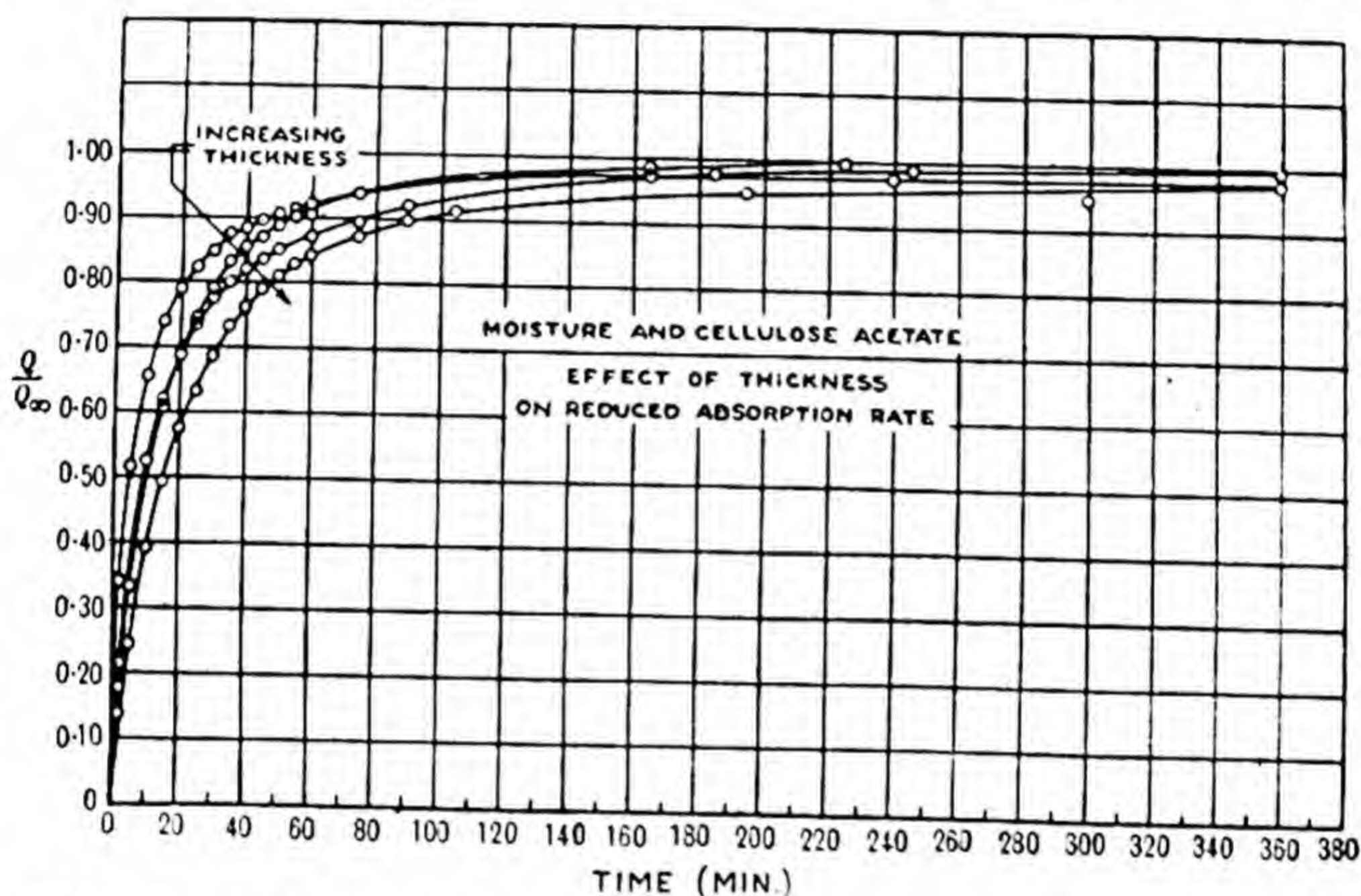
Fig. 154. Curves of relative sorption against time for water-acetyl cellulose systems [46]. The form of the curve $\frac{Q}{Q_\infty}$ against t is dependent on the membrane thickness.

On the other hand, in non-rigid swelling membranes of rubber [47] or cellulose acetate (Fig. 154) the departures were considerable.

The sorption velocity of water in rubber samples increases as the temperature rises. The amount sorbed after a period of 20 hr. (Q_{20}) is given below for a typical case:

Temp. ° C.	Amount sorbed in 20 hr. (Q_{20})
24	0·0110
60	0·0265
70	0·0390
100	0·079

Assuming that the parabolic diffusion law $(Q/Q_\infty)^2 = 4Dt/\pi l^2$ applies, the slope of the curve $\log Q$ [20] versus $1/T$ (T denotes °K.) gives an activation energy of 6900 cal./mol., a figure which may be compared with 6300 cal./atom for He-rubber to 11,900 cal./mol. for N_2-neoprene. Smoked rubber, para-rubber, and pale crepe rubber similarly gave values of the activation energy of 7000, 9800 and 9600 cal./mol. of water respectively.

When rubber swelled in benzene [49], or when paraffin [50] was absorbed by cured rubber and by rubber gum, the positive temperature coefficients of the sorption velocity suggested that in these and other organic solids vapours are sorbed by processes of activated diffusion. The occurrence of activated diffusion has already been established for gas-rubber [52], cellulose, -bakelite and similar systems (Chap. IX). In liquids also, diffusion constants [53] may be expressed by the equation $D = D_0 e^{-E/RT}$, although the values of E are usually smaller.

TABLE 118. *Diffusion constants in miscellaneous systems*

System	D (cm.^{2} sec.$^{-1}$)	Temp. ° C.
H_2O-cellulose acetate [51]	$0\cdot17$–$1\cdot7 \times 10^{-8}$	25
H_2O-leathers [41]	$0\cdot41$–$19\cdot5 \times 10^{-7}$	25
D_2O-H_2O [46]	$2\cdot5 \times 10^{-5}$	25
H_2-rubber	$0\cdot85 \times 10^{-5}$	25
N_2-rubber	$0\cdot11 \times 10^{-5}$	25
CH_3OH-C_2H_5OH	$2\cdot7 \times 10^{-5}$	19
$C_2H_2Cl_4$-$C_2H_2Br_4$	$0\cdot56 \times 10^{-5}$	19

The data in Table 118 permit a qualitative comparison of the diffusion constants of water, gases, and liquids in organic polymers and liquids.

A MODIFIED DIFFUSION LAW FOR SORPTION OF WATER BY RUBBERS

The presence of salts in rubbers and leathers alters the sorption of water by these colloids (p. 436). For this reason Daynes [8] advanced a theory of diffusion as an osmotic phenomenon, the water being sorbed to equalise salt concentration differences

inside and outside the membrane. The law was then for-mulated as

$$\frac{\partial C}{\partial t} = D_1 \frac{\partial^2 h}{\partial x^2},$$

where h denotes the humidity of the atmosphere which would be in equilibrium with the solution at x. The relation between C and h is given by the sorption isothermal. The diffusion equation may now be written

$$\frac{\partial h}{\partial t} = \left(\frac{\partial h}{\partial C} D_1\right) \frac{\partial^2 h}{\partial x^2}.$$

So long as $\partial C/\partial h$ is a constant (i.e. at low humidities), a simple Fick law where $D = \left(D_1 \dfrac{\partial h}{\partial C}\right)$ may be used. The tempo of diffusion is then governed by a single parameter $\theta = \dfrac{4l^2}{\pi^2 D}$,
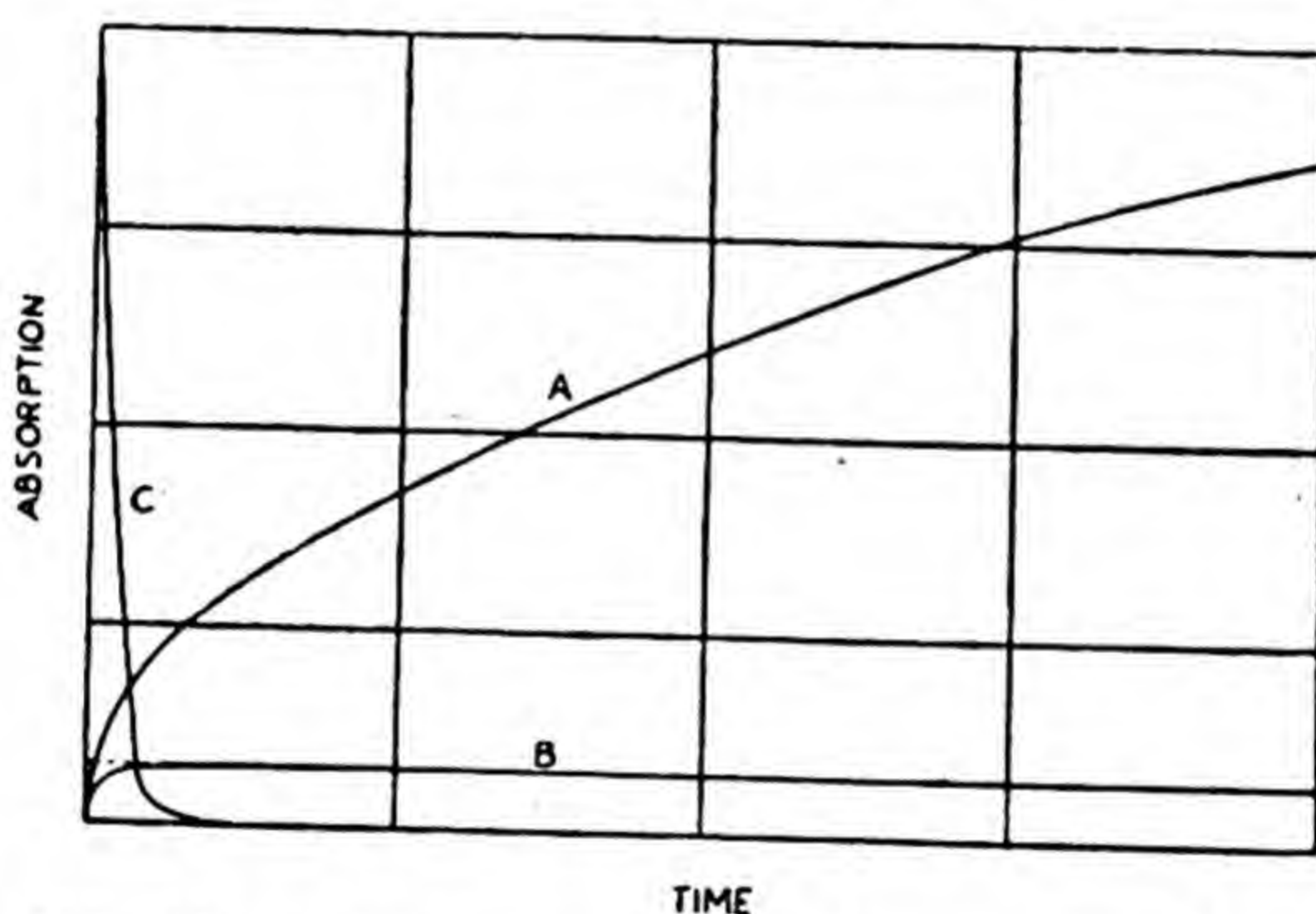
Fig. 155. Absorption and desorption rate curves in rubber[57].

but in the more complex case by the parameter $\theta' = \dfrac{4l^2}{\pi D_1} \dfrac{\partial C}{\partial h}$.

Because $\partial C/\partial h$, and therefore θ', increase rapidly at high humidity, sorption must proceed more and more slowly as humidity increases, or saturation is approached. In desorption, as humidity decreases, the converse is true, i.e. the desorption velocity steadily increases. The first prediction was fulfilled when water was sorbed by vulcanised and unvulcanised rubber[54, 8], gutta-percha, and paragutta[54]; and the second

was indicated by the data of Fry[55] and of Cooper and Scott[56] (Fig. 155[57]). The simple law $\dfrac{\partial C}{\partial t} = D \dfrac{\partial^2 C}{\partial x^2}$ would on the other hand require the ordinates of the asymptotes to the curves A and B to stand in the ratio $2 : 1$, while the curves A and C should be symmetrical.

THE PASSAGE OF VAPOURS OTHER THAN WATER THROUGH MEMBRANES

Although few studies have been made of the permeability of membranes to vapours other than water, the data are of considerable interest theoretically and practically. Typical data are those of Dewar[58] and Edwards and Pickering[27] (Table 119).

TABLE 119. *Permeability of rubber to vapours at room temperature*

Vapour	$10^6 \times$ permeability constant (c.c./sec./cm.^{2}/mm. thick/cm. Hg pressure)		Ratio of permeability constants for vapour and for hydrogen[23]
H_2O	2·41	[23]	55
C_2H_5OH	1·28	[56]	29·1
CH_3Cl	1·14	[56]	25·9
C_2H_5Cl	0·81	[23]	18·5
	8·75	[23]	·198

Kahlenberg[60] showed that if a cell H_2O/rubber/ethyl alcohol was set up the alcohol diffuses into the water more rapidly than water into alcohol. At 15° C. the vapour pressures are 12 mm. for water and 32 mm. for alcohol, so that, with the permeability constants of Dewar in Table 119, one could predict the direction of diffusion actually observed by Kahlenberg. As usual the permeation velocities bear no simple relationship to molecular size or mass, the large molecule, ethyl chloride, being transmitted ten times as fast as the smaller molecule, methyl chloride. The solubility of the diffusing substance in the membrane is one important factor in diffusion. Another must be the extent to which the mem-

brane swells. The swelling, which increases as the amount sorbed increases, causes the polyisoprene chains to separate more and more. One might then imagine that the looser the structure becomes the less its resistance to diffusion would be.

Payne and Gardner (59) also showed that the permeability of a membrane to a vapour depended upon the solvent capacity of the membrane for the vapour. They used smooth cellulose paper of thickness 0·1 mm. as support for the films, which in nearly every instance, in the form of a suitable varnish, penetrated the paper completely. The paper itself had only a slight impedance to diffusion of the vapour. Fig. 156 gives a summary of their relative permeability data for a large number of films, and diffusing substances.

The data of Fig. 156 give the following series for the relative permeabilities of a number of vapours:

Glue [water-soluble, but with macropores]:

$$H_2O > C_6H_6 > C_2H_5OH > CH_3COCH_3 > C_2H_2OCOCH_3.$$
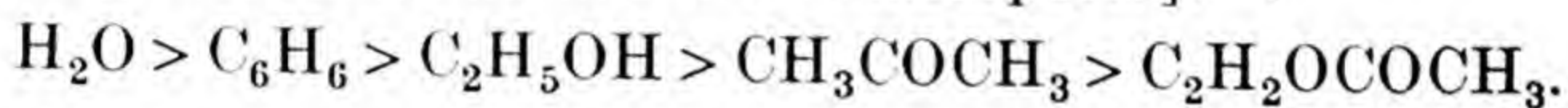
Rubber [soluble in C_6H_6, and partially in CH_3COCH_3]:

$$C_6H_6 > CH_3COCH_3 > C_2H_5OH > H_2O.$$
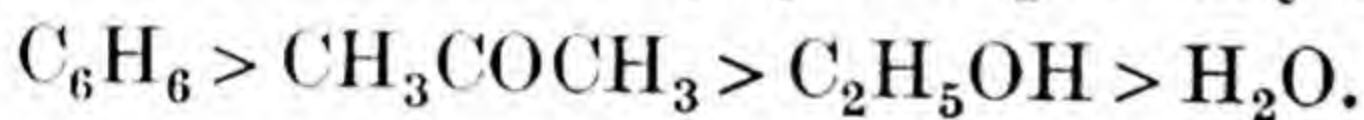
Paraffin wax [soluble in C_6H_6]:

$$C_6H_6 > CH_3COCH_3 > C_2H_5OCOCH_3 > C_2H_5OH > H_2O.$$
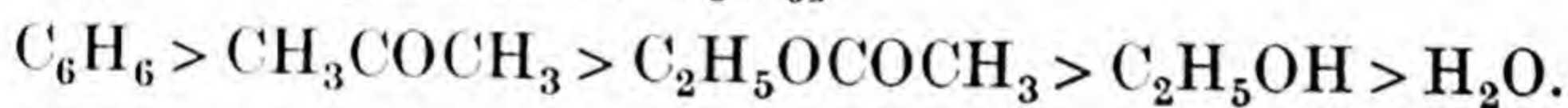
Cellulose nitrate [soluble in CH_3COCH_3, $C_2H_5OCOCH_3$]:

$$CH_3COCH_3 > C_2H_5OH > C_2H_5OCOCH_3 > C_6H_6 > H_2O.$$
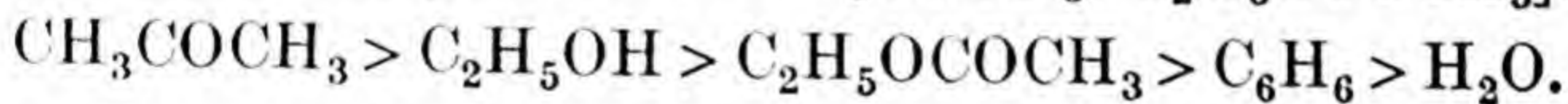
Raw linseed oil [soluble in CH_3COCH_3, $C_2H_5OCOCH_3$]:

$$C_2H_5OH,\ CH_3COCH_3 > C_2H_5OCOCH_3 > C_6H_6 > H_2O.$$
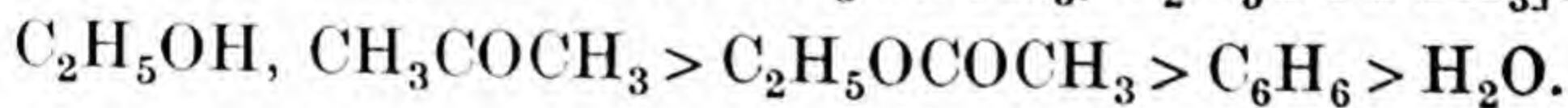
REMARKS ON THE PERMEATION AND DIFFUSION PROCESSES

The nature of the movement of water, organic vapours or gases depends primarily upon the manner in which the diffusing substance is held inside the solid, and on the nature of the channels. The sorption may be:

A. Van der Waals's sorption,

B. Dipole sorption in a monolayer,
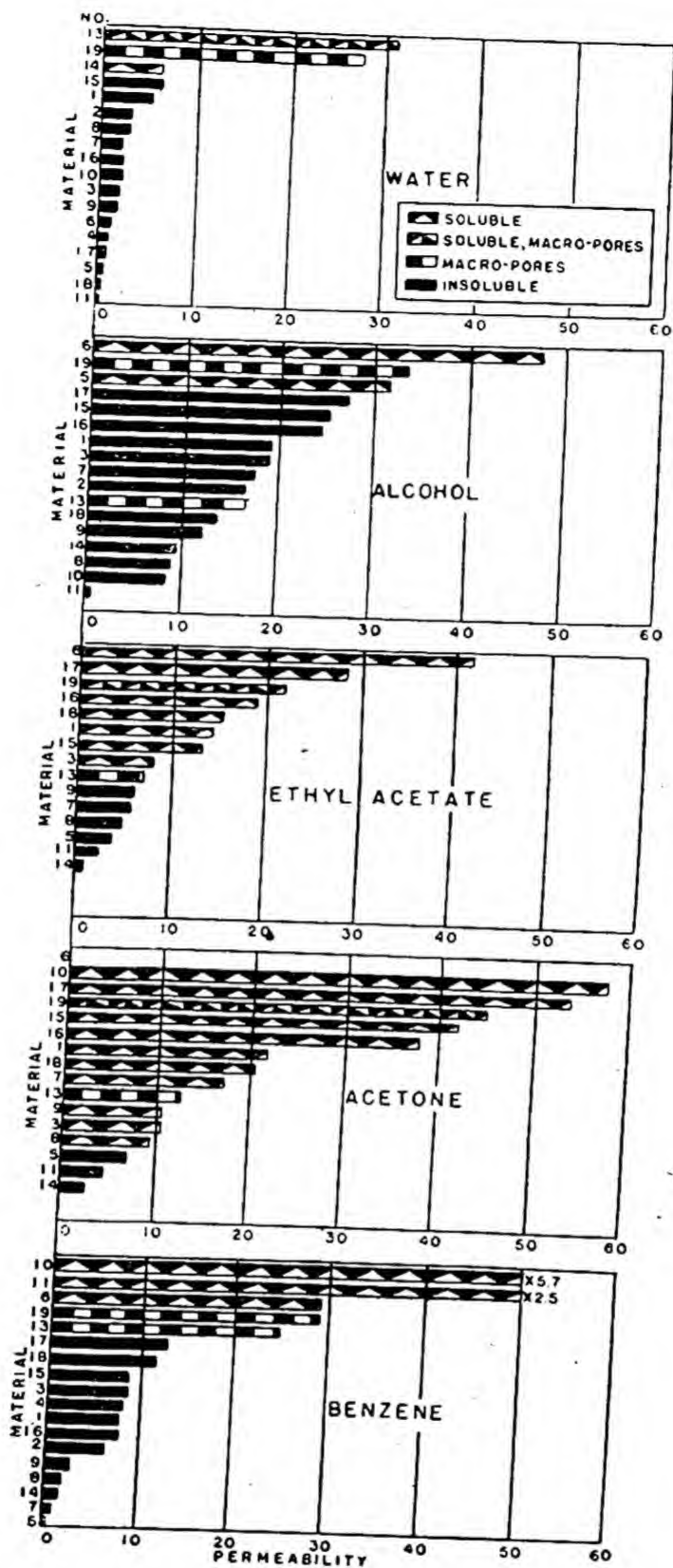
Fig. 156. Comparison of permeabilities of films.

1. Raw linseed oil
2. Bodied linseed oil
3. Rosin spar varnish
4. Phenolic varnish
5. Shellac
6. Rosin
7. Alkyd resin
8. Modified alkyd
9. Resin-oil modified alkyd
10. Rubber
11. Paraffin wax
13. Glue
14. Gelatin
15. Cellulose nitrate
16. Plasticized cellulose nitrate
17. Ester gum lacquer
18. Aluminum lacquer
19. Porous lacquer

C. Multilayer sorption at higher humidities, with possible orientation,

D. Capillary condensation in pores.

The sorbed substance may be in true solution within the solid, or it may be non-homogeneously distributed or per-sorbed. Very often, for example in cellulose (61), van der Waals sorption, or dipole sorption is superseded at higher pressures by capillary condensation. Occasionally, as in certain proteins, chemical effects are suspected (62). The mercerising of natural cellulose is thought to cause a re-orientation of the pyranose chains (see Fig. 137, Chap. IX, for a diagram of the unit cell) in the manner indicated in Fig. 157 (63), the hydration causing
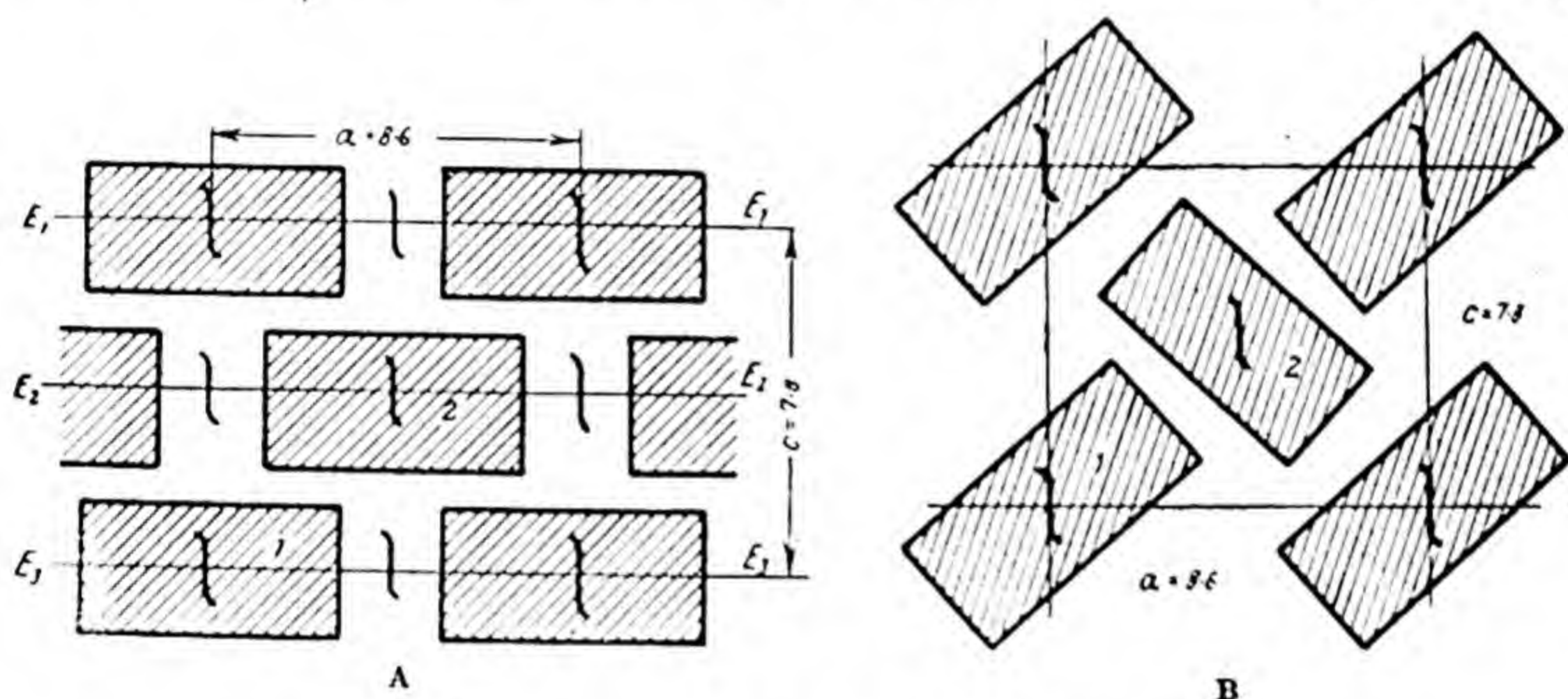
Fig. 157. A. Section of cell of native cellulose.
B. Section of cell of hydrated cellulose.

The b-axis is perpendicular to the plane of the diagram.

a contraction parallel to the cell direction and an expansion in directions normal to it. Ordinary sorption does not alter the cell, but may still affect membrane permeability since it was observed that while desiccated cellulose membranes were impermeable to air, the same membranes after sorbing water became permeable to air (64).

The dispersion of rubber in organic liquids is dependent upon the extent to which the isoprene chains are cross-linked by sulphur. Excessive vulcanisation causes a complete netting of rubber, and as would be anticipated, the extent of vulcanisa-tion conditions the extent of sorption of benzene (65, 66) or a

similar organic liquid (Fig. 158). The limiting case is represented by a membrane of polymerised p-divinyl benzene which neither swells in nor sorbs benzene appreciably. These phenomena must influence profoundly the permeability of the membrane, for it is not likely that netted membranes will be able to transmit large organic vapours readily, unless the transmission is intermicellar. Experiments on these aspects of permeability do not appear to have been made.
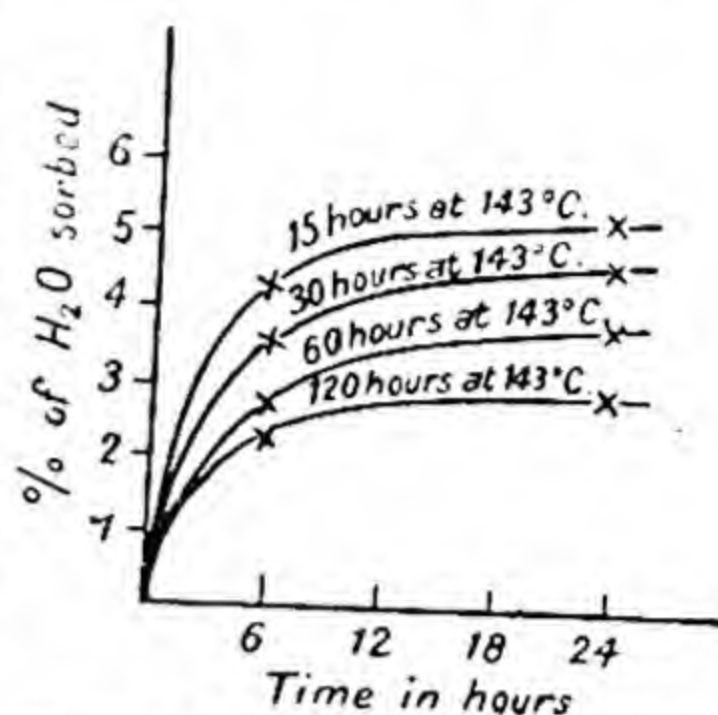
Fig. 158. Dependence of the amount and velocity of sorption upon the degree of vulcanisation.

The peculiar nature of some of the water-protein systems is best brought out by considering X-ray data. While certain natural proteins such as wool, silk, or horn are obtained, when desiccated, in crystalline form (67), others become denatured completely if they are dehydrated. They then fail to give X-ray patterns corresponding to a crystalline arrangement; but the X-ray patterns of the same forms when highly hydrated may indicate a remarkable degree of crystalline order (68). Thus the water is not only sorbed but sometimes plays a vital part in the protein structure. The diffusion of water in such gelatinous membranes might have interesting features owing to the unique role of the water in the gel.

It has been noted that the stronger the sorption of a vapour by an organic colloid the more quickly does the permeation process deviate from the Fick laws $P = D\dfrac{\partial C}{\partial x}$ and $\dfrac{\partial C}{\partial t} = D\dfrac{\partial^2 C}{\partial x^2}$, as the humidity increases. The classification of Wilson and Fuwa (69), which gives a rough measure of the capacity of various types of organic solid to sorb water, may therefore be used as a guide to the degree of applicability which the Fick laws might be expected to have. Some of the substances listed (finely divided inorganic solids, carbon black, silica gel, etc.) are permeable by hydrodynamic flow, but other membranes which have been considered in this chapter show permeation

rates which are independent of the hydrostatic head of pressure, and therefore do not transmit liquids by hydrodynamic flow.

REFERENCES

(1) Carson, F. *Misc. Publ. U.S. Bur. Stand.* M. 127 (1937).
(2) Kline, G. *Bur. Stand. J. Res., Wash.,* **18**, 235 (1937).
(3) Boggs, C. and Blake, J. *Industr. Engng Chem.* **18**, 224 (1926).
(4) For a summary of the data see J. W. McBain, *The Sorption of Gases and Vapours by Solids,* chap. XII. Routledge, 1932.
(5) McBain, J. W. *The Sorption of Gases and Vapours by Solids,* p. 372. Routledge, 1932.
(6) Lowry, H. and Kohman, G. *J. phys. Chem.* **31**, 23 (1927).
(7) Kubelka, V. *Kolloidzschr.* **51**, 331–6 (1930); also M. Bergmann, *J. Soc. Leath. Tr. Chem.* **14**, 307 (1930).
(8) E.g. Daynes, H. *Trans. Faraday Soc.* **33**, 531 (1937).
(9) Taylor, R., Herrmann, D. and Kemp, A. *Industr. Engng Chem.* **28**, 1255 (1936).
(10) Schumacher, E. and Ferguson, L. *Industr. Engng Chem.* **21**, 159 (1929).
(11) Wing, H. *Industr. Engng Chem.* **28**, 786 (1936).
(12) Wray, R. and van Vorst, A. *Industr. Engng Chem.* **25**, 842 (1933).
(13) Wosnessenski, S. and Dubnikow, L. M. *Kolloidzschr.* **74**, 183 (1936).
(14) Abrams, A. and Chilson, W. *Paper Tr. J.* **91**, T.S. 193 (1930).
(15) Charch, W. and Scroggie, A. G. *Paper Tr. J.* **101**, T.S. 201 (1935).
(16) Edwards, J. and Wray, R. *Industr. Engng Chem.* **28**, 549 (1936).
(17) Hunt, J. and Lansing, D. *Industr. Engng Chem.* **27**, 26 (1935).
(18) Staedel, W. *Papier Fabr.* **31**, 535 (1933).
(19) Stillwell, S. *Tech. Pap. For. Prod. Res., Lond.,* 1 (publ. 1926–36).
(20) Wilson, J. and Lines, G. *Industr. Engng Chem.* **17**, 570 (1925).
(21) Bergmann, M. *J. Soc. Leath. Tr. Chem.* **13**, 161 (1929).
(22) Martley, J. *Tech. Pap. For. Prod. Res., Lond.,* 2 (publ. 1926–36).
(23) Sager, T. P. *Bur. Stand. J. Res., Wash.,* **19**, 181 (1937).
(24) Schroeder, P. N. *Z. phys. Chem.* **45**, 75 (1903).
(25) Daynes, H. *Proc. Roy. Soc.* **97**A, 286 (1920).
(26) Bergmann, M. and Ludewig, S. *J. Soc. Leath. Tr. Chem.* **13**, 279 (1929).
(27) Edwards, J. and Pickering, S. *Sci. Pap. Bur. Stand.* **16**, 327 (1920).
(28) Levey, H. *Plastic Prod.* **11**, 52 (1934).
(29) Birdseye, C. *Industr. Engng Chem.* **21**, 573 (1929).
(30) Hyden, W. *Industr. Engng Chem.* **21**, 405 (1929).

(31) Fabel, K. *Kunstseide*, **15**, 383 (1933).

(32) Tressler, D. and Evers, C. *Paper Tr. J.* **101**, T.S. 113 (1935).

(33) Abrams, A. and Brabender, G. *Paper Tr. J.* **102**, T.S. 204 (1936).

(34) Harvey, A. *Paper Tr. J.* **78**, T.S. 256 (1924).

(35) Thomas, C. and Reboulet, H. *Industr. Engng Chem. Anal. ed.*, **2**, 390 (1930).

(36) Gregory, J. *J. Text. Inst.* **21**, T. 66 (1930).

(37) Trillat, J. and Matricon, M. *J. chim. Phys.* **32**, 101 (1935).

(38) Edwards, R. *J. Soc. Leath. Tr. Chem.* **16**, 439 (1932).

(39) Sale, P. and Hedrick, A. *Bur. Stand. Tech. Paper*, **18**, 540 (1924).

(40) Barr, G. *Second Rep. Fabrics Co-ord. Res. Committee, D.S.I.R. Gt Brit.* p. 113 (1930).

(41) Sager, T. P. *Bur. Stand. J. Res. J., Wash.*, **13**, 879 (1934).

(42) Bradley, H., McKay, A. and Worswick, B. *J. Soc. Leath. Tr. Chem.* **13**, 10, 87 (1929).

(43) Masson, O. and Richards, E. *Proc. Roy. Soc.* **78A**, 412 (1907).

(44) Hedges, J. *Trans. Faraday Soc.* **22**, 178 (1926).

(45) *Tech. Pap. For. Prod. Res., Lond.*, 1 and 2.

(46) Sheppard, S. and Newsome, P. *J. phys. Chem.* **34**, i, 1160 (1930).

(47) Andrews, D. and Johnston, J. *J. Amer. Chem. Soc.* **46**, 640 (1924).

(48) Leopold, H. and Johnston, J. *J. phys. Chem.* **32**, 876 (1928).

(49) Kirchof, F. *Kolloidchem. Beih.* **6**, 1 (1914).

(50) Lundal, A. E. *Ann. Phys., Lpz.*, **66**, 741 (1898).

(51) Ostwald, W. *Grundiss der Kolloidchemie*, p. 370.

(52) Barrer, R. M. *Trans. Faraday Soc.* **35**, 628 (1939).

(53) —— *Trans. Faraday Soc.* **35**, 644 (1939).

(54) Daynes, H. *India Rubb. J.* **84**, 376 (1932).

(55) Fry, J. *India Rubb. J.* **73**, 513 (1927).

(56) Cooper and Scott. *Lab. Circ. Res. Ass. Brit. Rubber Manuf.* no. 65 (1930).

(57) Daynes, H. *Rubber Tech. Conf., London*, May 23–5, 1938.

(58) Dewar, J. *Proc. Roy. Instn*, **21**, 813 (1914–16).

(59) Payne, H. and Gardner, W. *Industr. Engng Chem.* **29**, 893 (1937).

(60) Kahlenberg, L. *J. phys. Chem.* **10**, 141 (1906).

(61) Sheppard, S. *Trans. Faraday Soc.* **29**, 77 (1933).

(62) Bancroft, W. and Barnett, C. *J. phys. Chem.* **34**, 449, 753, 1217, 2433 (1930).

(63) Meyer, K. and Mark, H. *Ber. dtsch. chem. Ges.* **61**, 593 (1928).

(64) Alexejev, A. and Matalski, V. *J. chim. Phys.* **24**, 737 (1927).

(65) Kirchof, F. *Kolloidzschr.* **35**, 367 (1924).

(66) Stamberger, P. *Kolloidzschr.* **45**, 239 (1928).

(67) Astbury, W. and Woods, H. J. *Nature, Lond.*, **126**, 913 (1930); **127**, 663 (1931).

(68) Bernal, J., Fankuchen, I. and Perutz, M. *Nature, Lond.*, **141**, 528 (1938).

(69) Wilson, R. and Fuwa, T. *Industr. Engng Chem.* **14**, 915 (1922).

AUTHOR INDEX

SUBJECT INDEX

Absorption, *see* Sorption, Solution
— of alkali metals by alkali halides, 109–10, 111–15, 312, 316
— of alkali metals in tungsten, 354–5
— of ammonia, sulphur dioxide, and hydrochloric acid by alkali halides, 115
— and diffusion of gases in finely divided metals, 230–4
— of halogens by alkali halides, 109–10, 111–14, 312
— of hydrogen by alkali halides, 109–10, 111–14, 312
— of thallium by alkali halides, 113
Activated adsorption, 232–3
Activated diffusion, 71, 73, 106, 121–3, 132–3, 169, 207–8, 222–3, 382, 403, 409, 416, 436, 445
Activation energy for diffusion, 103, 141, 221, 222, 223, 225, 274, 275, 420, 421, 424, 425
— — for structure-sensitive diffusion, 327–9
— — for surface diffusion, 346, 360–1, 363, 364–6, 366–7, 370
Activation energy, radius and polarisability in alkali halides, 264–5
Adatoms, 347, 350
Ammoniate formation in natrolite, 105–6
Analogy between activated diffusion and chemical reaction, 427
Anionic conductors, 267

Base exchange, 240
Berthollide compounds, 249–50. *See also* Interstitial compounds

Calculation of conductivity, 293–7
— of diffusion constant, 293–6, 298–303. *See also* Models of conduction and diffusion processes, etc.
— of energy periodicity of crystal surfaces, 379
— of surface diffusion constant, 375–6
Capillary condensation, 450
Chemical composition of gases desorbed from metals, 227
— — of glasses in relation to permeability, 129–30, 137–9

Classification of some diffusion systems, 123
Colour centres in alkali halides, 109–10, 319–21
Condensation and aggregation of atom beams on surfaces, 339–47
Conductivity of salts, 240, 247–50, 251–3, 256, 257–65, 265–7, 268–72, 272–3, 274, 276–8, 283, 289, 294–7, 305. *See also* Structure-sensitive conductivity
— of solid solutions of salts, 256, 261–3, 323–5
— and space-charge redistribution, 325
— of thin films, 343–6
Criteria of stability in films, 339, 340–1
Critical nominal thickness of thin films, 344–6
Critical streaming density for aggregation of atom beams on solids, 377–8
Cross-linking and permeability of polymers, 393
— and solubility of polymers, 391
— and sorption by polymers, 450–1
Crystal growth, 337–9, 339–41, 341–3, 375, 377–8.

Degassing of metals, 31, 226–30
Degrees of freedom in diffusion processes, 299–300, 422–3, 425
Dependance of activation energy for diffusion upon concentration, 282–3, 367, 372, 374
— of tensile strength upon sorption, etching and fibre diameter, 315–16
Derivation of diffusion constants from solutions of Fick's laws, 47–9, 50, 97–8, 112–14, 214–19, 351–2, 355, 356–9, 412–13. *See also* Measurement of diffusion constants
Differential forms of the diffusion equation, 1–5
Diffusion anistropy, 98, 102–3, 193, 276–9, 327
Diffusion equation when the diffusion constant depends upon concentration, 47–9, 101, 443, 446
— coupled with interface reactions, 37–43, 174–5, 176–8, 179–83, 191
— in cylinders, 31–7